Regulation of Reserve Carbohydrates in Hull-less Barley Grain

Wai Li Lim, B.Sc (Hons)

A thesis submitted to the University of Adelaide in fulfilment of the requirements for the degree of Doctor of Philosophy

The University of Adelaide
Faculty of Sciences
School of Agriculture, Food and Wine
Waite Campus

Date of submission: February 2018

Table of Contents

Declaration

I, Wai Li Lim certify that this work contains no material which has been accepted for the award of any other degree of diploma in my name, in any university or other tertiary institution and, to the best of my knowledge and belief, contains no material previously published or written by another person, except where due reference has been made in the text. In addition, I certify that no part of this work will, in the future, be used in a submission in my name, for any other degree or diploma in any university or other tertiary institution without the prior approval of the University of Adelaide and where applicable, any partner institution responsible for the joint-award of this degree.

I give consent to this copy of my thesis when deposited in the University Library, being made available for loan and photocopying, subject to the provisions of the Copyright Act 1968.

The author acknowledges that copyright of published works contained within this thesis resides with the copyright holder(s) of those works.

I also give permission for the digital version of my thesis to be made available on the web, via the University's digital research repository, the Library search catalogue and also through web search engines, unless permission has been granted by the University to restrict access for a period of time.

Wai Li Lim Date: 8th February 2018

Acknowledgments

My PhD experience with ARC Centre of Excellence in Plant Cell Walls has been rewarding and fulfilling. Firstly, I am very thankful to my supervisors, Rachel Burton, Helen Collins and Caitlin Byrt for their continued supervision, encouragement and support. I am grateful to be able to work with the PCW members, especially Jelle Lahnstein, Neil Shirley, Kuok Yap, Grace Ang, David Matthew, Natalie Kibble, Emma Drew, Stav Manafis, Kylie Neumann, Matthew Aubert, Matthew Tucker, Maple Ang, Sandy Khor, Chao Ma, Ali Hassan, George Dimitroff, Sophia Tsinivits, Jamil Chowdhury, Juanita Lauer, Lisa O'Donovan, Ghazwan Karem, Robyn McBride, Ashley Tan and Kendall Corbin. I would also like to thank to the collaborators of this project, Andrea Matros and Manuela Peukert for their supervision and assistance with MALDI-MSI during my training in IPK.

I would like to thank the Adelaide Graduate Research Scholarship from the University of Adelaide and ARC CoE Plant Cell Walls for their financial support. Finally yet importantly, I would like to thank my husband, Kek Jern Lim and my family for always showing their 100% support and love throughout my journey.

List of Publications

1. **Lim W.L.,** Collins H.M., Singh R.R., Kibble N.A., Yap K., Taylor J., Fincher G.B., Burton R.A. (2017) Method for hull-less barley transformation and manipulation of grain mixed-linkage beta-glucan. J Integr Plant Biol. doi: 10.1111/jipb.12625 **(Published)**

2. **Lim, W.L.,** Collins, H., Byrt, C., Lahnstein, J., Shirley. N., Aubert, M., Tucker, M., Peukert, M., Matros, A., Burton, R.A. Overexpression of *CslF6* gene in hull-less barley grain alters carbohydrate partitioning and impairs grain development. (**Unpublished)**

3. **Lim, W.L.,** Collins, H., Byrt, C., Shirley. N., Lahnstein, J., Burton, R.A. How does the lack of (1,3;1,4)-β-glucan affect other barley grain components? (**Unpublished)**

4. Peukert, M., **Lim, W.L.**, Seiffert, U., and Matros, A. 2016. Mass spectrometry imaging of metabolites in barley grain tissues. Curr. Protoc. Plant Biol. 1:574-591. doi: 10.1002/cppb.20037 **(Published)**

Thesis Abstract

(1,3;1,4)-β-Glucans, which have many health benefits, represent the major cell wall component in barley endosperm. There have been a number of studies that have altered the amount of (1,3;1,4)-β-glucan in the grain, however, the effects of modifying (1,3;1,4)-β-glucan on various carbohydrate metabolic pathways and its impact on grain development have not previously been clearly defined. Here, we used transgenic grain with increased (1,3;1,4)-β-glucan and a (1,3;1,4)-β-glucanless (*bgl*) mutant (OUM125) supplied by Professor K. Sato (Okayama University), to investigate the link between carbohydrate metabolism and grain development in hull-less barley. Hull-less barley was investigated as it is more suitable for food use due to absence of maternal (husk) tissues.

High (1,3;1,4)-β-glucan barley grain (cv Torrens) was successfully generated by over-expressing *HvCslF6,* via agrobacterium-mediated transformation. Transgenic grain had up to 70% more (1,3;1,4)-β-glucan than the wild type. Examination of developing transgenic grain revealed a large fluid filled cavity in the endosperm, which resulted in shrunken grain at maturity. The endosperm transfer region of the developing grain was ruptured by 10 days after pollination (DAP), which became more pronounced through development. Quantitative real-time PCR (QPCR) analysis uncovered genes related to cell wall, starch, sucrose and fructan biosynthesis that were differentially expressed across grain development. Starch metabolic genes were downregulated in the early storage phase and the fructan biosynthetic gene, *6-SFT*, was upregulated during the later storage phase. Increased amounts of sucrose and fructan were found in the cavity and endosperm tissue of the transgenic grain.

The link between altered sugar homeostasis, the large endosperm cavity and the poorly formed endosperm transfer region in transgenic grain was explored by immuno-histochemical

microscopy. Cell walls in the endosperm transfer region were poorly formed and variations occurred in the abundance of mannan polysaccharides. Additionally, the development of both the subaleurone and aleurone layers were altered with regards to cell number, shape and position.

To further understand the relationship between cell wall, starch and fructan metabolism in barley, transcript profiles of genes related to their metabolism were examined in the (1,3;1,4)-β-glucanless OUM125 mutant. Inactive CSLF6 synthase activity in OUM125 resulted in upregulation of the *CslH1* gene from 19 DAP, resulting in traces of BG1 antibody labelling in the mutant pericarp. Other cell wall-related genes including *CslF3, CslF7, CslF10, CesA2, CesA3* and *Gsl2* were upregulated from 15 DAP in the mutant grain. Deposition of arabinoxylan, callose and cellulose was altered in the absence of (1,3;1,4)-β-glucan in the mutant endosperm. QPCR analysis identified changes in the expression of starch and fructan biosynthetic genes during the storage phase. At grain maturity, sucrose and fructan contents had increased, while the amount of starch remained unchanged.

Research findings from this project provide fundamental knowledge about carbon partitioning in grain across development and suggest that small changes in polysaccharide synthesis and deposition can have significant effects on other metabolic processes important for correct grain development. While decreasing the amount of (1,3;1,4)-β-glucan in the barley endosperm had a low impact on grain morphology and carbon partitioning, significantly increasing the (1,3;1,4)-β-glucan content had major deleterious effects on a number of key processes.

Chapter 1

General Introduction

1.1 Schematic Structure of the Thesis

Chapter 1: ***General Introduction***

- Schematic structure of the thesis
- Background
- Objectives of the study

Chapter 2: ***Method for hull-less barley transformation and manipulation of grain mixed-linkage beta-glucan***

- The chapter describes my contribution to this project, which includes characterisation of transgenic seedlings and microscopy analysis of transgenic grain

Chapter 3: ***Overexpression of HvCslF6 gene in Hull-less Barley Grain Alters Carbon Partitioning and Impairs Endosperm Development***

- This chapter describes carbohydrates profiles, grain morphology, distribution of cell wall polysaccharides, and genetic analysis of carbohydrate metabolic pathway across grain development

Chapter 4: ***How does the Lack of (1,3;1,4)-β-Glucan Affect Other Barley Grain Components?***

- This chapter describes carbohydrates profiles, distribution of cell wall polysaccharides, and genetic analysis of carbohydrate metabolic pathway across grain development

Chapter 5: ***Mass Spectrometry Imaging of Metabolites in Barley Grain Tissues***

- The chapter describes my contribution to this project, which includes a comparison of the ionisation efficiency of small sugars from barley grain extracts between 2,5-dihydroxybenzoic acid (DHB) and gold nanoparticle (GNP) matrix

Chapter 6: ***General Discussion***

- Summary of research findings
- Limitations
- Significance of the study
- Future directions

1.2 Literature Review

1.2.1 Introduction

Carbohydrates in cereal grain are essential energy sources in animal and human food, and for the malting process. In barley grain, starch is the predominant carbohydrate representing 50-65% of the dry mass, whilst non-starch carbohydrates include (1,3;1,4)-β-glucans (2-20% dry mass) (Havrlentova and Kraic, 2006) and fructans (1-4% dry mass) (Nemeth et al., 2014). (1,3;1,4)-β-Glucan has attracted considerable attention due to its impact on the final end use of the grain and thus there is demand for barley that is either low or high in (1,3;1,4)-β-glucan. For example, although high (1,3;1,4)-β-glucan is desirable for human consumption due to its important health benefits, in poultry diets it has anti-nutritive activity and results in negative impacts on poultry growth and performance (Annison, 1993). Moreover, high (1,3;1,4)-β-glucan content may result in incomplete hydrolysis by enzymes leading to residual malt (1,3;1,4)-β-glucan negatively impacting the brewing process (Bamforth, 1994; Jamar et al., 2011). Modification of (1,3;1,4)-β-glucan content in barley grain by modulating the genes involved in the biosynthetic pathway provides an opportunity to improve barley quality for human health, nutrition and malt quality (Tonooka et al., 2009; Burton et al., 2011; Han et al., 2017). However, changes in (1,3;1,4)-β-glucan content in the mature grain have been associated with altered amounts of other carbohydrates, such as starch and fructan (Clarke et al., 2008; Burton et al., 2011; Hu et al., 2014). Some of the modified grain displayed a shrunken phenotype and the physiological reason for this was not obvious (Andersson et al., 1999; Morell et al., 2003; Carciofi et al., 2012; Ma et al., 2014). The work carried out in this project aims to examine the determinants of amounts of (1,3;1,4)-β-glucan and other major polysaccharides including starch and fructan, at the biochemical and molecular levels in hull-less barley grain, and to investigate the biological changes occurring in the modified grain during development.

1.2.2 Carbohydrates in plants

Carbohydrates are products of photosynthesis, and are comprised of carbon (C), hydrogen (H) and oxygen (O) atoms. Carbohydrates are building blocks for plant tissues and they are essential throughout the process of growth and development. When the synthesis of carbohydrates is greater than needed, excess carbohydrates will be stored in specialised tissues until they are required. These carbohydrates are therefore known as reserve or storage carbohydrates. Carbohydrates can be categorised into simple and complex forms. In plants, simple carbohydrates include monosaccharides such as glucose, fructose and galactose, disaccharides exemplified by sucrose and maltose and oligosaccharides including raffinose and stachyose. Complex carbohydrates, often known as storage carbohydrates, include starch, fructans, and cell wall polysaccharides such as cellulose, (1,3;1,4)-β-glucan and xylan. Monosaccharides are building blocks for complex carbohydrates and supply the energy for many other biosynthetic processes such as making proteins, DNA and RNA. Thus in both plant and human metabolism, complex carbohydrates are broken down into simple carbohydrates which are subsequently metabolised to generate fuel to support many metabolic activities.

1.2.3 Synthesis of carbohydrates in plants

In plants, carbohydrates are produced during photosynthesis, via light-dependent and light-independent reactions. Light-dependent reactions take place on the thylakoid membranes of chloroplasts. In the presence of light, four major complexes, comprised of photosystem I (PSI), photosystem II (PSII), cytochrome b6f complex, and ATP synthase, catalyse the light-dependent reaction and produce ATP and NADPH (Allen et al., 2011; Roach and Krieger-Liszkay, 2014). Light-independent reactions, also known as the Calvin cycle, do not require light. Instead, they require ATP and NADPH produced from light-dependent reactions, and

they take place in the stroma of chloroplasts. In the Calvin cycle, ribulose bisphosphate carboxylase oxygenase (RuBisCO) fixes carbon dioxide from the atmosphere and converts ribulose 1,5-biphosphate (RuBP) into 3-phosphoglycerate (3-PGA). 3-PGA uses ATP and NADPH produced from the light-dependent reaction and forms glyceraldehyde 3-phosphate (G3P), also known as triose phosphate. Triose phosphate can be recycled, forming RuBP so that the Calvin cycle can be reiterated. Other G3P molecules can be reduced to form hexose phosphates, which are the building blocks for carbohydrates (Fig. 1).

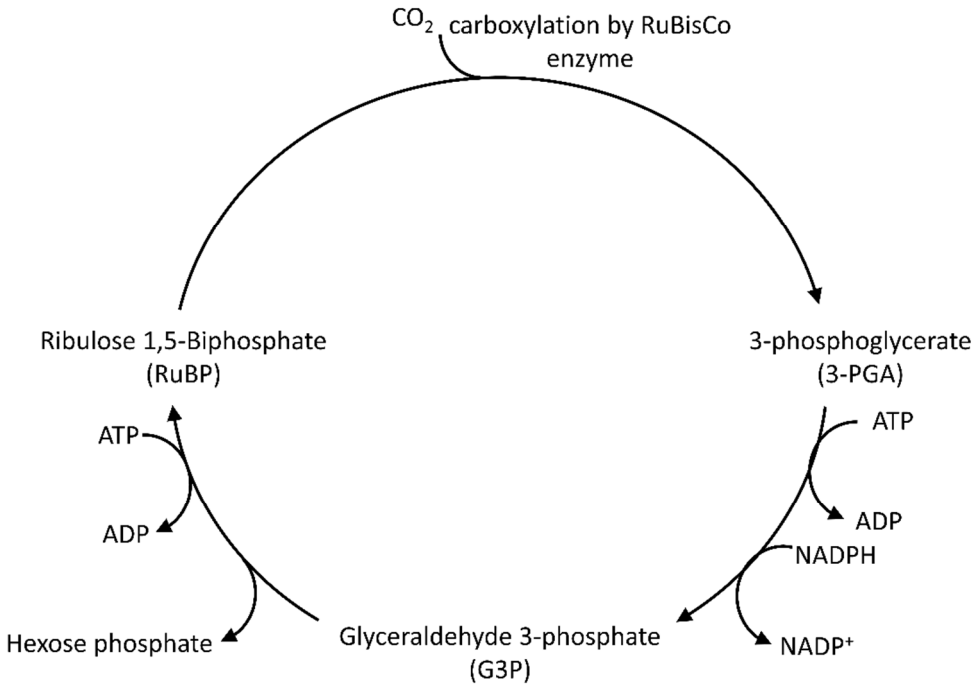

Figure 1: A simplified illustration of the Calvin cycle in plants. The cycle takes place in the stroma of chloroplasts without requiring light. Firstly, the RuBisCo enzyme captures carbon dioxide (CO_2) from the atmosphere and converts ribulose 1,5-biphosphate (RuBP) into a six-carbon intermediate which immediately splits into two molecules of 3-phosphoglycerate (3-PGA). Phosphoglycerate kinase uses ATP as a substrate to phosphorylate 3-PGA, forming 1,3-bisphosphoglycerate (1,3-BPGA) and ADP as products. Glyceraldehyde 3-phosphate

dehydrogenase subsequently reduces 1,3-BPGA using NADPH, forming glyceraldehyde 3-phosphate (G3P) and $NADP^+$. One molecule of G3P will be converted into hexose phosphate (carbohydrate), and the remaining G3P will be used to regenerate RuBP using ATP as a substrate.

1.2.4 Translocation of carbohydrates from source to sink tissues

1.2.4.1 In photosynthetic tissues (source)

In chloroplasts, triose phosphate from the Calvin cycle may be converted into ADP-glucose (ADP-Glc) which is a substrate for starch synthesis. Storage of starch in chloroplasts, however, is only short term. At night or when photosynthesis does not occur, starch in the chloroplasts may be broken down into glucose or maltose and exported to the cytoplasm. Hexoses in the cytoplasm, such as glucose and fructose, undergo modifications including phosphorylation, generating hexose-phosphate. Sucrose, a key carbon source for growth, development and defence, is primarily synthesised in the cytosol of all plant cells. Sucrose is synthesised by sucrose-phosphate synthase (SPS) and sucrose-phosphate phosphatase (SPP). In the sucrose synthesis pathway, SPS first uses UDP-Glc and fructose-6-phosphate as substrates to synthesise sucrose-6-phosphate, then SPP subsequently releases orthophosphate (Pi) from sucrose-6-phosphate, yielding sucrose as the final product (Fig. 2).

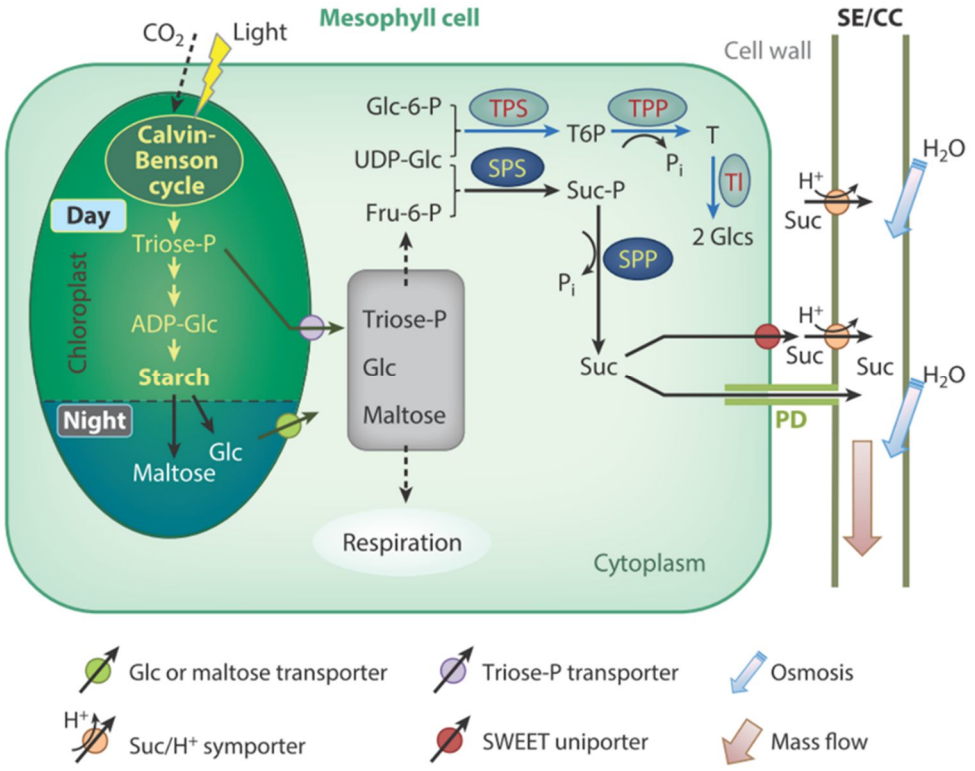

Figure 2: Carbohydrate synthesis in photosynthetic tissues and transportation of the carbohydrates via phloem loading. Triose-phosphate (triose-P), a product from the Calvin cycle, which takes place in the stroma of chloroplasts, is converted into ADP-glucose (ADP-Glc) which is a substrate for starch synthesis in the photosynthetic tissues. Storage of starch in the photosynthetic tissues is transient and starch is quickly degraded into glucose (Glc) or maltose for energy. Glc and maltose from chloroplasts may be exported to the cytoplasm and modified into glucose-6-phosphate (Glc-6-P). Glc-6-P isomerase may convert Glc-6-P into fructose-6-P (Fru-6-P). Triose-P may also be exported to the cytoplasm and used as building blocks for other metabolism. Trehalose is a product generated by trehalose-6-phosphate (T6P) synthase (TPS) and T6P phosphatase (TPP) using Glc-6-P and UDP-Glu as substrates. Trehalose is subsequently hydrolysed by trehalase (TI) into two molecules of Glc. For sucrose synthesis, sucrose-phosphate synthase (SPS) first uses Fru-6-P and UDP-Glc as substrates to produce sucrose-phosphate (Suc-P). The phosphate from Suc-P will be removed by sucrose-phosphate phosphatase (SPP) forming sucrose. Sucrose is then loaded into the phloem (comprised of sieve

elements and companion cells (SE/CC)) via symplastic (through plasmodesmata) and/or apoplastic pathways (via sugar transporters). Accumulation of sucrose in the phloem creates an osmotic potential and attracts water; this drives mass flow of assimilates toward the sink organs. Various sugar transporters are indicated. Additional abbreviations: orthophosphate (P_i), plasmodesmata (PD). Figure reproduced from Ruan, (2014).

Sucrose from source tissues will be translocated to the tissues that are not involved in photosynthesis, known as sink tissues. The translocation process from source to sink is conducted via the phloem, which is comprised of sieve tube elements and companion cells. Sieve tube elements are like a pipe for the transport of carbohydrates, and companion cells support sieve tube elements by carrying out metabolic functions (Fig. 3D) (van Bel and Knoblauch, 2000; Braun and Slewinski, 2009; Braun et al., 2013).

The translocation of carbohydrates from photosynthetic cells to phloem tissues is facilitated by both symplastic and apoplastic phloem loading (Patrick, 1997; Haupt et al., 2001). In the symplastic pathway, sucrose from the cytoplasm of photosynthetic cells diffuses down the concentration gradient to the neighbouring cells, the bundle sheath cells and vascular parenchyma cells, and is loaded into the phloem through plasmodesmata. Alternatively, sucrose can be exported to the neighbouring cells and to phloem via an apoplastic pathway, mediated by various sugar transporters (Fig 3A to 3C). The functioning of the phloem loading pathway varies between cereals, for example, barley, wheat, maize and sugarcane are reported to transport carbohydrates predominantly via the apoplastic pathway, whereas rice predominantly uses the symplastic pathway to transport nutrients to the sink organs (Braun and Slewinski, 2009).

A

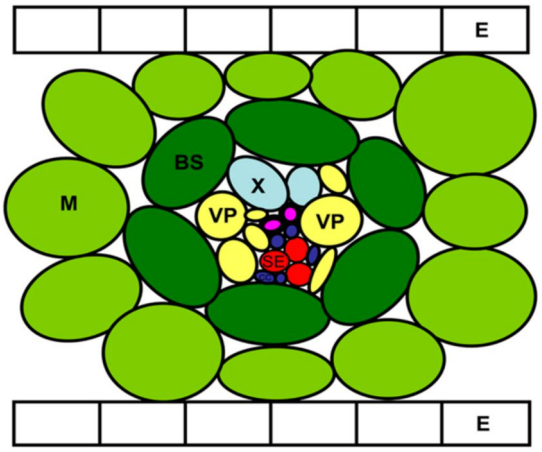

B

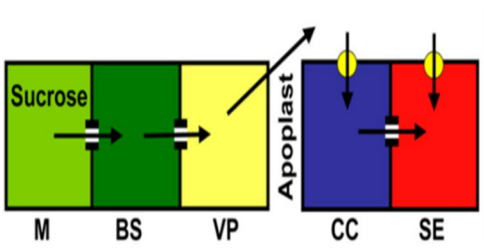

C

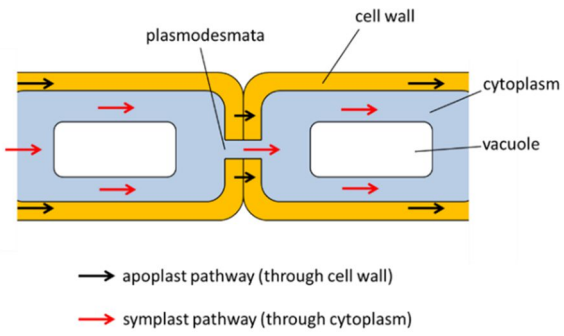

D

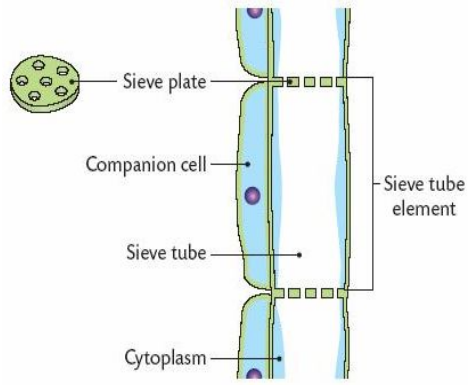

Figure 3: Schematic diagrams of leaf structure and the path of sucrose movement. (A) Arrangement of cells in a leaf. Mesophyll cells surround bundle sheath cells, which surround other cell types including vascular parenchyma cells, xylem and phloem. Image taken from Braun and Slewinski, (2009). (B) Sucrose moves to the bundle sheath and vascular parenchyma cells through plasmodesmata via a symplastic pathway. Sucrose in the vascular parenchyma cells is exported to the apoplast and imported into the companion cells and sieve tube elements by transporter proteins (yellow circles). Image taken from Braun and Slewinski, (2009). (C) Symplastic phloem loading involves the transportation of nutrients within the cytoplasm,

whereas apoplastic phloem loading involves an extracellular step in the transportation of nutrients. (D) Phloem consists of sieve tube elements and companion cells. Image taken from Flowering Plants, (2017). Abbreviations: epidermal cells (E), mesophyll cells (M), bundle sheath cells (BS), vascular parenchyma cells (VP), xylem (X), thin-walled sieve elements (SE), companion cells (CC). Thick-walled sieve elements are coloured pink.

1.2.4.2 In non-photosynthetic tissues (sink)

Sucrose from the phloem is unloaded into sink tissues either apoplasmically or symplasmically. For apoplastic loading, sucrose can be imported via sucrose transporters, and can be hydrolysed into glucose and fructose by cell wall invertase prior to entering the cytosol. Sucrose in the cytosol may be hydrolysed by cytoplasmic invertase and sucrose synthase, while sucrose in the vacuole may be hydrolysed by vacuolar invertase. The intracellular hexose is used for consumption and storage (Fig. 4) (Poorter and Villar, 1997). Approximately 35-40% of carbohydrates are used by sink organs as an energy source for growth and development. The remaining carbohydrates are used in metabolism and to make the structural components of plant cells, such as cellulose and non-cellulosic polysaccharides, or stored as reserve carbohydrates (Hall and Rao, 1999). Sugars may also enter the nucleus and be involved in mediating the expression of genes (Fig. 4) (Ruan, 2014).

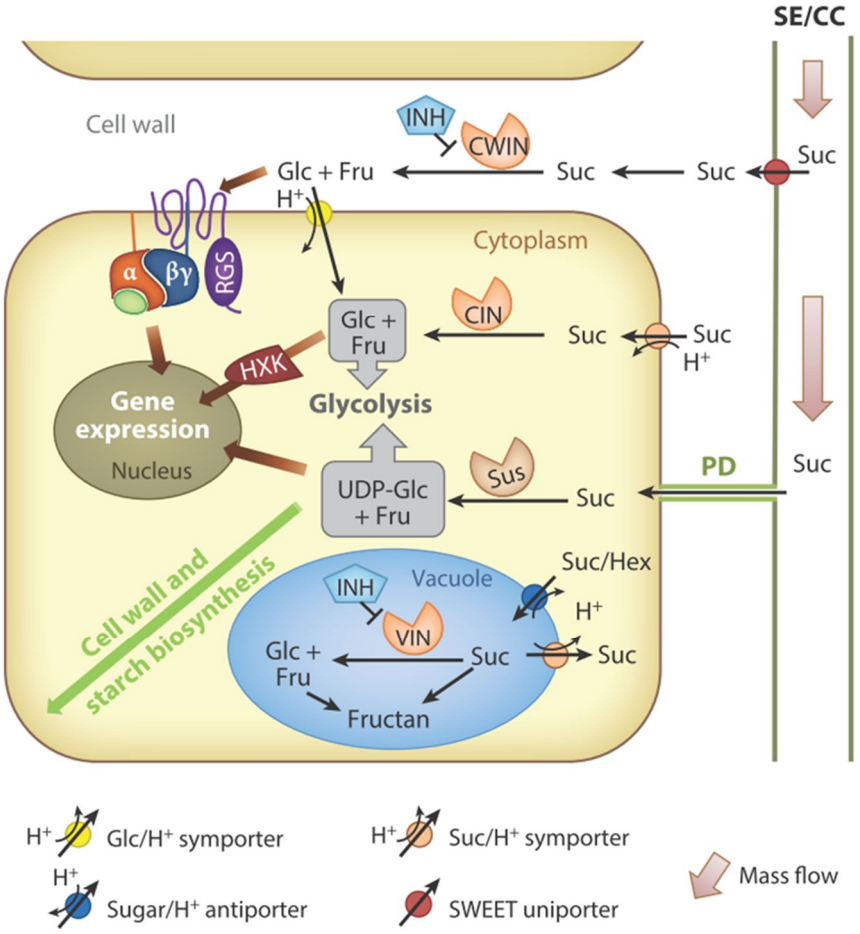

Figure 4: Sucrose metabolism in sink tissues. Sucrose is unloaded from the phloem into sink tissues via apoplastic or/and symplastic pathways. In the apoplastic pathway, sucrose may be hydrolysed by cell wall invertase (CWINV) into glucose (Glc) and fructose (Fru) prior to entering the cytoplasm through a receptor (regulator of G-protein signaling (RGS) coupled with a G protein for downstream signalling). After import via plasmodesmata (PD) or sucrose transporters, sucrose may be hydrolysed by cytoplasmic invertase (CIN) producing Glc and Fru, and sucrose synthase (SuS) producing UDP-Glucose (UDP-Glc) and fructose (Fru). Cytosolic sucrose may enter the vacuole via sucrose transporters and be hydrolysed by vacuolar invertase (VIN). The activity of CWINV, CIN and VIN are controlled by respective inhibitors (INHs). Hydrolysis of sucrose produces hexose (Hex) and modified hexose can enter the nucleus and serve as a gene regulator via binding to respective sugar-responsive elements. Various

transporters involved are indicated. Figure reproduced from Ruan, (2014). Additional abbreviations: sieve element/companion cell complex (SE/CC), hexokinase (HXK).

1.2.5 Reserve carbohydrates

In grasses, excess carbohydrates can be stored as reserve carbohydrates in the form of starch, fructans and (1,3;1,4)-β-glucan (Vijn and Smeekens, 1999; Burton and Fincher, 2009; Kermode, 2011). These have different chemical structures and properties, such as their composition, type and the position of linkages, orientation and arrangement of structures, distribution and solubility. Under conditions where the demand for energy exceeds the photosynthetic supply, such as low intensity light, extreme environments for growth and low leaf area, reserve carbohydrates supply energy for plant development (Brown and Blaser, 1965).

Reserve carbohydrates in plants are a major food source for humans and animals. Cereals, vegetables, fruits, tubers and legumes are examples of sources of dietary carbohydrates. These are important because they provide energy for our metabolism and they also provide dietary fibre which is beneficial for human health (Mann et al., 2007; Kermode, 2011). The carbohydrates in plants are also used as chemical energy for the production of biofuels (Smith, 2008).

Storage of carbohydrates in the form of starch, fructans and (1,3;1,4)-β-glucan within plant species may vary depending on the developmental stages and environmental conditions (Pollock and Lloyd, 1987; Coleman et al., 1995; Downing and Gamroth, 2007; Scofield et al., 2009). For example, the starch content in the peduncle and leaf of wheat plants is abundant before anthesis and decreased after anthesis (Scofield et al., 2009). Fructan accumulates in the

wheat peduncle at the early stage of development, and after 16 days after anthesis (DAA), fructan is remobilised for grain filling (Gebbing, 2003). In maize root, (1,3;1,4)-β-glucan accumulates in the elongating cells and remains high even after the elongation process ceased, but the structure of (1,3;1,4)-β-glucan is different at different stages of root elongation (Kozlova et al., 2012).

Environmental factors, or stresses, can also influence the accumulation of carbohydrates in plants. For example, the starch content in Timothy grass (*Phleum pretense* L.) is affected by nitrogen fertilization and the stage of development (Ould-Ahmed et al., 2014), and under cold conditions fructan accumulates in wheat plants and contributes to freezing tolerance (Kawakami and Yoshida, 2002).

The carbohydrate content in plants also varies depending on the plant organ and cell type in question. Ryegrass stems contain higher levels of fructan compared to leaf blades at vegetative, elongation and reproductive stages of development (Liu et al., 2011). (1,3;1,4)-β-Glucans are much more abundant, nearly 3-fold greater, in the starchy endosperm cell walls of barley compared to those of the aleurone (Harris and Fincher, 2009).

Reserve carbohydrates have important roles in plant growth and development, reproduction and stress responses. For example, during cereal development, a portion of the carbon fixed in the source organs is temporarily stored in the leaves and stems which then become vegetative sink organs. Stored carbohydrate in these vegetative organs may be subsequently remobilized to the reproductive sink organs which are usually seeds or grain during grain filling (Scofield et al., 2009).

1.2.6 Cereal grain formation

Grain is an important sink organ of many cereal crops. Mature cereal grains are rich in nutrients which are sources of energy and dietary fibres in human food. Like other flowering plants, cereal grain formation is initiated via a double fertilisation event in the embryo sac. A mature embryo sac consists of an egg cell accompanied by two synergid cells at the micropylar end, a large vacuolated central cell with two polar nuclei, and antipodal cells which cluster in the chalazal region of the embryo sac adjacent to the side walls (Fig. 5A and 5B) (Mogensen, 1982; Engell, 1989). Within one hour after pollination, the pollen tube carrying two sperm cells reaches the micropylar end of the ovule and enters the embryo sac. Within the embryo sac, one of the haploid sperm cells fuses with a haploid egg cell to form a diploid zygote, while the second haploid sperm fuses with two haploid polar nuclei in the central cell to form a triploid cell. The diploid zygote further develops into an embryo while the triploid cells undergo repeated rounds of cell division without cell wall formation, forming a multinucleate syncytium (Fig. 5A), which lasts for about 60 hours (Mogensen, 1982; Engell, 1989; Faure, 2001; Faure et al., 2003). During this stage, the syncytium nuclei migrate toward the peripheral cytoplasmic layer surrounding the central vacuole (Olsen, 2001; Sabelli and Larkins, 2009) and the nutrients that are required to support this process are released from the dying antipodal cells (Engell, 1989; An and You, 2004).

Cellularisation of the endosperm is accompanied by differentiation of the nucellar projection. The maternal nucellus surrounding the embryo sac undergoes programmed cell death except for the nucellus tissue facing the vascular bundle, which differentiates into the nucellar projection (Sreenivasulu et al., 2010; Domínguez and Cejudo, 2015). Endosperm cellularisation involves deposition of anticlinal cell walls between adjacent endosperm coenocytes to form

open-tubular alveoli (Brown et al., 1994; Olsen, 2001; Sabelli and Larkins, 2009). This process occurs around 3 to 4 days after pollination (DAP) and begins in the outermost cell row adjacent to the nucellar projection (Thiel, 2014). The nucleus within each open-ended alveolus undergoes mitotic division and this is followed by formation of periclinal cell walls (Fig. 5C). The cellularisation process completes around 6 DAP when the central cell cavity is filled with cells (Sabelli and Larkins, 2009). Completion of cellularisation is followed by differentiation of the endosperm, which forms different endosperm cell types (Olsen, 2001).

In barley grain, the endosperm tissue is comprised of three major cell types: 1) endosperm transfer cells, 2) aleurone and 3) starchy endosperm (Fig. 5D and 5E). Differentiation of aleurone and starchy endosperm cell types are controlled by signalling in response to their surface position which has been demonstrated in maize in an *in-vitro* study (Becraft and Asuncion-Crabb, 2000; Gruis et al., 2006). In contrast, differentiation of endosperm transfer cells requires signals released from the maternal tissues, such as hormones (Gruis et al., 2006; Thiel et al., 2008).

A

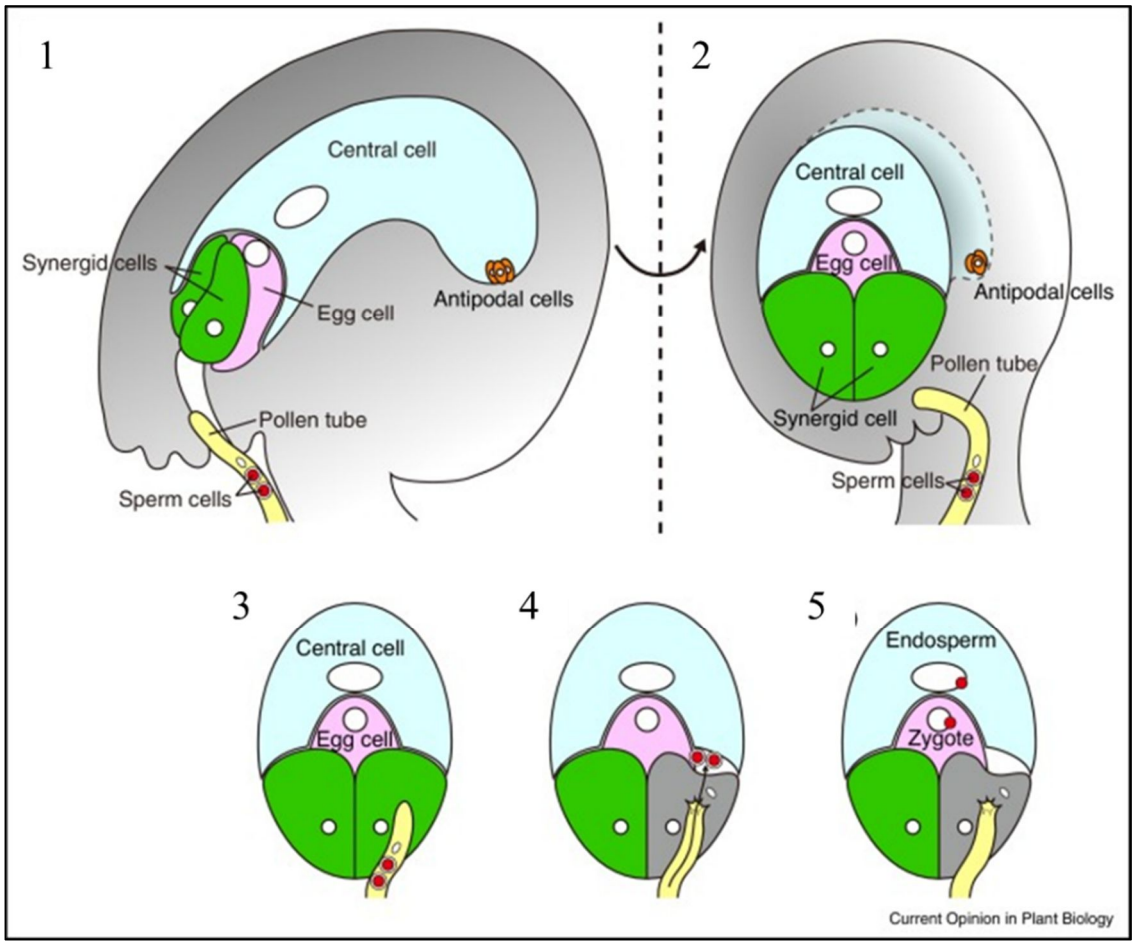
1
Central cell
Synergid cells
Egg cell
Antipodal cells
Pollen tube
Sperm cells
2
Central cell
Egg cell
Antipodal cells
Pollen tube
Synergid cell
Sperm cells
3
Central cell
Egg cell
4
5
Endosperm
Zygote
Current Opinion in Plant Biology

B

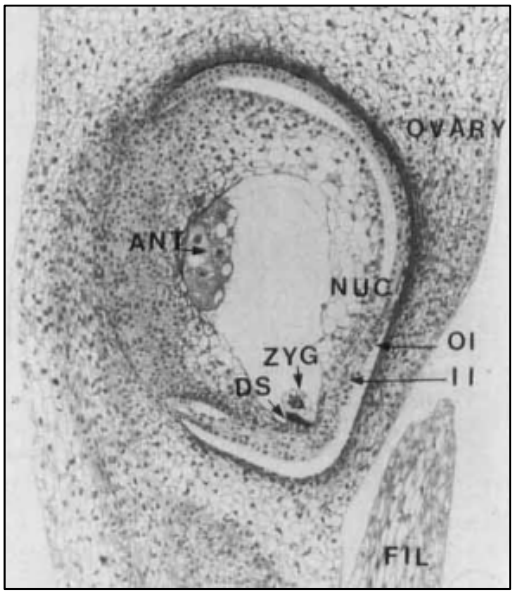
OVARY
ANT
NUC
OI
ZYG
II
DS
FIL

C

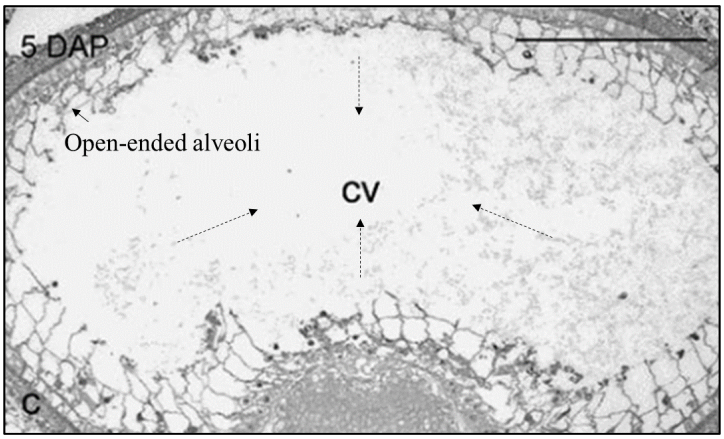

D

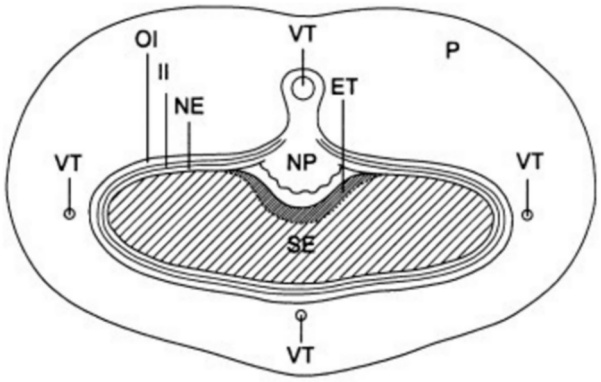

E

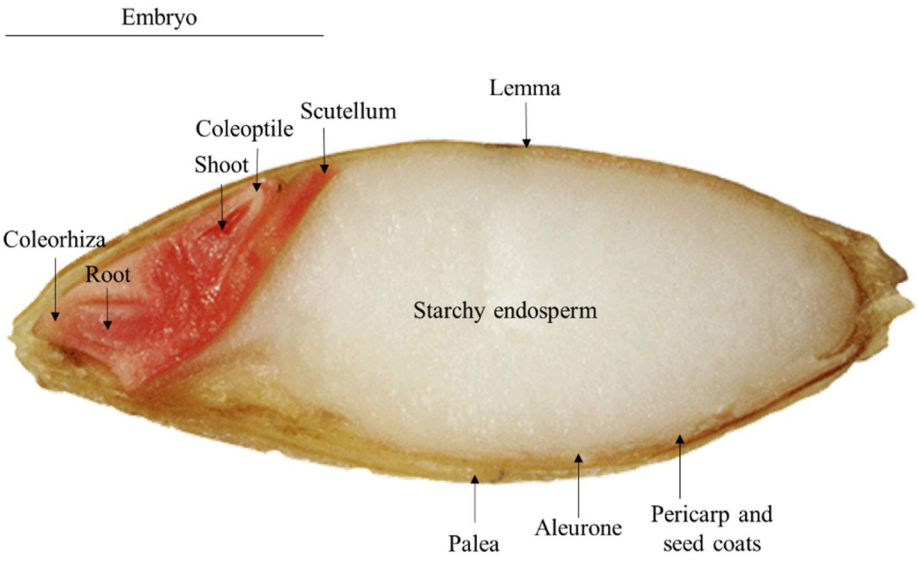

Figure 5: Grain development. (A) Schematic representation of double fertilisation using *Arabidopsis* as a model (process 1 to 5). An unfertilised ovule consists of antipodal cells, a central cell and an egg cell accompanied by two synergid cells. Pollen tube developed from a male gametophyte carrying two sperm cells is attracted toward the ovule (1: side view and 2: front view). 3: Pollen tube arrives at one of the synergid cells. 4: Pollen tube discharges two sperm cells. 5: One of the two sperms fuse with the egg to form a diploid zygote, while the other sperm fuses with two female polar nuclei in the central cell which later develops into the endosperm. Image taken from Maruyama and Higashiyama, (2016). (B) An ovule of barley (*Hordeum vulgare* cv. Bomi). Image taken from Engell, (1989). (C) Cellularisation occurs in barley endosperm at 5 DAP. A solid arrow indicates an open-end alveoli undergoing repeated rounds of periclinal wall formation. A dotted arrow indicates periclinal wall formation towards the central vacuole. Image taken from Wilson et al., (2006). (D) A schematic representation of a cross-section of a barley grain at 6 DAP. Image taken from Weschke et al., (2000). (E) A longitudinal-section of a mature barley grain stained with tetrazolium. Image taken from Britain, (2011). Abbreviations: antipodal cell (ANT), zygote (ZYG), degenerated synergid (DS), nucellus (NUC), outer integument (OI), inner integument (II), filament (remnant of stamen)

(FIL), central vacuole (CV), endosperm transfer cells (ET), nucellar epidermis (NE), nucellar projection (NP), pericarp (p), starchy endosperm (SE), vascular tissue (VT).

1.2.7 Endosperm transfer cells

Endosperm transfer cells (ETCs) are highly specialised modified cells positioned at the maternal-filial boundary which are involved in nutrient transfer from the maternal to the filial tissues (Thiel, 2014). ETCs can be distinguished from the other cell types by their thickened cell walls and the wall ingrowth architecture, of either the "flange" or "reticulate" type (Talbot et al., 2002). Flange wall ingrowths form parallel ribs that resemble the secondary cell wall thickenings of tracheary elements (Fig. 6A and 6B) (Talbot et al., 2002) whereas reticulate wall ingrowths are initiated as discrete papillar projections that appear to be randomly deposited (Fig. 6C) (Talbot et al., 2001). These cell wall characteristics greatly enhance the surface area of ETCs to facilitate the transfer of nutrients (McCurdy et al., 2008). In cereal grains including maize, barley and wheat, the wall ingrowths of ETCs appear to be of the "flange" type (Zheng and Wang, 2010, 2011; Thiel et al., 2012b).

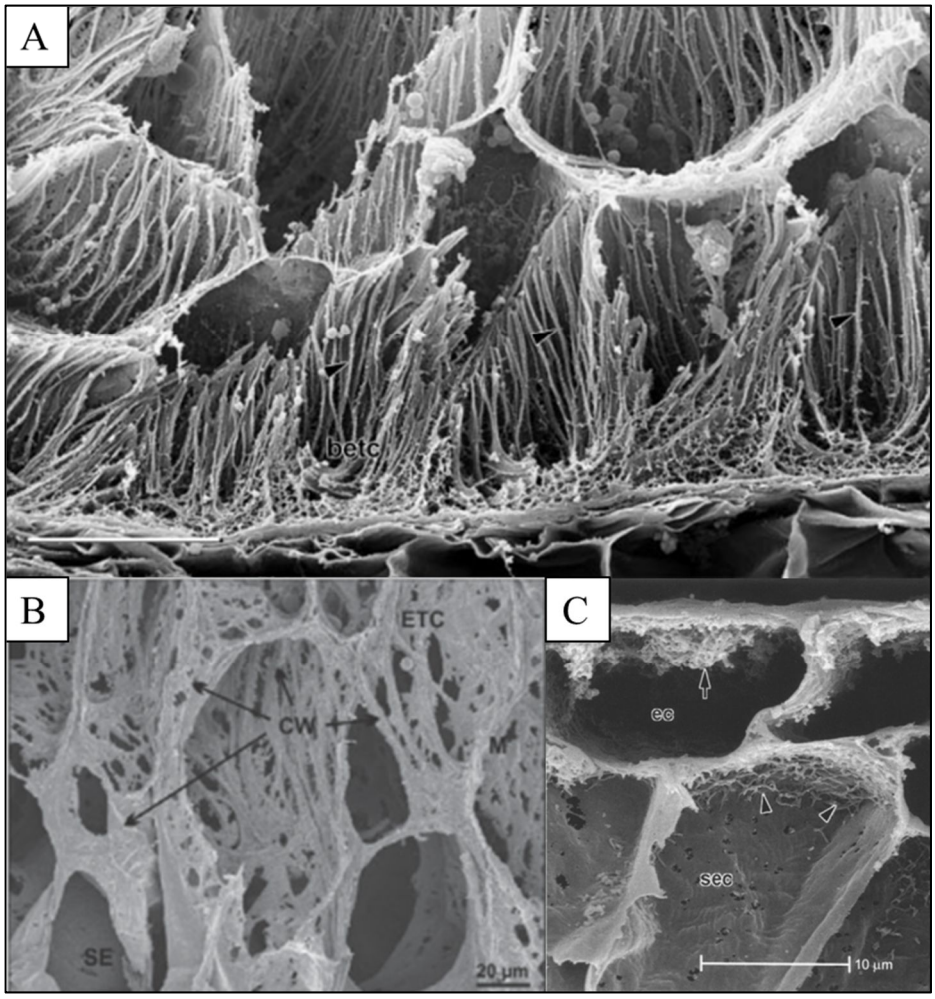

Figure 6: Scanning electron micrographs of endosperm transfer cells (ETC) wall ingrowth morphologies in cereal grains. (A) Flange-like wall ingrowths (arrow heads) in basal ETCs of maize (*Zea mays*) grain. Image taken from Talbot et al., (2002). (B) Flange-like wall ingrowths (arrow) in ETCs of barley (*Hordeum vulgare*) grain at 7 DAP. Image taken from Thiel et al., (2012b). (C) Deposition of wall ingrowth material in the epidermal cells of cotyledons of developing *Vicia faba* seed. Reticulate-like wall ingrowths (arrow heads) in the subepidermal cell. Image taken from Talbot et al., (2001). Abbreviations: basal endosperm transfer cell (betc), cell wall (CW), endosperm transfer cell (ETC), starchy endosperm (SE), epidermal cell (ec), subepidermal cell (sec).

In barley grain. ETC walls appear to be thin from 5 to 7 DAP (Fig. 7A) (Thiel et al., 2012b). At 7 DAP, wall ingrowths and thickenings in the ETCs become pronounced. Additionally, the intracellular compartments in the ETCs appear to be dense and filled with numerous cell organelles including small vacuoles, small starch granules, mitochondria and banded endoplasmic reticulum (Fig. 7B). By 10 DAP, the cell walls become thicker and compact, and parallel rib-shaped projections appear, while the cells become flattened in a plane perpendicular to the long axis of the endosperm (Fig. 7C). By 12 DAP, wall thickenings in ETCs appear irregularly and the cytoplasm is less dense compared to the earlier stages, with fewer mitochondria, lipid bodies, starch granules and vesicles (Fig. 7D) (Thiel et al., 2012b; Thiel, 2014). During grain development, the volume of ETCs increases 9-fold from 5 to 10 DAP and decreases 1.5-fold from 10 to 14 DAP. In contrast, the endosperm volume does not change from 3 to 7 DAP, but increases 14-fold from 7 to 14 DAP. These observations indicate that the ETCs have already fully developed before the size of the endosperm increases exponentially (Thiel et al., 2012b; Thiel, 2014).

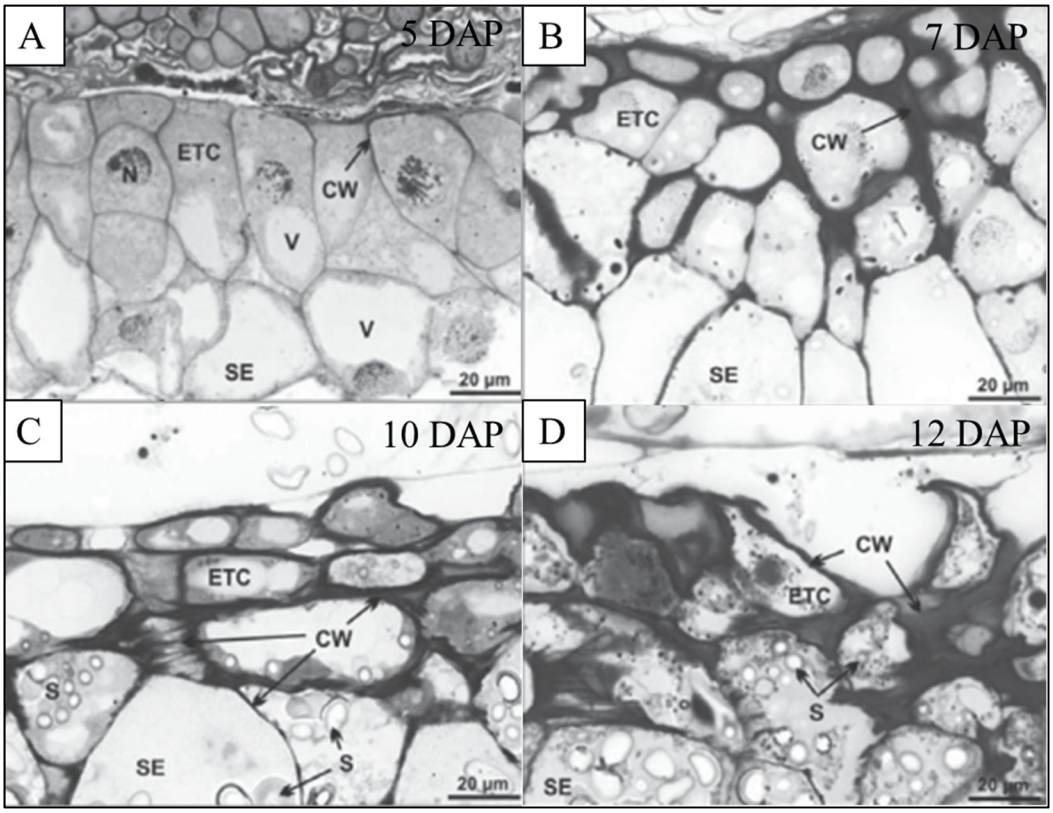

Figure 7: Morphologies of ETCs in developing barley grain under light microscopy. (A) At 5 DAP, ETC walls appear to be thin. (B) At 7 DAP, ETC wall ingrowths and thickenings become pronounced. (C) At 10 DAP, cell walls of ETC appear to be thicker and show parallel rib-shaped projections. The cells are flattened in a plane perpendicular to the long axis of the endosperm. (D) At 12 DAP, ETC walls are thicker and appear irregular compared to earlier stages. Figures reproduced from Thiel et al., (2012b). Abbreviations: endosperm transfer cell (ETC), cell wall (CW), vacuole (V), starchy endosperm (SE), starch (S).

1.2.7.1 Signals that regulate ETC specification and differentiation

The *END1* gene in barley has been linked to differentiation of ETCs based on the evidence of mRNA localisation exclusively in the endosperm coenocyte facing the nucellar projection, which further develops into ETCs (Doan et al., 1996). Additional transfer cell-specific genes which have been identified in other cereal grains include *ZmMRP-1* in maize, which encodes a

MYB-related R1-type transcription factor specific for transfer cell-specific genes including *BETL1* (Gómez et al., 2002), *Meg1* (Gutiérrez-Marcos et al., 2004) and *ZmTCRR-1* (Muñiz et al., 2006). However, the exact functions of these transfer cell-specific genes in controlling the cell fate specification are unknown. A laser-assisted microdissection and transcriptome sequencing study identified high expression of genes encoding the regulatory elements of a two-component signalling (TCS) system (West and Stock, 2001) specifically in the barley ETCs (Thiel et al., 2012a). For example, *histidine kinase 1* (*HK1*) genes in barley are highly expressed at 3 DAP, a transition stage between the syncytium and cellularisation (Thiel et al., 2012a). There are 3 subgroups of histidine kinases: 1) the ethylene receptor family (Gamble et al., 1998), 2) the cytokinin receptor family (Tran et al., 2007) and 3) the 'classical' histidine kinases which are involved as osmosensors (Wohlbach et al., 2008). The genes encoding putative ethylene receptors, histidine-containing phosphotransfer proteins (HPts) and response regulator (RRs) are highly expressed between 3 and 5 DAP (Thiel et al., 2012a). At 5 DAP, the genes encoding key enzymes in ethylene biosynthesis such as S-adenosylmethionine (SAM) synthase and aminocyclopropanecarboxylate (ACC) oxidase, are upregulated in barley ETCs. External abscisic acid (ABA) was shown to induce the expression of the *HvHK1* gene through interaction with ABA-associated transcription factors (Thiel et al., 2012a). In *Vicia faba* cotyledons, reactive oxygen species (ROS) which act downstream of ethylene, activates wall ingrowth formation (Andriunas et al., 2012). This suggests involvement of ethylene and ABA in ETC development and wall ingrowths in barley (Thiel et al., 2012b).

The role of ETCs in nutrient transport is supported by the high expression of the *sucrose transporter 1* (*HvSUT1*) gene in the ETCs during the stage when starch begins to accumulate in the endosperm (Weschke et al., 2000; Thiel et al., 2012b). In addition, *HvSTP1* gene which encodes a hexose transporter, is highly expressed in the syncytial endosperm at 3 DAP and

ETCs at 7 DAP. This is essential to maintain the hexose gradient to support endosperm growth (Weschke et al., 2003).

1.2.8 Aleurone

The aleurone tissue is modified endosperm cells positioned in the outermost layer of the starchy endosperm except for the layer facing the endosperm cavity which forms endosperm transfer cells (Thiel, 2014). Aleurone cells contain dense granular cytoplasm due to the presence of inclusion bodies in the vacuoles (Buttrose, 1963), which are rich in protein and lipid (Jones, 1969; Morrison et al., 1975; Olsen, 2001). Aleurone cells remain living in mature grain unlike the starchy endosperm which undergoes programmed cell death (Bradbury et al., 1956; Young and Gallie, 2000). During grain germination, aleurone cells secrete hydrolytic enzymes such as α-amylase, in response to exogenous gibberellic acid (GA), to break down storage carbohydrates in the starchy endosperm (Ranki and Sopanen, 1984). Completion of germination is then followed by aleurone cell death (Kuo et al., 1996; Wang et al., 1996; Bethke et al., 1999; Fath et al., 2000).

1.2.8.1 Aleurone study in barley grain

Regulation of aleurone development is broadly studied in maize plants. In barley grain, a barley *ltp2* gene is localised specifically in the aleurone layer and it is widely used as an aleurone marker gene (Kalla et al., 1994). The information of signalling pathway involved in the aleurone differentiation in barley grain remains scarce, and additional genes that control the number of aleurone cells in other cereal species remains unknown.

1.2.8.2 Aleurone cell fate and differentiation

Differentiation of outermost endosperm cells into aleurone is initiated around 8 DAP (Bosnes et al., 1992) and it is determined by signals released from the peripheral starchy endosperm (Becraft and Asuncion-Crabb, 2000; Gruis et al., 2006), although the position cues for aleurone cell fate are still not fully understood. The ability of aleurone cells to redifferentiate into starchy endosperm and vice versa was evident in a maize mutant lacking the *dek1* gene (Fig. 8A and 8B) (Becraft and Asuncion-Crabb, 2000; Gruis et al., 2006; Becraft and Yi, 2010). The *dek1* gene encodes an integral membrane protein in the plasma membrane (Lid et al., 2002; Tian et al., 2007). The DEK1 membrane protein consists of an extracellular loop and a cytoplasmic domain with an active calpain protease, which are essential elements for signalling transduction (Wang et al., 2003). The plasticity of aleurone cell fate remains throughout endosperm development (Becraft and Asuncion-Crabb, 2000).

In addition, maize with a recessive *crinkly4 (cr4)* gene showed sporadic patches of aleurone cells on the abgerminal face of the grain (Fig. 8C) (Becraft et al., 1996). The maize *crinkly4 (cr4)* gene encodes a receptor-like kinase that is involved in differentiation of epidermis tissues (Becraft et al., 1996; Jin et al., 2000). A protein co-localisation study showed interactions between CR4 and DEK1 proteins in the plasma membrane and in endocytic vesicles (Tian et al., 2007) indicating that *cr4* and *dek1* genes have an overlapping biological function in aleurone development (Becraft et al., 2002).

The number of aleurone layers varies amongst cereal grains. Maize (Kyle and Styles, 1977) and wheat (Morrison et al., 1975) have one cell layer; rice has one to three (Hoshikawa, 1993) and barley has three to four aleurone cell layers (Jones, 1969). The signalling pathway that gives rise to a different number of aleurone cells is still unknown. A mutant for the *supernumerary*

aleurone layers 1 (*sal1*) gene in maize contains up to seven layers of aleurone (Fig. 8D) compared to the wild type, indicating that the *sal1* gene has a negative regulatory function for aleurone cell fate (Shen et al., 2003). The *Sal1* gene is a homolog of the human *CHMP1* gene, which has a role in vesicle trafficking (Howard et al., 2001) and chromatin modification (Stauffer et al., 2001). It was proposed that loss of function of the *sal1* gene may result in increased expression of CR4 receptors in the peripheral endosperm layer that usually become starchy endosperm cells (Shen et al., 2003).

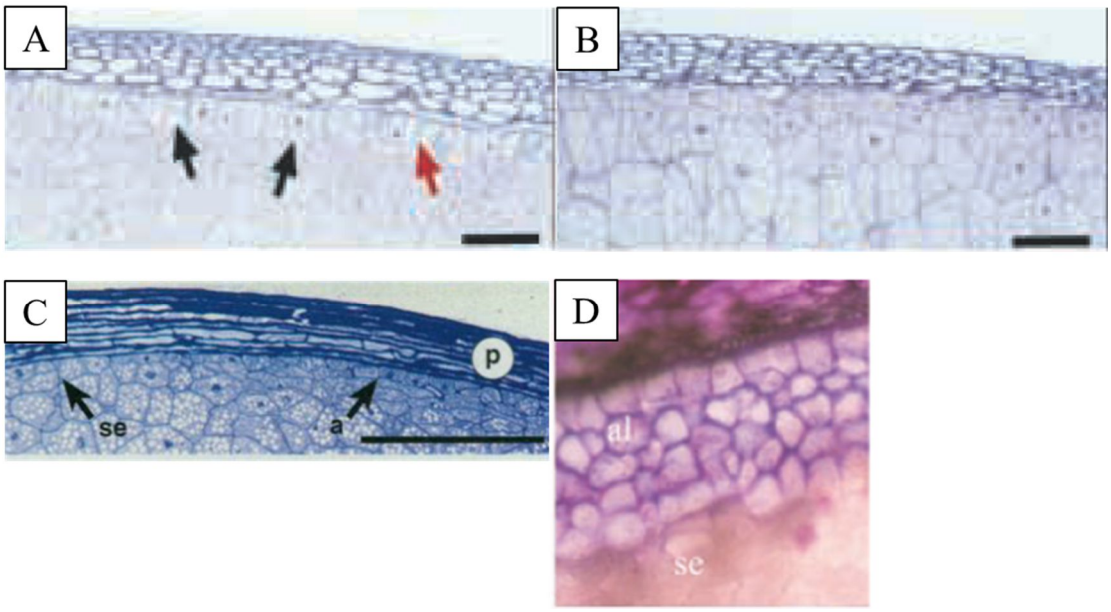

Figure 8: Morphologies of aleurone cell layers in maize endosperm. (A) A wild type maize endosperm consists of a single aleurone cell layer (red arrow) whereas the black arrows indicate formation of periclinal walls during mitosis. (B) The outermost endosperm layer of a *dek1* maize mutant becomes starchy endosperm. A and B are taken from Becraft and Asuncion-Crabb, (2000). (C) The outermost endosperm layer in the *cr4* mutant contains cells characteristic of both starchy endosperm and aleurone (black arrows). Image taken from Becraft et al., (1996). (D) The homozygous *sal1-1*-defective maize endosperm. The aleurone cells are stained red with Sudan red. A cross section of the homozygous *sal1-1*-defective kernel shows multilayered

aleurone. Image taken from Shen et al., (2003). Abbreviations: starchy endosperm (se), aleurone (a and al), pericarp (p).

1.2.8.3 Involvement of hormones in aleurone cell differentiation

Abscisic acid (ABA) and gibberellic acid (GA) play a key role in aleurone development during grain maturation and germination (Bethke et al., 1999; Fath et al., 2000; Bethke et al., 2006). On the other hand cytokinin and auxin may be involved in aleurone differentiation during early grain development. Overexpression of the *isopentenyl transferase (IPT)* gene, encoding a cytokinin biosynthetic enzyme, in maize results in formation of interspersed patches of aleurone and starchy endosperm cells at the outermost endosperm layer (Geisler-Lee and Gallie, 2005). Furthermore, maize plants treated with N-1-naphthylphthalamic acid (NPA), an auxin transport inhibitor, contain multilayered aleurone in the grain (Forestan et al., 2010).

1.2.9 Cell wall polysaccharides in barley endosperm

The cell walls in barley grain contain cellulose and non-cellulosic polysaccharides, including (1,3;1,4)-β-glucan, arabinoxylan, callose, xyloglucan, heteromannan and pectins. The deposition pattern and amount of these cell wall polysaccharides are varied in different barley tissues. The spatial and temporal appearance of cell wall polysaccharides can be detected by various microscopy techniques using antibodies that are specific for cell wall antigens (Wilson et al., 2006; Robert et al., 2011).

At 3 DAP before the formation of the first anticlinal wall between adjacent endosperm coenocytes, callose was first detected in the central cell walls surrounding the central vacuole

(Fig. 9A) (Wilson et al., 2006). As the first anticlinal walls are formed at 3 DAP, callose was first detected (Fig. 9B) (Wilson et al., 2006; Wilson et al., 2012). Deposition of callose persisted in the periclinal cell wall at 5 DAP (Fig. 9C) but by 6 DAP, the callose labelling began to diminish. From 7 to 28 DAP, callose was detected only in the regions restricted to plasmodesmata (Fig. 9D) (Wilson et al., 2006). Another short-lived component, xyloglucan was deposited in the nucellar epidermis at 3 DAP (Fig. 9E), in the developing endosperm at 4 DAP (Fig. 9F) persisting up to 6 DAP (Fig. 9G) (Wilson et al., 2012).

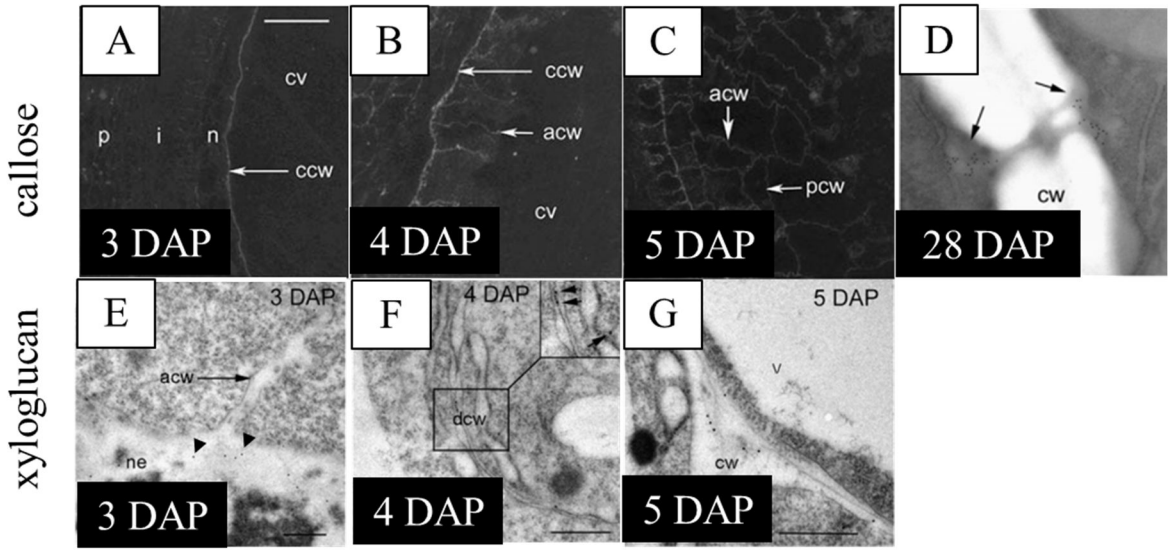

Figure 9: Deposition of callose and xyloglucan in developing barley grain. Callose was detected using silver-enhanced (1,3)-β-glucan antibody labelling visualised under a light microscope (panels A to C) and using a gold-conjugated (1,3)-β-glucan antibody visualised under a transmission electron microscope (panel D). (A) At 3 DAP, intense labelling with the (1,3)-β-glucan antibody was detected in the central cell wall surrounding the central vacuole before the formation of anticlinal cell walls. (B) At 4 DAP, (1,3)-β-glucan antibody labelling was distributed uniformly in the newly formed anticlinal cell walls. (C) At 5 DAP, labelling from (1,3)-β-glucan antibody was detected in the periclinal cell walls. (D) At 28 DAP, the gold labelling was restricted to the region surrounding plasmodesmata (black arrows). Transmission

electron micrographs of developing endosperm labelled with xyloglucan antibody, LM15 (panels E to G) (Marcus et al., 2008). (E) At 3 DAP, LM15 antibody labelling was detected in the nucellar epidermis only (arrow heads). (F) At 4 DAP, LM15 antibody labelling was detected in the developing cell walls (arrows). (G) At 5 DAP, LM15 antibody labelling was detected in the endosperm. A to C are taken from Wilson et al., (2006). D to G are taken from Wilson et al., (2012). Abbreviations: pericarp (p), integuments (i), nucellus (n), central cell wall (ccw), central vacuole (cv), anticlinal cell wall (acw), periclinal cell wall (pcw), cell wall (cw), nucellar epidermis (ne), developing cell wall (dcw), vacuole (v).

(1,3;1,4)-β-Glucan is initially deposited in both anticlinal and periclinal cell walls around 5 DAP (Fig. 10A). From 5 DAP onwards, (1,3;1,4)-β-glucan continually accumulates in the cell walls of cellularised endosperm (Fig. 10B and 10C) (Wilson et al., 2006) and by 10 DAP, (1,3;1,4)-β-glucan is uniformly distributed throughout the endosperm tissues. At 12 DAP, (1,3;1,4)-β-glucan labelling was absent in the peripheral endosperm layer until 16 DAP (Fig. 10D and 10E). At 28 DAP, the (1,3;1,4)-β-glucan labelling was intense in the cell walls of aleurone and starchy endosperm. This observation was supported by the chemical analysis which showed high (1,3;1,4)-β-glucan accumulation between 16 to 36 DAP (Wilson et al., 2012). Heteromannan is laid down in the developing endosperm around 5 DAP (Fig. 10F and 10G) and by 10 DAP, heteromannan is uniformly distributed throughout the endosperm tissues (Fig. 10H and 10I). At 28 DAP, heteromannan labelling was not detected in the aleurone layer (Fig. 10J and 10K).

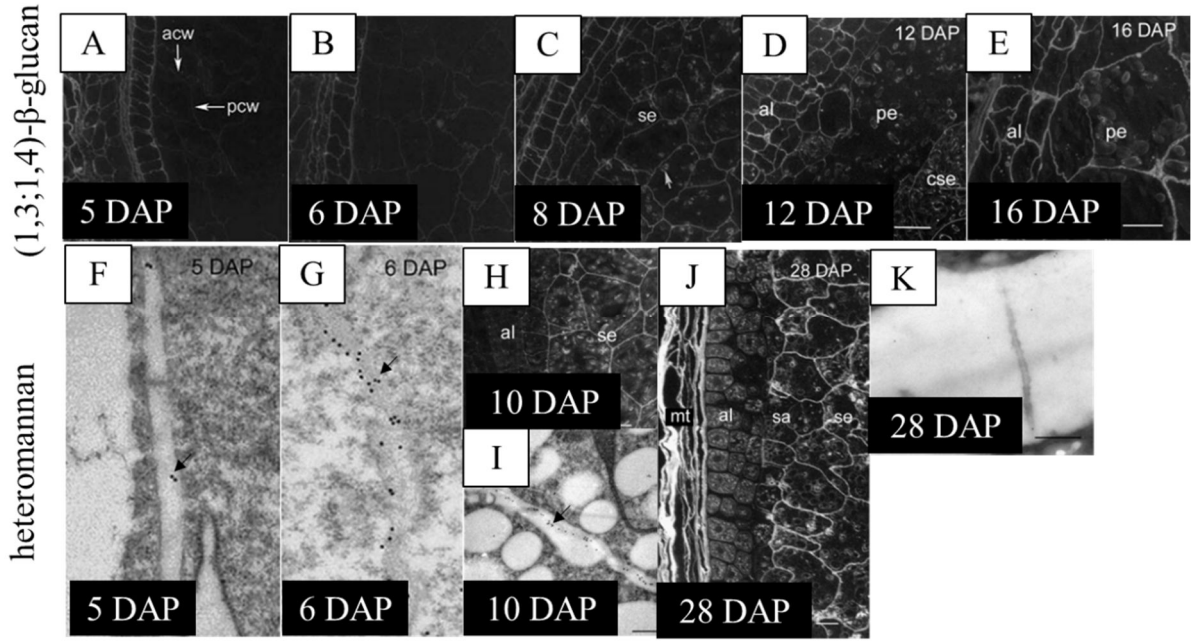

Figure 10: Deposition of (1,3;1,4)-β-glucan and heteromannan in developing barley grain. (1,3;1,4)-β-glucan was detected using silver-enhanced (1,3;1,4)-β-glucan antibody labelling (Meikle et al., 1994) and visualised under a light microscope (panels A to E). (A) (1,3;1,4)-β-Glucan was detected in the anticlinal and periclinal cell wall at 5 DAP. (B) At 6 DAP, (1,3;1,4)-β-glucan labelling was detected in the cell walls of cellularising endosperm. (C) At 8 DAP, the labelling intensity was enhanced as the endosperm was fully cellularised. (D) At 12 DAP, the (1,3;1,4)-β-glucan antibody labelled the central starchy endosperm and differentiating aleurone, except for the peripheral endosperm layer. (E) (1,3;1,4)-β-glucan labelled uniformly throughout the endosperm tissues. Light (panels H and J) and transmission electron micrographs (panel F, G, I and K) of heteromannan deposition using (1-4)-β-mannan and galacto-(1-4)-β-mannan antibody (Pettolino et al., 2001). (F and G) Heteromannan labelling was detected in the cell walls of cellularising endosperm at 5 and 6 DAP (black arrows). (H) At 10 DAP, heteromannan labelling was detected throughout the endosperm tissues including aleurone cell walls as shown in the transmission electron micrograph (black arrows) (panel I). (J) At 28 DAP, heteromannan was found in the maternal tissues, subaleurone and starchy endosperm, except for the aleurone layer as confirmed by gold-labelled sections (panel K). A, B, C, F and G are taken from Wilson

et al., (2006). D, E, H, I, J and K are taken from Wilson et al., (2012). Abbreviations: anticlinal cell wall (acw), periclinal cell wall (pcw), starchy endosperm (se), aleurone (al), peripheral endosperm (pe), central starchy endosperm (cse), maternal tissues (mt), subaleurone (sa).

From 4 to 7 DAP, arabinoxylan is only detected in the cell walls of vascular tissue (Fig. 11A and 11B). The first appearance of arabinoxylan occurs around 8 DAP where the labelling was found in the endosperm cell walls adjacent to the crease region (Fig. 11C and 11D) (Wilson et al., 2006). However, pre-treatment of sections with α-L-arabinofuranosidase (an enzyme that hydrolyses the α-1,2- and α-1,3-linked L-arabinofuranose residues from arabinoxylans) before labelling with LM11 confirms the presence of highly-substituted arabinoxylan in the cell walls of cellularising endosperm at 5 and 8 DAP (Fig. 11G and 11H) (Wilson et al., 2012). At 10 DAP, arabinoxylan labelling was intense in the crease region and by 12 DAP, the labelling was detected in the aleurone and central starchy endosperm cell walls, except for the subaleurone layer. However, pre-treatment with α-L-arabinofuranosidase revealed the presence of highly substituted arabinoxylan in the subaleurone (Wilson et al., 2012). At 16 DAP, arabinoxylan labelling was detected in all endosperm tissues, and the intensity in the aleurone became stronger at later stages (Fig 11E and 11F) (Wilson et al., 2012).

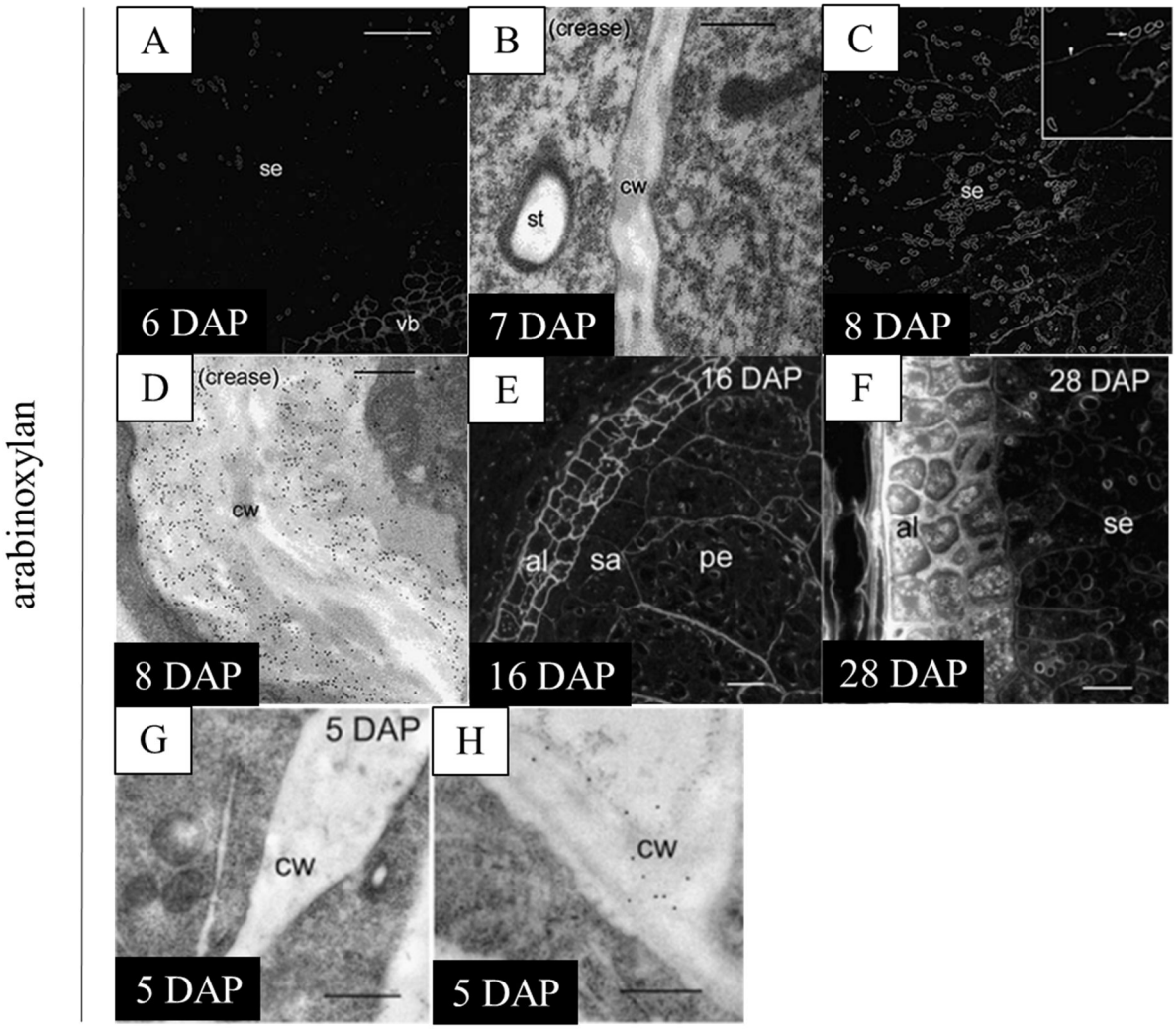

Figure 11: Deposition of arabinoxylan in developing barley grain. Arabinoxylan was detected using silver-enhanced arabinoxylan antibody (LM11) labelling (McCartney et al., 2005) and visualised using light microscopy (panels A, C, E and F), while a gold-conjugated LM11 antibody was used for transmission electron microscopy (panels B, D, G and H). (A) At 6 DAP, LM11 antibody labelling was only detected in the vascular bundles. (B) At 7 DAP. LM11 antibody labelling was absent in the endosperm cell walls adjacent to the crease region. (C and D), At 8 DAP, LM11 antibody labelled in the endosperm cell walls at the crease. (E) At 16 DAP, all endosperm tissues were labelled with LM11 antibody. (F) An intense labelling in the thickened cell walls of aleurone. A comparison of sections at 5 DAP without (G) and with pre-treatment of sections with α-L-arabinofuranosidase (H). Pre-treatment of sections with α-L-arabinofuranosidase revealed presence of LM11 antibody labelling in the cell walls of

cellularising endosperm which was not detected on the non-treated section. A to D are taken from Wilson et al., (2006). E to H are taken from Wilson et al., (2012). Abbreviations: starchy endosperm (se), vascular bundles (vb), starch granule (st), cell wall (cw), aleurone (al), subaleurone (sa), peripheral endosperm (pe).

For cellulose detection, there is no specific antibody for cellulose developed and the carbohydrate binding module CBM3a recognises both cellulose and xyloglucan (Hernandez-Gomez et al., 2015). Detection of cellulose with CBM3a during early grain development therefore may not be accurate as xyloglucan was detected as early as 3 DAP (Fig. 9E). However, as the xyloglucan labelling disappears from 6 DAP onwards and previous analysis showed absence of xyloglucan in mature grain (Fincher, 1975). Chemical analysis shows 3 to 4% w/w of cellulose in a mature barley grain (Fincher, 1975), hence the CBM3a is suitable for detection of cellulose deposition during the later stages of grain development.

1.2.10 Cell wall polysaccharides in barley endosperm transfer cells

There is little information about the spatial-temporal distribution of cell wall polysaccharides in the barley endosperm transfer cells. In wheat, arabinoxylan is the major cell wall component in the transfer cells from 5 to 23 DAP and it is more highly substituted compared to the structure of arabinoxylan in aleurone cell walls (Robert et al., 2011). Transcriptome data reported by Thiel et al., (2012a) and Thiel et al., (2012b) revealed differential expression of cell wall-related genes in the barley endosperm transfer cells throughout grain development. At 5 DAP, genes encoding (1,3)-β-glucan synthases/transferases are upregulated and followed by an upregulation of (1,3)-β-glucanases, suggesting accumulation of callose with a high turnover rate. At 5 to 7 DAP, genes related to the biosynthesis of mannan, xyloglucans, glucuronoxylans,

arabinoxylans and esterified pectin are upregulated. Between 7 to 10 DAP, cellulose synthase A (*CesA*) genes are upregulated, implying that cellulose is synthesized later than hemicelluloses.

1.2.11 (1,3;1,4)-β-Glucan

(1,3;1,4)-β-Glucans, also referred to as mixed-linkage glucans, are linear non-cellulosic polysaccharides composed of chains of glycosyl residues linked by β-glycosidic bonds, which may be either (1,3)- or (1,4)-linkages. The (1,3)- and (1,4)-linkage arrangement is commonly patterned as two or three (1,4)-linkages separated by a randomly inserted (1,3)-linkage which also induces a kink in the molecular chain. This results in asymmetric (1,3;1,4)-β-glucan molecules which are not able to align and aggregate, contributing to the flexibility and solubility of the polysaccharide (Fig. 12A) (Woodward et al., 1983; Collins et al., 2010). (1,3;1,4)-β-Glucans are composed of randomly arranged cellotriosyl (G4G4G; DP3) and cellotetraosyl (G4G4G4G; DP4) units that are separated by a single (1,3)-linkage (Fig. 12B). The ratio of the DP3:DP4 units can be used to predict the solubility and rheological behaviour of (1,3;1,4)-β-glucan (Papageorgiou et al., 2005). (1,3;1,4)-β-Glucans with very high or very low DP3:DP4 ratios are less soluble relative to the (1,3;1,4)-β-glucan which has an intermediate DP3:DP4 ratio, which for example in Poaceae range from 2–3:1 (Burton et al., 2010; Trafford et al., 2012). The ratio of DP3:DP4 in cereal grains varies across species and the polysaccharides with lower DP3:DP4 ratios are more soluble than those with higher ratio (Fig. 12C) (Burton and Fincher, 2012). In barley, approximately 90% of the adjacent (1,4)-β-linked glucosyl residues in the (1,3;1,4)-β-glucan structure are comprised of DP3 and DP4 oligosaccharides, and the remaining oligosaccharides have a DP of 12 to 15 (Woodward et al., 1983; Nemeth et al., 2010).

A

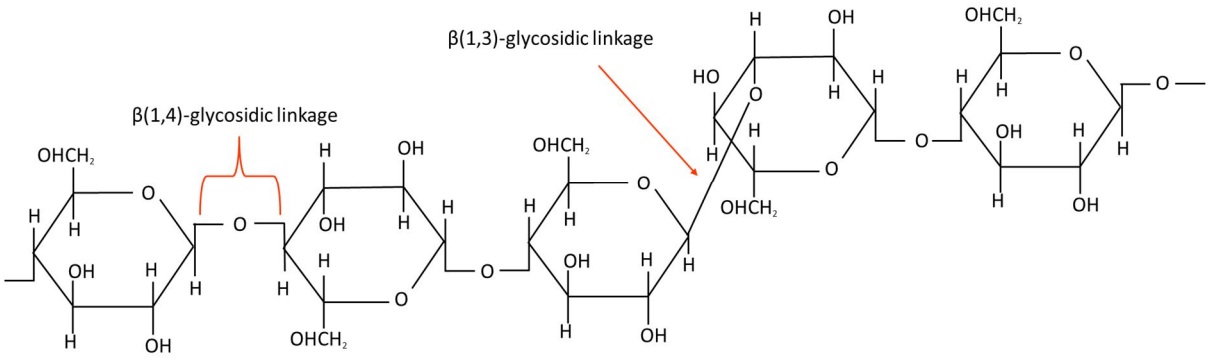

B

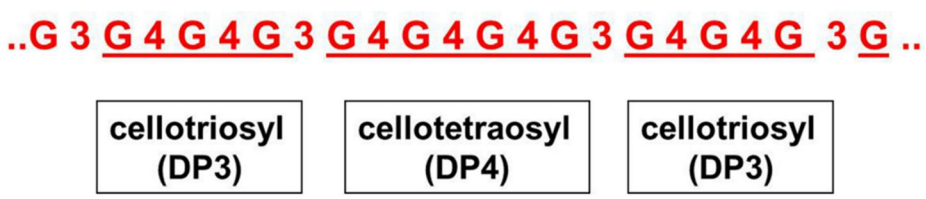

C

Species	(1,3;1,4)-β-glucan (% w/w)	DP3:DP4 ratio	Solubility in water (%)	Starch (% w/w)
Oats	6–8	1.5–2.3:1	~80	~60
Barley	4–10	2.6:1	~20	~57
Wheat	1	3.2:1	0	~57
Brachypodium	40	5.9:1	Insoluble	<10
Rice	<0.06	1:1.4	?	80
Maize	Trace	2.5:1	?	70–80
Sorghum	0.07–0.2	2.8:1	?	70–80

Figure 12: Structure of (1,3;1,4)-β-glucan. (A) (1,3;1,4)-β-glucans consist of linear glucosyl residues joined by (1,3)- and (1,4)-glycosidic linkages. (B) (1,3;1,4)-β-glucans contain cellotriosyl (DP3) and cellotetraosyl (DP4) units linked by (1,3)-linkages. (C) The levels of

(1,3;1,4)-β-glucans, DP3:DP4 ratio, solubility of (1,3;1,4)-β-glucans in water and starch content in various cereal grains. Figures reproduced from Burton and Fincher, (2012).

(1,3;1,4)-β-Glucans are a component of both primary and secondary cell walls of most Poaceae, including cereals and grasses (Burton and Fincher, 2009). Occurrence of (1,3;1,4)-β-glucans have also been reported in the cell walls of *Equisetum* species (Monro et al., 1976; Fry et al., 2008), algae (Ford and Percival, 1965; Nevo and Sharon, 1969; Eder et al., 2008; Salmeán et al., 2017), bacteria (Lee and Hollingsworth, 1997; Pérez-Mendoza et al., 2015), fungi (Pettolino et al., 2009) and some lichen species (Honegger and Haisch, 2001).

1.2.11.1 Biosynthesis of (1,3;1,4)-β-glucan

Cellulose-synthase (*CesA*) superfamily genes are the major genes involved in the biosynthesis of cell wall polysaccharides such as cellulose. Other families, such as *Cellulose-synthase-like* (*Csl*) gene families are divided into subgroups designated *CslA* to *CslJ* (Fig. 13) (Burton et al., 2006). *CslF* and *CslH* genes are responsible for the biosynthesis of (1,3;1,4)-β-glucans in grasses and cereals (Burton et al., 2006; Doblin et al., 2009; Burton et al., 2011). The deposition of (1,3;1,4)-β-glucans was observed in the cell wall of *Arabidopsis* plants when rice *CslF*, and later a barley *CslH1* gene, were overexpressed in *Arabidopsis* plants (Burton et al., 2006; Doblin et al., 2009). In barley, overexpression of the *HvCslF6* gene results in a significant increase in the amount of (1,3;1,4)-β-glucans in both vegetative and grain tissues (Burton et al., 2011).

There are contradicting studies in relation to the location of (1,3;1,4)-β-glucan biosynthesis in grasses which have yet to reach consensus. There are two subcellular locations proposed for the

biosynthesis of (1,3;1,4)-β-glucan: 1) in the Golgi apparatus (Urbanowicz et al., 2004; Carpita and McCann, 2010; Kim et al., 2015) or 2) at the plasma membrane (Philippe et al., 2006; Wilson et al., 2015). According to the study from Wilson et al., (2015), the barley CSLF6 protein is localised mainly in the plasma membrane and Golgi-derived vesicles, whereas the barley CSLH1 protein is found mainly in the endoplasmic reticulum, Golgi and post-Golgi vesicles. Another study shows that the *Brachypodium distachyon* CSLF6 protein is localised in the Golgi apparatus (Kim et al., 2015). A different observation for the recognition of (1,3;1,4)-β-glucan in the golgi could be associated with the role of CSLF6 derived from different plant species (Kim et al., 2015; Wilson et al., 2015).

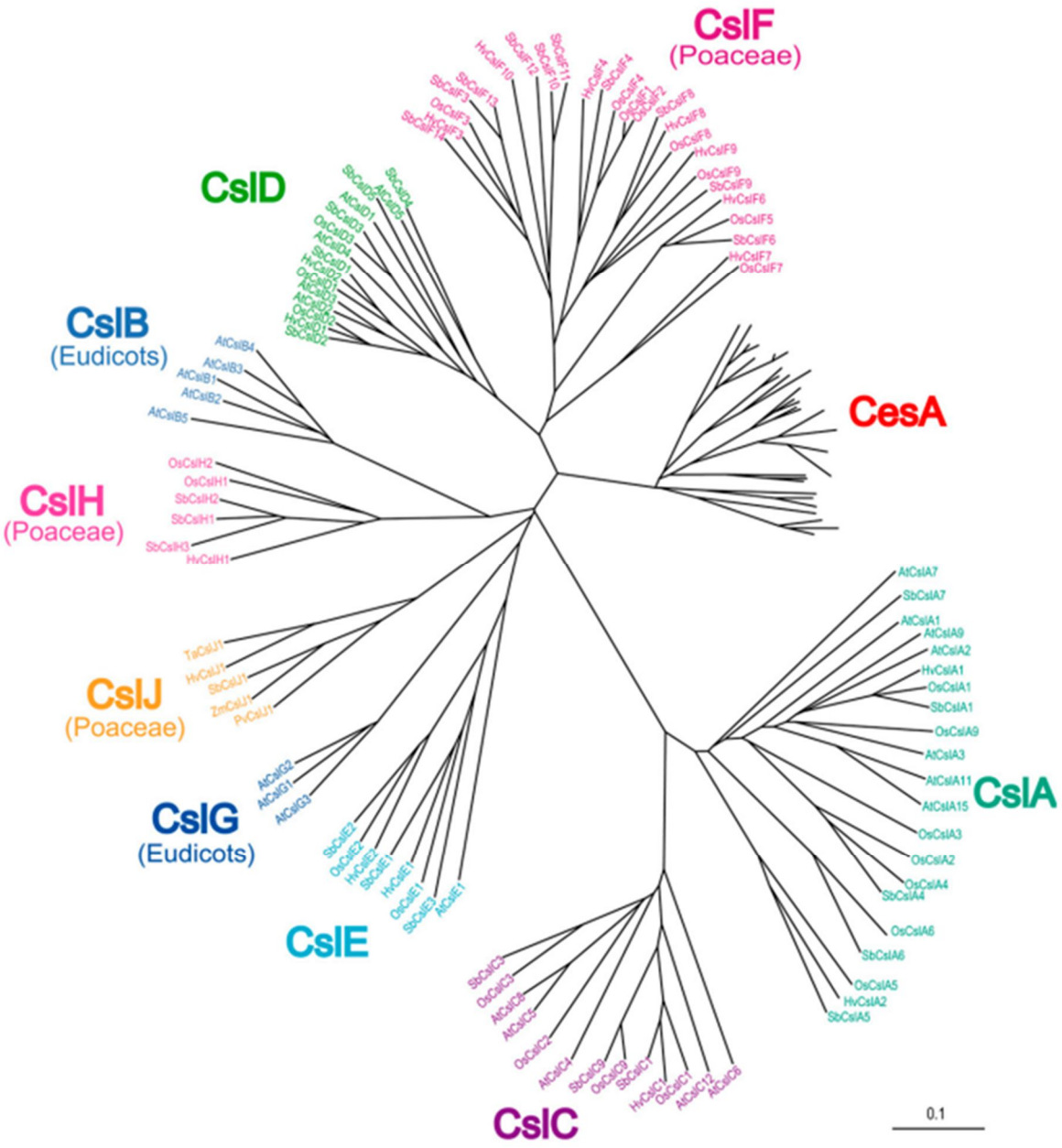

Figure 13: Phylogenetic tree of *cellulose synthase* and *cellulose synthase-like* gene families in higher plants. Picture taken from Fincher, (2009).

1.2.11.2 Hydrolysis of (1,3;1,4)-β-glucan

Degradation of (1,3;1,4)-β-glucans into oligosaccharides requires the action of a (1,3;1,4)-glucanase, also referred to as (1,3;1,4)-glucan-endohydrolase or lichenase. (1,3;1,4)-Glucanase cleaves the (1,4)-linkages and releases tri- and tetrasaccharides as the major products, with

oligosaccharides of up to ten or more units as a minor product. The (1,3;1,4)-β-oligosaccharides released by (1,3;1,4)-β-glucanase are further hydrolysed by β-glucan-exohydrolase and β-glucosidase enzymes. The action of β-glucan-exohydrolase involves breaking down the (1,3)- and (1,4)-linkages of the oligosaccharides and releasing glucose units as end products (Jamar et al., 2011). (1,3;1,4)-β-Glucanase cleaves the (1,4)-linkages on the reducing terminal side of (1,3)-β-glucosyl residues and releases oligosaccharides that contain a variable number of (1,4)-β-glucosyl residues with a single (1,3)-β-glucosyl residue (Fig. 14). The action of lichenase is specific because it does not hydrolyse pure (1,3)-β-glucans or (1,4)-β-glucans (Simmons et al., 2013).

Figure 14: Mode of action of (1,3;1,4)-β-glucanase on (1,3;1,4)-β-glucans. (1,3;1,4)-β-Glucanase cleaves the (1,4)-linkages adjacent to a (1,3)-β-glucosyl residue of the chain and releases tri- and tetrasaccharides (G4G3G and G4G4G3G). G represents a β-D-glucosyl residue, 3 and 4 are (1,3)- and (1,4)-linkages, respectively. Figure reproduced from Hrmova and Fincher, (2001).

In barley, (1,3;1,4)-β-glucanase exists in two isoforms, isozyme EI and EII which are encoded by *Glb* genes. EI is encoded by the *Glb 1* gene on chromosome 1H, whereas EII is encoded by the *Glb 2* gene on chromosome 7H (Jamar et al., 2011). Isozyme EI and EII share 92% nucleotide sequence similarity and similar kinetic properties towards (1,3;1,4)-β-glucan, however, EII has a greater thermostability than EI, with optimum temperatures at 45 and 37°C respectively, which is likely due to an additional glycosylation site on EII (Woodward et al., 1983; Litts et al., 1990; Wolf, 1991; Doan and Fincher, 1992; Jamar et al., 2011). Specific

amino acid substitutions have recently been shown to improve the structural stability and catalytic efficiency of the EII enzyme, which is essential for barley malting (Lauer et al., 2017)

In barley grain, EI mRNA is expressed in the scutellum tissue and aleurone layer whereas EII mRNA is only expressed in the aleurone (Slakeski and Fincher, 1992) During barley grain germination, (1,3;1,4)-β-glucanase is secreted from the aleurone and scutellum tissue to degrade the (1,3;1,4)-β-glucan in the endosperm cell walls (Fincher et al., 1986; Jin et al., 2004). *(1,3;1,4)-β-glucanase EII* gene is expressed exclusively in germinating grain while *(1,3;1,4)-β-glucanase EI* gene is expressed in various tissues during seedling growth (Slakeski and Fincher, 1992). During grain filling, the *(1,3;1,4)-β-glucanase EI* gene and its protein levels are highly expressed in the developing barley endosperm (Finnie et al., 2006; Burton et al., 2008), indicating that it has a significant role in (1,3;1,4)-β-glucan metabolism during barley grain development.

1.2.12 Starch

Starch is the primary storage polysaccharide in many tissues of plants, such as maize, barley, wheat, sorghum and rice grains and potato tubers (Végh, 2009). Starch is a polymer of glucose residues joined by α(1,4)-glycosidic bonds (Fig. 15). When plants require energy, starch granules are hydrolysed to produce glucose, which is the fuel source for many biological activities (Fontaine et al., 1942; Zeeman et al., 2007). Starch is important for many industries including for food, paper and biofuel (Burrell, 2003). In the food industry, starch provides calories in the human diet and is sourced from higher plants including cereals, legumes and tubers (Végh, 2009). The human digestive system contains α-amylases which hydrolyse starch into glucose prior to absorption, and the glucose provides energy to the body 2011 (Butterworth

et al., 2011). Starch can exist in resistant forms, which is not hydrolysed by α-amylase and pullulanase (Englyst et al., 1982; Englyst et al., 1992). Similar to the role of non-starch polysaccharides, resistant starch shows positive physiological effects in the human gastrointestinal tract (Cummings et al., 1996; Topping and Clifton, 2001). In the biofuel industry, starch from grain crops such as maize and sorghum is converted to bioethanol (Makkar, 2012).

1.2.12.1 Structure of starch

Starch consists of amylose and amylopectin molecules which interact to form a semi-crystalline granule with varying polymorphic types and degrees (Yamaguchi et al., 1979; Buléon et al., 1998). Amylose is a linear polymer of glucan units joined by α(1,4)-glycosidic bonds. It consists of approximately 1000 glucose residues and contains few branch points. Amylopectin is a highly branched polymer, consisting of linear α(1,4)-glucan chains and α(1,6)-glucan linkages at the branch points. Amylopectin consists of 100000 to 1000000 glucose residues with branch points every 20-25 glucose units (Jeon et al., 2010; Streb and Zeeman, 2012).

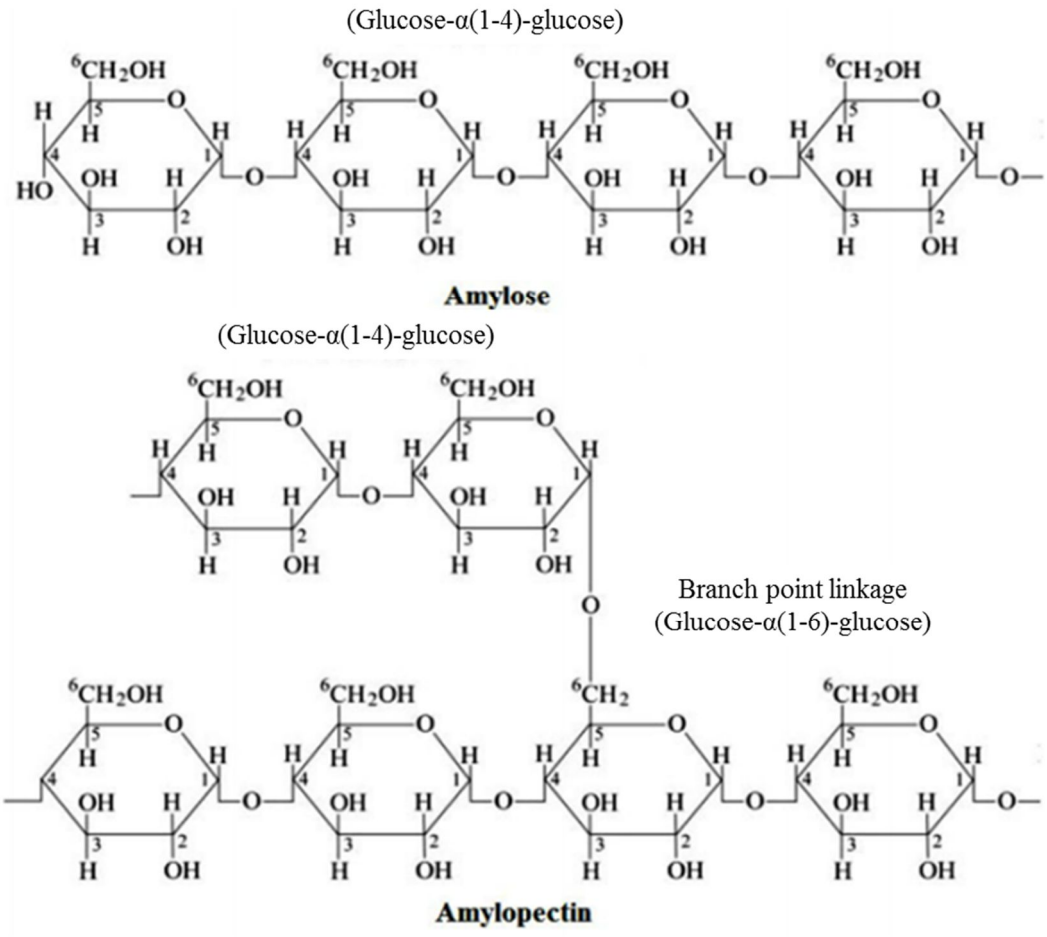

Figure 15: Amylose is composed of a linear chain of α(1,4)-linked glucose units, whereas amylopectin consists of α(1,4)-linked glucose chains and α(1,6)-linked glucose units at the branch points. Figures reproduced from Streb and Zeeman, (2012).

In the starch granule, the ratio of amylose and amylopectin may vary between plant species and between organs of the same plant (Burrell, 2003). Generally, amylose accounts for about 30% while amylopectin is comprised of about 70% of the granule mass and therefore responsible for the granule crystallinity (French, 1984; Zobel, 1988; Gallant et al., 1997). In the granule, amylose exists in a single helical structure whereas amylopectin forms double helices between neighbouring chains. The double helices that aligned in the same cluster form a structure of

alternating crystalline and amorphous lamellar composition (Buléon et al., 1998; Vermeylen et al., 2004) (Streb and Zeeman, 2012).

Starch granule is comprised of A-type (large) and B-type (small). In barley, large granules contain diameters in the range from 10 to 40 μm whereas small granules range from 1 to 10 μm (Palmer, 1972; Chmelik et al., 2001). The small granules account for about 87% of the total granules, however, only represent 11% of the starch by weight (Bathgate and Palmer, 1972). The amylose content in the small granules is about 41%, which is greater than the large granules (25%) (Bathgate and Palmer, 1972). During early stage of development, large granule is formed and the size is increased during grain maturation, whereas small granules remain small, although the number of granules increased (Karlsson et al., 1983). A recent study shows that high resistant starch barley genotypes are associated with reduced granule size and increased proportions of small granules (B-type) with altered granule morphology (Ahmed et al., 2016). Furthermore, modification of genes related to starch metabolic pathway appears to affect the starch granule structure (Burton et al., 2002; Morell et al., 2003; Regina et al., 2010; Shaik et al., 2016).

1.2.12.2 Biosynthesis of starch

The biosynthesis of starch components, amylose and amylopectin, involve the coordinated activities of multiple enzymes. For example, amylose is synthesised by ADP glucose pyrophosphorylase (AGPase) and granule-bound starch synthase (GBSS), whereas amylopectin is synthesised by AGPase, soluble starch synthase (SS), starch branching enzyme (BE), and starch debranching enzyme (DBE). Moreover, the initiation process of starch biosynthesis may also involve plastidial starch phosphorylase (Pho) (Jeon et al., 2010).

Starch biosynthesis takes place in the plastids of photosynthetic cells, such as chloroplasts (Nomura et al., 1967), and non-photosynthetic cells, called amyloplasts (Tyson and Ap Rees, 1988). In chloroplasts, glucose-6-phosphate, which is produced during photosynthesis, is retained for the synthesis of starch (Fig. 16A). In amyloplasts, ATP and glucose-6-phosphate from the cytosol are imported into the cell for starch biosynthesis (Fig. 16B). Glucose-6-phosphate in cells is then converted into glucose-1-phosphate by the plastidial phosphoglucomutase (pPGM). Subsequently, glucose-1-phosphate and ATP are used as substrates by the ADPG pyrophosphorylase (AGP) producing ADP-glucose (ADPG) for starch biosynthesis (Fig. 16A and 16B) (Bahaji et al., 2011).

A

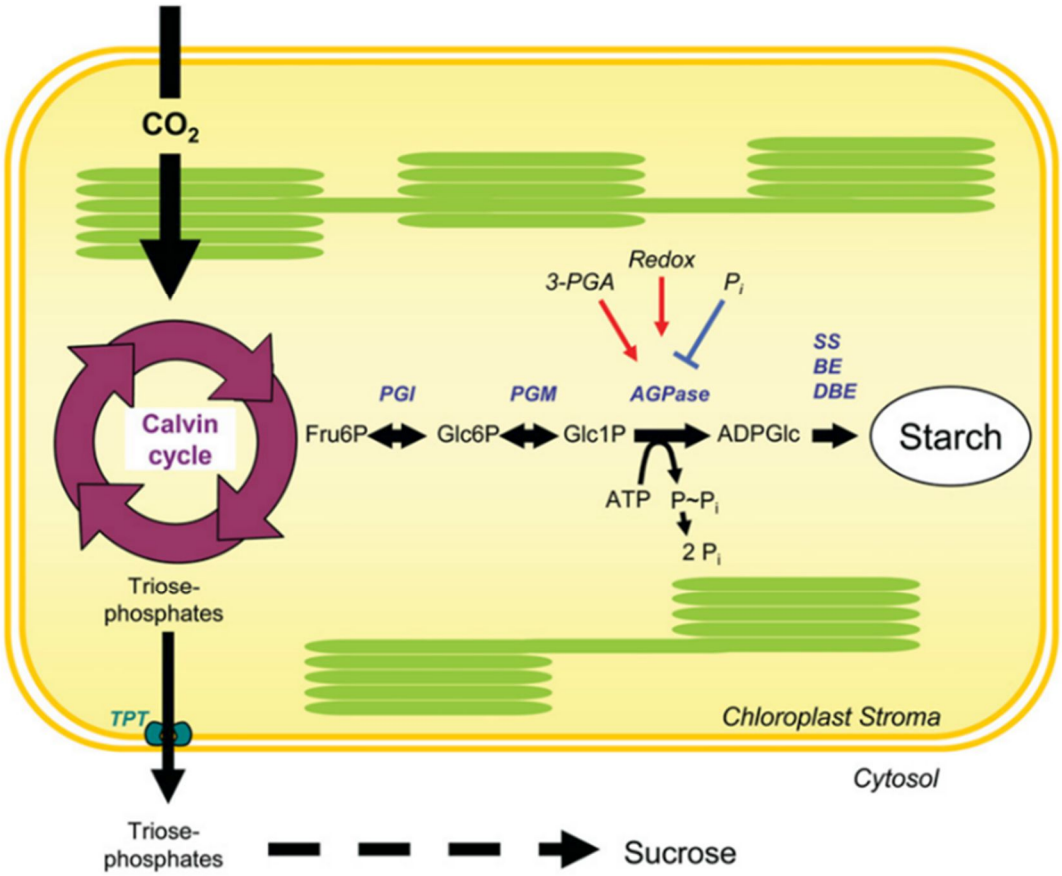

B

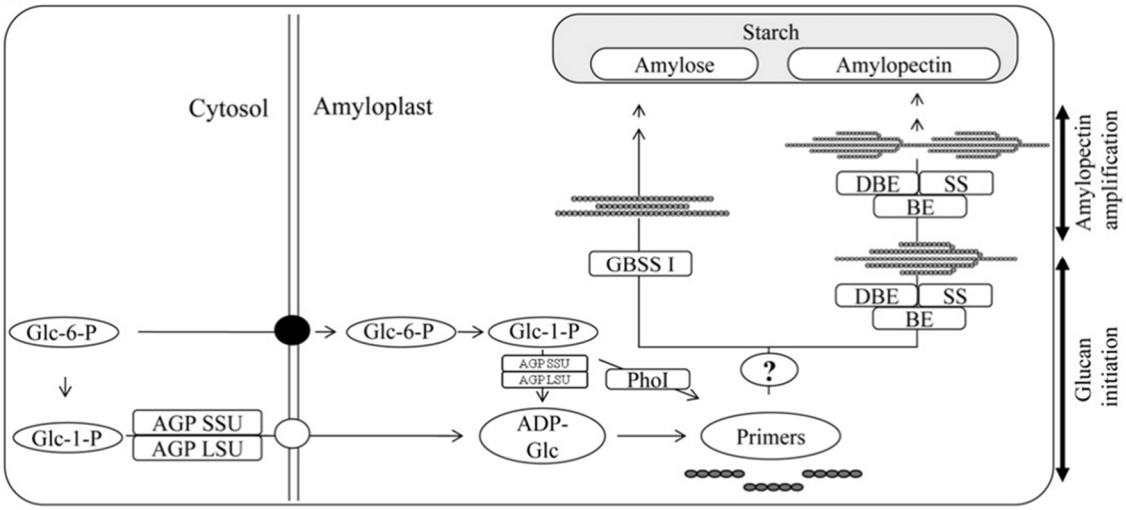

Figure 16: Models of starch biosynthesis in photosynthetic and non-photosynthetic cells. (A) The pathway of starch biosynthesis in photosynthetic cells. A portion of carbon assimilated via the Calvin cycle remains in the chloroplast for starch synthesis. Briefly, Fru6P, which is an intermediate of the Calvin cycle, is converted into Glc6P by PGI. Glc6P is converted to Glc1P by PGM1. Glc1P is subsequently converted into ADP-glucose by AGPase in the presence of ATP. ADP-glucose is used as a substrate by SS which transfers glucose to the pre-existing α(l-4)-linked glucosyl chain. BE cleaves the α(1,4)-linked glucosyl chain and reattaches α(1,6)-linked glucose units at the branch points. Excess α(1,6)-linked glucosyl chains are removed by DBE. Figure reproduced from Zeeman et al., (2007). (B) The pathway of starch biosynthesis in non-photosynthetic cells. Glc6P and Glc1P from the cytosol are transported into the amyloplast via transporters, and are used as substrates for the synthesis of amylose and amylopectin. Figure reproduced from Jeon et al., (2010). Abbreviations: fructose-6-phosphate (Fru6P), glucose-6-phosphate (Glc6P or Glc-6-P), glucose-1-phosphate (Glc1P or Glc-1-P), ADP-glucose (ADPGlc or ADP-Glc), plastidial phosphoglucose isomerase (PGI), plastidial phosphoglucomutase (PGM1), ADP-glucose pyrophosphorylase (AGPase), small subunits (SSU), large subunits (LSU), starch synthase (SS), branching enzyme(BE), debranching

enzyme (DBE), plastidial starch phosphorylase (Pho), granule-bound starch synthase I (GBSS I), triose-phosphate/phosphate translocator (TPT).

The literature suggests that plastidial starch phosphorylase I (Pho I) initiates the process by extending short glucan chains, including malto-oligosaccharides (MOS) and branched malto-dextrins, via the transfer of glucosyl units from glucose-1-phosphate to the α-glucan chains (Satoh et al., 2003). For amylose biosynthesis, GBSS I acts to produce long linear α-(1,4)-glucan chains (Nelson and Pan, 1995). The synthesis of amylopectin involves SS, BE and DBE, which comprise different isoforms, producing different chain lengths and branch types in the amylopectin clusters (Boyer and Preiss, 1981). ADPG is synthesised by AGP from glucose-1-phosphate as a substrate (Ballicora et al., 2004). ADPG is used as a substrate by SS to elongate the glucan chains to predetermined chain lengths through an unknown mechanism (Fujita et al., 2006). Branch points of glucan chains are catalysed by BE, which cleaves the α-(1,4)-linkage and reattaches the α-(1,6)-linkage to the glucan chains (Nakamura, 2002; Nakamura et al., 2010), DBE maintains proper formation of amylopectin by hydrolysing α-(1,6)-glucosidic linkages which are improperly positioned in the chains during starch biosynthesis (Fig. 11A and 11B). DBE exists as two different types: isoamylase (ISA) and pullulanase (PUL), which may have an overlapping biological role during starch biosynthesis (Kubo et al., 1999; Jeon et al., 2010).

1.2.12.3 Hydrolysis of starch

Breakdown of starch releases oligosaccharides such as maltose, and smaller compounds such as glucose and glucose-1-phosphate, which can be used for plant cellular metabolism, and sucrose synthesis. Starch is made during the day, when photosynthesis occurs, while starch is

degraded during the night when respiration is taking place. Degradation of starch involves several key enzymes, such as α-glucan water dikinase (GWD), phosphoglucan water dikinase (PWD), phosphoglucan phosphatases such as Starch Excess 4 (SEX4) and Like Sex Four 2 (LSF2), β-amylase, α-amylase, debranching enzyme (DBE) and α-glucan phosphorylase (PHS1) (Streb and Zeeman, 2012).

GWD and PWD are enzymes which phosphorylate the glucan chains, resulting in disruption of amylopectin structure and destabilisation of amylopectin double helices. It is suggested that phosphorylation of glucan chains may solubilise the surface of the starch granules, enabling the degrading enzymes to attack the exposed glucan chains (Edner et al., 2007). Interestingly, phosphoglucan phosphatases, SEX4 and LSF2, which are able to remove the phosphate groups from the glucan chains, have also been reported to promote starch degradation. This indicates that the presence of the phosphate group on the glucan chains is tightly regulated in relation to starch degradation (Silver et al., 2014).

The modification of starch granules by α-glucan water dikinase (GWD and PWD) and phosphoglucan phosphatase (SEX and LSF) allows the attack of the α(1,4)-glucan chains by hydrolytic enzymes, β-amylase and α-amylase (Streb and Zeeman, 2012). β-Amylase, known as an exo-acting amylase, hydrolyses the external α-(1,4)-linkages, releasing the olisosaccharides from the non-reducing ends (Oyefuga et al., 2011). On the other hand, α-amylase, known as an endo-acting amylase, which is secreted by the aleurone layer and the scutellum surrounding the endosperm of germinated cereal seeds, hydrolyses the internal α-(1,4)-linkages, releasing linear or branched oligosaccharides (Ranki and Sopanen, 1984). It is noteworthy that the β- and α-amylases cannot hydrolyse the α-(1,6) branch points, hence DBE comes into play in hydrolysing the branch points of the glucan chains (Streb and Zeeman, 2012).

1.2.13 Fructan

Fructans are water-soluble polysaccharides that are stored in approximately 15% of plant species, including cereals, vegetables, ornamentals and forage grasses (Hendry and Wallace, 1993). Fructans consist of repeating fructose residues with a terminal sucrose unit (glucose and fructose). In cereals, fructans are stored in the stems, leaves and grains (Wagner and Wiemken, 1987; Van Den Ende et al., 2003; Huynh et al., 2008; Verspreet et al., 2013b; Nemeth et al., 2014). When energy is required, the fructans are hydrolysed into sucrose and hexoses and transported via the phloem, for example, to the kernel for storage (Verspreet et al., 2013b). Fructans function as osmoprotectors during drought and cold stress periods (Pilon-Smits et al., 1995; Yoshida et al., 1998). The mechanism involves the stabilization of membrane lipids via the interaction between fructans and lipids, which reduces the outflow of water from the membranes (Valluru and Van den Ende, 2008).

Fructans are important sources of dietary fibre and they are resistant to enzymes in the human digestive tract due to the β-configuration of the fructan linkages. Consequently, fructans are fermented by bacteria in the large bowel, such as *Bifidobacteria* and *Lactobacilli*, which leads to an increase of fecal mass and can lead to excess gas and discomfort in some individuals. (Flamm et al., 2001; Kleessen et al., 2001). Fermentation of fructans produces short-chain fatty acids such as acetate, propionate and butyrate, which are beneficial for human health (Kolida and Gibson, 2007; Louis and Flint, 2009).

Dietary fructans have been shown to increase the absorption of minerals such as calcium, magnesium and zinc in the large intestine and consequently increase bone mass (Coudray et al., 2003; Raschka and Daniel, 2005; Abrams et al., 2007). Fructans have been implicated in reducing inflammation and disease activity, including Crohn's disease in the intestinal tract

(Leenen and Dieleman, 2007). In the food industry, fructans are widely used in food products because short-chain fructans and long-chain fructans produce a natural sweet taste and a fat-like texture with a neutral taste (Vijn and Smeekens, 1999).

1.2.13.1 Structure of fructans

Fructans are polymers consisting of linear or branched repeating fructose residues with a terminal sucrose unit. Repeating fructose units are joined by either β(2-1)- or β(2-6)-fructofuranosyl linkages or contain both linkages. Different linkage positions between individual fructose residues determine the type of fructans, which can be found in different plant species. Five types of fructans have been identified: 1) inulin, 2) levan, 3), mixed-type levan, 4) inulin neoseries and 5) levan neoseries (Bonnett et al., 1997; Vijn and Smeekens, 1999).

1.2.13.1.1 Inulin-type fructan

Inulin-type fructan is a storage polysaccharide usually found in Asteraceae species (Pollock and Cairns, 1991), consisting of 2 to 100 fructose units, depending on the plant species, growth phase, harvesting date, and temperature of the extraction and post-extraction procedures (Koch et al., 1999; Saengthongpinit and Sajjaanantakul, 2005; Apolinário et al., 2014). Inulin-type fructan is joined by linear β(2-1)-fructofuranosyl linkages and it terminates with one glucose joined to one fructose molecule through an α(1-2)-glucopyranosyl link (Figure 17B). The shortest chain length of inulin is 1-kestose, which has only 2 fructose units and 1 glucose unit joined by a β(2-1)-fructofuranosyl linkage (Fig. 17A) (Waterhouse et al., 1991; Apolinário et al., 2014).

A

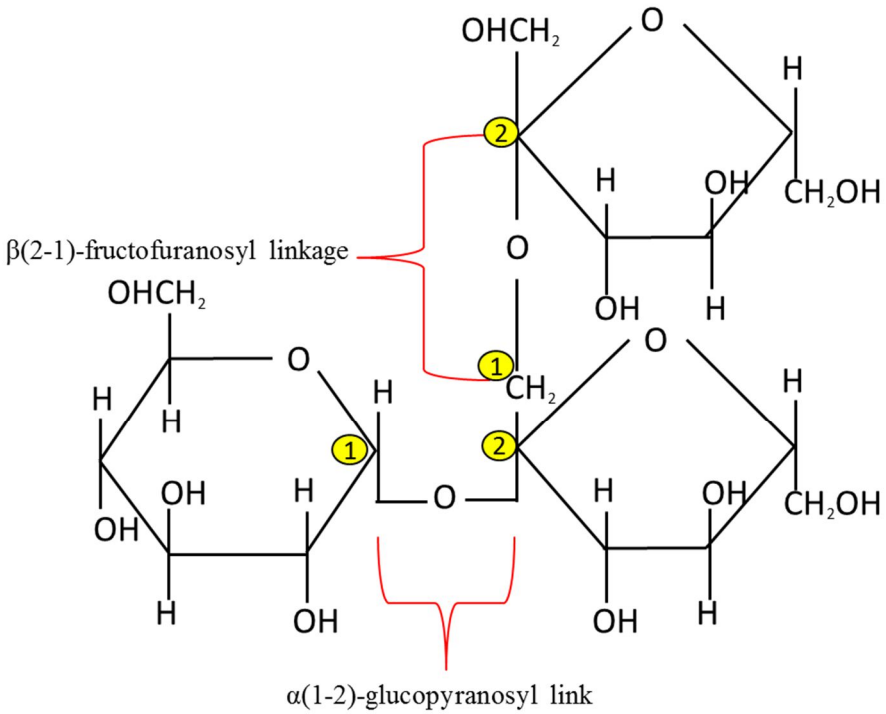

1-kestose

B

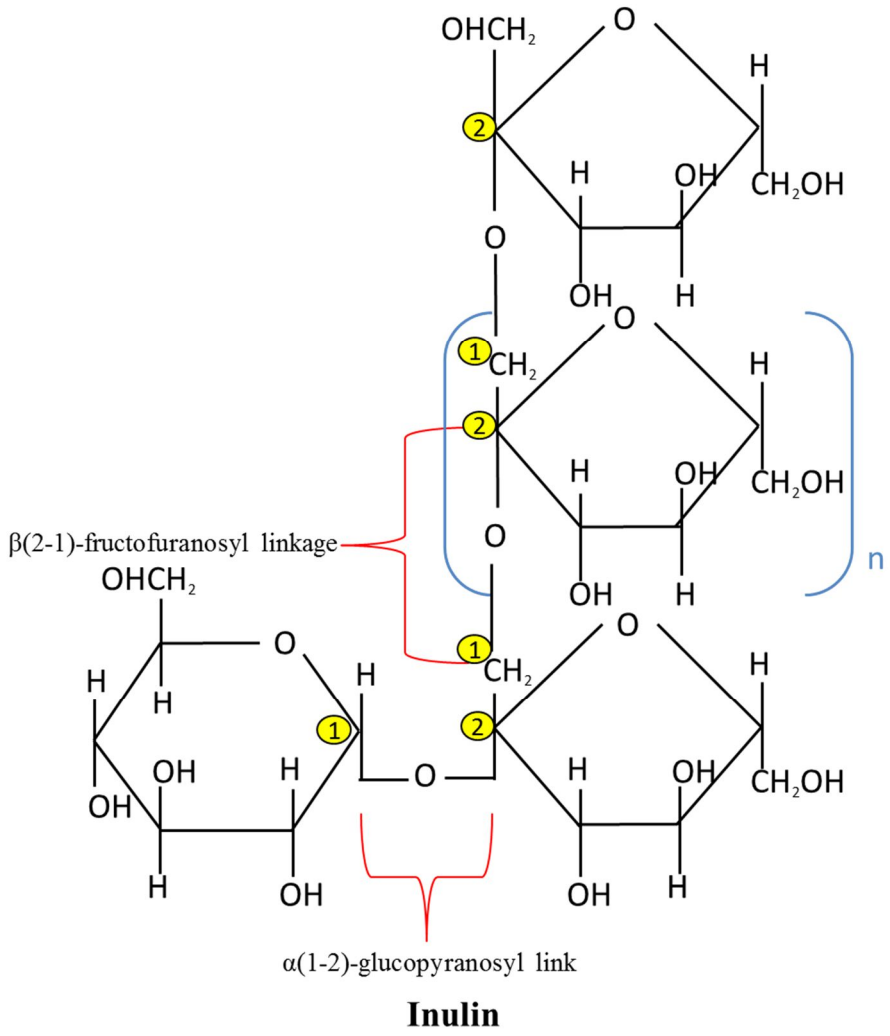

Figure 17: Inulin-type fructans. (A) 1-kestose consists of a fructose unit attached to C_1 of a fructose unit of the sucrose molecule via a β(2,1)-fructofuranosyl linkage. (B) Inulin consists of repeating numbers of fructose units (in blue brackets) attached to a sucrose molecule via β(2,1)-fructofuranosyl linkages. The number of the carbon atom is shown in a yellow circle.

1.2.13.1.2 Levan-type fructans

Levan-type fructans are storage polysaccharides consisting mainly of linear chains of fructose joined by β(2-6)-fructofuranosyl linkages (Fig. 18B). 6-Kestose is the shortest form of levan,

consisting of one β(2-6)-linked fructosyl unit terminating with one sucrose molecule (Fig. 18A) (Forsythe et al., 1990). Levan-type fructans are usually found in a wide range of bacterial groups, such as *Bacillus, Streptococcus, Pseudomonas, Erwinia,* and *Actinomyces* (Hendry and Wallace, 1993) and some cereals, such as wheat and barley (Van den Ende et al., 2011). The fructan polymers produced by bacteria leads to the formation of an extracellular matrix, protecting them from physical and environmental stresses, and they function as a nutrient storage source for biofilm development (Iztok et al., 2013; Jaco et al., 2013).

A

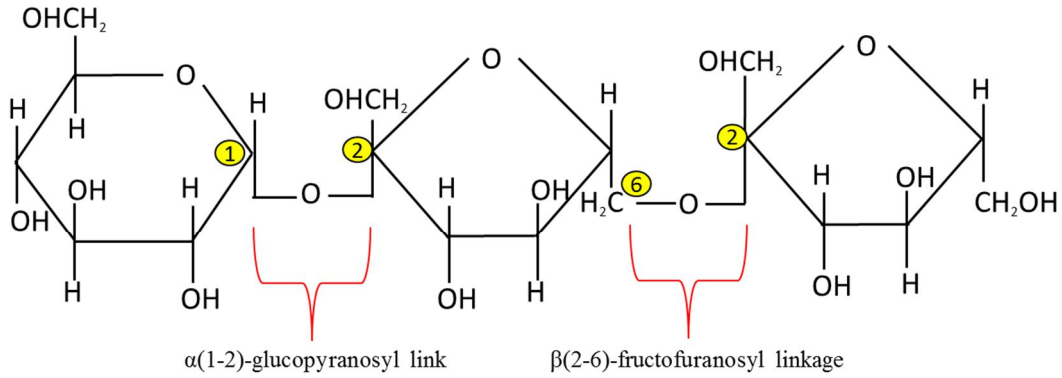

6-kestose

B

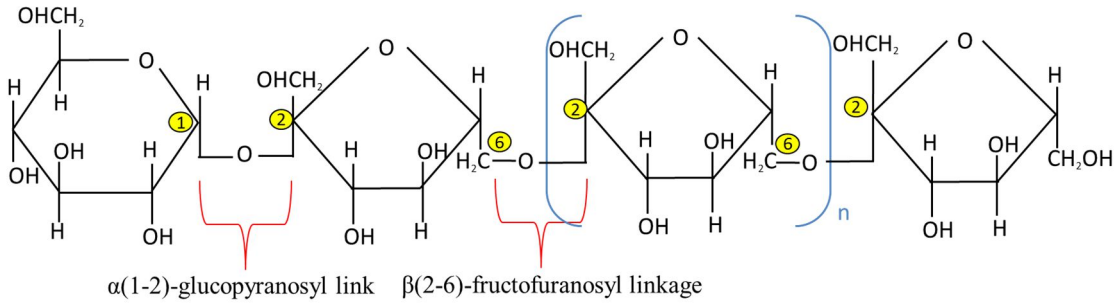

Levan

Figure 18: Levan-type fructans. (A) 6-kestose consists of a fructose unit linked to C_6 of a fructose residue of the sucrose molecule via a β(2,6)-fructofuranosyl linkage. (B) Levan-type fructan is a larger unit of 6-kestose consisting of repeat numbers of fructose units (in blue brackets) joined by β(2,6)-fructofuranosyl linkages. The number of the carbon atom is shown in a yellow circle.

1.2.13.1.3 Mixed-type levan

Mixed-type levan or graminan, contains both β(2-1)- and β(2-6)-fructofuranosyl linkages and these are typically found in the Poaceae, such as wheat and barley (Wei and Chatterton, 2001). The simplest form of mixed-type levan exists as bifurcose (Fig. 19).

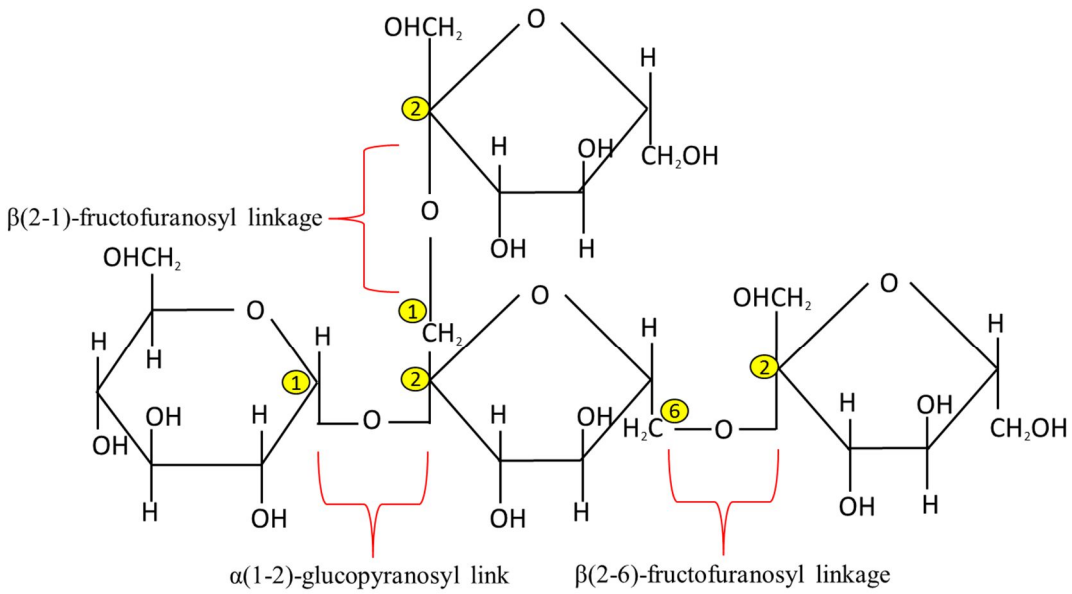

Bifurcose

Figure 19: Mixed-type levan. Bifurcose, the simplest form of mixed-type levan consisting of fructose units attached to a sucrose molecule via both a β(2,1)-fructofuranosyl and a β(2,6)-fructofuranosyl linkage. The number of the carbon atom is shown in a yellow circle.

1.2.13.1.4 Inulin neoseries

Inulin-neoseries-type fructans are composed of a fructose unit attached to both carbon 1 (C1) and carbon 6 (C6) of a glucose unit with repeating units to form a linear polymer with β(2-1)-fructofuranosyl linkages at either end of the glucose unit of the sucrose molecule (Fig. 20B) (Vijn et al., 1997). Inulin neoseries are found in the Liliaceae, such as onion and asparagus (Shiomi, 1989; Ritsema et al., 2003). The smallest form of the inulin neoseries is neokestose, consisting of a fructose unit attached to C6 of the glucose moiety of a sucrose molecule (Fig. 20A).

A

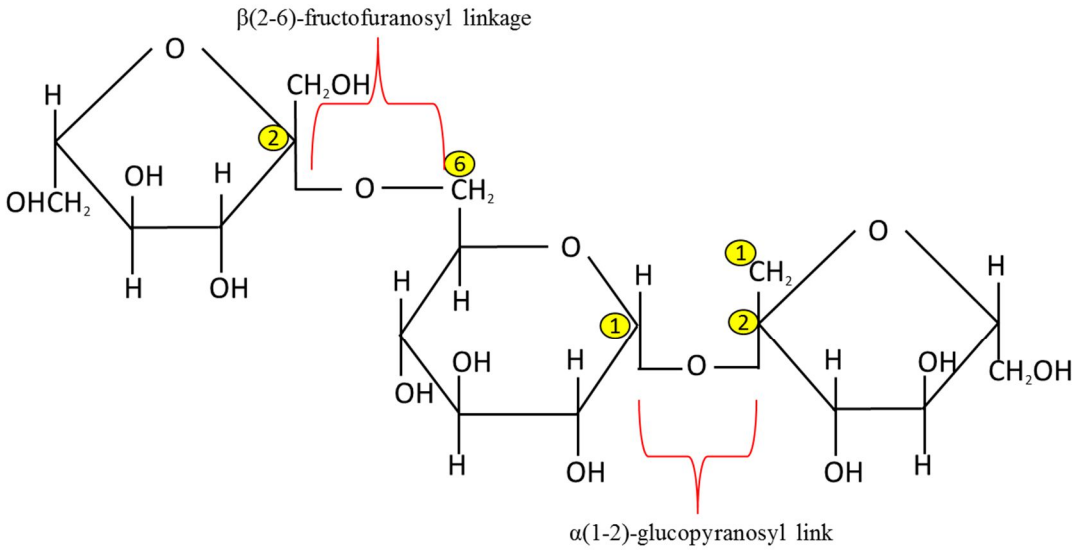

Neokestose

B

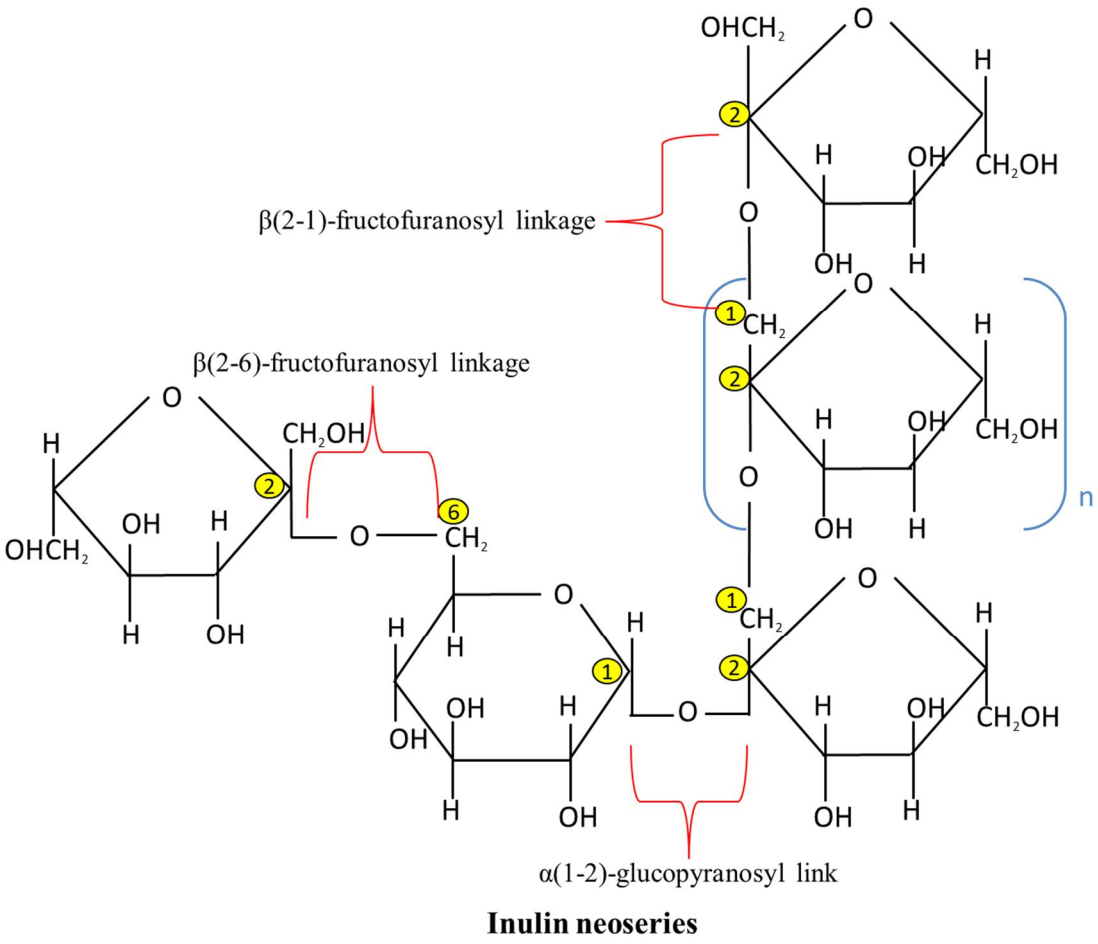

Figure 20: Inulin neoseries. (A) Neokestose, the simplest form of the inulin neoseries consisting of a fructose unit attached to C6 of the glucose moiety of a sucrose molecule. (B) Inulin neoseries consists of a fructose unit on both carbon 1 (C1) and carbon 6 (C6) of the glucose unit to form the repeating units with β(2-1)-fructofuranosyl linkages (in blue brackets) at either end of the glucose unit of the sucrose molecule. The number of the carbon atom is shown in a yellow circle.

1.2.13.1.5 Levan neoseries

Levan neoseries of fructans are composed of linear polymers of β(2-6)-linked fructosyl residues attached to either end of the glucose moiety of a sucrose molecule (Fig. 21) (Vijn and Smeekens, 1999). These fructans can be found in the Poaceae such as oats, wheat and barley (Yildiz, 2010).

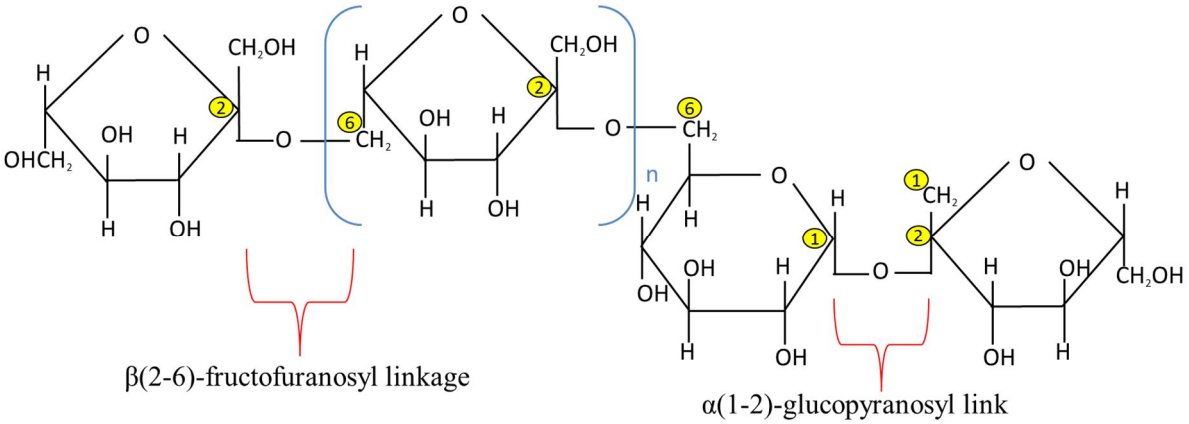

Figure 21: Levan neoseries. A polymer of fructosyl residues (in blue brackets) is joined to C_6 of the glucose unit of the sucrose molecule via β(2,6)-fructofuranosyl linkages. The number of the carbon atom is shown in a yellow circle.

1.2.13.2 Type of fructans in cereals

Dicotyledonous plants tend to store β(2-1)-linked fructans, whereas monocotyledonous plants tend to accumulate β(2-6)-linked fructans. Cereals, including barley, oats and wheat have fructans that contain both β(2-1)- and β(2-6)-fructofuranosyl linkages, also known as mixed-type fructans or graminans (Bonnett et al., 1997; Vijn and Smeekens, 1999). The fructan content in barley grain ranges from 1 to 4% w/w (Nemeth et al., 2014), wheat grain ranges from 0.7 to 2.9% w/w (Huynh et al., 2008) and rye ranges from 1.7 to 6.6% w/w (Henry and Saini, 1989; Karpinnen et al., 2003).

1.2.13.3 Biosynthesis of fructans

The amount of fructans in plants is determined by the balance between biosynthesis and hydrolysis reactions carried out by specific enzymes. The biosynthesis of fructans involves different synthesizing enzymes, known as fructosyltransferases, such as sucrose:sucrose 1 fructosyltransferase (1-SST), fructan:fructan 1 fructosyltransferase (1-FFT), sucrose:fructan 6-fructosyltransferase (6-SFT) and fructan:fructan 6-G fructosyltransferase (6G-FFT). Previous studies report that the biosynthesis of fructan occurs in the vacuole of plant cells (Darwen and John, 1989; Pollock and Cairns, 1991). In the vacuole, the synthesis of a fructan chain is initiated by 1-SST in the presence of sucrose, which is used as a starting molecule. 1-SST transfers a fructosyl unit from one sucrose molecule to another, forming 1-kestose with a β(2-1)-fructofuranosyl linkage. In addition, 1-SST also produces nystose (2 fructosyl units attached to C_1 of a fructose unit of the sucrose molecule) (Koops and Jonker, 1996), and possibly other fructooligosaccharides up to a degree of polymerization (DP) of 7 (Hellwege et al., 2000). 1-FFT is involved in the elongation of β(2-1)-linked fructan chains by transferring a fructosyl unit from one fructan to another (Edelman and Jeeeord, 1968; Van den Ende et al., 1996; Van Laere and Van Den Ende, 2002). Despite the overlapping function between 1-SST and 1-FFT in elongating fructan chains, the fructosyl donor used by 1-SST is sucrose, whereas fructan is used as the donor for 1-FFT.

Sucrose is used as the primary donor for the initiation of a fructan polymer, however, this may be inhibited when the sucrose level is too high. For example, at high concentrations sucrose competes with trisaccharides for a fructosyl unit, thus preventing the elongation of fructans by 1-FFT (Edelman and Jeeeord, 1968). The biosynthesis of levan is initated by 6-SFT, creating β(2-6)-linkages. 6-SFT uses sucrose as a donor or acceptor, producing 6-kestose, which is the shortest form of levan. 6-SFT continues to elongate 6-kestose to produce levan.

In addition to sucrose, 6-SFT also uses 1-kestose, which is the end product of the 1-SST reaction, to form bifurcose, which consists of both β(2-1)- and β(2-6)-fructofuranosyl linkages (Duchateau et al., 1995). 1-FFT and 6-SFT further elongate bifurcose to form branches of mixed-type levan or graminan (Sprenger et al., 1995; Kawakami and Yoshida, 2002; Kawakami and Yoshida, 2005). Similarly, 1-kestose or the low DP of inulin are also used by 6G-FFT as a fructose donor to synthesise neokestose, which consists of a fructosyl unit attached to C_6 of the glucose moiety of a sucrose molecule or oligofructan (Shiomi, 1989). 1-FFT or 6-SFT then elongates neokestose to form inulin neoseries or levan neoseries, respectively (Figure 22) (Vijn and Smeekens, 1999).

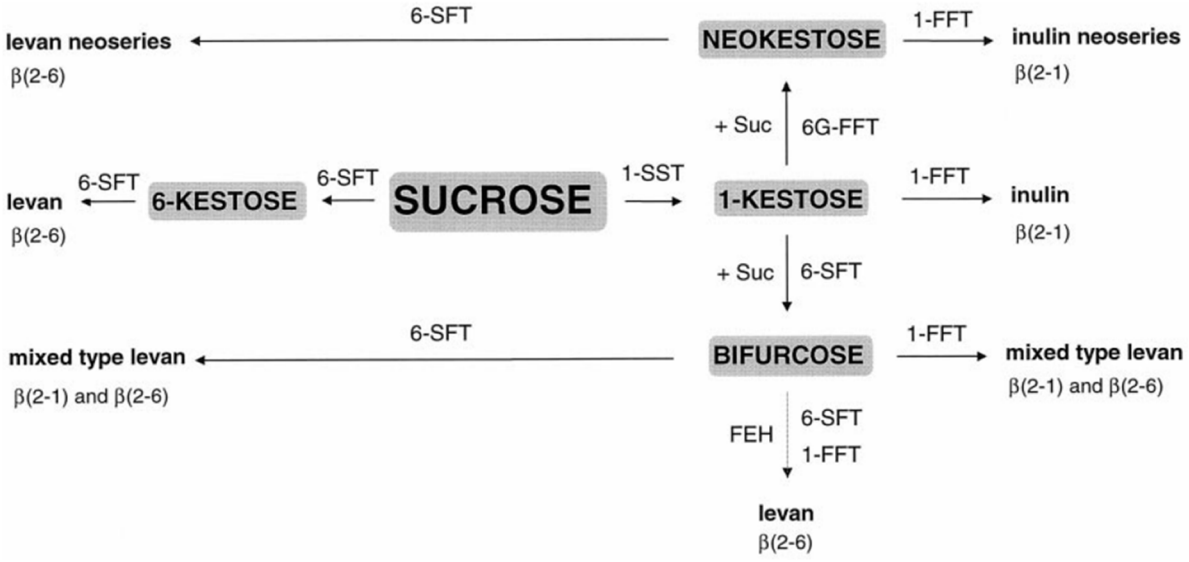

Figure 22: Model of the biosynthesis of fructans in plants. Sucrose (Suc) is the starting molecule used by different fructosyltransferases to produce various types of fructans. The dotted line shows an alternative route for the production of levan β(2,6). Abbreviations: sucrose:sucrose 1 fructosyltransferase (1-SST), fructan:fructan 1 fructosyltransferase (1-FFT), sucrose:fructan 6-fructosyltransferase(6-SFT), fructan:fructan 6-G fructosyltransferase (6G-FFT), fructan exohydrolases (FEH). Figure reproduced from Vijn and Smeekens, (1999).

1.2.13.4 Hydrolysis of fructan

Hydrolysis of fructans involves fructan exohydrolases (FEHs), including 1-FEH and 6-FEH. FEHs utilize a water molecule as an acceptor, degrading fructosyl linkages and releasing fructosyl units (Van den Ende et al., 2002). The location for the fructan hydrolysis has been reported to be within the vacuole (Wagner et al., 1986; Darwen and John, 1989; Van den Ende et al., 2000).

Fructan hydrolase exists as different isoenzymes, including 1-FEH, 6-FEH, 6&1-FEH and 6-KEH, which are differentially expressed in specific plant tissues under different environmental conditions (Van Den Ende et al., 2003; Kawakami et al., 2005; Van den Ende et al., 2005; Kawakami and Yoshida, 2012). Purification and characterisation of different FEH isoenzymes have previously been established in various plant species such as wheat (Van Den Ende et al., 2003; Van Riet et al., 2006), chicory roots (Van den Ende et al., 2000), oat (Henson and Livingston III, 1996), Jerusalem artichoke (Xu et al., 2015), barley (Henson and Livingston Iii, 1998) and daisy (Degasperi et al., 2003). In wheat stems 1-FEH enzyme activity was induced during fructan biosynthesis (in young stems) and during the degradation of fructan (in mature stems), indicating that 1-FEH may function both as a hydrolytic enzyme and a β(2-1)-trimmer during fructan biosynthesis (Van Den Ende et al., 2003). Van Den Ende et al., (2003) also demonstrated that 1-FEH preferentially hydrolyses 1-kestose and nystose compared to 6-kestose, indicating that 1-FEH is specific towards β(2-1)-linkages in a fructan chain.

Complete hydrolysis of mixed-type fructans requires cleavage of both β(2-1)- and β(2-6)-linkages. β(2-6)-linkages are exclusively cleaved by 6-FEH which releases only fructosyl units (Van Riet et al., 2006; Kawakami and Yoshida, 2012). The 6-FEH enzyme is also found in non-fructan containing plants such as sugar beet, indicating that 6-FEH may have other roles such

as protecting plants from pathogen invasion, possibly via induction of the pathogenesis-related (PR) enzymes (Van Den Ende et al., 2003).

6&1-FEH mRNA was expressed mainly in the wheat crown tissues (Kawakami et al., 2005) and although able to degrade both β(2-1)- and β(2-6)-linkages, it has a preference for β(2-6)-linkages in smaller fructans relative to β(2-1)-linkages. Similarly to 6&1-FEH, 6-KEH was detected in wheat crown tissues and found to be located in the apoplast. The 6-KEH enzyme specifically hydrolyses 6-kestose, releasing sucrose and fructose as the end products (Van den Ende et al., 2005).

1.2.13.4.1 β(2-1)-fructan I-fructanohydrolases (Invertase)

β(2-1)-Fructan I-fructanohydrolases, known as invertase, catalyses the hydrolysis of sucrose into glucose and fructose. Invertase exists in different isoforms with variable optimum pH requirements for activity, needing either acidic or neutral/alkaline conditions. Acid invertase includes cell wall invertases (insoluble) and vacuolar invertases (soluble), whereas the neutral/alkaline invertases includes cytosolic invertases (Fotopoulos, 2005).

Cell wall invertase is predominantly expressed in the plant cell wall. It catalyses the hydrolysis of sucrose into glucose and fructose. This function releases monosaccharides into the phloem for supplying carbohydrates to the sink tissues, and may serve as an extracellular indicator of pathogen infection (Roitsch et al., 2003; Roitsch and Gonzalez, 2004). Vacuolar invertase and cytosolic invertase are involved in plant growth and development (Paul Barratt et al., 2009; Welham et al., 2009).

Invertase is capable of hydrolysing both fructans and sucrose (Verspreet et al., 2013b), and this distinguishes it from FEHs. Interestingly, previous studies reported that fructosyltransferases also possess invertase activity, and act by transferring fructose units from sucrose to water molecules (Hochstrasser et al., 1998; Nagaraj et al., 2004; Kawakami and Yoshida, 2005; Jaco et al., 2013). Fructosyltransferases, such as 1-SST, release fructose units from fructans when incubated with 1-kestose, indicating that 1-SST has FEH activity (Koops and Jonker, 1996; Hochstrasser et al., 1998; Nagaraj et al., 2004). The fructosidase activity is also observed in 1-FFT (Van den Ende et al., 1996). Conversely, the literature has reported that invertase has fructosyltransferase activity that produces 1-kestose when the sucrose concentration is high. It is believed that fructosyltransferase, FEH and invertase have evolved from the same gene ancestor (Van den Ende et al., 2002; Ritsema et al., 2006; Huynh et al., 2012). The amino acid sequences of 1-FEH, 6-FEH, 6&1-FEH and 6-KEH are similar to cell wall-type invertase whereas fructosyltransferases are similar to vacuolar-type invertase (Kawakami and Yoshida, 2005; Van den Ende et al., 2005; Van Riet et al., 2006). The transformation of cell wall invertase to 1-FEH is determined by the Asp239 in the active site of cell wall invertase (Le Roy et al., 2007).This finding implies that the functions of fructosyltransferase, FEH and invertase can be overlapping and they can diverge from one another via single amino acid changes at strategic positions at the active site of the enzyme.

1.2.13.5 Remobilisation of fructans in cereal grains

Fructan metabolism during grain development has been reported in wheat (Verspreet et al., 2013b; Cimini et al., 2015) and barley (Peukert et al., 2014). In wheat grain, the levels of fructan peak during early grain development, before 9 DAP (Verspreet et al., 2013b; Cimini et al., 2015). The fructan levels decline as the grain begins to accumulate starch from 10 DAP onwards

(Verspreet et al., 2013b; Cimini et al., 2015). High levels of fructan before 9 DAP is accompanied by high levels of hexoses (glucose and fructose) and sucrose (Verspreet et al., 2013b; Cimini et al., 2015). Fructan accumulation has been observed in the growth zones of vegetative tissues in other plant species (Luscher and Nelson, 1995; Roth et al., 1997). Presence of fructans in developing tissues may be involved in osmoregulation by sequestering a surplus of imported sucrose (Fisher and Gifford, 1986) and to maintain the sucrose gradient between the vascular tissues and the sink tissues (Pollock, 1986). Furthermore, fructans can act as a scavenger of reactive oxygen species (ROS) which is produced in high amounts during cell division and expansion (Livanos et al., 2012; Peshev et al., 2013; Peukert et al., 2014; Matros et al., 2015).

Fructan metabolism is regulated through activities from multiple fructan metabolic enzymes during grain maturation, as shown by changes in fructan DP, gene expression and enzymatic activities (Peukert et al., 2014; Cimini et al., 2015). In developing wheat grain, 1-SST enzymes are the most active at 7 DAP compared to other biosynthetic enzymes, although the enzyme activity declines rapidly after 7 DAP. 1-FFT and 6-SFT enzymes show the greatest activities between 14 and 21 DAP, and both enzymes are involved in the synthesis of graminan (Cimini et al., 2015). Genes related to fructan hydrolysis, *1-FEH* and *6-FEH*, and *invertases*, show the greatest gene expression levels at 7 DAP and decline during grain maturation (Cimini et al., 2015). High turnover of fructans during early stages may contribute to a greater sink strength for grain filling.

The spatial information for fructan deposition has recently been resolved in barley grain utilising a mass spectrometry-based imaging approach (Peukert et al., 2014; Peukert et al., 2016) and various types of fructans in the endosperm cavity have been profiled using a high-

performance liquid chromatography HPLC approach (Peukert et al., 2014). The transcript profiles of the fructan metabolic genes in separated barley grain tissues have also been resolved by laser microdissection and QPCR (Peukert et al., 2014). During the first 7 DAP, *1-SST* and *6-SFT* transcripts are high in the developing endosperm, leading to accumulation of 6-kestose and bifurcose. Between 7 to 10 DAP, *1-SST* and *1-FFT* transcripts are the highest in the nucellar projection, resulting in a higher accumulation of inulin-type oligofructans such as 1-kestose and nystose in the endosperm cavity relative to whole grain (Peukert et al., 2014; Peukert et al., 2016). Despite our current knowledge of fructan metabolism in the barley cavity region, there are still significant gaps in our knowledge of the regulation of fructan in other barley grain tissues such as pericarp, endosperm and the embryo during development.

1.2.14 Other storage compounds in barley grain

In addition to carbohydrates, proteins, lipids and minerals are also storage compounds in barley grain which are mobilised to the embryo during grain germination. In a mature barley grain, there are approximately 80% carbohydrates (dry mass), 11% proteins, 3% lipids and the remainder are other minor substances including minerals, amino acids and peptides, and nucleic acids (Henry, 1988). In particular, the interaction of proteins and lipids with starch in the grain has been shown to affect the physicochemical and rheological properties of the end products (Dahle, 1971; Appelqvist and Debet, 1997; Kaur et al., 2016).

1.2.14.1 Storage proteins

Storage proteins in barley grain are mainly found in the starchy endosperm (70%), with the remainder (20%) in the aleurone layer and scutellum (Laidman, 1982). Hordeins are the major

protein components in barley grain (Wallace and Lance, 1988) and these can be separated into B type (sulphur rich), C type (sulphur poor), D type (high molecular weight) and γ type (sulphur rich) based on their electrophoretic motilities (Shewry et al., 1985). These hordein types are encoded by *hordein-1*, *hordein-2*, *hordein-3* and *hordein-5* genes (Giese et al., 1983; Kreis and Shewry, 1992). Hordeins are synthesized in rough endoplasmic reticulum during later stages of grain filling (Rahman et al., 1982) and stored in the form of protein bodies in starchy endosperm cells (Matthews and Miflin, 1980). Other proteins found in barley grain include Hordenin, Globulin and Albumin (Folkes and Yemm, 1956).

1.2.14.2 Storage lipids

Lipids are mainly stored in the embryo with relatively small amounts in the aleurone and endosperm tissues (Price and Parsons, 1979; Koehler and Wieser, 2013). The majority of lipids in barley grain are unsaturated fatty acids (Palmer, 1989), of which approximately 57% is linoleic acid and 5% is linolenic acid (Morrison, 1977). The unsaturated fatty acids can be converted into lipid peroxidase and subsequently to aldehydes, ketones and alcohols, via an oxidation process (Fastnaught et al., 2006). In the food industry, the presence of lipids in wort improves yeast growth during fermentation which positively contributes to the beer quality (Bravi et al., 2009)

1.2.15 Naturally occurring barley mutants with modified grain composition

Natural barley mutants are commonly generated through chemical mutagenesis from existing barley cultivars (Felker et al., 1985; Bosnes et al., 1987). In many cases, barley mutants with high (1,3;1,4)-β-glucan levels are associated with thicker endosperm cell walls and shrunken

endosperm. For example, Prowashonupana grain contains more (1,3;1,4)-β-glucan and the endosperm cell walls appear thicker than the wild type grain. In addition, Prowashonupan grain contains less starch, more storage proteins and other cell wall polysaccharides such as cellulose and arabinoxylan (Fig. 23A) (Andersson et al., 1999). Prowashonupana is now called Sustagrain® Barley patented by the ConAgra™ Specially Grain Products Company (U.S.A). The mutant barley has been made commercially available for human consumption due to its high dietary fibre content. Another barley mutant available for public consumption is M292 (cv Himalaya), which also has high (1,3;1,4)-β-glucan levels and the mutant grain appears shrunken (Fig. 23C), however the author did not report on cell wall thickness. Similar to Prowashonupana grain, M292 mutant contains less starch, more dietary constituents such as fructan, resistant starch, and more proteins (Clarke et al., 2008). M292 barley mutant is now known as BARLEYmax™ patented by CSIRO (Australia).

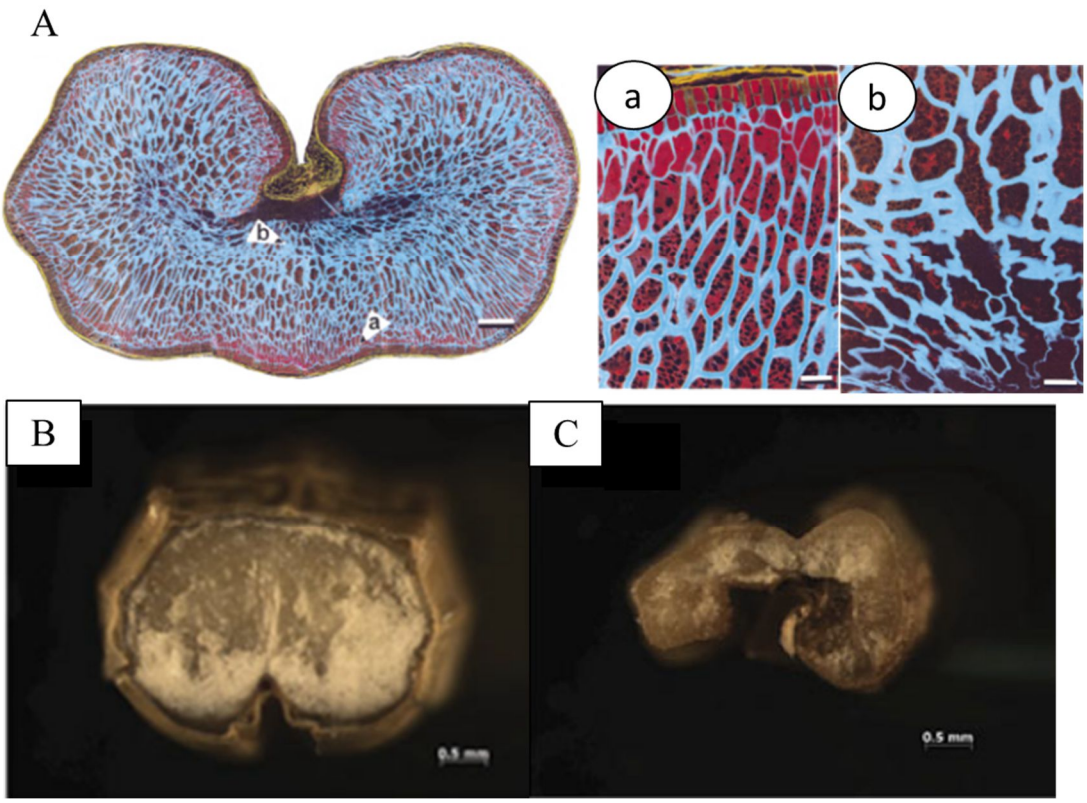

Figure 23: Examples of barley mutants with high (1,3;1,4)-β-glucan levels that appear shrunken. (A) Fluorescence micrographs of mature Prowashonupana cross-sectioned. Aleurone protein is stained red, endosperm protein is stained orange, cell walls are stained blue and starch is unstained (black). Cell walls in the endosperm close to the aleurone layer (a) and crease (b) are thickened. Image taken from Andersson et al., (1999). (B) A transverse section of a mature Himalaya wild type grain. C, M292 barley mutant has a shrunken endosperm compared to the wild type grain (panel B). Image taken from Li et al., (2011).

A shrunken endosperm in barley can be caused by mutations in the maternal tissues, *seg* (shrunken endosperm genetic) (Jarvi and Eslick, 1975; Felker et al., 1985) or in the endosperm tissues, *sex* (shrunken endosperm xenia) (Bosnes et al., 1987). The causal mutation for many of these mutants are not known, except the *sex6* mutant (also known as M292, Fig. 23C) in which the mutation has been identified in the *starch synthase IIa* gene (Morell et al., 2003). *seg8* mutants have an impaired nucellar projection which has been linked to an altered balance between abscisic acid and gibberellins (Weier et al., 2014). The impaired nucellar projection in *seg8* mutants results in low starch accumulation (Djarot and Peterson, 1991) and absence of trisaccharides in the region adjacent to the endosperm cavity (Peukert et al., 2014). In addition, the aleurone is impaired in one of the shrunken mutants called *defective seed5* (*des5*) (Fig. 24A to 24D) (Bosnes et al., 1987; Olsen et al., 2008). The pleiotropic effects resulting in shrunken endosperm are likely to be associated with perturbed endosperm developmental process (Bosnes et al., 1992; Olsen et al., 2008), which may be multi-genic and complex.

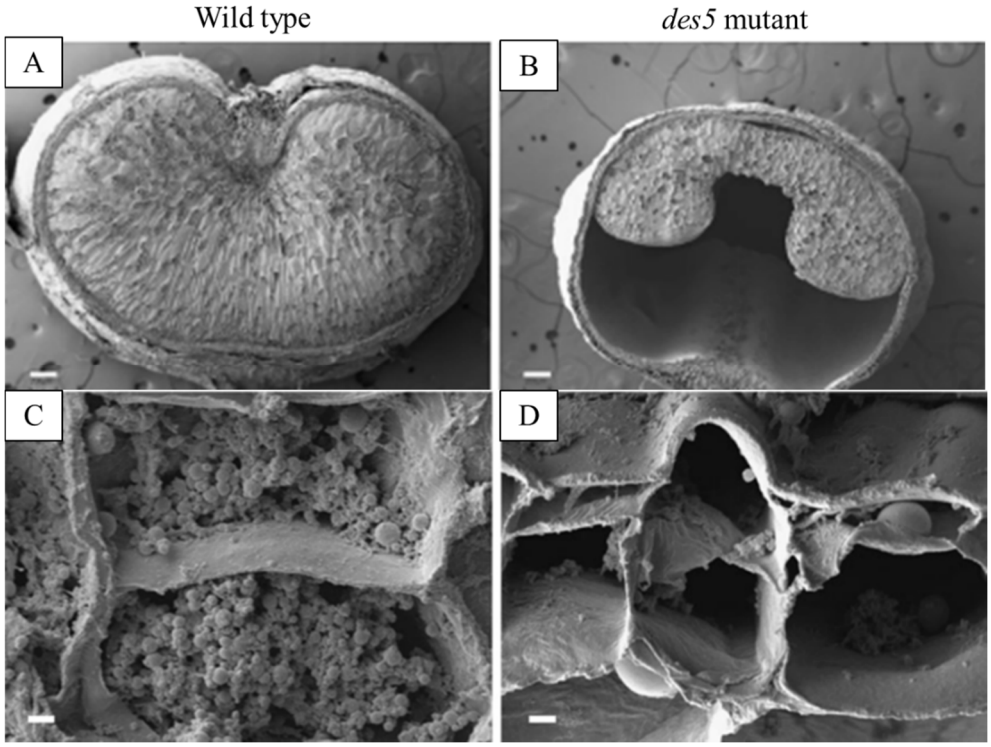

Figure 24: Scanning electron micrographs of transverse sections of wild type and *des5* barley mutant grain taken at 30 DAP (panels A and B) and 12 DAP (panels C and D). (A) Wild type barley grain has normal endosperm while in (B), the *des5* barley mutant appears shrunken due to developmental arrest of the endosperm and a prematurely aborted embryo. (C) The aleurone cells in wild type grain show cuboidal shapes. (D) The aleurone cells in *des5* mutant appear irregular in shape and lack cell content. Figure reproduced from Olsen et al., (2008).

Many shrunken barley mutants show an altered starch metabolism, leading to low starch content and altered granule morphology (Tyynelä et al., 1995; Li et al., 2011; Ma et al., 2014; Sparla et al., 2014). Many studies have consistently shown a shift from starch to (1,3;1,4)-β-glucan, protein and fructan accumulation (Munck et al., 2004; Clarke et al., 2008; Shaik et al., 2016). Failure of sugars to be converted into starch may result in accumulation of soluble sugars such as sucrose and fructan in the starch deficient grain, such as seen in lines with RNAi suppression of all Starch Branching Enzyme isoforms as observed by Shaik et al., (2016). In this case, the author suggests that large fluid-filled cavity in the RNAi lines is a result of deficient loading of

sugars from the cavity to the endosperm (Carciofi et al., 2012). However, it is also possible that the large fluid-filled cavity is attributed to impairment of transfer tissues, which were not examined by the author (Carciofi et al., 2012).

The shrunken phenotype in barley grain so far has not been reported for mutants with low (1,3;1,4)-β-glucan levels, including M-737 and the (1,3;1,4)-β-glucanless (*bgl)* mutant, where cell walls are noticeably thinner (Fig. 25A to 25D) (Aastrup, 1983; Tonooka et al., 2009). Despite changes in cell wall thickness, there is no significant difference in the amount of starch in these low (1,3;1,4)-β-glucan mutant lines (Aastrup, 1983; Tonooka et al., 2009). Of the thin-walled mutants, M-737 (cv Minerva) shows a shorter malting rate and mealy endosperm (Aastrup, 1983), whilst the *bgl* mutant grains are softer (Tonooka et al., 2009), which is also a favourable characteristics for malting (Palmer, 1993; Psota et al., 2007; Ferrari et al., 2010).

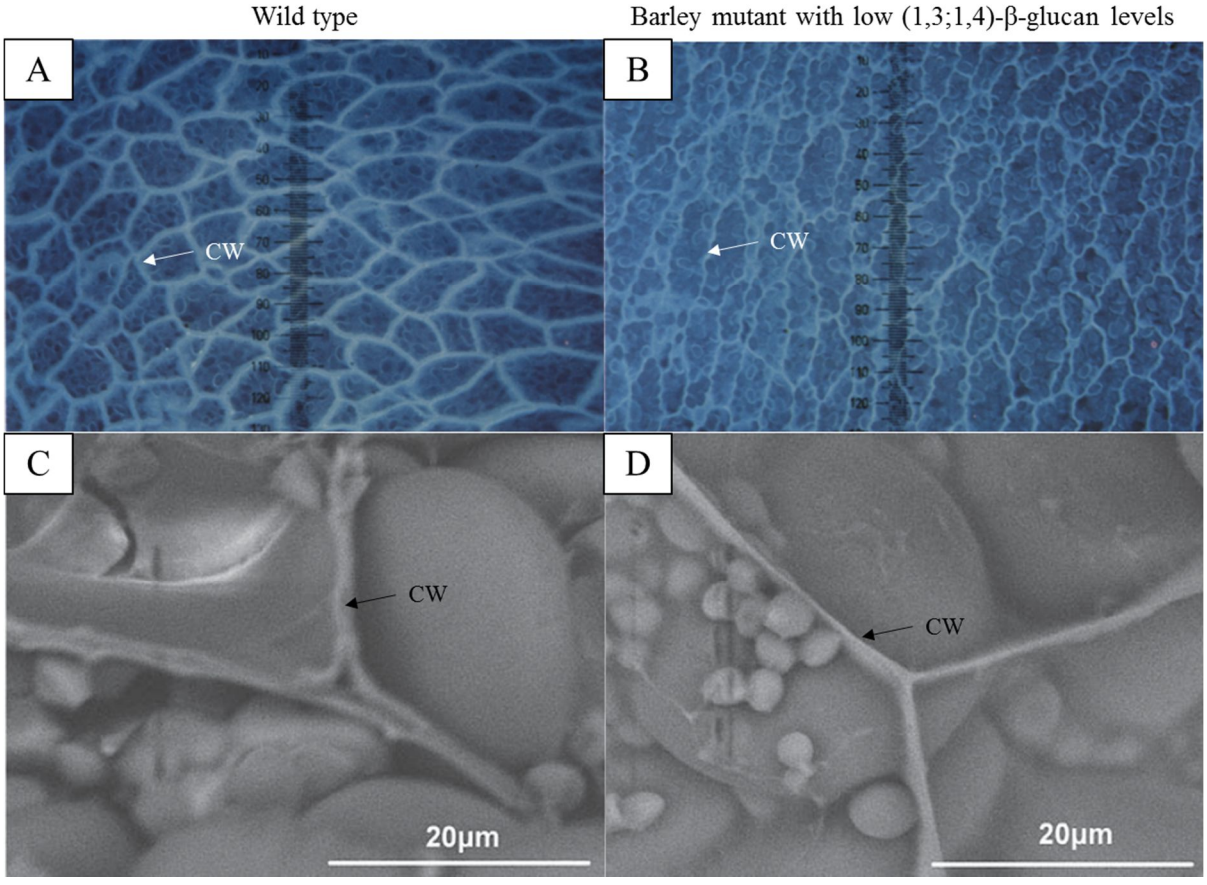

Figure 25: Barley mutants with low (1,3;1,4)-β-glucan levels. (A) Wild type Minerva and (B) M-737 barley mutant stained with Calcofluor and Fast Green with sections visualised using a fluorescence microscope. A and B taken from Aastrup, (1983). (C) Wild type Nishinohoshi (Ni) grain and (D) Ni(*bgl*) mutant grain under the scanning electron microscope. The cell walls in M-737 and *bgl* barley mutants are thinner relative to those of their parental lines. C and D taken from Tonooka et al., (2009). Abbreviation: cell walls (CW).

1.2.16 Manipulation of carbohydrate content in hull-less barley grain

Barley cultivars may be hulled or hull-less varieties. The difference between them is the presence or absence of an outer hull. For human consumption, hulled barley requires a pearling process to remove the outer hull, which also removes the germ (embryo) and bran (aleurone and part of the starchy endosperm) that are inedible. The bran layers are rich in minerals, proteins, vitamins and fibres, which provide numerous health benefits (Bhatty, 1993; El Rabey et al., 2013). Hull-less barley, on the other hand, does not have an outer hull attached. The hull-less phenotype is controlled by a single locus (*nud*) on the long arm of chromosome 7H (Taketa et al., 2008). Without undergoing a pearling process, the bran layer remains attached to the grain and hence retains most of the nutrients. Hull-less barley grain contains a higher proportion of starch, protein and (1,3;1,4)-β-glucan compared to hulled barley, which makes these varieties ideal for food applications (Bhatty, 1999). Although hull-less grain offers a significant advantage for food applications than hulled barley, cultivation of hull-less barley remains rare over recent years due to a much poorer crop yield compared to hulled barley (Box et al., 1999; Hulless Barley Potential Opportunities 2015). In Australia, Torrens was released by the South Australian Barley Improvement Program (SABIP) and was shown to have improved grain yield,

agronomy and feed quality relative to previously available varieties (Box and Barr, 2000; Box et al., 2005).

Manipulation of carbohydrate content, particularly (1,3;1,4)-β-glucan, in hull-less grain is a potential avenue for improvement of the nutritional quality for human consumption and brewing quality. However, research related to carbohydrate modifications in hull-less grain has been limited (Clarke et al., 2008; Tonooka et al., 2009; Taketa et al., 2012). A previous attempt to increase (1,3;1,4)-β-glucan content in barley grain was successful in Golden Promise (hulled barley). Golden Promise barley was transformed with the *HvCslF6* gene driven by an endosperm-specific oat globulin promoter (*AsGlo*), resulting in more than an 80% increase in (1,3;1,4)-β-glucan content compared to the wild type (Burton et al., 2011). In the project described here, we generated transgenic hull-less barley lines with high (1,3;1,4)-β-glucan content using a similar approach as described in Burton et al., (2011) and investigated the effects of high (1,3;1,4)-β-glucan on the fate of carbon in the grain across development. To study the converse effect of low (1,3;1,4)-β-glucan we investigated the carbon flow in a (1,3;1,4)-β-glucanless hull-less barley mutant supplied by Professor K. Sato (Okayama University). Research outputs from this project will advance our understanding of carbon partitioning and its significance for grain development. It will also help indicate whether the manipulation of cell wall components in a cereal such as barley is a feasible goal, especially using a transgenic route, which may also encounter additional resistance from the weight of public opinion. An understanding of the storage carbohydrate metabolism in hull-less barley varieties is important for informing future agricultural research and for improving hull-less crop yields and food quality, and may also be relevant to other important cereals and seeds consumed by humans.

1.2.17 Short descriptions of plant models used in this study

1.2.17.1 CslF6 transgenic barley

The hull-less barley variety (cv Torrens) was stably transformed with a *cellulose synthase-like F6 (CslF6)* gene, which encodes a (1,3;1,4)-β-glucan synthase. The *Agrobacterium tumefaciens*-mediated transformation method used in this study was a modified version of the conventional method as described in Burton et al., (2011). The transgene was driven by an endosperm-specific oat globulin promoter (*AsGlo*).

1.2.17.2 (1,3;1,4)-β-glucanless (bgl) barley mutant

The OUM125 mutant (*bgl*) (cv Akashinriki) seeds are kindly provided by Professor Kazuhiro Sato (Okayama University) as part of a collaboration with Associate Professor Matthew Tucker (ARC CoE Plant Cell Walls, University of Adelaide) to investigate the role of the *HvCslF6* gene in barley growth and development. The OUM125 barley mutant contains a single nucleotide substitution (from G to A at the 4275th position (1979th in coding region) in the coding region of the *CslF6* gene, resulting in a non-functional protein. Characterisation of OUM125 mutants showed undetectable levels of (1,3;1,4)-β-glucan in grain and vegetative tissues such as root, leaf and stem. Scanning electron micrographs revealed thinner endosperm cell walls in the mutant compared to the wild type grain (Fig. 25C and 25D). Assessment of the phenotype of the mutant plants revealed that they were sensitive to cold and developed chlorosis below the leaf tip (Tonooka et al., 2009; Taketa et al., 2012).

1.2.18 References

Aastrup S (1983) Selection and characterization of low β-glucan mutants from barley. Carlsberg Research Communications **48:** 307-316

Abrams SA, Hawthorne KM, Aliu O, Hicks PD, Chen Z, Griffin IJ (2007) An inulin-type fructan enhances calcium absorption primarily via an effect on colonic absorption in humans. J Nutr **137:** 2208-2212

Ahmed Z, Tetlow IJ, Falk DE, Liu Q, Emes MJ (2016) Resistant starch content is related to granule size in barley. Cereal Chemistry **93:** 618-630

Allen JF, de Paula WB, Puthiyaveetil S, Nield J (2011) A structural phylogenetic map for chloroplast photosynthesis. Trends Plant Sci **16:** 645-655

An L-H, You R-L (2004) Studies on nuclear degeneration during programmed cell death of synergid and antipodal cells in Triticum aestivum. Sexual plant reproduction **17:** 195-201

Andersson A, Andersson R, Autio K, Åman P (1999) Chemical composition and microstructure of two naked waxy barleys. Journal of Cereal Science **30:** 183-191

Andriunas FA, Zhang H-M, Xia X, Offler CE, McCurdy DW, Patrick JW (2012) Reactive oxygen species form part of a regulatory pathway initiating trans-differentiation of epidermal transfer cells in Vicia faba cotyledons. J Exp Bot **63:** 3617-3629

Annison G (1993) The role of wheat non-starch polysaccharides in broiler nutrition. Crop and Pasture Science **44:** 405-422

Apolinário AC, de Lima Damasceno BPG, de Macêdo Beltrão NE, Pessoa A, Converti A, da Silva JA (2014) Inulin-type fructans: A review on different aspects of biochemical and pharmaceutical technology. Carbohydrate Polymers **101:** 368-378

Appelqvist IA, Debet MR (1997) Starch-biopolymer interactions—a review. Food Reviews International **13:** 163-224

Bahaji A, Li J, Ovecka M, Ezquer I, Muñoz FJ, Baroja-Fernández E, Romero JM, Almagro G, Montero M, Hidalgo M, Sesma MT, Pozueta-Romero J (2011) Arabidopsis thaliana Mutants Lacking ADP-Glucose Pyrophosphorylase Accumulate Starch and Wild-type ADP-Glucose Content: Further Evidence for the Occurrence of Important Sources, other than ADP-Glucose Pyrophosphorylase, of ADP-Glucose Linked to Leaf Starch Biosynthesis. Plant and Cell Physiology **52:** 1162-1176

Ballicora MA, Iglesias AA, Preiss J (2004) ADP-glucose pyrophosphorylase: a regulatory enzyme for plant starch synthesis. Photosynthesis Research **79:** 1-24

Bamforth C (1994) -Glucan and -Glucanases in Malting and Brewing: Practical Aspects. Brewers Digest **69:** 12-12

Bathgate G, Palmer G (1972) A reassessment of the chemical structure of barley and wheat starch granules. Starch-Stärke **24:** 336-341

Becraft PW, Asuncion-Crabb Y (2000) Positional cues specify and maintain aleurone cell fate in maize endosperm development. Development **127:** 4039-4048

Becraft PW, Li K, Dey N, Asuncion-Crabb Y (2002) The maize dek1 gene functions in embryonic pattern formation and cell fate specification. Development **129:** 5217-5225

Becraft PW, Stinard PS, McCarty DR (1996) CRINKLY4: a TNFR-like receptor kinase involved in maize epidermal differentiation. SCIENCE-NEW YORK THEN WASHINGTON-**:** 1406-1408

Becraft PW, Yi G (2010) Regulation of aleurone development in cereal grains. J Exp Bot **62:** 1669-1675

Bethke PC, Hwang Y-s, Zhu T, Jones RL (2006) Global patterns of gene expression in the aleurone of wild-type and dwarf1 mutant rice. Plant Physiol **140:** 484-498

Bethke PC, Lonsdale JE, Fath A, Jones RL (1999) Hormonally regulated programmed cell death in barley aleurone cells. The Plant Cell **11:** 1033-1045

Bhatty R (1993) Physicochemical properties of roller-milled barley bran and flour. Cereal Chemistry **70:** 397-397

Bhatty R (1999) The potential of hull-less barley. Cereal Chemistry **76:** 589-599

Bonnett GD, Sims IM, Simpson RJ, Cairns AJ (1997) Structural diversity of fructan in relation to the taxonomy of the Poaceae. New Phytologist **136:** 11-17

Bosnes M, Harris E, Aigeltinger L, Olsen O (1987) Morphology and ultrastructure of 11 barley shrunken endosperm mutants. Theoretical and applied genetics **74:** 177-187

Bosnes M, Weideman F, Olsen OA (1992) Endosperm differentiation in barley wild-type and sex mutants. The Plant Journal **2:** 661-674

Box A, Barr A (2000) Identification of molecular markers associated with improved coleoptile length in hulless barley.

Box A, Jefferies S, Barr A (1999) Emergence and establishment problems of hulless barley—a possible solution. *In* Proceedings of the 9th Australian Barley Technical Symposium,

Box A, Washington J, Eglinton J (2005) Progress in Developing a Hulless Barley Industry.

Boyer CD, Preiss J (1981) Evidence for independent genetic control of the multiple forms of maize endosperm branching enzymes and starch synthases. Plant Physiol **67:** 1141-1145

Bradbury D, MacMasters MM, Cull IM (1956) Structure of the mature wheat kernel. III. Microscopic structure of the endosperm of hard red winter wheat. Cereal Chem **33:** 361-373

Braun DM, Slewinski TL (2009) Genetic control of carbon partitioning in grasses: roles of sucrose transporters and tie-dyed loci in phloem loading. Plant Physiol **149:** 71-81

Braun DM, Wang L, Ruan Y-L (2013) Understanding and manipulating sucrose phloem loading, unloading, metabolism, and signalling to enhance crop yield and food security. J Exp Bot **65:** 1713-1735

Bravi E, Perretti G, Buzzini P, Della Sera R, Fantozzi P (2009) Technological Steps and Yeast Biomass as Factors Affecting the Lipid Content of Beer during the Brewing Process. Journal of agricultural and food chemistry **57:** 6279-6284

Britain MAoG (2011) UK Malting Industry. *In*,

Brown R, Blaser R (1965) Relationships between reserve carbohydrate accumulation and growth rate in orchardgrass and tall fescue. Crop Science **5:** 577-582

Brown RC, Lemmon BE, Olsen OA (1994) Endosperm Development in Barley: Microtubule Involvement in the Morphogenetic Pathway. The plant cell **6:** 1241-1252

Buléon A, Colonna P, Planchot V, Ball S (1998) Starch granules: structure and biosynthesis. International journal of biological macromolecules **23:** 85-112

Burrell M (2003) Starch: the need for improved quality or quantity—an overview. J Exp Bot **54:** 451-456

Burton RA, Collins HM, Kibble NA, Smith JA, Shirley NJ, Jobling SA, Henderson M, Singh RR, Pettolino F, Wilson SM, Bird AR, Topping DL, Bacic A, Fincher GB (2011) Over-expression of specific HvCslF cellulose synthase-like genes in transgenic barley increases the levels of cell wall (1,3;1,4)-beta-d-glucans and alters their fine structure. Plant Biotechnol J **9:** 117-135

Burton RA, Fincher GB (2009) (1,3;1,4)-β-D-Glucans in Cell Walls of the Poaceae, Lower Plants, and Fungi: A Tale of Two Linkages. Molecular Plant **2:** 873-882

Burton RA, Fincher GB (2012) Current challenges in cell wall biology in the cereals and grasses. Front Plant Sci **3:** 130

Burton RA, Gidley MJ, Fincher GB (2010) Heterogeneity in the chemistry, structure and function of plant cell walls. Nat Chem Biol **6:** 724-732

Burton RA, Jenner H, Carrangis L, Fahy B, Fincher GB, Hylton C, Laurie DA, Parker M, Waite D, Van Wegen S (2002) Starch granule initiation and growth are altered in barley mutants that lack isoamylase activity. The Plant Journal **31:** 97-112

Burton RA, Jobling SA, Harvey AJ, Shirley NJ, Mather DE, Bacic A, Fincher GB (2008) The genetics and transcriptional profiles of the cellulose synthase-like HvCslF gene family in barley. Plant Physiology **146:** 1821-1833

Burton RA, Wilson SM, Hrmova M, Harvey AJ, Shirley NJ, Medhurst A, Stone BA, Newbigin EJ, Bacic A, Fincher GB (2006) Cellulose synthase-like CslF genes mediate the synthesis of cell wall (1,3;1,4)-beta-D-glucans. Science **311:** 1940-1942

Butterworth PJ, Warren FJ, Ellis PR (2011) Human α-amylase and starch digestion: An interesting marriage. Starch-Stärke **63:** 395-405

Buttrose M (1963) Ultrastructure of the developing aleurone cells of wheat grain. Australian Journal of Biological Sciences **16:** 768-774

Carciofi M, Blennow A, Jensen SL, Shaik SS, Henriksen A, Buléon A, Holm PB, Hebelstrup KH (2012) Concerted suppression of all starch branching enzyme genes in barley produces amylose-only starch granules. BMC Plant Biol **12:** 223

Carpita NC, McCann MC (2010) The maize mixed-linkage (1->3),(1->4)-beta-D-glucan polysaccharide is synthesized at the golgi membrane. Plant Physiol **153:** 1362-1371

Chmelik J, Krumlová A, Budinská M, Kruml T, Psota V, Bohacenko I, Mazal P, Vydrová H (2001) Comparison of size characterization of barley starch granules determined by electron and optical microscopy, low angle laser light scattering and gravitational field-flow fractionation. Journal of the Institute of Brewing **107:** 11-17

Cimini S, Locato V, Vergauwen R, Paradiso A, Cecchini C, Vandenpoel L, Verspreet J, Courtin CM, D'Egidio MG, Van den Ende W (2015) Fructan biosynthesis and

degradation as part of plant metabolism controlling sugar fluxes during durum wheat kernel maturation. Front Plant Sci **6:** 89

Clarke B, Liang R, Morell M, Bird A, Jenkins C, Li Z (2008) Gene expression in a starch synthase IIa mutant of barley: changes in the level of gene transcription and grain composition. Functional & integrative genomics **8:** 211-221

Coleman M, Dickson R, Isebrands J, Karnosky D (1995) Carbon allocation and partitioning in aspen clones varying in sensitivity to tropospheric ozone. Tree Physiology **15:** 593-604

Collins HM, Burton RA, Topping DL, Liao M-L, Bacic A, Fincher GB (2010) REVIEW: Variability in Fine Structures of Noncellulosic Cell Wall Polysaccharides from Cereal Grains: Potential Importance in Human Health and Nutrition. Cereal Chemistry Journal **87:** 272-282

Coudray C, Tressol JC, Gueux E, Rayssiguier Y (2003) Effects of inulin-type fructans of different chain length and type of branching on intestinal absorption and balance of calcium and magnesium in rats. Eur J Nutr **42:** 91-98

Cummings JH, Beatty ER, Kingman SM, Bingham SA, Englyst HN (1996) Digestion and physiological properties of resistant starch in the human large bowel. British Journal of Nutrition **75:** 733-747

Dahle L (1971) Wheat protein-starch interaction. I. Some starch-binding effects of wheat-flour proteins. Cereal Chemistry

Darwen CW, John P (1989) Localization of the Enzymes of Fructan Metabolism in Vacuoles Isolated by a Mechanical Method from Tubers of Jerusalem Artichoke (Helianthus tuberosus L.). Plant Physiol **89:** 658-663

Degasperi MI, Itaya NM, Buckeridge MS, Figueiredo-Ribeiro RDCL (2003) Fructan degradation and hydrolytic activity in tuberous roots of Viguiera discolor Baker

(Asteraceae), a herbaceous species from the cerrado. Brazilian Journal of Botany **26:** 11-21

Del Viso F, Puebla A, Fusari C, Casabuono A, Couto A, Pontis H, Hopp H, Heinz R (2009) Molecular characterization of a putative sucrose: fructan 6-fructosyltransferase (6-SFT) of the cold-resistant Patagonian grass Bromus pictus associated with fructan accumulation under low temperatures. Plant and Cell Physiology **50:** 489-503

Djarot I, Peterson D (1991) Seed development in a shrunken endosperm barley mutant. Annals of botany **68:** 495-499

Doan DN, Fincher GB (1992) Differences in the thermostabilities of barley (1→ 3, 1→ 4)-β-glucanases are only partly determined by N-glycosylation. FEBS Lett **309:** 265-271

Doan DNP, Linnestad C, Olsen O-A (1996) Isolation of molecular markers from the barley endosperm coenocyte and the surrounding nucellus cell layers. Plant Molecular Biology **31:** 877-886

Doblin MS, Pettolino FA, Wilson SM, Campbell R, Burton RA, Fincher GB, Newbigin E, Bacic A (2009) A barley cellulose synthase-like CSLH gene mediates (1,3;1,4)-beta-D-glucan synthesis in transgenic Arabidopsis. Proc Natl Acad Sci U S A **106:** 5996-6001

Domínguez F, Cejudo FJ (2015) Programmed cell death (PCD): an essential process of cereal seed development and germination. Advances in Seed Biology**:** 178

Downing TTW, Gamroth MJ (2007) Nonstructural carbohydrates in cool-season grasses. *In*. [Corvallis, Or.]: Oregon State University, Extension Service

Duchateau N, Bortlik K, Simmen U, Wiemken A, Bancal P (1995) Sucrose:fructan 6-fructosyltransferase, a key enzyme for diverting carbon from sucrose to fructan in barley leaves. Plant Physiol **107:** 1249-1255

Edelman J, Jeeeord TG (1968) The mechanism of fructosan metabolism in higher plants as exemplified in *Helianthus Tuberosus* New Phytologist **67:** 517-531

Eder M, Tenhaken R, Driouich A, Lütz-Meindl U (2008) Occurrence and characterization of arabinogalactan-like proteins and hemicelluloses in micrasterias (Streptophyta)1. Journal of Phycology **44:** 1221-1234

Edner C, Li J, Albrecht T, Mahlow S, Hejazi M, Hussain H, Kaplan F, Guy C, Smith SM, Steup M (2007) Glucan, water dikinase activity stimulates breakdown of starch granules by plastidial β-amylases. Plant Physiol **145:** 17-28

El Rabey HA, Al-Seeni MN, Amer HM (2013) Efficiency of barley bran and oat bran in ameliorating blood lipid profile and the adverse histological changes in hypercholesterolemic male rats. BioMed Research International **2013:** 10

Engell K (1989) Embryology of barley: time course and analysis of controlled fertilization and early embryo formation based on serial sections. Nordic journal of botany **9:** 265-280

Englyst H, Wiggins H, Cummings J (1982) Determination of the non-starch polysaccharides in plant foods by gas-liquid chromatography of constituent sugars as alditol acetates. Analyst **107:** 307-318

Englyst HN, Kingman S, Cummings J (1992) Classification and measurement of nutritionally important starch fractions. European journal of clinical nutrition **46:** S33-50

Fastnaught C, Berglund P, Dudgeon A, Hadley M (2006) Lipid changes during storage of milled hulless barley products. Cereal Chemistry **83:** 424-427

Fath A, Bethke P, Lonsdale J, Meza-Romero R, Jones R (2000) Programmed cell death in cereal aleurone. Plant Molecular Biology **44:** 255-266

Faure J-E (2001) Double fertilization in flowering plants: Discovery, study methods and mechanisms. Comptes Rendus de l'Académie des Sciences - Series III - Sciences de la Vie **324:** 551-558

Faure JE, Rusche ML, Thomas A, Keim P, Dumas C, Mogensen HL, Rougier M, Chaboud A (2003) Double fertilization in maize: the two male gametes from a pollen grain have the ability to fuse with egg cells. The Plant Journal **33:** 1051-1062

Felker FC, Peterson DM, Nelson OE (1985) Anatomy of immature grains of eight maternal effect shrunken endosperm barley mutants. American Journal of Botany**:** 248-256

Ferrari B, Baronchelli M, Stanca AM, Gianinetti A (2010) Constitutive differences between steely and mealy barley samples associated with endosperm modification. Journal of the Science of Food and Agriculture **90:** 2105-2113

Fincher GB (1975) Morphology and chemical composition of barley endosperm cell walls Journal of the Institute of Brewing **81:** 116-122

Fincher GB (2009) Revolutionary times in our understanding of cell wall biosynthesis and remodeling in the grasses. Plant Physiol **149:** 27-37

Fincher GB, Lock PA, Morgan MM, Lingelbach K, Wettenhall RE, Mercer JF, Brandt A, Thomsen KK (1986) Primary structure of the (1-->3,1-->4)-beta-D-glucan 4-glucohydrolase from barley aleurone. Proc Natl Acad Sci U S A **83:** 2081-2085

Finnie C, Bak-Jensen KS, Laugesen S, Roepstorff P, Svensson B (2006) Differential appearance of isoforms and cultivar variation in protein temporal profiles revealed in the maturing barley grain proteome. Plant Science **170:** 808-821

Fisher DB, Gifford RM (1986) Accumulation and conversion of sugars by developing wheat grains VI. Gradients along the transport pathway from the peduncle to the endosperm cavity during grain filling. Plant Physiol **82:** 1024-1030

Flamm G, Glinsmann W, Kritchevsky D, Prosky L, Roberfroid M (2001) Inulin and oligofructose as dietary fiber: a review of the evidence. Crit Rev Food Sci Nutr **41:** 353-362

Flowering Plants (2017). *In* Leavingbio.net,

Folkes B, Yemm E (1956) The amino acid content of the proteins of barley grains. Biochemical Journal **62:** 4

Fontaine F, Peterson W, McCoy E, Johnson MJ, Ritter GJ (1942) A new type of glucose fermentation by Clostridium thermoaceticum. Journal of bacteriology **43:** 701

Ford CW, Percival E (1965) 551. Polysaccharides synthesised by Monodus subterraneus. Part II. The cell-wall glucan. Journal of the Chemical Society (Resumed)**:** 3014-3016

Forestan C, Meda S, Varotto S (2010) ZmPIN1-mediated auxin transport is related to cellular differentiation during maize embryogenesis and endosperm development. Plant Physiol **152:** 1373-1390

Forsythe KL, Feather MS, Gracz H, Wong TC (1990) Detection of kestoses and kestose-related oligosaccharides in extracts of Festuca arundinacea, Dactylis glomerata L., and Asparagus officinalis L. Root cultures and invertase by C and H nuclear magnetic resonance spectroscopy. Plant Physiol **92:** 1014-1020

Fotopoulos V (2005) Plant invertases: structure, function and regulation of a diverse enzyme family. Journal of Biological Research **4:** 127 – 137

Frehner M, Keller F, Wiemken A (1984) Localization of fructan metabolism in the vacuoles isolated from protoplasts of Jerusalem artichoke tubers (Helianthus tuberosus L.). Journal of Plant Physiology **116:** 197-208

French D (1984) Organization of starch granules. Starch chemistry and technology**:** 183-247

Fry SC, Nesselrode BH, Miller JG, Mewburn BR (2008) Mixed-linkage (1-->3,1-->4)-beta-D-glucan is a major hemicellulose of Equisetum (horsetail) cell walls. New Phytol **179:** 104-115

Fujita N, Yoshida M, Asakura N, Ohdan T, Miyao A, Hirochika H, Nakamura Y (2006) Function and characterization of starch synthase I using mutants in rice. Plant Physiol **140:** 1070-1084

Gallant DJ, Bouchet B, Baldwin PM (1997) Microscopy of starch: evidence of a new level of granule organization. Carbohydrate Polymers **32:** 177-191

Gamble RL, Coonfield ML, Schaller GE (1998) Histidine kinase activity of the ETR1 ethylene receptor from Arabidopsis. Proceedings of the National Academy of Sciences **95:** 7825-7829

Gebbing T (2003) The enclosed and exposed part of the peduncle of wheat (Triticum aestivum)–spatial separation of fructan storage. New Phytologist **159:** 245-252

Geisler-Lee J, Gallie DR (2005) Aleurone Cell Identity Is Suppressed following Connation in Maize Kernels. Plant Physiol **139:** 204-212

Giese H, Andersen B, Doll H (1983) Synthesis of the major storage protein, hordein, in barley. Planta **159:** 60-65

Gómez E, Royo J, Guo Y, Thompson R, Hueros G (2002) Establishment of cereal endosperm expression domains identification and properties of a maize transfer cell–specific transcription factor, ZmMRP-1. The Plant Cell **14:** 599-610

Gruis D, Guo H, Selinger D, Tian Q, Olsen O-A (2006) Surface Position, Not Signaling from Surrounding Maternal Tissues, Specifies Aleurone Epidermal Cell Fate in Maize. Plant Physiol **141:** 898-909

Gutiérrez-Marcos JF, Costa LM, Biderre-Petit C, Khbaya B, O'Sullivan DM, Wormald M, Perez P, Dickinson HG (2004) maternally expressed gene1 is a novel maize endosperm transfer cell–specific gene with a maternal parent-of-origin pattern of expression. The Plant Cell **16:** 1288-1301

Hall, Rao (1999) Photosynthesis Ed 6th. Cambridge University Press

Han N, Na C, Chai Y, Chen J, Zhang Z, Bai B, Bian H, Zhang Y, Zhu M (2017) Over-expression of (1, 3; 1, 4)-β-D-glucanase isoenzyme EII gene results in decreased (1, 3;

1, 4)-β-D-glucan content and increased starch level in barley grains. Journal of the Science of Food and Agriculture **97:** 122-127

Harris P, Fincher G (2009) Distribution, fine structure and function of (1, 3; 1, 4)-β-glucans in the grasses and other taxa. *In*. Academic Press

Haupt S, Duncan GH, Holzberg S, Oparka KJ (2001) Evidence for symplastic phloem unloading in sink leaves of barley. Plant Physiol **125:** 209-218

Havrlentova M, Kraic J (2006) Content of beta-d-glucan in cereal grains. Journal of Food and Nutrition Research (Slovak Republic)

Hellwege EM, Czapla S, Jahnke A, Willmitzer L, Heyer AG (2000) Transgenic potato (Solanum tuberosum) tubers synthesize the full spectrum of inulin molecules naturally occurring in globe artichoke (Cynara scolymus) roots. Proc Natl Acad Sci U S A **97:** 8699-8704

Hendry GAF, Wallace RK (1993) The origin, distribution and evolutionary significance of fructans,

Henry R, Saini H (1989) Characterization of cereal sugars and oligosaccharides. Cereal Chem **66:** 362-365

Henry RJ (1988) The carbohydrates of barley grains—A review. Journal of the Institute of Brewing **94:** 71-78

Henson CA, Livingston III DP (1996) Purification and characterization of an oat fructan exohydrolase that preferentially hydrolyzes [beta]-2, 6-fructans. Plant Physiol **110:** 639-644

Henson CA, Livingston Iii DP (1998) Characterization of a fructan exohydrolase purified from barley stems that hydrolyzes multiple fructofuranosidic linkages. Plant Physiology and Biochemistry **36:** 715-720

Hernandez-Gomez MC, Rydahl MG, Rogowski A, Morland C, Cartmell A, Crouch L, Labourel A, Fontes CM, Willats WG, Gilbert HJ (2015) Recognition of xyloglucan by the crystalline cellulose-binding site of a family 3a carbohydrate-binding module. FEBS Lett **589:** 2297-2303

Hochstrasser U, Lüscher M, De Virgilio C, Boller T, Wiemken A (1998) Expression of a functional barley sucrose-fructan 6-fructosyltransferase in the methylotrophic yeast Pichia pastoris. FEBS Letters **440:** 356-360

Honegger R, Haisch A (2001) Immunocytochemical location of the (1→3) (1→4)-β-glucan lichenin in the lichen-forming ascomycete Cetraria islandica (Icelandic moss)1. New Phytologist **150:** 739-746

Hoshikawa K (1993) Anthesis, fertilization and development of caryopsis. Science of the rice plant **1:** 339-376

Howard TL, Stauffer DR, Degnin CR, Hollenberg SM (2001) CHMP1 functions as a member of a newly defined family of vesicle trafficking proteins. Journal of cell science **114:** 2395-2404

Hrmova M, Fincher G (2001) Structure-function relationships of β- D-glucan endo- and exohydrolases from higher plants. Plant Molecular Biology **47:** 73-91

Hu G, Burton C, Hong Z, Jackson E (2014) A mutation of the cellulose-synthase-like (CslF6) gene in barley (Hordeum vulgare L.) partially affects the β-glucan content in grains. Journal of Cereal Science **59:** 189-195

Hulless Barley Potential Opportunities (2015). *In* EaCD Alberta Agriculture and Forestry, Competitiveness and Market Analysis Branch ed,

Huynh B-L, Mather DE, Schreiber AW, Toubia J, Baumann U, Shoaei Z, Stein N, Ariyadasa R, Stangoulis JC, Edwards J (2012) Clusters of genes encoding fructan biosynthesizing enzymes in wheat and barley. Plant Molecular Biology **80:** 299-314

Huynh B-L, Palmer L, Mather DE, Wallwork H, Graham RD, Welch RM, Stangoulis JCR (2008) Genotypic variation in wheat grain fructan content revealed by a simplified HPLC method. Journal of Cereal Science **48:** 369-378

Iztok D, Mojca B, David S, Ines M-M (2013) Exopolymer diversity and the role of levan in Bacillus subtilis biofilms. PLoS ONE **8**

Jaco F, Bianca AB, Siew LT, Florian FB (2013) Biosynthesis of levan, a bacterial extracellular polysaccharide, in the Yeast Saccharomyces cerevisiae. PLoS ONE **8**

Jamar C, du Jardin P, Fauconnier M-L (2011) Cell wall polysaccharides hydrolysis of malting barley (Hordeum vulgare L.): a review. Revue de Biotechnologie, Agronomie, Société et Environnement **15**

Jarvi A, Eslick R (1975) Shrunken endosperm mutants in barley. Crop Science **15:** 363-366

Jeon J-S, Ryoo N, Hahn T-R, Walia H, Nakamura Y (2010) Starch biosynthesis in cereal endosperm. Plant Physiology and Biochemistry **48:** 383-392

Jin P, Guo T, Becraft PW (2000) The maize CR4 receptor-like kinase mediates a growth factor-like differentiation response. Genesis **27:** 104-116

Jin Y-L, Speers RA, Paulson AT, Stewart RJ (2004) Barley β-glucans and their degradation during malting and brewing. Technical Quarterly-Master Brewers Association of the Americas **41:** 231-240

Jones RL (1969) The fine structure of barley aleurone cells. Planta **85:** 359-375

Kalla R, Shimamoto K, Potter R, Nielsen PS, Linnestad C, Olsen OA (1994) The promoter of the barley aleurone-specific gene encoding a putative 7 kDa lipid transfer protein confers aleurone cell-specific expression in transgenic rice. The Plant Journal **6:** 849-860

Karlsson R, Olered R, Eliasson AC (1983) Changes in starch granule size distribution and starch gelatinization properties during development and maturation of wheat, barley and rye. Starch-Stärke **35:** 335-340

Karpinnen S, Myllymaki O, Forssell P, Poutanen K (2003) Fructan content of rye and rye products. Cereal Chemistry **80:** 168

Kaur A, Shevkani K, Katyal M, Singh N, Ahlawat AK, Singh AM (2016) Physicochemical and rheological properties of starch and flour from different durum wheat varieties and their relationships with noodle quality. Journal of Food Science and Technology **53:** 2127-2138

Kawakami A, Yoshida M (2002) Molecular characterization of sucrose:sucrose 1-fructosyltransferase and sucrose:fructan 6-fructosyltransferase associated with fructan accumulation in winter wheat during cold hardening. Biosci Biotechnol Biochem **66:** 2297-2305

Kawakami A, Yoshida M (2005) Fructan:fructan 1-fructosyltransferase, a key enzyme for biosynthesis of graminan oligomers in hardened wheat. Planta **223:** 90-104

Kawakami A, Yoshida M (2012) Graminan breakdown by fructan exohydrolase induced in winter wheat inoculated with snow mold. J Plant Physiol **169:** 294-302

Kawakami A, Yoshida M, Van den Ende W (2005) Molecular cloning and functional analysis of a novel 6&1-FEH from wheat (Triticum aestivum L.) preferentially degrading small graminans like bifurcose. Gene **358:** 93-101

Kermode AR (2011) Plant storage products (Carbohydrates, Oils and Proteins). *In* eLS. John Wiley & Sons, Ltd

Kim S-J, Zemelis S, Keegstra K, Brandizzi F (2015) The cytoplasmic localization of the catalytic site of CSLF6 supports a channeling model for the biosynthesis of mixed-linkage glucan. The Plant Journal **81:** 537-547

Kleessen B, Hartmann L, Blaut M (2001) Oligofructose and long-chain inulin: influence on the gut microbial ecology of rats associated with a human faecal flora. Br J Nutr **86:** 291-300

Koch K, Andersson R, Rydberg I, Åman P (1999) Influence of harvest date on inulin chain length distribution and sugar profile for six chicory (Cichorium intybus L) cultivars. Journal of the Science of Food and Agriculture **79:** 1503-1506

Koehler P, Wieser H (2013) Chemistry of cereal grains. *In* Handbook on sourdough biotechnology. Springer, pp 11-45

Kolida S, Gibson GR (2007) Prebiotic Capacity of Inulin-Type Fructans. The Journal of Nutrition **137:** 2503S-2506S

Koops AJ, Jonker HH (1996) Purification and characterization of the enzymes of fructan biosynthesis in tubers of Helianthus tuberosus Colombia (II. Purification of sucrose:sucrose 1-fructosyltransferase and reconstitution of fructan synthesis in vitro with purified sucrose:sucrose 1-fructosyltransferase and fructan:fructan 1-fructosyltransferase). Plant Physiol **110:** 1167-1175

Kozlova L, Snegireva A, Gorshkova T (2012) Distribution and structure of mixed linkage glucan at different stages of elongation of maize root cells. Russian journal of plant physiology **59:** 339-347

Kreis M, Shewry PR (1992) The control of protein synthesis in developing barley seeds.

Kubo A, Fujita N, Harada K, Matsuda T, Satoh H, Nakamura Y (1999) The starch-debranching enzymes isoamylase and pullulanase are both involved in amylopectin biosynthesis in rice endosperm. Plant Physiol **121:** 399-410

Kuo A, Cappelluti S, Cervantes-Cervantes M, Rodriguez M, Bush DS (1996) Okadaic acid, a protein phosphatase inhibitor, blocks calcium changes, gene expression, and cell death induced by gibberellin in wheat aleurone cells. The Plant Cell **8:** 259-269

Kyle DJ, Styles ED (1977) Development of aleurone and subaleurone layers in maize. Planta **137:** 185-193

Laidman D (1982) Control mechanisms in the mobilisation of stored nutrients in germinating cereals. The Physiology and biochemistry of seed development, dormancy and germination.(Ed. AA Khan). Elsevier Biomedical Press. Amsterdam**:** 371

Lauer JC, Yap K, Cu S, Burton RA, Eglinton JK (2017) Novel barley (1→ 3, 1→ 4)-β-glucan endohydrolase alleles confer increased enzyme thermostability. Journal of agricultural and food chemistry **65:** 421-428

Le Roy K, Lammens W, Verhaest M, De Coninck B, Rabijns A, Van Laere A, Van den Ende W (2007) Unraveling the difference between invertases and fructan exohydrolases: a single amino acid (Asp-239) substitution transforms Arabidopsis cell wall invertase1 into a fructan 1-exohydrolase. Plant Physiol **145:** 616-625

Lee J, Hollingsworth RI (1997) Oligosaccharide β-glucans with unusual linkages from Sarcina ventriculi. Carbohydr Res **304:** 133-141

Leenen CH, Dieleman LA (2007) Inulin and oligofructose in chronic inflammatory bowel disease. J Nutr **137:** 2572s-2575s

Li Z, Li D, Du X, Wang H, Larroque O, Jenkins CL, Jobling SA, Morell MK (2011) The barley amo1 locus is tightly linked to the starch synthase IIIa gene and negatively regulates expression of granule-bound starch synthetic genes. J Exp Bot **62:** 5217-5231

Li Z, Li D, Du X, Wang H, Larroque O, Jenkins CLD, Jobling SA, Morell MK (2011) The barley amo1 locus is tightly linked to the starch synthase IIIa gene and negatively regulates expression of granule-bound starch synthetic genes. J Exp Bot **62:** 5217-5231

Lid SE, Gruis D, Jung R, Lorentzen JA, Ananiev E, Chamberlin M, Niu X, Meeley R, Nichols S, Olsen O-A (2002) The defective kernel 1 (dek1) gene required for aleurone

cell development in the endosperm of maize grains encodes a membrane protein of the calpain gene superfamily. Proc Natl Acad Sci U S A **99:** 5460-5465

Litts JC, Simmons CR, Karrer EE, Huang N, Rodriguez RL (1990) The isolation and characterization of a barley 1,3-1,4-β-glucanase gene. European Journal of Biochemistry **194:** 831-838

Liu Z, Mouradov A, Smith KF, Spangenberg G (2011) An improved method for quantitative analysis of total fructans in plant tissues. Analytical biochemistry **418:** 253-259

Livanos P, Galatis B, Quader H, Apostolakos P (2012) Disturbance of reactive oxygen species homeostasis induces atypical tubulin polymer formation and affects mitosis in root-tip cells of Triticum turgidum and Arabidopsis thaliana. Cytoskeleton **69:** 1-21

Louis P, Flint HJ (2009) Diversity, metabolism and microbial ecology of butyrate-producing bacteria from the human large intestine. FEMS Microbiol Lett **294:** 1-8

Luscher M, Nelson CJ (1995) Fructosyltransferase activities in the leaf growth zone of tall fescue. Plant Physiol **107:** 1419-1425

Ma J, Jiang Q-T, Wei L, Wang J-R, Chen G-Y, Liu Y-X, Li W, Wei Y-M, Liu C, Zheng Y-L (2014) Characterization of shrunken endosperm mutants in barley. Gene **539:** 15-20

Makkar HPS (2012) Biofuel co-products as livestock feed - opportunities and challenges. FOOD AND AGRICULTURE ORGANIZATION OF THE UNITED NATIONS

Mann J, Cummings J, Englyst H, Key T, Liu S, Riccardi G, Summerbell C, Uauy R, Van Dam R, Venn B (2007) FAO/WHO scientific update on carbohydrates in human nutrition: conclusions. European journal of clinical nutrition **61:** S132

Marcus SE, Verhertbruggen Y, Hervé C, Ordaz-Ortiz JJ, Farkas V, Pedersen HL, Willats WG, Knox JP (2008) Pectic homogalacturonan masks abundant sets of xyloglucan epitopes in plant cell walls. BMC Plant Biol **8:** 60

Maruyama D, Higashiyama T (2016) The end of temptation: the elimination of persistent synergid cell identity. Current opinion in plant biology **34:** 122-126

Matros A, Peshev D, Peukert M, Mock H-P, Van den Ende W (2015) Sugars as hydroxyl radical scavengers: proof-of-concept by studying the fate of sucralose in Arabidopsis. The Plant Journal **82:** 822-839

Matthews JA, Miflin BJ (1980) In vitro synthesis of barley storage proteins. Planta **149:** 262-268

McCartney L, Marcus SE, Knox JP (2005) Monoclonal antibodies to plant cell wall xylans and arabinoxylans. Journal of Histochemistry & Cytochemistry **53:** 543-546

McCurdy DW, Patrick JW, Offler CE (2008) Wall ingrowth formation in transfer cells: novel examples of localized wall deposition in plant cells. Current opinion in plant biology **11:** 653-661

Meikle PJ, Hoogenraad NJ, Bonig I, Clarke AE, Stone BA (1994) A (1→ 3, 1→ 4)-β-glucan-specific monoclonal antibody and its use in the quantitation and immunocytochemical location of (1→ 3, 1→ 4)-β-glucans. The Plant Journal **5:** 1-9

Mogensen HL (1982) Double fertilization in barley and the cytological explanation for haploid embryo formation, embryoless caryopses, and ovule abortion. Carlsberg Research Communications **47:** 313-354

Monro JA, Penny D, Bailey RW (1976) The organization and growth of primary cell walls of lupin hypocotyl. Phytochemistry **15:** 1193-1198

Morell MK, Kosar-Hashemi B, Cmiel M, Samuel MS, Chandler P, Rahman S, Buleon A, Batey IL, Li Z (2003) Barley sex6 mutants lack starch synthase IIa activity and contain a starch with novel properties. The Plant Journal **34:** 173-185

Morrison IN, Kuo J, O'Brien TP (1975) Histochemistry and fine structure of developing wheat aleurone cells. Planta **123:** 105-116

Morrison W (1977) Cereal lipids. Proceedings of the Nutrition Society **36:** 143-148

Munck L, Møller B, Jacobsen S, Søndergaard I (2004) Near infrared spectra indicate specific mutant endosperm genes and reveal a new mechanism for substituting starch with (1→ 3, 1→ 4)-β-glucan in barley. Journal of Cereal Science **40:** 213-222

Muñiz LM, Royo J, Gómez E, Barrero C, Bergareche D, Hueros G (2006) The maize transfer cell-specific type-A response regulator ZmTCRR-1 appears to be involved in intercellular signalling. The Plant Journal **48:** 17-27

Nagaraj VJ, Altenbach D, Galati V, Lüscher M, Meyer AD, Boller T, Wiemken A (2004) Distinct regulation of sucrose: sucrose-1-fructosyltransferase (1-SST) and sucrose: fructan-6-fructosyltransferase (6-SFT), the key enzymes of fructan synthesis in barley leaves: 1-SST as the pacemaker. New Phytologist **161:** 735-748

Nakamura Y (2002) Towards a better understanding of the metabolic system for amylopectin biosynthesis in plants: rice endosperm as a model tissue. Plant and Cell Physiology **43:** 718-725

Nakamura Y, Utsumi Y, Sawada T, Aihara S, Utsumi C, Yoshida M, Kitamura S (2010) Characterization of the reactions of starch branching enzymes from rice endosperm. Plant and Cell Physiology **51:** 776-794

Nelson O, Pan D (1995) Starch synthesis in maize endosperms. Annual review of plant biology **46:** 475-496

Nemeth C, Andersson AA, Andersson R, Mangelsen E, Sun C, Åman P (2014) Relationship of grain fructan content to degree of polymerisation in different barleys. Food and Nutrition Sciences **5:** 581

Nemeth C, Freeman J, Jones HD, Sparks C, Pellny TK, Wilkinson MD, Dunwell J, Andersson AA, Aman P, Guillon F, Saulnier L, Mitchell RA, Shewry PR (2010)

Down-regulation of the CSLF6 gene results in decreased (1,3;1,4)-beta-D-glucan in endosperm of wheat. Plant Physiol **152:** 1209-1218

Nevo Z, Sharon N (1969) The cell wall of Peridinium westii, a non cellulosic glucan. Biochimica et Biophysica Acta (BBA) - Biomembranes **173:** 161-175

Nomura T, Nakayama N, Murata T, Akazawa T (1967) Biosynthesis of starch in chloroplasts. Plant Physiol **42:** 327-332

Olsen LT, Divon HH, Al R, Fosnes K, Lid SE, Opsahl-Sorteberg H-G (2008) The defective seed5 (des5) mutant: effects on barley seed development and HvDek1, HvCr4, and HvSal1 gene regulation. J Exp Bot **59:** 3753-3765

Olsen O-A (2001) Endosperm development: cellularization and cell fate specification. Annual review of plant biology **52:** 233-267

Ould-Ahmed M, Decau M-L, Morvan-Bertrand A, Prud'homme M-P, Lafrenière C, Drouin P (2014) Plant maturity and nitrogen fertilization affected fructan metabolism in harvestable tissues of timothy (Phleum pratense L.). Journal of Plant Physiology **171:** 1479-1490

Oyefuga O, Adeyanju M, OO A, Agboola F (2011) Purification and some properties of b-amylase from the nodes of sugar cane, Saccharium offinacium. International Journal of Plant Physiology and Biochemistry **3:** 117-124

Palmer G (1972) Morphology of starch granules in cereal grains and malts. Journal of the Institute of Brewing **78:** 326-332

Palmer G (1989) Cereals in malting and brewing. Cereal science and technology**:** 61-242

Palmer G (1993) Ultrastructure of endosperm and quality. Ferment **6:** 105-110

Papageorgiou M, Lakhdara N, Lazaridou A, Biliaderis C, Izydorczyk M (2005) Water extractable (1→ 3, 1→ 4)-β-D-glucans from barley and oats: An intervarietal study on

their structural features and rheological behaviour. Journal of Cereal Science **42:** 213-224

Patrick J (1997) Phloem unloading: sieve element unloading and post-sieve element transport. Annual review of plant biology **48:** 191-222

Paul Barratt DH, Derbyshire P, Findlay K, Pike M, Wellner N, Lunn J, Feil R, Simpson C, Maule AJ, Smith AM (2009) Normal growth of Arabidopsis requires cytosolic invertase but not sucrose synthase. Proceedings of the National Academy of Sciences

Pérez-Mendoza D, Rodríguez-Carvajal MÁ, Romero-Jiménez L, Farias GdA, Lloret J, Gallegos MT, Sanjuán J (2015) Novel mixed-linkage β-glucan activated by c-di-GMP in Sinorhizobium meliloti. Proceedings of the National Academy of Sciences **112:** E757-E765

Peshev D, Vergauwen R, Moglia A, Hideg É, Van den Ende W (2013) Towards understanding vacuolar antioxidant mechanisms: a role for fructans? J Exp Bot **64:** 1025-1038

Pettolino F, Sasaki I, Turbic A, Wilson SM, Bacic A, Hrmova M, Fincher GB (2009) Hyphal cell walls from the plant pathogen Rhynchosporium secalis contain (1,3/1,6)-β-d-glucans, galacto- and rhamnomannans, (1,3;1,4)-β-d-glucans and chitin. FEBS Journal **276:** 3698-3709

Pettolino FA, Hoogenraad NJ, Ferguson C, Bacic A, Johnson E, Stone BA (2001) A (1? 4)-ß-mannan-specific monoclonal antibody and its use in the immunocytochemical location of galactomannans. Planta **214:** 235-242

Peukert M, Lim WL, Seiffert U, Matros A (2016) Mass spectrometry imaging of metabolites in barley grain tissues. *In* Current Protocols in Plant Biology. John Wiley & Sons, Inc.

Peukert M, Thiel J, Mock H-P, Marko D, Weschke W, Matros A (2016) Spatiotemporal dynamics of oligofructan metabolism and suggested functions in developing cereal grains. Front Plant Sci **6**

Peukert M, Thiel J, Peshev D, Weschke W, Van den Ende W, Mock H-P, Matros A (2014) Spatio-temporal dynamics of fructan metabolism in developing barley grains. The Plant Cell **26:** 3728-3744

Philippe S, Saulnier L, Guillon F (2006) Arabinoxylan and (1→3),(1→4)-β-glucan deposition in cell walls during wheat endosperm development. Planta **224:** 449

Pilon-Smits E, Ebskamp M, Paul MJ, Jeuken M, Weisbeek PJ, Smeekens S (1995) Improved performance of transgenic fructan-accumulating tobacco under drought stress. Plant Physiol **107:** 125-130

Pollock C, Lloyd E (1987) The effect of low temperature upon starch, sucrose and fructan synthesis in leaves. Annals of botany **60:** 231-235

Pollock CJ (1986) Tansley review no5. Fructans and the metabolism of sucrose in vascular plants. New Phytologist **104:** 1-24

Pollock CJ, Cairns AJ (1991) Fructan metabolism in grasses and cereals. Annual Review of Plant Physiology and Plant Molecular Biology **42:** 77-101

Poorter, Villar (1997) The fate of acquired carbon in plants: chemical composition and construction costs. Plant resource allocation**:** 39-72

Price PB, Parsons J (1979) Distribution of lipids in embryonic axis, bran-endosperm, and hull fractions of hulless barley and hulless oat grain. Journal of agricultural and food chemistry **27:** 813-815

Psota V, Vejražka K, Faměra O, Hrčka M (2007) Relationship between grain hardness and malting quality of barley (Hordeum vulgare L.). Journal of the Institute of Brewing **113:** 80-86

Rahman S, Shewry P, Miflin B (1982) Differential protein accumulation during barley grain development. J Exp Bot **33:** 717-728

Ranki H, Sopanen T (1984) Secretion of α-amylase by the aleurone layer and the scutellum of germinating barley grain. Plant Physiol **75:** 710-715

Raschka L, Daniel H (2005) Mechanisms underlying the effects of inulin-type fructans on calcium absorption in the large intestine of rats. Bone **37:** 728-735

Regina A, Kosar-Hashemi B, Ling S, Li Z, Rahman S, Morell M (2010) Control of starch branching in barley defined through differential RNAi suppression of starch branching enzyme IIa and IIb. J Exp Bot **61:** 1469-1482

Ritsema T, Hernández L, Verhaar A, Altenbach D, Boller T, Wiemken A, Smeekens S (2006) Developing fructan-synthesizing capability in a plant invertase via mutations in the sucrose-binding box. The Plant Journal **48:** 228-237

Ritsema T, Joling J, Smeekens S (2003) Patterns of fructan synthesized by onion fructan : fructan 6G-fructosyltransferase expressed in tobacco BY2 cells – is fructan : fructan 1-fructosyltransferase needed in onion? New Phytologist **160:** 61-67

Roach T, Krieger-Liszkay A (2014) Regulation of photosynthetic electron transport and photoinhibition. Current Protein and Peptide Science **15:** 351-362

Robert P, Jamme F, Barron C, Bouchet B, Saulnier L, Dumas P, Guillon F (2011) Change in wall composition of transfer and aleurone cells during wheat grain development. Planta **233:** 393-406

Roitsch T, Balibrea ME, Hofmann M, Proels R, Sinha AK (2003) Extracellular invertase: key metabolic enzyme and PR protein. J Exp Bot **54:** 513-524

Roitsch T, Gonzalez MC (2004) Function and regulation of plant invertases: sweet sensations. Trends Plant Sci **9:** 606-613

Roth A, Lüscher M, Sprenger N, Boller T, Wiemken A (1997) Fructan and fructan-metabolizing enzymes in the growth zone of barley leaves. New Phytol **136:** 73-79

Ruan Y-L (2014) Sucrose metabolism: gateway to diverse carbon use and sugar signaling. Annual review of plant biology **65:** 33-67

Sabelli PA, Larkins BA (2009) The development of endosperm in grasses. Plant Physiol **149:** 14-26

Saengthongpinit W, Sajjaanantakul T (2005) Influence of harvest time and storage temperature on characteristics of inulin from Jerusalem artichoke (Helianthus tuberosus L.) tubers. Postharvest Biology and Technology **37:** 93-100

Salmeán AA, Duffieux D, Harholt J, Qin F, Michel G, Czjzek M, Willats WGT, Hervé C (2017) Insoluble (1 → 3), (1 → 4)-β-D-glucan is a component of cell walls in brown algae (Phaeophyceae) and is masked by alginates in tissues. Scientific reports **7:** 2880

Satoh H, Nishi A, Yamashita K, Takemoto Y, Tanaka Y, Hosaka Y, Sakurai A, Fujita N, Nakamura Y (2003) Starch-branching enzyme I-deficient mutation specifically affects the structure and properties of starch in rice endosperm. Plant Physiol **133:** 1111-1121

Scofield GN, Ruuska SA, Aoki N, Lewis DC, Tabe LM, Jenkins CL (2009) Starch storage in the stems of wheat plants: localization and temporal changes. Annals of botany **103:** 859-868

Shaik SS, Obata T, Hebelstrup KH, Schwahn K, Fernie AR, Mateiu RV, Blennow A (2016) Starch granule re-structuring by starch branching enzyme and glucan water dikinase modulation affects caryopsis physiology and metabolism. PLoS ONE **11:** e0149613

Shen B, Li C, Min Z, Meeley RB, Tarczynski MC, Olsen O-A (2003) sal1 determines the number of aleurone cell layers in maize endosperm and encodes a class E vacuolar sorting protein. Proceedings of the National Academy of Sciences **100:** 6552-6557

Shewry PR, Kreis M, Parmar S, Lew EJL, Kasarda DD (1985) Identification of γ-type hordeins in barley. FEBS Lett **190:** 61-64

Shiomi N (1989) Properties of fructosyltransferases involved in the synthesis of fructan in Liliaceous plants. Journal of Plant Physiology **134:** 151-155

Silver DM, Kötting O, Moorhead GB (2014) Phosphoglucan phosphatase function sheds light on starch degradation. Trends Plant Sci **19:** 471-478

Simmons TJ, Uhrin D, Gregson T, Murray L, Sadler IH, Fry SC (2013) An unexpectedly lichenase-stable hexasaccharide from cereal, horsetail and lichen mixed-linkage beta-glucans (MLGs): implications for MLG subunit distribution. Phytochemistry **95:** 322-332

Slakeski N, Fincher GB (1992) Developmental regulation of (1→ 3, 1→ 4)-β-glucanase gene expression in barley tissue-specific expression of individual isoenzymes. Plant Physiol **99:** 1226-1231

Smith AM (2008) Prospects for increasing starch and sucrose yields for bioethanol production. The Plant Journal **54:** 546-558

Sparla F, Falini G, Botticella E, Pirone C, Talamè V, Bovina R, Salvi S, Tuberosa R, Sestili F, Trost P (2014) New starch phenotypes produced by TILLING in barley. PLoS ONE **9:** e107779

Sprenger N, Bortlik K, Brandt A, Boller T, Wiemken A (1995) Purification, cloning, and functional expression of sucrose:fructan 6-fructosyltransferase, a key enzyme of fructan synthesis in barley. Proc Natl Acad Sci U S A **92:** 11652-11656

Sreenivasulu N, Borisjuk L, Junker BH, Mock H-P, Rolletschek H, Seiffert U, Weschke W, Wobus U (2010) Barley grain development: toward an integrative view. International Review of Cell and Molecular Biology **281:** 49-89

Stauffer DR, Howard TL, Nyun T, Hollenberg SM (2001) CHMP1 is a novel nuclear matrix protein affecting chromatin structure and cell-cycle progression. Journal of cell science **114:** 2383-2393

Streb S, Zeeman SC (2012) Starch metabolism in Arabidopsis. The Arabidopsis Book **10:** e0160

Taketa S, Amano S, Tsujino Y, Sato T, Saisho D, Kakeda K, Nomura M, Suzuki T, Matsumoto T, Sato K (2008) Barley grain with adhering hulls is controlled by an ERF family transcription factor gene regulating a lipid biosynthesis pathway. Proceedings of the National Academy of Sciences **105:** 4062-4067

Taketa S, Yuo T, Tonooka T, Tsumuraya Y, Inagaki Y, Haruyama N, Larroque O, Jobling SA (2012) Functional characterization of barley betaglucanless mutants demonstrates a unique role for CslF6 in (1, 3; 1, 4)-β-D-glucan biosynthesis. J Exp Bot **63:** 381-392

Talbot MJ, Franceschi VR, McCurdy DW, Offler CE (2001) Wall ingrowth architecture in epidermal transfer cells ofVicia faba cotyledons. Protoplasma **215:** 191-203

Talbot MJ, Offler CE, McCurdy DW (2002) Transfer cell wall architecture: a contribution towards understanding localized wall deposition. Protoplasma **219:** 197-209

Thiel J (2014) Development of endosperm transfer cells in barley. Front Plant Sci **5**

Thiel J, Hollmann J, Rutten T, Weber H, Scholz U, Weschke W (2012a) 454 Transcriptome sequencing suggests a role for two-component signalling in cellularization and differentiation of barley endosperm transfer cells. PLoS ONE **7:** e41867

Thiel J, Riewe D, Rutten T, Melzer M, Friedel S, Bollenbeck F, Weschke W, Weber H (2012b) Differentiation of endosperm transfer cells of barley: a comprehensive analysis at the micro-scale. The Plant Journal **71:** 639-655

Thiel J, Weier D, Sreenivasulu N, Strickert M, Weichert N, Melzer M, Czauderna T, Wobus U, Weber H, Weschke W (2008) Different hormonal regulation of cellular differentiation and function in nucellar projection and endosperm transfer cells: a microdissection-based transcriptome study of young barley grains. Plant Physiol **148:** 1436-1452

Tian Q, Olsen L, Sun B, Lid SE, Brown RC, Lemmon BE, Fosnes K, Gruis DF, Opsahl-Sorteberg H-G, Otegui MS (2007) Subcellular localization and functional domain studies of DEFECTIVE KERNEL1 in maize and Arabidopsis suggest a model for aleurone cell fate specification involving CRINKLY4 and SUPERNUMERARY ALEURONE LAYER1. The Plant Cell **19:** 3127-3145

Tonooka T, Aoki E, Yoshioka T, Taketa S (2009) A novel mutant gene for (1-3, 1-4)-β-D-glucanless grain on barley (Hordeum vulgare L.) chromosome 7H. Breeding Science **59:** 47-54

Topping DL, Clifton PM (2001) Short-chain fatty acids and human colonic function: roles of resistant starch and nonstarch polysaccharides. Physiological reviews **81:** 1031-1064

Trafford K, Fincher G, Shewry P (2012) Barley grain carbohydrates: starch and cell walls. Barley: chemistry and technology**:** 71

Tran L-SP, Urao T, Qin F, Maruyama K, Kakimoto T, Shinozaki K, Yamaguchi-Shinozaki K (2007) Functional analysis of AHK1/ATHK1 and cytokinin receptor histidine kinases in response to abscisic acid, drought, and salt stress in Arabidopsis. Proceedings of the National Academy of Sciences **104:** 20623-20628

Tyson R, Ap Rees T (1988) Starch synthesis by isolated amyloplasts from wheat endosperm. Planta **175:** 33-38

Tyynelä J, Stitt M, Lönneborg A, Smeekens S, Schulman AH (1995) Metabolism of starch synthesis in developing grains of the shx shrunken mutant of barley (Hordeum vulgare). Physiologia Plantarum **93:** 77-84

Urbanowicz BR, Rayon C, Carpita NC (2004) Topology of the maize mixed linkage (1->3),(1->4)-beta-d-glucan synthase at the Golgi membrane. Plant Physiol **134:** 758-768

Valluru R, Van den Ende W (2008) Plant fructans in stress environments: emerging concepts and future prospects. J Exp Bot **59:** 2905-2916

van Bel AJ, Knoblauch M (2000) Sieve element and companion cell: the story of the comatose patient and the hyperactive nurse. Functional Plant Biology **27:** 477-487

Van Den Ende W, Clerens S, Vergauwen R, Van Riet L, Van Laere A, Yoshida M, Kawakami A (2003) Fructan 1-exohydrolases. beta-(2,1)-trimmers during graminan biosynthesis in stems of wheat? Purification, characterization, mass mapping, and cloning of two fructan 1-exohydrolase isoforms. Plant Physiol **131:** 621-631

Van den Ende W, Coopman M, Clerens S, Vergauwen R, Le Roy K, Lammens W, Van Laere A (2011) Unexpected presence of graminan- and levan-type fructans in the evergreen frost-hardy eudicot Pachysandra terminalis (Buxaceae): purification, cloning, and functional analysis of a 6-SST/6-SFT enzyme. Plant Physiol **155:** 603-614

Van den Ende W, Michiels A, De Roover J, Van Laere A (2002) Fructan biosynthetic and breakdown enzymes in dicots evolved from different invertases. Expression of fructan genes throughout chicory development. ScientificWorldJournal **2:** 1281-1295

Van den Ende W, Michiels A, De Roover J, Verhaert P, Van Laere A (2000) Cloning and functional analysis of chicory root fructan1-exohydrolase I (1-FEH I): a vacuolar enzyme derivedfrom a cell-wall invertase ancestor? Mass fingerprint of the 1-FEH I enzyme. The Plant Journal **24:** 447-456

Van den Ende W, Roover JD, Van Laere A (1996) In vitro synthesis of fractofuranosyl-only oligosaccharides from inulin and fructose by purified chicory root fructan:fructan fructosyl transferase. Physiologia Plantarum **97:** 346-352

Van den Ende W, Yoshida M, Clerens S, Vergauwen R, Kawakami A (2005) Cloning, characterization and functional analysis of novel 6-kestose exohydrolases (6-KEHs) from wheat (Triticum aestivum). New Phytol **166:** 917-932

Van Laere A, Van Den Ende W (2002) Inulin metabolism in dicots: chicory as a model system. Plant, Cell & Environment **25:** 803-813

Van Riet L, Nagaraj V, Van den Ende W, Clerens S, Wiemken A, Van Laere A (2006) Purification, cloning and functional characterization of a fructan 6-exohydrolase from wheat (Triticum aestivum L.). J Exp Bot **57:** 213-223

Végh KR (2009) Starch bearing crops as food sources. Cultivated plants primarily as food sources **1:** 219-231

Vermeylen R, Goderis B, Reynaers H, Delcour JA (2004) Amylopectin molecular structure reflected in macromolecular organization of granular starch. Biomacromolecules **5:** 1775-1786

Verspreet J, Cimini S, Vergauwen R, Dornez E, Locato V, Le Roy K, De Gara L, Van den Ende W, Delcour JA, Courtin CM (2013b) Fructan metabolism in developing wheat (Triticum aestivum L.) kernels. Plant Cell Physiol **54:** 2047-2057

Vijn I, Smeekens S (1999) Fructan: more than a reserve carbohydrate? Plant Physiol **120:** 351-360

Vijn I, van Dijken A, Sprenger N, van Dun K, Weisbeek P, Wiemken A, Smeekens S (1997) Fructan of the inulin neoseries is synthesized in transgenic chicory plants (Cichorium intybus L.) harbouring onion (Allium cepa L.) fructan:fructan 6G-fructosyltransferase. Plant J **11:** 387-398

Wagner W, Wiemken A (1987) Enzymology of fructan synthesis in grasses: Properties of sucrose-sucrose-fructosyltransferase in barley leaves (Hordeum vulgare L. cv Gerbel). Plant Physiol **85:** 706-710

Wagner W, Wiemken A, Matile P (1986) Regulation of fructan metabolism in leaves of barley (Hordeum vulgare L. cv Gerbel). Plant Physiol **81:** 444-447

Wallace W, Lance R (1988) The protein reserves of the barley grain and their degradation during malting and brewing. Journal of the Institute of Brewing **94:** 379-386

Wang C, Barry JK, Min Z, Tordsen G, Rao AG, Olsen O-A (2003) The calpain domain of the maize DEK1 protein contains the conserved catalytic triad and functions as a cysteine proteinase. Journal of Biological Chemistry **278:** 34467-34474

Wang M, Oppedijk BJ, Lu X, Van Duijn B, Schilperoort RA (1996) Apoptosis in barley aleurone during germination and its inhibition by abscisic acid. Plant Molecular Biology **32:** 1125-1134

Waterhouse AL, Calub TM, French AD (1991) Conformational analysis of 1-kestose by molecular mechanics and by n.m.r. spectroscopy. Carbohydr Res **217:** 29-42

Wei J-Z, Chatterton NJ (2001) Fructan biosynthesis and fructosyltransferase evolution: Expression of the 6-SFT (sucrose : fructan 6-fructosyltransferase) gene in crested wheatgrass (Agropyron cristatum). Journal of Plant Physiology **158:** 1203-1213

Weier D, Thiel J, Kohl S, Tarkowská D, Strnad M, Schaarschmidt S, Weschke W, Weber H, Hause B (2014) Gibberellin-to-abscisic acid balances govern development and differentiation of the nucellar projection of barley grains. J Exp Bot**:** eru289

Welham T, Pike J, Horst I, Flemetakis E, Katinakis P, Kaneko T, Sato S, Tabata S, Perry J, Parniske M, Wang TL (2009) A cytosolic invertase is required for normal growth and cell development in the model legume, Lotus japonicus. J Exp Bot **60:** 3353-3365

Weschke W, Panitz R, Gubatz S, Wang Q, Radchuk R, Weber H, Wobus U (2003) The role of invertases and hexose transporters in controlling sugar ratios in maternal and filial tissues of barley caryopses during early development. The Plant Journal **33:** 395-411

Weschke W, Panitz R, Sauer N, Wang Q, Neubohn B, Weber H, Wobus U (2000) Sucrose transport into barley seeds: molecular characterization of two transporters and implications for seed development and starch accumulation. The Plant Journal **21:** 455-467

West AH, Stock AM (2001) Histidine kinases and response regulator proteins in two-component signaling systems. Trends in biochemical sciences **26:** 369-376

Wilson SM, Burton RA, Collins HM, Doblin MS, Pettolino FA, Shirley N, Fincher GB, Bacic A (2012) Pattern of deposition of cell wall polysaccharides and transcript abundance of related cell wall synthesis genes during differentiation in barley endosperm. Plant Physiol **159:** 655-670

Wilson SM, Burton RA, Doblin MS, Stone BA, Newbigin EJ, Fincher GB, Bacic A (2006) Temporal and spatial appearance of wall polysaccharides during cellularization of barley (Hordeum vulgare) endosperm. Planta **224:** 655

Wilson SM, Ho YY, Lampugnani ER, Van de Meene AM, Bain MP, Bacic A, Doblin MS (2015) Determining the subcellular location of synthesis and assembly of the cell wall polysaccharide (1, 3; 1, 4)-β-d-glucan in grasses. The Plant Cell **27:** 754-771

Wohlbach DJ, Quirino BF, Sussman MR (2008) Analysis of the Arabidopsis histidine kinase ATHK1 reveals a connection between vegetative osmotic stress sensing and seed maturation. The Plant Cell **20:** 1101-1117

Wolf N (1991) Complete nucleotide sequence of a Hordeum vulgare gene encoding (1→ 3, 1→ 4)-β-glucanase isoenzyme II. Plant Physiol **96:** 1382

Woodward JR, Fincher GB, Stone BA (1983) Water-soluble (1→3), (1→4)-β-D-glucans from barley (Hordeum vulgare) endosperm. II. Fine structure. Carbohydrate Polymers **3:** 207-225

Xu H, Liang M, Xu L, Li H, Zhang X, Kang J, Zhao Q, Zhao H (2015) Cloning and functional characterization of two abiotic stress-responsive Jerusalem artichoke (Helianthus tuberosus) fructan 1-exohydrolases (1-FEHs). Plant Molecular Biology **87:** 81-98

Yamaguchi M, Kainuma K, French D (1979) Electron microscopic observations of waxy maize starch. Journal of Ultrastructure Research **69:** 249-261

Yildiz F (2010) Advances in Food Biochemistry,

Yin Y, Huang J, Xu Y (2009) The cellulose synthase superfamily in fully sequenced plants and algae. BMC Plant Biol **9:** 99

Yoshida M, Abe J, Moriyama M, Kuwabara T (1998) Carbohydrate levels among winter wheat cultivars varying in freezing tolerance and snow mold resistance during autumn and winter. Physiologia Plantarum **103:** 8-16

Young TE, Gallie DR (2000) Programmed cell death during endosperm development. *In* Programmed Cell Death in Higher Plants. Springer, pp 39-57

Zeeman SC, Delatte T, Messerli G, Umhang M, Stettler M, Mettler T, Streb S, Reinhold H, Kötting O (2007) Starch breakdown: recent discoveries suggest distinct pathways and novel mechanisms. Functional Plant Biology **34:** 465-473

Zheng Y, Wang Z (2010) Current opinions on endosperm transfer cells in maize. Plant Cell Reports **29:** 935-942

Zheng Y, Wang Z (2011) Contrast observation and investigation of wheat endosperm transfer cells and nucellar projection transfer cells. Plant Cell Reports **30:** 1281-1288

Zobel H (1988) Molecules to granules: a comprehensive starch review. Starch-Stärke **40:** 44-50

Chapter 2

Method for Hull-less Barley Transformation and Manipulation of Grain Mixed-Linkage Beta-Glucan

Statement of Authorship

Title of Paper	Method for hull-less barley transformation and manipulation of grain mixed-linkage beta-glucan
Publication Status	☑ Published ☐ Accepted for Publication ☐ Submitted for Publication ☐ Unpublished and Unsubmitted w ork w ritten in manuscript style
Publication Details	Wai Li Lim, Helen M Collins, Rohan R Singh, Natalie AJ Kibble, Kuok Yap, Jillian Taylor, Geoffrey B Fincher and Rachel A Burton

Principal Author

Name of Principal Author (Candidate)	Wai Li Lim		
Contribution to the Paper	Characterisation of the *CslF6* transgenic lines including the phenotype of mature grain, phenotype of barley seedlings (embryo, shoot and root measurement) and all microscopy work. Helped prepare the manuscript.		
Overall percentage (%)	60%		
Certification:	This paper reports on original research I conducted during the period of my Higher Degree by Research candidature and is not subject to any obligations or contractual agreements with a third party that would constrain its inclusion in this thesis. I am the primary author of this paper.		
Signature		Date	2 August 2017

Co-Author Contributions

By signing the Statement of Authorship, each author certifies that:

i. the candidate's stated contribution to the publication is accurate (as detailed above);
ii. permission is granted for the candidate in include the publication in the thesis; and
iii. the sum of all co-author contributions is equal to 100% less the candidate's stated contribution.

Name of Co-Author	Helen M Collins		
Contribution to the Paper	Conceived project and helped to design experiments. Performed some of the biochemical analyses, analysed data and contributed to the preparation of the manuscript.		
Signature		Date	31/7/2017

Name of Co-Author	Rohan R Singh		
Contribution to the Paper	Performed transformation work and assisted in preparation of the manuscript.		
Signature		Date	31/7/2017.

Name of Co-Author	Natalie AJ Kibble		
Contribution to the Paper	Helped to design the experiments and assisted with manuscript preparation.		
Signature		Date	1/8/2017

Name of Co-Author	Kuok Yap		
Contribution to the Paper	Performed some of the biochemical analyses.		
Signature		Date	28/7/2017

Name of Co-Author	Jillian Taylor		
Contribution to the Paper	Performed instron analysis. Jill has left the University		
Signature		Date	3/8/2017

Name of Co-Author	Geoffrey B Fincher		
Contribution to the Paper	Conceived project, helped to design experiments. and secured finance		
Signature		Date	3/8/2017

Name of Co-Author	Rachel A Burton		
Contribution to the Paper	Conceived project and helped to design experiments. Assisted with manuscript preparation.		
Signature		Date	31/7/2017

Descriptions of Candidate's Contribution to This Project

Introduction

(1,3;1,4)-β-Glucans are structural and storage polysaccharides in cell walls of many grasses, including the cereals. They are made up of glucose monomers joined by β(1,3)- and β(1,4)-linkages and their unique structure makes them soluble in aqueous environments. Humans possess no digestive enzymes to break them down in the gastrointestinal tract but they are efficiently fermented by parts of the microbiome to yield valuable short chain fatty acids. There is evidence that consumption of food containing high levels of (1,3;1,4)-β-glucans are beneficial to human health by improving blood glucose levels (Reid, 1971) and lowering "bad" low-density lipoprotein (LDL) and improving "good" high-density lipoprotein (HDL) cholesterol levels (McCleary et al., 1981; Buckeridge, 2010; Rodríguez-Gacio et al., 2012) which potentially may reduce the risk of heart disease. In cereal grains, the amount of (1,3;1,4)-β-glucans varies amongst species. For example, (1,3;1,4)-β-glucans in barley grain ranges between 3 to 11% w/w (weight per weight), oats contain 3 to 7% w/w, rye contains 1 to 2% w/w, while maize, rice and wheat contain less than 1% (Handford et al., 2003).

An attempt to increase (1,3;1,4)-β-glucan content in the hulled barley variety Golden Promise was previously accomplished by transformation with an over-expression construct of (1,3;1,4)-the β-glucan synthase gene, *CslF6,* via *Agrobacterium tumefaciens* (Burton et al., 2011). The transgenic barley lines contained more than an 80% increase in (1,3;1,4)-β-glucan content in grain (Burton et al., 2011). However, hulled barley grain is not suitable for human consumption without processing due to the adherent outer hull which creates an undesirable mouthfeel. Hence, the use of barley for human food is more suited to hull-less barley cultivars, where the outer hull can easily be removed and there is no need for pearling.

To broaden the use of hull-less barley cultivars in the health industry, a highly reproducible *Agrobacterium*-mediated transformation protocol for hull-less variety Torrens has been developed. As a proof of concept, Torrens was transformed with over-expression constructs for the *CslF6* and *CslH1* genes driven by the oat globulin starchy endosperm-specific promoter *(::AsGlo*). Both genes encode barley (1,3;1,4)-β-glucan synthases (Doblin et al., 2009; Burton et al., 2011). In this project, my contribution was to verify the total *HvCslF6* transcript levels in selected transgenic *CslF6* lines using a real time quantitative PCR method and to characterise the grain phenotypes of transgenic *CslF6* lines containing higher amounts of (1,3;1,4)-β-glucans. Grain characterisation included generating toluidine-blue stained sections, immuno-histochemical analysis of (1,3;1,4)-β-glucan using the (1,3;1,4)-β-glucan antibody (BG1), describing the phenotypes of grain germination, seedling and embryo. The manuscript for this project was published in Journal of Integrative Plant Biology (Thesis page 138).

Microscopy analysis indicated a stronger fluorescent signal strength from the (1,3;1,4)-β-glucan (BG1) antibody in the transgenic aleurone, subaleurone and starchy endosperm tissues when compared with the wild type (WT) grain. Furthermore, the transgenic grain developed malformed endosperm transfer cells, aleurone and subaleurone cells during development. At maturity, the endosperm of transgenic grain was shrunken and in some cases the embryo contributed a significantly larger portion of whole grain weight. Germinated grain had lower root lengths and shoot mass, but the germination efficiency was unaffected compared to WT.

Materials and Methods

Plant materials

Wild type (*Hordeum vulgare* L. cv Torrens) and transformed barley were generated. The transformation protocol was described in Thesis page 138. Seeds produced from transformed plants (F6-15-3, F6-18-6, F6-25-5, F6-16-5), Torrens (WT) and WT from tissue culture (WT(tc)) were analysed. All plants were grown in a glasshouse under a day/night temperature regime of 23°C/15°C.

Grain (1,3;1,4)-β-glucan assay

(1,3;1,4)-β-Glucan content of mature grain was measured on 15 mg flour using a scaled down version of the Megazyme mixed-linkage beta-glucan assay (McCleary and Codd, 1991) as outlined in Burton et al. (2011).

Seed germination

A total of 100 seeds (20 seed sample + 80 sacrificial seeds) were placed on 2 sheets of 90 mm Whatman filter paper in a 10 cm petri dish. A 4 ml aliquot of Milli-Q water was added to the Petri dish and it was sealed with parafilm. The seeds were allowed to germinate in a dark incubator at 20°C for 72 h. Seeds which had chitted were counted and removed every 24 h. The percentage of seeds chitted every 24 h was calculated.

Measurement of shoot and root length, shoot and embryo weight

To measure the shoot and root length of seedlings, 10 seeds for each line were placed in a Petri dish and incubated at 4°C, in dark and moist conditions for 24 h. Seeds for each line were transferred to a seed germination pouch (Phytotc) (Beijing Bioconsumable Tech,Ltd., China) and incubated at 20°C for 1 week in the dark. The shoot and root of each seed was measured, then each shoot was collected, lyophilised and the dry weight was measured. To measure the embryo weight from mature seeds, seeds were soaked in water for 6 h. Embryos were carefully removed from the mature seed with a scalpel, collected in a 2 ml Eppendorf tube, lyophilised and weighed. The embryo weight was expressed as a percentage of the total grain weight.

Tissue fixation, embedding and microscopy for developing grain

Thick tissue slices from the centre of developing grain (15 DAP) were fixed in 0.25% glutaraldehyde, 4% paraformaldehyde and 4% sucrose in phosphate buffered saline (PBS), pH 7.2 for 16 h, washed twice in PBS for a period of 8 h and dehydrated in an ethanol series. Samples were infiltrated and embedded in LR White resin and polymerised at 58°C. Embedded tissue was sectioned at 1 μm thickness on an Ultramicrotome (Leica EM UC6) using a diamond knife, and collected on polylysine coated slides (Thermo Fisher Scientific, Scoresby Vic, Australia). For detection of (1,3;1,4)-β-glucans, sections were re-hydrated with 1 X PBS, incubated with 0.05 M glycine to inactivate residual aldehyde groups for 20 min, and blocked with 1% (w/v) bovine serum albumin (BSA) in 1 X PBS (blocking buffer) for 10 min (3 times). Sections were incubated with BG1 (Biosupplies Australia, Parkville, Vic., Australia) murine monoclonal antibodies raised against barley (1,3;1,4)-β-glucan for 1 h at room temperature under moist conditions. After washing 3 times with blocking buffer, sections were incubated with DyLight®550 goat anti-mouse IgG (H+L) (Thermo Fisher Scientific, Scoresby Vic,

Australia) for 1 h at room temperature in the dark. Sections were washed 3 times with blocking buffer, incubated with 0.1% (w⁄v) Calcofluor White 2MR (Sigma-Aldrich, St.Louis, MO) for 90 s and rinsed with water before being mounted with 90% (v/v) glycerol. Images were taken using a Carl Zeiss fluorescence microscope (Axio Imager M2; Carl Zeiss, Oberkochen, Germany). Signals from the DyLight®550-conjugated secondary antibody were observed under the Alexa Fluor 555 filter set at 538-562 nm excitation and 570-640 nm emission wavelengths. Signals from Calcofluor White 2MR were observed under the DAPI filter set at 335-383 nm excitation and 420-470 nm emission wavelengths. Tissue sections were stained with Toluidine blue for morphology examination.

RNA isolation, cDNA synthesis and real-time quantitative PCR

Developing endosperm tissue was collected from ten randomly selected T1 grain (*HvCslF6*), pooled as a bulk sample for total RNA extraction, followed by cDNA synthesis as per Burton et al. (2008) and Betts et al. (2017). Real-time quantitative PCR was performed according to Burton et al. (2008) using the primers HvCslF6_F: TGGGCATTCACCTTCGTCAT, HvCslF6_R: TCAATGGAGCCAGCCATAGAG. Data was normalised using the reference genes *HvCyclophilin*, *HvGAPdH2*, *HvHSP70*, and *HvTubulin* (Burton et al. 2008).

Results

Barley grain over-expressing *HvCslF6* had higher levels of *HvCslF6* transcript in the endosperm compared to WT

The transcript levels of the *HvCslF6* transgene and endogenous genes in WT Torrens and transgenic grain were measured using real-time quantitative PCR on cDNA from developing T1 grain endosperm at 11 days after pollination (DAP). Total transcript levels were markedly higher in the transgenic lines (F6-15, F6-16, F6-18 and F6-25) compared to WT and WT(tc) grain, as shown for a subset of the transformants (Fig. 1).

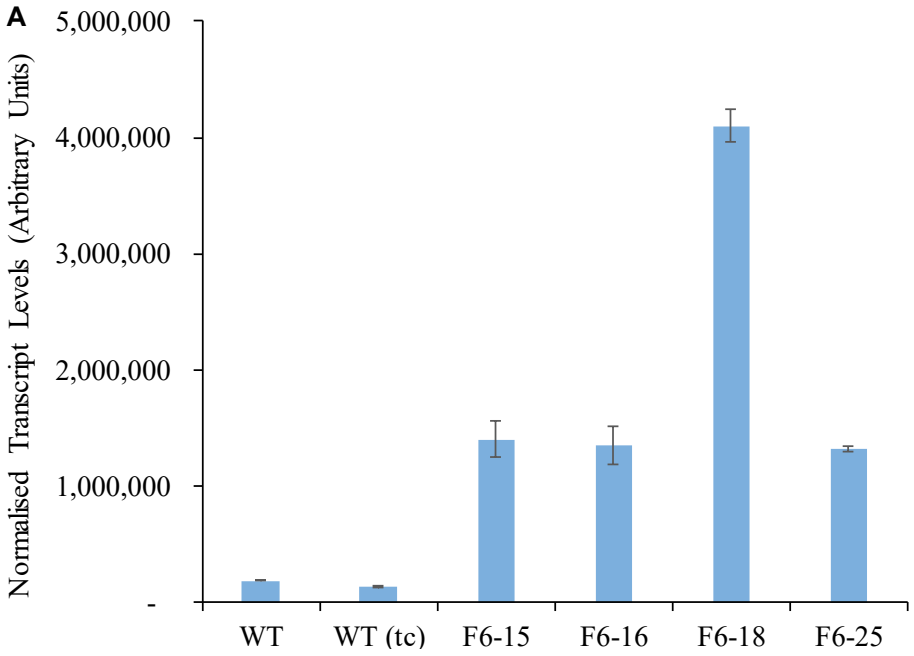

Figure 1: Total combined levels of the *HvCslF6* transcript derived from both the transgene and endogenous gene in developing T1 grain endosperm at 11 DAP. Levels of the total *HvCslF6* transcripts are observed to be lower in the wild type (WT) Torrens and wild type grain from plants put through the tissue culture process (WT (tc)) in comparison to the transgenic lines.

The mature grain of barley over-expressing *HvCslF6* were shrunken and darkened

Transgenic barley lines over-expressing *HvCslF6* appeared to be shrunken and darker in colour at mature stage. The dark colouration was consistently found in T2 transgenic grains (F6-16-5, F6-18-6, F6-25-5). The grain parts which were darkened were different between the transgenic lines. For example, F6-16-5 appeared darkened for the whole starchy endosperm, F6-18-6 appeared darkened in the peripheral endosperm region and F6-25-5 grain appeared darkened only in some parts of the endosperm (Fig. 2A). (1,3;1,4)-β-Glucan content in mature endosperm from each line was measured. In comparison to the WT grain, transgenic grains (F6-15-3, F6-16-5, F6-18-6 and F6-25-5) had about a 100% increase in (1,3;1,4)-β-glucan content while WT(tc) showed approximately a 50% increase.

A

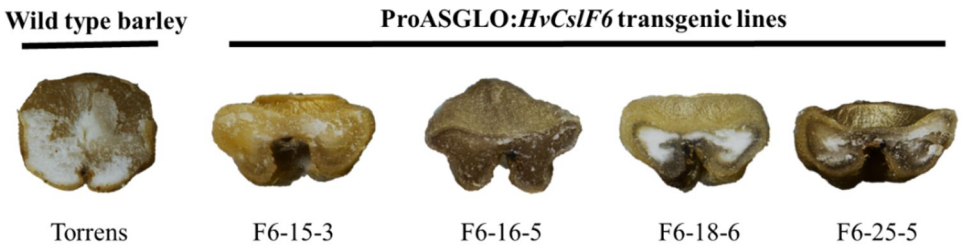

B

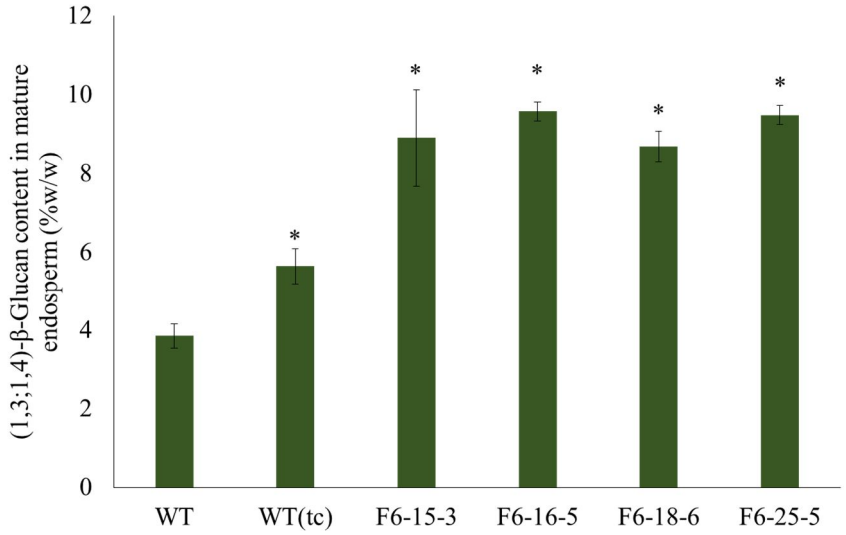

Figure 2: (A) Cross-sections of mature barley grain. (B) (1,3;1,4)-β-Glucan content in mature endosperm on a weight for weight basis (%w/w). * indicates a significant difference from WT according to a t-test with a P-value < 0.05.

Grain of barley over-expressing *HvCslF6* gene had larger cavity compared to the WT grain

The morphology of transgenic and WT grain was examined at 15 DAP using a toluidine blue stain. Developing transgenic grain had a larger cavity size than the WT grain (Fig 3A and 3B). The endosperm transfer cells in transgenic grain were missing in places whereas the endosperm transfer cells in WT grain remained intact (Fig 3A and 3B).

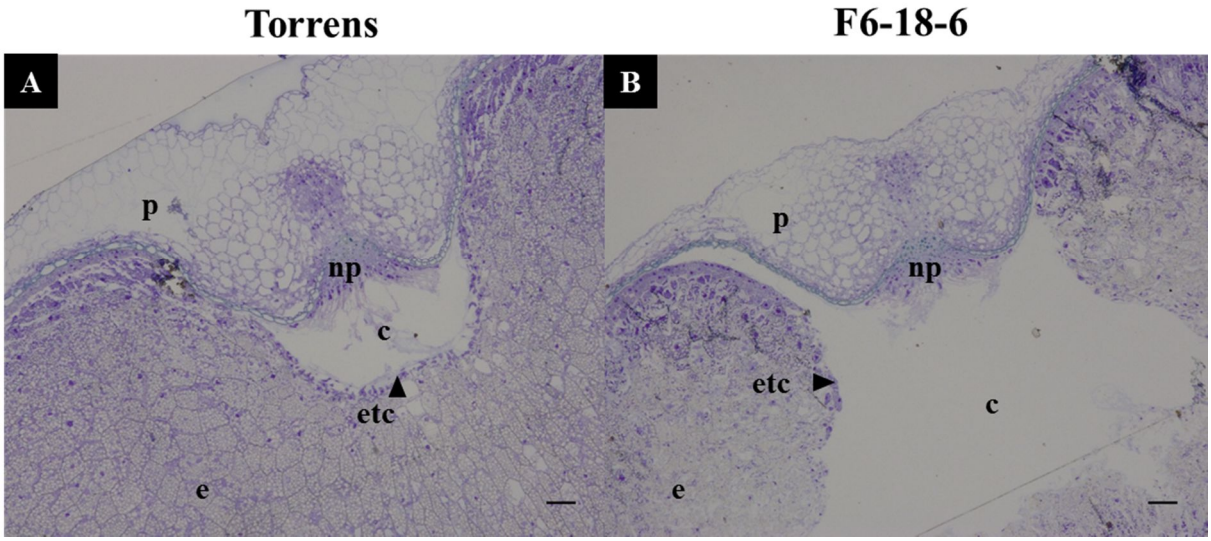

Figure 3: Examination of the endosperm cavity and endosperm transfer cells in barley grain at 15 DAP stained with toluidine blue. The endosperm cavity in transgenic grain (F6-18-6) was larger than WT grain. The endosperm transfer cells in F6-18-6 were less apparent and seemed to be poorly formed, while the endosperm transfer cells in WT grain remained intact (arrow

head). Abbreviations: pericarp (p), nucellar projection (np), cavity (c), endosperm transfer cells (etc), endosperm (e). Scale bar represents 100 μm.

Abnormal aleurone and subaleurone in barley grain over-expressing *HvCslF6*

At 15 DAP, the aleurone layer in transgenic grain was about 3 cell layers thick, while the aleurone layer in WT grain was about 2 cell layers wide. (Fig. 4A and 4B). The aleurone cells had a pronounced square shape compared with the WT grain with much thicker walls. The subaleurone cells in transgenic grain appeared irregular shape and the cellular contents were also missing. Overall the grain appeared to resemble a much more mature stage at around 22 DAP, as previously described in Wilson et al., (2012). When the grain sections were stained with calcofluor white and labelled with (1,3;1,4)-β-glucan fluorescent antibody (BG1), it was more apparent that the cells of subaleurone and starchy endosperm in WT grain were regular in shape but appeared much more irregular in the transgenic grain (Fig 4C to 4F).

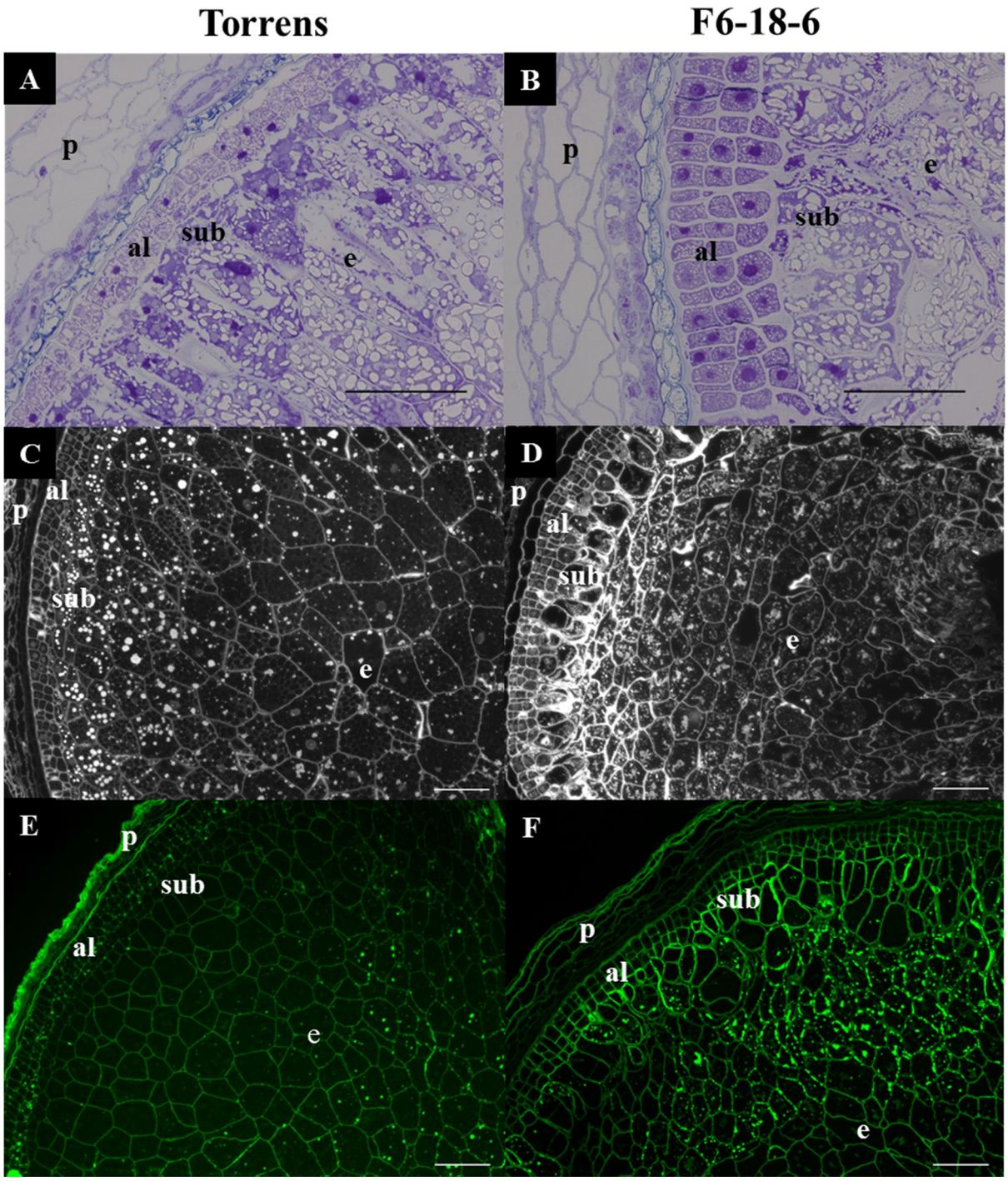

Figure 4: Morphologies of endosperm in barley grain. (A and B) Grain sections at 15 DAP stained with toluidine blue indicating that the transgenic grain had a thicker aleurone layer (about 3 cell layers thick) compared to WT where this layer was only 2 cell layers thick. The cell contents of the subaleurone in the transgenic grain were different compared to the WT grain. (C and D) Grain sections at 15 DAP stained with calcofluor white displayed an irregular

arrangement of endosperm cells and greater staining intensity of the peripheral endosperm cell walls in the transgenic compared to the WT grain. (E and F) Immunolabeling with the (1,3;1,4)-β-glucan fluorescent antibody (BG1) indicating the distribution of (1,3;1,4)-β-glucan in the endosperm cell walls of both transgenic and WT grain. Scale bar represents 100μm. Abbreviations: pericarp (p), aleurone (al), subaleurone (sub), endosperm (e).

***HvCslF6* over-expression changed the grain phenotype but not germination capacity**

Despite the altered grain structure, there was no significant difference in germination rate between transgenic and WT grain. Grain from WT, WT(tc) and transgenic lines reached 100% germination after two days (Fig. 5A). The length of seedling roots and shoots of all lines were measured and compared. At one week old, the seedlings from the *HvCslF6* transgenic lines had shorter roots than WT and WT(tc) (Fig. 5B and 5C). Although there was no significant difference in shoot length between transgenic lines and WT, the weight of seedling shoots was significantly less for transgenic lines compared to WT and WT(tc) (Fig. 5C and 5D). The embryo from F6-18-6 transgenic grain appeared to be the largest compared to the other lines and had a greater embryo proportion per whole grain (50% increase) compared to the WT (Fig. 5E and 5F). Measurements indicated a delayed growth rate for the F6-18-6 transgenic line compared to WT barley (Fig. 5G).

A

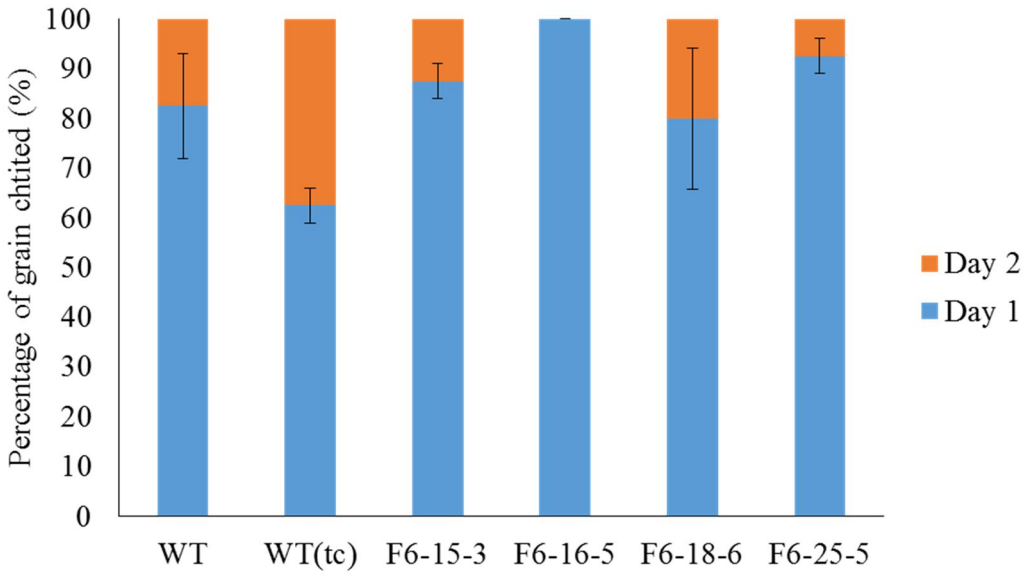
Percentage of grain chtited (%)
100
90
80
70
60
50
40
30
20
10
0
WT
WT(tc)
F6-15-3
F6-16-5
F6-18-6
F6-25-5
Day 2
Day 1

B

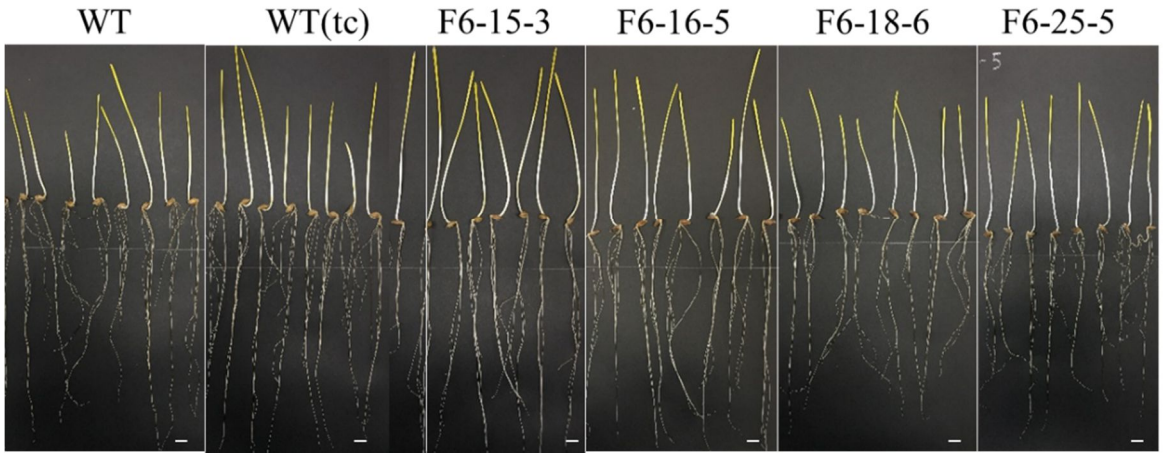
WT
WT(tc)
F6-15-3
F6-16-5
F6-18-6
F6-25-5

C

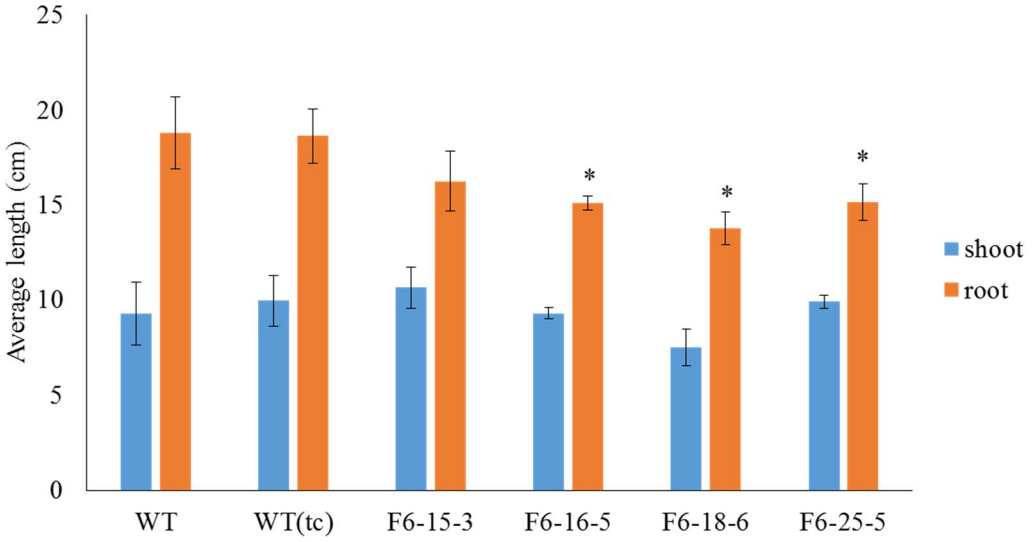
25
20
15
10
5
0
Average length (cm)
shoot
root
*
*
*
WT
WT(tc)
F6-15-3
F6-16-5
F6-18-6
F6-25-5

D

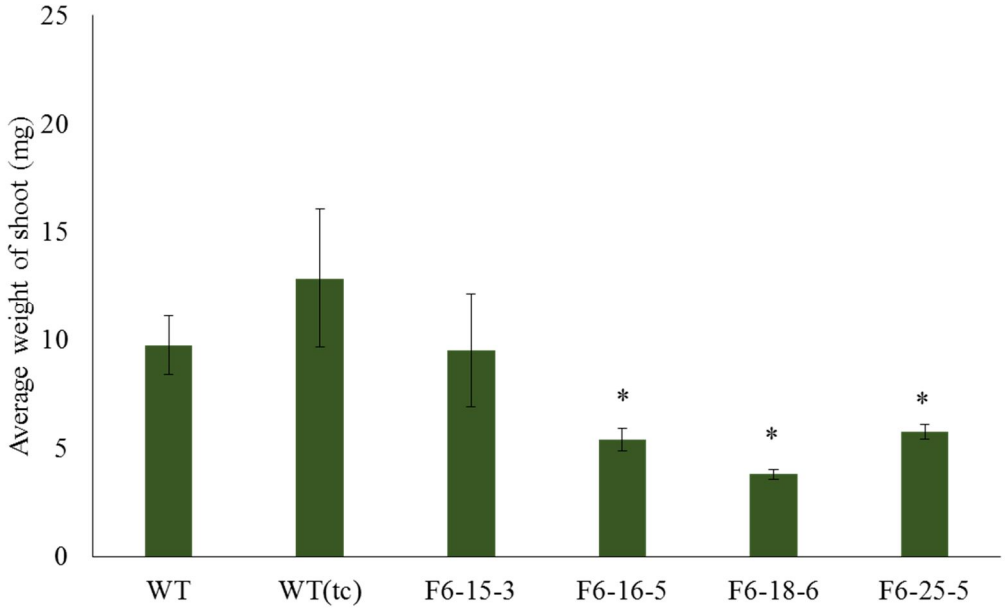
25
20
15
10
5
0
Average weight of shoot (mg)
*
*
*
WT
WT(tc)
F6-15-3
F6-16-5
F6-18-6
F6-25-5

E

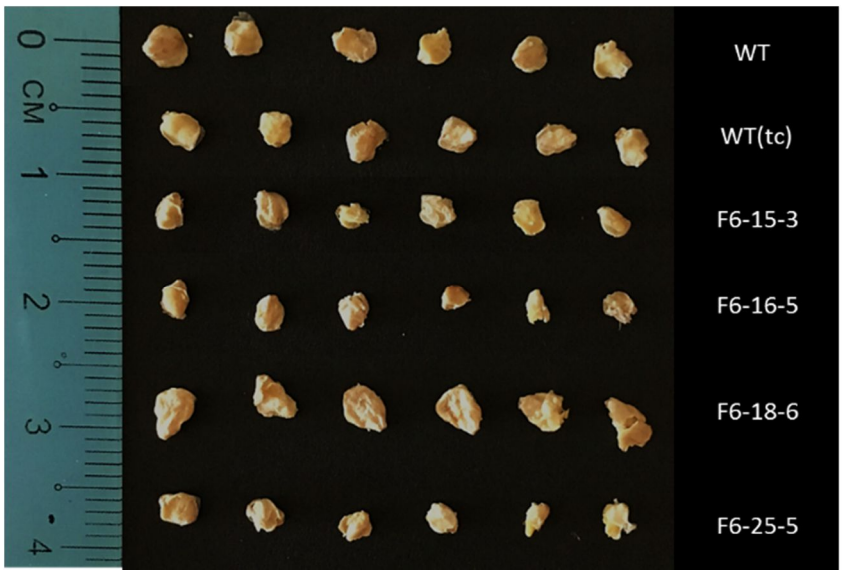
WT
WT(tc)
F6-15-3
F6-16-5
F6-18-6
F6-25-5

F

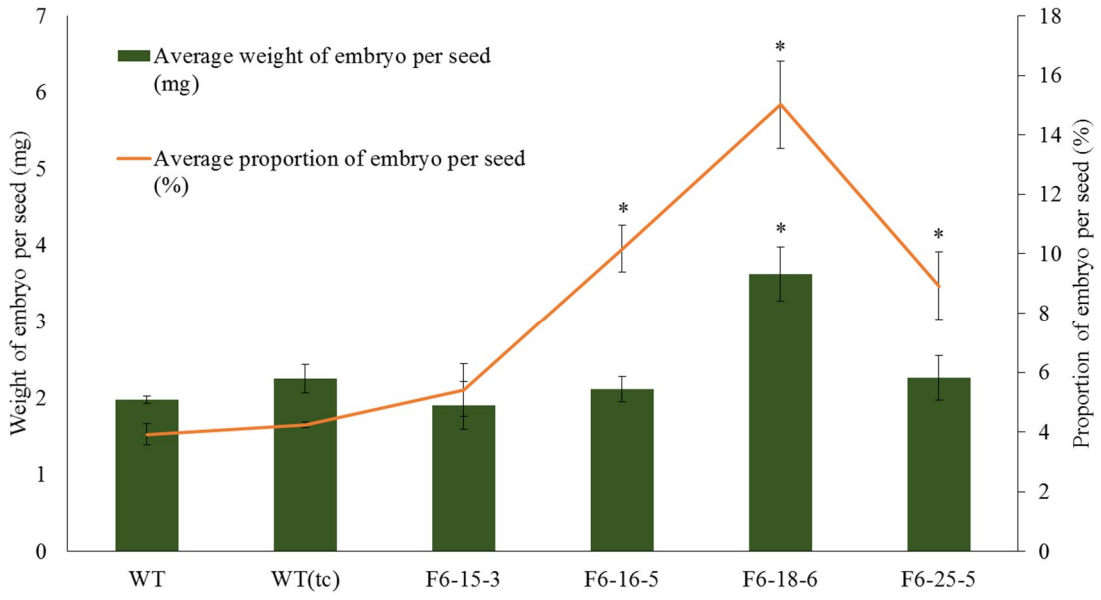
Average weight of embryo per seed (mg)
Average proportion of embryo per seed (%)
Weight of embryo per seed (mg)
Proportion of embryo per seed (%)
0
1
2
3
4
5
6
7
0
2
4
6
8
10
12
14
16
18
*
WT
WT(tc)
F6-15-3
F6-16-5
F6-18-6
F6-25-5

G

Figure 5: The phenotype of barley plants. (A) Seed germination rate across all barley lines on days 1 and 2. (B) Phenotype of barley seedlings. (C and D) Transgenic lines had shorter root length and reduced shoot weight compared to WT and WT(tc) lines. (E) Phenotype of embryos from mature grain. (F) Transgenic grain had a larger embryo size, with a greater proportion of embryo per seed (orange) and greater weight of embryo per seed (green). (G) At 50 days old, transgenic plants showed a slower growth rate compared to WT plants. * Significantly different to WT according to a t-test with a P-value < 0.05.

Discussion

Successful *Agrobacterium*-mediated transformation for the hull-less barley cultivar Torrens has now been demonstrated using a slight modification to the standard *Agrobacterium*-mediated protocol. The modified protocol includes addition of acetosyringone to the co-cultivation medium (Shrawat et al., 2007; Hensel et al., 2008) and the transfer of co-cultivated scutella to a 'resting' medium containing Timentin® but no selection agent (Shrawat et al., 2007). Either individual or combined treatments yielded a 1.8% transformation frequency plus a 50% increase in transformation frequency of hulled cultivars (WI4330 and Golden Promise). The modified transformation protocol was applied to the Torrens variety, producing transgenic plants with over-expression of *HvCslF6* (Fig. 1) and *HvCslH1* construct respectively. Transgenic Torrens overexpressing *HvCslF6* gene had more than 70% increase in (1,3;1,4)-β-glucan content (Fig. 2B) in the grain while transgenic Torrens overexpressing *CslH1*gene did not show any difference in (1,3;1,4)-β-glucan content compared to the WT grain (Thesis page 137).

Although the promoter used to drive transgene expression was specific to the endosperm tissue (Vickers et al., 2006), the effects appeared to extend to the embryo, affecting seedling phenotype and plant growth (Fig. 5C to 5G). There was no effect on seed germination efficiency, or rate, despite the shrunken endosperm and larger embryo size of the transgenic grain (Fig. 2A, 5E and 5F).

Over-expression of the *HvCslF6* gene in Torrens grain appeared to impair grain development, based on the observation of an enlarged endosperm cavity and abnormal aleurone and subaleurone cells (Fig. 3A, 3B, 4A to 4F). These abnormal grain phenotypes could be related to alterations in carbon flux as a result of the modified (1,3;1,4)-β-glucan level. In addition, the

transgenic grain had a reduced starch content and lower grain weight, indicating a deficient loading of sugars into the endosperm cells. This is likely a result of stress response and may induce reactive oxygen species (ROS) accumulation in the transgenic grain (Rosa et al., 2009; Tanou et al., 2009; Xie et al., 2011; Kosová et al., 2014; Matros et al., 2015; Arshad et al., 2017). Previous studies showed that oligofructans can act as a ROS scavenger, in order to protect the transfer tissues from oxidative damage to ensure nutrient supply to the endosperm (Matros et al., 2015; Peukert et al., 2016). Fructans have also been shown to interact with the plasma membrane to stabilise the membrane during drying (Valluru and Van den Ende, 2008; Livingston et al., 2009). During early stages of grain development, oligofructans are abundant in the endosperm cavity (Peukert et al., 2014; Peukert et al., 2016) which can act as a ROS scavenger (Peukert et al., 2014; Matros et al., 2015). In this study, we propose more fructans are accumulated in the transgenic cavity compared to the WT grain (Hisano et al., 2004; Kawakami et al., 2008; den Ende, 2013) due to their roles in antioxidant activity and protection of cell membrane.

Nonetheless, the shrunken nature of the grain may be related to the presence of a large fluid-filled cavity and reduced starch filling, and as the grain dries, the cavity empties and tissues collapse. Interestingly, this phenotype does not appear in transgenic Golden Promise over-expressing *HvCslF6* (Burton et al., 2011), although it resembles the phenotype of transgenic barley lines with RNAi suppression of all Starch Branching Enzyme isoforms (Carciofi et al., 2012). This suggests that the hull-less cultivar may be more sensitive to attempts to modify cell wall composition. In the next chapter, differences in structural and cell wall composition in the endosperm transfer region between the transgenic grain and WT, which could cause the size of cavity to increase, are explored. In addition, we investigated how manipulation of (1,3;1,4)-β-glucan in the engineered barley resulted in modification of metabolism of other carbohydrates

including sucrose and fructans. This information may be valuable in helping us understand how the changes in carbohydrate metabolic networks that occur as a consequence of environmental stress or gene modification are regulated.

References

Arshad MS, Farooq M, Asch F, Krishna JSV, Prasad PVV, Siddique KHM (2017) Thermal stress impacts reproductive development and grain yield in rice. Plant Physiology and Biochemistry **115:** 57-72

Betts NS, Berkowitz O, Liu R, Collins HM, Skadhauge B, Dockter C, Burton RA, Whelan J, Fincher GB (2017) Isolation of Tissues and Preservation of RNA from Intact, Germinated Barley Grain. Plant J **91:** 754–765

Buckeridge MS (2010) Seed cell wall storage polysaccharides: models to understand cell wall biosynthesis and degradation. Plant Physiol **154:** 1017-1023

Burton RA, Collins HM, Kibble NA, Smith JA, Shirley NJ, Jobling SA, Henderson M, Singh RR, Pettolino F, Wilson SM, Bird AR, Topping DL, Bacic A, Fincher GB (2011) Over-expression of specific HvCslF cellulose synthase-like genes in transgenic barley increases the levels of cell wall (1,3;1,4)-beta-d-glucans and alters their fine structure. Plant Biotechnol J **9:** 117-135

Burton RA, Jobling SA, Harvey AJ, Shirley NJ, Mather DE, Bacic A, Fincher GB (2008) The genetics and transcriptional profiles of the cellulose synthase-like HvCslF gene family in barley. Plant Physiol **146:** 1821-1833

Carciofi M, Blennow A, Jensen SL, Shaik SS, Henriksen A, Buléon A, Holm PB, Hebelstrup KH (2012) Concerted suppression of all starch branching enzyme genes in barley produces amylose-only starch granules. BMC Plant Biol **12:** 223

den Ende WV (2013) Multifunctional fructans and raffinose family oligosaccharides. Front Plant Sci **4:** 247

Doblin MS, Pettolino FA, Wilson SM, Campbell R, Burton RA, Fincher GB, Newbigin E, Bacic A (2009) A barley cellulose synthase-like CSLH gene mediates (1,3;1,4)-beta-D-glucan synthesis in transgenic Arabidopsis. Proc Natl Acad Sci U S A **106:** 5996-6001

Handford MG, Baldwin TC, Goubet F, Prime TA, Miles J, Yu X, Dupree P (2003) Localisation and characterisation of cell wall mannan polysaccharides in Arabidopsis thaliana. Planta **218:** 27-36

Hensel G, Valkov V, Middlefell-Williams J, Kumlehn J (2008) Efficient generation of transgenic barley: The way forward to modulate plant–microbe interactions. Journal of Plant Physiology **165:** 71-82

Hisano H, Kanazawa A, Kawakami A, Yoshida M, Shimamoto Y, Yamada T (2004) Transgenic perennial ryegrass plants expressing wheat fructosyltransferase genes accumulate increased amounts of fructan and acquire increased tolerance on a cellular level to freezing. Plant Science **167:** 861-868

Kawakami A, Sato Y, Yoshida M (2008) Genetic engineering of rice capable of synthesizing fructans and enhancing chilling tolerance. Journal of experimental botany **59:** 793-802

Kosová K, Vítámvás P, Prášil IT (2014) Proteomics of stress responses in wheat and barley—search for potential protein markers of stress tolerance. Front Plant Sci **5**

Livingston DP, 3rd, Hincha DK, Heyer AG (2009) Fructan and its relationship to abiotic stress tolerance in plants. Cell Mol Life Sci **66:** 2007-2023

Matros A, Peshev D, Peukert M, Mock H-P, Van den Ende W (2015) Sugars as hydroxyl radical scavengers: proof-of-concept by studying the fate of sucralose in Arabidopsis. The Plant Journal **82:** 822-839

McCleary BV, Amado R, Waibel R, Neukom H (1981) Effect of galactose content on the solution and interaction properties of guar and carob galactomannans. Carbohydr Res **92:** 269-285

McCleary BV, Codd R (1991) Measurement of (1 → 3),(1 → 4)-β-D-glucan in barley and oats: A streamlined enzymic procedure. Journal of the Science of Food and Agriculture **55:** 303-312

Peukert M, Thiel J, Mock H-P, Marko D, Weschke W, Matros A (2016) Spatiotemporal Dynamics of Oligofructan Metabolism and Suggested Functions in Developing Cereal Grains. Front Plant Sci **6**

Peukert M, Thiel J, Peshev D, Weschke W, Van den Ende W, Mock H-P, Matros A (2014) Spatio-temporal dynamics of fructan metabolism in developing barley grains. The Plant Cell **26:** 3728-3744

Reid JG (1971) Reserve carbohydrate metabolism in germinating seeds of Trigonella foenum-graecum L.(Leguminosae). Planta **100:** 131-142

Rodríguez-Gacio MdC, Iglesias-Fernández R, Carbonero P, Matilla ÁJ (2012) Softening-up mannan-rich cell walls. J Exp Bot **63:** 3976-3988

Rosa M, Prado C, Podazza G, Interdonato R, González JA, Hilal M, Prado FE (2009) Soluble sugars—Metabolism, sensing and abiotic stress: A complex network in the life of plants. Plant Signal Behav **4:** 388-393

Shrawat AK, Becker D, Lörz H (2007) Agrobacterium tumefaciens-mediated genetic transformation of barley (Hordeum vulgare L.). Plant Science **172:** 281-290

Tanou G, Molassiotis A, Diamantidis G (2009) Induction of reactive oxygen species and necrotic death-like destruction in strawberry leaves by salinity. Environmental and experimental botany **65:** 270-281

Valluru R, Van den Ende W (2008) Plant fructans in stress environments: emerging concepts and future prospects. J Exp Bot **59:** 2905-2916

Vickers CE, Xue G, Gresshoff PM (2006) A novel cis-acting element, ESP, contributes to high-level endosperm-specific expression in an oat globulin promoter. Plant Molecular Biology **62:** 195-214

Wilson SM, Burton RA, Collins HM, Doblin MS, Pettolino FA, Shirley N, Fincher GB, Bacic A (2012) Pattern of deposition of cell wall polysaccharides and transcript

abundance of related cell wall synthesis genes during differentiation in barley endosperm. Plant Physiol **159:** 655-670

Xie YJ, Xu S, Han B, Wu MZ, Yuan XX, Han Y, Gu Q, Xu DK, Yang Q, Shen WB (2011) Evidence of Arabidopsis salt acclimation induced by up-regulation of HY1 and the regulatory role of RbohD-derived reactive oxygen species synthesis. The Plant Journal **66:** 280-292

Research Article

Method for hull-less barley transformation and manipulation of grain mixed-linkage beta-glucan

Running title: Transgenic hull-less barley

Wai Li Lim†, Helen M Collins†, Rohan R Singh, Natalie AJ Kibble, Kuok Yap, Jillian Taylor, Geoffrey B Fincher and Rachel A Burton*

ARC Centre of Excellence in Plant Cell Walls, School of Agriculture, Food and Wine, University of Adelaide, Waite Campus, Glen Osmond, South Australia, 5064, Australia

†These authors contributed equally to the project

***Correspondence:** Rachel A Burton (rachel.burton@adelaide.edu.au)

Edited by: Tobias I. Baskin, University of Massachusetts, USA

Received: November 15, 2017; Accepted: December 13, 2017

ABSTRACT

Hull-less barley is increasingly offering scope for breeding grains with improved characteristics for human nutrition; however recalcitrance of hull-less cultivars to transformation has limited use of these varieties. To overcome this, we have sought to develop an effective transformation system for hull-less barley using the cultivar Torrens. Torrens yielded a transformation efficiency of 1.8%, using a modified *Agrobacterium* transformation method. This method was used to over-express genes encoding synthases for the important dietary fibre component, (1,3;1,4)-β-glucan (mixed-linkage glucan), primarily found in starchy endosperm cell walls. Over-expression of the *HvCslF6* gene driven by an endosperm-specific promoter produced lines where mixed-linkage glucan content increased on average by 45%, peaking at 70% in some lines, with smaller increases in transgenic *HvCslH1*grain. Transgenic *HvCslF6* lines displayed alterations where grain had a darker colour, were more easily crushed than wild type and were smaller. This was associated with an enlarged cavity in the central endosperm and changes in cell morphology, includingaleurone and sub-aleurone cells. This work provides proof-of-concept evidence that mixed-linkage glucan content in hull-less barley grain can be increased by over-expression of the *HvCslF6* gene, but also indicates that hull-less cultivars may be more sensitive to attempts to modify cell wall composition.

INTRODUCTION

Barley grain develops from a caryopsis that is surrounded by a thick hull or husk, which consists of remnants of the outer palea and inner lemma. In hulled, or covered, barley varieties these tissues remain attached to the pericarp epidermis via a lipid layer during grain maturation, while the hull-less phenotype is controlled by a single *nud*gene on chromosome 7H (Taketa et al. 2008) and is associated with non-adherence of the pericarp and hull. Non-adherent hulls of barley can be readily removed during threshing in a manner similar to that observed for wheat and rice grains (Bhatty 1986). However, the majority of barley grown worldwide has an attached hull.

The potential for wider use of barley grain in healthy human foods is becoming increasingly recognised, but the hull represents a major impediment in the adoption of barley for food purposes because it causes problems with undesirable mouth feel rendering covered grain unpalatable for human consumption. For existing food applications the hull of covered barley grain is usually removed by pearling, but this causes concomitant losses in nutrient-rich embryo, aleurone and starchy endosperm tissues. As a result, there has been renewed interest in hull-less barley cultivars where these losses can be easily circumvented, and palatability is improved. Thus, hull-less barleys have lower processing costs and retain more valuable nutrients normally lost during pearling.

The major components of dietary fibre in barley and other cereal grains are the two cell wall polysaccharides, mixed-linkage glucans and arabinoxylans, together with fructans and resistant starch. In barley, (1,3;1,4)-β-glucan (mixed-linkage glucan) is the most abundant of these components and is therefore an important determinant of the overall level of soluble dietary fibre in grain, the consumption of which has been shown to improve human health by lowering the risk of serious dietary related diseases such as type II diabetes, cardiovascular disease and colorectal cancer (Collins et al. 2010; El Khoury et al. 2012).

Mixed-linkage glucans are polysaccharides consisting of unbranched, unsubstituted (1,3)- and (1,4)-linked β-glucosyl residues. Approximately 90% of the molecule is made up of blocks of two or three adjacent (1,4)-linkages separated by single (1,3)-linkages, which are irregularly spaced in such a way that prevents alignment of the polysaccharide (Burton et al. 2011). Consequently, large mixed-linkage glucan molecules are often soluble in water where they form solutions of high viscosity. The high viscosity of glucan solutions is thought to contribute to the health benefits of mixed-linkage glucan in human diets (Dikeman and Fahey 2006),while extensive bacterial fermentation of this polysaccharide in the human gastrointestinal tract is also a key determinant of its efficacy as desirable dietary fibre (El Khoury et al. 2012).

The synthesis of mixed-linkage glucan in barley is mediated by members of the *cellulose synthase-like* gene families, *CslF* and *CslH*(Burton et al. 2006; Doblin et al. 2009). Amongst these, *HvCslF6* is the most highly transcribed and is believed to be the most important gene for glucan synthesis in barley grain (Burton et al. 2008). This was confirmed in *cslf6* mutant lines (called *beta-glucanless* or *bgl*) that have very low levels of mixed-linkage glucan(Tonooka et al. 2009). Furthermore, *Agrobacterium*-mediated transformation of the hulled barley cultivar Golden Promise with the *HvCslF6* gene resulted in increases of more than 80% in mixed-linkage glucan content and 50% in the dietary fibre of transgenic grain (Burton et al. 2011). *Agrobacterium*-mediated transformation of Golden Promise is an established procedure in many laboratories world-wide with transformation frequencies ranging from 2 to 87% (Tingay et al. 1997; Matthews et al. 2001; Trifonova et al. 2001; Fang et al. 2002; Murray et al. 2004; Travella et al. 2005; Lange et al. 2006; Shrawat et al. 2007; Bartlett et al. 2008; Hensel et al. 2008). Attempts to transform other barley cultivars using this procedure have either failed completely or delivered variable transformation frequencies ranging from less than 1% up to approximately 8% (Murray et al. 2004; Hensel et al. 2008).

The experiments reported here were conducted to develop a robust and reproducible *Agrobacterium*-mediated transformation protocol for hull-less barley cultivars. This would provide the capability to make transgenic lines in newly released cultivars or key elite breeding lines and to assess the potential for increasing mixed-linkage glucan content in grain of a hull-less barley for human health benefits. The hull-less cultivar Torrens was transformed with over-expression constructs of the *HvCslF6* and *HvCslH1* genes, driven by the oat globulin starchy endosperm-specific promoter (*AsGlo*) (Vickers et al. 2006), and the physiological effects in the grain were compared with those of hulled transgenic Golden Promise carrying the same constructs (Burton et al. 2011).

RESULTS

Production of transformed callus and regeneration of transgenic plants

The standard conditions employed to transform Golden Promise served as a useful starting point to assess how amenable the hull-less varieties, Torrens, Macumba, and Finniss were to *Agrobacterium*-mediated transformation. At the end of the callus selection phase, the scutella had produced a mixture of callus types. The scutella of Torrens, typically generated a watery, transparent non-embryogenic callus that was occasionally interspersed with hard, nodular, slow-growing embryogenic callus, which was resistant to the selection agent (Figure 1A). By comparison, the scutella of WI4330 and Golden Promise predominantly produced large quantities of high quality, well developed, compact embryogenic callus under the selection conditions (Figure 1B and C). Overall, Golden Promise showed the highest frequency of callus induction at 100%, followed by WI4330 (82%), Finniss (80%), Torrens (74%) and Macumba (42%). The non-responsive scutella turned brown and failed to develop any hygromycin-resistant callus sectors (data not shown). Embryogenic callus of all five genotypes were transferred to regeneration medium to stimulate the production of transgenic plants. Both WI4330 and Golden Promise (Figure 1E and 1F) successfully produced plants but none were forthcoming from the transformed callus of the hull-less cultivars.

The use of cultured scutella in combination with the addition of acetosyringone to the co-cultivation medium and the transfer of co-cultivated scutella to callus induction medium containing Timentin for a week prior to callus selection were investigated in an attempt to regenerate plants from transformed callus of the hull-less cultivars. Not surprisingly, the response of the scutella to either the separate or combined treatments were highly variable (Supplementary Table 1), but in each case successful plant regeneration was achieved from transformed Torrens callus (Figure 1D). The transformation frequency (number of successful transgenic plants generated from the total number of scutella) for Torrens in these experiments ranged from 0.5 to 2.6% at an average of 1.8%. Putative Torrens transformants were successfully transferred to soil and the presence of the selectable marker gene was confirmed by Southern hybridisation analysis (Supplementary Figure 1). These modifications were not trialled with cultivar ‘Macumba”, while cultured ‘Finniss” scutella subjected to a “resting” step yielded a transformation frequency of 1.6%. An additional valuable observation was that the use of cultured scutella without added acetosyringone or Timentin was sufficient to boost the transformation frequencies of WI4330 from 1.3 to 7.3% and Golden Promise from 22.3 to 45%.

Transformation of Torrens with*AsGlo::HvCslF6* and *HvCslH1* constructs

The modified transformation protocol was used to regenerate seven independent transgenic *AsGlo::HvCslF6* andten*AsGlo*::*HvCslH1* Torrens plants which survived the transfer to soil and successfully produced grain. The transcript levels of the endogenous genes, *HvCslF6*transgene and *HvCslH1* transgene were measured using real-time quantitative PCR on cDNA from developing T_1 grain at 11 days after pollination (*HvCslF6*) and mature T_2 grain (*HvCslH1*). Total transcript levels were markedly higher in grain from transgenic lines compared to wild type plants, as shown for a subset of the transformants (Figure 2). Initial observations of the grain indicated a strong visible phenotype for the lines over-expressing *HvCslF6* (Figure 3B and 3C) when compared with wild type Torrens (Figure 3A) and the *HvCslH1* lines (Figure 3D) in that the transgenic grain was shrunken and very dark in colour. The four *HvCslF6* transgenic lines with the most severe phenotype were chosen for further detailed analysis. When placed on a light box, grains of wild type Torrens (Figure 3E) and the *HvCslH1* lines (Figure 3H) were translucent while some or all grain of the lines carrying the *HvCslF6* transgene were opaque (Figure 3F and 3G). When the dry transgenic grain was cut in half, the internal structure appeared altered compared with wild type grain (Figure 3I - M). The severity of this varied; for some grain the entire interior was darkened (Figure 3K) whilst for others the effect was more patchy (Figure 3J, L and M) but all darkened grain was severely shrunken (Figure 3J - M). None of the *HvCslH1* grain was observed to be shrunken (Figure 3D and 3H). PCR genotyping (data not shown) of the T_2 plants showed a consistent correlation with the presence of the *HvCslF6* transgene (Figure 2) and the dark grain phenotype (Figure 3).

The shrunken grain phenotype was quantified when grain weight was measured in the T_3 generation (Figure 4A). The weight of the Torrens wild type lines ranged from 34.7 to 49.5 g per 1000 grains, while the weight of the Torrens *HvCslF6* lines were generally lower and ranged from 11.4 to 41.0 g per 1000 grains. The grain weight of the *HvCslH1* lines were similar to the controls at between 29.3 to 40.3g (Figure 4A).

Barley lines transformed with*HvCslF6* and *HvCslH1* have altered levels of mixed-linkage glucanand reduced starch content

Mixed-linkage glucan levels in *HvCslF6* Torrens T3 transgenic grain lines were increased by up to 70% compared with wild type Torrens on a weight for weight basis (Figure 4B). However, to take into account the smaller grain sizes of some transgenic lines, the glucan content was also expressed on a per grain basis (Figure 4C). Due to the shrunken nature of the grain and reduced endosperm area, the amount of mixed-linkage glucan deposited in each grain was very low in many cases. There is variability between sister lines derived from the same T_0parent for the traits presented in Figure 4 that is likely to be due to the random selection of the grain for analysis, where some may still be

segregating for transgene copy number. By contrast, the mean mixed-linkage glucan (% w/w) content of Torrens lines transformed with *HvCslH1* was not significantly different to wild type (Figure 4B). However, two siblings of transgenic line H-26 contained significantly higher amounts when expressed on a per grain basis (Figure 4C). As with a previous study where the hulled Golden Promise cultivar was transformed with HvCslF6 (Burton et al. 2011), essentially all the Torrens transgenic lines over-expressing *HvCslF6* showed a reduced DP3:DP4 ratio (Figure 4D), typically from about 2.4:1 down to 2.0:1. The DP3:DP4 ratio is a measure of the ratio between the 3-O-β-cellobiosyl-D-glucose (DP3) and 3-O-β-cellotriosyl-D-glucose (DP4) oligosaccharides released after hydrolysis with (1,3;1,4)-β-glucanase (EC 3.2.1.73, lichenase).It gives an indication of the fine structure of the mixed-linkage glucan polysaccharide. This shift was not evident in the transgenic *HvCslH1* grain with most of the lines showing either similar or higher ratios to the controls (Figure 4D).

The starch content was measured in a subset of *HvCslF6* lines since some lines produced only a limited number of small-sized grain making them unsuitable for analysis (Figure 4E). Those lines analysed showed a significantly reduced starch content compared with the controls. One of the sibling lines of Torrens F6-16 had a very low grain weight at 11.4g per 1000 grains (Figure 4A) and a particularly low starch content of 22% (Figure 4E). There was no overall change in grain starch content of the Torrens *HvCslH1* lines (Figure 4E).

The force required to crush individual grains was measured using a flat anvil on the Instron. Significantly less force was needed to crush grain from Torrens lines F6-18 and F6-25 compared with the wild type grain (Figure 5).

Differences in embryo size and seedling development in *HvCslF6*transgenic lines

Adult T_2 plants of *HvCslF6* Torrens lines containing the greatest increases of grain mixed-linkage glucan, in particular F6-18, were slower growing than the wild type Torrens plants (Figure 6A). We observed that T_3 excised embryos of F6-18were bigger (Figure 6B) and contributed a significantly larger portion of whole grain weight, at 15% of the total grain weight, compared with just 4% of the total weight for the wild type grain (Figure 6C). The larger embryos did not appear to affect either germination speed or success rate since germination, as assessed by chitting, after two days from the start of imbibition, was 100%. For some lines the embryo also comprised a larger proportion of mature grain weight, for example F6-16, and F6-25 (Figure 6C) which can be attributed to the reduced size of the endosperm. Shoot and root lengths were measured for 7 day old T_2 seedlings (Figure 7A). Shoot length was consistent between lines (Figure 7A and 7B) but primary root length was significantly reduced for three out of the four *HvCslF6* over-expressing seedling lines as

compared with wild type control seedlings (Figure 7B). The dry weight of seedling shoots was measured and although there were no visible differences in the shoot length of the *HvCslF6* transgenic lines, they were thinner and weighed significantly less than the controls (Figure 7C). The dry weight of the roots was not measured as intact roots could not be rescued from the growing medium.

Internal grain morphology is perturbed in Torrens *HvCslF6* lines

The developing grain at 15 days after pollination was visually examined using light and immunofluorescence microscopy.The Torrens linesover-expressing *HvCslF6* were observed to contain a much larger cavity in the centre of the grain compared with wild type Torrens grain (Figure 8A and 8B). During development of wild type grain, the cells around the edge of the nucellar projection adjacent to the crease differentiate into specialised transfer cells (Figure 8C; Bewley and Black,1994). In the *HvCslF6* transgenic lines, these cells appeared to be deformed and in places were completely missing (Figure 8D) contributing to a more uneven and indeterminate cavity edge. Perturbations were also observed in the transgenic aleurone that were on average three cell layers thick, with strongly defined walls and a pronounced square shape (Figure 8F) compared with the wild type parent, which at this equivalent stage had only two layers of more oblong cells with evidence of the inner aleurone layer still differentiating (Figure 8E). In the transgenic lines, the sub-aleurone region was also missing and overall appeared to resemble much more mature grain at around 22 days after pollination as previously documented by Wilson et al. (2012). Brighter staining of mixed-linkage glucan was observed on the transgenic grain sections of F6-18when compared with the wild type grain, as indicated bystronger fluorescence signal strength in the aleurone, sub-aleurone and starchy endosperm tissues(Figure 8G and 8H).

DISCUSSION

Plant transformation is a crucial technology platform that underpins research into the functional analysis of genes, including those involved in cell wall biosynthesis and grain development in cereals. A widely used, standard *Agrobacterium*-mediated protocol developed for the tissue culture responsive cultivar Golden Promise (Tingay et al. 1997; Matthews et al. 2001) is usually adopted for the production of transgenic barley lines. This method has been successfully applied to other barley varieties, including to a set of Australian cultivars, although these consistently demonstrated lower transformation frequencies compared with Golden Promise (Murray et al. 2004; Hensel et al. 2008) and two Egyptian cultivars (Ibrahim et al. 2010). However, all but one of the transformed cultivars reported have been of the hulled variety, which have limited application for some end-uses including human food.

For a particular barley genotype, success of the transformation process was reliably indicated by the percentage of scutella producing embryogenic callus and the frequency of plant regeneration on selective callus induction and regeneration media.In this current study, all three hull-less varieties produced scutellum-derived callus at variable rates that resembled the highly regenerable material of the control cultivars Golden Promise and the breeding line WI4330, but none regenerated plants using the standard transformation regime. Freshly isolated scutella endure significant stresses following contact with *Agrobacterium* and immediate exposure to the selection agent following co-cultivation. To address these issues, minor modifications were made to the transformation procedure for cultivar Torrens. One day old cultured scutella were used for transformation and the inclusion of two further explant handling steps, namely the addition of acetosyringone to the co-cultivation medium (Shrawat et al. 2007; Hensel et al. 2008) and the transfer of co-cultivated scutella to a 'resting' medium containing Timentin but no selection agent (Shrawat et al. 2007), either individually or jointly, generated transgenic Torrens plants. Acetosyringone is a chemotactic compound released by some plant cells following wounding that both attracts *Agrobacterium* to the wound site and activates its virulence (*vir*) genes, triggering the initiation of T-DNA transfer (Godwin et al. 1991). The application of this compound boosts transformation efficiency of other monocots, including wheat (Wu et al. 2003), and so it is likely that its inclusion here renders the same effect. Presumably, the stress of *Agrobacterium* infection was reduced by using cultured scutella for transformation, while the more favourable tissue culture conditions achieved with the non-selective 'resting' step supported the recovery and growth of transformed cells in the scutellar mass, leading to sustained callus development and plant differentiation under selection pressure. Transformation frequencies for Golden Promise and WI4330 were also significantly increased when one day old cultured scutella were used for transformation even without a rest period or acetosyringone. Together, these modifications are likely to also be of value in the transformation of a range of other barley cultivars, broadening the portfolio of transformable cultivars in general.

Since an effective transformation protocol was successfully developed for the hull-less barley variety, Torrens, it was used in a proof-of-concept experiment aimed at defining the effects of specific candidate genes on quality characteristics relating to human health and nutrition applications. Therefore, as the initial test we chose to use genes that might improve the quality of barley grain in the context of human health by manipulating the dietary fibre content. Torrens barley was transformed with the *HvCslF6* and *HvCslH1* genes, which are known to encode mixed-linkage glucan synthases (Burton et al. 2006; Doblin et al. 2009). Mixed-linkage glucan is a major cell wall polysaccharide found in the endosperm tissues of a number of cereals (Welch and Lloyd 1989; Wood et al. 1991; Rudi et al. 2006; Pritchard et al. 2011), and it is an important component of dietary fibre in the human diet (Collins et al. 2010). Previous proof-of-function experiments in transgenic lines of the hulled Golden Promise variety demonstrated that over-expression of the barley cellulose synthase-

like *HvCslF6* gene increased grain mixed-linkage glucan levels by 80% and dietary fibre content by at least 50% (Burton et al. 2011), providing results that could be directly compared to those obtained with the hull-less cultivar Torrens transformed in the current study.

The results showed that over-expression of the *HvCslF6* gene often had an undesirable reduction in grain weight (Figure 4A) accompanied by striking changes to the visible phenotype of the grain, including a shrunken profile and darkened surface (Figure 3). These changes were also associated with the presence of a large cavity in the central endosperm of the grain where the bordering transfer cell layer was stretched and ragged (Figure 8A and 8B). Perturbations in the aleurone layer number and maturity were also evident and the amount of starch was reduced commensurate with increases in mixed-linkage glucan (Figure 4B and 4E). Grain of the most severely affected transgenic line (F6-18) also had larger embryos (Figure 6B) that did not appear to translate to effects on germination capability but impacted root length and shoot mass (Figure 7).

The reasons underlying the pleotropic effects in these linespotentially caused by the change in amount of mixed-linkage glucan, and possibly starch, are unclear. The promoter used to drive the transgene has been shown to be limited to the endosperm (Vickers et al. 2006). Changes in the endosperm of the transgenic lines may have deleterious effects on embryo development which may in turn affect the growth at the seedling stage. This implies that there may be a feedback loop in operation during grain development that has far-reaching effects.

We are as not yet able to explain the dark coloration of the hull-less transgenic grains, or the irregularly pigmented endosperm, observed in the current work (Figure 3). Most of the pigments in barley grain, which include anthocyanins, proanthocyanins, flavonols, phenolic acids and phenol glycosides are located in the hull and outer layers of the barley grain (Lampi et al. 2004) but in the transgenic *HvCslF6* lines discolouration is clearly found throughout the grain (Figure 3) leading to their opacity on the light box. Sincesuchgrain pigments have been shown to have benefits in human health (Katsube et al. 2003; Lila 2004) the production of the dark grain may represent a fortuitous advantage, especially as hull-less grain is not required to be pearled before consumption.

The shrunken nature of the grain is likely to be related to the presence of the large cavity in the endosperm during development. As the grain matures and dries, the cavity empties and tissues collapse inwards. This is seen for other barley shrunken endosperm mutants, for example the *seg1* to *seg8* series, where a range of different defects in developing grain cause the shrunken phenotype, many of which are still undefined(Felker et al. 1985). Why this effect is more severe in hull-less Torrens grain with a higher mixed-linkage glucan content compared with the similarly manipulated transgenic hulled Golden Promise described previously (Burton et al. 2011) remains unclear, and it will be informative to examine the nature of the cavity and its contents in future work.

The brittle nature of the mature transgenic hull-less grain is also unusual and implies that there are changes in the coherence or adhesion of the grain tissues or cell walls that allow the grain to be crushed more easily than the wild type grain. This is not due to the presence of an air-filled "bubble", since the inner cavity has already collapsed in mature grain so the presence of more aleurone cell layers with their thicker and less flexible cell walls may play a role in this and will require closer examination. At this stage, the distorted and discoloured appearance of the transgenic hull-less grain would not be conducive to consumer acceptance, should genetically modified barley become more widely received in the future.

Although the levels of mixed-linkage glucan were variable in the transgenic grains, a consistent effect in all the *HvCslF6* transgenic lines was the reduction in DP3:DP4 ratios in the polysaccharides (Figure 4D). Similar results were obtained when the hulled variety Golden Promise was transformed with an over-expression construct of the *HvCslF6* gene (Burton et al. 2011). This observation is presumably related to the particular three-dimensional structure of each glucan synthase protein (Jobling 2015; Dimitroff et al. 2016) where the protein derived from the transgene differs from the endogenous form. However, the reduced DP3:DP4 ratio would predict an increase in the percentage of the mixed-linkage glucan that is soluble in water, and it is the water-soluble fraction that is believed to impart the greatest benefit for human health (Collins et al. 2010).

When the Torrens barley was transformed with the *HvCslH1* gene, which also encodes a glucan synthase (Doblin et al. 2009), there was no reduction in grain size and only two sister lines showed an increase in mixed-linkage glucan content on a per grain basis and a change in the DP3:DP4 ratios of this polysaccharide (Figure 4). This is probably explained by the fact that the *HvCslH1* gene is normally expressed at very low levels in the developing barley grain (Burton et al. 2008; Doblin et al. 2009) and possibly implies that necessary additional protein co-factors for glucan synthesis were not present in this tissue.

In summary, we have developed a method for the transformation of the hull-less barley variety, Torrens, at acceptable frequencies, using modifications that also significantly enhance the transformation rate of established hulled cultivars and which can now be more widely applied. We have shown that the mixed-linkage glucan level of transgenic hull-less grain can be increased by over-expression of the *HvCslF6* gene. In addition, the fine structure of the polysaccharide, as measured by the DP3:DP4 ratio, is altered in the *HvCslF6* lines in such a direction that would presumably be beneficial in human health applications. However, these changes are accompanied by significant morphological and end-use penalties in the hull-less grain, including a reduced size, shrunken and darkened appearance and perturbations in the organisation of the inner grain tissues, including a large central cavity in the endosperm and abnormal aleurone cells. Over-expression of the *HvCslF6* gene also caused a reduction in the starch content of the grain. These pleotropic effects are much more

severe than those reported for similarly manipulated transgenic hulled barley grain and the underlying metabolic changes will be the subject of on-going research.

MATERIALS AND METHODS

Plant Material and barley transformation

Details of the barley germplasm used in this study are supplied in Supplementary Table 2. Donor plants of three hull-less cultivars Torrens, Macumba and Finniss and two hulled positive controls, Golden Promise and the elite Australian breeding line WI4330 were grown under conditions described previously by Burton et al. (2011).The *AsGlo::HvCslF6* construct (Burton et al. 2011) and the *AsGlo::HvCslH1* construct built in the same binary vector with a full-length *HvCslH1* cDNA (Doblin et al. 2009) were transformed into barley using the standard *Agrobacterium*-mediated transformation protocol developed by Tingay et al. (1997) for Golden Promise and modified by Matthews et al. (2001). Further modifications of this procedure were performed including the culture of scutella on callus induction medium in the dark at room temperature for a day prior to the infection step, the addition of 500µMacetosyringone to the co-cultivation medium (Shrawat et al. 2007; Hensel et al. 2008) and the use of a "resting" step, whereby co-cultivated scutella were transferred to callus induction medium containing Timentin at 150mg/l (SmithKline Beecham, Pty, Ltd., Melbourne, Australia) at 22ºC for a week prior to callus selection (Shrawat et al. 2007).

Southern hybridisation analysis

The transgenic status of independent lines and the number of transgene insertion loci were determined by Southern hybridisation analysis using the restriction endonuclease, *Eco*RV, which cuts the genomic DNA of transformed plants once in the T-DNA region and in the genomic DNA flanking the site of transgene insertion.

Plant DNA was extracted from leaf tissue using the protocol described by Guidet et al. (1991). The DNA pellet was dissolved in TE buffer (10mM Tris-HCl, 1mM EDTA, pH 8.0) containing 40µg/ml RNAse A. Digested DNA (15µg) was separated on a 1% (w/v) agarose gel and transferred to a Hybond-XL nylon membrane (GE Healthcare Ltd, Little Chalfont, Buckinghamshire, UK) with 0.4M NaOH, according to the manufacturer's instructions.

A 1.1kb *Xho*I DNA fragment, excised from plasmid pCAMBIA1390, was used as a probe to detect *hpt* sequences in the genomic DNA of the transformed plants. This was extracted from an agarose gel fragment using the Nucleospin Extract II kit (Macherey-Nagel, Düren, Germany), according to the

manufacturer's instructions. The probe was labelled by random priming (Feinberg and Vogelstein 1983) using the MegaPrime DNA labelling system (GE Healthcare Ltd). Unincorporated nucleotides were separated from the radioactively labelled DNA by gel filtration through a Sephadex G-100 column. Membrane hybridisation was conducted at 65ºC in a 0.5M phosphate buffer, pH 7.2, containing 7% (w/v) SDS and 10mM Na_2EDTA, as described in the product booklet supplied with the membrane. Following hybridisation, the membrane was washed with 0.1x SSC, 0.1% (w/v) SDS at 65ºC for 20 min, air-dried and exposed to X-ray film (RX Fuji Medical X-ray film; RX-U, Tokyo, Japan).

Assessment of transgenic lines

Primary transformants were grown to maturity under standard glasshouse conditions (Burton 2004).The presence of the transgene was confirmed using the REDExtract-N-AmpPlant PCR-Kit (Sigma-Aldrich, Australia) as outlined in Burton et al. (2011) and in some cases verified by Southern hybridisation. Wild type control plants were grown alongside each batch of plants. Mature grain was hand harvested and threshed. The 1000 grain weight values were calculated from the weight of 100 grains from each line. Ten randomly selected T_3 grain from each line, including controls, were ground using a Capmix dental amalgam mixer to provide a bulk flour sample. All analyses were performed on this bulk flour sampleusing duplicate technical replications and calculated on a dry weight whole grain basis.

RNA isolation, cDNA synthesis and real-time quantitative PCR

Developing endosperm tissue was collected from ten randomly selected T_1 grain (*HvCslF6*) or mature T_2 grain (*HvCslH1*), pooled as a bulk sample for total RNA extraction, followed by cDNA synthesis as per Burton et al. (2008) and Betts et al. (2017). Real-timequantitative PCR was performed according to Burton et al. (2008) using the primers HvCslF6_F: TGGGCATTCACCTTCGTCAT,HvCslF6_R: TCAATGGAGCCAGCCATAGAG, HvCslH1_F: TGCTGTGGCTGGATGGTGTT and HvCslH1_R: AACGCAGCCACAATCAAACCA. Data was normalised using the reference genes *HvCyclophilin*, *HvGAPdH2*, *HvHSP70*, and *HvTubulin*(Burton et al. 2008)

Grain mixed-linkage glucan and starch assays

Grain mixed-linkage glucan was measured on 15mg flour using a scaled down version of the Megazyme mixed-linkage beta-glucan assay (McCleary and Codd 1991) as outlined in Burton et al. (2011). Results are presented as both a percentage ofmixed-linkage glucan per gram of flour (%w/w) and on a mg per grain basis.

After hydrolysis with lichenase [EC 3.2.1.73; 1,3-1,4-beta-D-glucan 4-glucanohydrolase], a portion of the hydrolysate was collected and stored at -20°C for HPAEC analysis of the G4G3G (DP3) and G4G4G3G (DP4) oligosaccharides. Hydrolysates were separated on a solid phase extraction (SPE) cartridge packed with graphitized carbon (Varian Bond Elute Carbon 50mg-1) as outlined in Ermawar et al. (2015). The oligosaccharides were dissolved in 1mL water and analysed using high pH anion exchange chromatography (HPAEC) on a Dionex ICS-5000 using a DionexCarboPAC PA-200 column (3x250mm) as outlined by Ermawar et al. (2015). The areas under peaks were compared with standards of DP3 and DP4 oligosaccharide standard curves.

Starch content was measured on 25mg flour using a small-scale version of the Megazyme Total Starch Assay (amyloglucosidase⁄ α-amylase method) (McCleary et al. 1994)and presented as a percentage of starch per gram of flour (%w/w).

All analyses were performed using duplicate technical replications.

Grain germination, seedling and embryo phenotyping

The viability of wild type Torrens, Null and transgenic *CslF6* lines, F6-15, F6-16, F6-18 and F6-25 (20 T_3grains each) were placed in 10cm Petri dishes lined with two sheets of 90mm Whatman filter paper. . An additional 80 wild type grains were added to the Petri dish. These grains were kept separate and were discarded once germinated. A 4 mL aliquot of water was added, and the grain was allowed to germinate in the dark at 20°C for 72h. Chitted grains were counted and removed every 24 h.

To measure the shoot and root length of seedlings, 10 grains of each line were placed in a Petri dish and incubated in dark and moist conditions for 24h at 4°C before being transferred to seed germination pouches (PhytoTC) at 20°C for one week. The length of the shoots and roots were measured and the average length calculated. The shoots were collected, weighed, freeze-dried and re-weighed.

To determine embryo weight, mature grain was imbibed in water for 6h. The embryo was excised with a scalpel blade, collected in a 2 mL Eppendorf tube and freeze dried. A total of 20 embryos were collected for each line. The average embryo weight was expressed as a percentage of the total grain weight.

ImmunofluorescentLight Microscopy

Developing T_3 grain 15 days after pollination was fixed in 0.25% (v/v) glutaraldehyde, 4% (w/v) paraformaldehyde and 4% (w/v) sucrose in Phosphate Buffered Saline (PBS), pH 7.2, dehydrated and embedded in LR White resin according to Burton et al. (2011). Embedded tissue was sectioned (1µm thickness) on an ultramicrotome using a diamond knife and dried onto polysine coated microscope slides (ThermoFisher Scientific).

Immuno-chemical analysis of mixed-linkage glucans was performed according to Burton et al. (2011) using the primary BG1 murine monoclonal antibody (Biosupplies Australia, Parkville, Vic., Australia) raised against barley mixed-linkage glucan. This was followed by the secondary antibody Dylight 555 goat anti-mouse IgG (H+L) (Invitrogen, Australia) for 1h at room temperature. Sections were washed with 1% (w/v) bovine serum albumin in PBS, stained with 0.1% (w/v) Calcofluor White 2MR (Sigma-Aldrich, St.Louis, MO) for 90sec, rinsed with water and mounted with 90% (v/v) glycerol. Images were captured using an Axio Imager M2 mounted on a Carl Zeiss fluorescence microscope (Carl Zeiss, Oberkochen, Germany).

Mechanical properties

To measure mechanical strength, T_3grains were compressed and monitored for their break point. A small flat-faced puncture probe (2mm^2 at tip) was mounted in a single column Instron 5543 testing system (Instron, 825 University Ave., Norwood, MA, USA) and penetration resistance at maximum load (Newtons) was determined at an anvil movement rate of 100mm/min. The penetration was set to stop when the peak penetration load dropped sharply by 30%.

Statistical analysis

ANOVA was performed using the software package IBM SPSS statistics 24. Data was omitted from analysis when there were fewer than two biological replicates.

ACKNOWLEDGMENTS

This research was supported by funding from the Adelaide Graduate Research Scholarship (AGRS), Australian Research Council Centre of Excellence in Plant Cell Walls and the CSIRO Flagship Collaboration Fund. We would like to thank Caitlin Byrt for valuable discussion on the manuscript, and Neil Shirley and Sandy Khor for assistance with the QPCR. The authors gratefully acknowledge Amanda Box from the University of Adelaide Barley Breeding Program for supplying Torrens, Macumba and Finniss grain for experimental purposes, Robin Hosking, Lidia Mischis and Kylie Neumann for their glasshouse assistance, the Centre for the Application of Molecular Biology to International Agriculture for providing gene construct pCAMBIA1390. We also would like to thank

Ian Dundas and Dawn Verlin for the use of their laboratory equipment to perform the Southern hybridisation analyses and Gwen Mayo, from Adelaide Microscopy, Waite Facility, University of Adelaide for assistance with microscopic analysis.

AUTHOR CONTRIBUTIONS

W.L.L., H.M.C, N.A.J.K, G.B.F and R.A.B conceived the project and designed the experiments. W.L.L., J.T. and K.Y. performed the biochemical and physical analysis. W.L.L and H.M.C analysed the data. W.L.L., H.M.C, N.A.J.K and R.A.B wrote and edited the manuscript.

REFERENCES

Bartlett JG, Alves SC, Smedley M, Snape JW, Harwood WA (2008) High-throughput Agrobacterium-mediated barley transformation. **Plant Methods** 4: 1-12

Betts NS, Berkowitz O, Liu R, Collins HM, Skadhauge B, Dockter C, Burton RA, Whelan J, Fincher GB (2017) Isolation of Tissues and Preservation of RNA from Intact, Germinated Barley Grain. **Plant J** 91: 754–765

Bewley JD, Black M (1994) *Seeds: Physiology of development and germination.* 2nd edn.Springer Science & Business Media, US

Bhatty RS (1986) The potential of hull-less barley. A review. **Cereal Chem** 63: 97-103

Burton RA, Collins HM, Kibble NAJ, Smith JA, Shirley NJ, Jobling SA, Henderson M, Singh RR, Pettolino F, Wilson SM, Bird AR, Topping DL, Bacic A, Fincher GB (2011) Over-expression of specific *HvCslF* cellulose synthase-like genes in transgenic barley increases the levels of cell wall (1,3;1,4)-ß-D-glucans and alters their fine structure. **Plant Biotechnol J** 9: 117-135

Burton RA, Jobling SA, Harvey AJ, Shirley NJ, Mather DE, Bacic A, Fincher GB (2008) The genetics and transcriptional profiles of the cellulose synthase-like HvCslF gene family in barley. **Plant Physiol** 146: 1821-1833

Burton RA, Shirley, N.J., King, B.J., Harvey, A.J., Fincher, G.B., (2004) The CesA gene family of barley. Quantitative analysis of transcripts reveals two groups of co-expressed genes. **Plant Physiol** 134: 224-236

Burton RA, Wilson SM, Hrmova M, Harvey AJ, Shirley NJ, Stone BA, Newbigin EJ, Bacic A, Fincher GB (2006) Cellulose synthase-like CslF genes mediate the synthesis of cell wall (1,3;1,4)-beta-D-glucans. **Science** 311: 1940-1942

Collins HM, Burton RA, Topping DL, Liao M-L, Bacic A, Fincher GB (2010) Variability in fine structures of noncellulosic cell wall polysaccharides from cereal grains: Potential Importance in Human Health and Nutrition. **Cereal Chem** 87: 272-282

Dikeman CL, Fahey GC (2006) Viscosity as related to dietary fiber: A review. **Crit Rev Food Sci** 46: 649-663

Dimitroff G, Little A, Lahnstein J, Schwerdt JG, Srivastava V, Bulone V, Burton RA, Fincher GB (2016) (1,3;1,4)-β-Glucan biosynthesis by the CSLF6 Enzyme: Position and flexibility of catalytic residues influence product fine structure. **Biochemistry** 55: 2054-2061

Doblin MS, Pettolino FA, Wilson SM, Campbell R, Burton RA, Fincher GB, Newbigin E, Bacic A (2009) A barley *cellulose synthase-like CSLH* gene mediates (1,3;1,4)-beta-D-glucan synthesis in transgenic *Arabidopsis*. **Proc Natl Acad Sci USA** 106: 5996-6001

El Khoury D, Cuda C, Luhovyy BL, Anderson GH (2012) Beta glucan: Health benefits in obesity and metabolic syndrome. **J Nutr Metabolism** 2012: 28

Ermawar RA, Collins HM, Byrt CS, Betts NS, Henderson M, Shirley NJ, Schwerdt J, Lahnstein J, Fincher GB, Burton RA (2015) Distribution, structure and biosynthetic gene families of (1,3;1,4)-beta-glucan in *Sorghum bicolor*. **J Integr Plant Biol** 57: 429-445

Fang Y-D, Akula C, Altpeter F (2002) Agrobacterium-mediated barley (*Hordeum vulgare* L.) transformation using green fluorescent protein as a visual marker and sequence analysis of the T-DNA∝barley genomic DNA junctions. **J Plant Physiol** 159: 1131-1138

Feinberg AP, Vogelstein B (1983) A technique for radiolabeling DNA restriction endonuclease fragments to high specific activity. **Anal Biochem** 132: 6-13

Felker FC, Peterson DM, Nelson OE (1985) Anatomy of immature grains of eight maternal effect shrunken endosperm barley mutants. **Am J Bot**: 248-256

Godwin I, Todd G, Ford-Lloyd B, Newbury HJ (1991) The effects of acetosyringone and pH on Agrobacterium-mediated transformation vary according to plant species. **Plant Cell Rep** 9: 671-675

Guidet F, Rogowsky P, Taylor C, Song W, Langridge P (1991) Cloning and characterisation of a new rye-specific repeated sequence. **Genome** 34: 81-87

Hensel G, Valkov V, Middlefell-Williams J, Kumlehn J (2008) Efficient generation of transgenic barley: The way forward to modulate plant–microbe interactions. **J Plant Physiol** 165: 71-82

Ibrahim AS, El-Shihy OM, Fahmy AH (2010) Highly efficient *Agrobacterium tumefaciens*-mediated transformation of elite Egyptian barley cultivars. **Am Eurasian J Sustain Agric** 4: 403-413

Jobling SA (2015) Membrane pore architecture of the CslF6 protein controls (1-3,1-4)-β-glucan structure. **Science Advances** 1: e1500069

Katsube N, Iwashita K, Tsushida T, Yamaki K, Kobori M (2003) Induction of apoptosis in cancer cells by bilberry (*Vaccinium myrtillus*) and the anthocyanins. **J Agr Food Chem** 51: 68-75

Lampi A-M, Moreau RA, Piironen V, Hicks KB (2004) Pearling barley and rye to produce phytosterol-rich fractions. **Lipids** 39: 783-787

Lange M, Vincze E, Møller MG, Holm PB (2006) Molecular analysis of transgene and vector backbone integration into the barley genome following Agrobacterium-mediated transformation. **Plant Cell Rep** 25: 815-820

Lila MA (2004) Anthocyanins and human health: An in vitro investigative approach. **J Biomed Biotechnol** 2004: 306-313

Matthews PR, Wang M-B, Waterhouse PM, Thornton S, Fieg SJ, Gubler F, Jacobsen JV (2001) Marker gene elimination from transgenic barley, using co-transformation with adjacent `twin T-DNAs' on a standard Agrobacterium transformation vector. **Mol Breeding** 7: 195-202

McCleary BV, Codd R (1991) Measurement of (1;3),(1;4)-beta-D-glucan in barley and oats - A streamlined enzymatic procedure. **J Sci Food Agr** 55: 303-312

McCleary BV, Solah V, Gibson TS (1994) Quantitative Measurement of Total Starch in Cereal Flours and Products. **J Cereal Sci** 20: 51-58

Murray F, Brettell R, Matthews P, Bishop D, Jacobsen J (2004) Comparison of Agrobacterium-mediated transformation of four barley cultivars using the GFP and GUS reporter genes. **Plant Cell Rep** 22: 397-402

Pritchard JR, Lawrence GJ, Larroque O, Li Z, Laidlaw HKC, Morell MK, Rahman S (2011) A survey of β-glucan and arabinoxylan content in wheat. **J Sci Food Agr** 91: 1298-1303

Rudi H, Uhlen AK, Harstad OM, Munck L (2006) Genetic variability in cereal carbohydrate compositions and potentials for improving nutritional value. **Anim Feed Sci Tech** 130: 55-65

Shrawat AK, Becker D, Lörz H (2007) *Agrobacterium tumefaciens*-mediated genetic transformation of barley (Hordeum vulgare L.). **Plant Sci** 172: 281-290

Taketa S, Amano S, Tsujino Y, Sato T, Saisho D, Kakeda K, Nomura M, Suzuki T, Matsumoto T, Sato K, Kanamori H, Kawasaki S, Takeda K (2008) Barley grain with adhering hulls is controlled by an ERF family transcription factor gene regulating a lipid biosynthesis pathway. **Proc Natl Acad Sci USA** 105: 4062-4067

Tingay S, McElroy D, Kalla R, Fieg S, Wang M, Thornton S, Brettell R (1997) *Agrobacterium tumefaciens*-mediated barley transformation. **Plant J** 11: 1369-1376

Tonooka T, Aoki E, Yoshioka T, Taketa S (2009) A novel mutant gene for (1,3;1,4)-beta-D-glucanless grain on barley (*Hordeum vulgare* L.) chromosome 7H. **Breeding Sci** 59: 47-54

Travella S, Ross SM, Harden J, Everett C, Snape JW, Harwood WA (2005) A comparison of transgenic barley lines produced by particle bombardment and Agrobacterium-mediated techniques. **Plant Cell Rep** 23: 780-789

Trifonova A, Madsen S, Olesen A (2001) Agrobacterium-mediated transgene delivery and integration into barley under a range of in vitro culture conditions. **Plant Sci** 161: 871-880

Vickers CE, Xue GP, Gresshoff PM (2006) A novel cis-acting element, ESP, contributes to high-level endosperm-specific expression in an oat globulin promoter. **Plant Mol Biol** 62: 195-214

Welch RW, Lloyd JD (1989) Kernel (1-3) (1-4)-beta-D-glucan content of oat genotypes. **J. Cereal Sci** 9: 35-40

Wilson SM, Burton RA, Collins HM, Doblin MS, Pettolino F, Shirley N, Fincher GB, Bacic A (2012) Pattern of deposition of cell wall polysaccharides and transcript abundance of related cell wall synthesis genes during differentiation in barley (*Hordeum vulgare*) endosperm. **Plant Physiol**159: 655-670

Wood PJ, Weisz J, Fedec P (1991) Potential for beta-glucan enrichment in brans derived form oat (Aven-Sativa L) cultivars of diffeent (1-3),(1-4)-beta-D-glucan concentrations. **Cereal Chem** 68: 48-51

Wu H, Sparks C, Amoah B, Jones H (2003) Factors influencing successful Agrobacterium-mediated genetic transformation of wheat. **Plant Cell Rep** 21: 659-668

Supplementary Figure 1. Southern hybridisation analysis of a subset of the Torrens T_0*HvCslF6*transformants. Genomic DNA of transformants (F6-15 to -18) and a non-transformed plant (WT) was digested with EcoRV and hybridised with a radiolabelled fragment of the hygromycin B phosphotranferase gene used for selection of the transgenic plants. The sizes of the DNA marker fragments are indicated on the left-hand side of the autoradiogram.

Supplementary Table 1: The effects of acetosyringone and a "resting" step on the transformation of 'Torrens' with *proAsGlo::HvCslF6* (a) and *proAsGlo::HvCslH* (b)

Supplementary Table 2: Information about the five barley genotypes used in this study

Figure legends:

Figure 1. The emergence of scutellum-derived, embryogenic (*) callus and plant regeneration on selection media. A, DTorrens, B,EWI4330 and C, F Golden Promise

Figure 2. Real time quantitative PCR analysis of transgenic grain. A. Total combined levels of the *HvCslF6* transcript derived from both the transgene and endogenous gene in developing T_1 grain 11 days after pollination B. Total combined levels of the *HvCslH1* transcript derived from both the transgene and endogenous gene in mature T_2 grain. Levels of the endogenous *HvCslF6* and *HvCslH1* transcripts are observed to be lower in the wild type (WT Torrens) and wild type grain from plants put through the tissue culture process (WT (tc)) in comparison to the transgenic lines carrying the respective transgenes.

Figure 3. The visual phenotype of transgenic barley grain.T_1transgenic barley graintransformed with*HvCslF6* or *HvCslH1*.A, E: wild type (WT) Torrens. B, F: Torrens F6-18. C, G: Torrens F6-24. D, H: Torrens H-25. E-H were photographed on a light box:I-M: the internal structures of wild type Torrens (I) and the transgenic *HvCslF6* lines (J-M). Scale bar: 5mm

Figure 4. Compositional analysis of transgenic (T_3) barley grain over-expressing *HvCslF6* and *HvCslH1*.A: 1000 grain weight (g). B: Mixed-linkage glucan (% w/w). C: Mixed-linkage glucan (mg per grain). D: DP3:DP4 oligosaccharide ratio after treatment with (1,3;1,4) -β-glucanase. E: starch (% w/w), error bars standard deviation n = 2-6, where no error bars are shown n≤2, WT: wild type Torrens, WT(tc): wild type from tissue culture. Ten T_3 grain were randomly selected and ground to a bulk flour which was subsequently used for all analyses. Line names in common are sister lines derived from the same T_0 transgenic event. *significantly different to the wild type Torrens (WT) ($P<0.05$)

Figure 5. Test of the strength of the grain of transgenic (T_3) barley lines over-expressing *HvCslF6* by Instron crush test. WT: wild type Torrens, WT(tc): wild type from tissue culture. *significantly different to the parent ($p<0.01$)

Figure 6. Plant and embryo phenotypes of transgenic Torrens barley lines over-expressing *HvCslF6*.A: 50 day old plants of wild type Torrens and a T_2 plant of line F6-18. B: Embryos excised from mature grain (T_3). C: Average weight of embryo (mg) (red) and the proportion of embryo per seed (blue), WT: wild type Torrens, WT(tc): wild type from tissue culture. *Significantly different to wild type Torrens ($P<0.05$)

Figure 7. Phenotypic analyses of transgenic (T_3) Torrens barley seedlings over-expressing *HvCslF6.*A: germinated grain showing root and shoot length. B: length of shoots (blue) and roots (red) average of 10 grains, C: average dry shoot weight, *significantly different to wild type Torrens ($P<0.05$). Scale bar: 1cm

Figure 8. Detailed internal morphology of developing grain(15 days after pollination) ofwild type Torrens (A, C, E, G) and F6-18 transgenic barley over-expressing *HvCslF6* (B, D, F, H). A and B; thick sections photographed over a light box. C, D, E and F; toluidine blue stained sections. G and H; immuno-histochemical analysis of mixed-linkage glucan with the antibody BG1. np: nucellar projection, ec: endosperm cavity, etc: endosperm transfer cells, p/t: pericarp and testa, a: aleurone, sa: sub-aleurone, se: starchy endosperm. Scale bar: 100µm

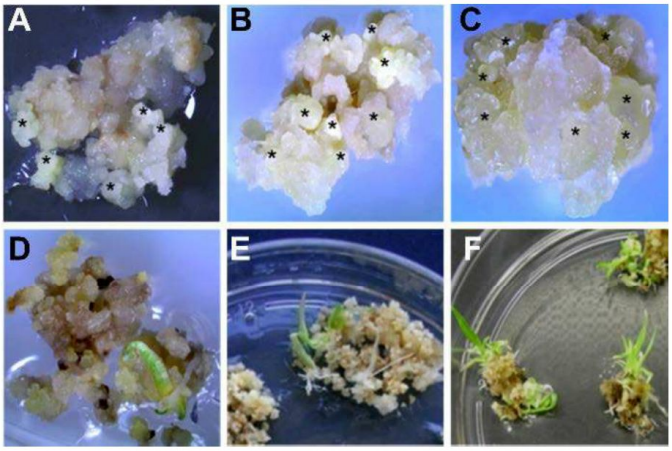

Figure 1b

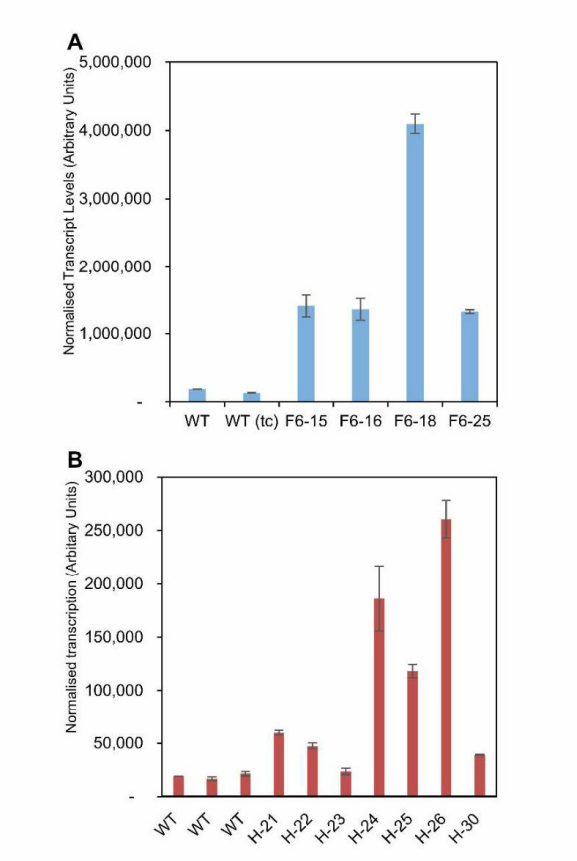

Figure 2

Figure 3c

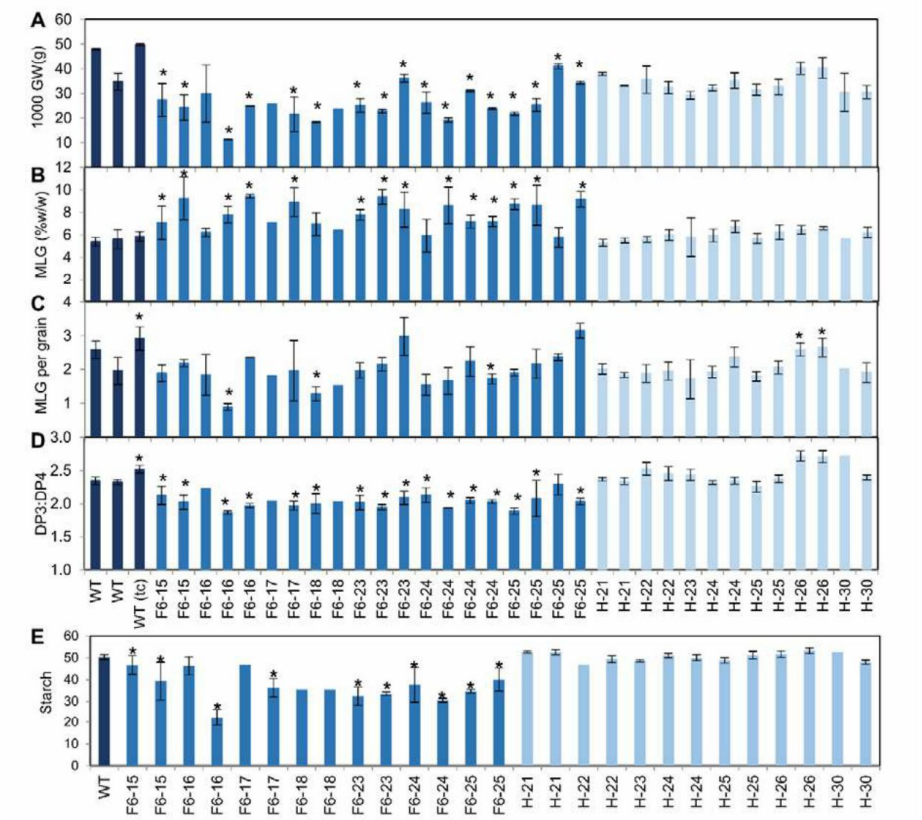

Figure 4b

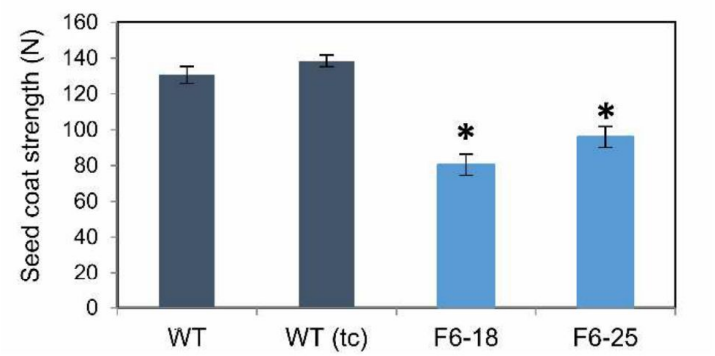

Figure 5

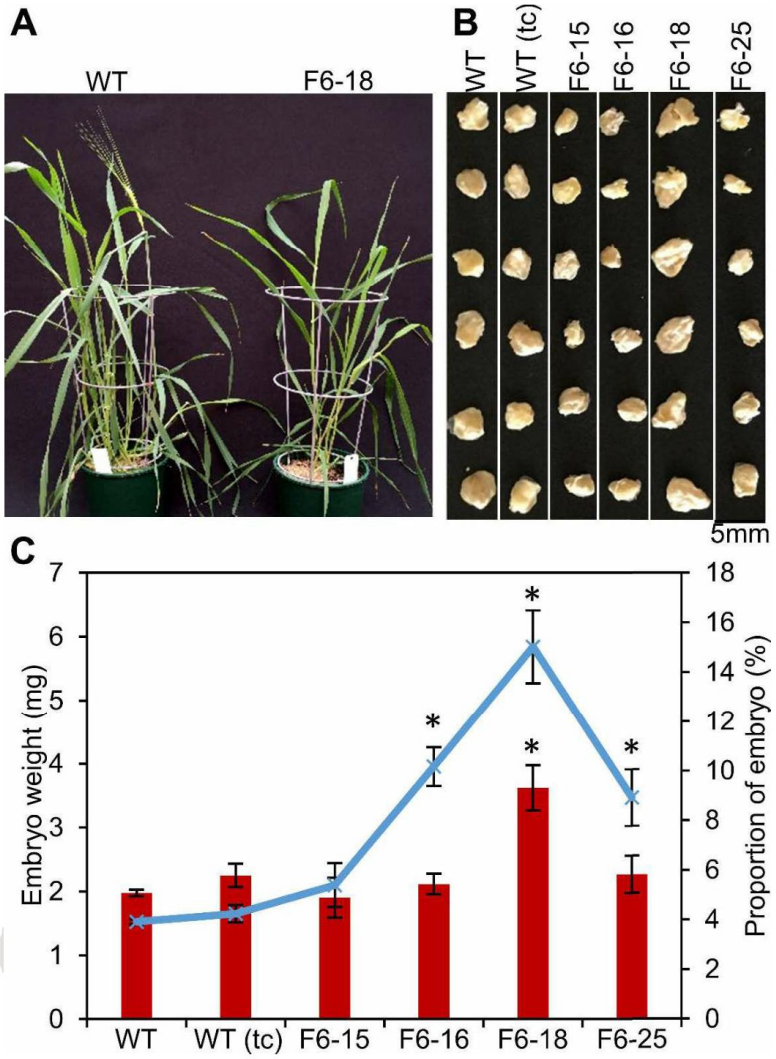

Figure 6b

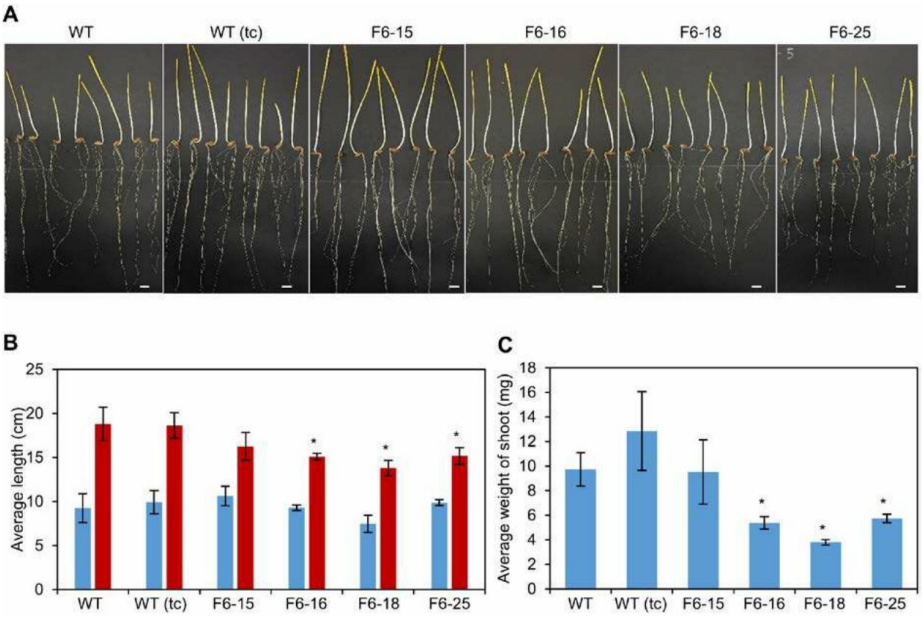

Figure 7b

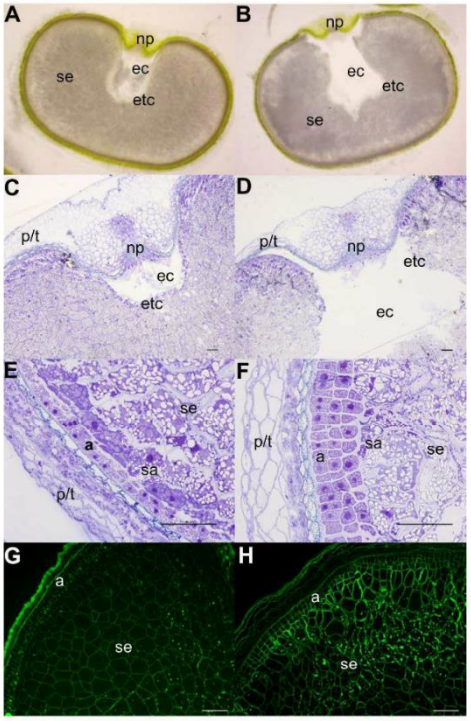

Figure 8c

Chapter 3

Overexpression of *HvCslF6* gene in Hull-less Barley Grain Alters Carbon Partitioning and Impairs Endosperm Development

Statement of Authorship

Title of Paper	Over-expression of *CslF6* gene in hull-less barley grain alters carbohydrate partitioning and impairs grain development
Publication Status	☐ Published ☐ Accepted for Publication ☐ Submitted for Publication ☑ Unpublished and Unsubmitted w ork w ritten in manuscript style
Publication Details	Wai Li Lim, Helen Collins, Caitlin Byrt, Jelle Lahnstein, Neil Shirley, Matthew Aubert, Matthew Tucker, Manuela Peukert, Andrea Matros and Rachel Burton

Principal Author

Name of Principal Author (Candidate)	Wai Li Lim		
Contribution to the Paper	Grew plants and prepared barley tissues. Performed all analytical experiments, all microscopy work, MALDI-MSI analysis, protein work, designed primers and prepared cDNA for qPCR and prepared manuscript.		
Overall percentage (%)	80		
Certification:	This paper reports on original research I conducted during the period of my Higher Degree by Research candidature and is not subject to any obligations or contractual agreements with a third party that would constrain its inclusion in this thesis. I am the primary author of this paper.		
Signature		Date	27 July 2017

Co-Author Contributions

By signing the Statement of Authorship, each author certifies that:

iv. the candidate's stated contribution to the publication is accurate (as detailed above);
v. permission is granted for the candidate in include the publication in the thesis; and
vi. the sum of all co-author contributions is equal to 100% less the candidate's stated contribution.

Name of Co-Author	Helen Collins		
Contribution to the Paper	Supervised experiment design, data analysis and interpretation. Assisted with manuscript.		
Signature		Date	31/7/2017

Name of Co-Author	Caitlin Byrt		
Contribution to the Paper	Supervised experiment design, data analysis and interpretation. Assisted with manuscript.		
Signature		Date	21/7/17

Name of Co-Author	Jelle Lahnstein		
Contribution to the Paper	Assisted with HPLC work.		
Signature		Date	21 July 2017

Name of Co-Author	Neil Shirley		
Contribution to the Paper	Performed all qPCR work.		
Signature		Date	21/7/17

Name of Co-Author	Matthew Aubert		
Contribution to the Paper	Performed AsGlo-YFP transgenic work.		
Signature		Date	21/07/2017

Name of Co-Author	Matthew Tucker		
Contribution to the Paper	Assisted with AsGlo-YFP transgenic work.		
Signature		Date	21/7/17

Name of Co-Author	Manuela Peukert		
Contribution to the Paper	Supervised experimental design, data analysis and interpretation. Assisted with MALDI-MSI experiments and manuscript.		
Signature		Date	27/06/2017

Name of Co-Author	Andrea Matros		
Contribution to the Paper	Supervised experimental design, data analysis and interpretation. Assisted with MALDI-MSI experiments and manuscript.		
Signature		Date	26.06.2017

Name of Co-Author	Rachel Burton		
Contribution to the Paper	Conceived project and designed experiments. Assisted with manuscript.		
Signature		Date	31/7/2017

Over-expression of *CslF6* Gene in Hull-less Barley Grain Alters Carbohydrate Partitioning and Impairs Grain Development

Wai Li Lim[1], Helen Collins[1], Caitlin Byrt[1,2], Jelle Lahnstein[1], Neil J. Shirley[1], Matthew K. Aubert[1], Matthew R. Tucker[1], Manuela Peukert[3], Andrea Matros[3] and Rachel A. Burton[1*]

[1]ARC Centre of Excellence in Plant Cell Walls, School of Agriculture, Food and Wine, University of Adelaide, Waite Campus, Glen Osmond, SA, 5064, Australia.

[2]Australian Research Council Centre of Excellence in Plant Energy Biology, University of Adelaide, Waite Campus, Urrbrae, SA, Australia.

[3]Applied Biochemistry Group, Leibniz Institute of Plant Genetics and Crop Plant Research (IPK-Gatersleben), Gatersleben, Germany.

*Corresponding Author

Corresponding author email: rachel.burton@adelaide.edu.au

Abstract

During cereal grain development, sugar in the form of sucrose is converted into storage carbohydrates such as starch, fructan and (1,3;1,4)-β-glucan. Previous studies showed that overexpression of the *HvCslF6* gene in a hull-less barley variety, under the control of an endosperm-specific promoter, resulted in high (1,3;1,4)-β-glucan and low starch content in the grain. Associated morphological changes included elongated aleurone cells and irregular cell shapes in the peripheral endosperm. Here we explore the physiological basis for these defects by testing how changes in the carbohydrate composition of developing grain impact mature grain morphology. We observed that an increase in (1,3;1,4)-β-glucans coincided with increased levels of soluble carbohydrates in the grain cavity and endosperm tissue. The transcript levels of genes relating to cell wall, starch, sucrose and fructan metabolism were perturbed. Evidence from microscopy indicated that the cell walls of endosperm transfer cells (ETCs) in transgenic grain were thinner and contained a reduced amount of mannan relative to wild type. Matrix-assisted laser desorption/ionization (MALDI) mass spectrometry imaging (MSI) and quantitative HPLC measurements showed excess soluble sugars in the developing grain cavity, suggesting an interference of sugar flow from the cavity to the endosperm. Our findings demonstrate the importance of regulating carbon partitioning in maintenance of grain structure, cellularisation and filling processes.

Introduction

Photoassimilates are the energy storing carbon products of photosynthesis. A portion of these assimilates are converted into more complex organic carbon compounds known as storage carbohydrates. Plant storage carbohydrates are not only important food sources for humans and animals, they are also sources of fermentable carbon for alcohol production (Burton and Fincher, 2014; Koehler and Wieser, 2013; Vijn and Smeekens, 1999). Examples of storage carbohydrates in cereal grains are starch, fructan and (1,3;1,4)-β-glucan. In Hordeum vulgare L. (barley) grain, starch represents the major storage polysaccharide and contributes between 52-72% of the dry weight (Henry, 1988). In contrast, fructan constitutes 1-4% and (1,3;1,4)-β-glucan contributes between 4-10% of the total dry weight (Åman et al., 1985; Burton and Fincher, 2012; Henry and Saini, 1989; Nemeth et al., 2014). The relative amount of storage compounds in barley grain is important for many industrial applications. Therefore, an understanding of carbon partitioning is key for future development of barley varieties with application-specific grain quality.

In grain, allocation of carbon occurs as soon as the grain begins to form and this process remains throughout development. During the pre-storage phase (0 to 6 DAP), the maternal pericarp receives sucrose from the main vascular tissue and is converted into hexoses for transient starch reserves (Radchuk et al., 2009; Sreenivasulu et al., 2010; Wobus et al., 2005). Concurrently, the maternal nucellus begins to disintegrate to support cell division and cellularisation events in the early endosperm (Domínguez and Cejudo, 2015). Whilst the (1,3;1,4)-β-glucan is first deposited in the early formed cell walls between 4 to 5 DAP (Kohorn et al., 2006), oligofructans are detected in the vacuole (Peukert et al., 2016b; Peukert et al., 2014). Differentiation of endosperm begins around 3 DAP when the cells opposite to the vascular bundle form the

transfer tissues, meanwhile the remaining nucellus tissue adjacent to the vascular bundle differentiates into the nucellar projection (NP) (Sreenivasulu et al., 2010).

From 6 to 8 DAP, grain undergoes a transition phase, involving expression of genes related to energy production and storage (Sreenivasulu et al., 2010; Wobus et al., 2005). Starch storage in the endosperm begins at 9 DAP (Olsen, 2001; Sreenivasulu et al., 2010; Wobus et al., 2005), which coincided with a high sucrose-to-hexose ratio (Wobus et al., 2005). Maintaining cytosolic sucrose homeostasis has been shown indispensable for proper starch synthesis in developing grains of barley plants with RNAi-mediated repression of the vacuolar sucrose transporter *HvSUT2*. Transgenic endosperms accumulated less starch and dry weight, although overall sucrose and hexose content was higher, likely due to suppressed sucrose efflux from the vacuoles (Radchuk et al., 2017).

Carbohydrate metabolic enzymes are key components controlling final grain composition. For example, starch is synthesized by enzymes including granule bound starch synthase (GBSS), starch synthase (SS), isoamylase (Iso), limit dextrinase (LD), pullulanase (PUL), starch branching enzyme (SBE) and amylase (Amy) (Jeon et al., 2010; Keeling and Myers, 2010; Radchuk et al., 2009). Fructans are synthesized by sucrose:sucrose-1-fructosyltransferase (1-SST), fructan:fructan-1-fructosyltransferase (1-FFT), sucrose:fructan-6-fructosyltransferase (6-SFT) and fructan:fructan-6G-fructosyltransferase (6G-FFT). Hydrolysis of fructans is mediated by fructan 1-exohydorolase (1-FEH) and fructan 6-exohydorolase (6-FEH) (Vijn and Smeekens, 1999). (1,3;1,4)-β-glucans accounts for 70% of cell wall material in barley endosperm (Burton and Fincher, 2014; Fincher, 1975; Guillon et al., 2011). The cellulose synthase-like genes (CslF6 and CslH1) are involved in the biosynthesis of (1,3;1,4)-β-glucans (Burton et al., 2011a; Doblin et al., 2009) while (1,3;1,4)-β-glucanases (isozyme EI and EII)

are involved their degradation (Harvey et al., 2001; Hrmova and Fincher, 2001; Hrmova et al., 1996; Jamar et al., 2011).

Manipulation of genes associated with carbohydrate metabolic pathways is a common strategy to produce crops with desired grain composition. However, this may result in significant impacts on grain development and its composition. Previous studies showed that mutation in the starch synthase IIa (SSIIa) gene (M292 barley mutant) resulted in a shrunken grain phenotype. Moreover, the reduction in starch content in M292 mutant coincided with significantly increased sucrose, fructan and (1,3;1,4)-β-glucan content (Clarke et al., 2008). The shrunken grain phenotype was also reported in low-starch barley lines with RNAi suppression of all Starch Branching Enzyme isoforms (Carciofi et al., 2012). This may be a result of deficient sugar loading from the cavities into the endosperm, causing excessive accumulation of water and the appearance of enlarged grain central cavities (Carciofi et al., 2012; Shaik et al., 2016). Interestingly, large grain cavities were also observed in barley lines overexpressing the *HvCslF6* gene, which showed an increased level of (1,3;1,4)-β-glucan and reduced starch content (Lim et al., 2017). These observations indicate that a balance between different types of carbon storage is important, although the relationships and interplay between pathways that regulate the accumulation of different storage compounds and grain development is not fully understood.

In this study, transgenic grains overexpressing the *HvCslF6* gene were utilised as a system to investigate the effects of increased (1,3;1,4)-β-glucan on carbohydrate metabolism during grain development, cavity formation and cell identity. Our data reveals altered transcript levels of genes related to starch, fructan and sucrose metabolism, increased accumulation of soluble carbohydrates and malformed endosperm. The results provide fundamental information relating

to the effect of modified carbon storage on hull-less grain composition, development and cell morphology. These findings are also important from an applied perspective, since modification of (1,3;1,4)-β-glucan levels in hull-less grain is a potential avenue for improvement of brewing quality and nutritional quality for human consumption.

Materials and Methods

Plant materials

Wild type (WT) (*Hordeum vulgare* L. cv Torrens) and transformed barley plants were grown as described in Burton *et al.*, (2011) and Lim et al., (2017) in a glasshouse under a day/night temperature regime of 23°C/15°C. Plant transformation has previously been described in Lim et al., (2017). Four independent transformed plants (15-3, 18-6, 25-5, 16-5) from the T_3 generation, Torrens (WT) and wild type plants regenerated from tissue culture (WT(tc)) were selected and analysed. Developing grains from individual plants were collected from the middle of the spike at 7, 11, 15, 19 and 24 DAP. The pericarp, endosperm and embryo tissues were separated using a scalpel and fine forceps and snap-frozen in liquid nitrogen. Frozen tissues were kept at -80°C until required.

Vector construction

DNA fragments were synthesized by Genscript (USA) and inserted into the pUC57 vector. The 2.6kb 3xnls-YFP gene (MA044) was adapted from Ueda et al., (2011) and codon optimized for barley using the online tool at https://sg.idtdna.com/CodonOpt. The sequence for the 994 bp oat globulin AsGlo1 promoter sequence (pAsGLO1; MA003) was obtained from Vickers et al., (2006) and modified to include 5'-HindIII and 3'-KpnI restriction sites. The HindIII/KpnI AsGlo1 fragment from MA003 was excised and inserted into the Gateway-compatible pMDC32 vector (Curtis and Grossniklaus, 2003) in place of the double 35S promoter, creating MA009. The 3xnls-YFP sequence was amplified from pUC57 using pUC57-attL1_FWD (5'-ACCTCGCGAATGCATCTAGATCA-3') and SacI-attL2 REV (5'-CAAATAATGATTTTATTTTGACTGATAGTGACCTGTTCGTTGCAACAAATTGATGAGCAATTATTTTTTATAATGCCAACTTTGTACAAGAAAGCTGGGTTCATTATTTGGA

GCTC-3') primers and HiFi Platinum Taq (ThermoFisher, Scoresby Vic, Australia) resulting in a PCR fragment flanked by attL1 and attL2 gateway compatible sites. The 3xnlsYFP insert was transferred into the MA009 (pAsGlo1:pMDC32) vector using LR clonase II (ThermoFisher, Scoresby Vic, Australia) according to the manufacturer's instructions. The resulting vector MA032 (pAsGlo1:3xnlsYFP) was transformed into *Agrobacterium tumefaciens* strain AGL1 prior to use in barley transformation.

Agrobacterium-mediated barley transformation

The transformation protocol followed Tingay et al., (1997), as modified by Matthews et al., (2001) and Burton et al., (2011b). One modification was the replacement of Hordeum vulgare cv. Golden Promise with Hordeum vulgare cv. Torrens. All plants were grown under standard glasshouse conditions following Burton et al., (2004).

(1,3;1,4)-β-Glucan assay

Freeze-dried samples from developing and mature barley grain were ground and weighed to produce 10 mg aliquots. To remove free sugars and chlorophyll, powdered materials were pre-treated with 70% ethanol (EtOH) (0.01 w/v %) at 97°C for 30 min, centrifuged at 5000 rpm for 5 min and the supernatants were removed. The pellets were then treated with 100% EtOH (0.01 w/v %) at 97°C for 10 min, centrifuged at 5000 rpm for 5 min and the supernatants were removed. The same pellets were used to analyse (1,3;1,4)-β-glucan content using a scaled down version of the Megazyme mixed-linkage beta-glucan assay (McCleary and Codd, 1991).

Starch assay

The starch content of developing tissues and mature grain was measured using a scaled down version of Megazyme Total Starch Assay (Megazyme International) according to the manufacturer's instructions (McCleary et al., 1994), with approximately 10 mg of freeze-dried samples, pre-treated with 70% ethanol (30 min, 97°C) and 100% ethanol (10min, 97°C) respectively.

Soluble sugar analysis

Extraction of soluble sugars and fructans from barley grains were performed as described in Verspreet et al., (2012). Briefly, developing grains from each biological replicate were ground and weighed at approximately 10 mg. The soluble sugars were extracted in 80% EtOH at 85°C for 30 min followed by Milli-Q water at 50°C for 30 min in a final dilution of 1:40 w/v. The supernatants from each extraction were combined. For cavity sap, 10 barley grains were cut in half using a scalpel and fluids from the endosperm cavity were extracted using a microsyringe (Hamilton, Reno, Nevada, United States). Cavity sap was heated at 90°C to inactivate endogenous enzymes and diluted in Milli-Q water to produce a final dilution of 1:100 v/v. The diluted sample extracts from grain tissues and cavity extracts, were treated with and without fructanase (Megazyme fructan assay kit, Deltagen, Kilsyth VIC, Australia), incubated at 40°C for 2 h for complete hydrolysis, and then heated at 90°C for 5 min. Sample extracts were separated using a high pH anion exchange chomatography with pulsed amperometric detection (HPAEC–PAD) on a Dionex ICS-5000. A 25 µL aliquot was injected onto a DionexCarboPACTMPA-20 column (3 x 150 mm) with a guard column (3 x 50 mm) kept at 30 °C and operated at a flow rate of 0.5 mL min-1. The eluents used were (A) 0.1 M sodium

hydroxide and (B) 0.1 M sodium hydroxide with 1 M sodium acetate. The gradient was started with 0% (B) from 0 to 9 min, 10% (B) from 9 to 10 min, 100% (B) from 10 to 12 min, 0% (B) from 12 up to 20 min. Temperature of the detector was maintained at 20°C and data collection was at 2 Hz. The Gold Standard PAD waveform (std. quad. potential) was used to detect carbohydrates. Standards used were: glucose, fructose, sucrose, raffinose, 1-kestose and nytose at concentrations of 4, 2, 1, 0.5, 0.25 and 0.125 mg/L respectively. Total fructan content was calculated according to the methods from Huynh et al., (2008) and Verspreet et al., (2013b). Total fructan (μM) equals the sum of glucose and fructose after hydrolysis minus the sum of free glucose, fructose, sucrose and raffinose (before hydrolysis), taking into account the loss of one water molecule per monosaccharide (x0.9).

Monosaccharide analysis

Monosaccharide analysis from barley grain was carried out as described by Hassan et al., (2017) using a reversed phase HPLC coupled to Diode Array Detector (Agilent Technologies, Mulgrave VIC, Australia). Total arabinoxylan content (% weight per weight (w/w)) was calculated from the combined amount of % L-arabinose and % D-xylose, taking into account the loss of one water molecule per monosaccharide (x0.9).

RNA isolation and cDNA synthesis

Total RNA was extracted from all tissue homogenates using a phenolguanidine reagent, treated with the DNA-free kit (Ambion®, Thermo Fisher Scientific, Scoresby Vic, Australia), and used as the template for cDNA synthesis as described in Burton et al., (2008)

Real-time quantitative PCR (qPCR)

Gene specific primers were designed from the 3' untranslated regions of full-length cDNAs. Fragments amplified using the gene specific primers were purified using HPLC as described in Burton et al. (2008) and sequenced at the Australian Genome Research Facility, Adelaide, South Australia. The PCR primer sequences are provided in Supplementary Table S3. qPCR analysis was carried out as described in Burton et al., (2004) with the modifications reported in Burton et al. (2008). Heatmap representation generated using MultiExperiment Viewer (MeV) software (http://mev.tm4.org/).

Preparation of microsomal membranes

The method for preparation of the microsomes from barley grain was according to Song et al., (2015). Briefly, frozen grain tissues from 10 seeds were homogenized using acid washed sand in 500 µL extraction buffer containing 50 mM HEPES-KOH (pH 6.8), 0.4 M sucrose, 1 mM dithiothreitol (DTT), 5 mM MnCl2, 5mM MgCl2 and complete EDTA-free proteinase inhibitor cocktail tablet (Roche, Basel, Switzerland). The homogenate was filtered through two layers of miracloth (Merck Millipore, Billerica, MA, US) and the filtrate was centrifuged at 3000g for 20 min at 4°C. The supernatant was collected and centrifuged at 100,000 X g for 30 min at 4°C in 10 ml ultracentrifuge tubes (Beckman Coulter, Australia). The supernatant was decanted, and the pellets were suspended in 30 µl of extraction buffer. Protein concentration was measured using the BCA protein assay kit (Thermo Scientific, Rockford, IL, US). The bovine serum albumin (BSA) provided in the kit was used as the standard.

SDS-PAGE and immunoblotting

Protein gel electrophoresis was performed following the protocol of Wilson et al., (2015). Briefly, 30 µg of protein was reduced with 100 mM DTT and 1 X NuPAGE sample buffer. Proteins were separated on Bis-Tris 4 to 12% gradient gels (Novex; Life Technologies) together with a molecular mass marker (Precision Plus Protein Kaleidoscope (BioRad, NSW, Australia). Gels were run with MOPS buffer at 200 V. After electrophoresis, the gel was removed from the cassette and transferred onto nitrocellulose membrane (Nitrobind, 0.22 µm; ThermoFisher Scientific) using the XCell II Blot Module (Invitrogen) according to the manufacturer's protocol. The membrane was blocked overnight in Tris-buffered saline (TBS; 20 mM Tris base, 150 mM NaCl) containing 3% skim milk powder in 1 X TBS (blocking solution) before incubation for 1 h at room temperature. The membrane was subsequently incubated with a polyclonal CslF6 primary antibody (Wilson et al., 2015) at 1:2000 dilution in blocking solution overnight at 4°C, washed 3 times in 1 X TBST (0.05% Tween 20 detergent in 1 X TBS), then incubated in anti-rabbit HP conjugate (BioRad, NSW, Australia) at a 1:10,000 dilution diluted in blocking solution for 2 h at room temperature. Finally, the membrane was washed 3 times in 1 X TBST before signal was detected with SuperSignal West Pico or Femto Maximum Sensitivity chemiluminescent substrate (Thermo Scientific) according to the manufacturer's instructions. Chemiluminescence was captured digitally using a ChemiDoc MP Imaging System (BioRad, NSW, Australia).

Tissue preparation for MALDI-MSI measurement

Sectioning of barley grains and matrix application was performed as described in Peukert et al., (2014). The MSI measurements were performed using an ultrafleXtreme MALDI time-of- flight

(TOF)/TOF device (Bruker Daltonics, Germany) following the protocol described in Peukert et al., (2016a).

Tissue fixation, embedding and microscopy for barley grain

Developing grains were halved using a razor blade and fixed in 0.25% glutaraldehyde, 4% paraformaldehyde and 4% sucrose in phosphate buffered saline (PBS), pH 7.2, dehydrated and embedded in LR White resin according to Burton et al., (2011). Embedded tissue was sectioned (1 μm) on an ultramicrotome using a diamond knife and dried onto polylysine coated microscope slides (ThermoFisher Scientific). Immuno-chemical analysis of cell wall polysaccharides was performed according to Burton et al., (2011) using primary antibodies including (1,3)-β-glucan, hetero-(1,4)-β-mannan (Pettolino et al., 2001), BG1 (Biosupplies Australia, Parkville, Vic., Australia), LM11 (McCartney et al., 2005), LM19 (PlantProbes) and a recombinant crystalline cellulose CBM3a protein (PlantProbes). For detection of crystalline cellulose, a monoclonal anti-polyHistidine antibody (Sigma-Aldrich, Castle Hill, NSW, Australia) (1:100 dilution in 1 X PBS with 1% w/v BSA) was applied after CBM3a (Blake et al., 2006). For detection of arabinoxylan, sections were incubated in α-L-arabinofurosidase (Megazyme International, Deltagen, Kilsyth VIC, Australia) under moist conditions at 40°C for 2 h prior to LM11 antibody incubation (Wilson et al., 2012). For detection of homogalacturonan, sections were either not treated or treated with 0.1 M sodium carbonate (Na2CO3) for 1 h at room temperature prior to LM19 antibody incubation (Verhertbruggen et al., 2009). Alexa Fluor® 555 goat anti-mouse IgG (H+L) Secondary antibody (ThermoFisher, Scoresby Vic, Australia) was used against BG1, (1,3)-β-glucan and anti-polyHistidine antibodies) while Alexa Fluor® 555 goat anti-rat IgG (H+L) (ThermoFisher, Scoresby Vic, Australia) secondary antibody was used against LM11 and LM19 antibodies. Sections were incubated with

secondary antibodies for 1 h at room temperature in the dark. Images were taken using a Carl Zeiss fluorescence microscope (Axio Imager M2; Carl Zeiss, Oberkochen, Germany). Tissue sections were stained with Toluidine blue for morphological examination and were photographed using a Nikon Ni-E optical microscope. For environmental scanning electron microscopy (ESEM), individual mature grains were mounted on SEM stubs and coated with carbon and gold. Samples were examined in a Philips XL30 Field Emission scanning electron microscope at an accelerating voltage of 5 kV.

Protein content

The amount of nitrogen in mature grain samples was analysed using the Dumas combustion method as described in Jung et al., (2003). Protein content was calculated from the nitrogen content of the material, using a nitrogen conversion factor of 6.25.

Starch granule size measurement

Ground barley flour was mixed with 1 ml of 2% sodium dodecyl sulfate (SDS) (Sigma-Aldrich, Castle Hill, NSW, Australia) and 5 µL of DTT (Sigma-Aldrich, Castle Hill, NSW, Australia) for 10 min. The sample mixture was centrifuged for 10 min and the supernatant was decanted. The pellet was then washed in 1 ml of Milli-Q water, centrifuged for 10 min and the supernatant was decanted. The pellet was resuspended in 150 µL of Lugol's iodine solution containing 2% potassium iodine (KI) (E. Merck, Darmstadt, Germany) and 1% Iodine (I) (Sigma-Aldrich, Castle Hill, NSW, Australia) and dilute further with 300 µL of Milli-Q water. A drop of the mixed sample was placed on a Bright-Line Hemacytometer (Hausser Scientific, Horsham, USA) and covered with a coverslip. Images were taken using a Nikon Ni-E optical microscope and

measurement of starch particles from the images were performed using Image J software (http://imagej.net/Fiji).

Results

pAsGlo:HvCslF6 is expressed in the peripheral endosperm and correlates with increased CslF6 protein and (1,3;1,4)-β-glucan abundance

To determine the abundance of CslF6 protein in transgenic grain, a specific CslF6 antibody was used (Fig. 1A). Consistent with Wilson et al., (2015), a strong doublet band of CslF6 protein at a size of between 80 to 100 kDa was observed in endosperm extracts of transgenic and WT barley grain at 15 DAP, although the predicted size for the CslF6 protein is 105 kDa (Wilson et al., 2015). Levels of CslF6 protein were greatest in the endosperm of transgenic 16-5, 15-3, 25-5 and 18-6 compared to the WT. A weaker band corresponding to the CslF6 protein was observed in the pericarp sample from 18-6 transgenic grain (Fig. 1A).

Accumulation of *HvCslF6* transcript was measured in control and transgenic barley grain tissues across a range of days after pollination (DAP) using real-time quantitative PCR (qPCR). From 7 to 19 DAP, *HvCslF6* transgene transcript levels were higher in transgenic pericarp and endosperm tissues compared to WT and WT(tc). In the pericarp, *HvCslF6* transgene transcript levels were also slightly higher at 24 DAP compared to the WT. In the embryo, only the 18-6 transgenic grain showed higher *HvCslF6* gene transcript levels at 19 DAP (Supplementary Fig. S1A).

To examine the tissue specificity of the *AsGlo* promoter (*pAsGlo*), barley grain from plants transformed with an *pAsGlo:3xnlsYFP* transcriptional fusion construct were observed under a fluorescent microscope. Fluorescence from YFP was first detected around 7 DAP (data not shown) and by 20 DAP was seen specifically in the peripheral endosperm of the grain. No signal was detected in aleurone or pericarp tissues (Fig. 1B to 1D).

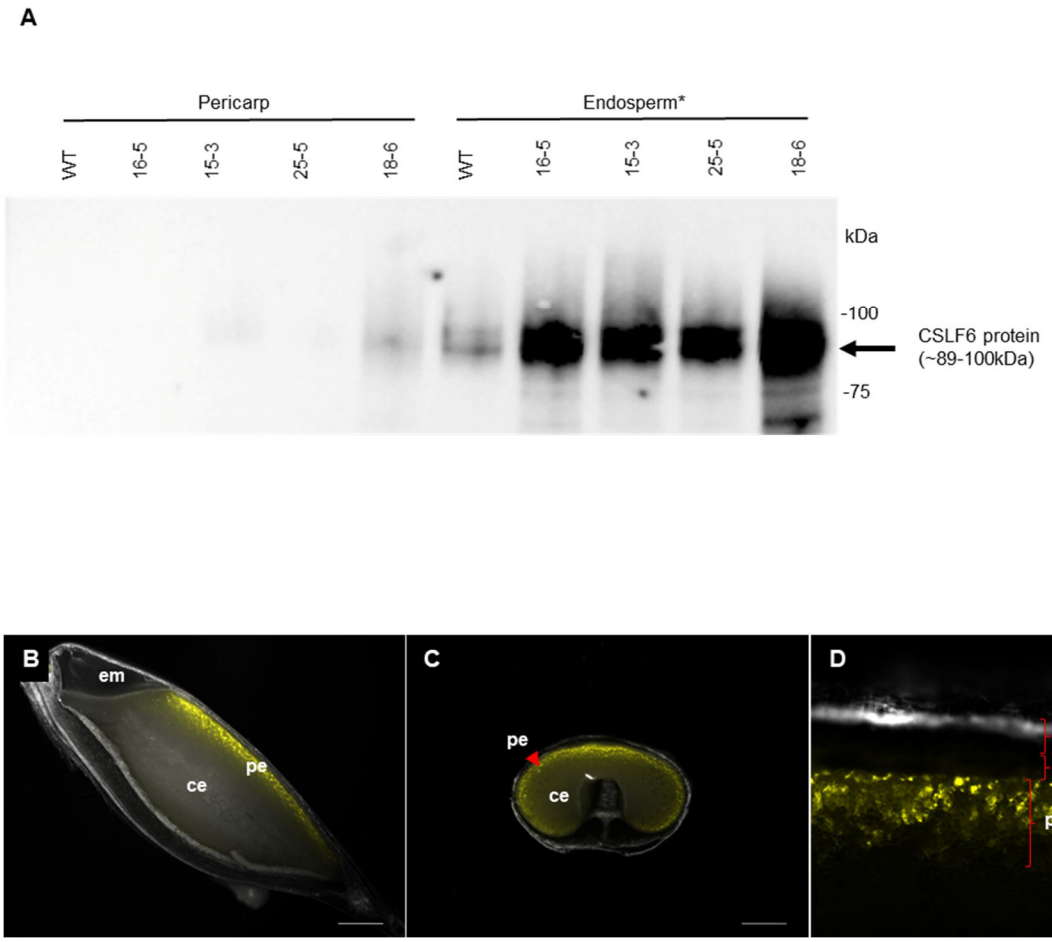

Figure 1: Total CslF6 protein levels and fluorescent microscopy of *pAsGLO:3xnlsYFP* construct at 20 DAP under DAPI channel in developing barley grain. (A) Total CslF6 protein levels in the transgenic grains are slightly higher in pericarp and clearly upregulated in endosperm tissues relatively to WT at 15 DAP. (B) to (D) Fluorescence from YFP is detected in the peripheral endosperm of barley grain. Images from (B) and (C) are under 1x magnification with scale bars equivalent to 1000 µm. Image from (D) is under 10x magnification with a scale bar equivalents to 100 µm. Abbreviations: peripheral endosperm (pe), central endosperm (ce), aleurone (al), pericarp (p), embryo (em).

To establish whether any contamination from the peripheral endosperm tissue had carried over into the manually prepared samples. Transcript levels of the barley aleurone-specific gene, *lipid transfer protein 2 (Ltp2)* from barley (Kalla et al., 1994) and the *GBSS1a* gene, which is not

detectable in barley pericarp (Radchuk et al., 2009) were examined in both WT and transgenic samples (Supplementary Fig. S1D and S1E). Both WT and transgenic grains had greater transcript levels of *HvLtp2* in the pericarp compared to endosperm and embryo tissue. The 18-6 transgenic pericarp at 24 DAP had the highest *HvLtp2* transcript level compared to all other barley lines and grain tissues, indicating that significant numbers of aleurone cells had adhered to the pericarp tissue when it was harvested from the grain at this stage. We also found considerably higher transcript levels of *HvGBSS1a* in the pericarp of WT samples than previously reported by Radchuk et al., (2009) (Supplementary Fig. S1E), but *HvGBSS1a* transcript levels in the embryo tissue were low in all lines tested (Supplementary Fig. S1E). Taken together, these results suggest that a considerable proportion of peripheral endosperm is present in manual preparations of pericarp tissues of all samples.

Distribution of (1,3;1,4)-β-glucan was examined using the (1,3;1,4)-β-glucan monoclonal antibody (BG1) (Fig. 2A to 2D). At 7 DAP, fluorescent signals from BG1 antibody labelling were evenly detected for both WT and 18-6 transgenic grain (data not shown). At 11 and 24 DAP, the fluorescent signals from the BG1 antibody were uniformly distributed across the tissue cell walls in WT grain (Fig. 2A and 2C), whereas for 18-6 transgenic grain, the fluorescent signals appeared to be stronger in the peripheral endosperm cell walls (Fig. 2B and 2D), which matched with the *pAsGlo:3xnlsYFP* expression pattern (Fig. 1C). BG1-associated fluorescence also indicated that peripheral and central endosperm cells in transgenic grain were irregularly arranged and the central endosperm cells appeared as well to be ‘squashed’ (Fig. 2D).

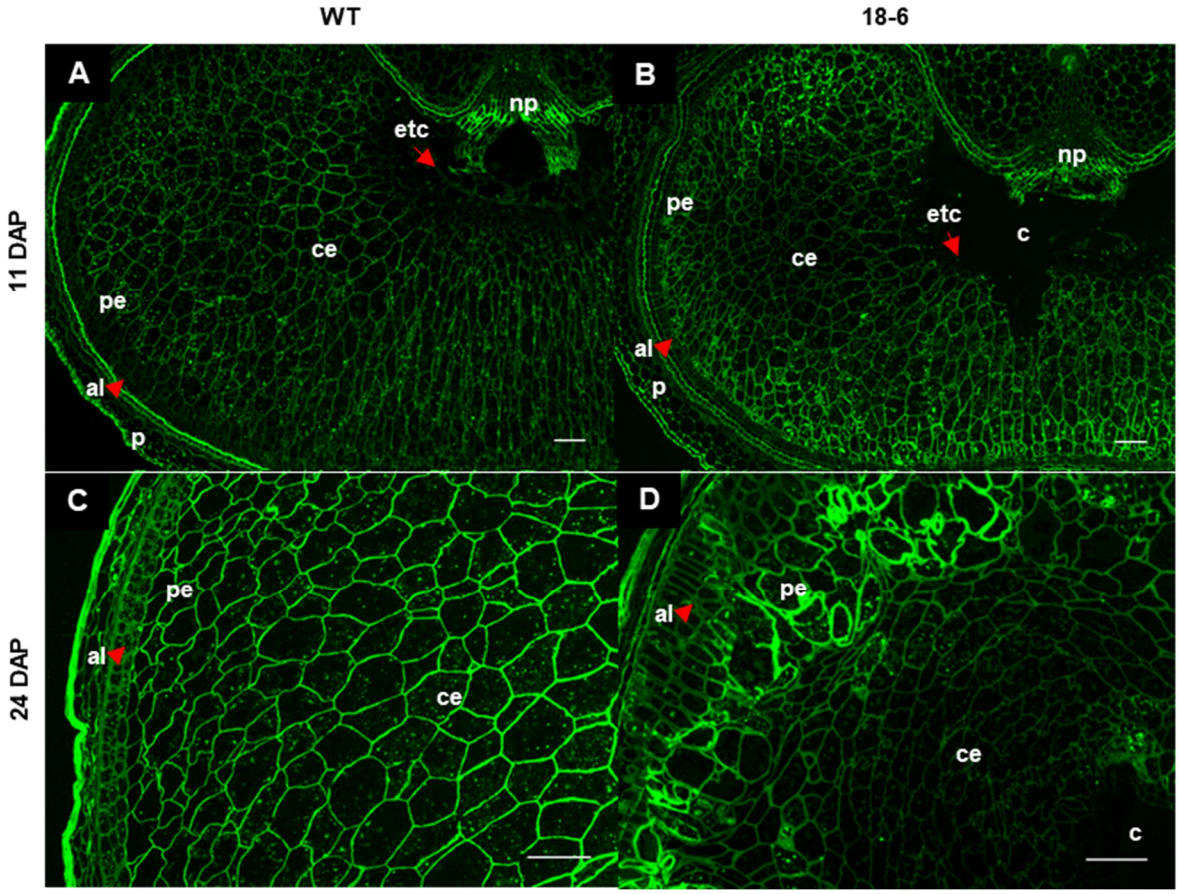

Figure 2: Fluorescence microscopy of developing barley grain. Immunolabeling with (1,3;1,4)-β-glucan (BG1) monoclonal antibody shows stronger fluorescent signals in the peripheral endosperm of transgenic grain at (B) 11 DAP and (D) 24 DAP relative to WT (A) and (C). (A) and (B) are under 5x magnification; (C) and (D) are under 10x magnification. Scale bars in (A) to (D) are equivalent to 100 µm. Abbreviations: pericarp (p), aleurone (al), peripheral endosperm (pe), central endosperm (ce), endosperm transfer cells (etc), cavity (c), nucellar projection (np).

Starch granules are smaller in *pAsGlo:HvCslF6* transgenic grain

The 'squashed' endosperm cells in 18-6 transgenic grain were packed with starch granules which appeared smaller than WT A-granule (big) but much larger than WT B-granule (small) (Fig. 3A and 3B). Small starch granules were also found in the peripheral endosperm layer of

18-6 transgenic grain, while the equivalent cells in WT contained fewer, larger granules (Fig. 3C and 3D). Moreover, the cell walls surrounding the starch granules were more obvious in WT endosperm compared to transgenic endosperm (Fig. 3A and 3B).

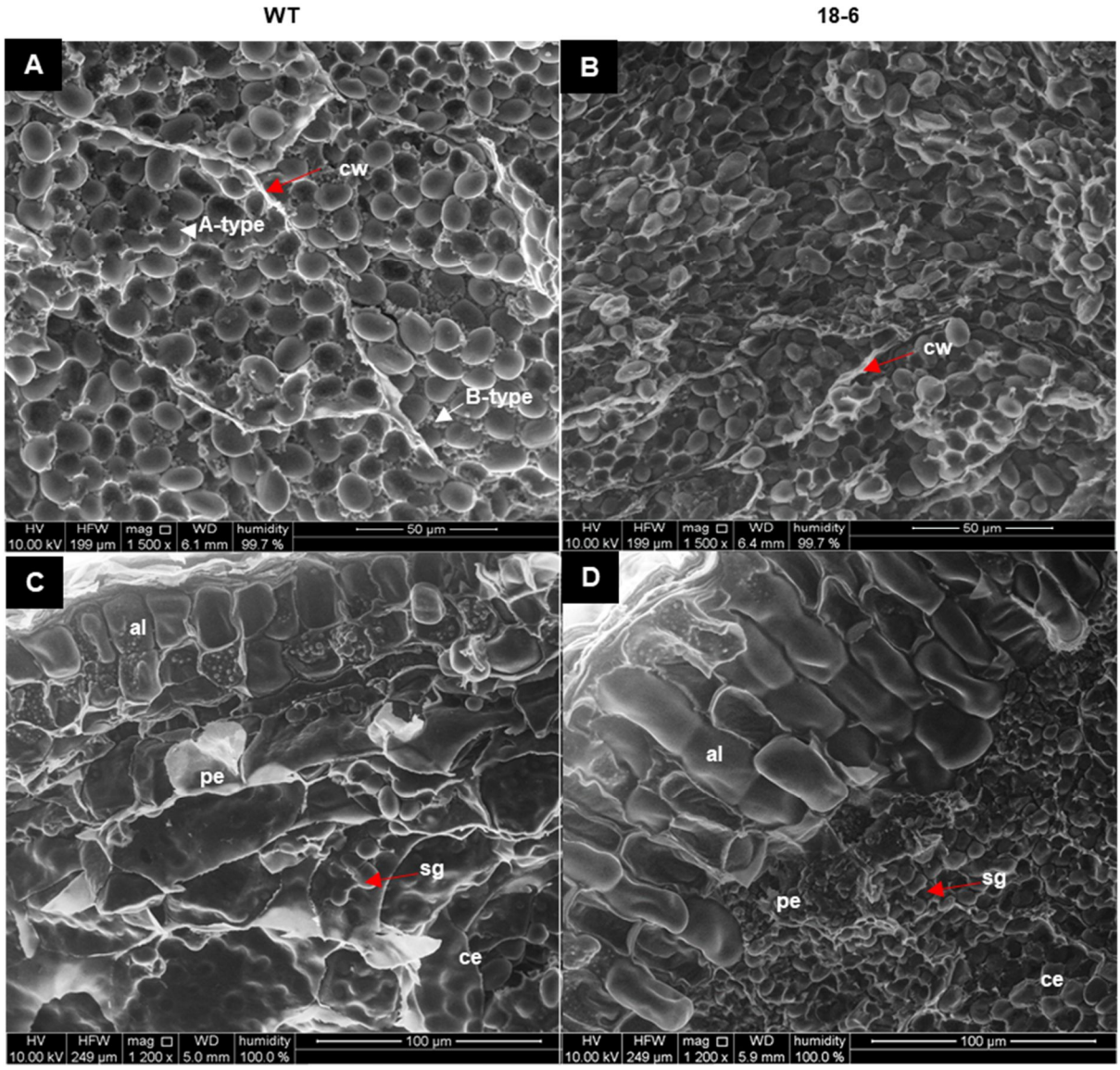

Figure 3: Environmental scanning electron micrographs of starch granules of mature barley grain. (A) Starch granules in WT endosperm consists of A-type granule (big) and B-type granule (small) and the cell walls surrounding the starch granules are apparent. (B) The size of the starch granules in the transgenic endosperm appear in an intermediate size between A-type and B-type from the WT grain. Starch granules are packed and the cell walls are not apparent

compared to the WT grain. (C) Aleurone cells in WT appear squared, while those of 18-6 transgenic grain appear elongated. (D) Starch granules are packed in the peripheral endosperm layer of F6-18-6 transgenic grain. (A) and (B) are taken in the middle and distal regions of cross-sectioned grains. (C) and (D) are taken around the aleurone layer. (A) and (B) are under 1500x magnification with scale bars equivalent to 50 µm whereas (C) and (D) are under 1200x magnification with scale bars equivalent to 100 µm. Abbreviations: aleurone (al), peripheral endosperm (pe), starch granule (sg), central endosperm (ce), cell wall (cw).

Starch granules in grain flour of WT, WT(tc) and all transgenic lines were further examined by iodine staining and light microscopy. The size of A and B-type granules was determined by diameter measurement using ImageJ (Table 1). From previous studies, barley grain starch is comprised of big granules with diameters in the range of 10 to 40 µm whereas small granules range from 1 to 10 µm (Chmelik et al., 2001; Palmer, 1972). Therefore, granules with diameters less than 10 µm were grouped as small granules (B-type) while granules with diameters greater than 10 µm were grouped as big granules (A-type). WT, WT(tc), 15-3, 16-5 and 25-5 had small granules with diameters ranging between 4.4 µm to 5 µm whereas the 18-6 line had diameters above 5 µm. The 18-6 line had the smallest “big” granules, with average diameter approximately 15 µm, whereas those of controls, WT and WT(tc), and other transgenic lines were above 20 µm, and ranged between 20 µm and 26 µm (Table 1).

Table 1: ImageJ analysis of starch granules in mature barley grain

Line	Average diameter of small granules (<10µm) ± SD	Average diameter of large granules (>10µm) ± SD
WT	4.60±0.12	22.99±0.71
WT(tc)	4.93±0.02	25.77±0.65
15-3	4.51±0.12	22.34±0.99
16-5	4.29±0.21	20.64±0.68
18-6	5.49±0.12	15.24±0.41
25-5	4.39±0.05	20.45±0.25

Abbreviation: Standard deviation (SD)

Abnormal structures of cavity and endosperm transfer cells in *pAsGlo:HvCslF6* transgenic grain

18-6 transgenic line had a smaller endosperm area than WT due to the presence of the large central cavity as reported in Lim et al., (2017). Moreover, the endosperm transfer cells (ETCs) surrounding the central cavity were deformed and sporadically missing. This phenotype was consistent across all transgenic lines but was absent in the WT and WT(tc) grain. Here, we investigated histological changes during the transition phase of grain development (8 to 14 DAP), where cellularisation of transfer tissues has been completed and storage product accumulation starts. Toluidine blue sections enabled comparisons between the structure of the cavity in transgenic and WT grain (Fig. 4A to 4F, Supplementary Fig. S2A to S2D). As early as 8 DAP, rupture of tissue in the cells adjacent to the NP, the newly forming cavity, can be observed in the transgenic grain while other transfer tissues appear similar to WT (Fig. 4A and 4B). At 9 DAP, the cavity size in the transgenic grain was larger compared to the WT and the ETCs remained intact (Supplementary Fig. S2A and S2B). At 10 DAP, the ETCs in transgenic grain were ruptured (Fig. 4C and 4D). The rupture in this region became increasingly

pronounced during subsequent development, whereas the ETCs remained intact in WT grain (Fig. 4E and 4F, Supplementary Fig. S2C and S2D). The cell wall morphology of ETCs was compared between the 18-6 transgenic and WT grain (Fig. 4G and 4H). In the WT grain the cell walls of the ETCs were denser and thicker (Fig. 4G) compared to those of transgenic grain which were thinner and surrounded by much less regular shaped cells (Fig. 4H). These results suggest that perturbed formation of the cavity and ETCs in transgenic grains coincides the time when assimilate transport increases drastically.

Altered cell wall composition in the endosperm transfer cells and endosperm of *pAsGlo:HvCslF6* transgenic grain

To determine whether ETC collapse might be associated with changes in cell wall composition, sections of WT and 18-6 transgenic grain were investigated. At 9 DAP, the labelling intensity for mannan antibody was similar between WT and transgenic grain (Fig. 4I and 4J), although the width of labelled cell walls was much broader in WT (Fig. 4G to 4J). At 10 and 11 DAP, the mannan labelling pattern in WT and transgenic grain appeared similar to that at 9 DAP (data not shown). Labelling with LM11 (Supplementary Fig. S3A and S3B), BG1 (Fig. 2A and 2B), (1,3)-β-glucan (Supplementary Fig. S3C and S3D), CBM3a (Supplementary Fig. S3G and S3H), LM19 (Supplementary Fig. S4A and S4B) and LM20 antibodies (data not shown) was not detected in the endosperm transfer cells of either WT or transgenic grain.

Contrasting this, clear differences were observed in the abundance of arabinoxylan, crystalline cellulose and callose in the endosperm of WT and 18-6 grain (Supplementary Fig. S5A to S5H). Transgenic grain showed stronger labelling intensities of LM11 and (1,3)-β-glucan antibodies in endosperm cell walls relative to WT (Supplementary Fig. S5A to S5D). Moreover, more

intense labelling of (1,3)-β-glucan antibody and CBM3a was detected in the peripheral endosperm of transgenic grains relative to WT, similar to that detected for BG1 (Fig. 2A to 2D, Supplementary Fig. S5C to S5F). The labelling intensity of mannan (Supplementary Fig. S5G and S5H) was similar between WT and transgenic grain, as was that of LM19, which was mainly detected in maternal grain tissues but only after pre-treatment with 0.1 M sodium carbonate (Na_2CO_3; Supplementary Fig. S4E to S4H).

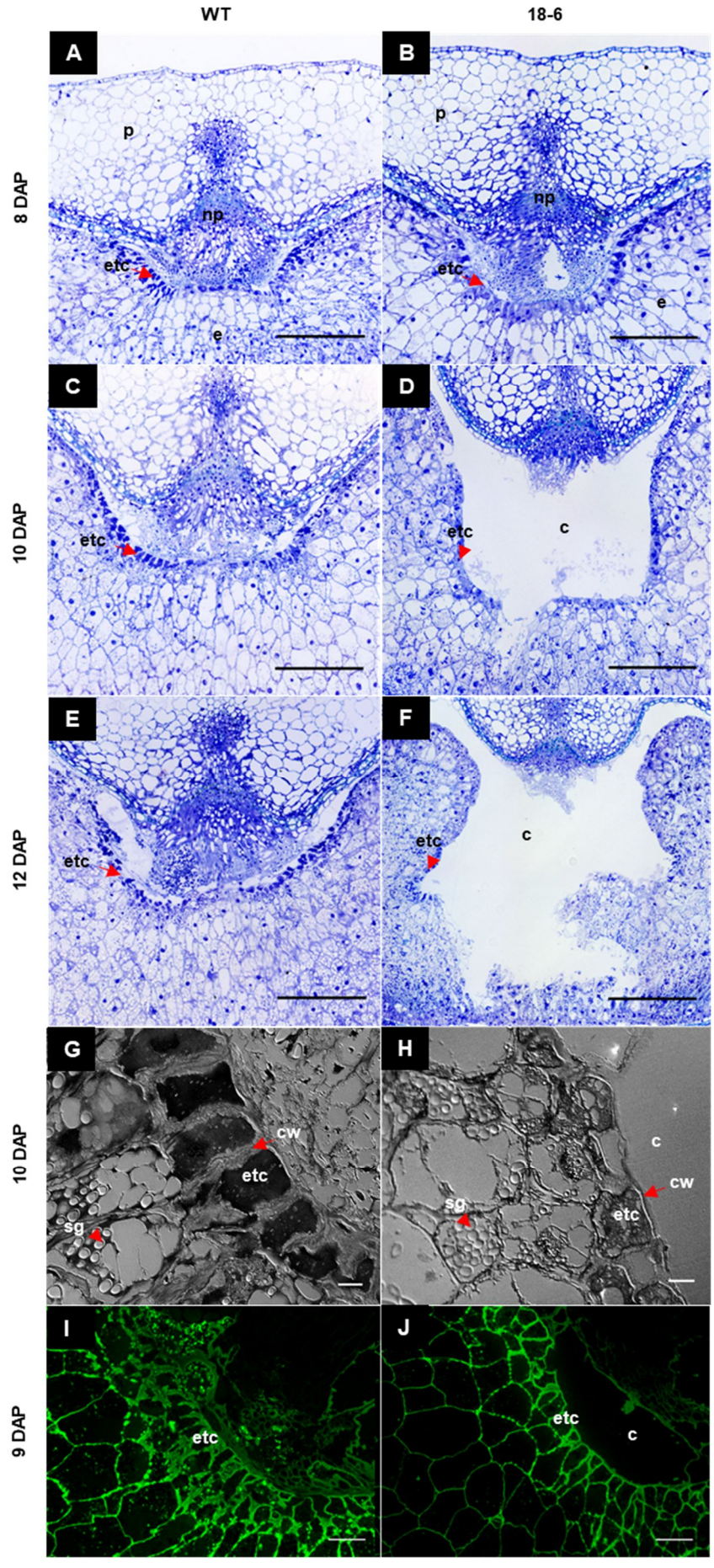
WT
18-6
8 DAP
10 DAP
12 DAP
10 DAP
9 DAP
A
B
C
D
E
F
G
H
I
J
p
np
etc
e
c
cw
sg

Figure 4: Microscopy images of endosperm transfer regions in WT and transgenic (18-6) barley grain. Grain sections in (A) to (F) are stained with toluidine blue. The endosperm transfer cells (ETCs) in WT appear intact while the ETC in transgenic grain are poorly formed. (G) ETCs in WT grain are denser with thicker cell walls compared to the thinner walls in transgenic grain (H). Immuno-histochemical analysis of mannan with the (1-4)-β-D-mannan and galacto-(1-4)-β-D-mannan antibody shows differences in fluorescent signals in the cell walls of ETCs between WT and transgenic grain at 9 DAP. (A) to (F) are under 4x magnification with scale bars equivalent to 100 µm. (G) and (H) are under 60x magnification with scale bars equivalent to 10 µm. (I) and (J) are under 20x magnification with scale bars equivalent to 50 µm. Abbreviations: pericarp (p), nucellar projection (np), cavity (c), endosperm transfer cells (etc), endosperm (e), cell wall (cw), starch granule (sg).

Modified aleurone cell shape in *pAsGlo:HvCslF6* transgenic grain

The formation of aleurone cells in 18-6 transgenic and WT grain was examined from 9 to 24 DAP (Supplementary Fig. S6A to S6H). The cells in the peripheral endosperm appeared deformed in shape in the 18-6 transgenic line compared to WT from 9 to 24 DAP (Supplementary Fig. S6A to S6H). At 12 and 14 DAP, the size of aleurone cells in transgenic grain appeared larger relative to WT (Supplementary Fig. S6C to S6F). At 24 DAP, the aleurone cells were notably elongated in 18-6 transgenic grain while the equivalent cells remained cube-shaped in WT (Supplementary Fig. S6G and S6H).

To compare the size of the aleurone cells, the dimensions of the cells were measured using ZEN imaging software. At 24 DAP, the average length of aleurone cells in 18-6 transgenic grain was 44.8 µm +/- 0.2 (standard error (SE)) and the width was 16.1 µm +/-0.3 (SE). For WT, the

average length of aleurone cells was 18.7 µm +/- 0.5 (SE) and the average width was 17.8 µm +/- 0.2(SE). This confirmed that WT aleurone cells were cuboid and transgenic cells were over twice as long, but the same width, as WT (data not shown). The aleurone cells in 18-6 remained elongated through to grain maturity (Fig. 3D).

pAsGlo:HvCslF6 transgenic barley grains accumulate more (1,3;1,4)-β-glucan, sucrose and total fructan and less starch in the endosperm compared to WT

The dynamics of storage carbohydrate deposition, including starch, (1,3;1,4)-β-glucan, sucrose and total fructan were examined in whole grain in WT, WT(tc) and all transgenic lines from 7 DAP until maturity (Fig. 5A to 5F). WT and WT(tc) grain accumulated starch and (1,3;1,4)-β-glucan throughout grain development (Fig. 5A and 5B). In the transgenic lines, the levels of starch and (1,3;1,4)-β-glucan declined after 24 DAP (Fig. 5C to 5F). WT and WT(tc) grain had maximum total fructan levels at 11 DAP at approximately 1.2 mg while the maximum levels of total fructan in transgenic lines ranged between 1.2 to 1.5 mg from 11 to 24 DAP (Fig. 5C to 5F). The sucrose levels in WT and WT(tc) grain were constant from 11 DAP to the mature stage at approximately 0.5 mg per grain, while the sucrose levels in all transgenic lines inclined from 11 to 19 DAP, ranging between 0.7 to 1 mg (Fig. 5C to 5F). At maturity, all transgenic lines contained more (1,3;1,4)-β-glucan but less starch compared to the WT in the endosperm on a per grain basis (Supplementary Table S1A), while soluble carbohydrates including glucose, fructose, sucrose and total fructan levels were comparable to those of WT and WT(tc) (Supplementary Table S1A). On a weight per weight basis, all transgenic lines contained more (1,3;1,4)-β-glucan, sucrose, total fructan but less starch than WT in developing and mature endosperm (Supplementary Fig. S7A and S7C, S8A and S8C, Supplementary Table S1A).

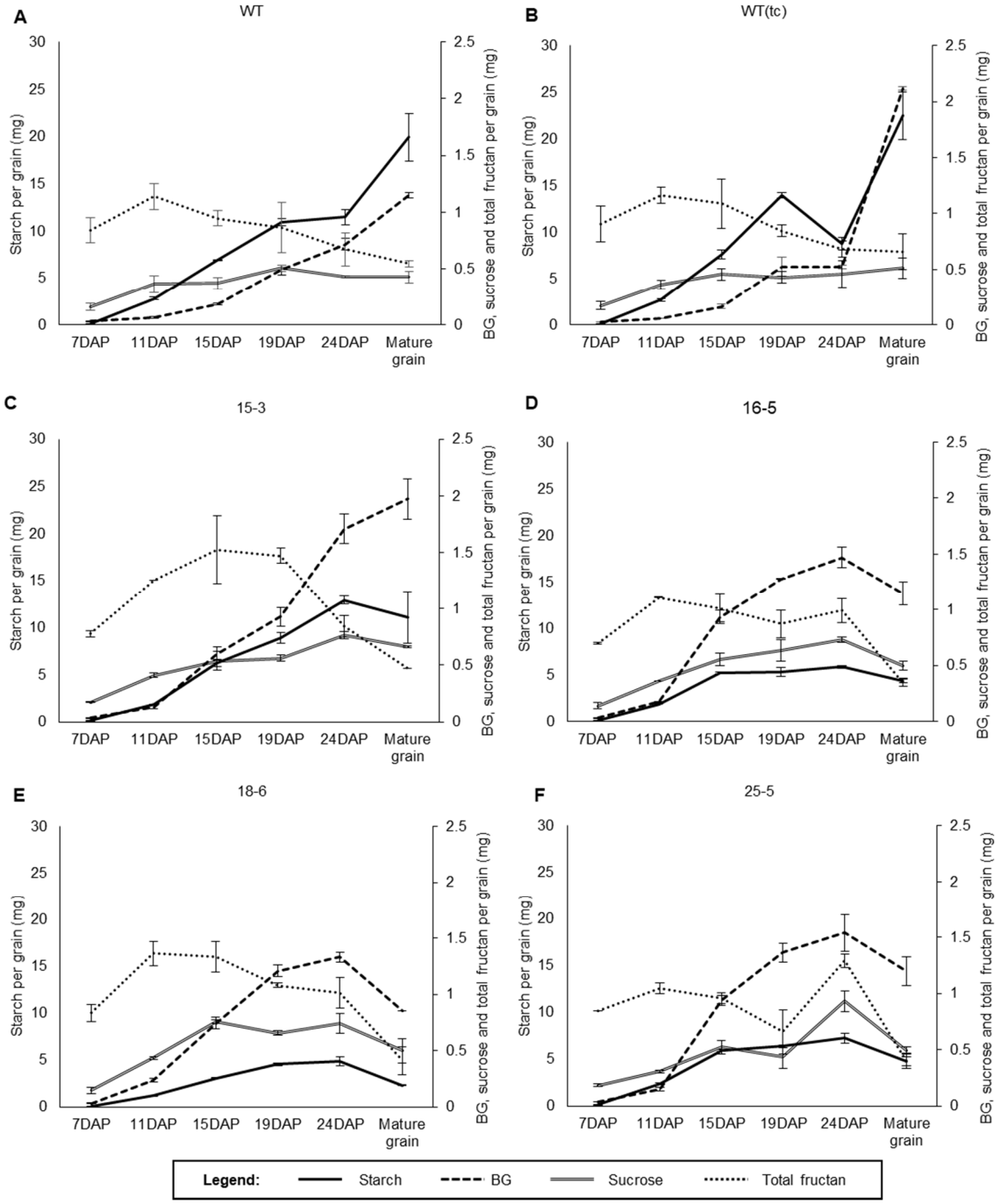

Figure 5: The carbohydrates content: (1,3;1,4)-β-glucan (BG), starch, sucrose and total fructan during barley grain development on a per grain basis (milligram, mg). (A) WT, (B) WT(tc) and *pAsGlo:HvCslF6* transgenic grains (C) 15-3, (D) 16-5, (E) 18-6, (F) 25-5. For BG measurement, each developing grain contains the pericarp, endosperm and embryo tissues while embryo is removed from the mature grain. For starch measurement, each developing grain contains the endosperm and embryo tissues while embryo is removed from the mature grain. For sucrose

and total fructan measurement, developing grain and mature grain contain the pericarp, endosperm and embryo tissues.

Sucrose and fructans accumulate in the *pAsGlo:HvCslF6* grain

The drastic morphological changes in the ETCs of transgenic grain coincided with the early phase of storage product formation (9 to 14 DAP) (Fig. 4A to 4F, Supplementary Fig. S7A to S7D), suggesting a possible relationship with disturbed carbohydrate homeostasis. This assumption is supported by pronounced differences in endosperm storage product accumulation from 15 DAP (Fig. 5A to 5F, Table 2, Supplementary Fig. S7A to S7D, S8A to S8D). A MALDI MSI technique was used to visualise the spatio-temporal distribution of sugar oligosaccharides in WT and 18-6 transgenic grain at both 15 and 24 DAP (Fig. 6A to 6H). At 15 DAP, MALDI-MSI revealed accumulation of disaccharides (DP2) in the region adjacent to the cavity of both transgenic and WT grain at a similar signal intensity (Fig. 6C), while the intensity signals for trisaccharides (DP3) and tetrasaccharides (DP4) were higher in the solid endosperm and the region between the endosperm and embryo of transgenic grain (Fig. 6E and 6G). At 24 DAP, the signal intensity for DP2 was higher in the region adjacent to the cavity and embryo of both transgenic and WT grain (Fig. 6D) and the signal intensities for DP3 and DP4 remained stronger in the transgenic grain, also mainly in the region adjacent to the cavity and endosperm (Fig. 6F and 6H).

Fluids from the endosperm cavity of barley grain were extracted using a microsyringe and the volume was measured. At 15 DAP, there was more than a two-fold increase in the volume of cavity fluids from single barley grain from transgenic lines compared to the WT grain (Supplementary Fig. S9). Quantitative measurement of soluble sugars revealed glucose,

fructose, sucrose and total fructan levels in the cavity, as a proportion of the total sugars from one whole grain, was similar between WT and transgenic grain at 11 DAP (Table 2). At 15 DAP, there was a significant increase in glucose, sucrose and total fructan levels in the transgenic cavity compared to WT (Table 2). At 24 DAP, sucrose and total fructan levels remained higher in the transgenic cavity compared to WT (Table 2).

The ratio of sucrose to hexose (glucose/fructose) was calculated based on mean values (Supplementary Fig. S8A, S10A and S10C, Table 2). In developing grain, sucrose-to-glucose ratios in the endosperm of all transgenic lines were similar to WT from 7 to 11 DAP, but varied from 15 to 24 DAP (Supplementary Fig. S11A). In contrast, sucrose-to-fructose ratios were similar to WT from 7 to 11 DAP, and the ratios became greater than WT from 15 to 24 DAP across all transgenic lines (Supplementary Fig. S11B). In the cavity of developing grain, sucrose-to-glucose or fructose ratios were higher across all transgenic lines at 15 and 24 DAP (Supplementary Fig. S11C and S11D). In mature grain, a greater proportion of sucrose relative to glucose or fructose, was consistently found in the endosperm, while a greater sucrose-to-fructose ratio was found in the embryo of all transgenic lines (Supplementary Fig. S11E and S11F). All transgenic lines consistently showed a greater sucrose-to-hexose ratios from 15 DAP. Given that there was less starch in the transgenic endosperm, high sucrose levels are likely used for (1,3;1,4)-β-glucan and fructan synthesis or due to failure to convert to starch synthesis.

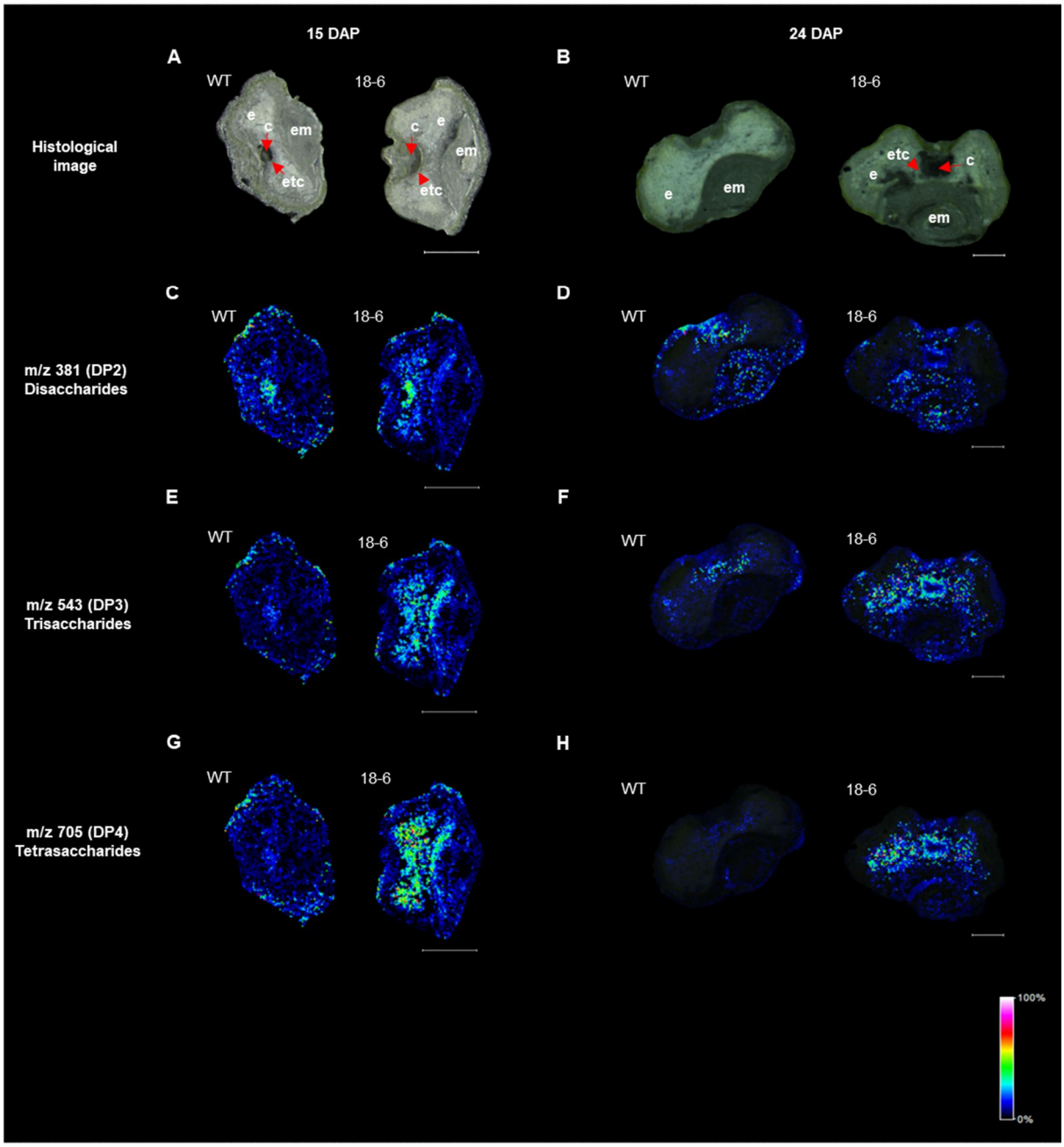

Figure 6: Visualization of oligosaccharides in WT and 18-6 transgenic grain at 15 and 24 DAP using a MALDI-MSI approach. (A) and (B) are histological images of WT and transgenic grain at 15 and 24 DAP respectively. (C) At 15 DAP, disaccharides (DP2) are mostly accumulated in and around the endosperm cavity of WT and transgenic grain. (D) At 24 DAP, DP2 signal intensity is the highest in the endosperm cavity and embryo of WT and transgenic grain. (E) and (G) show stronger signal intensities of trisaccharides (DP3) and tetrasaccharides (DP4) in the endosperm and tissues adjacent to embryo of transgenic grain relative to WT at 15 DAP. (F

and H) show stronger signal intensities of DP3 and DP4 in the endosperm and endosperm cavity of transgenic grain relative to WT at 24 DAP. Scale bars in (A), (C), (E) and (G) are equivalent to 500 µm. Scale bars in (B), (D), (F) and (H) are equivalent to 200 µm. Colours used in the single ion intensity maps correspond to signal intensity scaling displayed at the bottom right. Abbreviations: endosperm (e), endosperm transfer cells (etc), cavity (c), embryo (em).

Table 2. Percentage of soluble sugar content (glucose, fructose, sucrose and total fructan) in the endosperm cavity per total corresponding sugar from a single grain at 11 DAP, 15 DAP and 24 DAP on a weight per weight basis (w/w). *pASGLO:HvCslF6* transgenic grains contain greater amount of glucose in the cavity than WT at 15 DAP. No difference in fructose content between the transgenic grain and WT in the cavity at 15 DAP and 24 DAP was observed. Sucrose and Total fructan content are greater in the cavity of transgenic relative to the WT grain at 15 DAP and 24 DAP. The error bars show the standard deviation of the mean. * indicates a significant difference from the WT by t-test with P-values of < 0.05

	Glucose (%w/w)			Fructose (%w/w)			Sucrose (%w/w)			Total fructan (%w/w)		
	11 DAP	15 DAP	24 DAP	11 DAP	15 DAP	24 DAP	11 DAP	15 DAP	24 DAP	11 DAP	15 DAP	24 DAP
WT	0.33±0.01	0.40±0.32	0.48±0.27	0.26±0.02	0.17±0.13	0.24±0.18	0.26±0.02	0.19±0.09	0.02±0.03	0.32±0.02	0.22±0.14	0.06±0.06
WT(tc)	0.23±0.18	0.37±0.41	0.66±0.79	0.17±0.14	0.28±0.32	0.35±0.44	0.16±0.13	0.03±0.03*	0.02±0.01	0.20±0.16	0.07±0.02*	0.10±0.02
15-3	0.50±0.34	0.75±0.00*	0.94±0.54	0.24±0.18	0.17±0.00	0.33±0.24	0.42±0.29	0.47±0.05*	0.31±0.20*	0.51±0.39	0.52±0.09*	0.60±0.34*
16-5	0.31±0.25	0.84±0.09*	0.85±0.62	0.22±0.18	0.28±0.03	0.28±0.19	0.30±0.16	0.82±0.07*	0.15±0.03*	0.39±0.27	0.81±0.11*	0.39±0.13*
18-6	0.27±0.20	1.04±0.72*	0.19±0.02*	0.13±0.06*	0.72±0.66	0.18±0.08	0.25±0.17	0.52±0.14*	0.08±0.00*	0.28±0.16	0.75±0.29*	0.14±0.03*
25-5	0.10±0.07*	0.82±0.08*	0.83±0.23	0.07±0.06*	0.27±0.07	0.25±0.07	0.13±0.13*	0.57±0.06*	0.24±0.05*	0.13±0.12*	0.63±0.06*	0.58±0.17*

Carbohydrate metabolic pathways are altered in *pAsGlo:HvCslF6* grain

The transgenic lines had altered carbohydrate profiles compared to WT from early storage phase. To address this, genes that are associated with the regulation of various carbon pathways were analysed for their transcript levels and normalized to the WT samples in different grain tissues (pericarp, endosperm and embryo) across development. All transgenic lines were analysed, however, only the 18-6 transgenic line is presented in this study because it showed the highest CslF6 protein level (Fig. 1A) and the grain showed the most pronounced phenotype. The genes analysed include cell wall-related genes (*CslF6, CslH1, endo-β-(1,3;1,4)-glucanase E1 (Endo E1), cellulose synthase 2 (CesA2)* and *cellulose synthase-like F9 (CslF9)*), starch-related genes (*GBSS1a, starch synthase 2 (SS 2), SBE2a, SBE2b, Iso1*, *LD* and *sucrose synthase1 (SuSy1)*), sucrose metabolism genes (*cell wall invertase 1 (CWINV1)* and *vacuolar invertase (VIN)*, *sucrose phosphate synthase (SPS)*, *sucrose phosphate phosphatase (SPP), sucrose transporter 1 (SUT1)* and *sucrose transporter 2 (SUT2))* and fructan biosynthetic genes (*1-SST*, *1-FFT* and *6-SFT*). The *HORVU6H1G011260* and *HORVU2H1G109120* genes were selected due to their putative role in hydrolysing glycosidic bonds between two carbohydrate molecules, including fructans (Fig. 7 and Supplementary Table S3).

The changes in transcript levels of the genes of interest in pericarp, endosperm and embryo tissues are represented in a heat map in Figure 7. Genes where the maximum transcript value was lower than 2000 arbitrary units were not included in the heat map.

Consistent with additional expression from the *pAsGlo:HvCslF6* construct, *CslF6* transcript was upregulated in endosperm from the 18-6 transgenic line at 7 and 11 DAP and then declined until 24 DAP. In contrast, the *CslH1* gene was upregulated in the endosperm from 15 to 24 DAP (Fig. 7). Upregulation of the *CslF6* and *CslH1* gene was also detected in the endosperm

of other transgenic lines, including 15-3, 16-5 and 25-5 (data not shown). In the embryo tissue, the *CslF6* gene was upregulated at 19 DAP. The *Endo E1* transcript which encodes a protein responsible for the hydrolysis of (1,3;1,4)-β-glucan, was downregulated in the transgenic endosperm and embryo across development (Fig. 7). Other cell wall-related genes such as *CslF9* were downregulated in the transgenic endosperm from 7 to 15 DAP (Supplementary Fig. S11B) while the *HvCesA2* gene encoding a cellulose synthase (Burton et al., 2004; Desprez et al., 2007), had very low transcript levels in the endosperm of both WT and transgenic lines (Supplementary Fig. S1C).

The expression of starch metabolic genes: *SS2, SBE2a, SBE2b, GBSS1a, Iso1* and *LD*, was downregulated in transgenic endosperm across development with lowest levels at 24 DAP. In contrast, the *SBE1* gene expression was highly upregulated compared to WT in all tissues during development (Fig. 7). The starch metabolic gene profiles in the 18-6 transgenic line were similar in 15-3, 16-5 and 25-5 (data not shown). Sucrose is hydrolysed by invertases, including cell wall invertase (*CWINV*) and vacuolar invertase (*VIN*). The *CWINV1* gene was downregulated in the transgenic endosperm and embryo at late grain filling phase from 19 to 24 DAP. Of the genes involved in the fructan metabolic pathway, the *6-SFT* gene was upregulated in the transgenic endosperm from 11 to 19 DAP and there was only no remarkable increase in *6-SFT* gene expression levels in the transgenic embryo compared to the WT. The *HORVU2H1G109120* gene was upregulated concurrently with the *6-SFT* gene in the transgenic endosperm, while the *HORVU6H1G011260* gene transcript levels were counter-directional to those of *6-SFT*.

The sucrose transporter gene, *SUT1* gene was upregulated in the transgenic endosperm at 19 DAP and downregulated in the transgenic embryo at 15 DAP. The *SuSy1, SPS* and *SPP* genes

which are involved in sucrose metabolism showed only small changes in transcript levels compared to WT (Fig. 7). In overall during the storage phase (15 to 24 DAP), there was an upregulation of fructan biosynthetic gene (*6-SFT*) and sucrose transporter gene (*SUT1*), downregulation of invertase genes and starch metabolic genes in the transgenic endosperm, which coincided with the increased sucrose and fructan content, and decreased starch content as shown in the sugar quantitative data (Supplementary Fig. S7C and S7D, S8A, S8C and S8 D).

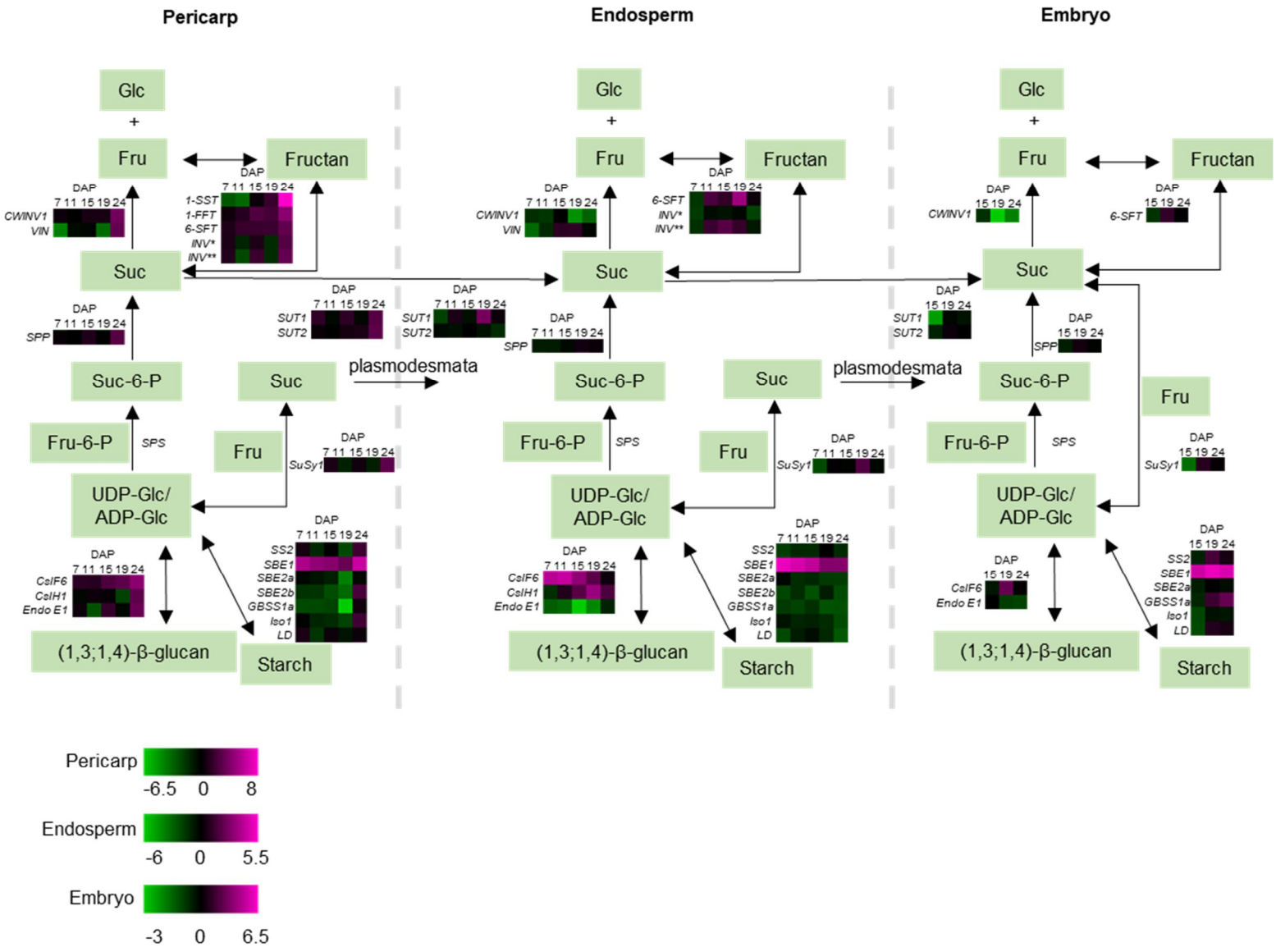
Pericarp
Endosperm
Embryo
Glc
+
Fru
Fructan
Suc
Suc-6-P
Fru-6-P
SPS
UDP-Glc/
ADP-Glc
(1,3;1,4)-β-glucan
Starch
plasmodesmata
DAP
7 11 15 19 24
CWINV1
VIN
1-SST
1-FFT
6-SFT
INV*
INV**
SUT1
SUT2
SPP
SuSy1
CslF6
CslH1
Endo E1
SS2
SBE1
SBE2a
SBE2b
GBSS1a
Iso1
LD
Pericarp
-6.5 0 8
Endosperm
-6 0 5.5
Embryo
-3 0 6.5

Figure 7: Schematic diagram of carbohydrate metabolic pathway in pericarp, endosperm and embryo of a barley grain and the transcript expression of involved genes in 18-6 transgenic grain from 7 to 24 DAP. The expression of *CslF6* transcripts includes the transgene and wild type gene expression. For each tissue, the transcript expression values are normalized against wild type (WT) and calculated as $\log_2$. Vertical dashed lines separate the three grain tissues. UDP-glucose (UDP-Glc) and ADP-glucose (ADP-Glc) are substrates for the biosynthesis of (1,3;1,4)-β-glucan and starch respectively. INV* indicates *HORVU6Hr1G011260* gene. INV** indicates *HORVU2Hr1G109120* gene, which are both involved in the hydrolysis of glycosidic bond between the carbohydrates, including fructans. Abbreviations: Glucose (Glc), Fructose (Fru), Sucrose (Suc), Sucrose-6-phosphate (Suc-6-P), Fructose-6-phosphate (Fru-6-P). Magenta indicates increased expression while green indicates decreased expression.

Discussion

Specificity of *pAsGlo* promoter activity in barley grain

The increase in the endosperm (1,3;1,4)-β-glucan content in the *pAsGlo:HvCslF6* transgenic lines is consistent with the early activity of the *pAsGlo* promoter shortly after the completion of endosperm cellularisation (Wilson et al., 2006), specifically in the peripheral endosperm (Fig. 1B to 1D), and matching the upregulation of the *CslF6* transgene transcript detected at 7 DAP (Supplementary Fig. S1A). Whereas the *pAsGlo* driven yellow fluorescent protein (YFP) was not detected in the transgenic pericarp and embryo (Fig. 1B), higher transcript levels of the *CslF6* transgene were detected in these tissues (Supplementary Fig. S1A). We observed high expression levels of *Ltp2* and *GBSS1a* in the transgenic pericarp which is indicative of possible RNA contamination from the peripheral endosperm layer (Supplementary Fig. S1D and S1E). Similar contaminations were reported in a recent study of endosperm transcriptome datasets and these authors suggest that hand dissection is likely to cause RNA contamination (Schon and Nodine, 2017). Considering the specificity of expression of *pAsGlo:YFP* in the peripheral endosperm, and the evidence of RNA contamination in the pericarp tissue from adherent underlying cells, we assume that the *CslF6* transgene was overexpressed exclusively in the endosperm, and not in the pericarp or embryo.

Aleurone development in *pAsGlo:HvCslF6* transgenic barley

The aleurone cells in 18-6 transgenic grain appeared elongated by 24 DAP which persisted to maturity (Fig. 3D and Supplementary Fig. S6H). Differentiation of aleurone cells is initiated around 8 DAP (Bosnes et al., 1992) and it is determined by signals released from the peripheral starchy endosperm (Becraft and Asuncion-Crabb, 2000; Gruis et al., 2006), although the position cues for aleurone cell fate are still not fully understood. There are a number of genes

which have been reported to be involved in regulating aleurone cell fate and differentiation in cereal grains, for example, *defective kernel1 (dek1)*, *crinkly4* (*cr4)* and *supernumerary aleurone1 (sal1)* (Lid et al., 2002; Olsen et al., 2008). Aleurone development has also been associated with regulation by hormones (Bethke et al., 1999; Gómez-Cadenas et al., 2001; Smeekens, 2000). In maize, upregulation of the *isopentenyl transferase (IPT)* gene which encodes a cytokinin biosynthetic enzyme, resulted in interspersed patches of aleurone and starchy endosperm cells, suggesting that cytokinin suppresses aleurone cell identity (Geisler-Lee and Gallie, 2005). Another study showed that maize kernels treated with an auxin transporter inhibitor, *N*-1-naphthylphthalamic acid (NPA) had up to four aleurone cell layers compared to the WT, which has only one aleurone cell layer (Forestan et al., 2010). Moreover, the number of aleurone cells has been linked to endosperm and embryo development. For example, *disorgal* maize mutants which had an increased number of aleurone cells, had a shrunken endosperm with reduced starch granule density, and a smaller embryo (Lid et al., 2004); *defective seed5 (des5)* barley mutants with a reduced number of aleurone cells had shrunken endosperm, altered starch granule types, and the embryo had prematurely aborted (Olsen *et al.*, 2008). The peripheral endosperm cells in these *pAsGlo:HvCslF6* transgenic lines, where the *CslF6* transgene is expressed (Fig. 1B to 1D), appeared to be structurally different from the WT from 9 DAP (Supplementary Fig. S6A to S6H). This is likely because the cells in the peripheral endosperm layer failed to retain their cell identities, which could be a result of downstream signalling pathways which are yet to be identified. To test this, targeted laser capture assisted RNAseq experiments would be required.

Morphology and cell wall composition in the endosperm transfer cells of *pAsGlo:HvCslF6* transgenic barley

The morphology of developing grain revealed an increase in cavity size in the transgenic grain relative to WT from 9 DAP (Supplementary Fig. S2A and S2B) while the ETC began to rupture at 10 DAP (Fig. 4D). During this stage, the cell walls of ETC in the transgenic grain were thinner than those in WT (Fig. 4G and 4H) and showed variations in mannan abundance (Fig. 4I and 4J). This was in contrast to the cell walls in the endosperm, which appeared thicker than WT (Supplementary Fig. S6F and S6H). In the ETC walls, no labelling was observed using BG1 ((1;3;1,4)-β-glucan) (Fig. 2B), LM11 (arabinoxylan) (Supplementary Fig. S3B), (1,3)-β-glucan (callose) (Supplementary Fig. S3D), CBM3a (crystalline cellulose) (Supplementary Fig. S3H) and LM20 (pectin) (data not shown), while the labelling from LM19 antibody appears to be from the remnants from the nucellus (Supplementary Fig. S4A to S4D) (Greenwood et al., 2005). Interestingly, these results did not match the transcriptome analysis by Thiel et al., (2012b), who demonstrated upregulation of genes related to callose and cellulose metabolism at the same time point (10 DAP). Failure of antibodies to detect other cell wall polysaccharides besides mannan, could be due to the way they are arranged in the cell walls of transfer region, such that their epitopes are masked and unavailable for binding. Therefore, it is difficult to determine if weakening and tearing of ETC in the 18-6 transgenic grain is solely dependent on the dominance of mannan polysaccharides based on our fluorescence immunolabeling results. A more precise examination of the cell wall polysaccharides in ETCs could be achieved using immunogold labelling and transmission electron microscopy (TEM), with appropriate unmasked techniques. Alternatively, laser-microdissection and transcriptome analysis of precise regions of the grain, mainly of ETCs and surrounding endosperm would be ideal to look at gene expression

Altered ETC morphology may trigger abnormal accumulation of sucrose and fructans in the grain cavity and endosperm

In barley, proper formation of ETCs is important to ensure nutrient transfer from the cavity to the endosperm for development and storage of carbohydrates. A study by Felker et al., (1985) showed that some barley mutants with abnormal endosperm had missing ETCs, such as *seg2, seg4, seg5 a*nd *seg8*, and starch filling in the endosperm was affected. Here, the importance of ETCs in carbon storage during grain filling was further explored in *CslF6* transgenic grain. Whilst the starch levels were reduced, there was a significant increase in sucrose and total fructan content in the transgenic grain cavity and endosperm compared to WT (Table 2, Supplementary Fig. S8A to S8D). We hypothesise that the high sucrose and fructan pools in the cavity at 15 DAP may be due to early perturbations in ETC differentiation (Fig. 4D and 4H), which subsequently interferes with and perturbs the flow of sucrose and fructans into the endosperm tissue as grain development progresses. However, a detailed histological examination of ETCs at much earlier stages (3 to 6 DAP) is required to confirm what is happening.

With large sections of ETC missing, sucrose and fructans from the cavity could diffuse into the endosperm symplastically. Furthermore, the concomitant increased sucrose-to-glucose and sucrose-to-fructose ratios at 15 DAP in the cavity and endosperm of transgenic grain suggest a shift towards the sucrose signalling pathways for fructan biosynthesis (Ruan, 2014; Vijn and Smeekens, 1999; Weichert et al., 2010). In the transgenic endosperm, there was an upregulation of a fructosyltransferase gene, *6-SFT* (Fig. 7), which encodes protein responsible for catalysing the formation of branched and levan-type fructans containing β(2,6) linkages (Vijn and Smeekens, 1999). Downregulation of *CWINV1* and *VIN* in the transgenic endosperm may also

be responsible for the increased amounts of sucrose and total fructan, and small amounts of glucose (Fig. 7, Supplementary Fig. S8A, S8C and S8D, Supplementary Fig. S10A).

Starch metabolism in the endosperm of *pAsGlo:HvCslF6* transgenic barley

Transgenic grain overexpressing *HvCslF6* showed an upregulation of the *CslH1* and a downregulation of the *Endo E1* gene in the endosperm (Fig. 7). Together, changes in the *CslF6*, *CslH1* and *Endo E1* gene abundance contributed to the increased amount of (1,3;1,4)-β-glucan in the transgenic endosperm (Fig. 7, Supplementary Fig. 7A and 7B). High (1,3;1,4)-β-glucan content is likely to be balanced by a lower starch content as previously reported (Burton et al., 2011a; Munck et al., 2004; Seefeldt et al., 2009). This study showed that reduction in starch content was also associated with downregulation of starch biosynthetic genes (Fig. 7). In contrast, the *SBE1* gene was consistently upregulated in the endosperm of 18-6 and other transgenic lines (Fig. 7). The SBE1 enzyme is involved in producing long-chain amylopectin. Mutation in the *SBE1* gene in rice results in decreased long chains with DP≥37 and short chains with DP 12 to 21, and increased shorter chain molecules with DP≤10 and an intermediate chains with DP 24 to 32 (Satoh et al., 2003). It is unclear whether the upregulation of the *SBE1* gene contributed to the reduced amount of starch in the transgenic grain which also showed different starch granule types (Fig. 3A and 3B, Table 1). Altered starch granule sizes were also reported in the *des5* barley mutant (Olsen et al., 2008), *seg* mutants (Ma et al., 2014) and the *sex6* mutant (Morell et al., 2003), however, genes that are responsible for the altered granule phenotypes have not been identified so far. It is possible that changes in starch granule phenotypes are due to pleiotropic effects from more general perturbations in carbon partitioning.

Cell wall metabolism in the endosperm of *pAsGlo:HvCslF6* transgenic barley

Biosynthesis of (1,3;1,4)-β-glucan, cellulose and callose, requires the conversion of sucrose to nucleotide sugars to be used as substrates (Dugger and Palmer, 1986; Gleason and Chollet, 2011; Ray et al., 1969). Strong fluorescent labelling from the LM11, callose antibodies and CBM3a indicated greater amounts of these polysaccharides in the transgenic endosperm (Supplementary Fig. S5A to S5F), which may be attributed to the possible increased UDP-glucose availability. Conversion of UDP-glucose or glucose-6-phosphate to UDP-xylose for arabinoxylan biosynthesis is mediated by an indirect reaction, via an intermediate UDP-glucuronic acid (Bindschedler et al., 2005; Loewus and Loewus, 1980; Reiter and Vanzin, 2001). There may have been greater UDP-glucose and UDP-xylose availability in the transgenic grain relative to WT, however testing this would involve tissue specific measurement of the nucleotide sugars and analysis of genes related to cellulose, callose and arabinoxylan biosynthesis.

Conclusions

Increased levels of (1,3;1,4)-β-glucan are desirable in relation to human health benefits. However, high levels of (1,3;1,4)-β-glucan in barley grain from early development affect general directions of carbohydrate metabolism, leading to impairment in grain development during the storage phase. Here, we have developed a schematic model to encapsulate the downstream effects of increased (1,3;1,4)-β-glucan metabolism in Torrens grain (Fig. 8). These changes affect the cell wall structure and composition in the ETCs, resulting in weakening of the cells. A continuous supply of sucrose from the maternal tissue together with the perturbed sucrose transport into the endosperm result in excessive accumulation of sucrose and fructans in the cavity and tearing of the transfer region. Thus, our study revealed that the shrunken phenotype of the *CslF6* transgenic grain is attributed to the increased amount of cavity fluids and reduced accumulation of starch in the endosperm during grain development. Our investigation of the metabolic, gene expression and morphological changes associated with increasing (1,3;1,4)-β-glucan early in grain development has shown the importance of regulation of sucrose homeostasis in controlling grain phenotypes.

Acknowledgements

The authors wish to acknowledge Dr. Wei Zeng (University of Melbourne), Dr. Gwenda Mayo, Dr. Lisa O'Donovan, Mr. Ken Neubauer, Dr. Rohan Singh, Ms. Katherine Allder, Ms Kylie Neumann (University of Adelaide) for their technical assistance, Dr. Hans-Peter Mock (Leibniz Institute of Plant Genetics and Crop Plant Research (IPK), for the stimulating discussions. This work was supported by Adelaide Graduate Research Scholarship (AGRS), an Australian Research Council (ARC) Centre of Excellence in Plant Cell Walls (CE110001007) and German Academic Exchange Service (DAAD) G08 Australia Germany Exchange Program.

Supporting Information

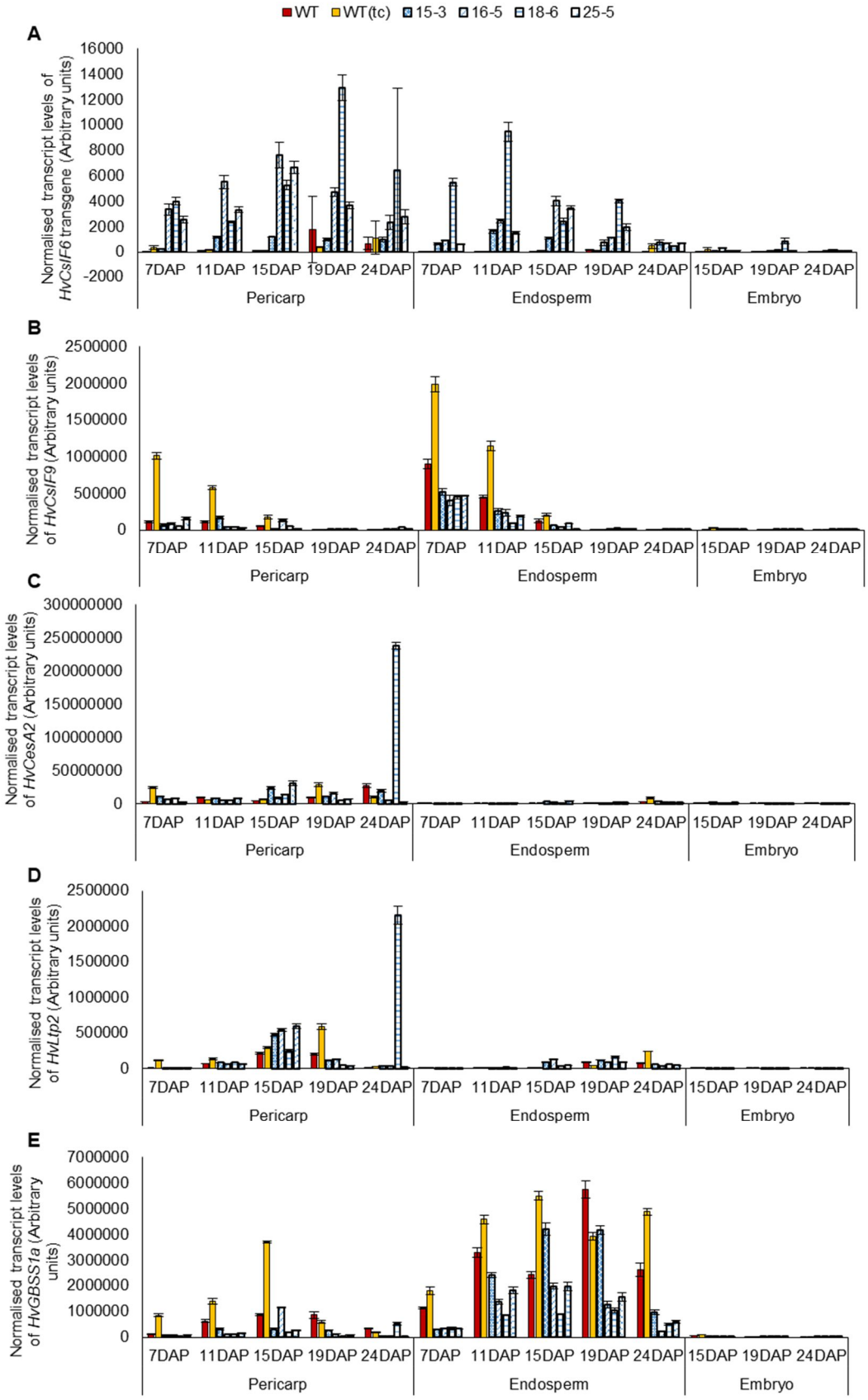

Supplementary figure 1: Normalized transcript levels of *HvCslF6* transgene, *HvCslF9, HvCesA2, HvLtp2* and *HvGBSS1a* in developing grain tissues. The error bars show the standard deviation of the mean. qPCR was performed based on one biological replicate.

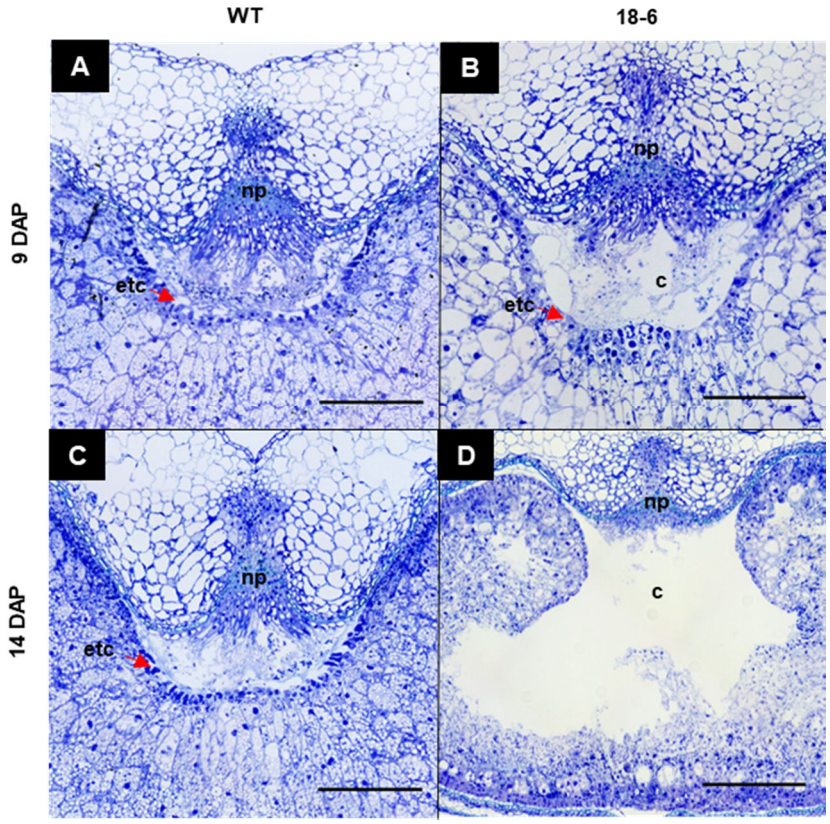

Supplementary figure 2: Morphology of endosperm cavity in WT and 18-6 transgenic grain at (A) and (B) 9 and (C) and (D) 14 DAP. Grain sections are stained with toluidine blue. All images are under 4x magnification with scale bars equivalent to 100 µm. Abbreviations: nucellar projection (np), cavity (c), endosperm transfer cells (etc), endosperm (e).

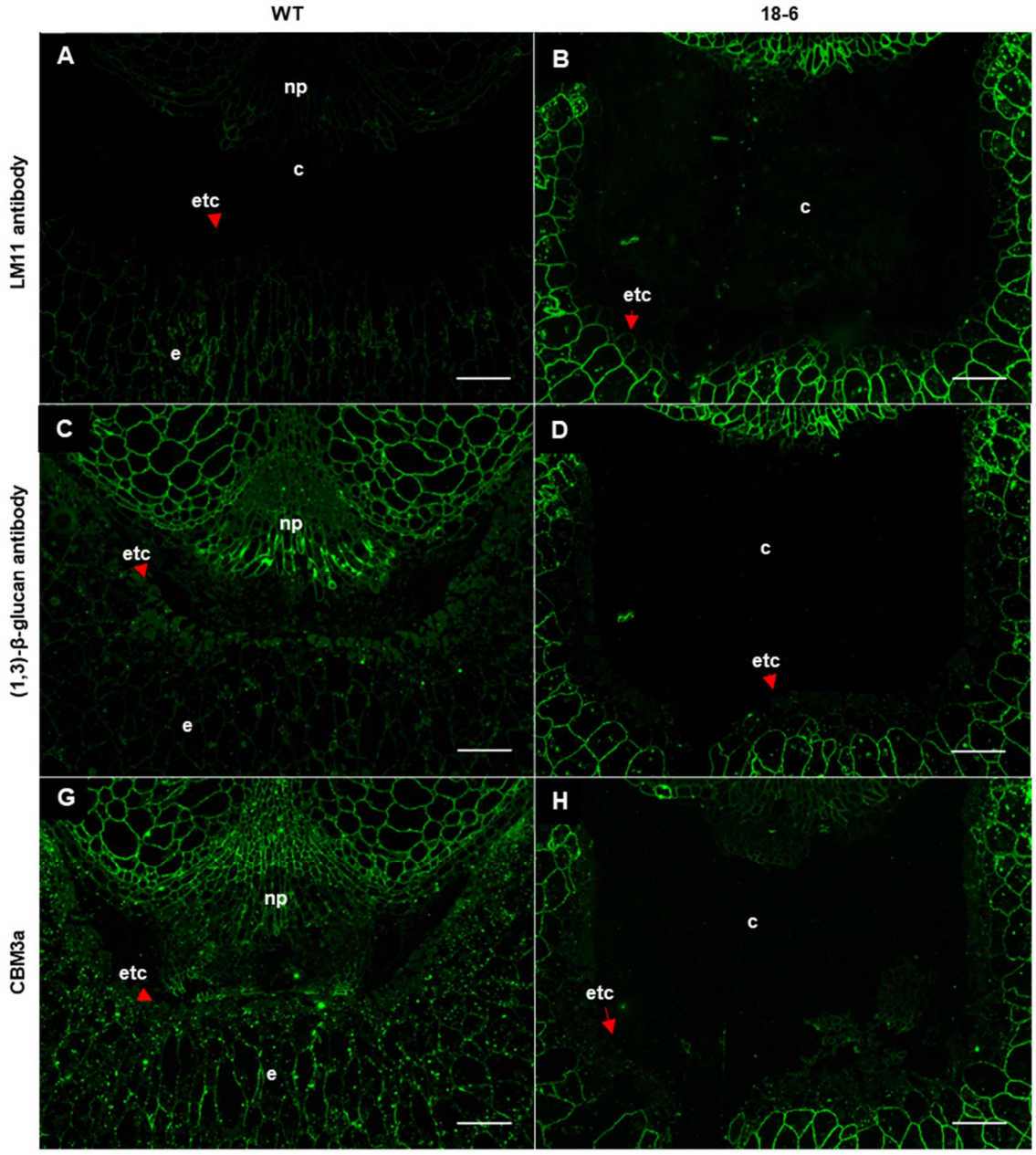

Supplementary figure 3: Immuno-histochemical analysis of arabinoxylan (LM11 antibody), callose ((1,3)-β-glucan antibody), crystalline cellulose (CBM3a) and mannan (1-4)-β-D-mannan and galacto-(1-4)-β-D-mannan antibody in ETC walls at 10 DAP. The fluorescent signals from LM11 antibody, (1,3)-β-glucan antibody and CBM3a are absent in the endosperm transfer cells in both WT and transgenic grain All images are under 10x magnification with scale bars equivalent to 100 µm. Abbreviations: nucellar projection (np), endosperm transfer cells (etc), cavity (c), endosperm (e), pericarp (p), aleurone (al).

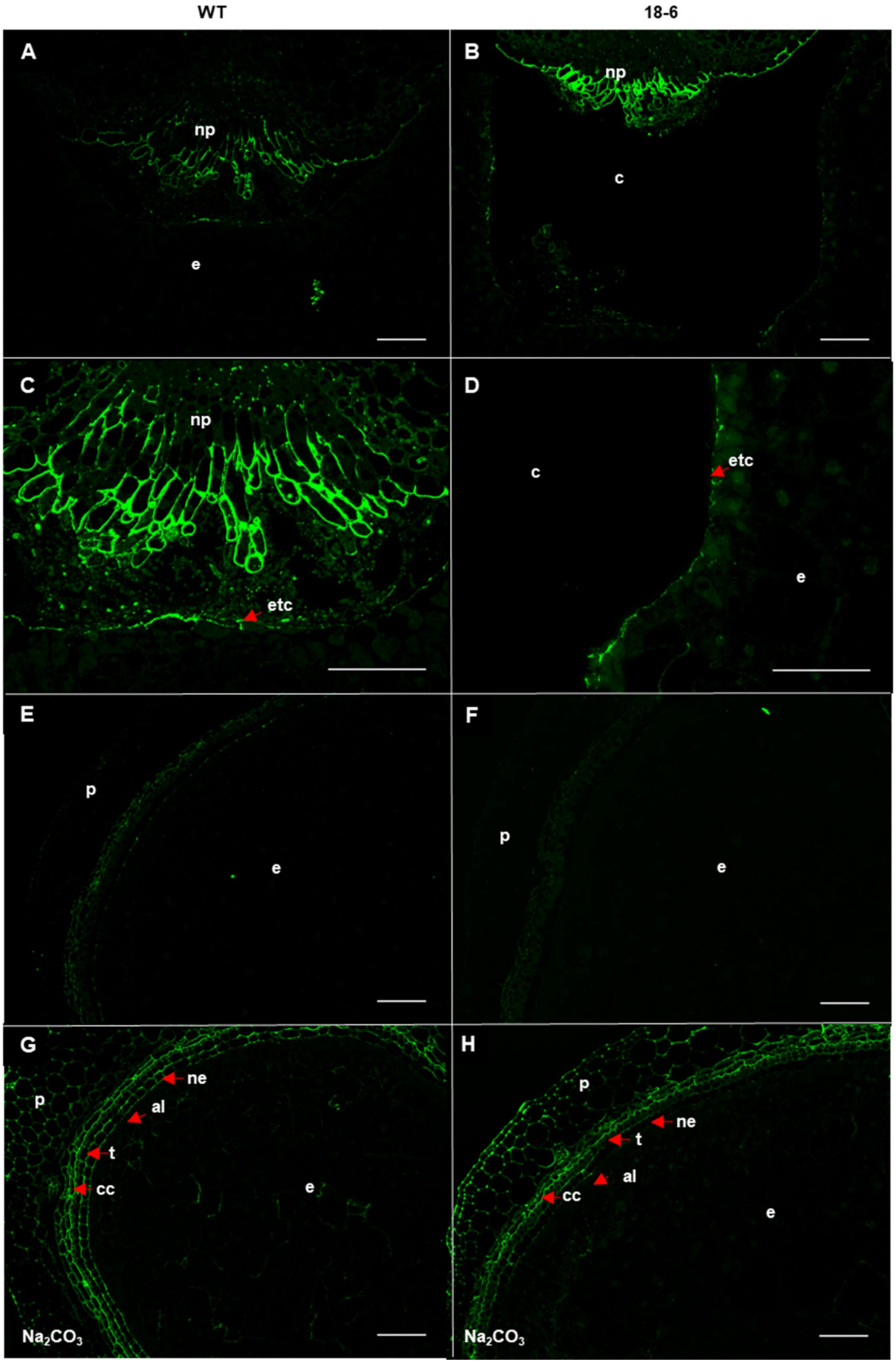

Supplementary figure 4: Immuno-histochemical analysis of pectins with LM19 antibody on barley grain sections at 10 DAP. (A) to (D) The fluorescent signals from LM19 antibody

labelled the cell walls of nucellar projection and the walls of endosperm transfer cells adjacent to the cavity in both transgenic and WT grain. In comparison to the untreated sections (E) and (F), grain sections pre-treated with 0.1 M sodium carbonate (Na_2CO_3) for 1 h prior to LM19 antibody labelling show stronger labelling intensities in the pericarp, cross cells, testa and nucellar epidermis (G) and (H). (A), (B), (E), (F), (G) and (H) are under 10x magnification. (C) and (D) are 20x magnification. All images have scale bars equivalent to 100 µm. Abbreviations: nucellar projection (np), endosperm transfer cells (etc), cavity (c), endosperm (e), pericarp (p), nucellar epidermis (ne), testa (t), cross cells (cc) and aleurone (al).

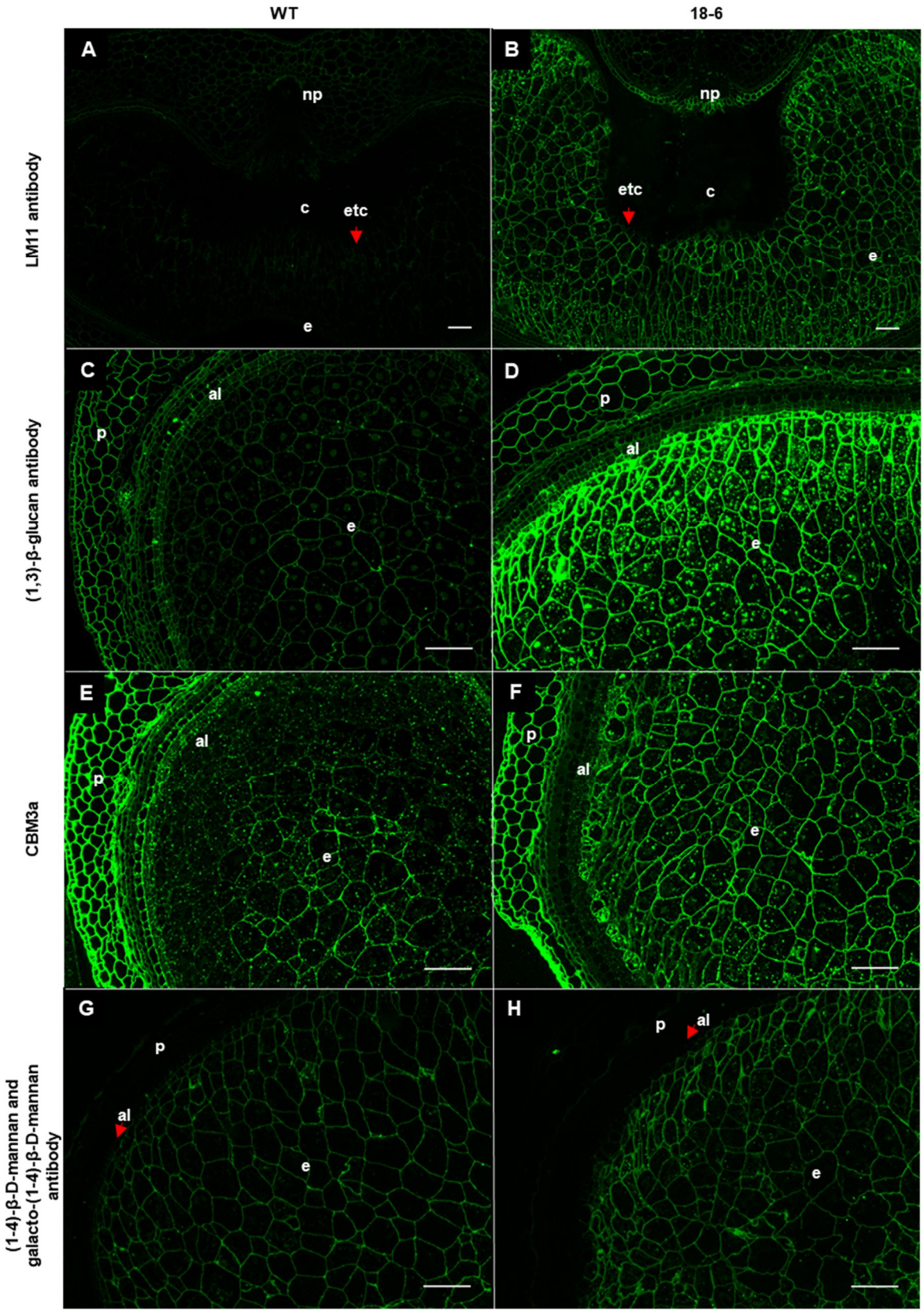

Supplementary figure 5: Immuno-histochemical analysis of arabinoxylan (LM11 antibody), callose (1,3)-β-glucan antibody), crystalline cellulose (CBM3a) and mannan (1-4)-β-D-mannan

and galacto-(1-4)-β-D-mannan antibody in endosperm cell walls at 10 DAP. The intensities of fluorescent signals from arabinoxylan, (1,3)-β-glucan are stronger in 18-6 transgenic grain relative to WT. Fluorescent signals from CBM3a and mannan are labelled uniformly in the trasngenic endosperm relative to WT. (A) and (B) are under 5x magnification. (C) to (H) are under 10x magnification. All images have scale bars equivalent to 100 μm. Abbreviations: nucellar projection (np), endosperm transfer cells (etc), cavity (c), endosperm (e), pericarp (p), aleurone (al).

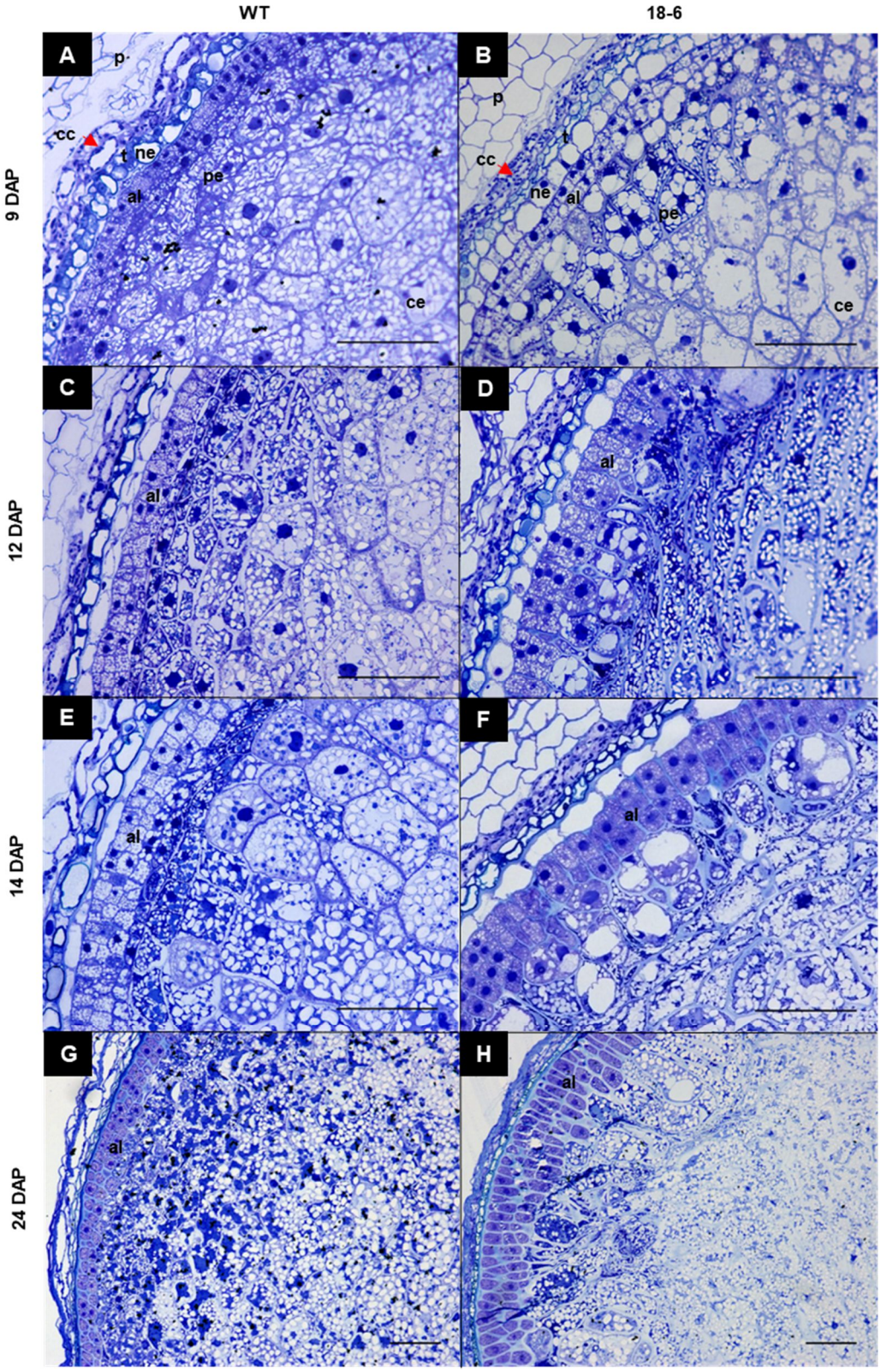

Supplementary figure 6: Morphology of aleurone cells in WT and 18-6 transgenic grain during grain development. Grain sections are stained with toluidine blue. (A) to (F) are under 20x magnification. (G) and (H) are under 10x magnification. All images have scale bars

equivalent to 100 μm. Abbreviations: pericarp (p), cross cells (cc), testa (t), nucellar epidermis (ne), aleurone (al), peripheral endosperm (pe), central endosperm (ce).

Supplementary table 1: Carbohydrates content in (A) mature barley grain (embryo removed) and (B) mature embryo on a weight per weight basis (w/w) and per grain basis (milligram, mg). * indicates a significant difference from the WT by t-test with P-values of < 0.05.

A

	WT	WT(tc)	15-3	16-5	18-6	25-5
1000 pericarp and endosperm weight (g)	31.2±2.8	40.2±3.7	21.2±3.3	14.4±2.9	13.4±4.2	15.9±3.9
Beta glucan (%w/w)	3.9±0.3	5.6±0.5*	8.9±1.2*	9.6±0.2*	8.7±0.4*	9.5±0.2*
Starch (%w/w)	66.6±1.6	59.8±2.5*	49.1±1.0*	36.5±0.6*	23.6±0.2*	37.7±1.2*
Total fructan (%w/w)	1.6±0.2	1.5±0.3	1.5±0.0	2.4±0.1*	3.9±0.0*	2.7±0.6*
Glucose (%w/w)	0.1±0.0	0.1±0.0	0.0±0.0	0.1±0.0	0.1±0.0	0.1±0.0
Fructose (%w/w)	0.1±0.0	0.1±0.0	0.0±0.0	0.0±0.0	0.0±0.0	0.1±0.0
Sucrose (%w/w)	0.9±0.2	1.0±0.2	1.8±0.2*	3.2±0.0*	5.0±0.1*	3.0±0.4*
Raffinose (%w/w)	0.3±0.0	0.3±0.0	0.3±0.0	1.4±0.2*	1.3±0.3*	0.8±0.1*
Arabinoxylan (%w/w)	4.4±0.4	4.3±0.3	6.6±1.2*	9.1±0.4*	13.2±0.5*	8.2±0.0*
Protein (%w/w)	21.0±1.7	17.6±2.1	17.6±4.6	21.3±1.8	23.0±0.9	21.9±0.5
Other (%w/w)	1.2	9.7	14.0	16.5	21.2	16.1
Beta glucan (mg)	1.1±0.0	2.1±0.0*	2.0±0.2*	1.1±0.1*	0.9±0.0	1.2±0.1*
Starch (mg)	20.8±1.0	24.0±1.0*	10.4±0.2*	5.3±0.1*	3.2±0.0*	6.0±0.2*
Total fructan (mg)	0.5±0.1	0.6±0.1	0.3±0.0	0.3±0.0	0.5±0.0	0.4±0.1
Glucose (mg)	0.0±0.0	0.0±0.0	0.0±0.0	0.0±0.0	0.0±0.0	0.0±0.0
Fructose (mg)	0.0±0.0	0.0±0.0	0.0±0.0	0.0±0.0	0.0±0.0	0.0±0.0
Sucrose (mg)	0.3±0.1	0.4±0.1	0.4±0.1	0.5±0.0	0.7±0.0	0.5±0.1
Raffinose (mg)	0.1±0.0	0.1±0.0	0.1±0.0	0.2±0.0	0.2±0.0	0.1±0.0
Arabinoxylan (mg)	1.4±0.1	1.7±0.1*	1.4±0.3	1.3±0.1	1.8±0.1*	1.3±0.0
Protein (mg)	6.6±0.5	7.1±0.9	3.7±1.0*	3.1±0.3*	3.1±0.1*	3.5±0.1*

B

	WT	WT(tc)	15-3	16-5	18-6	25-5
1000 embryo weight (g)	1.2±0.7	1.3±0.5	0.9±0.2	1.3±0.4	1.8±0.6	1.0±0.3
Total fructan (%w/w)	5.2±0.6	5.9±0.4	5.0±0.2	4.0±0.2*	5.0±0.6	4.5±0.5
Glucose (%w/w)	0.1±0.0	0.1±0.0	0.1±0.0	0.1±0.0	0.1±0.0	0.1±0.0
Fructose (%w/w)	0.1±0.0	0.1±0.0	0.0±0.0	0.0±0.0	0.0±0.0	0.0±0.0
Sucrose (%w/w)	9.2±1.1	9.9±0.1	9.1±0.4	7.3±0.8*	9.3±1.3	8.3±0.7
Raffinose (%w/w)	12.7±0.9	12.0±0.2	10.0±1.2*	13.0±0.9	11.7±0.0	11.8±0.1
Other (%w/w)	72.7	72.0	75.8	75.7	73.9	75.3
Total fructan (mg)	0.1±0.0	0.1±0.0	0.0±0.0	0.0±0.0	0.1±0.0	0.0±0.0
Glucose (mg)	0.0±0.0	0.0±0.0	0.0±0.0	0.0±0.0	0.0±0.0	0.0±0.0
Fructose (mg)	0.0±0.0	0.0±0.0	0.0±0.0	0.0±0.0	0.0±0.0	0.0±0.0
Sucrose (mg)	0.1±0.0	0.1±0.0	0.1±0.0	0.1±0.0	0.2±0.0	0.1±0.0
Raffinose (mg)	0.1±0.0	0.2±0.0	0.1±0.0	0.2±0.0	0.2±0.0	0.1±0.0

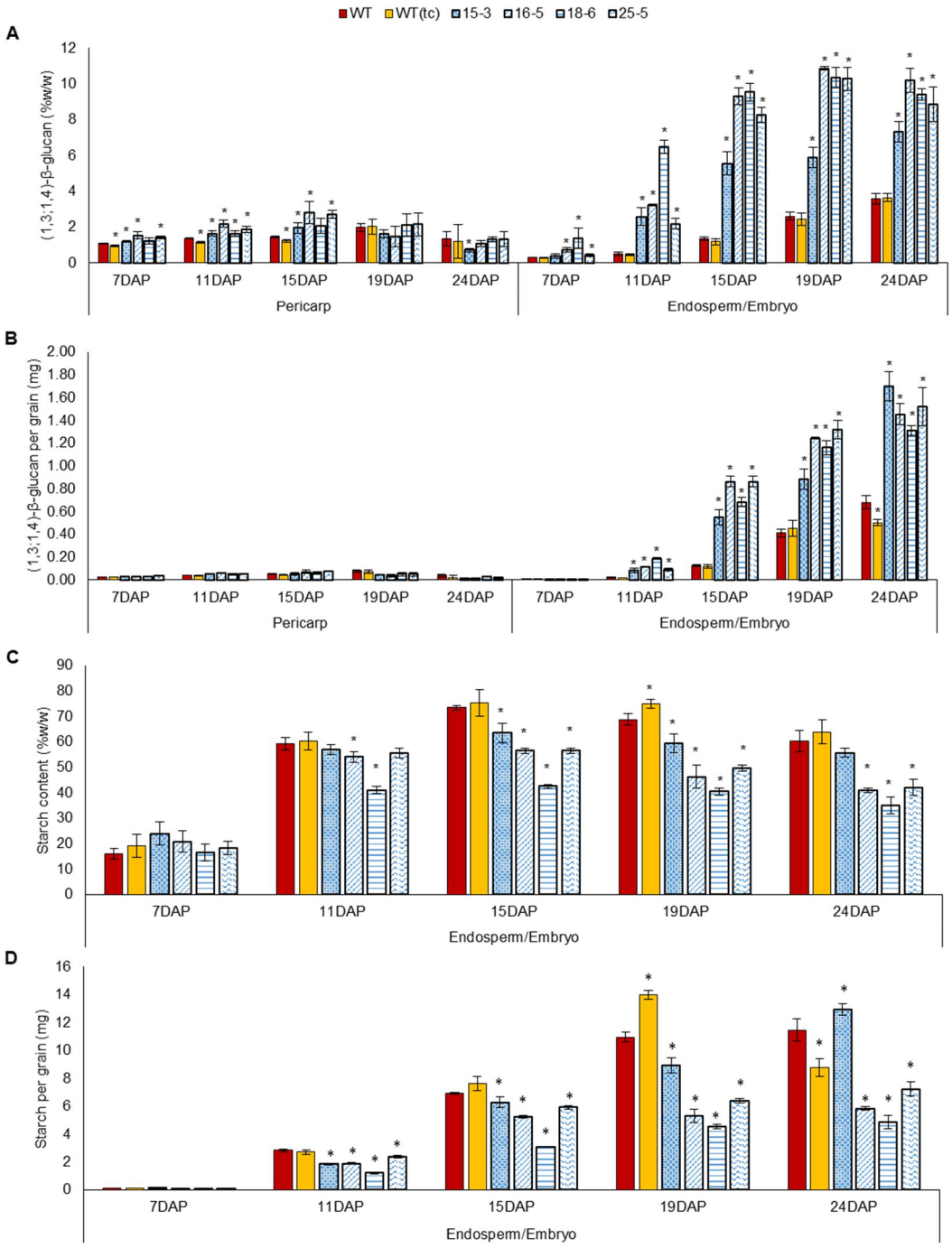

Supplementary figure 7: (A) and (B) (1,3;1,4)-β-glucan and (C) and (D) starch content in developing barley grain on a weight per weight basis (w/w) and on a per grain basis (milligram, mg). The error bars show the standard deviation of the mean. * indicates a significant difference from the WT by t-test with P-values of < 0.05.

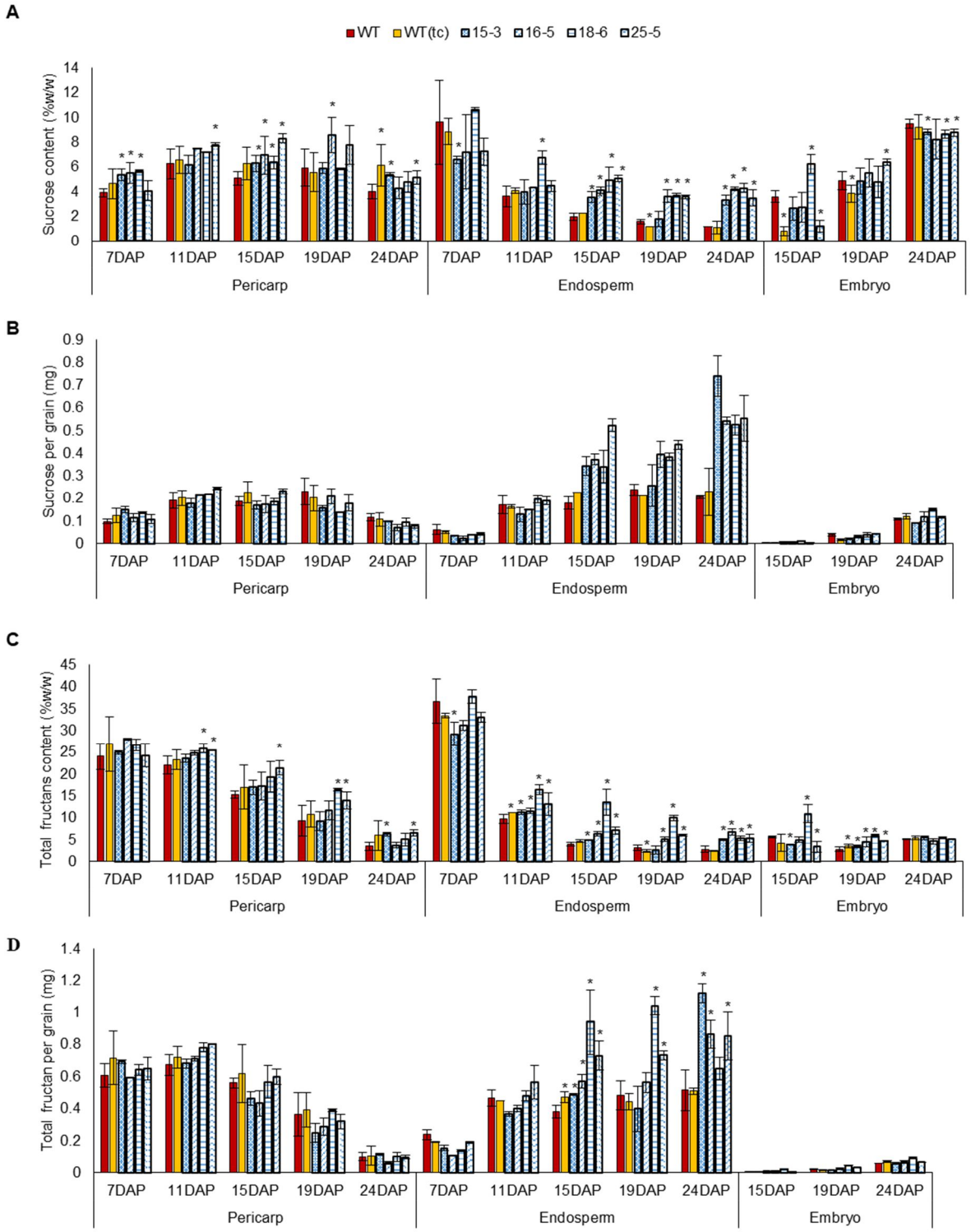

Supplementary figure 8: (A) and (B) Sucrose and (C) and (D) total fructan content in developing barley grain on a weight per weight basis (w/w) and on a per grain basis (milligram, mg). The error bars show the standard deviation of the mean. * indicates a significant difference from the WT by t-test with P-values of < 0.05.

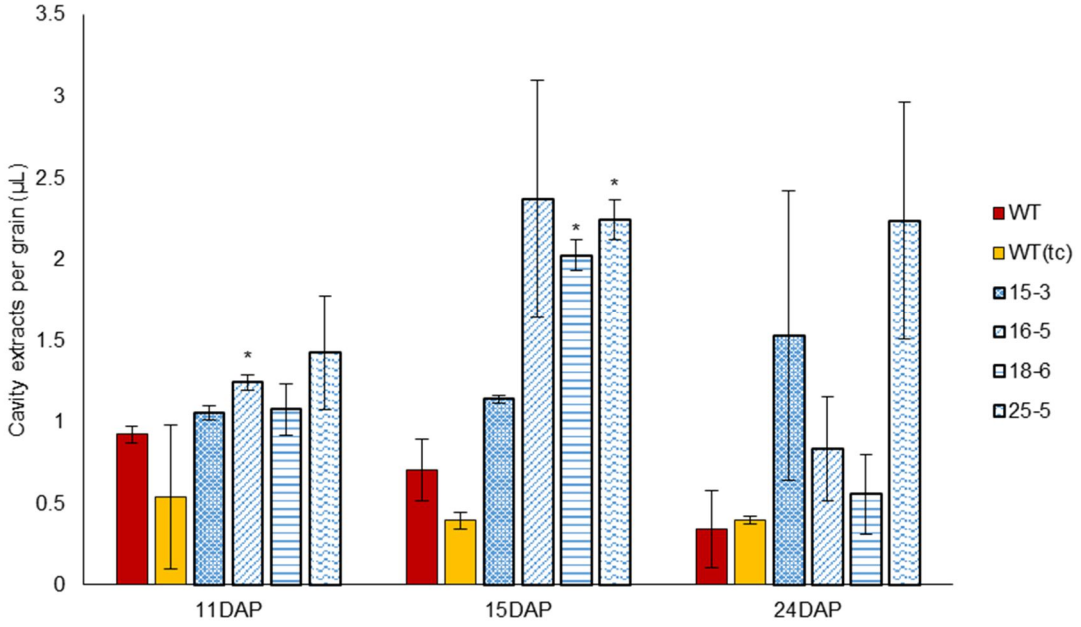

Supplementary figure 9: Total volume of fluids in the endosperm cavity extracted from a single grain (microliter, µL). *pAsGlo:HvCslF6* transgenic grains contain a greater amount of fluids in the endosperm cavity of a single grain at 15 DAP relative to WT. The error bars show the standard deviation of the mean. * indicates a significant difference from the WT by t-test with P-values of < 0.05

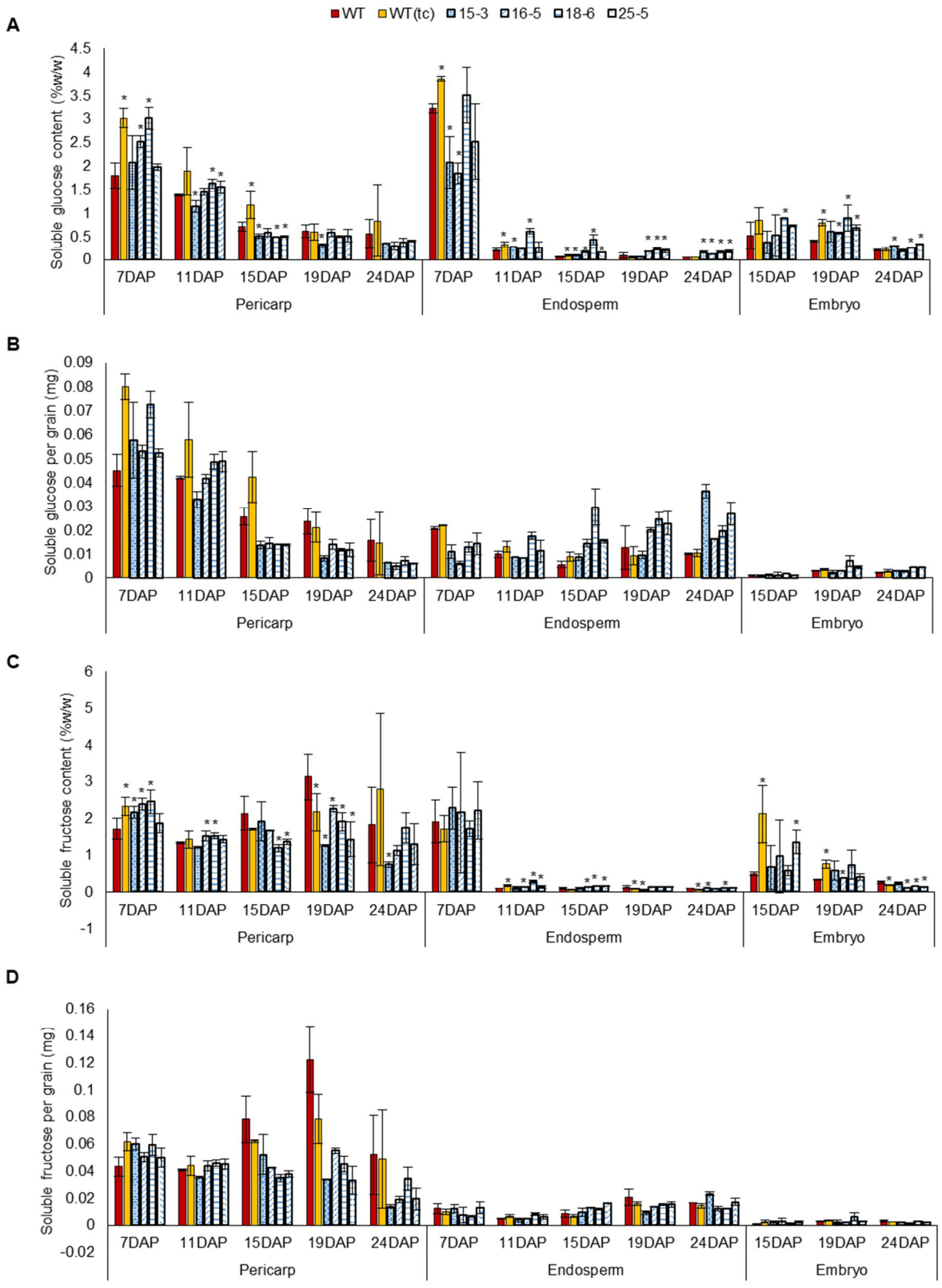

Supplementary figure 10: (A) and (B) Soluble glucose and (C) and (D) soluble fructose content in developing barley grain on a weight per weight basis (w/w) and on a per grain basis

(milligram, mg). The error bars show the standard deviation of the mean. * indicates a significant difference from the WT by t-test with P-values of < 0.05.

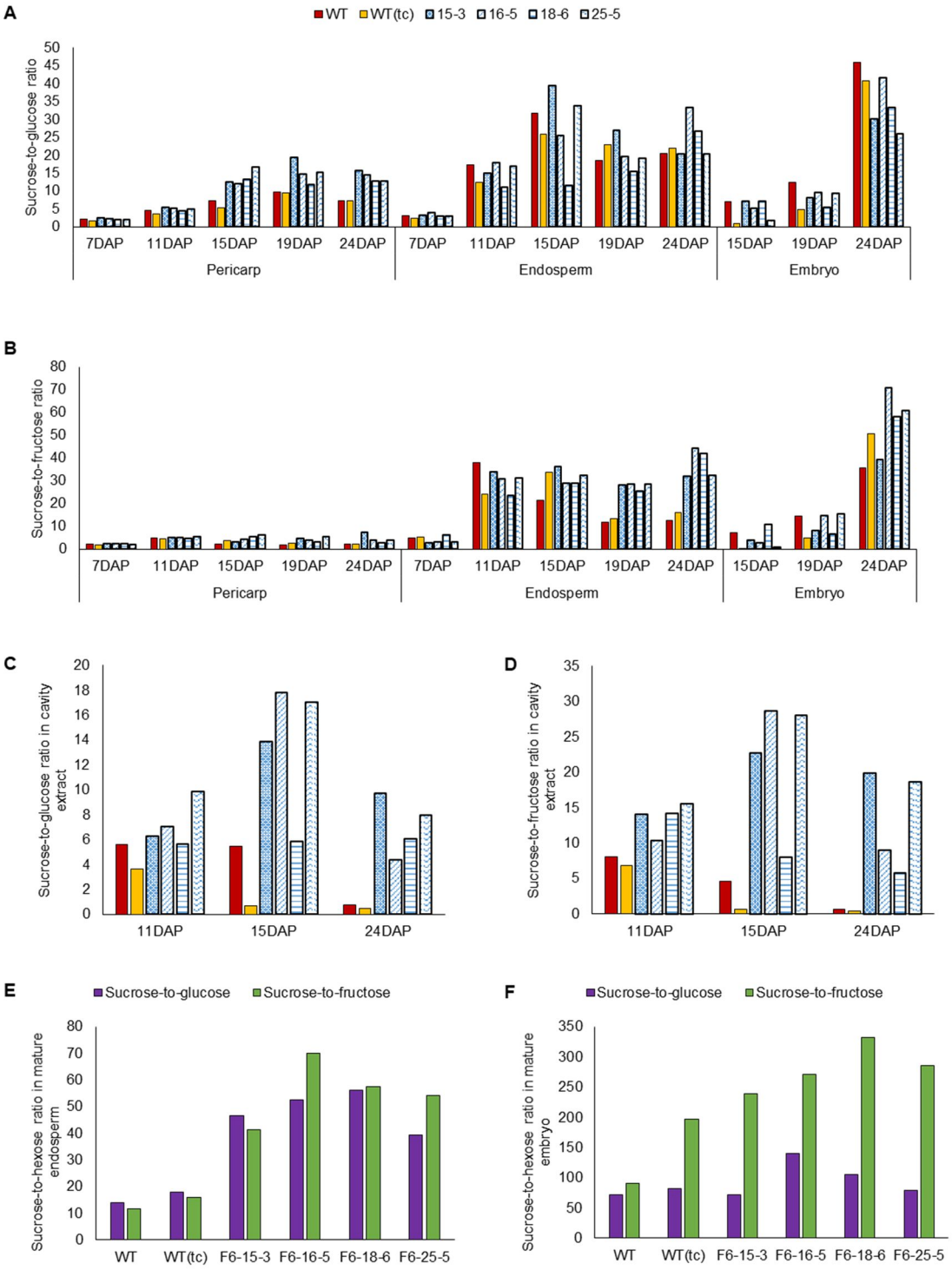

Supplementary figure 11: The ratios of sucrose-to-hexoses based on mean in developing and mature barley grain. (A) Sucrose-to-glucose and (B) sucrose-to-fructose ratio in developing barley tissues. (C) Sucrose-to-glucose and (D) sucrose-to-fructose ratio in the barley cavity extracts. Sucrose-to-hexose ratio in (E) mature endosperm and (F) mature embryo.

Supplementary table 2: List of primers used for real-time quantitative PCR. * indicates primers that bind between the *HvCslF6* gene and NOS terminator. ** indicates *β-fructofuranosidase* (also known as invertase) genes which are involved in cleaving the fructosyl-fructose linkages.

Gene full name	Gene	HORVU/Accession number	Sequence for forward primer (5'->3')	Sequence for reverse primer (5'->3')
Granule bound starch synthase 1a	*GBSS 1a*	FN179380.1	AGGACGTGCTTCTGGAACTG	CGAGAACCCTGAAGATGGAA
Starch synthase 2	*SS2*	AH011942.2	GCCTCAACACGTACTGGAACT	ATCGCGTGATCCTTGGTTACT
Starch branching enzyme 1	*SBE1*	FN179382.1	AACTTTGTCTTCCGGTCACCT	TTTACACAGCTCGATAATACTGCT
Starch branching enzyme 2b	*SBE2b*	AF064561	CGGAAACACGAGGAAGATAAG	TGGAGCATAGACAACACAGGT
Starch branching enzyme 2a	*SBE2a*	AK373114.1	ACCAAGTAGCCGTTTTGGAAC	TGTGTATCAGTGCCATCGAAA
Isoamylase 1	*Iso1*	AF490375.1	AGATGAAACAAAAGGCGAGAT	AGGGCGTGATACAAGGATGAC
Limit dextrinase	*LD*	AF252635.1	AAGTGAAAAGAACGAAGATAA	CCATCTCGGGGCTCTCACCTC
Cellulose synthase-like F6	*CslF6 (wild type)*	KP260639.1	TGGGCATTCACCTTCGTCAT	TGTCCGGGCAAACTCATCAA
Cellulose synthase-like F6	*CslF6 (transgene)*	n/a*	TGGGCATTCACCTTCGTCAT	TGATAATCATCGCAAGACCG
Cellulose synthase-like H1	*CslH1*	FJ459581.1	TGCTGTGGCTGGATGGTGTT	GCTTTATTATTGAGAGAGATTGGGAGA
Cellulose synthase-like F9	*CslF9*	EU267184.1	CTGCCACCGCGTCCGTGTA	AGGTTTTGCAGCATTACTTGA
(1,3;1,4)-beta-glucanase E1	*Endo E1*	AK252046.1	AACGAGAACCAGAAGGACAAC	TACGGACATACGGGCACTA
Cellulose synthase 2	*CesA2*	AY483152.1	CAGCCAGCCAGCAATTCTTTAT	AACCGCATTCTTGCCTTACAGA
Sucrose synthase 1	*SuSy1*	X65871.1	GTACGTGAGCAACCTGGAGAG	AATGTGCCGAGACATCAAATC
Sucrose-phosphate synthase	*SPS*	AK366557	AACCACAGCGCTACCAGACT	TGATCCGCATTTGTATTGGA
Sucrose-phosphatase	*SPP*	AF493562.1	AAGTACCGATCATGGGTGGA	CTCAACCCCGGGATATTCTT
Sucrose transporter 1	*SUT1*	AM055812.1	TCGCATAGGCGTCGTAACTA	GGTTTGCTACACGCAAGTCA
Sucrose transporter 2	*SUT2*	AJ272308.1	ACAAGGAAGGAAGGCAGGTT	CCCACGGAGGAAAGTAACAA
Cell wall invertase 1	*CWINV1*	AJ534447.1	CTCCGAGGGTATGGACGTAG	TTTTTCACTCATCCGGCAAT
Vacuolar invertase	*VIN*	JQ411255.1	CGGTGAGGCTCTATGTGTGA	CTAAGACGTCGAGGCCATCT
Sucrose:sucrose-1-fructosyltransferase	*1-SST*	AK366020.1	GGGCTACGGTACGACTGG	GGGTCTTCTCGTCAAGCTC
Fructan:fructan 1-fructosyltransferase	*1-FFT*	JQ411253.1	GACGACCGGCGAGACTATTACG	GACGCGTCGTACCTGCCATA
Sucrose:fructan 6-fructosyltransferase	*6-SFT*	JQ411254.1	GACCCGGAGCTCGACTTG	CCGGGTCTTCTCATCCAGAG
*β-fructofuranosidase***	*INV*	HORVU6Hr1G011260	TTATTGTCACAGAAGAGCAATGTG	GATAACCATACATAGTTGAGCAATTT
*β-fructofuranosidase***	*INV*	HORVU2Hr1G109120 /AK367512.1	CCAATTGTGGCTCAGGTGTA	GGGCATGCGTGCTATACTTT
Lipid transfer protein 2	*Ltp2*	X69793.1	TGTGCCAGTACGTCAAGGAC	GCTAGCCAGGAAGCAAGCTA

References

Åman P, Hesselman K, Tilly A-C (1985) The variation in chemical composition of Swedish barleys. Journal of Cereal Science **3:** 73-77

Becraft PW, Asuncion-Crabb Y (2000) Positional cues specify and maintain aleurone cell fate in maize endosperm development. Development **127:** 4039-4048

Bethke PC, Lonsdale JE, Fath A, Jones RL (1999) Hormonally regulated programmed cell death in barley aleurone cells. The Plant Cell **11:** 1033-1045

Bindschedler LV, Wheatley E, Gay E, Cole J, Cottage A, Bolwell GP (2005) Characterisation and expression of the pathway from UDP-glucose to UDP-xylose in differentiating tobacco tissue. Plant Molecular Biology **57:** 285-301

Blake AW, McCartney L, Flint JE, Bolam DN, Boraston AB, Gilbert HJ, Knox JP (2006) Understanding the biological rationale for the diversity of cellulose-directed carbohydrate-binding modules in prokaryotic enzymes. Journal of Biological Chemistry **281:** 29321-29329

Bosnes M, Weideman F, Olsen OA (1992) Endosperm differentiation in barley wild-type and sex mutants. The Plant Journal **2:** 661-674

Burton RA, Collins HM, Kibble NA, Smith JA, Shirley NJ, Jobling SA, Henderson M, Singh RR, Pettolino F, Wilson SM, Bird AR, Topping DL, Bacic A, Fincher GB (2011) Over-expression of specific HvCslF cellulose synthase-like genes in transgenic barley increases the levels of cell wall (1,3;1,4)-beta-d-glucans and alters their fine structure. Plant Biotechnol J **9:** 117-135

Burton RA, Collins HM, Kibble NAJ, Smith JA, Shirley NJ, Jobling SA, Henderson M, Singh RR, Pettolino F, Wilson SM, Bird AR, Topping DL, Bacic A, Fincher GB (2011) Over-expression of specific *HvCslF* cellulose synthase-like genes in transgenic

barley increases the levels of cell wall (1,3;1,4)-beta-D-glucans and alters their fine structure. Plant Biotechnology Journal **9:** 117-135

Burton RA, Fincher GB (2012) Current challenges in cell wall biology in the cereals and grasses. Front Plant Sci **3:** 130

Burton RA, Fincher GB (2014) Evolution and development of cell walls in cereal grains.

Burton RA, Jobling SA, Harvey AJ, Shirley NJ, Mather DE, Bacic A, Fincher GB (2008) The genetics and transcriptional profiles of the cellulose synthase-like HvCslF gene family in barley. Plant Physiology **146:** 1821-1833

Burton RA, Shirley NJ, King BJ, Harvey AJ, Fincher GB (2004) The *CesA* gene family of barley. Quantitative analysis of transcripts reveals two groups of co-expressed genes. Plant Physiology **134:** 224-236

Carciofi M, Blennow A, Jensen SL, Shaik SS, Henriksen A, Buléon A, Holm PB, Hebelstrup KH (2012) Concerted suppression of all starch branching enzyme genes in barley produces amylose-only starch granules. BMC Plant Biol **12:** 223

Chmelik J, Krumlová A, Budinská M, Kruml T, Psota V, Bohacenko I, Mazal P, Vydrová H (2001) Comparison of size characterization of barley starch granules determined by electron and optical microscopy, low angle laser light scattering and gravitational field-flow fractionation. Journal of the Institute of Brewing **107:** 11-17

Clarke B, Liang R, Morell M, Bird A, Jenkins C, Li Z (2008) Gene expression in a starch synthase IIa mutant of barley: changes in the level of gene transcription and grain composition. Functional & integrative genomics **8:** 211-221

Curtis MD, Grossniklaus U (2003) A gateway cloning vector set for high-throughput functional analysis of genes in planta. Plant Physiology **133:** 462-469

Desprez T, Juraniec M, Crowell EF, Jouy H, Pochylova Z, Parcy F, Höfte H, Gonneau M, Vernhettes S (2007) Organization of cellulose synthase complexes involved in primary

cell wall synthesis in Arabidopsis thaliana. Proceedings of the National Academy of Sciences **104:** 15572-15577

Doblin MS, Pettolino FA, Wilson SM, Campbell R, Burton RA, Fincher GB, Newbigin E, Bacic A (2009) A barley cellulose synthase-like CSLH gene mediates (1,3;1,4)-beta-D-glucan synthesis in transgenic Arabidopsis. Proc Natl Acad Sci U S A **106:** 5996-6001

Domínguez F, Cejudo FJ (2015) Programmed cell death (PCD): an essential process of cereal seed development and germination. Advances in Seed Biology**:** 178

Dugger W, Palmer RL (1986) Incorporation of UDPglucose into cell wall glucans and lipids by intact cotton fibers. Plant Physiol **81:** 464-470

Felker FC, Peterson DM, Nelson OE (1985) Anatomy of immature grains of eight maternal effect shrunken endosperm barley mutants. American Journal of Botany**:** 248-256

Fincher GB (1975) Morphology and chemical composition of barley endosperm cell walls Journal of the Institute of Brewing **81:** 116-122

Forestan C, Meda S, Varotto S (2010) ZmPIN1-Mediated Auxin Transport Is Related to Cellular Differentiation during Maize Embryogenesis and Endosperm Development. Plant Physiol **152:** 1373-1390

Geisler-Lee J, Gallie DR (2005) Aleurone Cell Identity Is Suppressed following Connation in Maize Kernels. Plant Physiol **139:** 204-212

Gleason F, Chollet R (2011) Plant biochemistry. Jones & Bartlett Publishers

Gómez-Cadenas A, Zentella R, Walker-Simmons MK, Ho T-HD (2001) Gibberellin/Abscisic Acid Antagonism in Barley Aleurone Cells: Site of Action of the Protein Kinase PKABA1 in Relation to Gibberellin Signaling Molecules. The Plant Cell **13:** 667

Greenwood JS, Helm M, Gietl C (2005) Ricinosomes and endosperm transfer cell structure in programmed cell death of the nucellus during Ricinus seed development. Proc Natl Acad Sci U S A **102:** 2238-2243

Gruis D, Guo H, Selinger D, Tian Q, Olsen O-A (2006) Surface Position, Not Signaling from Surrounding Maternal Tissues, Specifies Aleurone Epidermal Cell Fate in Maize. Plant Physiol **141:** 898-909

Guillon F, Bouchet B, Jamme F, Robert P, Quéméner B, Barron C, Larré C, Dumas P, Saulnier L (2011) Brachypodium distachyon grain: characterization of endosperm cell walls. J Exp Bot **62:** 1001-1015

Harvey AJ, Hrmova M, Fincher GB (2001) Regulation of genes encoding β-d-glucan glucohydrolases in barley (Hordeum vulgare). Physiologia Plantarum **113:** 108-120

Hassan AS, Houston K, Lahnstein J, Shirley N, Schwerdt JG, Gidley MJ, Waugh R, Little A, Burton RA (2017) A Genome Wide Association Study of arabinoxylan content in 2-row spring barley grain. PLoS ONE **12:** e0182537

Henry R, Saini H (1989) Characterization of cereal sugars and oligosaccharides. Cereal Chem **66:** 362-365

Henry RJ (1988) The carbohydrates of barley grains—A review. Journal of the Institute of Brewing **94:** 71-78

Hrmova M, Fincher G (2001) Structure-function relationships of β- D-glucan endo- and exohydrolases from higher plants. Plant Molecular Biology **47:** 73-91

Hrmova M, Harvey AJ, Wang J, Shirley NJ, Jones GP, Stone BA, Hoj PB, Fincher GB (1996) Barley beta-D-glucan exohydrolases with beta-D-glucosidase activity. Purification, characterization, and determination of primary structure from a cDNA clone. J Biol Chem **271:** 5277-5286

Huynh B-L, Palmer L, Mather DE, Wallwork H, Graham RD, Welch RM, Stangoulis JCR (2008) Genotypic variation in wheat grain fructan content revealed by a simplified HPLC method. Journal of Cereal Science **48:** 369-378

Jamar C, du Jardin P, Fauconnier M-L (2011) Cell wall polysaccharides hydrolysis of malting barley (Hordeum vulgare L.): a review. Revue de Biotechnologie, Agronomie, Société et Environnement **15**

Jeon J-S, Ryoo N, Hahn T-R, Walia H, Nakamura Y (2010) Starch biosynthesis in cereal endosperm. Plant Physiology and Biochemistry **48:** 383-392

Jung S, Rickert D, Deak N, Aldin E, Recknor J, Johnson L, Murphy P (2003) Comparison of Kjeldahl and Dumas methods for determining protein contents of soybean products. Journal of the American Oil Chemists' Society **80:** 1169-1173

Kalla R, Shimamoto K, Potter R, Nielsen PS, Linnestad C, Olsen OA (1994) The promoter of the barley aleurone-specific gene encoding a putative 7 kDa lipid transfer protein confers aleurone cell-specific expression in transgenic rice. The Plant Journal **6:** 849-860

Keeling PL, Myers AM (2010) Biochemistry and genetics of starch synthesis. Annual review of food science and technology **1:** 271-303

Koehler P, Wieser H (2013) Chemistry of cereal grains. *In* Handbook on sourdough biotechnology. Springer, pp 11-45

Kohorn BD, Kobayashi M, Johansen S, Riese J, Huang L-F, Koch K, Fu S, Dotson A, Byers N (2006) An Arabidopsis cell wall-associated kinase required for invertase activity and cell growth. The Plant Journal **46:** 307-316

Lid SE, Al RH, Krekling T, Meeley RB, Ranch J, Opsahl-Ferstad H-G, Olsen O-A (2004) The maize disorganized aleurone layer 1 and 2 (dil1, dil2) mutants lack control of the

mitotic division plane in the aleurone layer of developing endosperm. Planta **218:** 370-378

Lid SE, Gruis D, Jung R, Lorentzen JA, Ananiev E, Chamberlin M, Niu X, Meeley R, Nichols S, Olsen O-A (2002) The defective kernel 1 (dek1) gene required for aleurone cell development in the endosperm of maize grains encodes a membrane protein of the calpain gene superfamily. Proc Natl Acad Sci U S A **99:** 5460-5465

Lim WL, Collins HM, Singh RR, Kibble NA, Yap K, Taylor J, Fincher GB, Burton RA. 2017. Method for hull-less barley transformation and manipulation of grain mixed-linkage beta-glucan. J Integr Plant Biol

Loewus MW, Loewus FA (1980) The C-5 hydrogen isotope-effect in myo-inositol 1-phosphate synthase as evidence for the myo-inositol oxidation-pathway. Carbohydr Res **82:** 333-342

Ma J, Jiang Q-T, Wei L, Wang J-R, Chen G-Y, Liu Y-X, Li W, Wei Y-M, Liu C, Zheng Y-L (2014) Characterization of shrunken endosperm mutants in barley. Gene **539:** 15-20

Matthews PR, Wang MB, Waterhouse PM, Thornton S, Fieg SJ, Gubler F, Jacobsen JV (2001) Marker gene elimination from transgenic barley, using co-transformation with adjacent 'twin T-DNAs' on a standard *Agrobacterium* transformation vector. Molecular Breeding **7:** 195-202

McCartney L, Marcus SE, Knox JP (2005) Monoclonal antibodies to plant cell wall xylans and arabinoxylans. Journal of Histochemistry & Cytochemistry **53:** 543-546

McCleary B, Solah V, Gibson T (1994) Quantitative measurement of total starch in cereal flours and products. Journal of Cereal Science **20:** 51-58

McCleary BV, Codd R (1991) Measurement of (1 → 3),(1 → 4)-β-D-glucan in barley and oats: A streamlined enzymic procedure. Journal of the Science of Food and Agriculture **55:** 303-312

Morell MK, Kosar-Hashemi B, Cmiel M, Samuel MS, Chandler P, Rahman S, Buleon A, Batey IL, Li Z (2003) Barley sex6 mutants lack starch synthase IIa activity and contain a starch with novel properties. The Plant Journal **34:** 173-185

Munck L, Møller B, Jacobsen S, Søndergaard I (2004) Near infrared spectra indicate specific mutant endosperm genes and reveal a new mechanism for substituting starch with (1→ 3, 1→ 4)-β-glucan in barley. Journal of Cereal Science **40:** 213-222

Nemeth C, Andersson AA, Andersson R, Mangelsen E, Sun C, Åman P (2014) Relationship of grain fructan content to degree of polymerisation in different barleys. Food and Nutrition Sciences **5:** 581

Olsen LT, Divon HH, Al R, Fosnes K, Lid SE, Opsahl-Sorteberg H-G (2008) The defective seed5 (des5) mutant: effects on barley seed development and HvDek1, HvCr4, and HvSal1 gene regulation. J Exp Bot **59:** 3753-3765

Olsen O-A (2001) Endosperm development: cellularization and cell fate specification. Annual review of plant biology **52:** 233-267

Palmer G (1972) Morphology of starch granules in cereal grains and malts. Journal of the Institute of Brewing **78:** 326-332

Pettolino FA, Hoogenraad NJ, Ferguson C, Bacic A, Johnson E, Stone BA (2001) A (1? 4)-ß-mannan-specific monoclonal antibody and its use in the immunocytochemical location of galactomannans. Planta **214:** 235-242

Peukert M, Lim WL, Seiffert U, Matros A (2016) Mass Spectrometry Imaging of Metabolites in Barley Grain Tissues. *In* Current Protocols in Plant Biology. John Wiley & Sons, Inc.

Peukert M, Thiel J, Mock H-P, Marko D, Weschke W, Matros A (2016) Spatiotemporal Dynamics of Oligofructan Metabolism and Suggested Functions in Developing Cereal Grains. Front Plant Sci **6**

Peukert M, Thiel J, Peshev D, Weschke W, Van den Ende W, Mock H-P, Matros A (2014) Spatio-temporal dynamics of fructan metabolism in developing barley grains. The Plant Cell **26:** 3728-3744

Radchuk V, Riewe D, Peukert M, Matros A, Strickert M, Radchuk R, Weier D, Steinbiß H-H, Sreenivasulu N, Weschke W (2017) Down-regulation of the sucrose transporters HvSUT1 and HvSUT2 affects sucrose homeostasis along its delivery path in barley grains. Journal of Experimental Botany **68:** 4595-4612

Radchuk VV, Borisjuk L, Sreenivasulu N, Merx K, Mock H-P, Rolletschek H, Wobus U, Weschke W (2009) Spatiotemporal Profiling of Starch Biosynthesis and Degradation in the Developing Barley Grain. Plant Physiol **150:** 190-204

Ray PM, Shininger TL, Ray MM (1969) Isolation of β-glucan synthetase particles from plant cells and identification with Golgi membranes. Proceedings of the National Academy of Sciences **64:** 605-612

Reiter W-D, Vanzin GF (2001) Molecular genetics of nucleotide sugar interconversion pathways in plants. Plant Molecular Biology **47:** 95-113

Ruan Y-L (2014) Sucrose metabolism: gateway to diverse carbon use and sugar signaling. Annual review of plant biology **65:** 33-67

Satoh H, Nishi A, Yamashita K, Takemoto Y, Tanaka Y, Hosaka Y, Sakurai A, Fujita N, Nakamura Y (2003) Starch-branching enzyme I-deficient mutation specifically affects the structure and properties of starch in rice endosperm. Plant Physiol **133:** 1111-1121

Schon MA, Nodine M (2017) Widespread contamination of Arabidopsis embryo and endosperm transcriptome datasets. The Plant Cell**:** tpc. 00845.02016

Seefeldt HF, Blennow A, Jespersen BM, Wollenweber B, Engelsen SB (2009) Accumulation of mixed linkage (1→ 3)(1→ 4)-β-d-glucan during grain filling in barley: A vibrational spectroscopy study. Journal of Cereal Science **49:** 24-31

Shaik SS, Obata T, Hebelstrup KH, Schwahn K, Fernie AR, Mateiu RV, Blennow A (2016) Starch Granule Re-Structuring by Starch Branching Enzyme and Glucan Water Dikinase Modulation Affects Caryopsis Physiology and Metabolism. PLoS ONE **11:** e0149613

Smeekens S (2000) Sugar-induced signal transduction in plants. Annual review of plant biology **51:** 49-81

Song L, Zeng W, Wu A, Picard K, Lampugnani ER, Cheetamun R, Beahan C, Cassin A, Lonsdale A, Doblin MS (2015) Asparagus spears as a model to study heteroxylan biosynthesis during secondary wall development. PloS one **10:** e0123878

Sreenivasulu N, Borisjuk L, Junker BH, Mock H-P, Rolletschek H, Seiffert U, Weschke W, Wobus U (2010) Barley grain development: toward an integrative view. International Review of Cell and Molecular Biology **281:** 49-89

Thiel J (2014) Development of endosperm transfer cells in barley. Front Plant Sci **5**

Thiel J, Riewe D, Rutten T, Melzer M, Friedel S, Bollenbeck F, Weschke W, Weber H (2012b) Differentiation of endosperm transfer cells of barley: a comprehensive analysis at the micro-scale. The Plant Journal **71:** 639-655

Tingay S, McElroy D, Kalla R, Fieg S, Wang MB, Thornton S, Brettell R (1997) *Agrobacterium tumefaciens*-mediated barley transformation. Plant Journal **11:** 1369-1376

Ueda M, Zhang ZJ, Laux T (2011) Transcriptional activation of *Arabidopsis* axis patterning genes *WOX8/9* links zygote polarity to embryo development. Developmental Cell **20:** 264-270

Verhertbruggen Y, Marcus SE, Haeger A, Ordaz-Ortiz JJ, Knox JP (2009) An extended set of monoclonal antibodies to pectic homogalacturonan. Carbohydr Res **344:** 1858-1862

Verspreet J, Cimini S, Vergauwen R, Dornez E, Locato V, Le Roy K, De Gara L, Van den Ende W, Delcour JA, Courtin CM (2013b) Fructan metabolism in developing wheat (Triticum aestivum L.) kernels. Plant Cell Physiol **54:** 2047-2057

Verspreet J, Pollet A, Cuyvers S, Vergauwen R, Van den Ende W, Delcour JA, Courtin CM (2012) A simple and accurate method for determining wheat grain fructan content and average degree of polymerization. Journal of agricultural and food chemistry **60:** 2102-2107

Vickers CE, Xue GP, Gresshoff PM (2006) A novel *cis*-acting element, ESP, contributes to high-level endosperm-specific expression in an oat globulin promoter. Plant Molecular Biology **62:** 195-214

Vijn I, Smeekens S (1999) Fructan: more than a reserve carbohydrate? Plant Physiol **120:** 351-360

Weichert N, Saalbach I, Weichert H, Kohl S, Erban A, Kopka J, Hause B, Varshney A, Sreenivasulu N, Strickert M, Kumlehn J, Weschke W, Weber H (2010) Increasing Sucrose Uptake Capacity of Wheat Grains Stimulates Storage Protein Synthesis. Plant Physiol **152:** 698-710

Wilson SM, Burton RA, Collins HM, Doblin MS, Pettolino FA, Shirley N, Fincher GB, Bacic A (2012) Pattern of deposition of cell wall polysaccharides and transcript abundance of related cell wall synthesis genes during differentiation in barley endosperm. Plant Physiol **159:** 655-670

Wilson SM, Burton RA, Doblin MS, Stone BA, Newbigin EJ, Fincher GB, Bacic A (2006) Temporal and spatial appearance of wall polysaccharides during cellularization of barley (Hordeum vulgare) endosperm. Planta **224:** 655

Wilson SM, Ho YY, Lampugnani ER, Van de Meene AM, Bain MP, Bacic A, Doblin MS (2015) Determining the subcellular location of synthesis and assembly of the cell wall polysaccharide (1, 3; 1, 4)-β-d-glucan in grasses. The Plant Cell **27:** 754-771

Wobus U, Sreenivasulu N, Borisjuk L, Rolletschek H, Panitz R, Gubatz S, Weschke W (2005) Molecular physiology and genomics of developing barley grains. Recent research developments in plant molecular biology **2:** 1-29

Chapter 4

How does the Lack of (1,3;1,4)-β-Glucan Affect Other Barley Grain Components?

Statement of Authorship

Title of Paper	How does the Lack of (1,3;1,4)-β-Glucan Affect Other Barley Grain Components?
Publication Status	☐ Published ☐ Accepted for Publication ☐ Submitted for Publication ☑ Unpublished and Unsubmitted w ork w ritten in manuscript style
Publication Details	Wai Li Lim, Helen Collins, Caitlin Byrt, Jelle Lahnstein, Neil Shirley and Rachel Burton

Principal Author

Name of Principal Author (Candidate)	Wai Li Lim		
Contribution to the Paper	Grew plants and prepared barley tissues. Performed all analytical experiments, all microscopy work, designed primers and prepared cDNA for qPCR and prepared manuscript.		
Overall percentage (%)	85		
Certification:	This paper reports on original research I conducted during the period of my Higher Degree by Research candidature and is not subject to any obligations or contractual agreements with a third party that would constrain its inclusion in this thesis. I am the primary author of this paper.		
Signature		Date	27 July 2017

Co-Author Contributions

By signing the Statement of Authorship, each author certifies that:

i. the candidate's stated contribution to the publication is accurate (as detailed above);
ii. permission is granted for the candidate in include the publication in the thesis; and
iii. the sum of all co-author contributions is equal to 100% less the candidate's stated contribution.

Name of Co-Author	Helen Collins		
Contribution to the Paper	Supervised experiment design, data analysis and interpretation. Assisted with manuscript.		
Signature		Date	31/7/2017

Name of Co-Author	Caitlin Byrt		
Contribution to the Paper	Supervised experiment design, data analysis and interpretation. Assisted with manuscript.		
Signature		Date	21/7/17

Name of Co-Author	Jelle Lahnstein		
Contribution to the Paper	Assisted with HPLC work.		
Signature		Date	21 July 2017

Name of Co-Author	Neil Shirley		
Contribution to the Paper	Performed all qPCR work.		
Signature		Date	21/7/17

Name of Co-Author	Rachel Burton		
Contribution to the Paper	Conceived project and designed experiments. Assisted with manuscript.		
Signature		Date	31/7/2017

How does the Lack of (1,3;1,4)-β-Glucan Affect Other Barley Grain Components?

Wai Li Lim[1], Helen Collins[1], Caitlin Byrt[1,2], Neil Shirley[1], Jelle Lahnstein[1] and Rachel A. Burton[1*].

[1]ARC Centre of Excellence in Plant Cell Walls, School of Agriculture, Food and Wine, University of Adelaide, Waite Campus, Glen Osmond, SA, 5064, Australia.

[2]ARC Centre of Excellence in Plant Energy Biology, School of Agriculture, Food and Wine, University of Adelaide, Waite Campus, Glen Osmond, SA, 5064, Australia.

*Corresponding Author

Corresponding author email: rachel.burton@adelaide.edu.au

Abstract

(1,3;1,4)-β-Glucans function both as cell wall polysaccharides and storage compounds in many cereal crops, including barley (*Hordeum vulgare* L.). The (1,3;1,4)-β-glucan content of barley grain is important in the food and brewing industries. Consumption of (1,3;1,4)-β-glucan in human diets is desirable because it is associated with health benefits whereas in the brewing industry, (1,3;1,4)-β-glucan can increase wort viscosity, which may cause filtration problems and affect final beer quality. The biosynthesis of (1,3;1,4)-β-glucan in barley grain is mediated predominantly by the *CslF6* gene (Burton et al., 2011). A (1,3;1,4)-β-glucanless barley mutant (OUM125) was generated by Tonooka et al. (2009) which has a single nucleotide substitution in the coding region of the *CslF6* gene. The OUM125 mutant therefore has a non-functional CSLF6 synthase and has been reported to lack any detectable (1,3;1,4)-β-glucan in either grain or vegetative tissues (Tonooka et al., 2009; Taketa et al., 2012). Here we investigate how the lack of (1,3;1,4)-β-glucan impacts other components of the grain based on the hypothesis that there are likely to be differences in carbon partitioning between OUM125 and control grain. Biochemical analyses of OUM125 indicated that there was an increase in the amount of arabinoxylan, sucrose and fructan, but no change in starch content in the mature grain compared to the parental line. Immunolabeling of grain sections revealed the presence of lichenase resistant material bound by the BGI antibody in the pericarp, a decrease in labelling intensity of callose, and a different binding pattern by the carbohydrate binding module 3a (CBM3a) and the pontamine fast scarlet (S4B) stain, which are used to detect cellulose, compared to the control grain. We observed that OUM125 mutant plants were shorter in height and flowered later than the parental line. These results suggest that the lack of (1,3;1,4)-β-glucan in the OUM125 mutant, due to a non-functional CSLF6 protein, affects vegetative development but contrary to our expectations has no significant impact on the carbon partitioning pathways that influence mature grain composition.

Introduction

Barley (*Hordeum vulgare* L.) is a cereal belonging to the grass family in the Poaceae. It ranks fourth in cereal production globally and is an important staple food in countries such as Morocco, Ethiopia, Algeria and Afghanistan. In addition, barley is also grown as animal feed and for beer production, and barley straw and hulls are potential biofuel feedstocks (Glithero et al., 2013; Hyeon et al., 2014). Barley grain composition influences food and brewing product quality and is comprised of; starch (~60% w/w dry weight) (Greenwood and Thomson, 1959; Åman et al., 1985), non-starch polysaccharides, including ~4% w/w cellulose (MacLeod and Napier, 1959), ~4-10% (1,3;1,4)-β-glucan (Burton and Fincher, 2012), ~3-7% w/w arabinoxylan (Izydorczyk et al., 2003; Zhang et al., 2013), ~1-4.2% w/w fructan (Nemeth et al., 2014), ~2% w/w lipids and ~11% w/w proteins (Koehler and Wieser, 2013). However, the grain composition varies between different cultivars and it is influenced by environmental factors (Triboï et al., 2003; Holtekjølen et al., 2006; Zhang et al., 2013; Mutwali et al., 2016).

Grain carbon is stored predominantly in polysaccharides such as starch (Palmiano and Juliano, 1972; Perata et al., 1997; Dirk et al., 1999), fructans (Verspreet et al., 2013b; Cimini et al., 2015) and cell wall polysaccharides such as (1,3;1,4)-β-glucan and arabinoxylan (Fincher, 1975; Buckeridge et al., 2000; Burton and Fincher, 2014). In cereals, endosperm acts as the primary storage organ from which nutrients are mobilised to support embryo growth during seed germination (Yan et al., 2014). In barley endosperm, starch is the predominant storage polysaccharide which is stored in starch granules. Storage polysaccharides are also found in cell walls. In barley starchy endosperm, 70% w/w of the cell wall is (1,3;1,4)-β-glucan, 25% w/w is arabinoxylan and less than 3% is cellulose and heteromannan (Fincher, 1975; Burton and Fincher, 2014). Aleurone, which is part of the endosperm tissue, has a different cell wall

composition, where 26% w/w is (1,3;1,4)-β-glucan and 71% w/w is arabinoxylan (Bacic and Stone, 1981a, 1981b).

The fate of assimilated carbon during carbon partitioning and the deposition of storage carbohydrates are under the influence of a complex network of competing factors driven by suites of metabolic enzymes. In many plants, assimilated carbon is transported mainly as sucrose which is a key substrate for the biosynthesis of other carbohydrates (Ruan, 2014). Increasing sucrose uptake in grain via upregulation of sucrose transporter genes has been linked to higher grain yield (Weschke et al., 2000; Weichert et al., 2010). Thus, manipulation of genes involved in sucrose metabolism (Wang et al., 2008; Li et al., 2013) and starch biosynthesis are promising targets for increasing starch content and grain yield (Li et al., 2011; Cakir et al., 2015). It has been proposed that there is a relationship between starch and (1,3;1,4)-β-glucan content (Munck et al., 2004; Clarke et al., 2008; Seefeldt et al., 2009; Burton et al., 2011; Han et al., 2017). Starch consists of amylose and amylopectin, which are glucose polymers predominantly linked by α(1,4)-glycosidic bonds with α(1,6)-glucosidic bonds at the branch points (Jeon et al., 2010; Streb and Zeeman, 2012) whereas (1,3;1,4)-β-glucan is a linear polysaccharide made up of glycosyl monomers joined by β(1,3)- and β(1,4)- linkages (Burton et al., 2010). The demand for cereal foods with high levels of (1,3;1,4)-β-glucan, and more recently of resistant starch, is increasing due to their potential in promoting health benefits, including lowering blood cholesterol levels (De Deckere et al., 1993; Delaney et al., 2003), reducing undesirable glycemic responses (Raben et al., 1994; Cavallero et al., 2002; Hallfrisch et al., 2003; Behall et al., 2006) and may promote weight loss (Smith et al., 2008; Robertson, 2012; Higgins, 2014). Genetic modification and chemically-induced mutagenesis are proven approaches to producing grains with higher or lower levels of starch or (1,3;1,4)-β-glucans (Aastrup, 1983; Clarke et al., 2008; Burton et al., 2011; Sparla et al., 2014; Han et al., 2017).

When optimising grain composition it is important to understand how the modification of one storage polysaccharide influences the others. Studies have indicated that there is a correlation between grain starch and (1,3;1,4)-β-glucan levels There may also be an association between starch and fructan content, as based on observations of transgenic potato (Van Der Meer et al., 1994) and maize (Caimi et al., 1996) transformed with a fructosyltransferase gene from *Bacillus subtilis* (*SacB*). These transgenic plants had reduced starch content as a result of the high accumulation of fructans (Van Der Meer et al., 1994; Caimi et al., 1996). The deposition pattern of storage carbohydrates in developing grain has been described previously for wheat, where fructans mainly accumulated in grain during cell division and expansion expansion (0 to 11 days after pollination (DAP), followed by the accumulation of starch, (1,3;1,4)-β-glucan and arabinoxylan during grain filling (11 to 35 DAP) (Verspreet et al., 2013b). The spatio-temporal deposition of storage carbohydrates in developing barley grain with altered (1,3;1,4)-β-glucan metabolism, due to overexpression of the *CslF6* gene, has been described in Chapter 3, where change in (1,3;1,4)-β-glucan amount was associated with altered metabolism of fructan and starch and the phenotype of the transgenic barley was severely affected both in vegetative tissues and grain (Chapter 2 and Chapter 3). This indicates the importance of carbohydrate regulation in controlling plant development and grain composition.

If increasing barley grain (1,3;1,4)-β-glucan is associated with increased fructan and decreased starch contents then decreasing barley grain (1,3;1,4)-β-glucan might also alter grain starch and fructan amounts. As there is an absence of (1,3;1,4)-β-glucan in OUM125 due to a single mutation in the *CslF6* gene, this mutant is a valuable resource to investigate the effect of decreasing barley grain (1,3;1,4)-β-glucan. Mutation of the *CslF6* gene in the OUM125 barley line was the result of chemically-induced mutagenesis of the Akashinriki parent cultivar

(Konishi, 1979; Tonooka et al., 2009). The OUM125 mutant has a G to A substitution at the 4275th nucleotide position (1979th in the CDS), which results in an amino acid change at the 660th position from glycine (G) to aspartic acid (D). Consequently, the (1,3;1,4)-β-glucan synthase enzyme is non-functional, resulting in undetectable levels of (1,3;1,4)-β-glucan content in grain, roots and leaves (Taketa et al., 2012). Previous studies have indicated that the starch content in OUM125 grain is similar to wild type and the grain is softer, with thinner cell walls, which may be ideal for brewing (Sadosky et al., 2002; Speers et al., 2003) and animal feed (Annison, 1993). However, the plants were sensitive to cold environments and the yield was low, making them less favourable in the agronomic sector (Tonooka et al., 2009).

Here we examine the deposition of water-soluble polysaccharides such as fructans and sucrose in the OUM125 mutant grain during development. We use immunolabeling techniques to explore what happens to the deposition of other cell wall polysaccharides such as arabinoxylan, cellulose, mannan and callose, as a result of the absence of (1,3;1,4)-β-glucan in the cell walls of OUM125 mutant grain, and the transcript levels of genes related to the metabolism of each component are measured in developing pericarp and endosperm tissues using quantitative real-time PCR (qPCR).

Materials and Methods

Plant materials

Wild type *Hordeum vulgare* L. cv Akashinriki, which is listed under the two accession numbers AGG400237BARLI and AGG407909BARLI, were obtained from the Australian Grains Genebank and the OUM125 mutant barley grain was kindly provided by Professor Kazuhiro Sato (Okayama University) as part of a collaboration with Associate Professor Matthew Tucker (University of Adelaide) to investigate the role of the *HvCslF6* gene in barley growth and development. All plants were grown in a glasshouse under a day/night temperature regime of 23°C/15°C. Developing grains were collected at 7, 11, 15, 19 and 24 DAP. Pericarp, endosperm and embryo tissues were separated using a scalpel and fine forceps and snap-frozen in liquid nitrogen. Frozen tissues were kept at -80°C until required.

Starch assay

The starch content of developing tissues was measured using a scaled down version of the Megazyme Total Starch Assay (Megazyme International, Deltagen, Kilsyth VIC, Australia) according to the manufacturer's instructions (McCleary et al., 1994). Approximately 10 mg of freeze-dried sample was weighed for the assay and the starch content was calculated on a dry weight basis.

(1,3;1,4)-β-Glucan assay

Freeze-dried samples from developing barley grain were ground and weighed to produce 10 mg aliquots. To remove free sugars and chlorophyll, powdered materials were pre-treated with 70% ethanol (EtOH) (0.01 w/v %) at 97°C for 30 min, centrifuged at 5000 rpm for 5 min and

the supernatants were removed. The pellets were then treated with 100% EtOH (0.01 w/v %) at 97°C for 10 min, centrifuged at 5000 rpm for 5 min and the supernatants were removed. The same pellets were used to analyse (1,3;1,4)-β-glucan content using a scaled down version of the Megazyme mixed-linkage beta-glucan assay (McCleary and Codd, 1991).

Monosaccharide analysis

The total arabinoxylan content was calculated from the amount of arabinose and xylose in each line by reverse phase HPLC (Agilent Technologies, Mulgrave VIC, Australia) following Comino et al., (2013) with some modifications. Samples were initially hydrolysed in 1 M sulphuric acid at 100°C for 3 h. The hydrolysate was diluted (1:20) and derivatised with 1-phenyl-3-methyl-5-pyrazolone (PMP) at the anomeric carbon atoms. A Phenomenex Kinetex 2.6 µm C18 100 x 3 mm 100Å column at 30°C and a flow rate of 0.8 mL/min was used to perform the chromatography. Eluents for the separation of PMP-monosaccharide derivatives were (A) 10% acetonitrile, 40 mM ammonium acetate, and (B) 70% acetonitrile. The starting condition was 85% eluent A and 15% eluent B and the gradient was 8 to 16% eluent B over 12 min. Detection was carried out at 250 nm. Calibration curves of standards of monosaccharides were used to quantify the area under the peaks. Total arabinoxylan was calculated from the combined amount of % L-arabinose and % D-xylose, taking into account the loss of one water molecule per monosaccharide (x 0.88).

Soluble sugar analysis

Extraction of soluble sugars and fructans from barley grains were performed as described in Verspreet et al., (2012). Briefly, developing grains from each biological replicate were ground

and weighed at approximately 10 mg. The soluble sugars were extracted in 80% EtOH at 85°C for 30 min followed by Milli-Q water at 50°C for 30 min in a final dilution of 1:40 w/v. The supernatants from each extraction were combined. For cavity sap, 10 barley grains were cut in half using a scalpel and fluids from the endosperm cavity were extracted using a microsyringe (Hamilton, Reno, Nevada, United States). Cavity sap was heated at 90°C to inactivate endogenous enzymes and diluted in Milli-Q water to produce a final dilution of 1:100 v/v. The diluted sample extracts from grain tissues and cavity extracts, were treated with and without fructanase (Megazyme fructan assay kit, Deltagen, Kilsyth VIC, Australia), incubated at 40°C for 2 h for complete hydrolysis, and then heated at 90°C for 5 min. Sample extracts were separated using a high pH anion exchange chomatography with pulsed amperometric detection (HPAEC–PAD) on a Dionex ICS-5000. A 25 µL aliquot was injected onto a DionexCarboPACTMPA-20 column (3 x 150 mm) with a guard column (3 x 50 mm) kept at 30 °C and operated at a flow rate of 0.5 mL min-1. The eluents used were (A) 0.1 M sodium hydroxide and (B) 0.1 M sodium hydroxide with 1 M sodium acetate. The gradient was started with 0% (B) from 0 to 9 min, 10% (B) from 9 to 10 min, 100% (B) from 10 to 12 min, 0% (B) from 12 up to 20 min. Temperature of the detector was maintained at 20°C and data collection was at 2 Hz. The Gold Standard PAD waveform (std. quad. potential) was used to detect carbohydrates. Standards used were: glucose, fructose, sucrose, raffinose, 1-kestose and nytose at concentrations of 4, 2, 1, 0.5, 0.25 and 0.125 mg/L respectively. Total fructan content was calculated according to the methods from Huynh et al., (2008) and Verspreet et al., (2013b). Total fructan (µM) equals the sum of glucose and fructose after hydrolysis minus the sum of free glucose, fructose, sucrose and raffinose (before hydrolysis), taking into account the loss of one water molecule per monosaccharide (x0.9).

RNA isolation and cDNA synthesis

Total RNA was extracted from all tissue homogenates using a phenolguanidine reagent, treated with the DNA-free kit (Ambion®, Thermo Fisher Scientific, Scoresby Vic, Australia), and used as the template for cDNA synthesis following Burton et al., (2004; 2011) except that Superscript III reverse transcriptase (Invitrogen) was used in preference to Superscript II and the reaction was incubated at 50°C.

Real-time quantitative PCR (qPCR)

Gene specific primers were designed from the 3' untranslated regions of full-length cDNAs. Fragments amplified using the gene specific primers were purified using HPLC as described in Burton et al. (2008) and sequenced at the Australian Genome Research Facility, Adelaide, South Australia. The PCR primer sequences are provided in Supplementary Table 1. qPCR analysis was carried out as described in Burton et al., (2004) with the modifications reported in Burton et al. (2008). Heatmap representation generated using MultiExperiment Viewer (MeV) software (http://mev.tm4.org/).

Tissue fixation, embedding and microscopy for mature grain

Mature grain was embedded following Burton et al., (2011). Embedded tissue was sectioned at 2 μm thickness on an Ultramicrotome using a diamond knife (DiATOME, Nidau, Switzerland) and collected on polylysine coated slides (Thermo Fisher Scientific, Scoresby Vic, Australia). Sections were re-hydrated with 1 X PBS, incubated with 0.05 M glycine for 20 min to inactivate residual aldehyde groups and blocked with 1% (w/v) bovine serum albumin (BSA) (Sigma-

Aldrich, Castle Hill NSW, Australia) in 1 X phosphate-buffered saline (PBS) (blocking buffer) for 10 min (3 times). The distribution and relative abundance of polysaccharides in the developing grain of wild type and mutant were detected using monoclonal antibodies raised against specific polysaccharide epitopes including (1,3)-β-glucan (Biosupplies Australia, Parkville, Vic., Australia), (1,3;1,4)-β-glucan (Biosupplies Australia, Parkville, Vic., Australia), hetero-(1,4)-β-mannan (Pettolino et al., 2001), arabino-(1,4)-β-xylan LM11 (specific for unsubstituted xylan and arabinoxylan) (McCartney et al., 2005) and a family 3 carbohydrate-binding module (CBM3a) (PlantProbes). Sections were incubated in primary antibodies (1:50 dilution in 1 X PBS with 1% (w/v) BSA) for 2 h at room temperature under moist conditions. For crystalline cellulose, a monoclonal anti-polyHistidine antibody (Sigma-Aldrich, Castle Hill, NSW, Australia) (1:100 dilution in 1 X PBS with 1% w/v BSA) was applied after CBM3a incubation (Blake et al., 2006). For detection of arabinoxylan, sections were incubated in α-L-arabinofurosidase under moist conditions at 40°C for 2 h prior to primary antibody incubation. Other enzymes used included endo-1,4-β-Xylanase M6 (Megazyme), Lichenase (endo-1,3,1,4-β-Glucanase) (Megazyme) and Cellulase (endo-1,4-β-D-glucanase) (E-CELAN Megazyme). After washing 3 times with blocking buffer, sections were incubated with either anti-mouse or anti-rat secondary antibodies (depending on the primary antibody used) conjugated to Alexa Fluor® 488 (Thermo Fisher Scientific, Scoresby Vic, Australia), Alexa Fluor® 555 (Thermo Fisher Scientific, Scoresby Vic, Australia a) or DyLight® 550 (Thermo Fisher Scientific, Scoresby Vic, Australia) (1:100 dilution in 1 X PBS with 1% (w/v) BSA) for 1 h at room temperature in the dark. Sections were washed 3 times with blocking buffer and rinsed with water before being mounted with 90% (v/v) glycerol. Images were taken using a Carl Zeiss fluorescence microscope (Axio Imager M2; Carl Zeiss, Oberkochen, Germany). For environmental SEM (ESEM), individual mature grains were mounted on scanning electron

microscope stubs and coated with carbon and gold. Samples were examined in a Philips XL30 Field Emission scanning electron microscope at an accelerating voltage of 5 kV.

Results

Carbohydrate composition of OUM125 barley grain

The OUM125 mutant is in the background 'Akashinriki'. Two accessions of 'Akashinriki' (AGG400237BARLI and AGG407909BARLI) were available from the Australian Grains Genebank. These lines had different flowering periods and plant phenotypes (Fig. 1A and 1B). AGG400237BARLI (237) flowered about one month earlier than AGG407909BARLI (909), and the OUM125 mutant plants flowered one month later than the 909 control with a greater sterility rate. The 237 line was similar in height to the OUM125 mutant plants at 51 days of growth, whereas the height of the 909 line was twice that of the OUM125 mutant plants. The OUM125 mutant grain weight was significantly lower than that of either the 237 or 909 line, although there was a significant difference in grain weight between the 237 and 909 lines (Fig. 1C). Compositional analyses of mature 'Akashinriki' grains from lines 237 and 909 indicated that there was no significance difference between the two lines in the amount of (1,3;1,4)-β-glucan, arabinoxylan and soluble carbohydrates, except for the starch content (Table 1). Previous studies reported that mutations in the *CslF6* gene in barley and rice both decreased plant heights (Taketa et al., 2012; Vega-Sanchez et al., 2012). Hence, the 909 line was chosen for further analysis and treated as the parental control for the OUM125 mutant.

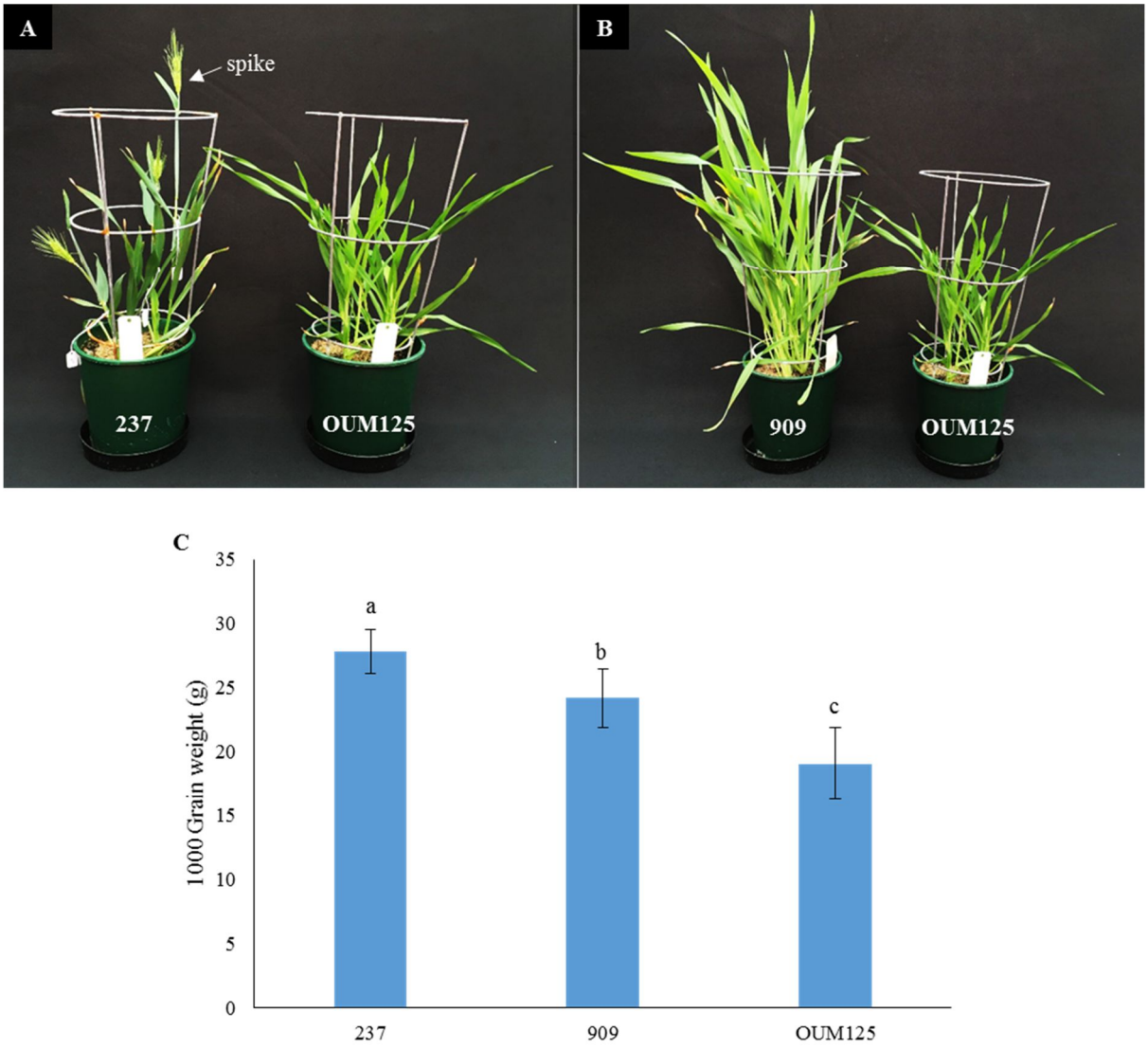

Figure 1: Phenotypes of barley plants. (A) Phenotype of parental lines 237 and 909 and the OUM125 mutant at 51 days. (B) 1000 grain weight (g) of mature 237 and 909 and OUM125 barley grain. a, b and c indicate a significant difference according to a t-test with a P-value < 0.05.

Table 1: Sugar composition in mature 237 and 909 and OUM125 barley grain measured on a weight per weight basis or mg per grain basis. a, b and c indicate a significant difference according to a t-test with a P-value < 0.05. %w/w represents percentage of weight per weight

	%w/w			mg per grain		
	237	909	OUM125	237	909	OUM125
Cell wall polysaccharides						
(1,3;1,4)-β-glucan	6.39±0.83a	5.84±0.46a	0.01±0.01b	1.78±0.23a	1.41±0.11b	0.00±0.00c
Arabinoxylan	5.96±0.18a	6.12±0.16a	7.23±0.45b	1.66±0.05a	1.48±0.04b	1.38±0.09b
Soluble carbohydrates						
Glucose	0.07±0.01a	0.06±0.01a	0.16±0.03b	0.02±0.00a	0.02±0.00b	0.03±0.01c
Fructose	0.09±0.01a	0.09±0.01a	0.16±0.06b	0.03±0.00a	0.02±0.00b	0.03±0.01ab
Sucrose	1.28±0.16a	1.23±0.20a	1.90±0.65b	0.36±0.04a	0.30±0.05b	0.36±0.12ab
Raffinose	0.45±0.03a	0.43±0.01a	0.63±0.13b	0.13±0.01a	0.10±0.00b	0.12±0.02ab
Total fructan	1.45±0.19a	1.34±0.23a	2.11±0.23b	0.40±0.05a	0.32±0.05b	0.40±0.04a
Starch	57.79±2.92a	48.13±1.10b	52.64±5.00ab	16.1±1.32a	11.64±0.27b	10.03±0.95c

The deposition of storage carbohydrates in 909 and OUM125 grain was examined at developing stages (from 7 to 24 DAP) in pericarp and endosperm. In 909, the storage of (1,3;1,4)-β-glucan increased as the endosperm developed and the (1,3;1,4)-β-glucan content in the developing pericarp stayed constant. Consistent with previous observations by Taketa et al., (2012), the level of (1,3;1,4)-β-glucan in OUM125 was undetectable in developing pericarp and endosperm tissues (Fig. 2A). Both 909 and OUM125 grain had similar storage patterns for fructan, arabinoxylan, starch, sucrose, soluble glucose and fructose in the pericarp and endosperm from 7 to 24 DAP (Fig. 2B, 2C, 2D, 3A, 3B and 3C). However, there was a greater (20%) proportion of starch in the endosperm of OUM125 compared to 909 from 15 to 24 DAP (Fig. 2D).

The carbohydrate content of mature grain was measured using whole grain samples. On a weight per weight basis, there was a significantly greater proportion of arabinoxylan, soluble glucose, fructose, sucrose, raffinose and total fructan in OUM125 grain compared to 909. Interestingly, there was no difference in starch content between 909 (about 48% w/w) and

OUM125 mature grain (about 53% w/w) (Table 1). The amount of storage compounds unaccounted for comprised 37% w/w and 36% w/w respectively in 909 and OUM125 grain respectively (Fig. S5).

On a per grain basis, there was relatively less arabinoxylan and starch in OUM125 mature grain compared to 909 grain, whilst soluble glucose and total fructan contents were significantly greater in OUM125 (Table 1). A non-functional CSLF6 protein in OUM125 did not appear to alter the deposition pattern for other carbohydrates including arabinoxylan and starch during grain development, although the fructan content in 909 peaked at 11 DAP and declined up to mature stage (Fig. S6A), while the fructan content in OUM125 grain increased from 15 to 19DAP and stayed constant up to mature stage (Fig. S6B).

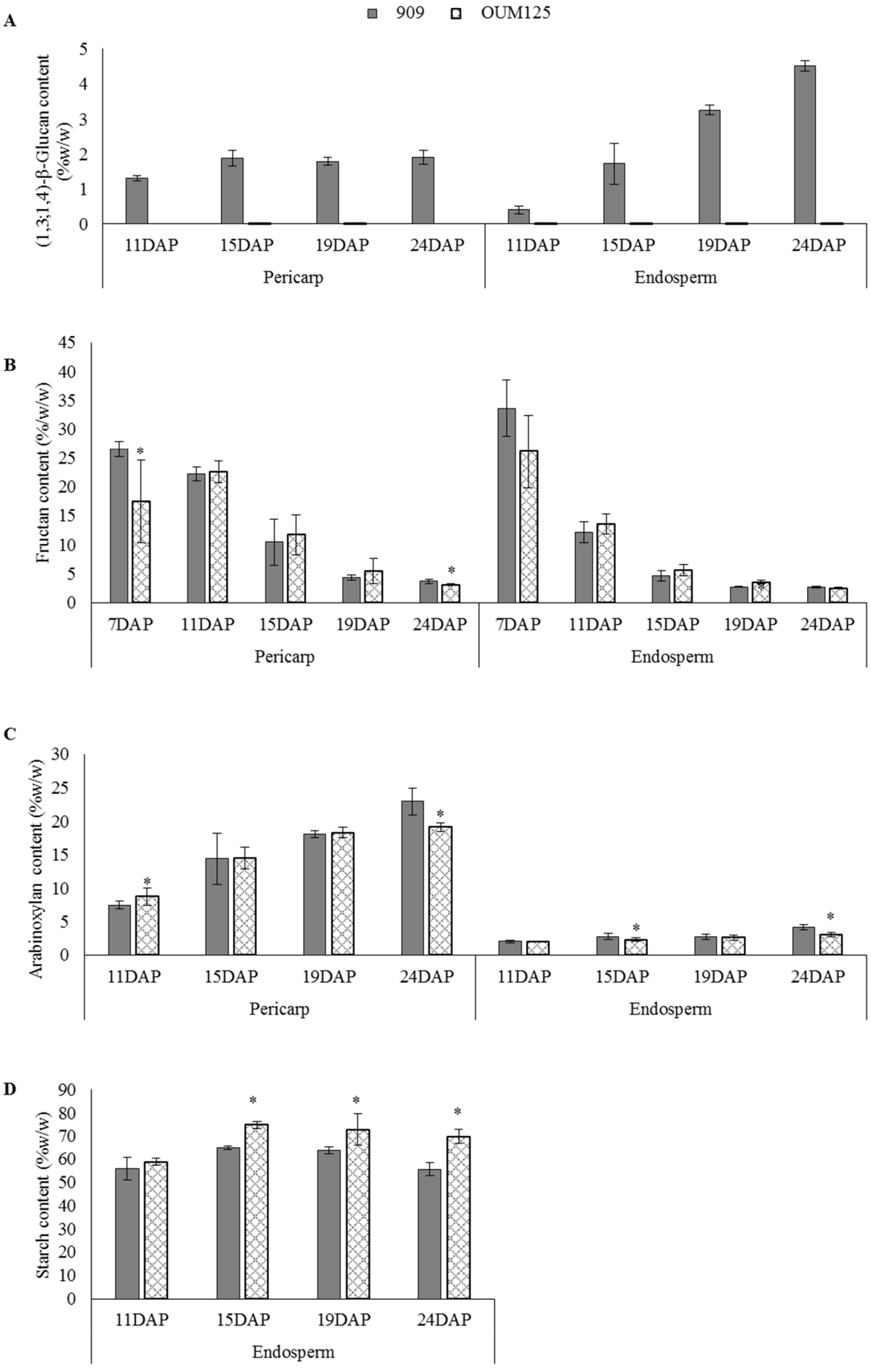
A
909
OUM125
(1,3;1,4)-β-Glucan content (%w/w)
0
1
2
3
4
5
11DAP
15DAP
19DAP
24DAP
Pericarp
Endosperm
B
Fructan content (%w/w)
0
5
10
15
20
25
30
35
40
45
7DAP
11DAP
15DAP
19DAP
24DAP
Pericarp
Endosperm
C
Arabinoxylan content (%w/w)
0
5
10
15
20
25
30
11DAP
15DAP
19DAP
24DAP
Pericarp
Endosperm
D
Starch content (%w/w)
0
10
20
30
40
50
60
70
80
90
11DAP
15DAP
19DAP
24DAP
Endosperm

Figure 2: Storage carbohydrate content in pericarp and endosperm of developing barley grain on a weight per weight basis. (A) (1,3;1,4)-β-glucan, (B) Total fructan, (C) Arabinoxylan and (D) Starch. * Significantly different to parental line according to a t-test with a P-value < 0.05.

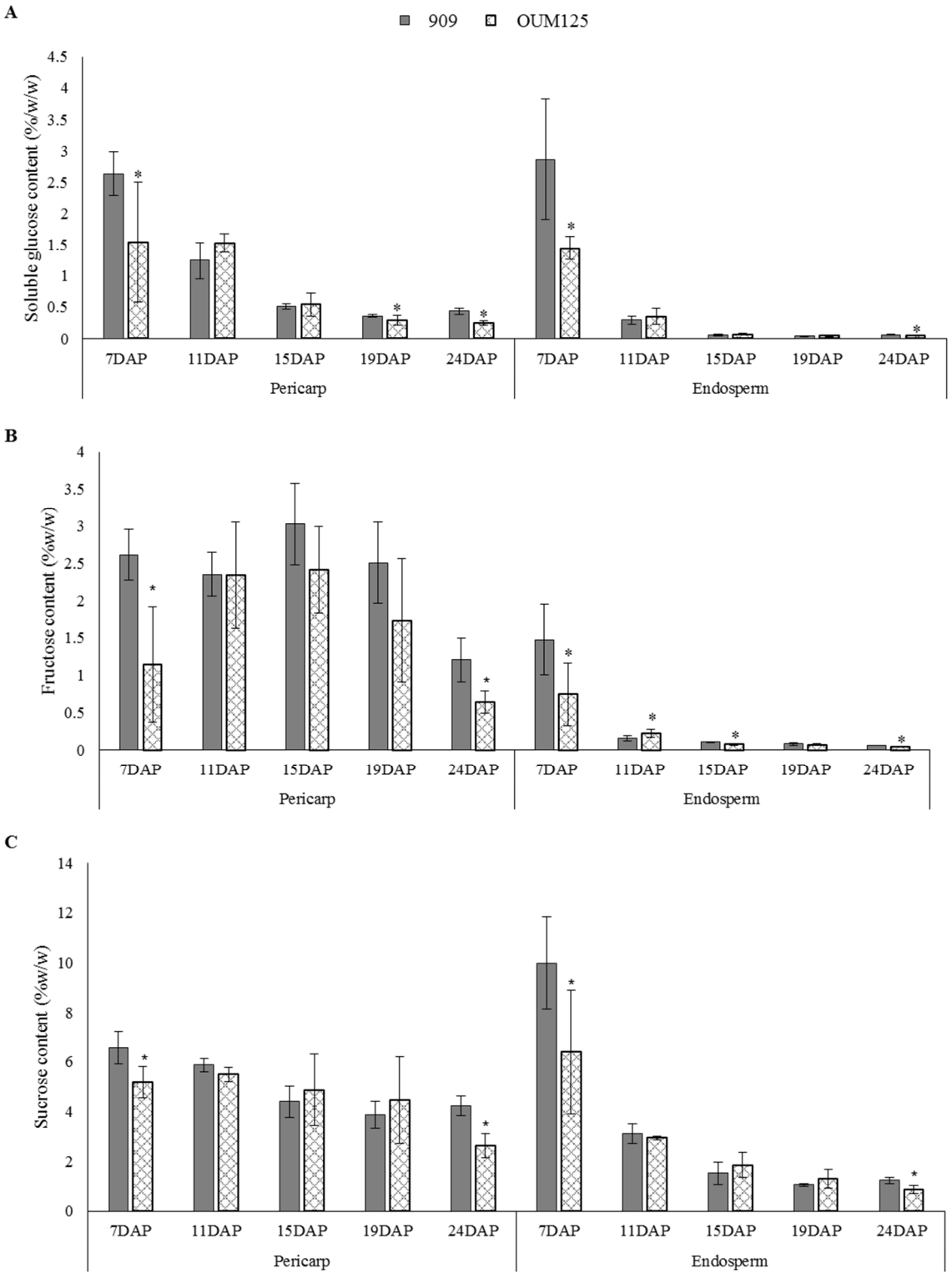

Figure 3: Soluble sugar content in pericarp and endosperm of developing barley grain on a weight per weight basis. (A) Glucose, (B) Fructose and (C) Sucrose. * Significantly different to parental line according to a t-test with a P-value < 0.05.

Relative transcript levels of carbohydrate metabolic genes

Transcripts for genes related to cell wall, fructan, starch and sucrose metabolism were investigated in the (1,3;1,4)-β-glucanless mutant in comparison to 909 grain (Table S1, Fig. S8A to S8F1). A heat map was generated to show the transcript profiles in OUM125 relative to 909 grain (Fig. 4A to 4H) and individual profiles are shown in Fig. S8A to S8F1. Transcripts with levels below 2000 arbitrary units were not included in the heat map. The raw data is presented in Appendix 2. The *HORVU6Hr1G011260* and *HORVU2Hr1G109120* genes containing the pfam00251 and pfam08244 domains respectively both encode β-fructofuranosidases, which have a function in hydrolysing the glycosidic bonds in carbohydrates, including fructans. The transcript levels for a number of genes differed in both pericarp and endosperm tissues of the mutant line relative to the parental control (Fig. 4A to 4H and Fig. S8A to S8F1). At 19 DAP, genes that were upregulated in the mutant pericarp include cell wall biosynthetic genes such as *CslH1, CslF10, CesA2, GT61* (*HORVU1Hr1G080720* and *HORVU5Hr1G013550*), *CesA3, Gsl2, CslF3, CslF7*, and *UGPase* (Fig. 4A), the fructan biosynthetic genes *6-SFT* and *1-FFT*, fructan hydrolases *CWINV 1*, *HORVU6Hr1G011260* and *VIN* genes (Fig. 4C), starch metabolic genes such as *SBE 1, GBSS 1a, GBSS 1b, SBE 2b, Isoamylase 1* and *Limit Dextrinase* genes (Fig. 4E) and sucrose transporter genes *SUT 1* and *SUT 2* (Fig. 4G). In the same tissue, the *Endo E1* transcript which is involved in (1,3;1,4)-β-glucan hydrolysis was upregulated at 7 DAP (Fig. 4A). To identify contamination in the pericarp from other tissues, the aleurone-specific gene, *lipid transfer protein 2* (*ltp 2)*, was examined for its transcript level. In contrast to the Torrens samples described in Chapter 3, both OUM125 and 909 tissues showed extremely low *ltp 2* transcript levels in the pericarp and endosperm tissues across development (Fig. S8G1). Hence, the *ltp 2* gene cannot be used as an indicator for tissue contamination in this study. However, it is still possible that the pericarp tissue is contaminated with some part of the endosperm tissue given that the grain was hand-

dissected (Schon and Nodine, 2017). In OUM125 endosperm, fructan biosynthetic genes *6-SFT* and *1-SST* were upregulated at 11 DAP, followed by fructan hydrolase genes *HORVU6Hr1G011260*, *HORVU2Hr1G109120* and *VIN* at 15 DAP (Fig. 4D). At 15 DAP, upregulation of cell wall biosynthetic genes such as *CslF7, CslF10, CesA2* and *Gsl2* (Fig. 4B), starch metabolic genes *GBSS 1a* and *SBE 1* (Fig. 4F) and *sucrose transporter 2 (SUT 2)* (Fig. 4H) was evident in OUM125 endosperm. At 24 DAP, *Endo E1*, *CesA3, GT61 (HORVU1Hr1G080720), 6-SFT, HORVU2Hr1G109120, SUT 1 and SUT 2* were all upregulated in mutant endosperm (Fig. 4B, 4D and 4H).

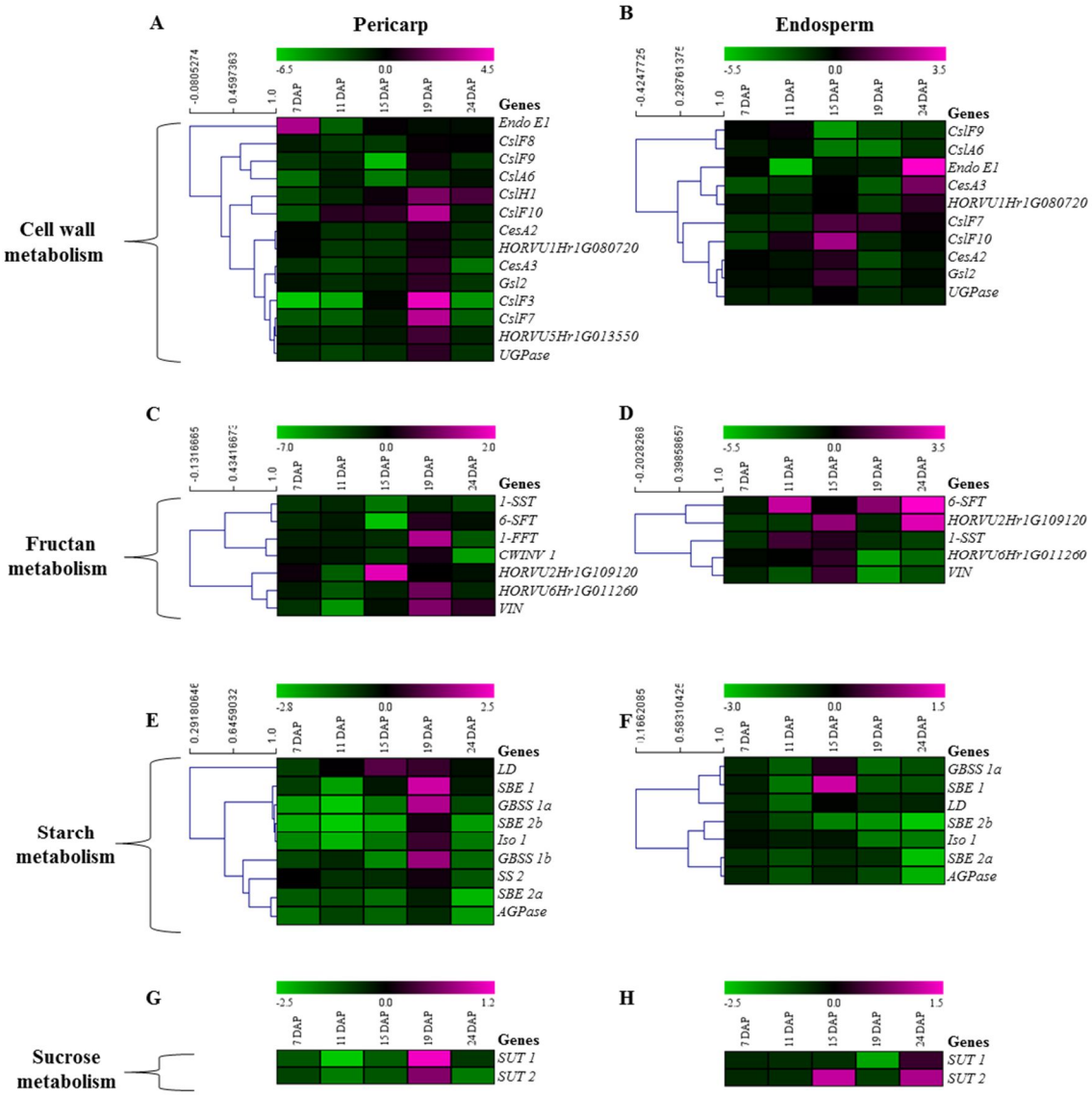

Figure 4: Relative expression of genes involved in the regulation of carbon storage in OUM125 mutant barley grain from 7 to 24 DAP in pericarp and endosperm tissues normalised against 909. The normalised expression values are calculated in $\log_2$. Developing stages are displayed vertically above each column. Gene names are displayed to the right of each row. Genes are hierarchically clustered based on the average Pearson's distance.

Morphology of starch granules

The morphology of starch granules were examined using environmental scanning electron microscopy. There was no morphology difference in starch granules between OUM125 and 909 under either low magnification (1200x) (Fig. 5C and 5D) or high magnification (2000x) (Fig. 5E and 5F). The cell walls surrounding the starch granules were clearly apparent in 909 sections but were not visible in OUM125 grain (Fig. 5A, 5B, 5E and 5F).

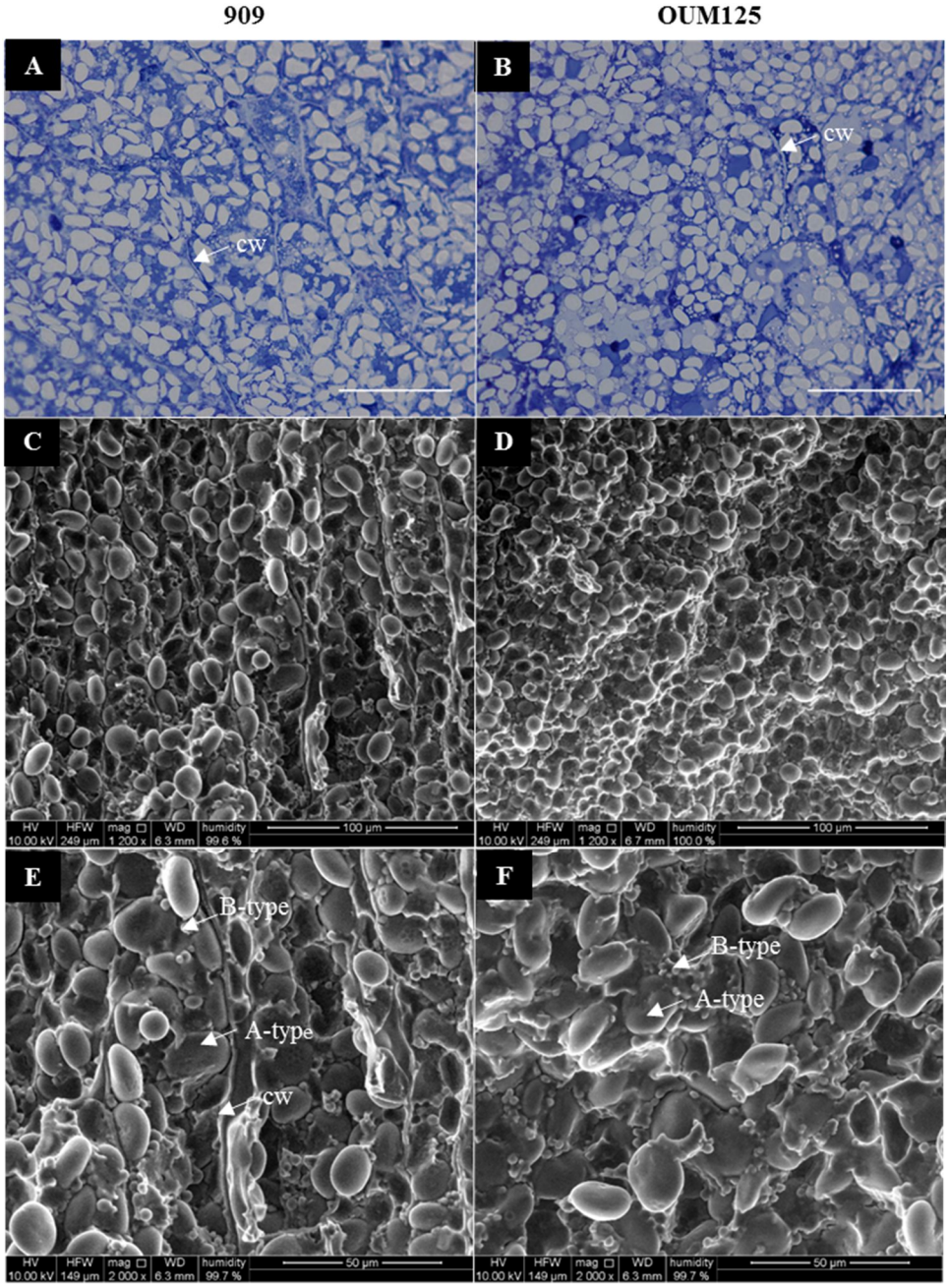

Figure 5: Toluidine blue and (A and B) electron scanning electron micrographs (C to F) of 909 and OUM125 grain. Panels A and B show thinner cell walls in the starchy endosperm of OUM125 grain at 24 DAP compared to 909 grain. Panels C to D show morphology of starch granules in mature grain. Panels A and B are at 20x magnification and scale bars represent 100μm. Panels C and D are at 1200x magnification. Panels E and F are at 2000x magnification. Abbreviations: cell wall (cw), A-type granule (A-type), B-type granule (B-type).

Deposition of arabinoxylan, callose, mannan and cellulose in OUM125

Distribution of cell wall polysaccharides in mature grain, including (1,3;1,4)-β-glucan, arabinoxylan, callose, mannan and cellulose was visualised using an immunolabeling technique with specific antibodies. In 909 grain, all cells were stained using calcofluor white, which binds non-specifically to β(1,3) and β(1,4)-linked polysaccharides including cellulose, (1,3;1,4)-β-glucan and callose (Fig. 6A). Using the same exposure time, there was no visible signal from calcofluor white in OUM125 grain (Fig. 6B). The 909 grain had uniform (1,3;1,4)-β-glucan labelling across the whole section (Fig. 6C), while no labelling was visible in OUM125 (Fig. 6D). Under a higher exposure time, (1,3;1,4)-β-glucan antibody labelling was detected in the pericarp and within the aleurone cells of OUM125 (Fig. 7B and 7C) which was not visible in the negative antibody control (Fig. 7H and 7I). To test whether the labelling in OUM125 was due to the presence of (1,3;1,4)-β-glucan, the section was treated with lichenase prior to the addition of the (1,3;1,4)-β-glucan antibody. After lichenase treatment, there was no obvious change in the extent of (1,3;1,4)-β-glucan antibody labelling (Fig. 7E and 7F).

Deposition of arabinoxylan was visualised using the LM11 antibody which binds to the xylan backbone (McCartney et al., 2005). Treatment with α-L-arabinofurosidase prior to LM11

labelling has previously been shown to increase the binding of the antibody to highly substituted arabinoxylan (Wilson et al., 2012). Similar intensities in LM11 labelling were observed in the 909 and OUM125 sections (Fig. 6E and 6F). The LM11 labelling was much stronger in the aleurone cell walls compared to other tissues (Fig. 6E and F). For 909, callose labelling was uniform across the section, including in the endosperm, aleurone layers and endosperm transfer layer (Fig. 6G), while in OUM125, callose was detected in the endosperm and aleurone layers but was absent from the endosperm transfer layer. However, the deposition pattern for callose was patchy and uneven in the endosperm (Fig. 6H). Immunolabeling with the mannan antibody revealed intense mannan labelling in the walls of the cells adjacent to the grain crease in both 909 and OUM125 grain. A patchy pattern of mannan labelling was detected in the 909 endosperm, while in OUM125, the labelling was concentrated adjacent to the grain crease (Fig. 6I and 6J).

The CBM3a and pontamine fast scarlet (S4B) stains are able to recognise crystalline (Blake et al., 2006) and microfibrillar cellulose (Anderson et al., 2010; Thomas et al., 2013), respectively. Absence of signal from both CBM3a and S4B in the OUM125 grain suggests that either they failed to bind because the antigen were blocked or there is an absence of cellulose in the cell walls (Fig. 6N). In an attempt to unmask the polysaccharides, sections were digested with α-L-arabinofurosidase and xylanase to remove the arabinoxylan from the cell walls. After digestion, CBM3a labelling was revealed, which was more intensive in the pericarp and aleurone cells than in the endosperm (Fig. 8D). The S4B stain provided no signal even after the sections were digested with α-L-arabinofurosidase and xylanase (Fig. 8B).

Differential binding specificity of S4B and CBM3a has been observed previously (Griffiths et al., 2014; Voiniciuc et al., 2015). Here the binding pattern for S4B appeared to be similar to the

(1,3;1,4)-β-glucan antibody BG1, although *in vitro* experiments have previously indicated that the S4B stain is specific only for cellulose (Anderson et al., 2010). This raised a question as to whether S4B binds to (1,3;1,4)-β-glucan in grain samples. To address this, 909 grain sections were treated with lichenase to remove the (1,3;1,4)-β-glucan in cell walls prior to S4B staining. We found that the S4B staining disappeared in the endosperm tissue after lichenase treatment, but persisted in the aleurone layers (Fig. S1D). In contrast, removal of (1,3;1,4)-β-glucan by lichenase enhanced the labelling intensity of CBM3a in the endosperm whilst any signal remained undetectable in the aleurone cell walls (Fig. S1F).

The specificity of the S4B for cellulose was further tested by cellulase treatment. Cellulase enzymes can digest both cellulose and (1,3;1,4)-β-glucan. Any cell wall components that were digested by cellulase but not the lichenase enzyme were considered to be cellulose. After cellulase treatment, no labelling was detected in the endosperm, while the labelling in aleurone cell walls remained (Fig. S2A and S2B).

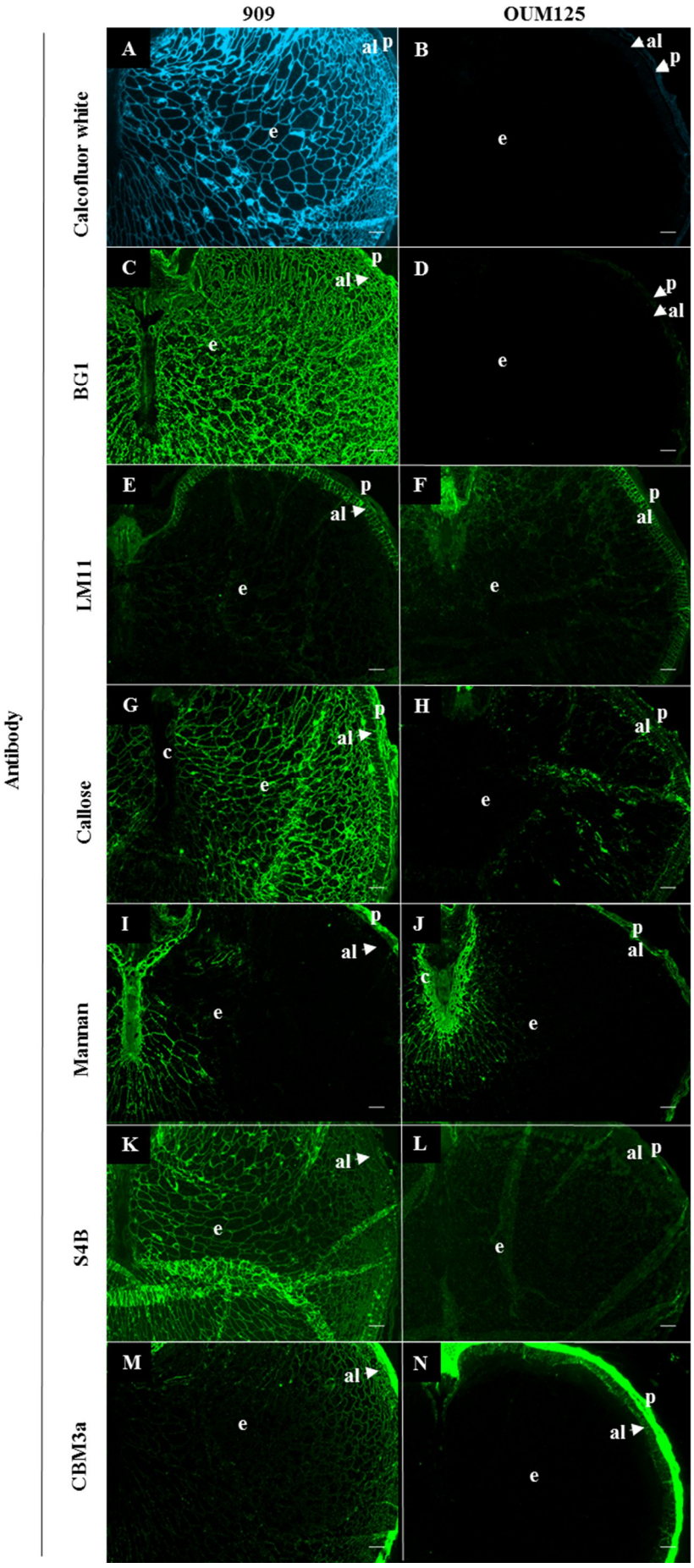
909
OUM125
Antibody
Calcofluor white
BG1
LM11
Callose
Mannan
S4B
CBM3a
A
B
C
D
E
F
G
H
I
J
K
L
M
N
al
p
e
c

Figure 6: Fluorescence micrographs of mature grain sections labelled with (A and B) Calcofluor white stain, (C and D) (1,3;1,4)-β-glucan (BG1), (E and F) LM11, (G and H) Callose, (I and J) Mannan, (K and L) Pontamine Fast Scarlet 4B (S4B) and (M and N) CBM3a. Scale bars represent 100 µm. Abbreviations: aleurone (al), endosperm (e), pericarp (p), cavity (c).

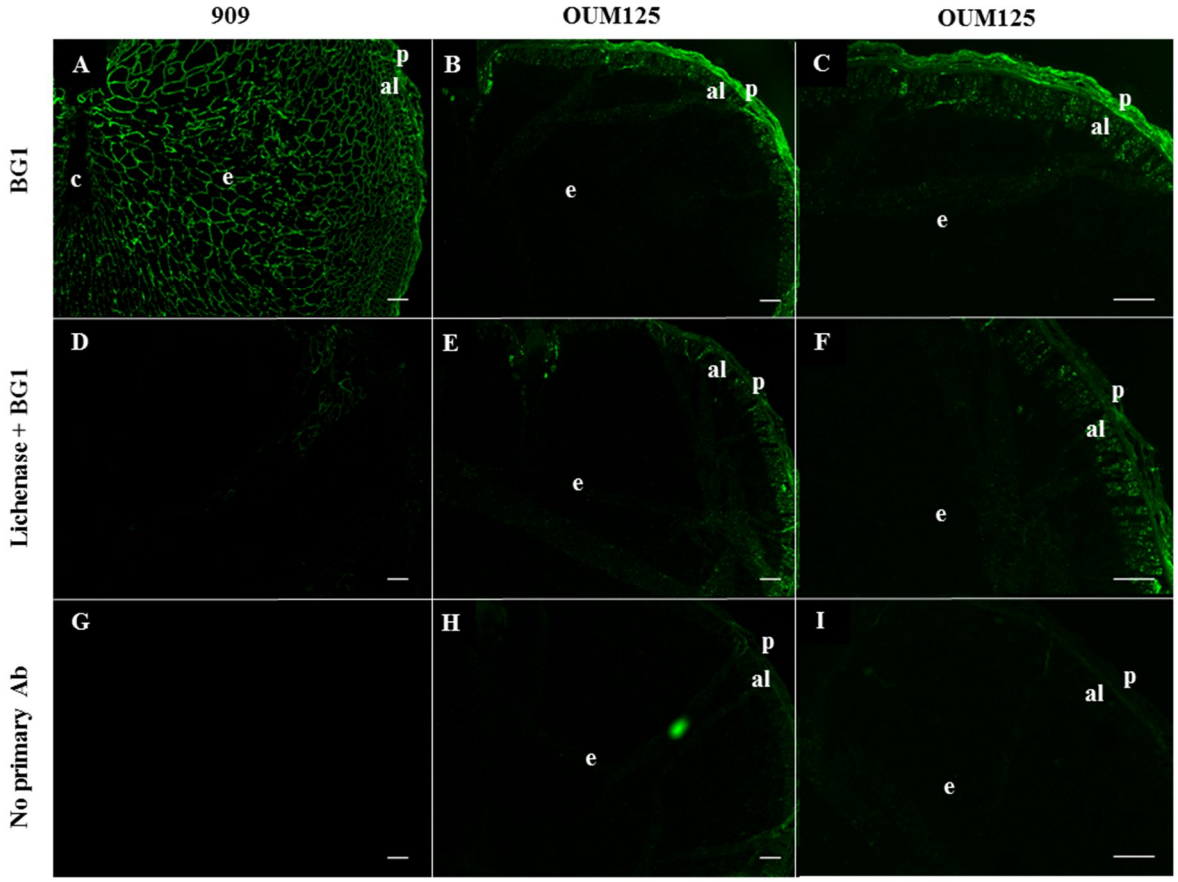

Figure 7: Fluorescence micrographs of (1,3;1,4)-β-glucan (BG1) labelling of mature barley grain. Panels A, B and C are non-treated sample. Panels D, E and F are treated with the lichenase enzyme for 2 hours at 40°C prior to BG1 labelling. Panels G, H and I are negative controls without the addition of BG1. Panels A, D and G are taken at 5x magnification with a 300 ms exposure time. Panels B, E and H are taken at 5x magnification with a 7.5 s exposure time. Panels C, F and I are taken at 10x magnification with a 850 ms exposure time. Scale bars represent 100 µm. Abbreviations: aleurone (al), endosperm (e), pericarp (p), cavity (c).

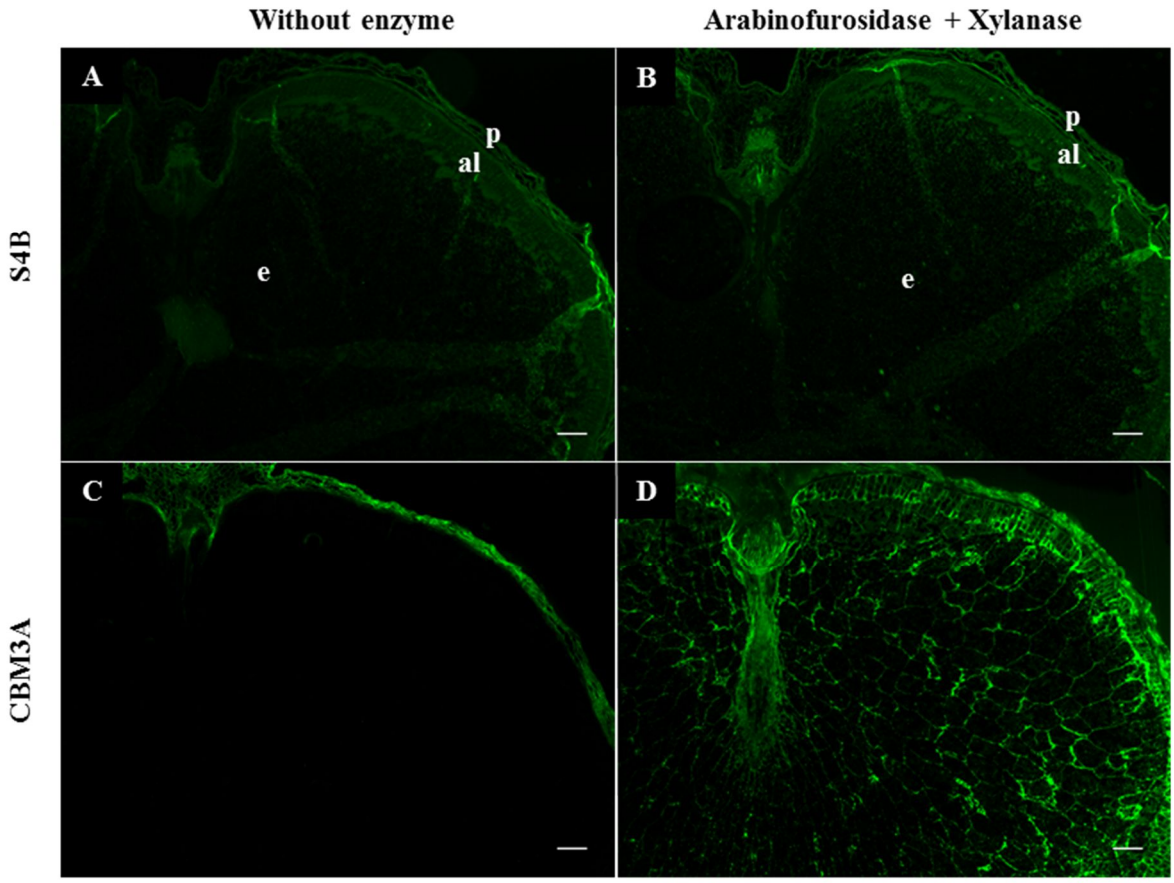

Figure 8: Fluorescence micrographs of Pontamine Fast Scarlet (S4B) and CBM3a labelling of mature OUM125 mutant barley grain. Panels A and C are non-treated samples. Panels B and D are treated with α-L-arabinofurosidase and xylanase enzymes for 2 hours at 40°C prior to S4B and CBM3a labelling. All images are taken at 5x magnification. Scale bars represent 100 µm. Abbreviations: aleurone (al), endosperm (e), pericarp (p), cavity (c).

Discussion

The OUM125 mutant is in an Akashinriki background. Two Akashinriki accessions were available from the Australian Grains Genebank; AGG400237BARLI (237) and AGG407909BARLI (909). These two accessions display phenotypic differences, hence it was not clear which accession would be most suitable to use as a control for comparison with the mutant. It is possible that the phenotypic differences are due to different sowing periods. No additional information about the source of the 237 and 909 lines is available from the Australia Grains Genebank. It would be possible in future studies to sequence the whole genome of 237, 909 and OUM125 mutant barley plants and compare which of the parental accessions share the highest degree of similarity compared to the OUM125 mutant. Genome sequencing would also be useful to identify other mutations in the OUM125 line which have not yet been removed by backcrossing.

We analysed the composition of storage carbohydrates in 237, 909 and OUM125 mature grain. On a weight per weight basis we found a significant reduction in starch content in 909 compared to 237, but there was no significant difference in (1,3;1,4)-β-glucan, arabinoxylan and fructan content between the two lines (Table 1). According to data reported by Taketa et al., (2012) and Vega-Sanchez et al., (2012), plants with a mutation in the *CslF6* gene were shorter in height compared to wild type plants and the OUM125 mutant displayed a reduction in plant height when compared to the 909 plants (Fig. 1B), while there was no obvious height difference between accession 237 and the OUM125 mutant (Fig. 1A). Hence, accession 909 was chosen for further characterisation and to be used to compare with the OUM125 mutant. The OUM125 line has a non-functional CSLF6 synthase, a protein mediating the biosynthesis of (1,3;1,4)-β-glucan, and this resulted in undetectable levels of (1,3;1,4)-β-glucan when measured according to the Megazyme protocol, consistent with observations by Taketa et al, (2012). Generally, the

cell walls of the starchy endosperm are comprised of ~70% of (1,3;1,4)-β-glucan and ~25% arabinoxylan (Fincher, 1975; Bacic and Stone, 1981b). Loss of (1,3;1,4)-β-glucan deposition in OUM125 resulted in increased levels of arabinoxylan and soluble carbohydrates including glucose, fructose, sucrose, raffinose and fructan. However, starch content was not significantly altered in the OUM125 mature grain (Table 1), consistent with previous findings (Tonooka et al., 2009).

The presence of (1,3;1,4)-β-glucan in OUM125 and 909 was investigated using the BG1 monoclonal antibody and the fluorescence microscope. Using a standard exposure time, there was no visible BG1 antibody labelling in OUM125 grain while BG1 labelling was uniform across all tissues in the 909 line (Fig. 6C and 6D). However, under a higher exposure time, we observed BG1 antibody labelling in the pericarp and within the aleurone cells of the OUM125 mutant grain (Fig. 7B, 7C, 7E and 7F). The fluorescent signals within the aleurone cells are from binding to unknown cellular contents, rather than to the walls of the cells, whilst the pericarp labelling is brighter and more even, although no individual walls are visible at this stage due to dehydration and collapse of the tissue. Interestingly, our qPCR data revealed an upregulation of the *CslH1* gene in the OUM125 pericarp. (Fig. 4A and S8A). The barley *CslH1* gene has been proposed to mediate the biosynthesis of (1,3;1,4)-β-glucan in older tissues, including the barley leaf tip (Doblin et al., 2009), and it is usually present in the grain in negligible levels compared with *CslF6*. In the absence of a functional CSLF6 protein it is possible that another site of CSLH1 action has been revealed where a relatively small amount of (1,3;1,4)-β-glucan has accumulated in the maternal tissues of OUM125 mutant grain.

Interestingly, BG1 labelling persisted in the pericarp of OUM125 grain even after treatment with the lichenase enzyme which hydrolyses the (1,4)-β-D-glucosidic linkages in β-glucans

containing (1,3)- and (1,4)-bonds. It has been shown that BG1 has a high affinity towards molecules as big as heptasaccharides (G3G4G4G3G4G4G$_R$) (G=glucose; 3=1,3 linkage; 4=1,4 linkage; GR=reducing terminal residue) (Meikle et al., 1994) but after this point the (1,3;1,4)-β-oligosaccharides become increasingly less soluble and so cannot be tested for affinity effectively. There are two explanations for the inability of the lichenase to remove material which was subsequently detected by the BG1 antibody in the mutant pericarp: 1) the BG1 antibody has a greater affinity towards (1,3;1,4)-β-glucan than the lichenase enzyme and/or 2) a resistant form of (1,3;1,4)-β-glucan is present in the OUM125 pericarp. A resistant form of (1,3;1,4)-β-glucan is possible, due to a different fine structure or conformation of the polysaccharide. For example, transgenic Arabidopsis overexpressing the *HvCslH1* gene released DP2 fragments (G3G$_R$) after lichenase digestion (Doblin et al., 2009), which was not found in transgenic *Nicotiana benthamiana* overexpressing the *HvCslF6* gene (Taketa et al., 2012), indicating that the (1,3;1,4)-β-glucan produced by the CSLH1 protein may have a different fine structure than that from the CSLF6 protein. With evidence of upregulation of *CslH1, CslF10, CslF3* and *CslF7* genes in the OUM125 pericarp, it is possible that *CslH* and other *CslF* genes act coordinately to mediate the biosynthesis of a resistant form of (1,3;1,4)-β-glucan which can be detected by the BG1 antibody (Fig. 4A) but cannot be detected by the Megazyme assay which relies on the activity of lichenase.

Compositional analysis indicated that the amount of arabinoxylan in the mature OUM125 grain was higher compared to 909 (Table 1), whilst genes encoding GT61, *HORVU1Hr1G080720* and *HORVU5Hr1G013550* which play a key role in arabinoxylan biosynthesis (Anders et al., 2012; Rennie and Scheller, 2014), were upregulated in OUM125 pericarp at 19 DAP and *HORVU1Hr1G080720* was upregulated in OUM125 endosperm at 24 DAP. Although the immunolabeling results with the LM11 antibody were similar for both (Fig. 6E and 6F), it is

possible that the higher levels of arabinoxylan in mature OUM125 grain could be attributed to water-soluble arabinoxylan which may not bind the antibody (Dervilly et al., 2002). The minority cell wall components including cellulose, callose and heteromannan were examined in 909 and OUM125 mature grain. (Fig. 6A to 6N). Callose has been associated with plant development through the regulation of plasmodesmata (Rinne and van der Schoot, 1998), cell plate formation (Thiele et al., 2009), wounding and pathogen infection responses (Jacobs et al., 2003; Nishimura et al., 2003; Chowdhury et al., 2014), and is deposited in cell walls surrounding plasmodesmata (Wilson et al., 2012). A previous study proposed that the *Gsl2* gene in barley may be involved in callose biosynthesis at later stages of endosperm development (Wilson et al., 2012). Callose antibody labelling indicated that OUM125 had a weaker labelling intensity with patchy patterns in the endosperm compared to 909 (Fig. 6G and 6H). Furthermore, we observed lower *Gsl2* transcript levels in OUM125 endosperm relative to 909 (Fig. 4B and S8J). To date, there is no accurate method available for quantifying callose, so based on the labelling intensity in the OUM125 grain, we propose a reduction in callose accumulation.

Heteromannan is one of the minority cell wall polysaccharides in barley grain, and its role in development is not known. It is first deposited in endosperm walls at 5 DAP (Wilson et al., 2006) and it is concentrated in the cell walls adjacent to the crease later in grain development (Wilson et al., 2012). *CslA* genes have been proposed to encode glucomannan synthases (Dhugga et al., 2004; Liepman et al., 2005). Accumulation of heteromannan at 10 DAP in barley grain was shown to coincide with upregulation of the *CslA6* gene which may be involved in its biosynthesis (Wilson et al., 2012). Our qPCR data showed relatively fewer *CslA6* gene transcripts in OUM125 pericarp and endosperm from 7 to 24 DAP (Fig. 4A, 4B and S8K) with the mannan antibody labelling concentrated in the region adjacent to the crease and relatively weakly in the endosperm compared to 909 grain (Fig. 6I and 6J). However, there was no

significant difference in the amount of mannose released from the monosaccharide analyses of 909 and OUM125 grain (Fig S3A and S3B).

Cellulose was not detectable in OUM125 grain using CBM3a and Pontamine fast scarlet (S4B) stains (Fig. 6L and 6N). However, removal of arabinoxylan with α-L-arabinofurosidase and xylanase unmasked the crystalline cellulose in OUM125 grain (Fig. 8C and 8D). This suggests that the amount of cellulose in OUM125 was extremely low compared to 909 where the crystalline cellulose could easily be detected without unmasking (Fig. 6M). It was noted that the cellulose in OUM125 was not stained by S4B even after digestion of arabinoxylan (Fig. 8B). Differential binding patterns of CBM3a and S4B stains on the OUM125 grain hints at the existence of different cellulose forms or conformations (Griffiths et al., 2014; Voiniciuc et al., 2015). Here we saw that S4B staining in the endosperm of 909 disappeared after lichenase digestion (Fig. S1D) which implies that it was binding to (1,3;1,4)-β-glucan even though S4B has been previously reported to bind to cellulose only (Anderson et al., 2010; Thomas et al., 2013). In our case, digestion of (1,3;1,4)-β-glucan by lichenase completely removed the labelling of S4B in endosperm, which also contained cellulose (Fig. S1C and S1D). Furthermore, there was no binding of S4B in the OUM125 grain which does not contain (1,3;1,4)-β-glucan in the endosperm (Fig. 6L). This indicates that S4B binds to (1,3;1,4)-β-glucan in barley grain as well as to cellulosic tissues such as wood, seed mucilage and Arabidopsis root (Anderson et al., 2010; Thomas et al., 2013; Griffiths et al., 2014). Here, the S4B binding did not seem to be affected in the aleurone cell walls upon lichenase treatment (Fig. S1D), possibly because (1,3;1,4)-β-glucan in the aleurone cell wall was not completely digested by lichenase, as we were able to observe traces of BG1 antibody labelling in the aleurone cell walls after the lichenase treatment (data not shown). Moreover, treatment with cellulase, which hydrolyses both cellulose and (1,3;1,4)-β-glucan, also did not remove S4B

binding in the aleurone cell walls (Fig. S2A and S2B). The binding pattern of S4B for the lichenase-treated sample appeared to be similar to the cellulase-treated sample (Fig. S1D and S2B), suggesting that (1,3;1,4)-β-glucan may not be completely digested by the cellulase allowing the remnants to be stained by S4B.

In the aleurone layer, there was an increased fluorescent signal from CBM3a after the cellulase treatment, indicating that the cellulase can access aleurone cell walls to hydrolyse the cellulose component (Fig. S2C and S2D). Binding of CBM3a to the aleurone cell wall after cellulase treatment was not due to unmasking of (1,3;1,4)-β-glucan since lichenase treatment did not promote binding of CBM3a (Fig. S1F and S2D). It is possible that digestion of cellulose by the cellulase in the aleurone and endosperm cell walls exposes an additional binding site for CBM3a, since the cellulase and CBM3a may have different carbohydrate-binding motifs. The cellulase enzyme provided by Megazyme was purified from *Aspergillus niger* (fungi), which has a family I cellulose-binding domain (CBD) (Carrard et al., 2000) while CBM3a was purified from *Clostridium thermocellum* (bacteria) and belongs to family III (Blake et al., 2006). This may explain the inability of cellulase to remove CBM3a staining in barley grain as the addition of cellulase partially digests the cellulose and actually improves the accessibility of the crystalline cellulose to CBM3a.

Conclusions

Where loss of the CSLF6 protein has been shown to severely affect vegetative growth and cold tolerance in both rice and barley, an almost complete lack of (1,3;1,4)-β-glucan has little effect on grain morphology or downstream processes such as germination. In OUM125 mutant grain compared to the 909 parental line, there was no difference in starch content but other storage carbohydrates such as arabinoxylan and fructan were more abundant but not at a level that generated notable physical changes. In the absence of a functional CSLF6 protein upregulation of *CslH1* and other *CslF* transcripts were seen in the pericarp, putatively leading to deposition of low levels of (1,3;1,4)-β-glucan that were resistant to lichenase digestions but which were detected by the BG1 antibody. The lack of large quantities of (1,3;1,4)-β-glucan also allowed a more accurate assessment of the binding specificities of the cellulose stains CBM3a and SB4. Overall, our findings indicate that whilst the *CslF6* gene plays an essential role for barley vegetative development it is not essential for barley grain development.

Acknowledgments

The authors wish to acknowledge Professor Kazuhiro Sato (Okayama University) and A/Professor Matthew Tucker for providing OUM125 seeds and Associate Professor Ken Chalmers for his contribution to this project.

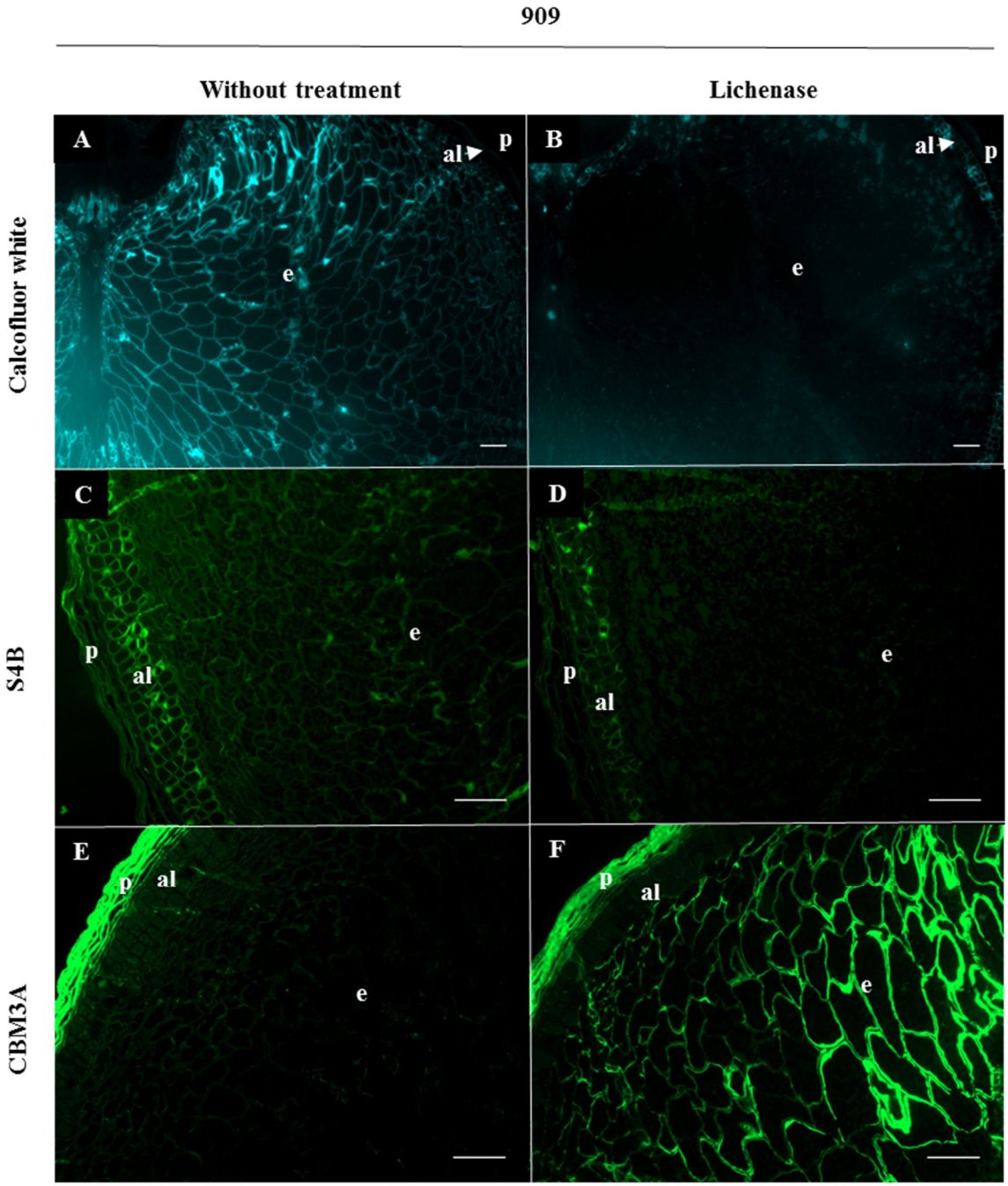

Supplementary figure 1: Fluorescence micrographs of Pontamine Fast Scarlet (S4B) and CBM3a labelling of mature 909 barley grain from control. Panels A, C and E are non-treated samples. Panels B, D and F are treated with the lichenase enzyme for 2 hours at 40°C prior to S4B and CBM3a labelling. Panels A and B are taken at 5x magnification while panels C, D E

and F are taken at 10x magnification. Scale bars represent 100 µm. Abbreviations: aleurone (al), endosperm (e), pericarp (p), cavity (c).

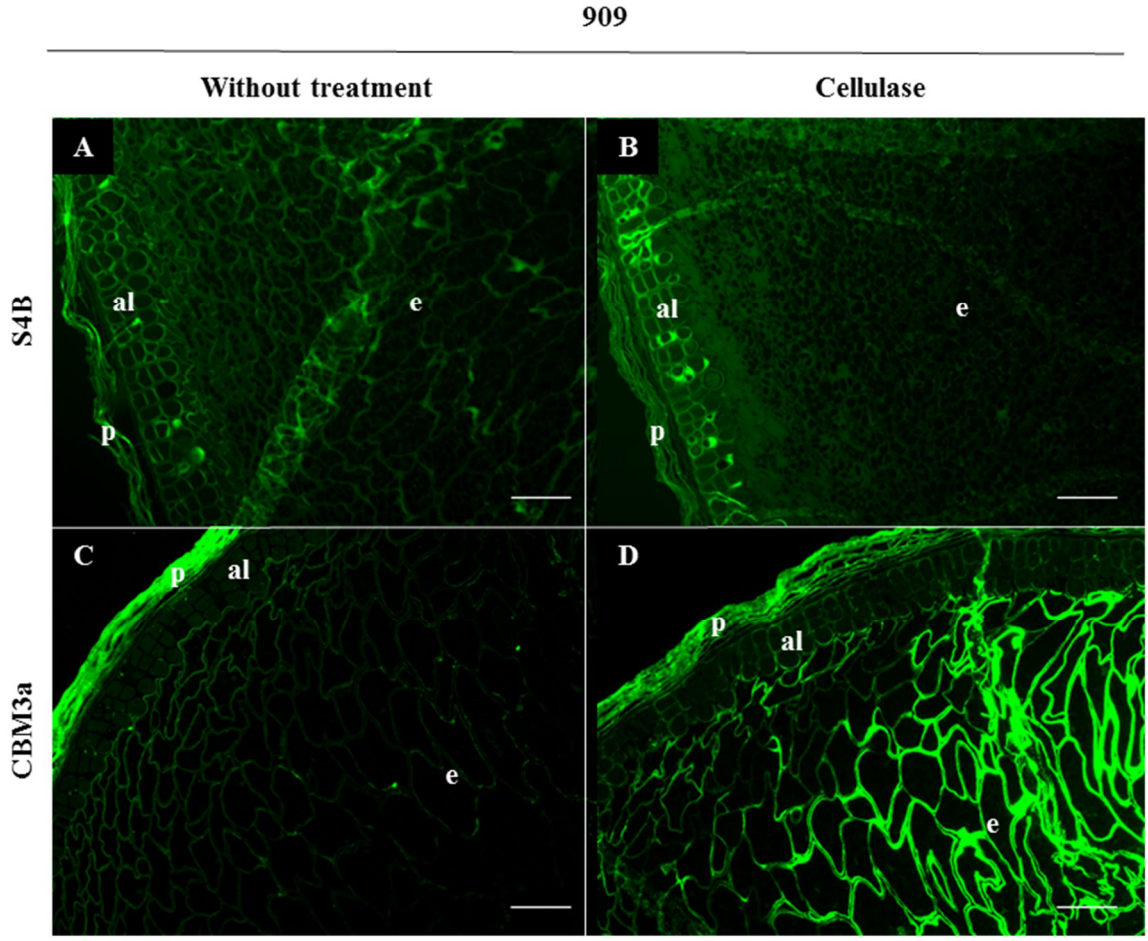

Supplementary figure 2: Fluorescence micrographs of Pontamine Fast Scarlet (S4B) labelling of mature 909 barley grain. (A) non-treated sample. (B) sample treated with cellulase for 24 hours at 40°C prior to S4B labelling. All images are taken at 10x magnification. Scale bars represent 100 µm. Abbreviations: aleurone (al), endosperm (e), pericarp (p).

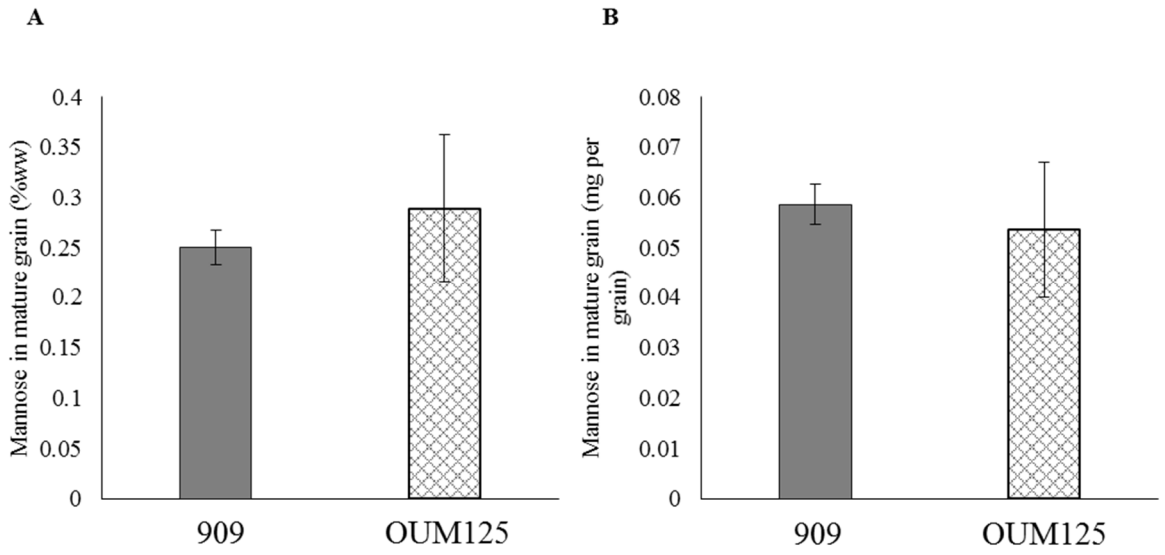

Supplementary figure 3: Mannose content in mature grain measured (A) on a weight per weight basis (w/w) and (B) on a per grain basis.

A

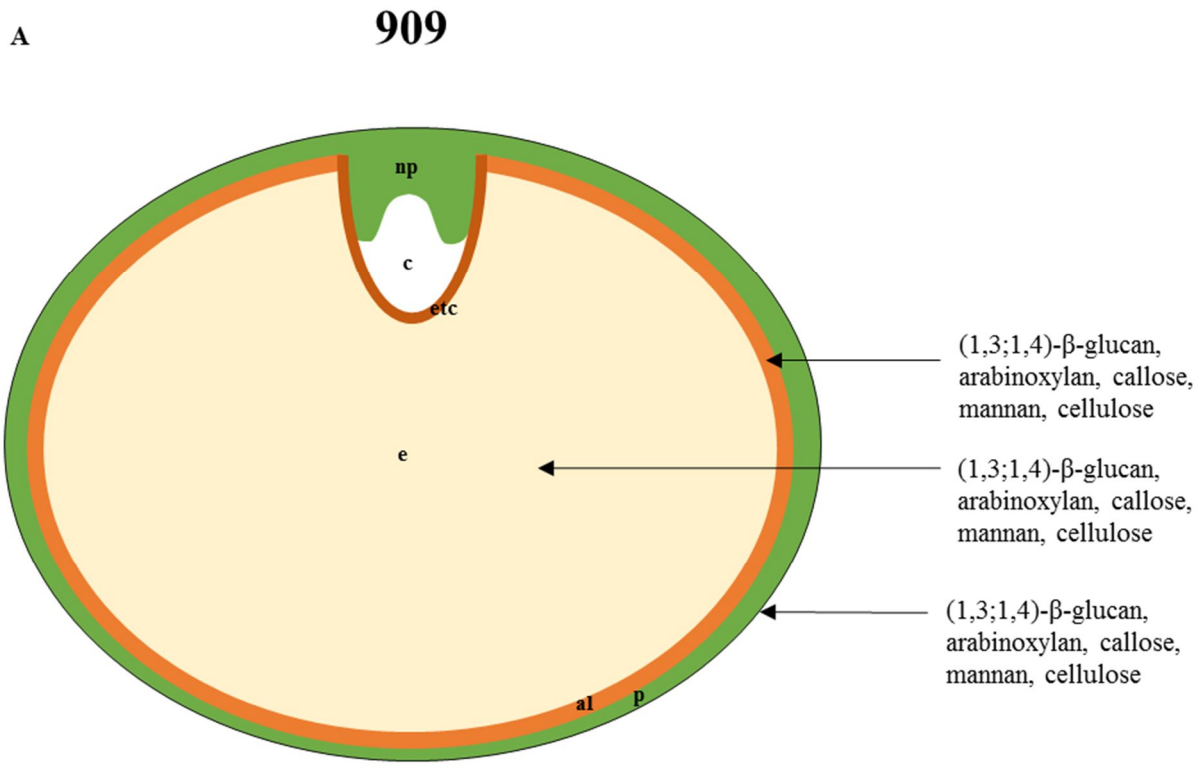
909
np
c
etc
e
al
p
(1,3;1,4)-β-glucan, arabinoxylan, callose, mannan, cellulose
(1,3;1,4)-β-glucan, arabinoxylan, callose, mannan, cellulose
(1,3;1,4)-β-glucan, arabinoxylan, callose, mannan, cellulose

B

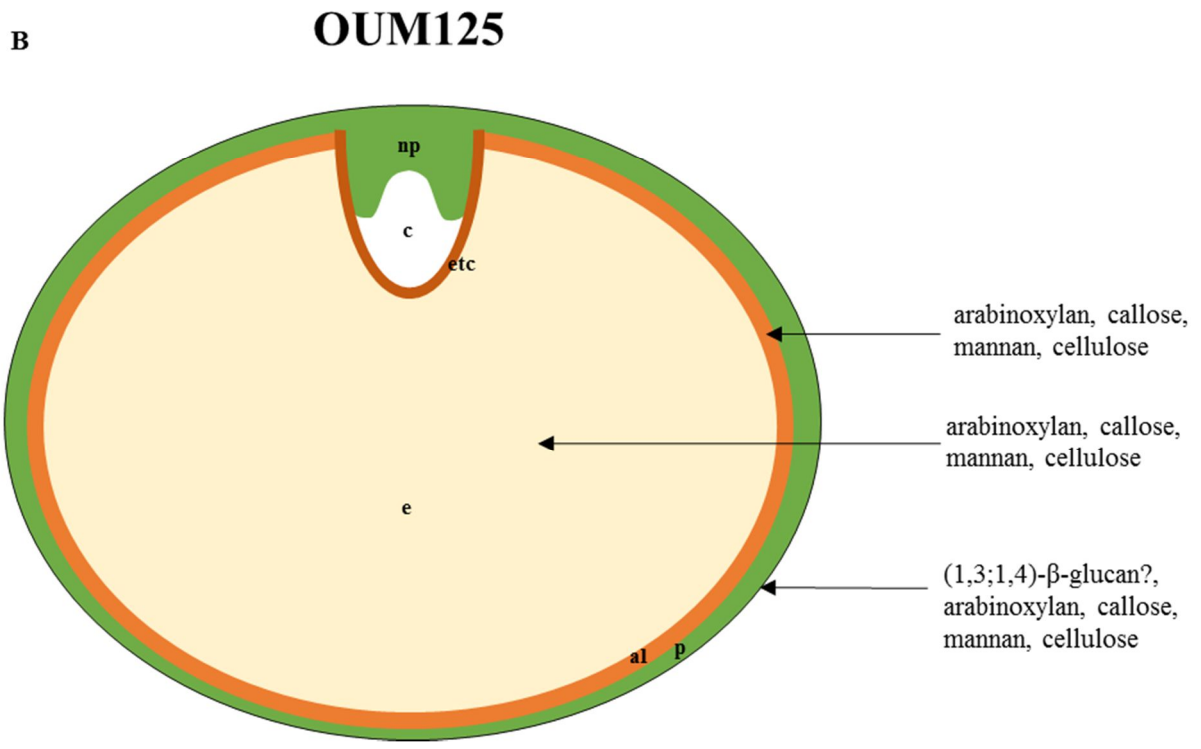
OUM125
np
c
etc
e
al
p
arabinoxylan, callose, mannan, cellulose
arabinoxylan, callose, mannan, cellulose
(1,3;1,4)-β-glucan?, arabinoxylan, callose, mannan, cellulose

Supplementary figure 4: Schematic diagram of mature 909 and OUM125 barley grain with their cell wall compositions in aleurone, endosperm and pericarp indicated. Abbreviations: aleurone (al), endosperm (e), pericarp (p), cavity (c), nucellar projection (np), endosperm transfer cell (etc).

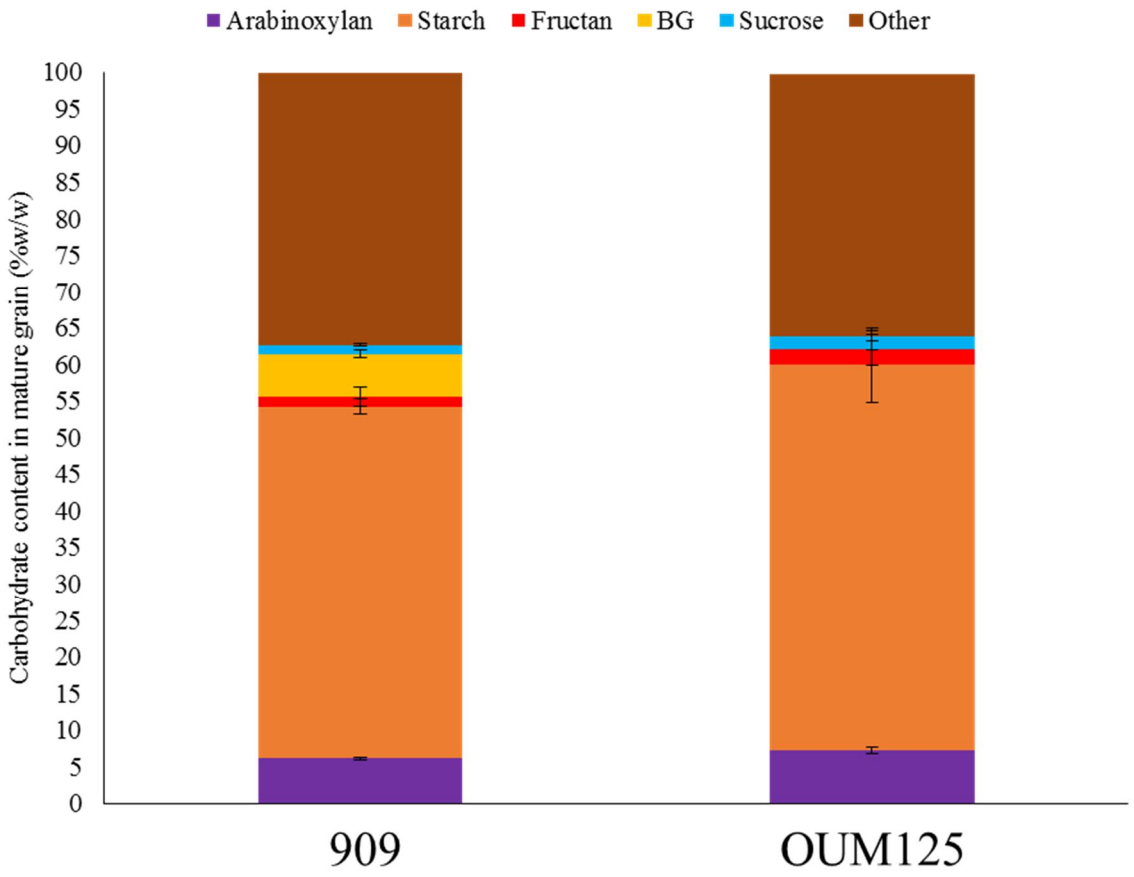

Supplementary figure 5: Carbohydrate content of mature barley grain measured on a percentage weight per weight basis.

A

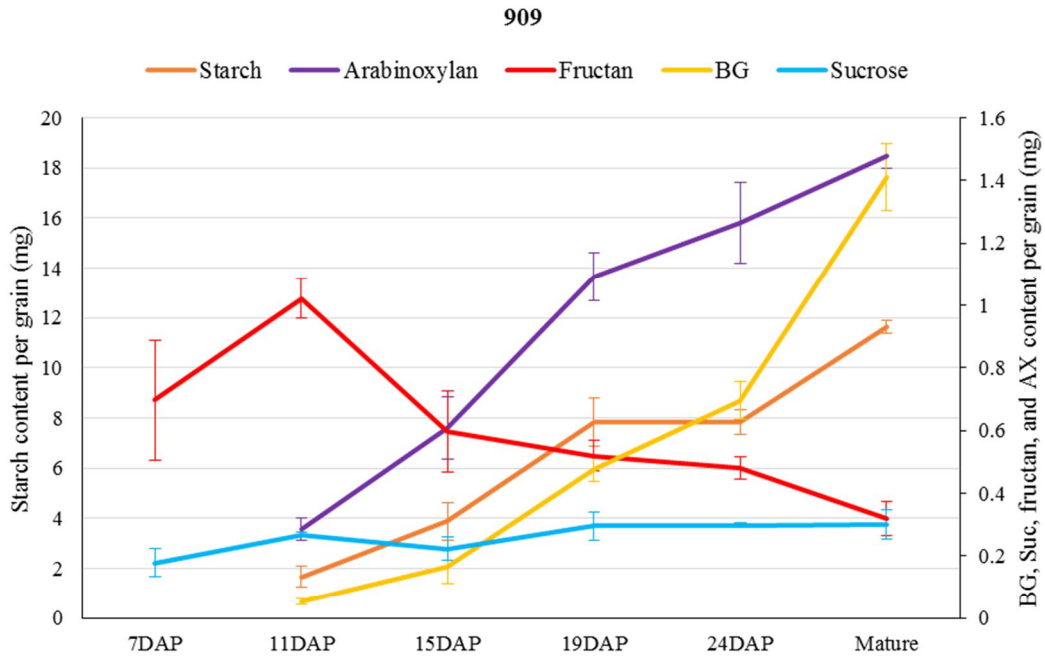

B

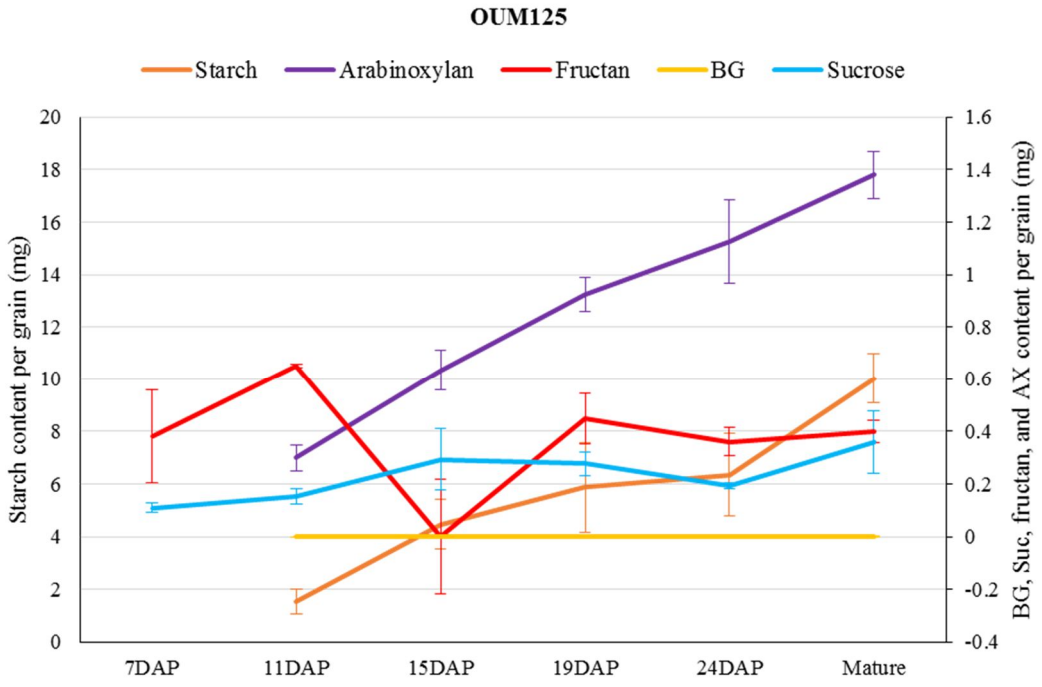

Supplementary figure 6: Carbohydrate content of barley grain from 7 DAP to mature measured on a mg per grain basis. Sugars from developing grain were measured in the pericarp

and endosperm, while the starch content in developing barley grain was measured in endosperm only. Sugars from mature grain were measured on a whole grain basis.

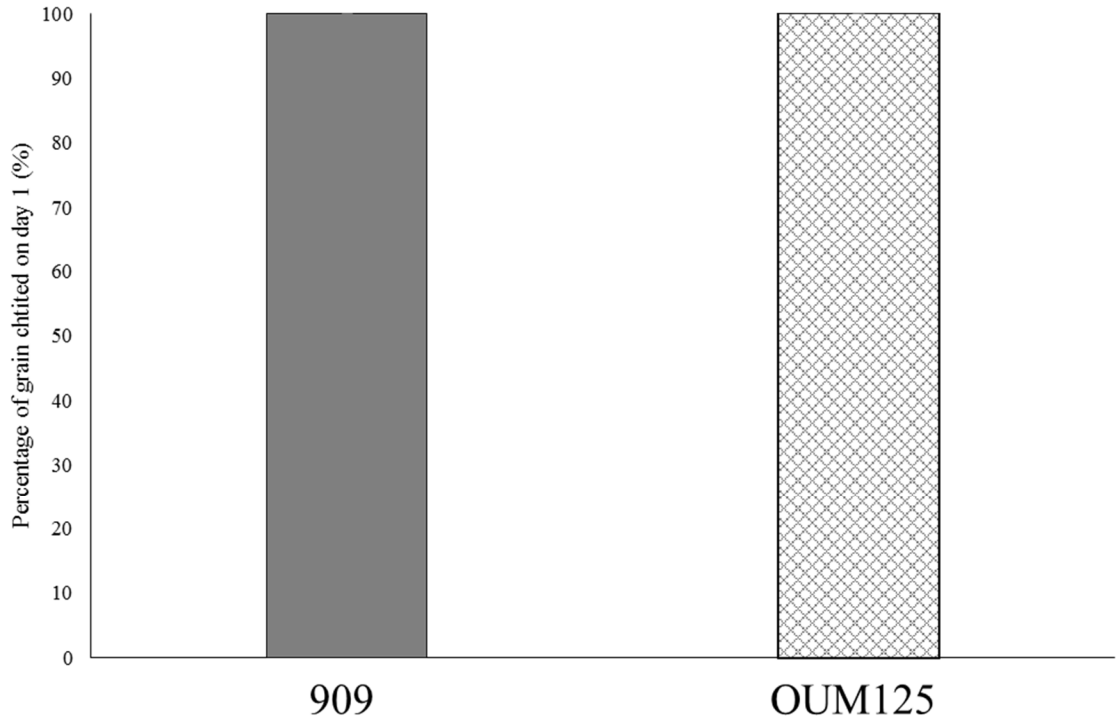

Supplementary figure 7: Seed germination test. Values are taken from 3 biological replicates for each line.

Supplementary table 1: List of primers used for real-time QPCR. * indicates β-fructofuranosidase (also known as invertase) genes which are involved in cleaving the fructofuranosyl linkages.

Gene full name	Gene	HORVU/Accession number	Sequence for forward primer (5' -> 3')	Sequence for reverse primer (5' -> 3')
Cellulose synthase-like H1	*CslH1*	FJ459581.1	TGCTGTGGCTGGATGGTGTT	GCTTTATTATTGAGAGAGATTGGGAGA
Cellulose synthase-like F3	*CslF3*	EU267179.1	CTTGTTGCCGGTTGCCTTTACA	TCAATTGGCTAAAATGGAAGAAAACTA
Cellulose synthase-like F7	*CslF7*	EU267182.1	CCCTGCTCTTGCTTGTCGTAG	TAGCCAAGCAATTGCATTT
Cellulose synthase-like F8	*CslF8*	EU267183.1	GCGTGGATTCTGGTGCTGATCTA	CCACCAATGCGATCAAAATAAAC
Cellulose synthase-like F9	*CslF9*	EU267184.1	CTGCCACCGCGTCCGTGTA	AGGTTTTGCAGCATTACTTGA
Cellulose synthase-like F10	*CslF10*	EU267185.1	GGCTATTGTTCAACCTGTGGATTA	TGGCCAAGAAAGCAATGGGTAGT
Cellulose synthase 2	*CesA2*	AY483152.1	CAGCCAGCCAGCAATTCTTTAT	AACCGCATTCTTGCCTTACAGA
Cellulose synthase 3	*CesA3*	AK365577.1	ACACGAGTCACTGGGCCAGA	CTGGTAAACTAGTCACCCGCTGA
(1,3;1,4)-beta-endoglucanase E1	*Endo E1*	AK252046.1	AACGAGAACCAGAAGGACAAC	TACGGACATACGGGCACTA
Glucan synthase like2	*Gsl2*	FJ853600.1	TGGGGCTGCTGCTCTTCAC	CGACGGCAATCTATCCATCTACC
Cellulose synthase-like A6	*CslA6*	AK376872.1	CTGCCGCTGCTTCTGCTACC	GCCGAATCCGATGACGAATG
Glycosyltransferase family 61	*GT61*	HORVU1Hr1G080720	TGCCATTGGCCATTGTATTA	TCATGGACATCCAAGCTTCA
Glycosyltransferase family 61	*GT61*	HORVU5Hr1G013550	TGACAAGGTTTGGGCCTATC	TCCCCGAAAAACAATTGAAG
Sucrose-sucrose-1-fructosyltransferase	*1-SST*	AK366020.1	GGGCTACGGTACGACTGG	GGGTCTTCTCGTCAAGCTC
Fructan-fructan 1-fructosyltransferase	*1-FFT*	JQ411253.1	GACGACCGGCGAGACTATTACG	GACGCGTCGTACCTGCCATA
Sucrose:fructan 6-fructosyltransferase	*6-SFT*	JQ411254.1	GACCCGGAGCTCGACTTG	CCGGGTCTTCTCATCCAGAG
*β-fructofuranosidase**	*INV*	HORVU6Hr1G011260	TTATTGTCACAGAAGAGCAATGTG	GATAACCATACATAGTTGAGCAATTT
*β-fructofuranosidase**	*INV*	HORVU2Hr1G109120	CCAATTGTGGCTCAGGTGTA	GGGCATGCGTGCTATACTTT
Cell wall invertase 1	*CWINV 1*	AJ534447.1	CTCCGAGGGTATGGACGTAG	TTTTTCACTCATCCGGCAAT
Vacuolar invertase	*VIN*	JQ411255.1	CGGTGAGGCTCTATGTGTGA	CTAAGACGTCGAGGCCATCT
Sucrose transporter 1	*SUT 1*	AM055812.1	TCGCATAGGCGTCGTAACTA	GGTTTGCTACACGCAAGTCA
Sucrose transporter 2	*SUT 2*	AJ272308.1	ACAAGGAAGGAAGGCAGGTT	CCCACGGAGGAAAGTAACAA
UTP-glucose-1-phosphate uridylyltransferase	*UGPase*	X91347.1	AAGGCTGGAGTCAAGTTGGA	AGCAGAATGCACACGAAAAA
ADP-glucose pyrophosphorylase large subunit	*AGPase*	AK362233.1	CCACATTCACCGCACCTACCT	GTCCTCAAGCACCCAGATAAA
Granule bound starch synthase 1a	*GBSS 1a*	FN179380.1	AGGACGTGCTTCTGGAACTG	CGAGAACCCTGAAGATGGAA
Granule bound starch synthase 1b	*GBSS 1b*	AK368223.1	GGCCCTTCTTAGCCTAGGAGT	CTTCGAACACCCTCCATGATA
Starch synthase 2	*SS 2*	FN179384.1	GCCTCAACACGTACTGGAACT	ATCGCGTGATCCTTGGTTACT
Starch branching enzyme 1	*SBE 1*	FN179382.1	AACTTTGTCTTCCGGTCACCT	TTTACACAGCTCGATAATACTGCT
Starch branching enzyme 2a	*SBE 2a*	AK373114.1	ACCAAGTAGCCGTTTTGGAAC	TGTGTATCAGTGCCATCGAAA
Starch branching enzyme 2b	*SBE 2b*	AF064561.1	CGGAAACACGAGGAAGATAAG	TGGAGCATAGACAACACAGGT
Limit Dextrinase	*LD*	AF252635.1	AAGTGAAAAGAACGAAGATAA	CCATCTCGGGGCTCTCACCTC
Isoamylase 1	*Iso 1*	AF490375.1	AGATGAAACAAAAGGCGAGAT	AGGGCGTGATACAAGGATGAC

A

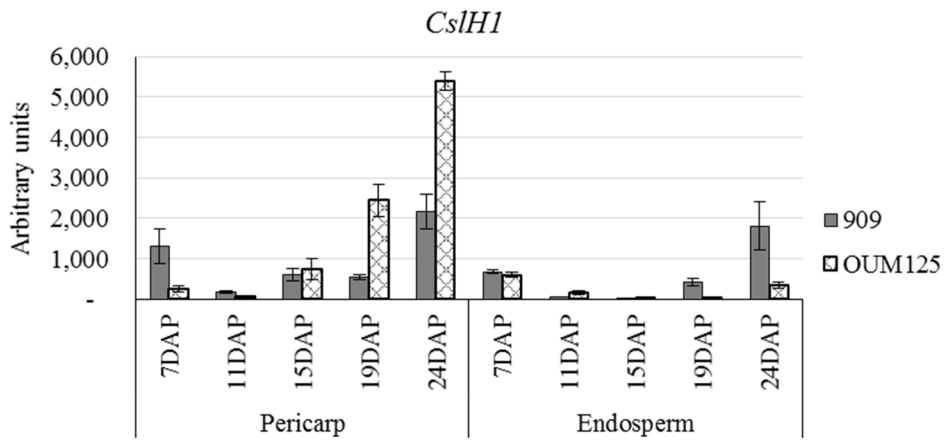
CslH1
Arbitrary units
6,000
5,000
4,000
3,000
2,000
1,000
-
7DAP
11DAP
15DAP
19DAP
24DAP
Pericarp
Endosperm
909
OUM125

B

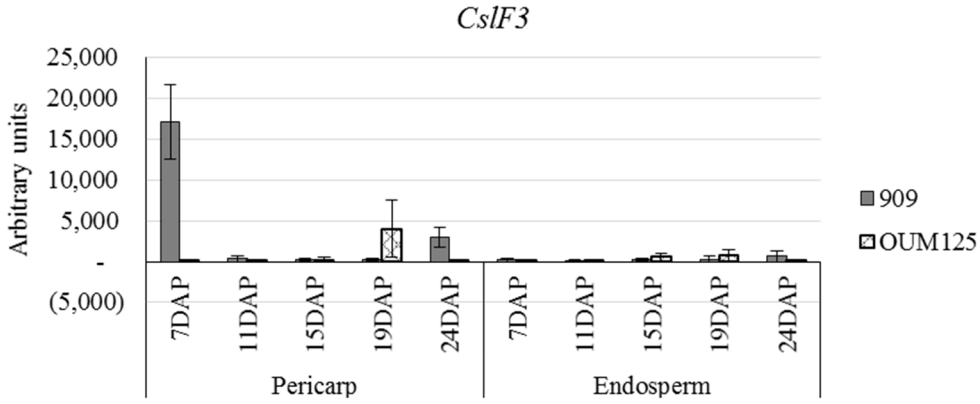
CslF3
Arbitrary units
25,000
20,000
15,000
10,000
5,000
-
(5,000)
7DAP
11DAP
15DAP
19DAP
24DAP
Pericarp
Endosperm
909
OUM125

C

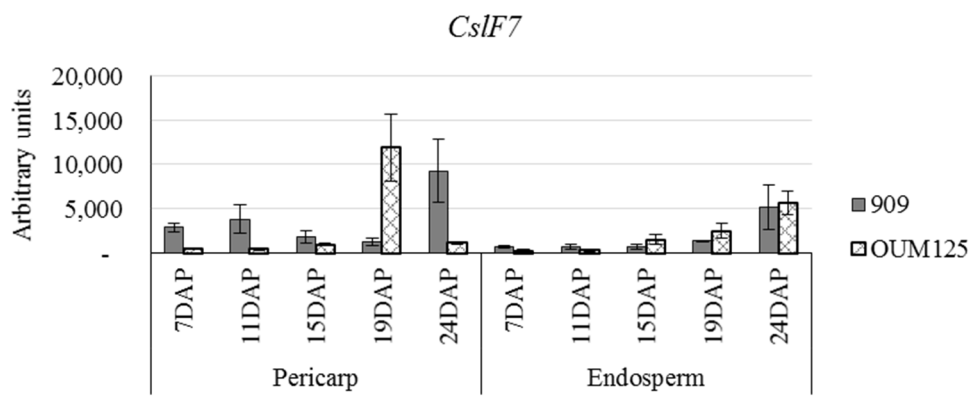
CslF7
Arbitrary units
20,000
15,000
10,000
5,000
-
7DAP
11DAP
15DAP
19DAP
24DAP
Pericarp
Endosperm
909
OUM125

D

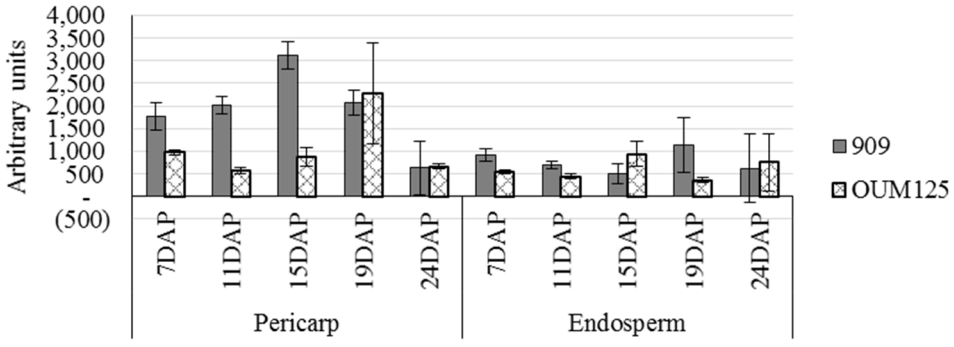
CslF8
Arbitrary units
4,000
3,500
3,000
2,500
2,000
1,500
1,000
500
-
(500)
7DAP
11DAP
15DAP
19DAP
24DAP
Pericarp
Endosperm
909
OUM125

E

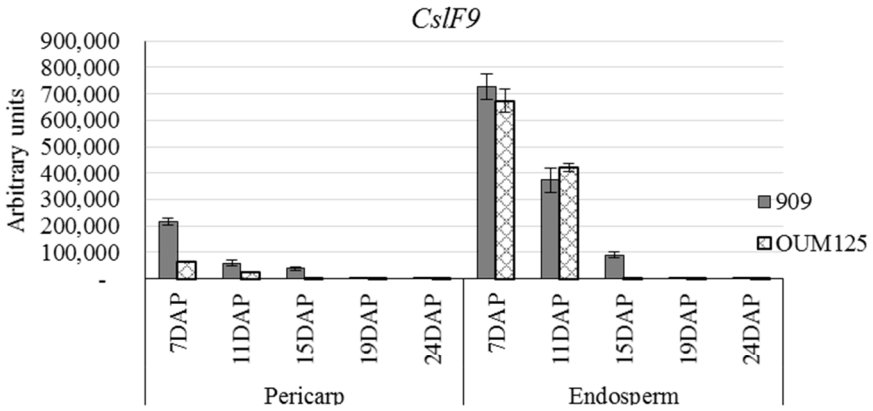
CslF9
Arbitrary units
900,000
800,000
700,000
600,000
500,000
400,000
300,000
200,000
100,000
-
909
OUM125
7DAP
11DAP
15DAP
19DAP
24DAP
Pericarp
Endosperm

F

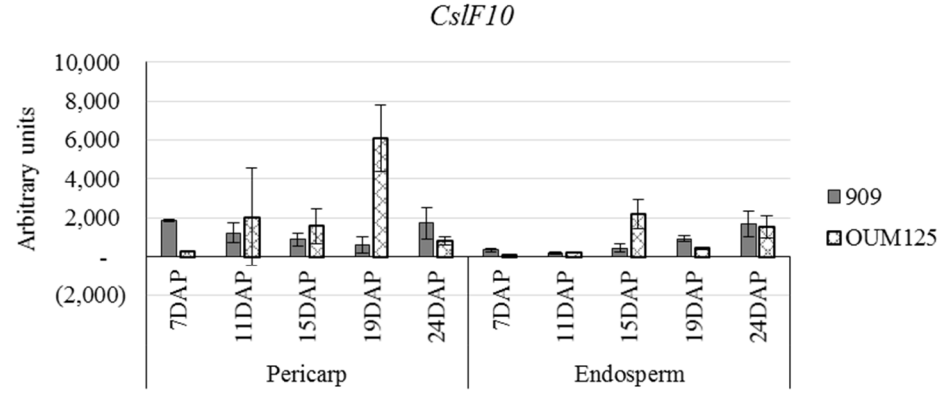
CslF10
Arbitrary units
10,000
8,000
6,000
4,000
2,000
-
(2,000)
909
OUM125
7DAP
11DAP
15DAP
19DAP
24DAP
Pericarp
Endosperm

G

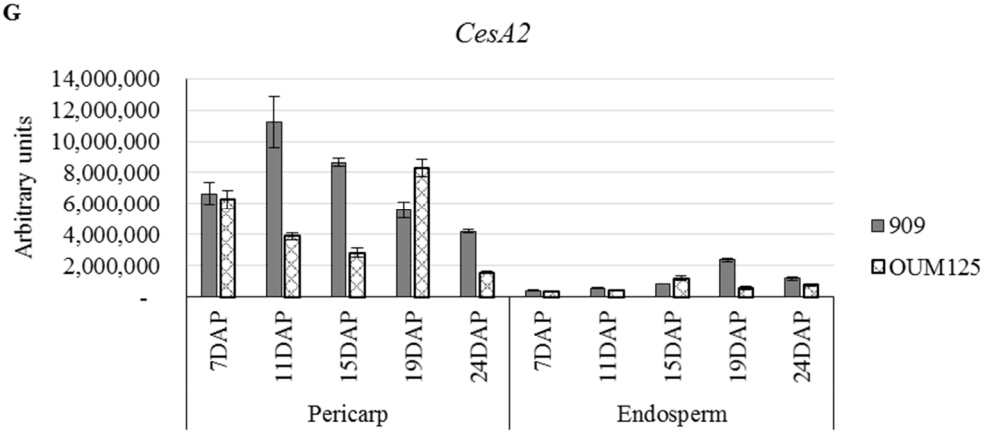
CesA2
Arbitrary units
14,000,000
12,000,000
10,000,000
8,000,000
6,000,000
4,000,000
2,000,000
-
909
OUM125
7DAP
11DAP
15DAP
19DAP
24DAP
Pericarp
Endosperm

H

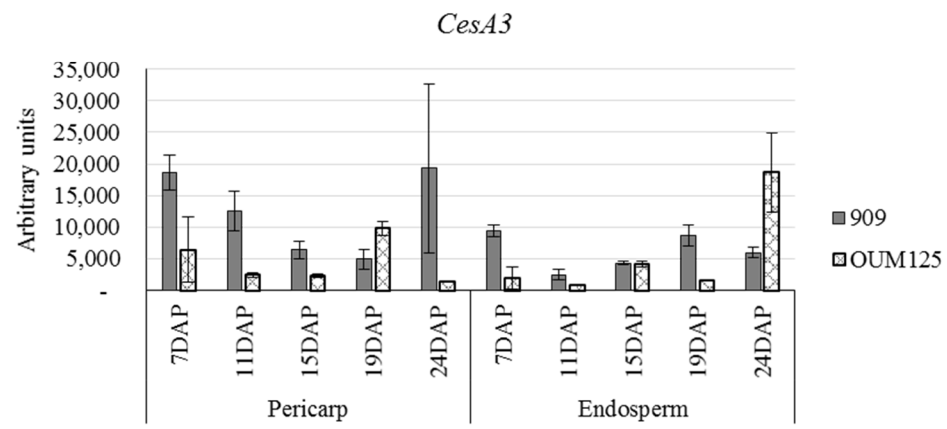
CesA3
Arbitrary units
35,000
30,000
25,000
20,000
15,000
10,000
5,000
-
909
OUM125
7DAP
11DAP
15DAP
19DAP
24DAP
Pericarp
Endosperm

I

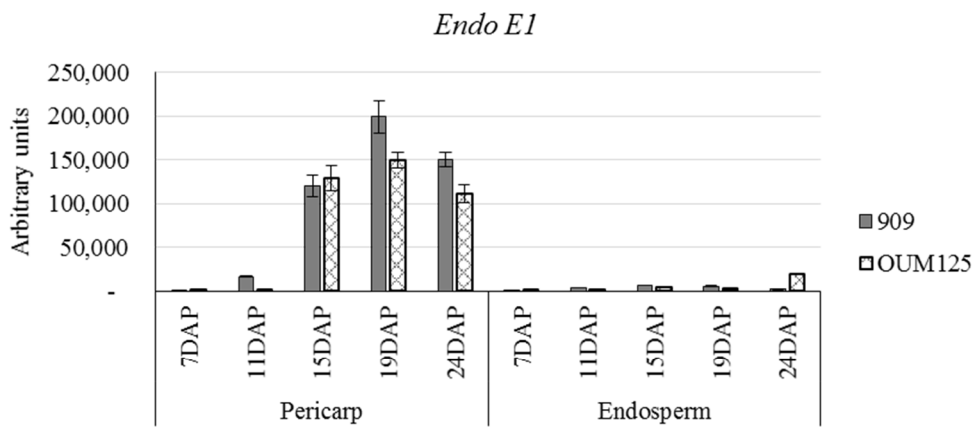
Endo E1
250,000
200,000
150,000
100,000
50,000
-
Arbitrary units
7DAP
11DAP
15DAP
19DAP
24DAP
Pericarp
Endosperm
909
OUM125

J

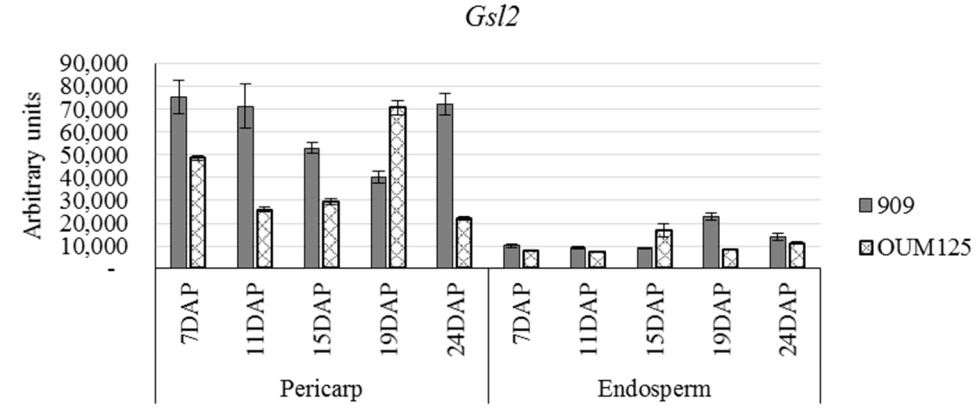
Gsl2
90,000
80,000
70,000
60,000
50,000
40,000
30,000
20,000
10,000
-
Arbitrary units
7DAP
11DAP
15DAP
19DAP
24DAP
Pericarp
Endosperm
909
OUM125

K

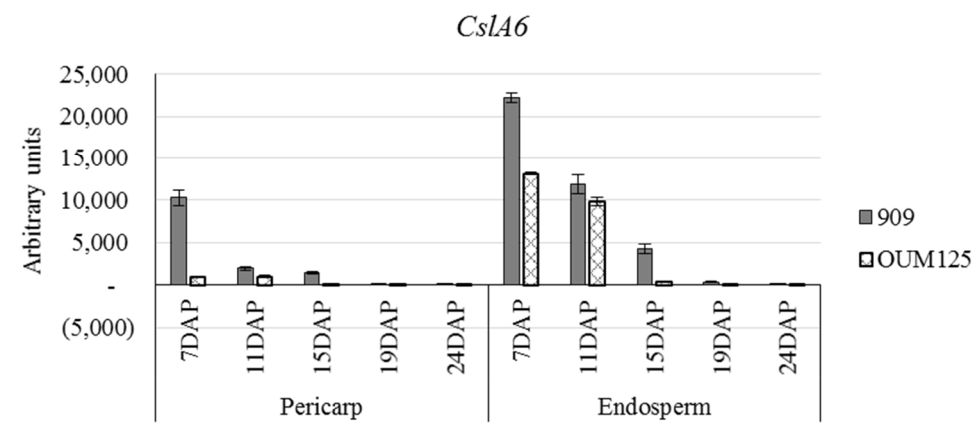
CslA6
25,000
20,000
15,000
10,000
5,000
-
(5,000)
Arbitrary units
7DAP
11DAP
15DAP
19DAP
24DAP
Pericarp
Endosperm
909
OUM125

L

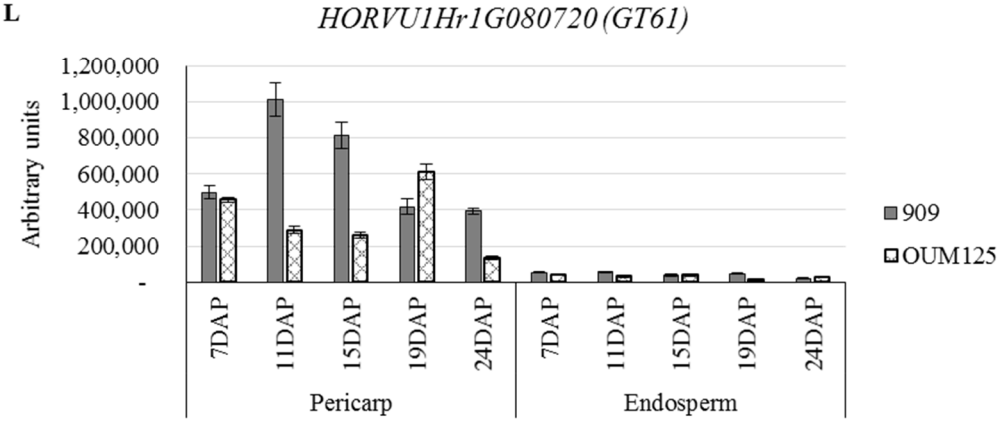
HORVU1Hr1G080720 (GT61)
1,200,000
1,000,000
800,000
600,000
400,000
200,000
-
Arbitrary units
7DAP
11DAP
15DAP
19DAP
24DAP
Pericarp
Endosperm
909
OUM125

M

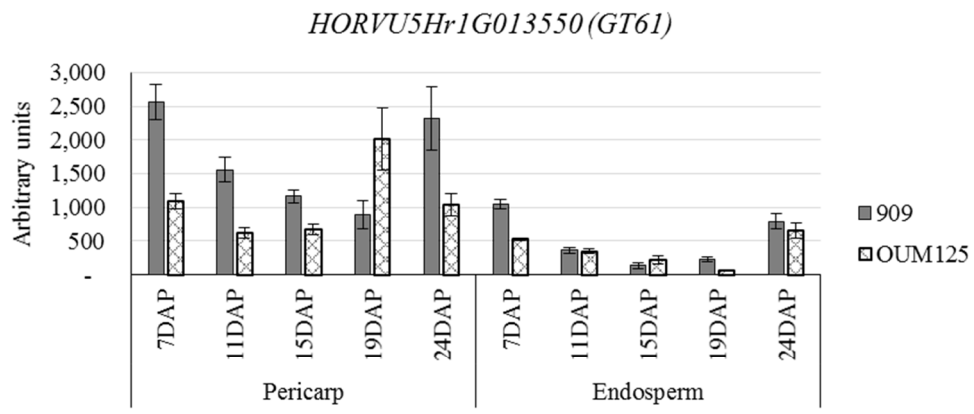
HORVU5Hr1G013550 (GT61)
Arbitrary units
3,000
2,500
2,000
1,500
1,000
500
-
7DAP
11DAP
15DAP
19DAP
24DAP
Pericarp
Endosperm
909
OUM125

N

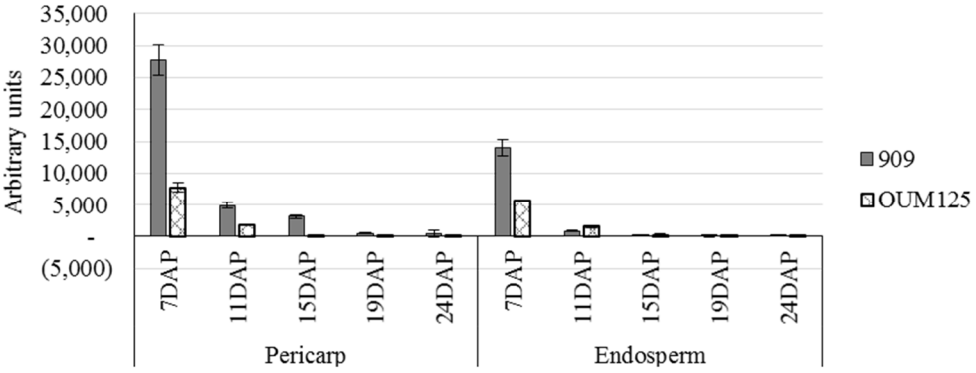
1-SST
Arbitrary units
35,000
30,000
25,000
20,000
15,000
10,000
5,000
-
(5,000)
7DAP
11DAP
15DAP
19DAP
24DAP
Pericarp
Endosperm
909
OUM125

O

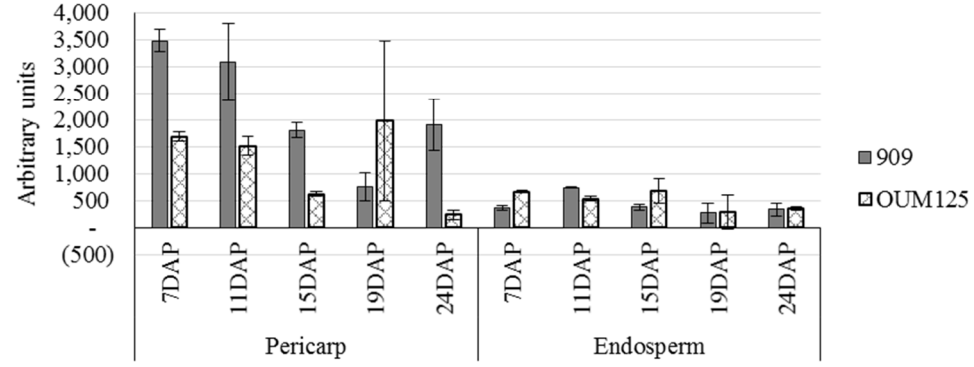
1-FFT
Arbitrary units
4,000
3,500
3,000
2,500
2,000
1,500
1,000
500
-
(500)
7DAP
11DAP
15DAP
19DAP
24DAP
Pericarp
Endosperm
909
OUM125

P

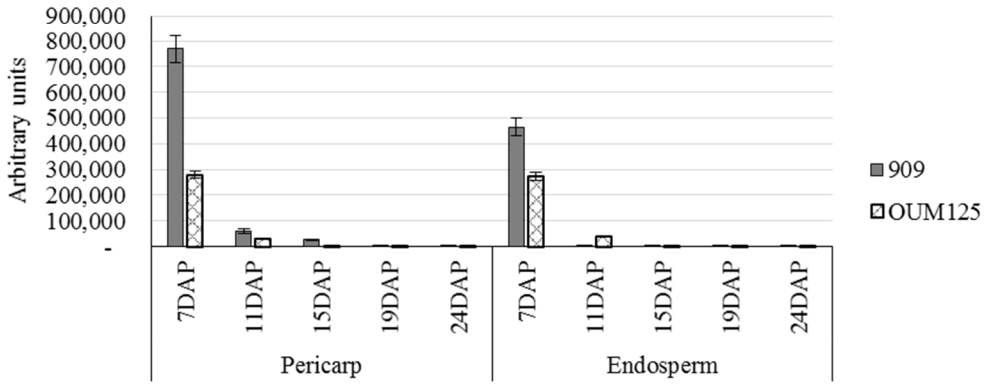
6-SFT
Arbitrary units
900,000
800,000
700,000
600,000
500,000
400,000
300,000
200,000
100,000
-
7DAP
11DAP
15DAP
19DAP
24DAP
Pericarp
Endosperm
909
OUM125

Q

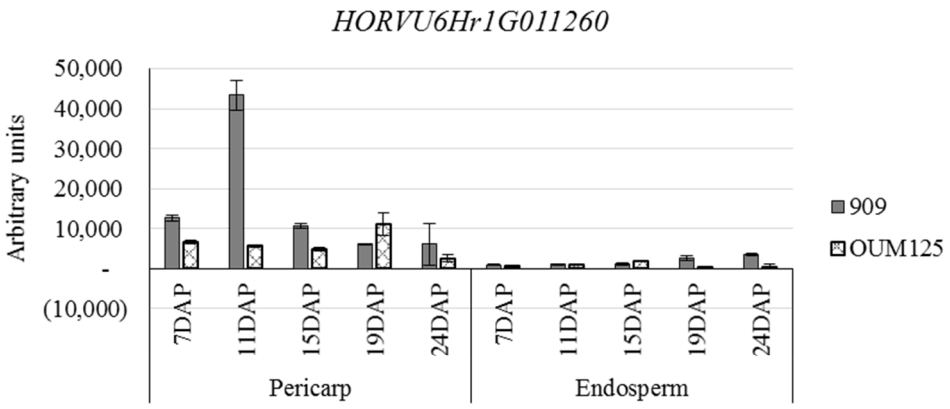
HORVU6Hr1G011260
Arbitrary units
50,000
40,000
30,000
20,000
10,000
-
(10,000)
7DAP
11DAP
15DAP
19DAP
24DAP
Pericarp
Endosperm
909
OUM125

R

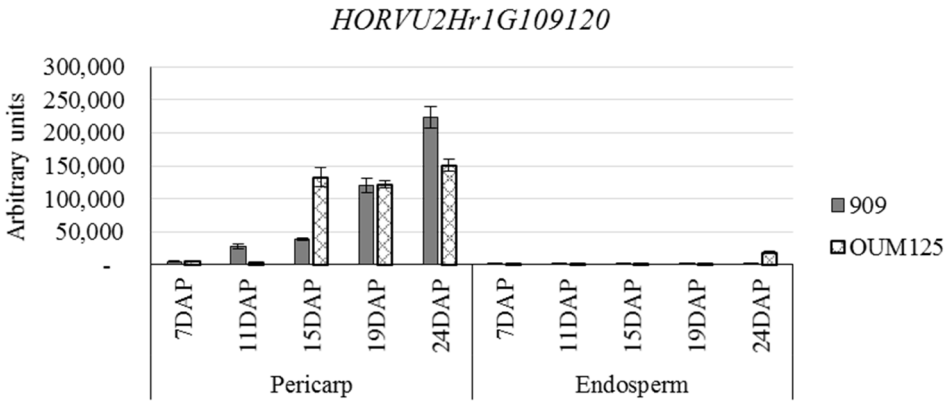
HORVU2Hr1G109120
Arbitrary units
300,000
250,000
200,000
150,000
100,000
50,000
-
7DAP
11DAP
15DAP
19DAP
24DAP
Pericarp
Endosperm
909
OUM125

S

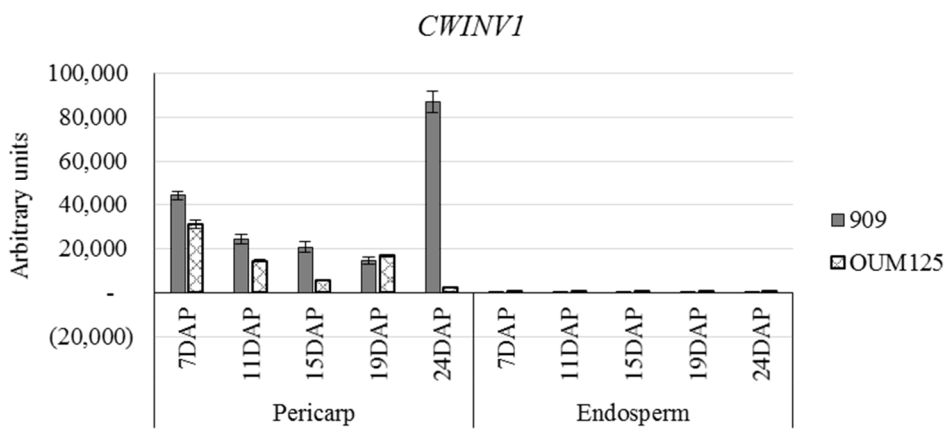
CWINV1
Arbitrary units
100,000
80,000
60,000
40,000
20,000
-
(20,000)
7DAP
11DAP
15DAP
19DAP
24DAP
Pericarp
Endosperm
909
OUM125

T

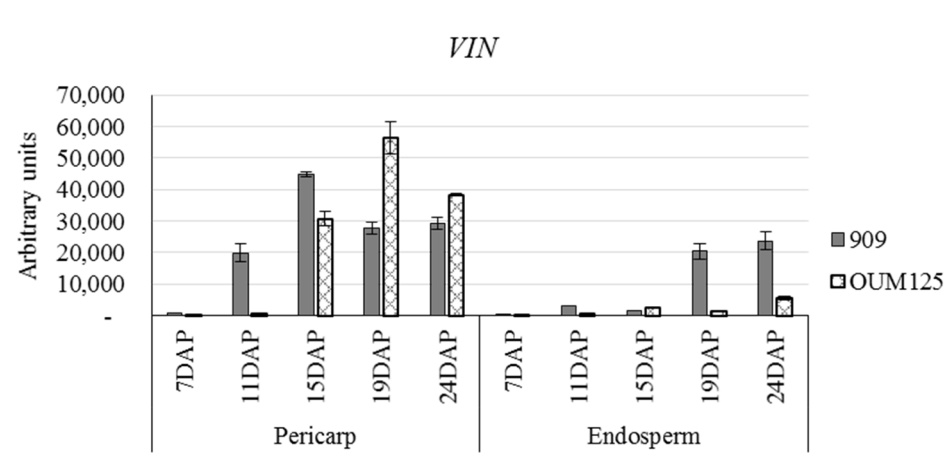
VIN
Arbitrary units
70,000
60,000
50,000
40,000
30,000
20,000
10,000
-
7DAP
11DAP
15DAP
19DAP
24DAP
Pericarp
Endosperm
909
OUM125

U

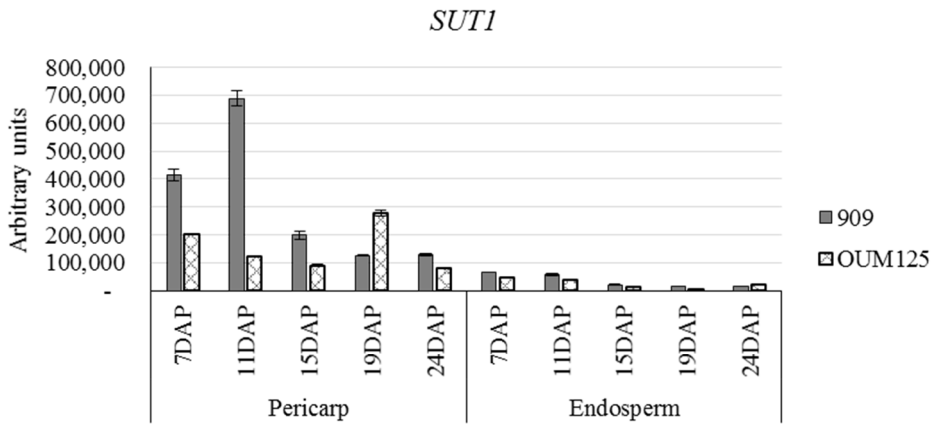
SUT1
Arbitrary units
800,000
700,000
600,000
500,000
400,000
300,000
200,000
100,000
-
7DAP
11DAP
15DAP
19DAP
24DAP
Pericarp
Endosperm
909
OUM125

V

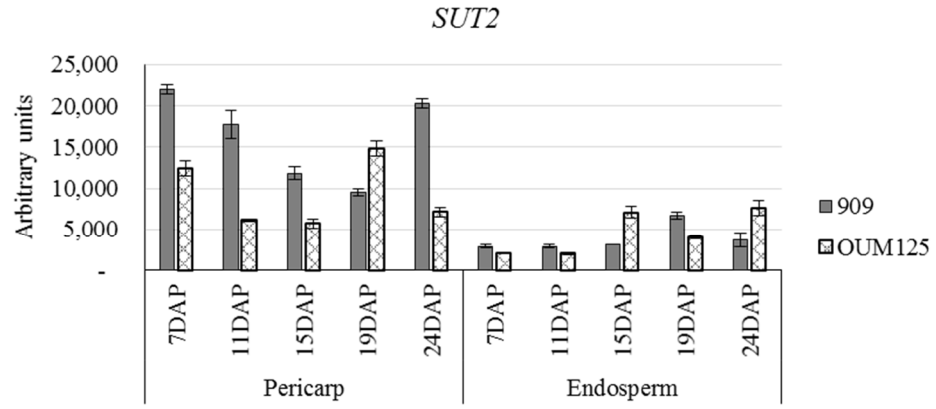
SUT2
Arbitrary units
25,000
20,000
15,000
10,000
5,000
-
7DAP
11DAP
15DAP
19DAP
24DAP
Pericarp
Endosperm
909
OUM125

W

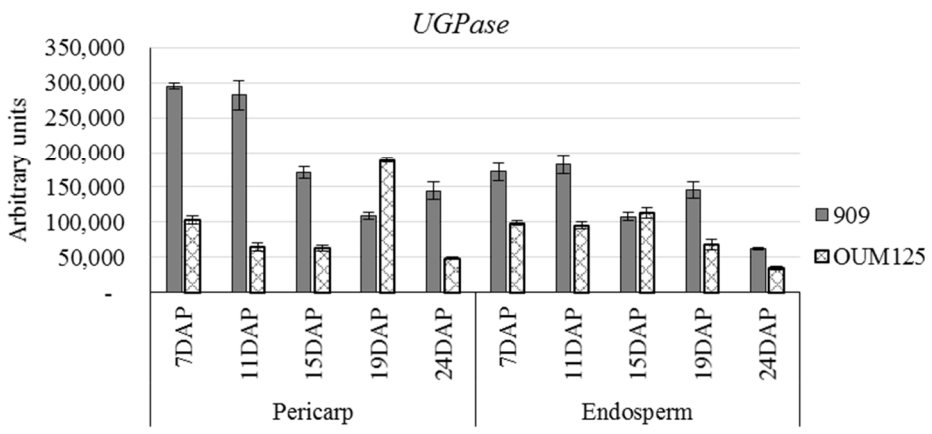
UGPase
Arbitrary units
350,000
300,000
250,000
200,000
150,000
100,000
50,000
-
7DAP
11DAP
15DAP
19DAP
24DAP
Pericarp
Endosperm
909
OUM125

X

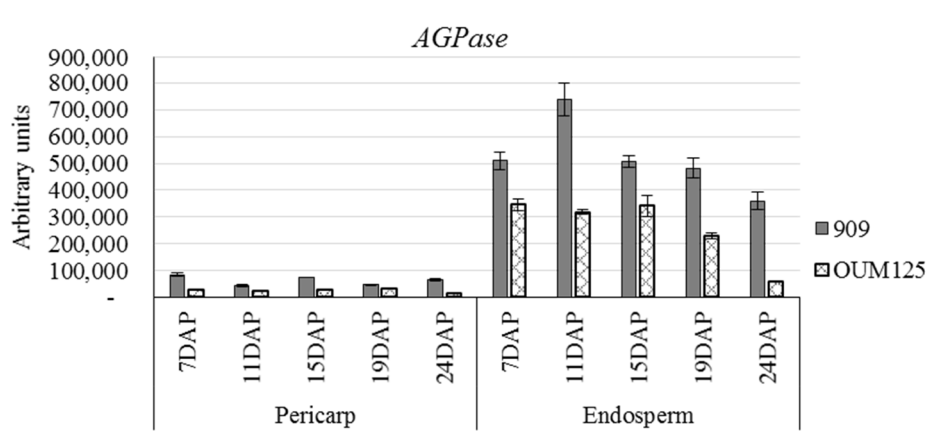
AGPase
Arbitrary units
900,000
800,000
700,000
600,000
500,000
400,000
300,000
200,000
100,000
-
7DAP
11DAP
15DAP
19DAP
24DAP
Pericarp
Endosperm
909
OUM125

Y

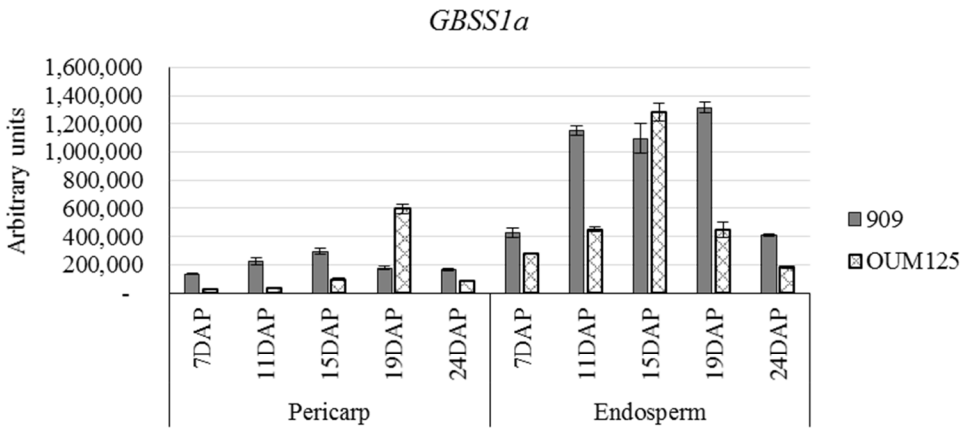
GBSS1a
Arbitrary units
1,600,000
1,400,000
1,200,000
1,000,000
800,000
600,000
400,000
200,000
-
7DAP
11DAP
15DAP
19DAP
24DAP
Pericarp
Endosperm
909
OUM125

Z

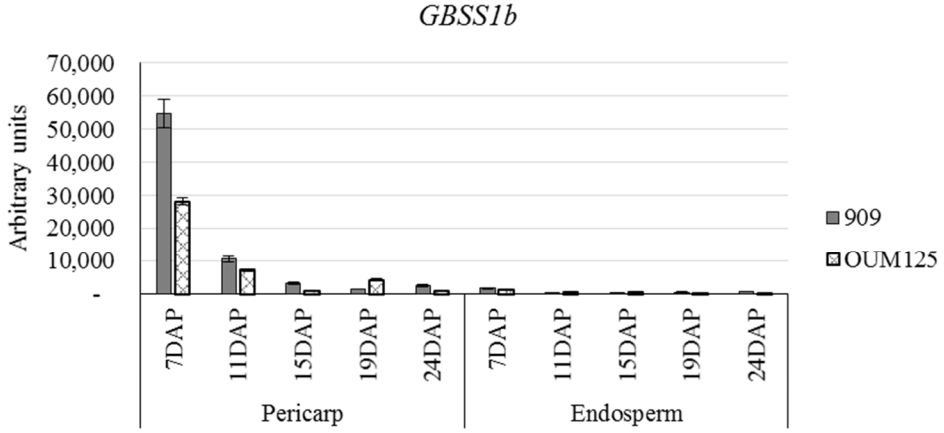
GBSS1b
Arbitrary units
70,000
60,000
50,000
40,000
30,000
20,000
10,000
-
7DAP
11DAP
15DAP
19DAP
24DAP
Pericarp
Endosperm
909
OUM125

A1

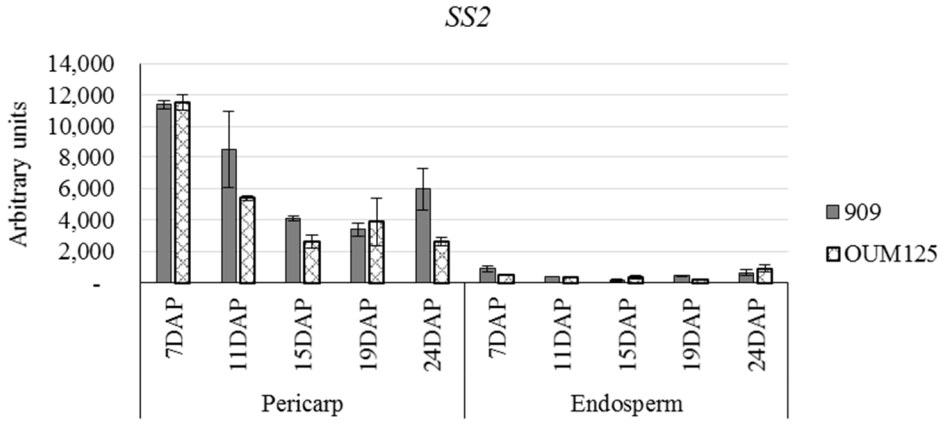
SS2
Arbitrary units
14,000
12,000
10,000
8,000
6,000
4,000
2,000
-
7DAP
11DAP
15DAP
19DAP
24DAP
Pericarp
Endosperm
909
OUM125

B1

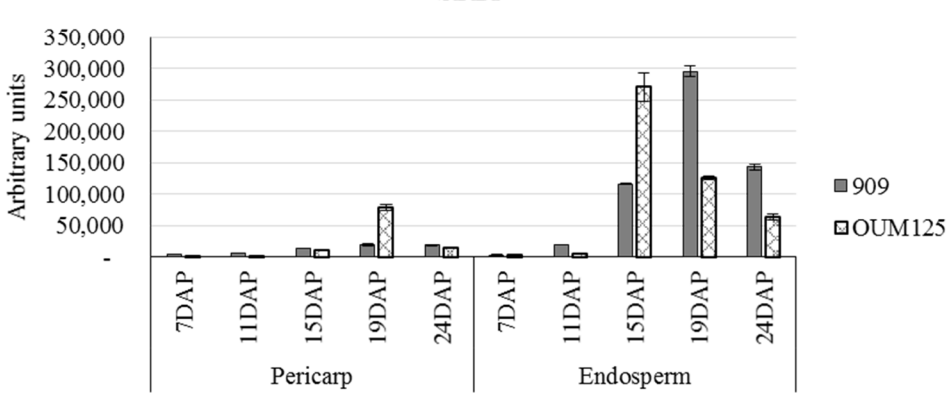
SBE1
Arbitrary units
350,000
300,000
250,000
200,000
150,000
100,000
50,000
-
7DAP
11DAP
15DAP
19DAP
24DAP
Pericarp
Endosperm
909
OUM125

C1

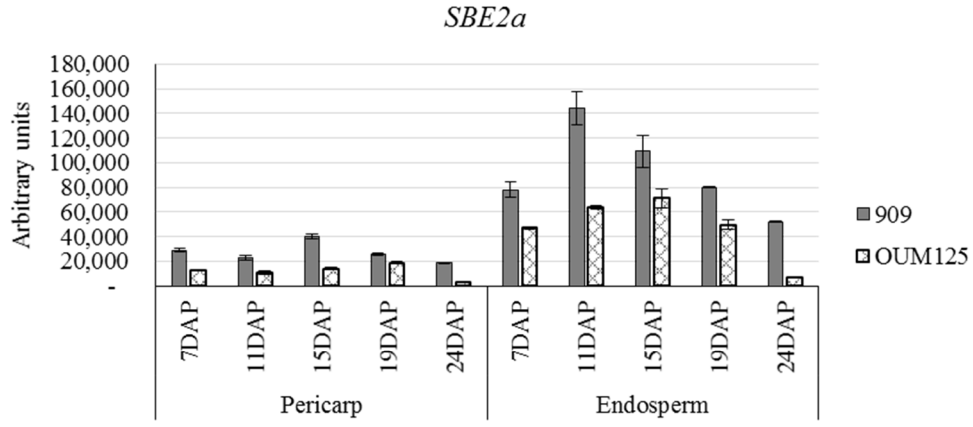
SBE2a
Arbitrary units
180,000
160,000
140,000
120,000
100,000
80,000
60,000
40,000
20,000
-
7DAP
11DAP
15DAP
19DAP
24DAP
Pericarp
Endosperm
909
OUM125

D1

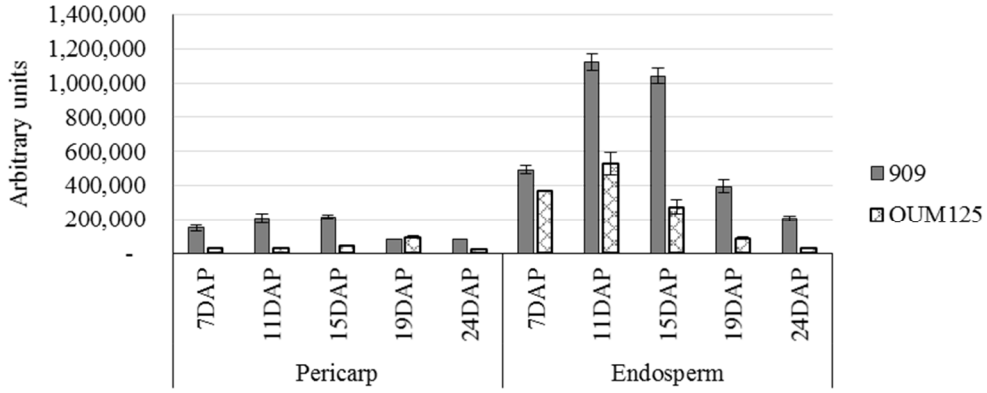
SBE2b
Arbitrary units
1,400,000
1,200,000
1,000,000
800,000
600,000
400,000
200,000
-
7DAP
11DAP
15DAP
19DAP
24DAP
Pericarp
Endosperm
909
OUM125

E1

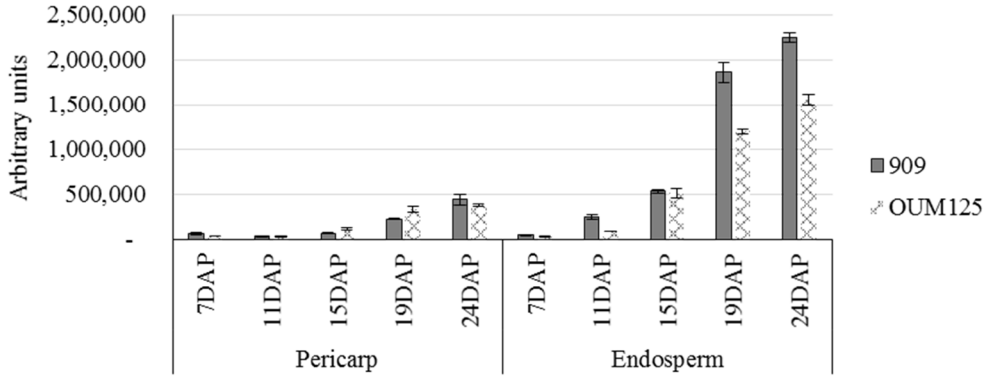
LD
Arbitrary units
2,500,000
2,000,000
1,500,000
1,000,000
500,000
-
7DAP
11DAP
15DAP
19DAP
24DAP
Pericarp
Endosperm
909
OUM125

F1

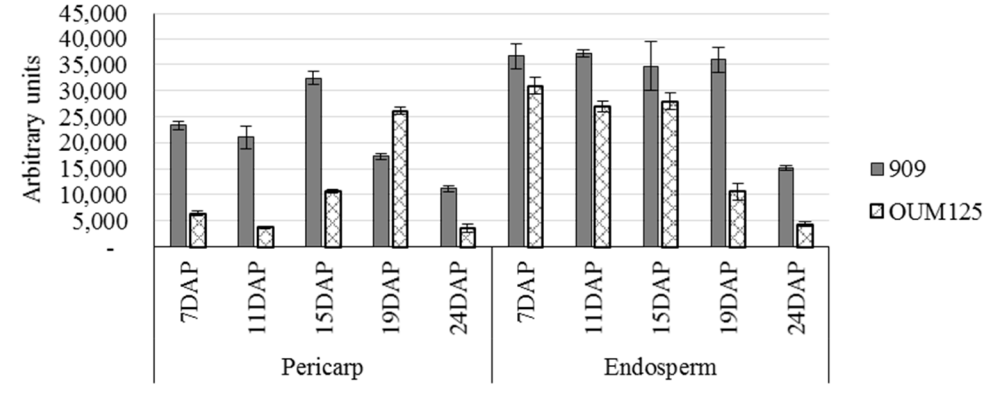
Iso 1
Arbitrary units
45,000
40,000
35,000
30,000
25,000
20,000
15,000
10,000
5,000
-
7DAP
11DAP
15DAP
19DAP
24DAP
Pericarp
Endosperm
909
OUM125

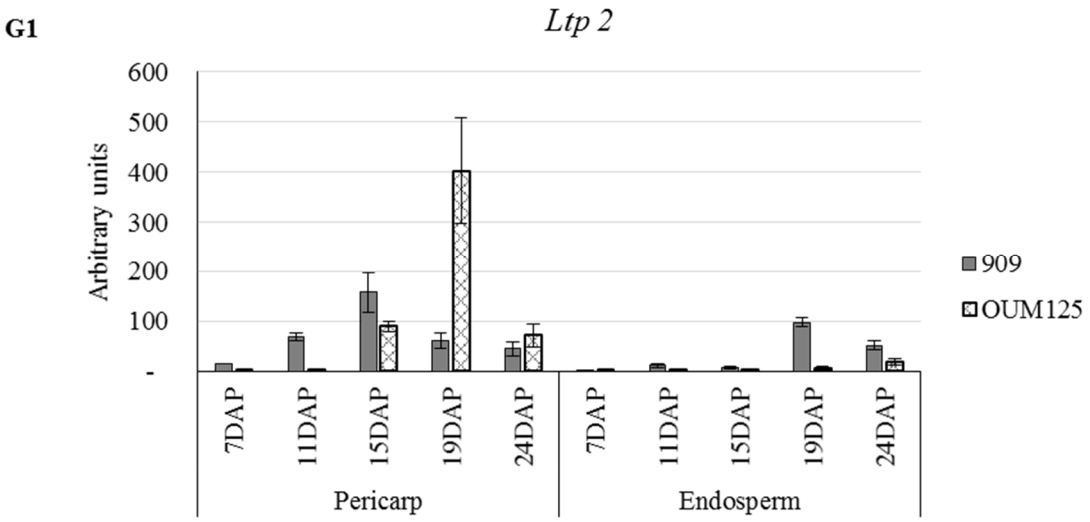

Supplementary figure 8: The expression levels of genes in the pericarp and endosperm of developing barley grain measured by real-time QPCR from 7 to 24 DAP for both 909 and OUM125.

References

Aastrup S (1983) Selection and characterization of low β-glucan mutants from barley. Carlsberg Research Communications **48:** 307-316

Åman P, Hesselman K, Tilly A-C (1985) The variation in chemical composition of Swedish barleys. Journal of Cereal Science **3:** 73-77

Anders N, Wilkinson MD, Lovegrove A, Freeman J, Tryfona T, Pellny TK, Weimar T, Mortimer JC, Stott K, Baker JM (2012) Glycosyl transferases in family 61 mediate arabinofuranosyl transfer onto xylan in grasses. Proceedings of the National Academy of Sciences **109:** 989-993

Anderson CT, Carroll A, Akhmetova L, Somerville C (2010) Real-time imaging of cellulose reorientation during cell wall expansion in Arabidopsis roots. Plant Phys **152**

Annison G (1993) The role of wheat non-starch polysaccharides in broiler nutrition. Crop and Pasture Science **44:** 405-422

Bacic A, Stone B (1981a) Isolation and ultrastructure of aleurone cell walls from wheat and barley. Functional Plant Biology **8:** 453-474

Bacic A, Stone B (1981b) Chemistry and Organization of Aleurone Cell Wall Components From Wheat and Barley. Functional Plant Biology **8:** 475-495

Behall KM, Scholfield DJ, Hallfrisch JG, Liljeberg-Elmstahl HG (2006) Consumption of both resistant starch and beta-glucan improves postprandial plasma glucose and insulin in women. Diabetes Care **29:** 976-981

Blake AW, McCartney L, Flint JE, Bolam DN, Boraston AB, Gilbert HJ, Knox JP (2006) Understanding the biological rationale for the diversity of cellulose-directed carbohydrate-binding modules in prokaryotic enzymes. Journal of Biological Chemistry **281:** 29321-29329

Buckeridge MS, Pessoa dos Santos H, Tiné MAS (2000) Mobilisation of storage cell wall polysaccharides in seeds. Plant Physiology and Biochemistry **38:** 141-156

Burton RA, Collins HM, Kibble NA, Smith JA, Shirley NJ, Jobling SA, Henderson M, Singh RR, Pettolino F, Wilson SM, Bird AR, Topping DL, Bacic A, Fincher GB (2011) Over-expression of specific HvCslF cellulose synthase-like genes in transgenic barley increases the levels of cell wall (1,3;1,4)-beta-d-glucans and alters their fine structure. Plant Biotechnol J **9:** 117-135

Burton RA, Fincher GB (2012) Current challenges in cell wall biology in the cereals and grasses. Front Plant Sci **3:** 130

Burton RA, Fincher GB (2014) Evolution and development of cell walls in cereal grains.

Burton RA, Gidley MJ, Fincher GB (2010) Heterogeneity in the chemistry, structure and function of plant cell walls. Nat Chem Biol **6:** 724-732

Burton RA, Jobling SA, Harvey AJ, Shirley NJ, Mather DE, Bacic A, Fincher GB (2008) The genetics and transcriptional profiles of the cellulose synthase-like HvCslF gene family in barley. Plant Physiology **146:** 1821-1833

Burton RA, Shirley NJ, King BJ, Harvey AJ, Fincher GB (2004) The *CesA* gene family of barley. Quantitative analysis of transcripts reveals two groups of co-expressed genes. Plant Physiology **134:** 224-236

Caimi PG, McCole LM, Klein TM, Kerr PS (1996) Fructan accumulation and sucrose metabolism in transgenic maize endosperm expressing a Bacillus amyloliquefaciens SacB gene. Plant Physiol **110:** 355-363

Cakir B, Tuncel A, Hwang S-K, Okita TW (2015) Increase of grain yields by manipulating starch biosynthesis. *In* Starch. Springer, pp 371-395

Carrard G, Koivula A, Söderlund H, Béguin P (2000) Cellulose-binding domains promote hydrolysis of different sites on crystalline cellulose. Proceedings of the National Academy of Sciences **97:** 10342-10347

Cavallero A, Empilli S, Brighenti F, Stanca AM (2002) High (1→3,1→4)-β-glucan barley fractions in bread making and their effects on human glycemic response. Journal of Cereal Science **36:** 59-66

Chowdhury J, Henderson M, Schweizer P, Burton RA, Fincher GB, Little A (2014) Differential accumulation of callose, arabinoxylan and cellulose in nonpenetrated versus penetrated papillae on leaves of barley infected with Blumeria graminis f. sp. hordei. New Phytologist **204:** 650-660

Cimini S, Locato V, Vergauwen R, Paradiso A, Cecchini C, Vandenpoel L, Verspreet J, Courtin CM, D'Egidio MG, Van den Ende W (2015) Fructan biosynthesis and degradation as part of plant metabolism controlling sugar fluxes during durum wheat kernel maturation. Front Plant Sci **6:** 89

Clarke B, Liang R, Morell M, Bird A, Jenkins C, Li Z (2008) Gene expression in a starch synthase IIa mutant of barley: changes in the level of gene transcription and grain composition. Functional & integrative genomics **8:** 211-221

Comino P, Shelat K, Collins H, Lahnstein J, Gidley MJ (2013) Separation and purification of soluble polymers and cell wall fractions from wheat, rye and hull less barley endosperm flours for structure-nutrition studies. Journal of agricultural and food chemistry **61:** 12111-12122

De Deckere E, Kloots WJ, Van Amelsvoort J (1993) Resistant starch decreases serum total cholesterol and triacylglycerol concentrations in rats. J Nutr **123:** 2142

Delaney B, Nicolosi RJ, Wilson TA, Carlson T, Frazer S, Zheng G-H, Hess R, Ostergren K, Haworth J, Knutson N (2003) β-Glucan fractions from barley and oats are similarly antiatherogenic in hypercholesterolemic syrian golden hamsters. J Nutr **133:** 468-475

Dervilly G, Leclercq C, Zimmermann D, Roue C, Thibault JF, Saulnier L (2002) Isolation and characterization of high molar mass water-soluble arabinoxylans from barley and barley malt. Carbohydrate Polymers **47:** 143-149

Dhugga KS, Barreiro R, Whitten B, Stecca K, Hazebroek J, Randhawa GS, Dolan M, Kinney AJ, Tomes D, Nichols S (2004) Guar seed ß-mannan synthase is a member of the cellulose synthase super gene family. Science **303:** 363-366

Dirk LMA, van der Krol AR, Vreugdenhil D, Hilhors HWM, Bewley JD (1999) Galactomannan, soluble sugar and starch mobilization following germination of Trigonella foenum-graecum seeds. Plant Physiology and Biochemistry **37:** 41-50

Doblin MS, Pettolino FA, Wilson SM, Campbell R, Burton RA, Fincher GB, Newbigin E, Bacic A (2009) A barley cellulose synthase-like CSLH gene mediates (1,3;1,4)-beta-D-glucan synthesis in transgenic Arabidopsis. Proc Natl Acad Sci U S A **106:** 5996-6001

Fincher GB (1975) Morphology and chemical composition of barley endosperm cell walls Journal of the Institute of Brewing **81:** 116-122

Glithero NJ, Wilson P, Ramsden SJ (2013) Straw use and availability for second generation biofuels in England. Biomass and Bioenergy **55:** 311-321

Greenwood C, Thomson J (1959) A comparison of the starches from barley and malted barley. Journal of the Institute of Brewing **65:** 346-353

Griffiths JS, Tsai AY-L, Xue H, Voiniciuc C, Šola K, Seifert GJ, Mansfield SD, Haughn GW (2014) SALT-OVERLY SENSITIVE5 mediates Arabidopsis seed coat mucilage adherence and organization through pectins. Plant Physiol **165:** 991-1004

Hallfrisch J, Scholfield DJ, Behall KM (2003) Physiological responses of men and women to barley and oat extracts (Nu-trimX). II. Comparison of glucose and insulin responses. Cereal Chemistry Journal **80:** 80-83

Han N, Na C, Chai Y, Chen J, Zhang Z, Bai B, Bian H, Zhang Y, Zhu M (2017) Over-expression of (1, 3; 1, 4)-β-D-glucanase isoenzyme EII gene results in decreased (1, 3; 1, 4)-β-D-glucan content and increased starch level in barley grains. Journal of the Science of Food and Agriculture **97:** 122-127

Higgins JA (2014) Resistant starch and energy balance: impact on weight loss and maintenance. Crit Rev Food Sci Nutr **54:** 1158-1166

Holtekjølen A, Uhlen A, Bråthen E, Sahlstrøm S, Knutsen S (2006) Contents of starch and non-starch polysaccharides in barley varieties of different origin. Food Chemistry **94:** 348-358

Hyeon JE, You SK, Kang DH, Ryu S-H, Kim M, Lee S-S, Han SO (2014) Enzymatic degradation of lignocellulosic biomass by continuous process using laccase and cellulases with the aid of scaffoldin for ethanol production. Process Biochemistry **49:** 1266-1273

Izydorczyk MS, Jacobs M, Dexter JE (2003) Distribution and structural variation of nonstarch polysaccharides in milling fractions of hull-less barley with variable amylose Content. Cereal Chemistry Journal **80:** 645-653

Jacobs AK, Lipka V, Burton RA, Panstruga R, Strizhov N, Schulze-Lefert P, Fincher GB (2003) An Arabidopsis callose synthase, GSL5, is required for wound and papillary callose formation. The Plant Cell **15:** 2503-2513

Jeon J-S, Ryoo N, Hahn T-R, Walia H, Nakamura Y (2010) Starch biosynthesis in cereal endosperm. Plant Physiology and Biochemistry **48:** 383-392

Koehler P, Wieser H (2013) Chemistry of cereal grains. *In* Handbook on sourdough biotechnology. Springer, pp 11-45

Konishi T (1979) Effects of induced dwarf genes on agronomic characters in barley. *In* Gamma field symposia,

Li B, Liu H, Zhang Y, Kang T, Zhang L, Tong J, Xiao L, Zhang H (2013) Constitutive expression of cell wall invertase genes increases grain yield and starch content in maize. Plant Biotechnol J **11:** 1080-1091

Li N, Zhang S, Zhao Y, Li B, Zhang J (2011) Over-expression of AGPase genes enhances seed weight and starch content in transgenic maize. Planta **233:** 241-250

Liepman AH, Wilkerson CG, Keegstra K (2005) Expression of cellulose synthase-like (Csl) genes in insect cells reveals that CslA family members encode mannan synthases. Proc Natl Acad Sci U S A **102:** 2221-2226

MacLeod AM, Napier J (1959) Cellulose distribution in barley. Journal of the Institute of Brewing **65:** 188-196

McCartney L, Marcus SE, Knox JP (2005) Monoclonal antibodies to plant cell wall xylans and arabinoxylans. Journal of Histochemistry & Cytochemistry **53:** 543-546

McCleary B, Solah V, Gibson T (1994) Quantitative measurement of total starch in cereal flours and products. Journal of Cereal Science **20:** 51-58

McCleary BV, Codd R (1991) Measurement of (1 → 3),(1 → 4)-β-D-glucan in barley and oats: A streamlined enzymic procedure. Journal of the Science of Food and Agriculture **55:** 303-312

Meikle PJ, Hoogenraad NJ, Bonig I, Clarke AE, Stone BA (1994) A (1→ 3, 1→ 4)-β-glucan-specific monoclonal antibody and its use in the quantitation and immunocytochemical location of (1→ 3, 1→ 4)-β-glucans. The Plant Journal **5:** 1-9

Munck L, Møller B, Jacobsen S, Søndergaard I (2004) Near infrared spectra indicate specific mutant endosperm genes and reveal a new mechanism for substituting starch with (1→ 3, 1→ 4)-β-glucan in barley. Journal of Cereal Science **40:** 213-222

Mutwali NIA, Mustafa AI, Gorafi YSA, Mohamed Ahmed IA (2016) Effect of environment and genotypes on the physicochemical quality of the grains of newly developed wheat inbred lines. Food Science & Nutrition **4:** 508-520

Nemeth C, Andersson AA, Andersson R, Mangelsen E, Sun C, Åman P (2014) Relationship of grain fructan content to degree of polymerisation in different barleys. Food and Nutrition Sciences **5:** 581

Nishimura MT, Stein M, Hou B-H, Vogel JP, Edwards H, Somerville SC (2003) Loss of a callose synthase results in salicylic acid-dependent disease resistance. Science **301:** 969-972

Palmiano EP, Juliano BO (1972) Biochemical Changes in the Rice Grain during Germination. Plant Physiol **49:** 751-756

Perata P, Guglielminetti L, Alpi A (1997) Mobilization of Endosperm Reserves in Cereal Seeds under Anoxia. Annals of botany **79:** 49-56

Pettolino FA, Hoogenraad NJ, Ferguson C, Bacic A, Johnson E, Stone BA (2001) A (1? 4)-ß-mannan-specific monoclonal antibody and its use in the immunocytochemical location of galactomannans. Planta **214:** 235-242

Raben A, Tagliabue A, Christensen NJ, Madsen J, Holst JJ, Astrup A (1994) Resistant starch: the effect on postprandial glycemia, hormonal response, and satiety. The American Journal of Clinical Nutrition **60:** 544-551

Rennie EA, Scheller HV (2014) Xylan biosynthesis. Current Opinion in Biotechnology **26:** 100-107

Rinne P, van der Schoot C (1998) Symplasmic fields in the tunica of the shoot apical meristem coordinate morphogenetic events. Development **125:** 1477-1485

Robertson MD (2012) Dietary-resistant starch and glucose metabolism. Current Opinion in Clinical Nutrition & Metabolic Care **15:** 362-367

Ruan Y-L (2014) Sucrose metabolism: gateway to diverse carbon use and sugar signaling. Annual review of plant biology **65:** 33-67

Sadosky P, Schwarz PB, Horsley RD (2002) Effect of arabinoxylans, β-glucans, and dextrins on the viscosity and membrane filterability of a beer model solution. Journal of the American Society of Brewing Chemists **60:** 153-162

Schon MA, Nodine M (2017) Widespread contamination of Arabidopsis embryo and endosperm transcriptome datasets. The Plant Cell**:** tpc. 00845.02016

Seefeldt HF, Blennow A, Jespersen BM, Wollenweber B, Engelsen SB (2009) Accumulation of mixed linkage (1→ 3)(1→ 4)-β-d-glucan during grain filling in barley: A vibrational spectroscopy study. Journal of Cereal Science **49:** 24-31

Slakeski N, Fincher GB (1992) Developmental regulation of (1→ 3, 1→ 4)-β-glucanase gene expression in barley tissue-specific expression of individual isoenzymes. Plant Physiol 99: 1226-1231

Smith KN, Queenan KM, Thomas W, Fulcher RG, Slavin JL (2008) Physiological effects of concentrated barley β-glucan in mildly hypercholesterolemic adults. Journal of the American College of Nutrition **27:** 434-440

Sparla F, Falini G, Botticella E, Pirone C, Talamè V, Bovina R, Salvi S, Tuberosa R, Sestili F, Trost P (2014) New starch phenotypes produced by TILLING in barley. PLoS ONE **9:** e107779

Speers RA, Jin YL, Paulson AT, Stewart RJ (2003) Effects of β-Glucan, Shearing and Environmental Factors on the Turbidity of Wort and Beer. Journal of the Institute of Brewing **109:** 236-244

Streb S, Zeeman SC (2012) Starch metabolism in Arabidopsis. The Arabidopsis Book **10:** e0160

Taketa S, Yuo T, Tonooka T, Tsumuraya Y, Inagaki Y, Haruyama N, Larroque O, Jobling SA (2012) Functional characterization of barley betaglucanless mutants demonstrates a unique role for CslF6 in (1, 3; 1, 4)-β-D-glucan biosynthesis. J Exp Bot **63:** 381-392

Thiele K, Wanner G, Kindzierski V, Jürgens G, Mayer U, Pachl F, Assaad FF (2009) The timely deposition of callose is essential for cytokinesis in Arabidopsis. The Plant Journal **58:** 13-26

Thomas J, Ingerfeld M, Nair H, Chauhan SS, Collings DA (2013) Pontamine fast scarlet 4B: a new fluorescent dye for visualising cell wall organisation in radiata pine tracheids. Wood Science and Technology **47:** 59-75

Tonooka T, Aoki E, Yoshioka T, Taketa S (2009) A novel mutant gene for (1-3, 1-4)-β-D-glucanless grain on barley (Hordeum vulgare L.) chromosome 7H. Breeding Science **59:** 47-54

Triboï E, Martre P, Triboï-Blondel AM (2003) Environmentally-induced changes in protein composition in developing grains of wheat are related to changes in total protein content. J Exp Bot **54:** 1731-1742

Van Der Meer IM, Ebskamp MJ, Visser RG, Weisbeek PJ, Smeekens SC (1994) Fructan as a new carbohydrate sink in transgenic potato plants. The Plant Cell **6:** 561-570

Vega-Sanchez ME, Verhertbruggen Y, Christensen U, Chen X, Sharma V, Varanasi P, Jobling SA, Talbot M, White RG, Joo M, Singh S, Auer M, Scheller HV, Ronald

PC (2012) Loss of Cellulose synthase-like F6 function affects mixed-linkage glucan deposition, cell wall mechanical properties, and defense responses in vegetative tissues of rice. Plant Physiol **159:** 56-69

Verspreet J, Cimini S, Vergauwen R, Dornez E, Locato V, Le Roy K, De Gara L, Van den Ende W, Delcour JA, Courtin CM (2013b) Fructan metabolism in developing wheat (Triticum aestivum L.) kernels. Plant Cell Physiol **54:** 2047-2057

Voiniciuc C, Schmidt MH-W, Berger A, Yang B, Ebert B, Scheller HV, North HM, Usadel B, Günl M (2015) MUCI10 produces galactoglucomannan that maintains pectin and cellulose architecture in Arabidopsis seed mucilage. Plant Physiol**:** pp. 00851.02015

Wang E, Wang J, Zhu X, Hao W, Wang L, Li Q, Zhang L, He W, Lu B, Lin H, Ma H, Zhang G, He Z (2008) Control of rice grain-filling and yield by a gene with a potential signature of domestication. Nat Genet **40:** 1370-1374

Weichert N, Saalbach I, Weichert H, Kohl S, Erban A, Kopka J, Hause B, Varshney A, Sreenivasulu N, Strickert M, Kumlehn J, Weschke W, Weber H (2010) Increasing Sucrose Uptake Capacity of Wheat Grains Stimulates Storage Protein Synthesis. Plant Physiol **152:** 698-710

Weschke W, Panitz R, Sauer N, Wang Q, Neubohn B, Weber H, Wobus U (2000) Sucrose transport into barley seeds: molecular characterization of two transporters and implications for seed development and starch accumulation. The Plant Journal **21:** 455-467

Wilson SM, Burton RA, Collins HM, Doblin MS, Pettolino FA, Shirley N, Fincher GB, Bacic A (2012) Pattern of deposition of cell wall polysaccharides and transcript abundance of related cell wall synthesis genes during differentiation in barley endosperm. Plant Physiol **159:** 655-670

Wilson SM, Burton RA, Doblin MS, Stone BA, Newbigin EJ, Fincher GB, Bacic A (2006) Temporal and spatial appearance of wall polysaccharides during cellularization of barley (Hordeum vulgare) endosperm. Planta **224:** 655

Yan D, Duermeyer L, Leoveanu C, Nambara E (2014) The functions of the endosperm during seed germination. Plant and Cell Physiology**:** pcu089

Zhang X-q, Xue D-w, Wu F-b, Zhang G-p (2013) Genotypic and environmental variations of arabinoxylan content and endoxylanase activity in barley grains. Journal of Integrative Agriculture **12:** 1489-1494

Chapter 5

Mass Spectrometry Imaging of Metabolites in Barley Grain Tissues

Statement of Authorship

Title of Paper	Mass Spectrometry Imaging of Metabolites in Barley Grain Tissues
Publication Status	☑ Published ☐ Accepted for Publication ☐ Submitted for Publication ☐ Unpublished and Unsubmitted w ork w ritten in manuscript style
Publication Details	Manuela Peukert, Wai Li Lim, Udo Seiffert and Andrea Matros

Principal Author

Name of Principal Author	Manuela Peukert		
Contribution to the Paper	Performed 90% of the experiments presented in this manuscript. Participated in drafting and revision of the manuscript.		
Overall percentage (%)	90		
Certification:	This paper reports on original research I conducted and is not subject to any obligations or contractual agreements with a third party that would constrain its inclusion in this thesis. I am the primary author of this paper.		
Signature		Date	27/06/2017

Co-Author Contributions

By signing the Statement of Authorship, each author certifies that:

iv. the candidate's stated contribution to the publication is accurate (as detailed above);

v. permission is granted for the candidate in include the publication in the thesis; and

vi. the sum of all co-author contributions is equal to 100% less the candidate's stated contribution.

Name of Co-Author (Candidate)	Wai Li Lim		
Contribution to the Paper	Contributed 5% of the experiments: Performed MALDI-MS measurement on different barley tissues using GNP and DHB matrix. Read, revised and approved the manuscript.		
Signature		Date	27 July 2017

Name of Co-Author	Udo Seiffert		
Contribution to the Paper	Contributed 5% of the experiments presented in this manuscript: Realized statistics and performed data visualization. Participated in drafting and revision of the manuscript.		
Signature		Date	26 JUNE 2017

Name of Co-Author	Andrea Matros		
Contribution to the Paper	Conceived project and designed experiments. Prepared the manuscript.		
Signature		Date	26.06.2017

Descriptions of Candidate's Contribution to This Project

Introduction

In plant biology, molecular compound analyses are frequently performed on extracts of whole plants or organs, such as roots, leaves or seeds, which results in loss of spatial information of intact molecules. However, this problem has now been resolved using a matrix-assisted laser desorption/ionisation mass spectrometry imaging (MALDI-MSI) technique. MALDI-MSI is widely used in medical and pharmaceutical research for diagnosis of tumours and cancers (Boyon et al.; Aikawa et al., 2016; Everest-Dass et al., 2016; Zhang et al., 2016). MALDI-MSI is highly sensitive, label-free and able to analyse a wide range of biological molecules such as peptides, lipids and other metabolites within the same tissue at a high spatial resolution based on their molecular mass.

MALDI-MSI has recently been applied to the study of a wide range of biomolecules in various plant samples and has successfully provided insights into native biochemical networks. These examples include cell wall polysaccharides such as (1,3;1,4)-β-glucan and arabinoxylan (Veličković et al., 2014), cuticular wax compounds (Cha et al., 2009), oligofructans (Peukert et al., 2014; Peukert et al., 2016), metabolic compounds (Jun et al., 2010; Brentan Silva et al., 2017), agrochemical compounds (Mullen et al., 2005) and endogenous peptides (Gemperline et al., 2016). The principle of MALDI-MSI is well established (Grassl et al., 2011; Kaspar et al., 2011; Peukert et al., 2012; Matros and Mock, 2013; Veličković and Rogniaux, 2014). Briefly, plant materials are sectioned and mounted onto glass slides. Mounted sections are covered with a matrix which helps promote the ionisation of molecular species. The choice of matrix, however, may influence the ionisation capacities of different molecular species (Peukert et al., 2012; Peukert, 2013). The sample is then transferred to the ion source of the MALDI-MSI instrument. The sample region of interest is selected and then sequentially irradiated by a

scanning laser beam. Charged particles are transferred to the mass analyser and separated according to their mass-to-charge (m/z) ratio. The data set is displayed as a sum mass spectrum, showing the ion signals accumulated across the measurement region as a function of the mass-to-charge ratio. Spatial distribution of individual ion signals based on m/z signal intensities is revealed by selecting single ion m/z values (Peukert et al., 2016).

Direct visualisation of intact molecules from barley grain sections using matrix assisted laser desorption/ionization (MALDI) mass spectrometry imaging (MSI) was previously performed by Dr. Andrea Matros and Dr. Manuela Peukert from Leibniz Institute of Plant Genetics and Crop Plant Research (IPK), Germany. In collaboration with Dr. Andrea Matros, a protocol for the analysis of metabolite distributions in cryo-sections of developing barley grains using MALDI-MSI approach was developed and is described in the manuscript attached in this thesis (Thesis page 342). My contribution to this publication was to examine the ionisation efficiency of small sugars from barley grain extracts utilising either a 2,5-dihydroxybenzoic acid (DHB) or a gold nanoparticle (GNP) matrix. My results showed that hexose, disaccharide (degree of polymerization (DP) 2) and trisaccharide (DP3) molecules ionised better using the GNP matrix, whereas oligomers with DP4-7 ionised better with the DHB matrix. This protocol, including my own contribution, is published in Current Protocols in Plant Biology.

Materials and Methods

Plant materials

Barley (cv Torrens) plants were grown in a greenhouse under a 16 h photoperiod, at 20°C day and 14°C night temperatures. Developing grains were collected at 14 and 15 day after pollination (DAP), snap-frozen in liquid nitrogen and stored at -80°C until required.

Sample preparation for relative quantification of oligosaccharides using an internal standard ^{13}C-sucrose

Barley grain at 14 DAP and 15 DAP were harvested from 3 biologically independent barley lines. Barley tissues, such as pericarp, endosperm and embryo, from 3 grains of each biological line, were separated, pooled and ground in liquid nitrogen. Barley grain at 15 DAP were halved (cross-section) and the sap from the internal cavity was extracted using a microsyringe Cavity sap was heated at 90°C for 5 min to inactivate endogenous enzymes. Pericarp, endosperm and embryo tissues were weighed and extracted in 80% ethanol and Milli-Q water at a 1:40 ratio (weight per volume (w/v)). The first extraction in 80% ethanol was carried out at 85°C for 30 min followed by an extraction in Milli-Q water at 50°C for 30 min. The supernatants from both extractions (80% ethanol and Milli-Q) were collected and combined. An internal standard ^{13}C-sucrose was dissolved in water and methanol at a 1:1 ratio to produce a working concentration of 10 mmol/L. An aliquot of 10 mmol/L of ^{13}C-sucrose standard was then added to each sample to produce a final concentration of 5 mmol/L. Samples with added ^{13}C-sucrose standard were then applied to the stainless steel sample plate and allowed to dry before the addition of the matrix (either Gold nanoparticle (GNP) or 2,5-dihydroxybenzoic acid (DHB)) on the same spot at a 1:1 ratio. The oligosaccharide contents were analysed and compared using MALDI Time-of-Flight (TOF) mass spectrometry (ultrafleXtreme, Bruker Daltonics).

MALDI TOF MS measurement

MALDI TOF MS measurement followed Peukert, (2013) and Peukert et al., (2016). Briefly, the sample plate was introduced into the ionization source of the MALDI-TOF MS instrument (ultrafleXtreme MALDI TOF/TOF, Bruker Daltonics). Measurement was performed in positive ionisation mode with a mass range of *m/z* 80-1300. The instrument was equipped with a Smartbeam-II laser with a repetition rate of 1000 Hz and calibrated with defined mass signals derived from a polyethylene glycol (PEG) mixture (1:1 mixture of PEG200 and 600, diluted 1:300 in 30% v/v acetonitrile and 0.1% w/v TFA), and from the matrix background (DHB or GNP) prior to each imaging run. The monoisotopic masses were determined by the chemical composition of the respective calibrants. The measurement of the laser raster spots was carried out in random order to eliminate influences of measurement order. The measurements were obtained from flexControl v3.3 (Bruker Daltonics) software.

Results and Discussion

The performance of the MALDI matrix in MALDI-MS is highly dependent on its ability to absorb the wavelength of the laser used, solubility of the matrix with each individual analyte and the ability to transfer energy during the ionisation process. Different matrices are carefully selected for the analysis of different substances. For example, 2,5-dihydroxybenzoic acid (DHB) is generally used for peptide and protein analysis (Strupat et al., 1991), although the DHB matrix has also been used for the analysis of polymers and metabolites from plant tissues (Pastor and Wilkins, 1997; Peukert, 2013); 1,8-Bis-(dimethylamino)-naphthalene (DMAN) is prefered for organic compounds (Shroff and Svatoš, 2009) whilst 2,5-Dihydroxyacetophenone (DHAP) is used for the analysis of peptides, proteins and glycoproteins (Wenzel et al., 2006). Each matrix produces its own background spectrum due to matrix fragmentation and cluster formation (Fig. 1) (Peukert, 2013). Hence, it is important to select a suitable matrix in which the background spectrum does not interfere with the actual spectrum from the samples. For the analysis of sugars and metabolites from seed extracts, the DHB matrix was selected because it produces the least background signals between *m/z* 400-1300 in positive ionisation mode, compared to other tested matrices such as 2,5-Dihydroxyacetophenone (DAHP), gold nanoparticle (GNP) and sinapinic acid (SA) as described in Peukert (2013). However, in our study, the signal intensity from hexose monomers (*m/z* 203 $[M+Na]^+$) was not detected when the DHB matrix was used (Fig. 2A).

Failure of hexose monomers to ionise can be an issue for analysing small products released from enzymatic digestion prior to mass spectrometry measurement (Peukert et al., 2014). To overcome this, a gold nanoparticle (GNP) matrix was tested and compared with the DHB matrix. Despite the complicated background signals below *m/z* 400 as reported in Peukert (2013) and shown in Fig. 1, the peaks from hexose (*m/z* 203 $[M+Na]^+$), disaccharide (*m/z* 365 $[M+Na]^+$)

and trisaccharide (*m/z* 527 $[M+Na]^+$) do not overlap with the GNP background signals (Fig. 3). In contrast, small oligomeric sugars with DP4-7 seemed to ionise better with the DHB matrix compared to the GNP matrix (Fig. 2B). Our findings showed that the GNP matrix produces a highly reproducible signal for the ionisation of small sugar monomers including hexose (*m/z* 203 $[M+Na]^+$) and small sugar oligomers such as DP2 (*m/z* 365 $[M+Na]^+$) and DP3 (*m/z* 527 $[M+Na]^+$) relative to the DHB matrix. Therefore, our study strengthens previous studies supporting the use of a GNP matrix for the analysis of small molecules (Spencer et al., 2008; Wu et al., 2009; Goto-Inoue et al., 2013)

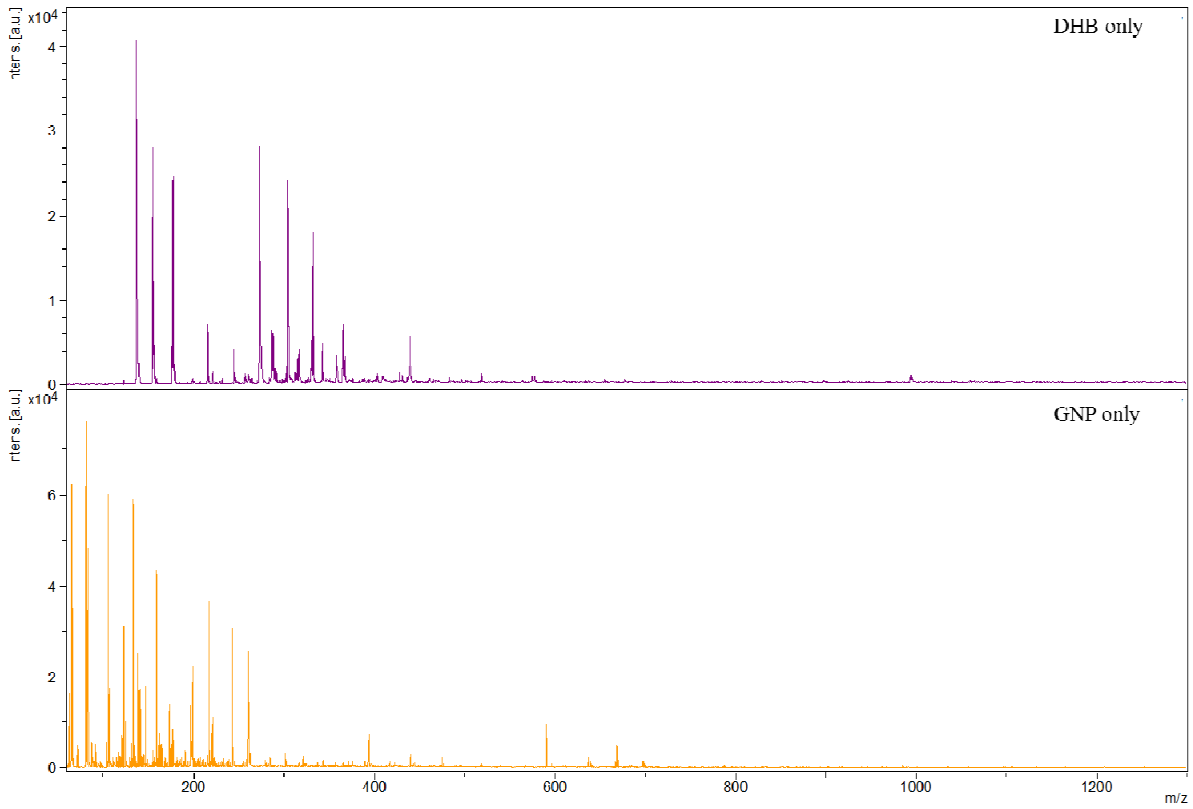

Figure 1: Background spectrum from DHB and GNP matrices. The DHB matrix produces intense background signals below *m/z* 400 and much reduced signal intensities beyond *m/z* 400. The GNP matrix produces intense background signals below *m/z* 300 and very low signal intensities beyond *m/z* 300.

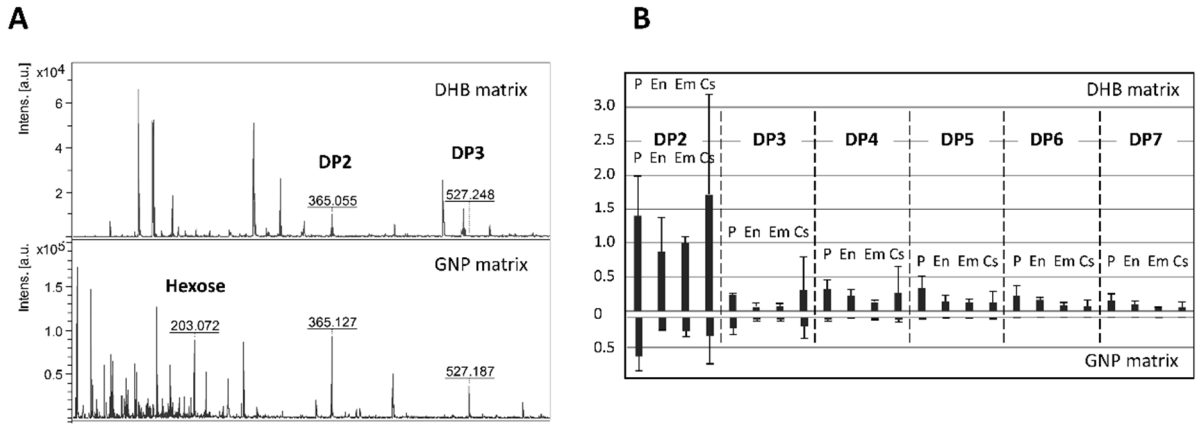

Figure 2: A: Embryos were manually separated from barley grains at 14 DAP. Extracts were analysed by MALDI-MS for their content of hexose and derived sugar oligomers. By using two different matrices, DHB and GNP, the molecular ion signals for the hexose and the hexose oligomers could be observed to vary in their intensity. For example, the DHB matrix is not suited to analyse the presence of the hexose monomer (*m/z* 203 $[M+Na]^+$). The GNP matrix showed best ionization capacity for sugar monomers, the dimer (*m/z* 365 $[M+Na]^+$), and the trisaccharide (*m/z* 527 $[M+Na]^+$). B: Barley grain tissues (P-pericarp, En-endosperm, Em-embryo, Cs-cavity sap) were manually separated (15 DAP) and extracts were analysed for their profiles of hexose and derived sugar oligomers with degrees of polymerization (DP) from two to seven by MALDI-MS utilizing DHB (top) and GNP (bottom) as a matrix. Tissue specific profiles could be distinguished for sugar oligomers of DP4 to DP7 with the DHB matrix, while those molecular ions were barely detectable using the GNP matrix. Relative intensity values were determined against an internal standard.

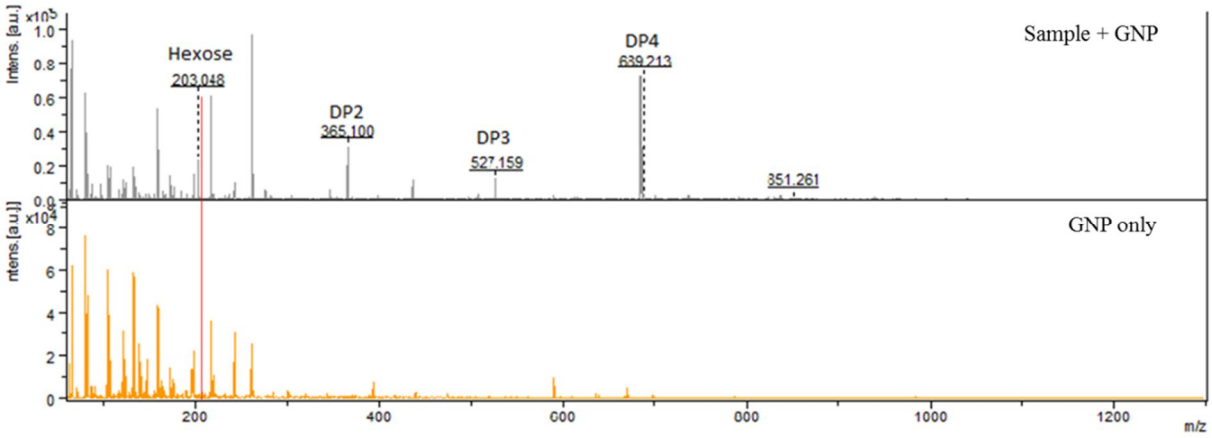

Figure 3: Matrix-derived signals from barley endosperm extract (ethanol and water extract). Red line indicates that the signal intensity from hexose (*m/z* 203 $[M+Na]^+$) does not overlap with background signals from the GNP matrix.

References

Aikawa H, Hayashi M, Ryu S, Yamashita M, Ohtsuka N, Nishidate M, Hamada A (2016) Abstract 350: Visualizing alectinib distribution in mice brain by using MALDI mass spectrometry imaging technique. Cancer Research **76:** 350

Boyon C, Longuespee R, Vinatier D, Fournier I, Salzet M, D'Ascq V MALDI imaging mass spectrometry in cancer

Brentan Silva D, Aschenbrenner A-K, Lopes NP, Spring O (2017) Direct analyses of secondary metabolites by mass spectrometry imaging (MSI) from Sunflower (Helianthus annuus L.) Trichomes. Molecules **22:** 774

Cha S, Song Z, Nikolau BJ, Yeung ES (2009) Direct profiling and imaging of epicuticular waxes on Arabidopsis thaliana by laser desorption/ionization mass spectrometry using silver colloid as a matrix. Analytical Chemistry **81:** 2991-3000

Everest-Dass AV, Briggs MT, Kaur G, Oehler MK, Hoffmann P, Packer NH (2016) N-glycan MALDI imaging mass spectrometry on formalin-fixed paraffin-embedded tissue enables the delineation of ovarian cancer tissues. Molecular & Cellular Proteomics **15:** 3003-3016

Gemperline E, Keller C, Jayaraman D, Maeda J, Sussman MR, Ané J-M, Li L (2016) Examination of endogenous peptides in Medicago truncatula using mass spectrometry imaging. Journal of proteome research **15:** 4403-4411

Goto-Inoue N, Hayasaka T, Setou M (2013) Application of gold nanoparticles for metabolite imaging Nanotechnology Research Journal **6:** 189

Grassl J, Taylor NL, Millar A (2011) Matrix-assisted laser desorption/ionisation mass spectrometry imaging and its development for plant protein imaging. Plant Methods **7:** 21

Jun JH, Song Z, Liu Z, Nikolau BJ, Yeung ES, Lee YJ (2010) High-spatial and high-mass resolution imaging of surface metabolites of Arabidopsis thaliana by laser desorption-ionization mass spectrometry using colloidal silver. Analytical Chemistry **82:** 3255-3265

Kaspar S, Peukert M, Svatos A, Matros A, Mock HP (2011) MALDI-imaging mass spectrometry–An emerging technique in plant biology. Proteomics **11:** 1840-1850

Matros A, Mock H-P (2013) Mass spectrometry based imaging techniques for spatially resolved analysis of molecules. Front Plant Sci **4**

Mullen AK, Clench MR, Crosland S, Sharples KR (2005) Determination of agrochemical compounds in soya plants by imaging matrix-assisted laser desorption/ionisation mass spectrometry. Rapid Communications in Mass Spectrometry **19:** 2507-2516

Pastor SJ, Wilkins CL (1997) Analysis of hydrocarbon polymers by matrix-assisted laser desorption / ionization-fourier transform mass spectrometry. Journal of the American Society for Mass Spectrometry **8:** 225-233

Peukert M (2013) Spatiotemporal distributions of metabolites involved in barley grain development with emphasis on endosperm formation. Halle (Saale), Universitäts-und Landesbibliothek Sachsen-Anhalt, Diss., 2013

Peukert M, Lim WL, Seiffert U, Matros A (2016) Mass spectrometry imaging of metabolites in barley grain tissues. *In* Current Protocols in Plant Biology. John Wiley & Sons, Inc.

Peukert M, Matros A, Lattanzio G, Kaspar S, Abadía J, Mock HP (2012) Spatially resolved analysis of small molecules by matrix-assisted laser desorption/ionization mass spectrometric imaging (MALDI-MSI). New Phytologist **193:** 806-815

Peukert M, Thiel J, Peshev D, Weschke W, Van den Ende W, Mock H-P, Matros A (2014) Spatio-temporal dynamics of fructan metabolism in developing barley grains. The Plant Cell **26:** 3728-3744

Shroff R, Svatoš A (2009) Proton sponge: A novel and versatile MALDI matrix for the analysis of metabolites using mass spectrometry. Analytical Chemistry **81:** 7954-7959

Spencer MT, Furutani H, Oldenburg SJ, Darlington TK, Prather KA (2008) Gold nanoparticles as a matrix for visible-wavelength single-particle matrix-assisted laser desorption/ionization mass spectrometry of small biomolecules. The Journal of Physical Chemistry C **112:** 4083-4090

Strupat K, Karas M, Hillenkamp F (1991) 2,5-Dihydroxybenzoic acid: a new matrix for laser desorption—ionization mass spectrometry. International Journal of Mass Spectrometry and Ion Processes **111:** 89-102

Veličković D, Rogniaux H (2014) In situ digestion of wheat cell-wall polysaccharides. Bio-protocol **4:** 1-13

Veličković D, Ropartz D, Guillon F, Saulnier L, Rogniaux H (2014) New insights into the structural and spatial variability of cell-wall polysaccharides during wheat grain development, as revealed through MALDI mass spectrometry imaging. J Exp Bot **65:** 2079-2091

Wenzel T, Sparbier K, Mieruch T, Kostrzewa M (2006) 2, 5-Dihydroxyacetophenone: a matrix for highly sensitive matrix-assisted laser desorption/ionization time-of-flight mass spectrometric analysis of proteins using manual and automated preparation techniques. Rapid Communications in Mass Spectrometry **20:** 785-789

Wu H-P, Yu C-J, Lin C-Y, Lin Y-H, Tseng W-L (2009) Gold nanoparticles as assisted matrices for the detection of biomolecules in a high-salt solution through laser desorption/ionization mass spectrometry. Journal of the American Society for Mass Spectrometry **20:** 875-882

Zhang C, Arentz G, Winderbaum L, Lokman N, Klingler-Hoffmann M, Mittal P, Carter C, Oehler M, Hoffmann P (2016) MALDI mass spectrometry imaging reveals

decreased CK5 levels in vulvar squamous cell carcinomas compared to the precursor lesion differentiated vulvar intraepithelial neoplasia. International Journal of Molecular Sciences **17:** 1088

Manuscript

Mass Spectrometry Imaging of Metabolites in Barley Grain Tissues

Manuela Peukert,[1] Wai Li Lim,[2] Udo Seiffert,[3] and Andrea Matros[4]

[1]Cluster of Excellence on Plant Sciences (CEPLAS), University of Cologne, Cologne, Germany
[2]Australian Research Council Centre of Excellence in Plant Cell Walls (ARC CoE), University of Adelaide, Urrbrae, Australia
[3]Biosystems Engineering, Fraunhofer Institute for Factory Operation and Automation IFF, Magdeburg, Germany
[4]Leibniz-Institute of Plant Genetics and Crop Plant Research (IPK), Applied Biochemistry Group, Gatersleben, Germany

Higher plants are composed of a multitude of tissues with particular functions, reflected by distinct profiles of transcripts, proteins, and metabolites. Although the rapid development of "omics" technologies has advanced plant science tremendously within recent years, analysis is frequently performed on whole organ or whole plant extracts, causing the loss of spatial information. Mass spectrometry–based imaging (MSI) approaches have become a powerful tool to decipher spatially resolved molecular information. Matrix-assisted laser desorption/ionization (MALDI) is the most widespread ionization method utilized for MSI and has recently been applied to plant science. A range of different plant organs and tissues has been successfully analyzed by MSI, and patterns of various classes of metabolites from primary and secondary metabolism have been obtained. This protocol describes a method for analysis of spatial metabolite distributions in cryosections of developing barley grains. Detailed procedures for sample preparation, mass spectrometry measurement, and data analysis are provided.

Keywords: barley grain • mass spectrometry imaging (MSI) • metabolite distribution • MALDI-MS imaging • on-tissue digestion

How to cite this article:
Peukert, M., Lim, W.L., Seiffert, U., and Matros, A. 2016. Mass spectrometry imaging of metabolites in barley grain tissues. *Curr. Protoc. Plant Biol.* 1:574-591.
doi: 10.1002/cppb.20037

INTRODUCTION

Matrix-assisted laser desorption/ionization (MALDI) mass spectrometry imaging (MSI) provides a means of resolving both the spatial distribution of many kinds of molecules (including metabolites and peptides) and their relative abundance from tissue sections. Generally, samples represent cryotome tissue sections that are fixed on a target plate and covered with a matrix compatible with the specific molecular species targeted for detection (typically proteins/peptides or metabolites). The target plate is then moved into the source of the MALDI-MS instrument, and mass spectra are generated by laser beam irradiation from an array of measurement points with defined spatial resolution in a defined sample area. Data can be displayed as an average spectrum. In addition, individual ion *m/z* values can be extracted and mapped back to the histological image, displaying their spatial distribution based on *m/z* signal intensities (single-ion intensity

Current Protocols in Plant Biology 1:574-591, December 2016
Published online December 2016 in Wiley Online Library (wileyonlinelibrary.com).
doi: 10.1002/cppb.20037

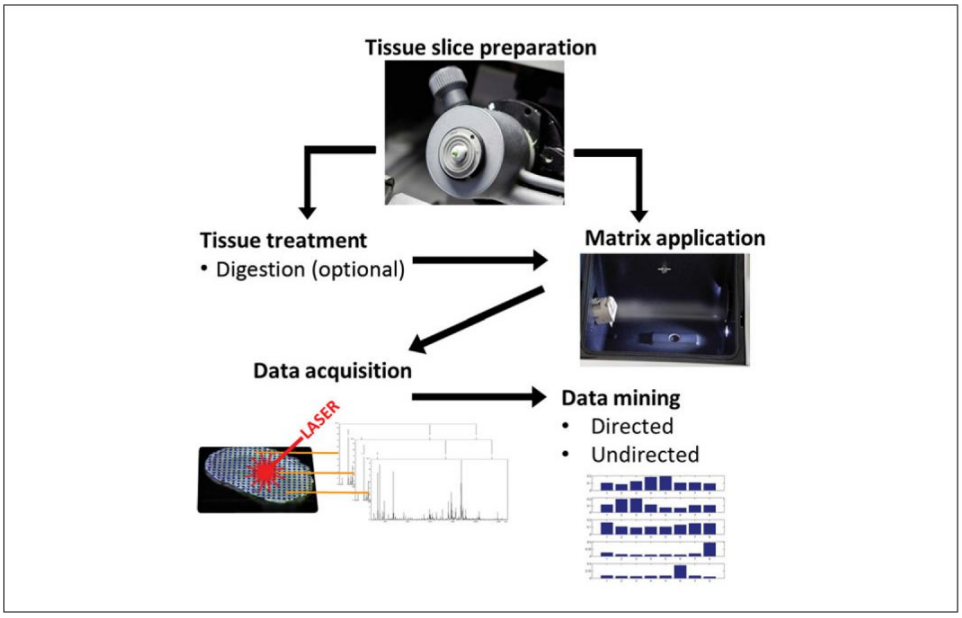

Figure 1 Workflow for MALDI-MS imaging (MSI) analysis of small molecules. The experiment starts with the preparation of tissue sections in a cryotome (Basic Protocol 1), after which an optional sample treatment (e.g., with a digestion reagent; see Support Protocol) can be performed. Next, a proper ionization matrix is applied on top of the sample (Basic Protocol 2). Spatially resolved mass spectrometry data are then acquired from the sample (Basic Protocol 3), and finally common distribution patterns of molecular signals are evaluated (Basic Protocol 4 or 5).

maps). Advanced data analysis strategies aim to evaluate groups of metabolites with similar distribution patterns across the region of measurement.

The following protocols describe MSI analysis of metabolite distributions in cryosections of developing barley grains. An overview of the described experimental steps is provided in Figure 1. The first protocol presents the steps needed to produce high-quality grain tissue sections using a cryotome (Basic Protocol 1). Next, the application of an ionization matrix is described (Basic Protocol 2), followed by the acquisition of MSI data (Basic Protocol 3). Finally, strategies for data analysis are described, particularly for resolving common distribution patterns of molecular signals in tissues of developing barley grains (Basic Protocols 4 and 5). Additionally, a Support Protocol is provided describing on-tissue digestion for annotation of specific molecular ions of interest.

CRYOSECTIONING OF DEVELOPING BARLEY GRAINS

BASIC PROTOCOL 1

Developing barley grains are composed of a multitude of tissue types (e.g., parenchymal, collenchymal, and vascular) whose three-dimensional structures need to be preserved as much as possible during sample preparation. At early developmental stages, grains contain a high proportion of water, making sample preparation fairly straightforward. In contrast, mature grains contain much less free water, requiring particular attention during sectioning. Standard histological procedures—e.g., slice preparation for immunostaining or dye staining—rely on embedding tissue in polymeric compounds such as synthetic resin (HM20) or the use of optimal cutting temperature (OCT) medium. However, embedding results in partial diffusion of metabolites, as well as suppression of ionization and interference of analytes during MSI measurements, and thus any contact of the tissue section with such polymeric compounds needs to be avoided. Instead, samples are simply fixed in the desired orientation with a small droplet of fixation medium on the cutting block of the cryotome. Sample fixation and cutting are described in this section.

Materials

Developing barley grains
Liquid nitrogen
Optimal cutting temperature (OCT) medium
White correction fluid (e.g., Wite-Out)

Cryotome, e.g., Leica CM3050 (Leica Microsystems)
Indium tin oxide (ITO)–coated glass slides (Bruker Daltonics)
Brush, forceps, razor blade
Desiccator and vacuum pump
Stereomicroscope (e.g., Leica MZ6) and digital camera (e.g., AxioCam ICc1, Zeiss) or similar microscopic image acquisition system

1. Harvest barley grains of various developmental stages, e.g., 3 to 24 days after pollination (DAP), from the middle part of the spike and immediately freeze in liquid nitrogen until further treatment.

   The plant material must be as fresh as possible. Long-term storage at −80°C causes freeze-drying of the material and hinders proper cutting by a conventional cryotome. Harvested grains can be stored up to 1.5 years. Sections should always be prepared fresh from the frozen grains prior to measurement.

2. Place a clean sectioning blade into the cryotome and adjust the cutting temperature to −20°C.

   If the non-embedded part of the sample is still flexible during the cutting process, lower temperatures should be used (i.e., down to −30°C). Conversely, higher temperatures (i.e., up to −10°C) can be tested for highly fragile samples.

3. Transfer the desired number of ITO-coated glass slides, a brush, forceps, and a razor blade into the cooled cryotome chamber.

4. Transfer a frozen grain sample into the cooled cryotome chamber and fix it onto the sample plate holder via a droplet of water (ice; for 3- to 7-DAP barley grains) or OCT medium (for 7- to 24-DAP barley grains).

   If necessary, precut the grain with a razor blade to a suitable length before fixation. Select a proper orientation for longitudinal or cross sections.

   OCT is a polymeric alcohol composed of polyvinyl alcohol and polyethylene glycol, and is widely used for embedding samples prior to cryosectioning (Turbett and Sellner, 1997).

5. Move the cutting block with the sample plate to start the sectioning process.

   Optimal section thickness for barley grains is 20 to 30 μm (Fig. 2; see Critical Parameters).

   To trim the tissue sample, a larger section thickness can be used until the desired morphological features are visible and then changed to the desired section thickness.

6. Transfer fine sections immediately onto precooled ITO-coated slides and fix the sections by touching the bottom of the slide, directly underneath the sample, with your fingertip for 20-30 sec.

   Touching the glass slide under the sample with a warm fingertip causes the ice in the section to melt and evaporate. This process is called thaw-mounting.

   More than one section can be placed per slide. The best section will be selected later for MSI measurement.

7. Place slides with sections in a desiccator, evacuate using a vacuum pump, and leave for 30 min until sections are completely dry.

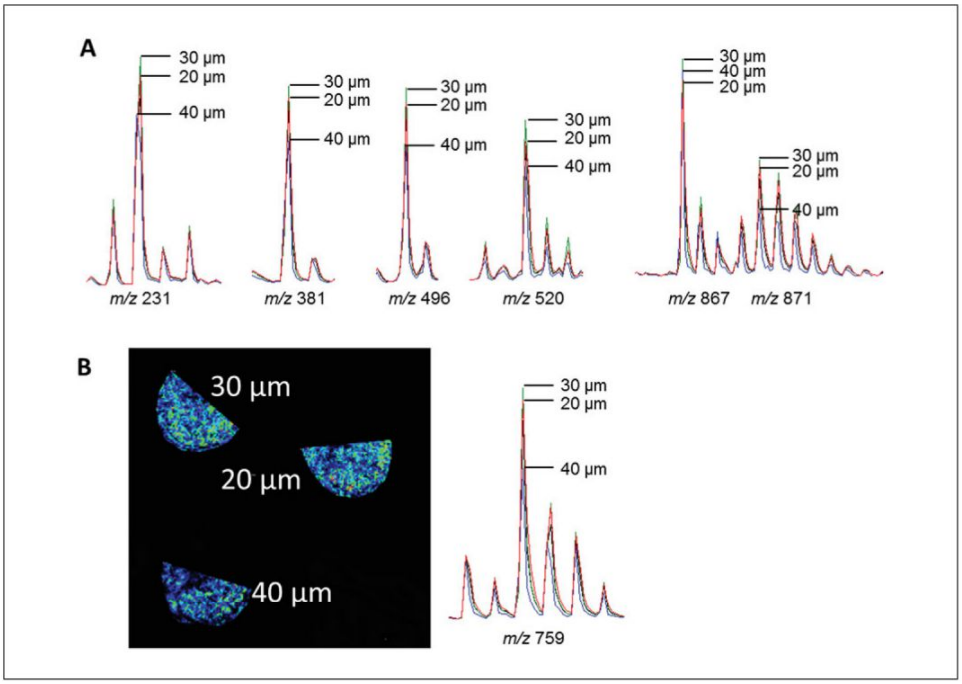

Figure 2 Effect of slice thickness on signal intensity. Sequential slices of different thicknesses were prepared from one barley grain and analyzed simultaneously by MALDI-MSI. Signal intensities of various molecular ions were then compared between sections. (**A**) Effect among different sample signals of various *m/z* values. (**B**) Single-ion intensity maps of the molecular ion *m/z* 759 from MSI measurements. In all cases, the 40-µm sections have reduced signal intensities compared to the 20- and 30-µm sections. Accordingly, 30 µm was chosen for all further sample preparations of developing barley grains.

The time needed for complete dryness varies, and is longest for samples with a high water content (young grains). For samples containing very little water, the drying step can be skipped.

8. Place at least three marks close to each sample using white correction fluid.

   This allows definition of sample position in the flexImaging software before the measurement is begun (see Basic Protocol 3). Fine edges are best.

9. Capture an optical image of the prepared slide using an appropriate image acquisition system, e.g., a slide scanner or stereomicroscope equipped with a digital camera.

   This image is used to designate the measurement region(s) (see Basic Protocol 3).

   For additional information on equipment, see Critical Parameters.

MATRIX APPLICATION AND SLIDE PREPARATION

BASIC PROTOCOL 2

MSI analyses are based on desorption and ionization of molecules from a sample surface mediated by a matrix compound and subsequent MS data recording. Depending on alterations in the ionizing capacity of different substrate groups to be analyzed, various matrix compounds have been proposed (Svatoš, 2010; van Hove et al., 2010; Kaspar et al., 2011). The proper choice of matrix depends on the molecules of interest. In small molecule applications, the matrix background often overlaps with sample signals (for additional information, see Critical Parameters). This protocol uses 2,5-dihydroxybenzoic acid (DHB), which is suitable for analysis of small primary metabolites such as sugars and lipids, as it generates less background in the mass range of the desired signals.

One of the most critical aspects of MSI is reproducible application of the matrix compound. The most widely used deposition techniques are spraying with a simple airbrush and vibration vaporization using a dedicated instrument. Spray application offers high spatial resolution (10-100 μm) compared to alternative approaches, such as microchip spotting (<20 μm) or sublimation (1 μm) (Kaletaş et al., 2009; Agar et al., 2010). This protocol describes the preparation of DHB matrix and its application by vibration vaporization using a Bruker Daltonics ImagePrep device. This instrument is able to apply a series of matrix layers with an incubation and drying period between deposition steps, as needed for multiple matrix layers and enzyme digestion on tissue sections.

Materials

Sample sections (see Basic Protocol 1 or Support Protocol)
2,5-Dihydroxybenzoic acid (DHB, Sigma-Aldrich)
Methanol, MS-grade
Water, MS-grade
Trifluoroacetic acid (TFA, >99%, Sigma-Aldrich)

Sonication bath
ImagePrep device (Bruker Daltonics)

1. Dilute DHB to 30 mg/ml in 50% (v/v) methanol containing 0.2% (v/v) TFA. Incubate at least 15 min in a sonication bath and check to be sure the DHB is dissolved completely.

   The matrix solution should always be freshly prepared. A preparation of 10 ml per experiment is sufficient.

   CAUTION: *TFA should be diluted in a properly ventilated chemical fume hood.*

2. Fill the matrix vial with pure methanol and set the global spray power adjustment for the instrument as described in the ImagePrep manual.

   ImagePrep spray plates can be used for several cycles of matrix deposition, but the metal mesh becomes porous after a number of cycles, resulting in larger droplets and a loss in achievable spatial resolution. Fine layers of matrix crystals can still be obtained, but this requires manual intervention during the spraying process. Thus, for best reproducibility, spray plates and the quality of the spray need to be checked.

3. Insert the slide with the dried sample into the ImagePrep instrument and adjust the slide position so that the light sensor is not covered by a section. Fill an appropriate amount of matrix solution (7–8 ml) into the reservoir of the spraying device.

4. Apply matrix solution via sensor-controlled vibration vaporization according to manufacturer's instructions.

   A number of spray protocols for particular matrices are provided by the manufacturer, and it is recommended that they be followed.

   The optical sensor of the ImagePrep monitors the wetness and thickness of the matrix by voltage differences of the sensor. As the spray power can decrease during an application run, an automatic spray power boost is implemented. If high-resolution images are desired, visual control of the spray application is helpful, as automatic spray power boost can result in less uniform spray coverage and a higher degree of wetness.

5. Use slide immediately or keep under dry conditions (e.g., in a desiccator) until further processing.

   Slides should be stored no more than 2-3 days prior to measurement.

6. Clean the spray head and spray chamber immediately with methanol after matrix application.

MALDI-MS MEASUREMENT OF SMALL MOLECULES

Generally, MSI approaches aim to achieve relative abundance profiles of molecules across a tissue surface or section. Technically, the MS instrument creates an array of mass spectra, where each spot represents its own *m/z* profile. Gradients of ion abundances are visualized across the sample by a two-dimensional reconstruction of the ion chromatograms afterwards. To achieve a high spatial assignment, while at the same time maintaining high molecular resolution and reproducibility, careful setting of instrument parameters is required. The following protocol steps provide a guide for setting up a MALDI-MSI run for small to medium plant tissue sections. They are described for a Bruker ultrafleXtreme device, but are generally applicable for Bruker MALDI-TOF instruments.

Materials

Sample sections with matrix deposited (see Basic Protocol 2)
Isopropanol

Low-lint cleaning wipes
ultrafleXtreme MALDI-TOF mass spectrometer (Bruker Daltonics)
FlexControl and flexImaging software (Bruker Daltonics)
MTP Slide-Adapter II (Bruker Daltonics)
Calibration solution: 1:1 mixture of polyethylene glycol (PEG) 200 and 600, diluted 1:300 in 30% (v/v) acetonitrile with 0.1 % (v/v) trifluoroacetic acid (TFA)

Prepare slide for measurement

1. Place a 1.5-µl droplet of calibration solution next to a sample on a slide.

   If more than one section will be measured within the same MSI run, the calibration solution should be placed in a region between the target samples, as resolution varies with the x-y position on the target.

2. Clean ~5 mm of the outer-left and outer-right surface of the matrix-coated slide with isopropanol using a low-lint cleaning wipe to enable a good fitting in the slide holder (adapter).

3. Fit the freshly prepared slide(s) into a Slide Adapter II MALDI target and introduce the adapter into the source of the MS instrument.

4. Select the required flexControl method. For MSI measurement of small molecules, select an *m/z* range of 80–1300 and a sample rate of 0.5 Gs/sec.

   These settings refer to 20,000–25,000 data points per spectrum. Make sure there is enough space on the hard disk.

5. Perform a mass calibration using the spot of calibration solution deposited on the slide.

   Calibration is performed using a text-editable list of calibration masses by means of the integrated calibration module of the flexControl software.

Perform MSI acquisition

6. Adjust the laser power and number of laser shots needed to gain a relative signal intensity of 25,000 by checking signal intensities from various regions of the target tissue section(s) or a section close to the target tissue section.

7. Open the flexImaging software and create a file for automated MSI measurements.

8. Select and load the optical image of the sample (see Basic Protocol 1, step 9).

9. Carefully, define the sample stage position based on the location marks (see Basic Protocol 1, step 8).

   This is needed to align the laser spot focus of the instrument (control the positioning after insertion of the slide holder into the source of the instrument). The laser shots should meet your desired position.

10. Designate the measurement region(s) and select a desired spatial resolution. For very small sections (e.g., from young seeds), use a 15-20 μm laser raster to ensure sufficient representation of the various tissues (see Critical Parameters). Mark an additional small measurement region (~25-35 laser raster points) with just matrix to use as a blank.

    In the experiments illustrated in this unit, 800 shots per raster spot were acquired with a laser beam width of 10 μm.

11. Choose an appropriate autoXecute method, which defines the number of laser shots and the flexControl method.

12. Perform MSI measurement. Acquire data from spots in random order to eliminate any influence of measurement order.

    This will result in approximately one-third longer acquisition times compared to FAST modus.

BASIC PROTOCOL 4

DIRECTED DATA ANALYSIS

The visualization of individual distribution patterns of molecular features is a key target in MSI data analysis that is achieved with the instrument vendor's software tools. These also allow for relative comparison and statistical analysis of molecular ion intensities between different regions of interest (ROIs) within a sample as well as between small numbers of samples. Methods are described here for flexImaging and ClinProTools software (Bruker Daltonics). First, using flexImaging, sum spectra can be generated and specific m/z signals can be selected for visualization. Next, calculation of average peak intensities from selected sample areas (ROIs) can be carried out using ClinProTools.

1. Open the flexImaging software and load the desired MSI experimental file.

2. Create sum spectra of the tissue measurement region and of the matrix blank region and visualize both in overlay mode.

   See Critical Parameters for additional discussion of matrix signals and blank regions.

3. For particular *m/z* values of interest, manually select single or multiple *m/z* signals from the sum spectrum for visualization of their distribution in the sample section.

   Examples for single-ion intensity maps representing particular molecular ion abundances in a barley grain section at 14 DAP are shown in Figure 3.

   If only particular signals are of interest, a mass filter list can be created and used as a default, but one should check that peak resolution and mass accuracy of the measurement fit the values set as default. By creating a mass filter list, diverse colors can be selected for the individual m/z values. Avoid selecting m/z values that overlay completely with signals derived from the matrix blank.

4. Use the "Region of interest" option to choose different parts of the measured sample for comparison of sum spectra according to these specific regions.

   For example, mark grain regions in the flexImaging software according to the histological properties of the sections, based on pictures taken prior to measurement (for example, see Fig. 5A).

5. Export the resulting sum spectra of the ROI's to ClinProTools.

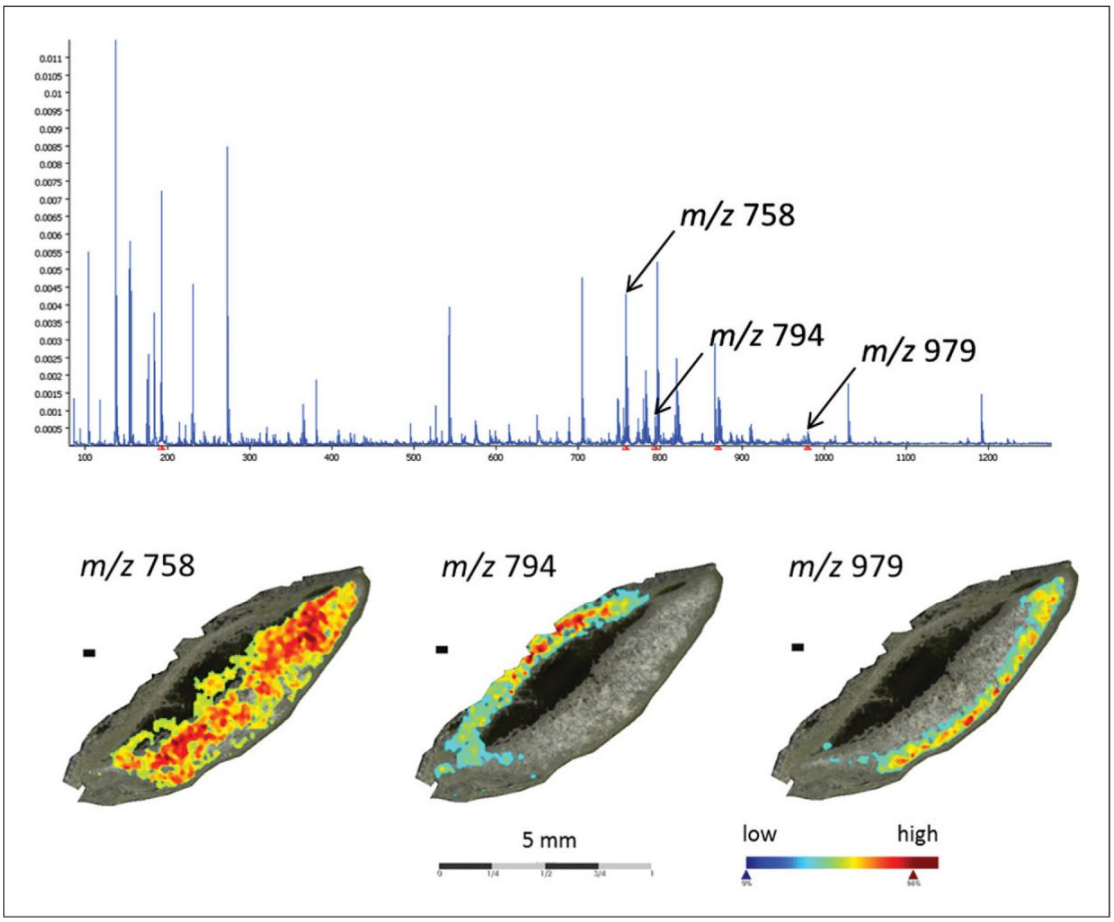

Figure 3 Tissue distribution of individual *m/z* values selected from the mean spectrum of a longitudinal section of a barley grain at 14 DAP. The mean spectrum can be used to select individual *m/z* values for analysis of their distribution over the sample surface. In targeted data analysis, a mass table containing signals of interest can be created for statistical analysis of their different distributions in particular sample regions (e.g., comparison of average signal intensities in labeled subregions of the sample slice).

Without data reduction, the number of exported single spectra for analysis by ClinProTools is limited to ~2000. Data reduction can be performed either by limiting the mass data frequency, resulting in loss of peak resolution, or by limiting the considered mass range.

6. In ClinProTools, select candidate peaks and determine the average intensities for each ROI.

Peak intensity lists can be prepared containing the data obtained by various independent experiments, and can be used further for multivariate statistical analysis, e.g., principle component analysis.

Because of different ionization capacities of molecules during the MALDI process (depending on applied matrix, matrix layer thickness, ionization mode, ionization suppression effects, and laser intensity, among others), the MALDI-MS technique is considered a semi-quantitative measurement. Thus, signal intensities of detected molecular ions can be compared relative to each other within a run, but not between different sample sets. To perform comparison between different sample sets/experiments, data normalization is needed, which has to be performed manually (see Basic Protocol 5, step 3a). Alternatively, the matrix background can be used as an internal standard, as long as it is always applied in the same concentration and with the same application method. We usually calculated the average signal intensity of five selected DHB background signals (m/z 137, 154, 177, 273, and 409) from the blank region measured simultaneously in all imaging runs. This

value was then set to 100% and signal intensities of particular ions were calculated as percentage relative to the mean DHB background.

BASIC PROTOCOL 5

UNDIRECTED DATA ANALYSIS

In contrast to directed data analysis, few robust biostatistical tools exist for evaluating extensive MSI data sets. This protocol presents two undirected data analysis approaches that have proved to be applicable for evaluating tissue-specific distribution patterns for groups of metabolites over a periodic study of barley grain development. The methods below are described for using either MATLAB (MathWorks) or SCiLS Lab (SCiLS) software.

The advantage of multivariate statistical tests is that prior knowledge of the sample structure is not entirely required. Furthermore, sufficient analysis of replicates in MSI experiments needs statistical tools that are capable of handling enormous amounts of data. These requirements are now fulfilled by the commercially available SCiLS Lab software. Alternatively, the MATLAB clustering approach can be conducted without expensive software utilizing standard numerical computing environments.

For cluster analysis using MATLAB

1a. Define relevant ROIs and export the resulting sum spectra to ClinProTools.

2a. Prepare peak intensity lists containing the data obtained for the particular experiments.

3a. To compare the distributions of molecular ions from independent experiments, normalize the total ion intensities of individual *m/z* values to relative signal intensities that display the contribution to the selected ROIs (e.g., to the sum of signal intensities of a particular *m/z* value over all ROIs = 1, which represents 100%).

In this way, the high dynamic range of the signals is excluded, displaying only the contribution of a selected molecular ion to a specific ROI.

These relative signal intensities can also be used to generate heat maps using Genesis software v1.7.6. (TU Graz).

4a. Perform cluster analysis.

In the example in Figure 4, the Neural Gas (NG) algorithm, implemented in MATLAB, was applied for cluster analysis. This algorithm was introduced by Martinetz and Schulten (1991) and is used to find common features (so called prototypes) in large data sets. It is a robust and initialization-tolerant alternative to the commonly utilized k-Means clustering, which often fails in cases of complex cluster formation. In an iterative learning process, all vectors of signal intensities (step 3a) are randomly presented to NG and compared to a set of prototypes. Within the course of the learning process, for each input sample (signal intensity vector), the best-matching prototype is determined and modified to represent the currently processed input sample even better. In this way, all prototypes converge towards one particular feature of the input samples. Hence, at the end of the learning process, the adapted prototypes represent the average pattern of all signal intensity patterns within one cluster.

The most critical parameter of NG is the number of prototypes, which equals the number of expected clusters that is typically a priori unknown. A rather straightforward solution is to systematically modify the number of prototypes within a realistic range (derived from the underlying biological application) and watch the decreasing distance between the best-matching prototype and the currently processed input vector along the learning process (learning progress). If the slope of this function drops towards a nearly constant value, convergence of the learning process has been reached. Each number of prototypes is associated with a particular constant convergence value. The optimal number of prototypes is the point where the aforementioned constant convergence value does not

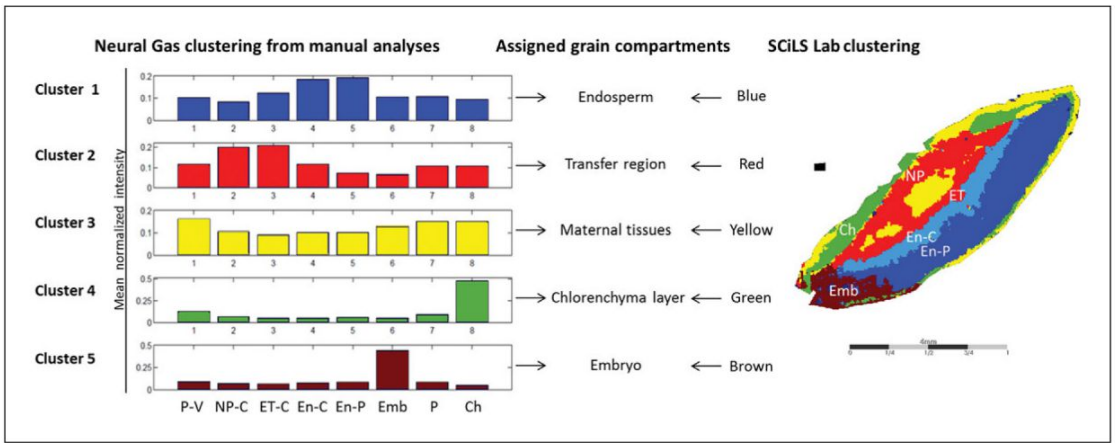

Figure 4 New tools for MALDI-MSI data mining allow time-saving multivariate statistical analysis. This example illustrates results obtained by manual data mining followed by Neural Gas clustering (left) and automated data mining using SCiLS Lab software (right). Left: Manual data analysis relies on careful observation of the sum of the mass spectra. Here, all sample peaks not interfering with the matrix background were selected from three replicates. Various regions in the tissue slices (related to particular seed tissues) were selected and the average peak intensities calculated. A Neural Gas cluster analysis was then performed to group signals showing similar intensity distributions across the samples. The generated prototypes representing the average abundance profile of the data within each cluster are shown. Right: In contrast, SCiLS Lab software allows automatic data normalization, peak picking, and peak alignment of replicates and of different sample types. Different statistical tools can then be applied to the samples. Here, the applied cluster analysis of the SCiLS Lab software resulted in a similar grouping of sample regions as gained by Neural Gas clustering from the same data set. The tissue regions characterized by common peak abundances are displayed as a color code mapped onto the measurement and analysis region. Abbreviations correspond to manually assigned tissue regions: P-V, pericarp-vascular tissues; NP-C, nucellar projection-cavity; ET-C, endospermal transfer cells-cavity; En-C, endosperm central; En-P, endosperm peripheral; Emb, embryo; P, pericarp; Ch, chlorenchyma layer.

decrease further with an increase of prototypes. In other words, the NG is saturated with prototypes. This number generally depends on the data structure of the underlying experiment. Typical values are in the range of 2 to ~10. Higher numbers often do not provide the desired level of granularity of the data representation by the obtained clusters.

Because NG is rather insensitive regarding the settings of learning parameters, all further parameters controlling its learning phase (e.g., initial learning rate and its decrease, initial neighborhood range and its decrease) can be kept at their defaults. For normalized data, the standard Euclidean metric as a similarity measure in NG is appropriate. Otherwise, a correlation-based metric can also be considered.

In Figure 4, the result from NG cluster analysis of MSI data sets for three individual experiments from barley grains at 14 DAP is shown. NG prototype patterns of five clusters were obtained. The grain parts that are accentuated in the respective clusters are indicated.

For cluster analysis using SCiLS Lab

1b. Load the flexImaging file directly into SCiLS Lab.

It is also possible to load several independent flexImaging files for simultaneous data processing and analysis.

2b. Perform simultaneous preprocessing of all data sets to ensure comparability between sample sets. In the preprocessing, include baseline subtraction, total ion count (TIC) normalization, and calculation of an overall mean spectrum.

3b. Perform an automated peak picking as implemented in the software (Alexandrov and Kobarg, 2011).

Generally, the peak picking process takes into account every 15th spectrum across the complete data set. For the analysis in Figure 4, the number of detected peaks was set to 400. This number can be further reduced by another peak alignment step, which we typically conduct on the local maxima within intervals of ±0.2 Da.

4b. To visualize individual or multiple *m/z* signal distributions across the sample/section as ion intensity maps, select individual or groups of *m/z* signals using the "Visualization" option of the software (Fig. 4).

Because MALDI-MSI data suffer from strong spectrum-to-spectrum variation, it may also be useful to apply spatial denoising prior to visualization of m/z images. The idea of spatial denoising is to average the intensities of a particular pixel and its adjacent neighbors. To avoid losing any details, edge-preserving spatial denoising (Alexandrov et al., 2010) is recommended.

5b. Subject the preprocessed and denoised data set to statistical analysis by bisectional k-means clustering and component analysis.

Here, the selection of an appropriate approach depends on the aims of the experiment. To dissect tissue regions that are preserved during the course of an experiment from those where complex changes occur according to their mass spectral appearance, bisectional k-means clustering has been found advantageous. On the other hand, to define groups of molecular signals with common abundance across the course of the experiment, a component analysis should be performed, in which a probabilistic latent semantic analysis (PLSA) is applied (Hanselmann et al., 2008). For PLSA, prior knowledge about the sample material is recommended to estimate the number of components that appropriately reflect the sample specificities.

The bisecting k-means divides a set of spectra into two sets that are maximally different. As metrics, the correlation distance and a minimal interval width of 0.4 Da can be used. For component analysis, a random initialization is usually chosen, and the number of components is set to six in our experiments. Generally, the number of components depends on the complexity of the sample, ranging from 2-4 for low-complexity samples up to 10 for samples with high structural diversity. The minimal interval width is also set to 0.4 Da.

SUPPORT PROTOCOL

STRUCTURAL ANALYSIS OF OLIGOMERIC SUGARS BY INVERTASE DIGESTION

Oligosaccharides are composed of hexose subunits that form glycosidic bonds by elimination of a water molecule. This reveals a nominal mass difference between the particular oligomers of *m/z* 162, which can be determined directly by MS/MS fragmentation of precursor ions from the tissue sections. At this point, identification of the hexose subunits is not possible, as hexoses such as fructose, glucose, and galactose, all share the same molecular mass. In barley grains, the most abundant disaccharide is sucrose, followed by maltose; oligosaccharides comprise members of the raffinose family (sucrose + galactose subunits) as well as the fructan family (sucrose + fructose subunits). To distinguish members of these oligosaccharide families, specific sugar-hydrolyzing enzymes can be utilized, such as α-galactosidase (specific for raffinose family oligosaccharides) and invertase and fructosyl 1-exohydrolase (specific for fructan family oligosaccharides).

Invertase degrades sucrose to fructose and glucose. In addition, it is capable of digesting fructosyl oligosaccharides such as 1-kestose (DP3) and nystose (DP4) and hydrolyzing them into monomers (Nelson and Spollen, 1987). This protocol describes on-tissue digestion with invertase and subsequent MALDI-MSI analysis. An example for the result obtained by this protocol is presented in Figure 5.

Materials

Yeast invertase (Sigma-Aldrich)
20 mM KH_2PO_4 (Sigma-Aldrich)

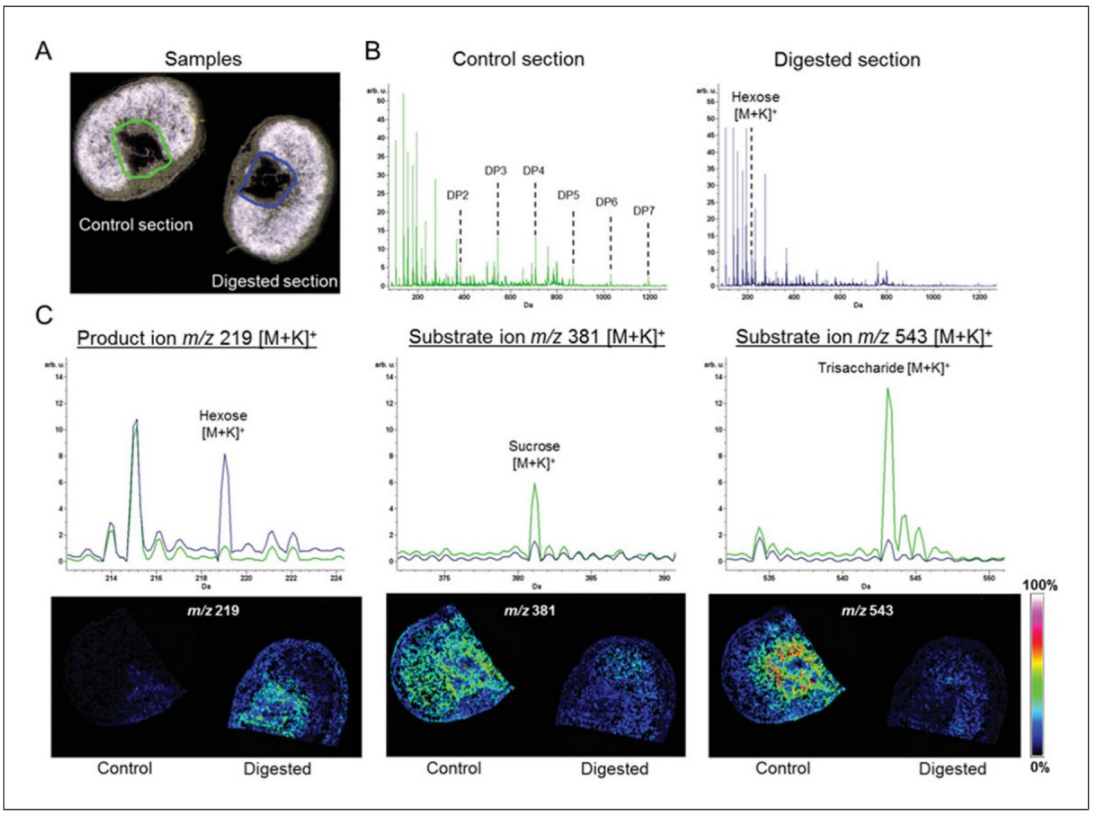

Figure 5 Spatially resolved on-tissue digestion and subsequent MSI analysis. Cryosections were treated with yeast invertase or buffer as a control. Sections were analyzed by MALDI-MSI. (**A**) Histological images of sections after digestion. (**B**) Average spectra of control and digested sections. Green (control) and blue (digested) correspond to areas outlined in (A). The control section shows the full complement of sugars (DP2-7), which are absent from the digested section. The hexose peak is the most abundant sugar signal. (**C**) Enlarged and overlaid spectra displaying signal for the hexose product ion (*m/z* 219) as well as the substrates sucrose (*m/z* 381) and trisaccharide (*m/z* 543). The corresponding MSI results are illustrated below each spectrum. Colors used in single-ion intensity maps correspond to signal intensities displayed at right. Reprinted from Peukert et al. (2014) (http://www.plantcell.org) with permission from the American Society of Plant Biologists.

20 mM K_2HPO_4 (Sigma-Aldrich)
Water, MS-grade
Methanol, MS-grade

Coverslips
ImagePrep device (Bruker Daltonics)
Moist chamber
55°C water bath

1. Prepare consecutive tissue sections with the cryotome as described (see Basic Protocol 1). Place two sections side by side on a slide for each digestion experiment.
2. Dissolve invertase at a concentration of 0.9 mg/ml (37 U/ml) in 20 mM KH_2PO_4 adjusted to pH 5 using 20 mM K_2HPO_4. Avoid foaming.
3. Mask the control section with a coverslip.
4. Load 400 µl invertase solution directly into the spray head of the ImagePrep device. Apply to the tissue section using 50 cycles consisting of 1.5 sec spraying and 30 sec drying.

For additional advice, see Basic Protocol 2.

5. Remove the coverslip from the control section and mask the treated section with a coverslip.
6. Repeat step 4 with control solution (KH_2PO_4/K_2HPO_4 without enzyme).
7. Carefully remove the slide from the ImagePrep device and incubate in a moist chamber above a water bath at 55°C for 1 h.

   Be sure to keep an atmosphere that is moist, but does not allow droplet formation on the slide.
8. Clean the ImagePrep device thoroughly with pure methanol using the "Clean" option on the instrument.
9. After incubation, remove slide from the incubation chamber, return it into the ImagePrep device, and proceed to deposition of matrix on the slide (see Basic Protocol 2).

   To directly compare signal intensities in the MALDI-MSI sum spectrum, consecutive slices are used and the treated and control sections measured simultaneously in random order. It is also helpful to cover part of the analyzed tissue with a coverslip before the application of invertase. The coverslip must be removed before matrix application. The covered area can serve as an internal control to evaluate the success of digestion.

   For comparative analysis and visualization of individual distribution patterns of molecular features, follow the procedure for directed data analysis (see Basic Protocol 4).

COMMENTARY

Background Information

Metabolites cannot be directly deduced from genomic information, but are essential parts of the complex network that determines the developmental and functional particularities of any biological system. There is enormous variance in the chemical properties of metabolites (e.g., hydrophilic vs. hydrophobic) and in the dynamic range of their concentrations (Kueger et al., 2012; Heinig et al., 2013). To understand systemic molecular networks down to tissue-specific functions, suitable technologies are needed that are capable of elucidating tissue-specific metabolite distribution patterns.

In this regard, MSI techniques have opened up a new avenue to obtain information on the spatial distribution of metabolites and proteins from biological tissues. Available technologies can be divided into measurement approaches that rely on special sample preparation (such as sectioning and matrix application) and techniques that directly scan the surface of a biological object. Recent reviews have summarized available technologies and applications (Bhardwaj and Hanley, 2014; El-Baba et al., 2014; Bartels and Svatoš, 2015). MSI techniques vary mostly in the process that forms molecular ions (ionization). The best-known soft ionization techniques currently used are matrix-assisted laser desorption/ionization (MALDI), secondary ion mass spectrometry (SIMS), and desorption electrospray ionization (DESI). Of these, MALDI-MSI is the most commonly used technique for molecular imaging of intact plant metabolites, peptides, and proteins (Svatoš, 2010; Grassl et al., 2011; Matros and Mock, 2013).

In MALDI-MSI, the relative abundances of molecules at specific positions in a tissue slice are observed (Kaspar et al., 2011). A great advantage to this technique is the ability to simultaneously detect several molecular species and the ability to map molecular ion abundances without any extraction protocol to two-dimensional coordinates of the original sample. Introduced by Spengler et al. (1994) and Caprioli et al. (1997), the technique was first used to visualize peptides and proteins in animal tissue sections. During the last decade, the technique has been applied widely in medical research and has provided a number of novel clinical markers for improved diagnosis or for pharmacological studies (Kriegsmann et al., 2015; Lahiri et al., 2016; Zhou et al., 2016). Investigations of plant tissues with MALDI-MSI are increasing, and recent reviews provide an excellent overview of its applications (Svatoš, 2010; Matros and Mock, 2013; Bartels and Svatoš, 2015; Boughton et al., 2016; Heyman and Dubery, 2016).

The MALDI-MSI method described in detail here is based on recent work evaluating particular spatiotemporal patterns of sugar

distributions in developing barley grains, which may relate to both differentiation and grain filling processes (Peukert et al., 2014).

Critical Parameters

Embedding of small, thin, and fragile plant samples

Embedding of sample tissues can strongly affect signal quality. In addition, from the outer sample surface, delocalization can occur during the thaw-mounting step. If possible, samples should be prepared without embedding by simply fixing them to the sample holder, as described. Very small, thin, or fragile samples may need some embedding. Trial experiments with methyl cellulose, stiffly beaten egg white, tragacanth, and ice have yielded promising results regarding signal intensities, signal suppression, and support during the cutting process for all tested media (unpub. observ.). Generally, the selection of an embedding medium should be based on the least amount of interfering molecular ion signals in the corresponding mass spectrum.

Additional information on critical parameters in sample preparation is provided in Peukert et al. (2012).

Image resolution affects histological evaluation

Image formats must be compatible with co-registration in the flexImaging software. Although optical images provide a reasonable overview of the sample and can serve as a reference image to define measurement areas at low resolution (<10,000 dpi), actual histological evaluation from such low-resolution images is impaired. Histological slide scanners (e.g., OpticLab H850, Plustek Technology) and microscope slide scanners (e.g., Pannoramic Desk device, 3D Histech, or ScanScope CS device, Aperio) provide an elegant alternative.

Slice thickness affects signal intensity

The structural diversity of plant material requires preliminary testing for the cutting procedure. Samples with a high water content are easier to cut than those with high proportions of aerenchyma or those that are dry or have wooden parts. In the authors' experience with developing barley grains, the more starch there is stored in the endosperm, the more fragile the samples. This can be circumvented by preparing thicker sections. On the other hand, thick slices may negatively impact signal intensity, as illustrated in Figure 2. To test which cutting thickness provides the best signal quality for the best sample quality (i.e., preservation of three-dimensional tissue structure), an MSI experiment with two to four different slice thicknesses should be performed beforehand.

Matrix background in small molecule analysis overlaps with sample signals

Be aware that, in small-molecule MALDI-MS analysis, the matrix-derived mass signals caused by matrix fragmentation and cluster formation often interfere with sample signals. It is critical to be sure they can be distinguished, i.e., by measuring a blank region from the sample slide. During data analysis, the sum of mass spectra of both measurement regions can be overlaid and compared. Signals that overlap with matrix background should be excluded from further analysis to avoid misinterpretation. Furthermore, isolation of such *m/z* values for MS/MS measurements carried out directly from the tissue section is not possible without getting interfering matrix fragmentation patterns. The interference of DHB-derived and 2,5-dihydroxyacetophenone (DHAP)–derived molecular ion signals with those generated from metabolite extracts of a barley grain sample is illustrated in Figure 6. For compounds of interest, conduct preliminary tests with standard compounds to elucidate interferences with matrix-derived MS signals.

Choice of matrix affects ionization of molecules

The selection of an appropriate matrix is essential before setting up a whole series of MSI experiments. Different matrices support ionization of different compound classes, and differences may even be observed within one compound class. As an example, Figure 7 illustrates an analysis of the ionization efficiency for hexose oligomers. Hexose and its disaccharide and trisaccharide ionize better when using the gold nanoparticle (GNP) matrix, whereas oligomers with a degree of polymerization (DP) of 4-7 ionize better with the DHB matrix.

High numbers of laser shots and acquired spectra perturb instrument performance

Generating a data set for developmental stages of barley grains implies largely varying sample sizes, i.e.., from ~1.5 mm at 3 DAP to large longitudinal slices (>5 × 10 mm) at 20 DAP. In addition, tissue differentiation increases during grain development, generating the need for high spatial resolution to preserve tissue-specific information. The size

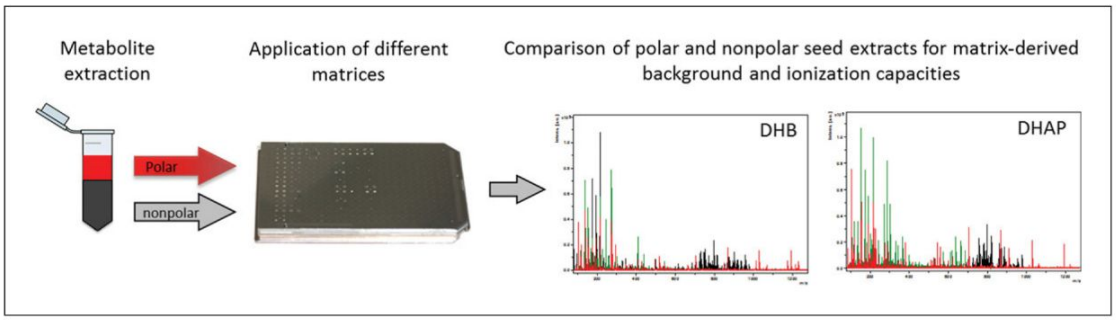

Figure 6 Overlap of matrix background with sample signals in small molecule analysis. Polar (red) and nonpolar (grey) metabolites were extracted from barley grains. Preparations of both extracts utilizing different matrices (DHB and DHAP) were deposited on a stainless steel target to check the amount of overlapping signals derived from the matrices (green). A high amount of matrix-derived signals was observed for both substances, especially in the low-molecular-mass range.

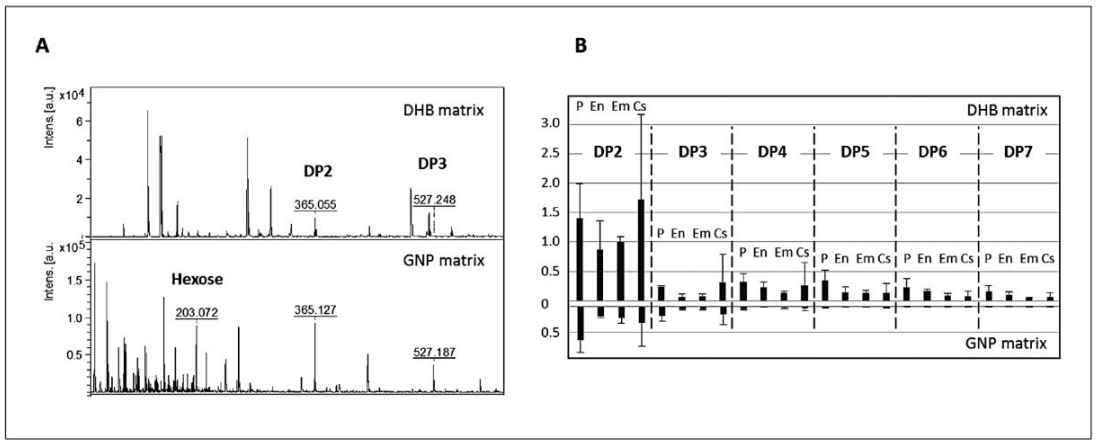

Figure 7 Choice of matrix affects ionization of hexose and hexose oligomers. (**A**) Embryos were manually separated from barley grains at 14 DAP and extracts were analyzed by MALDI-MS for their content of hexose and derived sugar oligomers. The intensity of molecular ion signals for hexose and hexose oligomers was observed to vary when using two different matrices (DHB and GNP). For example, the DHB matrix was not suited to analyze the presence of the hexose monomer (*m/z* 203 $[M+Na]^+$). The GNP matrix showed best ionization capacity for sugar monomers, the dimer (*m/z* 365 $[M+Na]^+$), and the trisaccharide (*m/z* 527 $[M+Na]^+$). (**B**) Barley grain tissues (P, pericarp; En, endosperm; Em, embryo; Cs, cavity sap) were manually separated (15 DAP) and extracts were analyzed for profiles of hexose and derived sugar oligomers with degrees of polymerization (DP) from 2 to 7 by MALDI-MS utilizing DHB (top) and GNP (bottom) as matrix. Tissue-specific profiles could be distinguished for sugar oligomers of DP4 to DP7 with DHB, whereas those molecular ions were barely detectable using GNP. Relative intensity values were determined against an internal standard (10 mM ^{13}C-sucrose).

of the measurement region and the chosen laser raster resolution define the number of acquired single spectra. A very high number of spectra in combination with a high number of laser shots per raster spot can result in a significant decrease in spectral intensity due to pollution of the MALDI source. Generally, a good maximum number of spectra per run is ~15,000. This is reached by a laser spot size of 35 μm for large samples or 15-20 μm for smaller samples. Also, the order of spot measurement should always be randomized to avoid positional influences on spectral quality from source pollution.

Targeted analyses are needed for compound identification

Generally, MSI data analysis provides a list of *m/z* signals relevant in the context of each specific experiment. To elucidate the chemical structure of the underlying compounds, additional experiments are required. These may include accurate mass measurements, MS/MS analysis, on-tissue digestion, extraction, and analysis of laser-dissected areas containing the unknown compound of interest, among other approaches. The choice of an appropriate strategy depends on the experimental context.

Anticipated Results

The provided protocols favor MSI analysis of the molecular distribution of phosphatidylcholines (PC) and oligosaccharides in cryosections of developing barley grains. Compound detection highly depends on the chosen matrix and on the chemical structure of the target molecules. The DHB matrix was found to be superior with regard to the amount of background signal and the ionization capacity for molecular ions from barley grain sections (see Critical Parameters and Figs. 3 and 4).

The over-representation of PCs compared to other lipids is explained by ionization suppression effects of this lipid class in complex lipid mixtures. Quaternary amines in PCs, lysophosphatidylcholines (LPCs), and sphingolipids (SLs) preform a positive charge that is thought to enhance their detectability in positive ionization mode and to suppress the signals of other phospholipids that are less cationic (Petković et al., 2001; Johanson et al., 2007; Emerson et al., 2010; Fuchs et al., 2010). Furthermore, the positive charge of the quaternary nitrogen in PC promotes the efficient release of the characteristic fragment ion (*m/z* 184) of the PC head group (Murphy and Axelsen, 2011). In MALDI-MSI experiments, the a priori exclusion of PC, LPC, or SL is impossible. Thus, the observed lipid profiles reflect the ionization capacities of those molecules rather than the real in vivo lipid concentrations. However, PC, LPC, and SL play key roles in living cells and a relative comparison of lipid amounts within the individual lipid classes (such as PC) was found convenient for MALDI-MSI experiments when compared to other methods (Horn et al., 2012).

Following the provided protocols, mono- and oligosaccharides are mainly detected in the form of their potassium adducts. This coincides with findings from Harvey (2011), who reported on the use of DHB matrix for oligosaccharide measurements. The high affinity of alkali metals for carbohydrates is also outlined in Wang et al. (1999). In recent MALDI-MSI applications to poplar stem and eggplant, oligosaccharides were detected as well by using the DHB matrix (Goto-Inoue et al., 2010; Jung et al., 2010).

Time Considerations

The best results are obtained when grain samples are prepared and measured on the same day. Sectioning in the morning will take ~2 hr, depending on the sample size and user experience. Drying the sample in a desiccator takes 30 min, and taking an optical image requires ~30 min. Preparation and application of matrix takes ~2 hr. It is important to monitor the application process to enable any necessary interventions, such as additional spray cycles or longer drying times between spray cycles. Setup of the measurement (including instrument calibration, laser intensity test, loading sample image, and labeling the measurement region) takes ~1 hr, depending on experience with the instrumentation. Measurement can take place overnight and depends on sample number and size of the measurement region. Cleaning the instrument requires ~1 hr, but may require several hours for the vacuum to become stable again.

Data mining requires careful consideration and no specific time frame can be provided, as this depends on the kind of analysis desired (directed or undirected), the number of replicates included, and the treatments being compared. Although an individual MSI measurement takes about a day, sufficient analysis of biological replicates is required for reliable interpretation of data. Also, the time needed for data evaluation varies depending on the target of the analysis, i.e., whether one wishes to examine the distribution of particular molecular ions or to dissect entire molecular networks. Thus, the total experimental time frame may vary from weeks to months.

Acknowledgements

The research of Manuela Peukert and Andrea Matros was supported by grants from the German Research Foundation (MA 4814/1-1) and the German Academic Exchange Service (DAAD, 57060105). Wai Li Lim received financial support from the DAAD G08 Australia Germany Exchange program, an Adelaide Graduate Research Scholarship (AGRS), and an ARC Centre of Excellence in Plant Cell Walls Scholarship (CE110001007). The authors thank Hans-Peter Mock, Winfriede Weschke, and Rachel Burton for continuous scientific support and fruitful discussions. Uta Siebert and Annegret Wolf are gratefully mentioned for their excellent technical assistance. Michael Becker (Bruker Daltonics GmbH, Bremen, Germany) is acknowledged for his profound initial technical support. The authors also thank Dennis Trede and Klaus Steinhorst from SCiLS GmbH (*http://scils.de/*) for their active support in unsupervised data analysis and provision of the software.

Literature Cited

Agar, N.Y.R., Kowalski, J.-M., Kowalski, P.J., Wong, J.H., and Agar, J.N. 2010. Tissue

preparation for the in situ MALDI MS imaging of proteins, lipids, and small molecules at cellular resolution. *Methods Mol. Biol.* 656:415-432. doi: 10.1007/978-1-60761-746-4_24.

Alexandrov, T. and Kobarg, J.H. 2011. Efficient spatial segmentation of large imaging mass spectrometry datasets with spatially aware clustering. *Bioinformatics* 27:i230-i238. doi: 10.1093/bioinformatics/btr246.

Alexandrov, T., Becker, M., Deininger, S.-O., Ernst, G.N., Wehder, L., Grasmair, M., von Eggeling, F., Thiele, H., and Maass, P. 2010. Spatial segmentation of imaging mass spectrometry data with edge-preserving image denoising and clustering. *J. Proteome Res.* 9:6535-6546. doi: 10.1021/pr100734z.

Amstalden van Hove, E.R., Smith, D.F., and Heeren, R.M.A. 2010. A concise review of mass spectrometry imaging. *J. Chromatogr. A* 1217:3946-3954. doi: 10.1016/j.chroma.2010.01.033.

Bartels, B. and Svatoš, A. 2015. Spatially resolved in vivo plant metabolomics by laser ablation-based mass spectrometry imaging (MSI) techniques: LDI-MSI and LAESI. *Front. Plant Sci.* 6:471. doi: 10.3389/fpls.2015.00471.

Bhardwaj, C. and Hanley, L. 2014. Ion sources for mass spectrometric identification and imaging of molecular species. *Nat. Prod. Rep.* 31:756-767. doi: 10.1039/c3np70094a.

Boughton, B.A., Thinagaran, D., Sarabia, D., Bacic, A., and Roessner, U. 2016. Mass spectrometry imaging for plant biology: A review. *Phytochem. Rev.* 15:445-488. doi: 10.1007/s11101-015-9440-2.

Caprioli, R.M., Farmer, T.B., and Gile, J. 1997. Molecular imaging of biological samples: Localization of peptides and proteins using MALDI-TOF MS. *Anal. Chem.* 69:4751-4760. doi: 10.1021/ac970888i.

El-Baba, T.J., Lutomski, C.A., Wang, B., Inutan, E.D., and Trimpin, S. 2014. Toward high spatial resolution sampling and characterization of biological tissue surfaces using mass spectrometry. *Anal. Bioanal. Chem.* 406:4053-4061. doi: 10.1007/s00216-014-7778-8.

Emerson, B., Gidden, J., Lay, J.O., and Durham, B. 2010. A rapid separation technique for overcoming suppression of triacylglycerols by phosphatidylcholine using MALDI-TOF MS. *J. Lipid Res.* 51:2428-2434. doi: 10.1194/jlr.D003798.

Fuchs, B., Süss, R., and Schiller, J. 2010. An update of MALDI-TOF mass spectrometry in lipid research. *Prog. Lipid Res.* 49:450-475. doi: 10.1016/j.plipres.2010.07.001.

Goto-Inoue, N., Setou, M., and Zaima, N. 2010. Visualization of spatial distribution of gamma-aminobutyric acid in eggplant (*Solanum melongena*) by matrix-assisted laser desorption/ionization imaging mass spectrometry. *Anal. Sci.* 26:821-825. doi: 10.2116/analsci.26.821.

Grassl, J., Taylor, N.L., and Millar, A. 2011. Matrix-assisted laser desorption/ionisation mass spectrometry imaging and its development for plant protein imaging. *Plant Methods* 7:1. doi: 10.1186/1746-4811-7-21.

Hanselmann, M., Kirchner, M., Renard, B.Y., Amstalden, E.R., Glunde, K., Heeren, R.M., and Hamprecht, F.A. 2008. Concise representation of mass spectrometry images by probabilistic latent semantic analysis. *Anal. Chem.* 80:9649-9658. doi: 10.1021/ac801303x.

Harvey, D.J. 2011. Analysis of carbohydrates and glycoconjugates by matrix-assisted laser desorption/ionization mass spectrometry: An update for the period 2005-2006. *Mass Spectrom. Rev.* 30:1-100. doi: 10.1002/mas.20265.

Heinig, U., Gutensohn, M., Dudareva, N., and Aharoni, A. 2013. The challenges of cellular compartmentalization in plant metabolic engineering. *Curr. Opin. Biotechnol.* 24:239-246. doi: 10.1016/j.copbio.2012.11.006.

Heyman, H.M. and Dubery, I.A. 2016. The potential of mass spectrometry imaging in plant metabolomics: A review. *Phytochem. Rev.* 15:297-316. doi: 10.1007/s11101-015-9416-2.

Horn, P.J., Korte, A.R., Neogi, P.B., Love, E., Fuchs, J., Strupat, K., Borisjuk, L., Shulaev, V., Lee, Y.-J., and Chapman, K.D. 2012. Spatial mapping of lipids at cellular resolution in embryos of cotton. *Plant Cell Online* 24:622-636. doi: 10.1105/tpc.111.094581.

Johanson, R.A., Buccafusca, R., Quong, J.N., Shaw, M.A., and Berry, G.T. 2007. Phosphatidylcholine removal from brain lipid extracts expands lipid detection and enhances phosphoinositide quantification by matrix-assisted laser desorption/ionization time-of-flight (MALDI-TOF) mass spectrometry. *Anal. Biochem.* 362:155-167. doi: 10.1016/j.ab.2006.12.026.

Jung, S., Chen, Y., Sullards, M.C., and Ragauskas, A.J. 2010. Direct analysis of cellulose in poplar stem by matrix-assisted laser desorption/ionization imaging mass spectrometry. *Rapid Commun. Mass Spectrom.* 24:3230-3236. doi: 10.1002/rcm.4757.

Kaletaş, B.K., van der Wiel, I.M., Stauber, J., Lennard, J.D., Güzel, C., Kros, J.M., Luider, T.M., and Heeren, R.M.A. 2009. Sample preparation issues for tissue imaging by imaging MS. *Proteomics* 9:2622-2633. doi: 10.1002/pmic.200800364.

Kaspar, S., Peukert, M., Svatoš, A., Matros, A., and Mock, H.P. 2011. MALDI-imaging mass spectrometry—an emerging technique in plant biology. *Proteomics* 11:1840-1850. doi: 10.1002/pmic.201000756.

Kriegsmann, J., Kriegsmann, M., and Casadonte, R. 2015. MALDI TOF imaging mass spectrometry in clinical pathology: A valuable tool for cancer diagnostics (review). *Int. J. Oncol.* 46:893-906. doi: 10.3892/ijo.2014.2788.

Kueger, S., Steinhauser, D., Willmitzer, L., and Giavalisco, P. 2012. High-resolution plant

metabolomics: From mass spectral features to metabolites and from whole-cell analysis to subcellular metabolite distributions. *Plant J.* 70:39-50. doi: 10.1111/j.1365-313X.2012.04902.x.

Lahiri, S., Sun, N., Buck, A., Imhof, A., and Walch, A. 2016. MALDI imaging mass spectrometry as a novel tool for detecting histone modifications in clinical tissue samples. *Exp. Rev. Proteomics* 13:275-284. doi: 10.1586/14789450.2016.1146598.

Martinetz, T.M. and Schulten, K.J. 1991. A neural-gas network learns topologies. *In* Artificial Neural Networks (T. Kohonen, K. Mäkisara, O. Simula, and J. Kangas, eds.) pp. 397-402. North-Holland Publishing Company, Amsterdam.

Matros, A. and Mock, H.P. 2013. Mass spectrometry based imaging techniques for spatially resolved analysis of molecules. *Front. Plant Sci.* 4:89. doi: 10.3389/fpls.2013.00089.

Murphy, R.C. and Axelsen, P.H. 2011. Mass spectrometric analysis of long-chain lipids. *Mass Spectrom. Rev.* 30:579-599. doi: 10.1002/mas.20284.

Nelson, C.J. and Spollen, W.G. 1987. Fructans. *Physiol. Plant* 71:512-516. doi: 10.1111/j.1399-3054.1987.tb02892.x.

Petković, M., Schiller, J., Müller, M., Benard, S., Reichl, S., Arnold, K., and Arnhold, J. 2001. Detection of individual phospholipids in lipid mixtures by matrix-assisted laser desorption/ionization time-of-flight mass spectrometry: Phosphatidylcholine prevents the detection of further species. *Anal. Biochem.* 289:202-216. doi: 10.1006/abio.2000.4926.

Peukert, M., Matros, A., Lattanzio, G., Kaspar, S., Abadía, J., and Mock, H.-P. 2012. Spatially resolved analysis of small molecules by matrix-assisted laser desorption/ionization mass spectrometric imaging (MALDI-MSI). *New Phytologist* 193:806-815. doi: 10.1111/j.1469-8137.2011.03970.x.

Peukert, M., Thiel, J., Peshev, D., Weschke, W., Van den Ende, W., Mock, H.-P., and Matros, A. 2014. Spatio-temporal dynamics of fructan metabolism in developing barley grains. *Plant Cell Online* 26:3728-3744. doi: 10.1105/tpc.114.130211.

Spengler, B., Hubert, M., and Kaufmann, R. 1994. MALDI ion imaging and biological ion imaging with a new scanning UV-laser microprobe. *In* Proceedings of the 42nd Annual Conference on Mass Spectrometry and Allied Topics, p. 1041. Chicago, Ill.

Svatoš, A. 2010. Mass spectrometric imaging of small molecules. *Trends Biotechnol.* 28:425-434. doi: 10.1016/j.tibtech.2010.05.005.

Turbett, G.R. and Sellner, L.N. 1997. The use of optimal cutting temperature compound can inhibit amplification by polymerase chain reaction. *Diagn. Mol. Pathol.* 6:298-303. doi: 10.1097/00019606-199710000-00009.

Wang, J., Sporns, P., and Low, N.H. 1999. Analysis of food oligosaccharides using MALDI-MS: Quantification of fructooligosaccharides. *J. Agricult. Food Chem.* 47:1549-1557. doi: 10.1021/jf9809380.

Zhou, L., Wang, K., Li, Q., Nice, E.C., Zhang, H., and Huang, C. 2016. Clinical proteomics-driven precision medicine for targeted cancer therapy: Current overview and future perspectives. *Exp. Rev. Proteomics* 13:367-381. doi: 10.1586/14789450.2016.1159959.

Chapter 6

General Discussion

Summary

The (1,3;1,4)-β-glucan polysaccharide in barley grain has major impacts on downstream applications for human food, animal feed and malting processes. (1,3;1,4)-β-Glucan has beneficial properties for human health due to its ability to form viscous solutions in the human gastrointestinal tract and its fermentability by the microbiome (Cavallero et al., 2002; Delaney et al., 2003; Yang et al., 2003; Behall et al., 2006; Queenan et al., 2007; Chen and Raymond, 2008; El Khoury et al., 2012; Shen et al., 2012; Arena et al., 2014). In contrast, (1,3;1,4)-β-glucan is regarded as an anti-nutritional factor in animal feeding, particularly for chickens again due to its viscous nature in their short digestive tracts (McNab and Smithard, 1992; Annison, 1993), and its natural viscous properties can cause filtration problems during malting processes thus affecting brew quality (Bamforth, 1994; Speers et al., 2003). Hence, it is important for a range of industries, and for us to understand what happens when we alter grain (1,3;1,4)-β-glucan, and whether manipulation of grain (1,3;1,4)-β-glucan influences other properties that are relevant to grain quality and subsequent applications.

Genetic manipulation of (1,3;1,4)-β-glucan content in barley grain can be achieved by modifying the carbon metabolic pathways associated with synthesis of storage polysaccharides (Clarke et al., 2008; Burton et al., 2011; Taketa et al., 2012; Hu et al., 2014; Han et al., 2017). For example, modified (1,3;1,4)-β-glucan content has been associated with altered starch (Munck et al., 2004; Clarke et al., 2008; Burton et al., 2011; Han et al., 2017) and fructan content (Clarke et al., 2008; Hu et al., 2014). However, grain from these engineered plants are commonly measured at the mature stage and often we lack information about the compositional changes that occur in developing grains and thus give rise to the final product. Changes in grain composition in barley may have effects on grain morphology (Andersson et al., 1999; Morell et al., 2003; Ma et al., 2014). The factors that affect grain morphology have not been fully

elucidated, and the extent to which altering metabolic pathways during grain development may lead to differences in morphology is a relatively unexplored research area. There are a number of examples of barley cultivars which have shrunken grain. Many of these have phenotypes associated with altered starch levels but the specific mutation or change that leads to the phenotype has not been defined, let alone the pleiotropic cascade which derives from the mutation. For these cultivars only one has been reported to have thicker cell walls whilst the M292 mutant is known to have an increase in (1,3;1,4)-β-glucan. It may be necessary to go to another species, *Brachypodium distachyon*, which has been shown to have the thickest endosperm cell walls yet described amongst the grasses (Trafford et al., 2012), with a commensurate reduction in starch content but with a smooth grain phenotype, to try and explore how thicker walls can "fit" into the grain. It certainly seems that a transgenic approach to induce this situation is not the solution. In terms of thinner endosperm cell walls, with less (1,3;1,4)-β-glucan, the OUM125 *CslF6* knockout mutant has achieved this with a much less severe effect on grain morphology but with a major penalty for plant fitness. There are other thin-walled mutants available with reduced (1,3;1,4)-β-glucan (Chapter 1) but the genetic lesions underlying this trait are unknown and so a direct comparison is not possible at this time.

To investigate the effects of modified (1,3;1,4)-β-glucan content on carbohydrate metabolic pathways from early grain development at 7 DAP, and to test how this might lead to differences in mature grain composition, specifically developed transgenic lines, the OUM125 mutant and relevant controls were examined. These line were transformed with the *HvCslF6* gene via an *Agrobacterium*-mediated transformation approach, which ultimately produced grain with high (1,3;1,4)-β-glucan content (Chapter 2 and Chapter 3). In contrast, the effects of significant reductions in grain (1,3;1,4)-β-glucan content on carbon flow was examined using a (1,3;1,4)-β-glucanless (*bgl*) mutant (OUM125) supplied by Professor K. Sato (Okayama University)

(Chapter 4). Both studies were carried out in the hull-less barley varieties cv Torrens and cv Akashinriki, respectively, due to the potential of hull-less varieties as a source of human food (Bhatty, 1999; Box et al., 2005).

We observed that Torrens barley overexpressing the *HvCslF6* gene had up to 70% more (1,3;1,4)-β-glucan content in the mature grain than wild type. We also tested transgenic lines overexpressing the *HvCslH1* gene and these lines had little difference in (1,3;1,4)-β-glucan content in mature grain compared to the wild type. The transgenic Torrens lines transformed with the *CslF6* gene had grain that were shrunken and darkened in colour. My contribution to Chapter 2 was the characterisation of transgenic seedlings for the F6-15-3, F6-16-5, F6-18-6 and F6-25-5 lines and application of microscopy techniques to examine the morphological changes in developing grain. The proportion of embryo per grain in the F6-18-6 transgenic line was significantly greater compared to the other transgenic lines and wild type (WT) and wild type that had been through tissue culture procedures WT(tc) controls. It was observed that along with the greater embryo size, seedling growth was affected. For example, decreased root lengths and decreased shoot weights were observed, although the germination capacity was not affected. The change in embryo size is likely to be associated with carbon flow and sugar signalling effects which are yet to be identified (Rolland et al., 2006; Ayre, 2011; Eveland and Jackson, 2012; Shang et al., 2015).

Examination of developing grain using toluidine blue stain revealed that there was a larger cavity in the transgenic grain at 9 DAP relative to wild type, with the cavity size becoming more pronounced from 10 DAP onwards throughout the carbon storage phases. Subsequent analyses focussed on the most severe line, F6-18-6, which was used as the prime example, but all lines showed common effects to various degrees. The endosperm transfer layer (ETL) facing

the nucellar projection began to rupture and a closer examination revealed thinner walls in the cells of the ETL in F6-18-6 transgenic grain compared to wild type. Fluorescence immunolabeling with various polysaccharide antibodies revealed that there was less mannan in the ETL at 9 and 10 DAP when the cavity size became larger and rupture began. No other common cell wall polysaccharides such as (1,3;1,4)-β-glucan, callose, cellulose, arabinoxylan and pectins were detected by fluorescent labelling in this tissue. In legumes, mannan polysaccharide has a role in both energy storage and maintaining structural integrity (Reid, 1971; Buckeridge et al., 2000; Handford et al., 2003) and it has been proposed to be involved in protecting cells from mechanical damage (McCleary et al., 1981; Rodríguez-Gacio et al., 2012) and pathogen defence (Handford et al., 2003). It is likely that less mannan in the walls of the ETL is a factor which contributed to a weaker cell wall structure, which in the absence of other strengthening polysaccharides became much more prone to rupture under pressure. Nevertheless, it is also possible that other cell wall polysaccharides were arranged in a complex way that their epitopes were unmasked and unavailable for binding.

The amount of fluids in the transgenic cavity at 15 DAP was about three fold greater and the concentrations of sucrose and fructans were up to four fold greater, compared to the wild type controls. This indicates that a higher osmotic pressure may have built up in the cavity of the transgenic grain, which is highly likely due to altered ETC morphology and possibly a greater sink strength in the transgenic grain. Combination of these two factors, may thus explain cavity expansion, which was particularly pronounced in F6-18-6 transgenic grain. Since barley grain loses its water content during maturation (Adams and Rinne, 1980; Cochrane, 1985), this dehydration and collapse of the cavity contributes to the shrivelling of the transgenic grain and gives rise to the distinct shrunken grain phenotype.

We observed that the F6-18-6 transgenic grain had a thicker aleurone tissue with elongated aleurone cells, consisting of about three to four cell layers at 24 DAP, compared to the wild type where the aleurone cells are square and only two to three cell layers deep. The subaleurone cells in the transgenic grain appeared irregular and displayed stronger signal intensities when labelled with calcofluor white, CBM3a (crystalline cellulose) and the BG1 ((1,3;1,4)-β-glucan), and callose antibodies when compared to other tissue regions. These observations indicate that the *CslF6* gene driven by the *AsGlo* promoter was expressed in the subaleurone region, which could mean that the sugar signalling in the subaleurone region was altered relative to wild type, and resulted in perturbed aleurone and subaleurone cell fate and shape in the transgenic lines.

The shrunken endosperm of the transgenic grain contained less starch and a different starch granule composition compared to the wild type. From early grain filling (11 DAP) less starch accumulated in the transgenic endosperm relative to wild type grain. The transcript analysis of starch metabolic genes revealed differences that are likely to be associated with the variable starch accumulation. The qPCR analysis of starch metabolic genes revealed downregulation of some key genes, such as *starch synthase 2, starch branching enzyme 2a, starch branching enzyme 2b, granule bound starch synthase 1a, isoamylase 1* and *limit dextrinase*, and upregulation of *starch branching enzyme 1* from 7 up to 24 DAP in the transgenic line relative to wild type. In previous studies pleiotropic effects from differential regulation of starch metabolic genes have been associated with differences in the granule size (Craig et al., 1998; Morell et al., 2003; Carciofi et al., 2012; McMaugh et al., 2014).

The reduced amount of starch in transgenic grain relative to wild type grain was accompanied with greater amounts of sucrose and fructan in the endosperm. Consistent with this observation, the qPCR analysis of transcript differences revealed upregulation of a fructosyltransferase gene,

6-SFT, downregulation of *cell wall invertase* and upregulation of *sucrose transporter 1* in the endosperm of the transgenic grain. This could be linked with an increase in sucrose uptake in the endosperm for fructan synthesis. It is possible that the increased sucrose pool in the transgenic endosperm is linked to the tearing of the ETL which might have enabled the sucrose to flow symplastically, rather than being regulated via membrane transporters. Based on the grain compositional differences we can deduce that the increased sucrose availability in the transgenic endosperm was used for cell wall biosynthesis, including the synthesis of (1,3;1,4)-β-glucan, cellulose, callose and arabinoxylan, rather than for starch biosynthesis. Previous studies have revealed that altered sucrose signalling pathways can lead to anthocyanin production (Teng et al., 2005; Solfanelli et al., 2006; Van den Ende and El-Esawe, 2014). Based on this we hypothesise that increased anthocyanin production might be linked to the dark appearance of the mature transgenic grain, and it would be interesting to test this hypothesis in the future.

To complement our investigation of what happens when grain (1,3;1,4)-β-glucan is increased we sourced material that would enable us to test what happens when grain (1,3;1,4)-β-glucan is decreased. Our strategy involved investigating the carbon metabolic pathways in a betaglucanless (*bgl*) barley mutant (OUM125). We were interested in testing whether loss of (1,3;1,4)-β-glucan had the opposite effect of increasing (1,3;1,4)-β-glucan or a different effect altogether. We observed that the mature mutant grain appeared smaller and had reduced grain weight compared to the wild type grain. However, there was no difference in grain morphology in the developing grains and the starch granules appeared similar to those of the wild type. Quantitative measurement of sucrose and fructan revealed a significant increase in the amounts of these sugars in mature mutant grain relative to the wild type grain, but there was no difference observed in the developing grains. Consistent with this we detected transcript differences in

fructosyltransferase genes, including *1-SST* and *6-SFT*, which were upregulated from 11 to 24 DAP while sucrose transporter genes, including *SUT1* and *SUT2*, were upregulated at 24 DAP in the mutant relative to wild type. The mutant grain generally had a higher starch content between 15 and 24 DAP, after it reverted to an amount similar to wild type grain. We observed that starch metabolic genes such as *granule bound starch synthase 1a, starch branching enzyme 1, starch branching enzyme 2a, starch branching enzyme 2b, limit dextrinase, isoamylase* and *ADP-Glucose Pyrophosphorylase*, were downregulated overall in the mutant relative to wild type, but the gene expression differences did not translate to differences in the final starch amounts in the mutant grain.

The effects of the absence of (1,3;1,4)-β-glucan on other cell wall components such as cellulose, callose, mannan and arabinoxylan, in mature grain were also investigated in this study using a combination of techniques such as HPLC and immunolabeling. An absence of (1,3;1,4)-β-glucan in the endosperm cell walls was linked to increased arabinoxylan, reduced callose and reduced cellulose. Cell wall-related genes such as *CslF3, CslF7, CslF10, CesA2, CesA3* and *Gsl2* were upregulated from 15 DAP in the mutant grain relative to wild type. We observed that the vegetative growth in the mutant differed to wild type. For example, the mutant plants were shorter than wild type plants and displayed chlorotic leaves and high sterility rates. Nonetheless, a grain germination test showed no difference in the rate between mutant and wild type grain.

We observed that increasing (1,3;1,4)-β-glucan content in barley grain by overexpressing the *CslF6* gene driven by an *AsGlo* promoter has negative impacts on grain development (Chapters 2 and 3), and morphology, particularly in the endosperm transfer layer, aleurone and subaleurone layer tissues. We hypothesise that these phenotypes manifested as a result of interference in complex sugar signalling pathways, which are yet to be fully defined. This

suggestion is based on the observations that increasing (1,3;1,4)-β-glucan content in barley grain results in high fructan and low starch contents. In contrast the absence of (1,3;1,4)-β-glucan in barley grain does not affect grain development and starch content, and although still affecting sucrose and fructan content, the ramifications on final grain fitness are a lot less severe.

The *CslF6* over-expressing hull-less transgenic grain has desirable characteristics, such as high fructan, low starch and potentially high polyphenol compounds, with high (1,3;1,4)-β-glucan levels, that may be of interest for future breeding programs targeted at producing healthy barley products for human consumption. However, the commercialisation of genetically modified or transgenic crops is currently not legalised in many countries and consumer acceptance of shrunken grain is not likely to be high. Alternative approaches to modifying these grain characteristics such as mutagenesis, TILLING (Targeting Induced Local Lesions in Genomes) and CRISPR Cas9 gene editing could be utilised to produce hull-less barley with high (1,3;1,4)-β-glucan content, although employing these approaches would be a significant investment and different gene targets, rather than the synthases themselves, would have to be found.

It is useful for brewing and animal feed industries to know that the absence of (1,3;1,4)-β-glucan in barley grain does not affect the starch content, which is an important sugar source for malting and an energy source for animals. This opens possibilities for using hull-less varieties for both these industries. Nevertheless, the mutant lines still require further backcrossing with other cultivars to eliminate the undesired plant phenotypes, such as reduced vegetative growth and leaf necrosis (Taketa et al., 2012) and to reduce the background mutation rate.

The outcomes of this research include gains in our fundamental understanding of the regulation of carbon flow in hull-less barley grain across development. This research has also contributed

a physiological explanation for the shrunken grain phenotype in the transgenic lines with increased (1,3;1,4)-β-glucan content, which may inform future strategies to develop grain with desirable carbohydrate content and morphological phenotypes. The data generated in this study has been used to develop a hypothetical model for the effects of increasing or decreasing (1,3;1,4)-β-glucan content in hull-less barley grain (Figure 1).

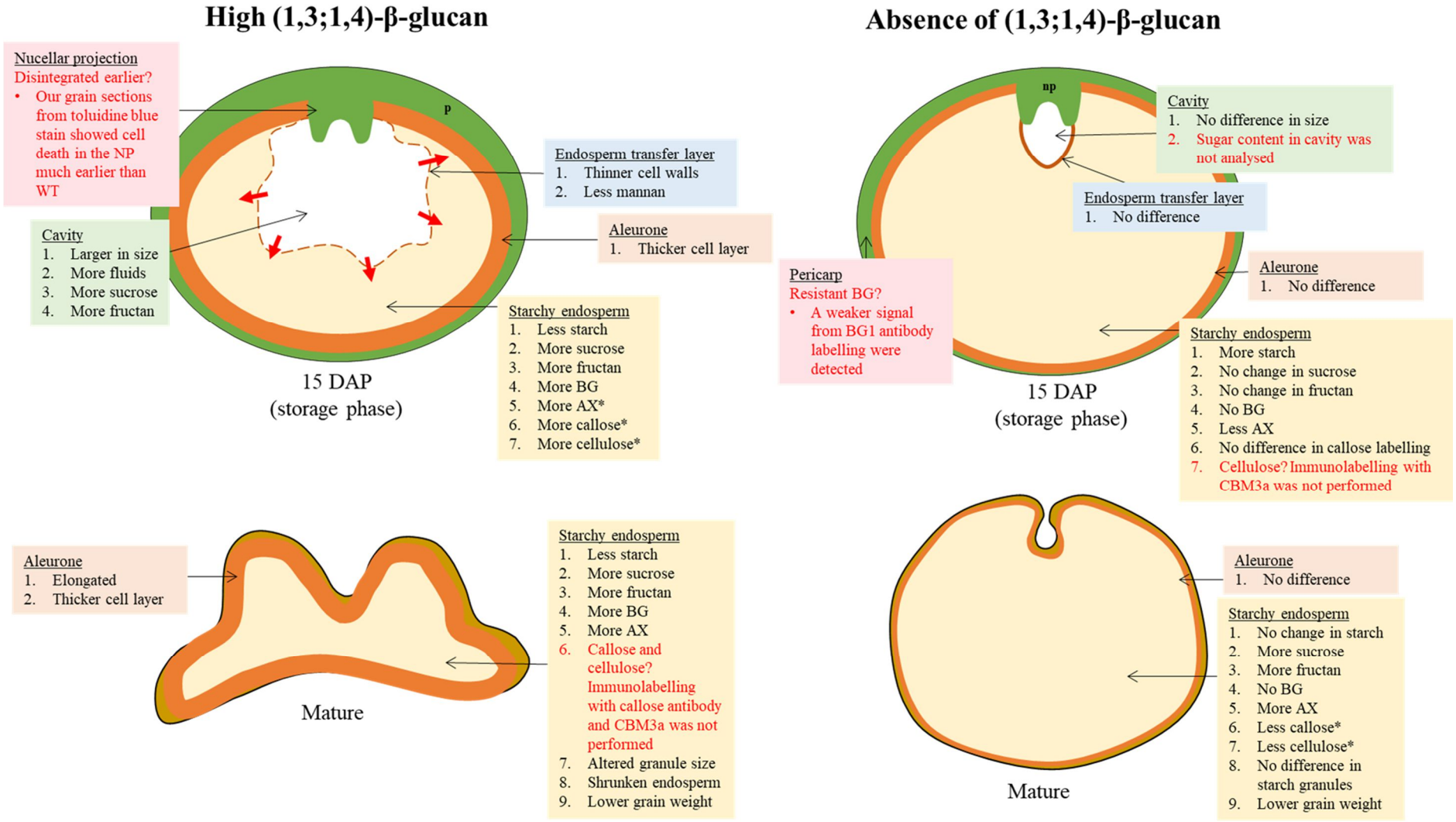
High (1,3;1,4)-β-glucan
Nucellar projection
Disintegrated earlier?
• Our grain sections from toluidine blue stain showed cell death in the NP much earlier than WT
p
Endosperm transfer layer
1. Thinner cell walls
2. Less mannan
Cavity
1. Larger in size
2. More fluids
3. More sucrose
4. More fructan
Aleurone
1. Thicker cell layer
Starchy endosperm
1. Less starch
2. More sucrose
3. More fructan
4. More BG
5. More AX*
6. More callose*
7. More cellulose*
15 DAP
(storage phase)
Aleurone
1. Elongated
2. Thicker cell layer
Starchy endosperm
1. Less starch
2. More sucrose
3. More fructan
4. More BG
5. More AX
6. Callose and cellulose? Immunolabelling with callose antibody and CBM3a was not performed
7. Altered granule size
8. Shrunken endosperm
9. Lower grain weight
Mature
Absence of (1,3;1,4)-β-glucan
np
Cavity
1. No difference in size
2. Sugar content in cavity was not analysed
Endosperm transfer layer
1. No difference
Pericarp
Resistant BG?
• A weaker signal from BG1 antibody labelling were detected
Aleurone
1. No difference
Starchy endosperm
1. More starch
2. No change in sucrose
3. No change in fructan
4. No BG
5. Less AX
6. No difference in callose labelling
7. Cellulose? Immunolabelling with CBM3a was not performed
15 DAP
(storage phase)
Aleurone
1. No difference
Starchy endosperm
1. No change in starch
2. More sucrose
3. More fructan
4. No BG
5. More AX
6. Less callose*
7. Less cellulose*
8. No difference in starch granules
9. Lower grain weight
Mature

Figure 1: A hypothetical model of the processes occurring in hull-less barley grain with high (1,3;1,4)-β-glucan (*CslF6* transgenic cv Torrens) and without (1,3;1,4)-β-glucan ((1,3;1,4)-β-glucanless cv Akashinriki). The differences in sugar amounts and grain morphology between the *CslF6* transgenics or the (1,3;1,4)-β-glucanless mutant and their respective wild type grains, Torrens or Akashinriki, in different grain tissues are listed in the shaded boxes. In *CslF6* transgenic grain at 15 DAP, perturbed ETC cell wall morphology may result in excessive accumulation of fluids in the cavity and subsequently lead to ETC ruptures (dotted brown line), following a direct flow of fluids from the cavity to the endosperm (red arrow). At maturity, there is a substantial loss in fluids in the transgenic cavity during the normal desiccation process, causing the grain to shrivel. The (1,3;1,4)-β-glucanless grain develops similarly to the wild type Akashinriki grain. Red font indicates unanswered questions. * indicates a comparison of cell wall polysaccharide content based on intensities from the fluorescent labelling method. Abbreviations: pericarp (p), nucellar projection (np), day after pollination (DAP), (1,3;1,4)-β-glucan (BG), arabinoxylan (AX).

Future Directions

Many of the consequences of altering (1,3;1,4)-β-glucan content in developing barley grain have been revealed as a result of this research. However, there are a number of outstanding questions that are yet to be addressed and which could form the basis for future work;

What are the complement of genes and proteins involved in regulating carbon partitioning during barley grain development?

To test the molecular basis of regulatory mechanisms many researchers have used RNA sequencing and proteomics profiling approaches. For example, regulatory mechanisms that change during plant development (Wang et al., 2016; Xu et al., 2016; Yu et al., 2016), the effects of pathogen infection (Blackman et al., 2015; Schaker et al., 2016), altered hormone levels (Yuan et al., 2016; Saini et al., 2017) and abiotic stress (Jin et al., 2016) have been reported. A similar approach could be used to determine the complement of genes and proteins involved in regulating carbon partitioning during barley grain development with and without modified *CslF6* function. Here we have demonstrated the key changes in plant growth, cell wall components and transcript of other cell wall-related genes that occur in *CslF6* transgenic grains and in grains of a betaglucanless mutant. However, global gene and protein profiling would provide the data needed to narrow down the which pathways of cell-wall signalling are involved and possibly identify the interactions between regulatory pathways for carbohydrate metabolism that change as a result of modified (1,3;1,4)-β-glucan in barley grain. It is likely that these are co-ordinately regulated by a suite of transcription factors so identification of one or more of these would be a key step forward.

Which metabolite and hormone changes are key in regulating carbon flux during grain development?

The regulation of hormones and metabolites influence plant tissue composition. Previous transcriptome profiling and sugar composition analyses from various plant tissues have demonstrated the effects of hormones on carbohydrate storage (Zhu et al., 2011; Chen and Wang, 2012; Chandrasekaran et al., 2014). For example, exogenous application of the hormone abscisic acid (ABA) to developing wheat kernels increased grain filling rate and starch content (Yang et al., 2014). A previous study of a barley shrunken endosperm mutant, *seg8*, revealed that spatio-temporal changes in the balance of gibberellin : abscisic acid (GA : ABA) impairs the differentiation of the nucellar projection during early grain development and potentially compromises the transfer of signals and assimilates from maternal to filial tissues. These observations reveal the influence of GA and ABA on endosperm differentiation (Sreenivasulu et al., 2010; Weier et al., 2014). To analyse a broader range of metabolites affected by (1,3;1,4)-β-glucan levels, future studies could test metabolite levels in developing grain using gas chromatography-mass spectrometry (GC-MS) (Weichert et al., 2010; Thiel et al., 2012b) and hormone levels could be similarly profiled (Sreenivasulu et al., 2008; Barrero et al., 2013).

Is there a dependent relationship in barley grain for the relative amounts (1,3;1,4)-β-glucan, starch and fructan in barley grain?

In many cases, high (1,3;1,4)-β-glucan in barley grain is associated with a low amount of starch (Munck et al., 2004; Clarke et al., 2008; Burton et al., 2011), whereas the amount of starch is not necessarily altered when the amount of (1,3;1,4)-β-glucan is decreased (Taketa et al., 2012; Hu et al., 2014; Han et al., 2017). However, information about the association between (1,3;1,4)-β-glucan and fructan in barley grain is limited. Our findings here support observations

by Clarke et al., (2008), that barley grain with high (1,3;1,4)-β-glucan contains a greater amount of fructans. However, high fructan content has also been observed in barley grain with low levels of (1,3;1,4)-β-glucan (Hu et al., 2014). Fructan can function as a scavenger for reactive oxygen species (Matros et al., 2015) and aid in plant stress tolerance (Vereyken et al., 2001; Valluru and Van den Ende, 2008) and is likely to be important in the ETL in particular. Here, it is difficult to determine whether the changes in the fructan amounts in transgenic Torrens grain and in the OUM125 mutant were simply a response to stress. To explore this further a correlation pattern analysis of fructan and other polysaccharides, for example, (1,3;1,4)-β-glucan, could be conducted using diverse barley cultivars containing a range of fructan contents in the grain under controlled environmental conditions. The fructan pathway is also defined providing the option to downregulate one of the enzymes using a CRISPR/Cas9 approach (Bikard and Marraffini, 2013; Bortesi and Fischer, 2015; Schaeffer and Nakata, 2015) to study the effects directly on grain from the edited plants. Fructans have been poorly studied overall in barley and as compounds that have considerable prebiotic potential (Pool-Zobel et al., 2002; Abrams et al., 2005; Kolida and Gibson, 2007; Van De Wiele et al., 2007) deserve to be more closely examined.

How can the composition and control of cell wall biosynthesis be more comprehensively examined in the endosperm transfer cells using the CslF6 transgenic lines?

In barley, the endosperm transfer cells (ETCs) have a different cell wall morphology and wall composition compared to other grain tissues. Using a combined approach of laser-microdissection and transcriptome sequencing, transcript profiles of genes related to cell wall biosynthesis, sugar transports and metabolites (Thiel et al., 2008; Thiel et al., 2012b) and cellularisation and differentiation of ETCs in barley grain have been reported (Thiel et al., 2008;

Thiel et al., 2012a). The wall composition in ETCs has previously been described in wheat grain, however the author examined only the (1,3;1,4)-β-glucan and arabinoxylan, whilst other cell wall polysaccharides such as mannan, which was found to be important here in the barley ETCs, were not reported (Robert et al., 2011; Wilson et al., 2012). Our study showed an abundance of mannan in the cell walls of ETCs in barley grain during early grain filling, between 8 to 10 DAP, whilst no other cell wall polysaccharides were detected. A precise deposition of the cell wall polysaccharides in ETCs could be achieved using immunogold labelling and transmission electron microscopy (TEM). However, examination of cell wall morphology in ETCs using TEM is likely to be technically challenging for *CslF6* transgenic samples due to the beam of high-energy electrons which is likely to cause the wall to tear apart. In addition, the scanning electron microscope (SEM) could be used to visualise the differences in cell wall morphology in the ETCs. Again, dehydration of transgenic grain, particularly in the central cavity, may cause the ETCs walls to collapse and lead to the appearance of artefacts.

Using a laser-assisted microdissection approach as described in Thiel's studies, cells in the ETL of the *CslF6* transgenic grain can be specifically isolated for transcriptome and proteomic analysis. This would allow us to identify genes and proteins associated with cell wall biosynthesis, hormone receptors and sugar transporters in the transgenic grain. Furthermore, the transcriptome analysis from Thiel's study was performed up to 12 DAP (Thiel et al., 2012a; Thiel et al., 2012b), whilst previous analysis from immunolabeling detected a strong gold-labelling with the arabinoxylan in the ETCs at 24 DAP (Wilson et al., 2012), hence it would be of interest to extend the transcriptome analysis of ETCs up to the late storage phase.

How can Brachypodium distachyon be further explored as a model for thick cell walls with very high (1,3;1,4)-β-glucan content?

In contrary to wheat and barley grain, which predominantly store starch, *Brachypodium distachyon* contains a greater proportion of (1,3;1,4)-β-glucan than starch and has a much thicker wall. A comparison of transcript profiles between barley and *B. distachyon* showed a lower abundance of starch metabolic transcripts, including *SS 1* and *SBE 1* and lower activities of starch biosynthetic enzymes, AGPase and SS across development whilst no difference in the abundance of *CslF6* transcripts was found (Trafford et al., 2012). In addition, *B. distachyon* contains only B-type granules (Chen et al., 2014). Trafford et al. suggest that the thick cell walls in *B. distachyon* are a result of smaller cells, most likely due to lower starch accumulation (Trafford et al., 2012). A greater proportion of (1,3;1,4)-β-glucan in *B. distachyon* implies that the carbon source is preferentially acquired for the biosynthesis of (1,3;1,4)-β-glucan rather than starch, although we are still not aware of the key switch between the starch and (1,3;1,4)-β-glucan synthesis pathways. Therefore, it would be of interest to investigate the effects of an overexpression of starch metabolic genes in *B. distachyon*, particularly on starch and (1,3;1,4)-β-glucan metabolism, as well as the impact on grain morphology. An overexpression of a fructosyltransferase gene, *6-SFT*, from wheat and timothy grass respectively, increases the fructan accumulation (about 8-fold) in transgenic *B. distachyon* under cold conditions (Tamura et al., 2014). Whether the increased amount of fructan in transgenic *B. distachyon* affected the starch and (1,3;1,4)-β-glucan, cell size and wall thickness, was not reported, and should be considered for future study.

Malformed endosperm transfer cells (ETCs) in maize

Poor formation of endosperm transfer cells has been reported in several maize maternal-effect mutants (Chettoor et al., 2016) such as *Maternally expressed gene1 (Meg1)* RNAi transgenic lines (Costa et al., 2012), *baseless1 (bsl1)* (Gutiérrez-Marcos et al., 2006), *empty pericarp4 (emp4)* (Gutiérrez-Marcos et al., 2007) and *globby1* (Costa et al., 2003). The poorly formed ETCs in the maize mutants was identified by using a GUS reporter system directed by the promoter of basal ETC-specific gene, *BET1* (Chettoor et al., 2016) or mRNA *in situ* hybridisation of basal ETC gene (Gutiérrez-Marcos et al., 2006). As a result of the poorly formed ETCs, the mutants have shrunken endosperm due to deficiencies in grain filing and carbon partitioning (Maitz et al., 2000; Costa et al., 2003; Gutiérrez-Marcos et al., 2006; Gutiérrez-Marcos et al., 2007; Chettoor et al., 2016). In barley, a detailed examination of ETCs, particularly in shrunken grain, is somewhat lacking (Felker et al., 1985), so the use of a similar GUS reporter system or mRNA *in situ* hybridisation using a barley ETC-specific marker, such as *END1* (Doan et al., 1996; Li et al., 2008) could help us to examine the malformed ETCs in barley mutants and provide more information about the role of ETCs in mediating barley grain development.

The use of labelled sucrose to track the movement of carbon

In Chapter 3, an increased amount of sucrose in the cavity of *CslF6* transgenic grain suggests that these grain have a greater sink strength compared to the wild type grain. In a previous study the endosperm tissue was directly exposed to the labelled sucrose solution and uptake measured using a scintillation counter (Wardlaw et al., 1995). However, this method does not represent the actual biological system since the tissue was excised as the uptake of labelled sucrose did not rely on the vascular transport system. Instead of exposing the endosperm directly to the

sucrose solutions, entire barley spikes could be used, however, this would also depend on the efficiency of the transporter activities in the phloem, such as the SWEET transporter (Ruan, 2014). An increased amount of fructan in the cavity could be due to higher fructan uptake or conversion of sucrose into fructans. One possible way to test this is to supply the barley spikes with [13C]sucrose and the labelled sugars can be separated and quantified using a HPLC coupled to a triple quadrupole mass spectrometer (TQMS) in multiple reaction monitoring (MRM) mode (Ross et al., 2004; Song et al., 2012; Garcia et al., 2013; Luo et al., 2015).

Concluding Remarks

This project provides one physiological explanation for the occurrence of a large cavity in the transgenic barley grain with increased (1,3;1,4)-β-glucan levels which significantly contributes to the shrunken grain phenotype. Our research findings demonstrate that marked changes in the cell wall structure of cells in the endosperm transfer layer occurred as a result of overexpressing the *CslF6* gene in the hull-less grain cultivar Torrens. Our fluorescence immunolabeling results showed that mannan is predominantly accumulated in the cell walls of the endosperm transfer layer and supports the structural integrity of this tissue during the grain storage phase, aligned with the specific role the endosperm transfer cells have in nutrient transfer during grain development (Thiel, 2014). However, we showed that poor formation of this layer does not affect the sucrose availability for carbohydrate synthesis in the endosperm. We also found that an increased level of (1,3;1,4)-β-glucan in hull-less barley grain introduced via a transgenic approach displays a more drastic change in carbon flow compared to a mutant grain with a severely reduced level of (1,3;1,4)-β-glucan. Overall, *CslF6* over-expressing transgenic and *betaglucanless* mutant plants provide ideal tools to study how changes in metabolic pathways have an influence on the carbon partitioning taking place in the barley grain during development and maturation.

References

Abrams SA, Griffin IJ, Hawthorne KM, Liang L, Gunn SK, Darlington G, Ellis KJ (2005) A combination of prebiotic short-and long-chain inulin-type fructans enhances calcium absorption and bone mineralization in young adolescents. The American Journal of Clinical Nutrition **82:** 471-476

Adams CA, Rinne RW (1980) Moisture content as a controlling factor in seed development and germination. International Review of Cytology **68:** 1-8

Andersson A, Andersson R, Autio K, Åman P (1999) Chemical composition and microstructure of two naked waxy barleys. Journal of Cereal Science **30:** 183-191

Annison G (1993) The role of wheat non-starch polysaccharides in broiler nutrition. Crop and Pasture Science **44:** 405-422

Arena MP, Caggianiello G, Fiocco D, Russo P, Torelli M, Spano G, Capozzi V (2014) Barley β-glucans-containing food enhances probiotic performances of beneficial bacteria. International Journal of Molecular Sciences **15:** 3025-3039

Ayre BG (2011) Membrane-transport systems for sucrose in relation to whole-plant carbon partitioning. Molecular Plant **4:** 377-394

Bamforth C (1994) -Glucan and -glucanases in malting and brewing: Practical Aspects. Brewers Digest **69:** 12-12

Barrero JM, Mrva K, Talbot MJ, White RG, Taylor J, Gubler F, Mares DJ (2013) Genetic, hormonal, and physiological analysis of late maturity α-amylase in wheat. Plant Physiol **161:** 1265-1277

Behall KM, Scholfield DJ, Hallfrisch JG, Liljeberg-Elmstahl HG (2006) Consumption of both resistant starch and beta-glucan improves postprandial plasma glucose and insulin in women. Diabetes Care **29:** 976-981

Bhatty R (1999) The potential of hull-less barley. Cereal Chemistry **76:** 589-599

Bikard D, Marraffini LA (2013) Control of gene expression by CRISPR-Cas systems. F1000prime reports **5**

Blackman LM, Cullerne DP, Torreña P, Taylor J, Hardham AR (2015) RNA-Seq analysis of the expression of genes encoding cell wall degrading enzymes during Infection of Lupin (Lupinus angustifolius) by Phytophthora parasitica. PLoS ONE **10:** e0136899

Bortesi L, Fischer R (2015) The CRISPR/Cas9 system for plant genome editing and beyond. Biotechnology advances **33:** 41-52

Box A, Washington J, Eglinton J (2005) Progress in developing a hulless barley industry.

Buckeridge MS, Pessoa dos Santos H, Tiné MAS (2000) Mobilisation of storage cell wall polysaccharides in seeds. Plant Physiology and Biochemistry **38:** 141-156

Burton RA, Collins HM, Kibble NA, Smith JA, Shirley NJ, Jobling SA, Henderson M, Singh RR, Pettolino F, Wilson SM, Bird AR, Topping DL, Bacic A, Fincher GB (2011) Over-expression of specific HvCslF cellulose synthase-like genes in transgenic barley increases the levels of cell wall (1,3;1,4)-beta-d-glucans and alters their fine structure. Plant Biotechnol J **9:** 117-135

Carciofi M, Blennow A, Jensen SL, Shaik SS, Henriksen A, Buléon A, Holm PB, Hebelstrup KH (2012) Concerted suppression of all starch branching enzyme genes in barley produces amylose-only starch granules. BMC Plant Biol **12:** 223

Cavallero A, Empilli S, Brighenti F, Stanca AM (2002) High (1→3,1→4)-β-glucan barley fractions in bread making and their effects on human glycemic response. Journal of Cereal Science **36:** 59-66

Chandrasekaran U, Xu W, Liu A (2014) Transcriptome profiling identifies ABA mediated regulatory changes towards storage filling in developing seeds of castor bean (Ricinus communis L.). Cell & Bioscience **4:** 33-33

Chen G, Zhu J, Zhou J, Subburaj S, Zhang M, Han C, Hao P, Li X, Yan Y (2014) Dynamic development of starch granules and the regulation of starch biosynthesis in Brachypodium distachyon: comparison with common wheat and Aegilops peregrina. BMC Plant Biol **14:** 198

Chen H-J, Wang S-J (2012) Abscisic acid enhances starch degradation and sugar transport in rice upper leaf sheaths at the post-heading stage. Acta Physiologiae Plantarum **34:** 1493-1500

Chen J, Raymond K (2008) Beta-glucans in the treatment of diabetes and associated cardiovascular risks. Vasc Health Risk Manag **4:** 1265-1272

Chettoor AM, Phillips AR, Coker CT, Dilkes B, Evans MMS (2016) Maternal gametophyte effects on seed development in maize. Genetics **204:** 233

Clarke B, Liang R, Morell M, Bird A, Jenkins C, Li Z (2008) Gene expression in a starch synthase IIa mutant of barley: changes in the level of gene transcription and grain composition. Functional & integrative genomics **8:** 211-221

Cochrane MP (1985) Assimilate uptake and water loss in maturing barley grains. J Exp Bot **36:** 770-782

Costa LM, Gutierrez-Marcos JF, Brutnell TP, Greenland AJ, Dickinson HG (2003) The globby1-1 (glo1-1) mutation disrupts nuclear and cell division in the developing maize seed causing alterations in endosperm cell fate and tissue differentiation. Development **130:** 5009-5017

Costa Liliana M, Yuan J, Rouster J, Paul W, Dickinson H, Gutierrez-Marcos Jose F (2012) Maternal control of nutrient allocation in plant seeds by genomic imprinting. Current Biology **22:** 160-165

Craig J, Lloyd JR, Tomlinson K, Barber L, Edwards A, Wang TL, Martin C, Hedley CL, Smith AM (1998) Mutations in the gene encoding starch synthase II profoundly alter amylopectin structure in pea embryos. The Plant Cell **10:** 413-426

Delaney B, Nicolosi RJ, Wilson TA, Carlson T, Frazer S, Zheng G-H, Hess R, Ostergren K, Haworth J, Knutson N (2003) β-Glucan fractions from barley and oats are similarly antiatherogenic in hypercholesterolemic Syrian Golden hamsters. J Nutr **133:** 468-475

Doan DNP, Linnestad C, Olsen O-A (1996) Isolation of molecular markers from the barley endosperm coenocyte and the surrounding nucellus cell layers. Plant Molecular Biology **31:** 877-886

El Khoury D, Cuda C, Luhovyy BL, Anderson GH (2012) Beta glucan: health benefits in obesity and metabolic syndrome. J Nutr Metab **2012:** 851362

Eveland AL, Jackson DP (2012) Sugars, signalling, and plant development. J Exp Bot **63:** 3367-3377

Felker FC, Peterson DM, Nelson OE (1985) Anatomy of immature grains of eight maternal effect shrunken endosperm barley mutants. American Journal of Botany**:** 248-256

Garcia AD, Chavez JL, Mechref Y (2013) Sugar nucleotide quantification using multiple reaction monitoring liquid chromatography/tandem mass spectrometry. Rapid Communications in Mass Spectrometry **27:** 1794-1800

Gutiérrez-Marcos JF, Costa LM, Evans MM (2006) Maternal gametophytic baseless1 is required for development of the central cell and early endosperm patterning in maize (Zea mays). Genetics **174:** 317-329

Gutiérrez-Marcos JF, Dal Prà M, Giulini A, Costa LM, Gavazzi G, Cordelier S, Sellam O, Tatout C, Paul W, Perez P (2007) empty pericarp4 encodes a mitochondrion-targeted pentatricopeptide repeat protein necessary for seed development and plant growth in maize. The Plant Cell **19:** 196-210

Han N, Na C, Chai Y, Chen J, Zhang Z, Bai B, Bian H, Zhang Y, Zhu M (2017) Over-expression of (1, 3; 1, 4)-β-D-glucanase isoenzyme EII gene results in decreased (1, 3; 1, 4)-β-D-glucan content and increased starch level in barley grains. Journal of the Science of Food and Agriculture **97:** 122-127

Handford MG, Baldwin TC, Goubet F, Prime TA, Miles J, Yu X, Dupree P (2003) Localisation and characterisation of cell wall mannan polysaccharides in Arabidopsis thaliana. Planta **218:** 27-36

Hu G, Burton C, Hong Z, Jackson E (2014) A mutation of the cellulose-synthase-like (CslF6) gene in barley (Hordeum vulgare L.) partially affects the β-glucan content in grains. Journal of Cereal Science **59:** 189-195

Jin H, Dong D, Yang Q, Zhu D (2016) Salt-responsive transcriptome profiling of Suaeda glauca via RNA sequencing. PLoS ONE **11:** e0150504

Kolida S, Gibson GR (2007) Prebiotic capacity of inulin-type fructans. The Journal of Nutrition **137:** 2503S-2506S

Li M, Singh R, Bazanova N, Milligan AS, Shirley N, Langridge P, Lopato S (2008) Spatial and temporal expression of endosperm transfer cell-specific promoters in transgenic rice and barley. Plant Biotechnol J **6:** 465-476

Luo P, Dai W, Yin P, Zeng Z, Kong H, Zhou L, Wang X, Chen S, Lu X, Xu G (2015) Multiple reaction monitoring-ion pair finder: a systematic approach to transform nontargeted mode to pseudotargeted mode for metabolomics study based on liquid chromatography–mass spectrometry. Analytical Chemistry **87:** 5050-5055

Ma J, Jiang Q-T, Wei L, Wang J-R, Chen G-Y, Liu Y-X, Li W, Wei Y-M, Liu C, Zheng Y-L (2014) Characterization of shrunken endosperm mutants in barley. Gene **539:** 15-20

Maitz M, Santandrea G, Zhang Z, Lal S, Hannah LC, Salamini F, Thompson RD (2000) rgf1, a mutation reducing grain filling in maize through effects on basal endosperm and pedicel development. The Plant Journal **23:** 29-42

Matros A, Peshev D, Peukert M, Mock H-P, Van den Ende W (2015) Sugars as hydroxyl radical scavengers: proof-of-concept by studying the fate of sucralose in Arabidopsis. The Plant Journal **82:** 822-839

McCleary BV, Amado R, Waibel R, Neukom H (1981) Effect of galactose content on the solution and interaction properties of guar and carob galactomannans. Carbohydr Res **92:** 269-285

McMaugh SJ, Thistleton JL, Anschaw E, Luo J, Konik-Rose C, Wang H, Huang M, Larroque O, Regina A, Jobling SA (2014) Suppression of starch synthase I expression affects the granule morphology and granule size and fine structure of starch in wheat endosperm. J Exp Bot**:** eru095

McNab J, Smithard R (1992) Barley β-glucan: An antinutritional factor in poultry feeding. Nutrition research reviews **5:** 45-60

Morell MK, Kosar-Hashemi B, Cmiel M, Samuel MS, Chandler P, Rahman S, Buleon A, Batey IL, Li Z (2003) Barley sex6 mutants lack starch synthase IIa activity and contain a starch with novel properties. The Plant Journal **34:** 173-185

Munck L, Møller B, Jacobsen S, Søndergaard I (2004) Near infrared spectra indicate specific mutant endosperm genes and reveal a new mechanism for substituting starch with (1→ 3, 1→ 4)-β-glucan in barley. Journal of Cereal Science **40:** 213-222

Pool-Zobel B, Van Loo J, Rowland I, Roberfroid M (2002) Experimental evidences on the potential of prebiotic fructans to reduce the risk of colon cancer. British Journal of Nutrition **87:** S273-S281

Queenan KM, Stewart ML, Smith KN, Thomas W, Fulcher RG, Slavin JL (2007) Concentrated oat β-glucan, a fermentable fiber, lowers serum cholesterol in hypercholesterolemic adults in a randomized controlled trial. Nutrition Journal **6:** 6

Reid JG (1971) Reserve carbohydrate metabolism in germinating seeds of Trigonella foenum-graecum L.(Leguminosae). Planta **100:** 131-142

Robert P, Jamme F, Barron C, Bouchet B, Saulnier L, Dumas P, Guillon F (2011) Change in wall composition of transfer and aleurone cells during wheat grain development. Planta **233:** 393-406

Rodríguez-Gacio MdC, Iglesias-Fernández R, Carbonero P, Matilla ÁJ (2012) Softening-up mannan-rich cell walls. J Exp Bot **63:** 3976-3988

Rolland F, Baena-Gonzalez E, Sheen J (2006) Sugar sensing and signaling in plants: conserved and novel mechanisms. Annu. Rev. Plant Biol. **57:** 675-709

Ross AR, Ambrose SJ, Cutler AJ, Feurtado JA, Kermode AR, Nelson K, Zhou R, Abrams SR (2004) Determination of endogenous and supplied deuterated abscisic acid in plant tissues by high-performance liquid chromatography-electrospray ionization tandem mass spectrometry with multiple reaction monitoring. Analytical biochemistry **329:** 324-333

Ruan Y-L (2014) Sucrose metabolism: gateway to diverse carbon use and sugar signaling. Annual review of plant biology **65:** 33-67

Saini K, Markakis MN, Zdanio M, Balcerowicz DM, Beeckman T, De Veylder L, Prinsen E, Beemster GTS, Vissenberg K (2017) Alteration in auxin homeostasis and Signaling by overexpression Of PINOID kinase causes leaf growth defects in Arabidopsis thaliana. Front Plant Sci **8**

Schaeffer SM, Nakata PA (2015) CRISPR/Cas9-mediated genome editing and gene replacement in plants: Transitioning from lab to field. Plant Science **240:** 130-142

Schaker PDC, Palhares AC, Taniguti LM, Peters LP, Creste S, Aitken KS, Van Sluys M-A, Kitajima JP, Vieira MLC, Monteiro-Vitorello CB (2016) RNAseq Transcriptional Profiling following Whip Development in Sugarcane Smut Disease. PLoS ONE **11:** e0162237

Shang X, Chai Q, Zhang Q, Jiang J, Zhang T, Guo W, Ruan Y-L (2015) Down-regulation of the cotton endo-1, 4-β-glucanase gene KOR1 disrupts endosperm cellularization, delays embryo development, and reduces early seedling vigour. J Exp Bot**:** erv111

Shen R-L, Dang X-Y, Dong J-L, Hu X-Z (2012) Effects of oat β-glucan and barley β-glucan on fecal characteristics, intestinal microflora, and intestinal bacterial metabolites in rats. Journal of agricultural and food chemistry **60:** 11301-11308

Solfanelli C, Poggi A, Loreti E, Alpi A, Perata P (2006) Sucrose-specific induction of the anthocyanin biosynthetic pathway in Arabidopsis. Plant Physiol **140:** 637-646

Song E, Pyreddy S, Mechref Y (2012) Quantification of glycopeptides by multiple reaction monitoring liquid chromatography/tandem mass spectrometry. Rapid Communications in Mass Spectrometry **26:** 1941-1954

Speers RA, Jin YL, Paulson AT, Stewart RJ (2003) Effects of β-glucan, shearing and environmental factors on the turbidity of wort and beer. Journal of the Institute of Brewing **109:** 236-244

Sreenivasulu N, Borisjuk L, Junker BH, Mock H-P, Rolletschek H, Seiffert U, Weschke W, Wobus U (2010) Barley grain development: toward an integrative view. International Review of Cell and Molecular Biology **281:** 49-89

Sreenivasulu N, Usadel B, Winter A, Radchuk V, Scholz U, Stein N, Weschke W, Strickert M, Close TJ, Stitt M (2008) Barley grain maturation and germination: metabolic pathway and regulatory network commonalities and differences highlighted by new MapMan/PageMan profiling tools. Plant Physiol **146:** 1738-1758

Taketa S, Yuo T, Tonooka T, Tsumuraya Y, Inagaki Y, Haruyama N, Larroque O, Jobling SA (2012) Functional characterization of barley betaglucanless mutants demonstrates a unique role for CslF6 in (1, 3; 1, 4)-β-D-glucan biosynthesis. J Exp Bot **63:** 381-392

Tamura K-i, Sanada Y, Tase K, Kawakami A, Yoshida M, Yamada T (2014) Comparative study of transgenic Brachypodium distachyon expressing sucrose:fructan 6-fructosyltransferases from wheat and timothy grass with different enzymatic properties. Planta **239:** 783-792

Teng S, Keurentjes J, Bentsink L, Koornneef M, Smeekens S (2005) Sucrose-specific induction of anthocyanin biosynthesis in Arabidopsis requires the MYB75/PAP1 gene. Plant Physiol **139:** 1840-1852

Thiel J (2014) Development of endosperm transfer cells in barley. Front Plant Sci **5**

Thiel J, Hollmann J, Rutten T, Weber H, Scholz U, Weschke W (2012a) 454 Transcriptome sequencing suggests a role for two-component signalling in cellularization and differentiation of barley endosperm transfer cells. PLoS ONE **7:** e41867

Thiel J, Riewe D, Rutten T, Melzer M, Friedel S, Bollenbeck F, Weschke W, Weber H (2012b) Differentiation of endosperm transfer cells of barley: a comprehensive analysis at the micro-scale. The Plant Journal **71:** 639-655

Thiel J, Weier D, Sreenivasulu N, Strickert M, Weichert N, Melzer M, Czauderna T, Wobus U, Weber H, Weschke W (2008) Different hormonal regulation of cellular differentiation and function in nucellar projection and endosperm transfer cells: a microdissection-based transcriptome study of young barley grains. Plant Physiol **148:** 1436-1452

Trafford K, Fincher G, Shewry P (2012) Barley grain carbohydrates: starch and cell walls. Barley: chemistry and technology**:** 71

Valluru R, Van den Ende W (2008) Plant fructans in stress environments: emerging concepts and future prospects. J Exp Bot **59:** 2905-2916

Van De Wiele T, Boon N, Possemiers S, Jacobs H, Verstraete W (2007) Inulin-type fructans of longer degree of polymerization exert more pronounced in vitro prebiotic effects. Journal of Applied Microbiology **102:** 452-460

Van den Ende W, El-Esawe SK (2014) Sucrose signaling pathways leading to fructan and anthocyanin accumulation: a dual function in abiotic and biotic stress responses? Environmental and experimental botany **108:** 4-13

Vereyken IJ, Chupin V, Demel RA, Smeekens SCM, De Kruijff B (2001) Fructans insert between the headgroups of phospholipids. Biochimica et Biophysica Acta (BBA) - Biomembranes **1510:** 307-320

Wang X, Chang L, Tong Z, Wang D, Yin Q, Wang D, Jin X, Yang Q, Wang L, Sun Y (2016) Proteomics profiling reveals carbohydrate metabolic enzymes and 14-3-3 proteins play important roles for starch accumulation during cassava root tuberization. Scientific reports **6:** 19643

Wardlaw I, Moncur L, Patrick J (1995) The response of wheat to high temperature following anthesis. Ii. Sucrose accumulation and metabolism by isolated kernels. Functional Plant Biology **22:** 399-407

Weichert N, Saalbach I, Weichert H, Kohl S, Erban A, Kopka J, Hause B, Varshney A, Sreenivasulu N, Strickert M, Kumlehn J, Weschke W, Weber H (2010) Increasing sucrose uptake capacity of wheat grains stimulates storage protein synthesis. Plant Physiol **152:** 698-710

Weier D, Thiel J, Kohl S, Tarkowská D, Strnad M, Schaarschmidt S, Weschke W, Weber H, Hause B (2014) Gibberellin-to-abscisic acid balances govern development and differentiation of the nucellar projection of barley grains. J Exp Bot**:** eru289

Wilson SM, Burton RA, Collins HM, Doblin MS, Pettolino FA, Shirley N, Fincher GB, Bacic A (2012) Pattern of deposition of cell wall polysaccharides and transcript abundance of related cell wall synthesis genes during differentiation in barley endosperm. Plant Physiol **159:** 655-670

Xu L, Wang J, Lei M, Li L, Fu Y, Wang Z, Ao M, Li Z (2016) Transcriptome Analysis of Storage Roots and Fibrous Roots of the Traditional Medicinal Herb Callerya speciosa (Champ.) ScHot. PLoS ONE **11:** e0160338

Yang D, Luo Y, Ni Y, Yin Y, Yang W, Peng D, Cui Z, Wang Z (2014) Effects of exogenous ABA application on post-anthesis dry matter redistribution and grain starch accumulation of winter wheat with different staygreen characteristics. The Crop Journal **2:** 144-153

Yang J-L, Kim Y-H, Lee H-S, Lee M-S, Moon YK (2003) Barley β-glucan lowers serum cholesterol based on the up-regulation of cholesterol 7α-hydroxylase activity and mRNA abundance in cholesterol-fed rats. Journal of nutritional science and vitaminology **49:** 381-387

Yu T, Li G, Dong S, Liu P, Zhang J, Zhao B (2016) Proteomic analysis of maize grain development using iTRAQ reveals temporal programs of diverse metabolic processes. BMC Plant Biol **16:** 241

Yuan S, Huang Y, Liu S, Guan C, Cui X, Tian D, Zhang Y, Yang F (2016) RNA-seq analysis of overexpressing ovine AANAT gene of melatonin biosynthesis in switchgrass. Front Plant Sci **7**

Zhu G, Ye N, Yang J, Peng X, Zhang J (2011) Regulation of expression of starch synthesis genes by ethylene and ABA in relation to the development of rice inferior and superior spikelets. J Exp Bot

Appendices

Appendix 1 Absolute transcript levels of metabolic genes related to cell walls, starch, sucrose and fructan, and lipid transfer protein in wild type Torrens (WT), wild type from tissue culture (WT(tc)) and *CslF6* transgenic barley grain.

Appendix 2: Absolute transcript levels of metabolic genes related to cell walls, starch, sucrose and fructan in wild type Akashinriki (WT) and a (1,3;1,4)-β-glucanless mutant grain (OUM125).

Line	DAP	Tissue	*CslF6 transgene*	*CslF6 total*	*CslH1*	*CslF9*	*Endo E1*	*Ces A2*	*CslF6 transgene*	*CslF6 total*	*CslH*	*CslF9*	*Endo E1*	*Ces A2*
WT Torrens	7	pericarp	56.54606492	129779.5411	1454.083677	111827.7093	107.2699141	3378208.356	11.13254104	618.0325978	270.2334643	8364.46741	54.62176628	52743.28743
WT Torrens	11	pericarp	97.94907272	143411.9098	3753.52286	116045.2886	9316.667304	10273748.04	30.24115079	13398.09712	638.0888293	12348.93352	731.5838852	543495.1963
WT Torrens	15	pericarp	96.07496981	114108.9963	5504.824059	50139.10165	72557.17254	5067905.74	41.61880608	3896.867095	398.8682583	5243.156587	2937.490575	96906.7006
WT Torrens	19	pericarp	1765.509109	130444.6233	8136.220229	4373.364568	123692.3792	9590369.795	2614.566628	10666.37105	448.1241346	546.3038709	709.1028852	879367.0989
WT Torrens	24	pericarp	680.135598	38044.70415	2557.690571	1820.330492	265954.5505	27538556.3	497.4940837	1778.364732	885.8678814	962.0645976	11239.26618	2333113.099
WT Torrens	7	endosperm	23.00443145	24592.43862	3489.675316	900790.173	187.8498212	1342989.093	6.593031753	2506.925217	93.59080057	65446.97462	16.78278735	79475.05544
WT Torrens	11	endosperm	19.64533638	56938.18837	1142.027211	453737.3139	22037.14377	930556.0735	8.685898015	338.3675244	37.22681197	18837.54412	1130.443266	58647.32939
WT Torrens	15	endosperm	40.91018098	68915.55845	1050.434258	122265.3373	32052.66624	925386.9911	16.73014154	922.3749695	82.85984415	26878.4688	1556.681116	50336.96632
WT Torrens	19	endosperm	174.165826	156578.3974	2890.955011	7754.353286	11445.54201	1760514.178	59.38161245	6699.09622	233.9361288	1434.144604	876.2650611	99243.1934
WT Torrens	24	endosperm	1.547325948	98078.18988	7489.263464	2830.444406	2247.829427	3366142.073	1.032254746	2688.362999	1153.469052	281.4594492	128.1989331	299110.352
WT Torrens	15	embryo	39.64310421	21925.18963	246.9956812	9492.802	1818.710285	1390603.528	14.32015297	194.9537533	36.78023391	1439.226308	66.93750602	60389.32855
WT Torrens	19	embryo	28.08006354	12836.19509	308.522713	3330.796716	10089.6357	1144026.842	23.20925914	236.5035184	36.67759068	185.3247232	25.46777481	96519.08731
WT Torrens	24	embryo	1.781063505	7827.129213	393.2934519	1645.347788	3546.378429	2055147.775	0.119517695	953.8605706	28.64703324	297.9356075	138.7588707	275299.7228
WT(tc)	7	pericarp	374.1233404	483300.726	8733.086792	1013799.867	1065.000486	24815049.56	153.334299	15123.58419	1144.993774	42837.35603	199.2385617	1533077.073
WT(tc)	11	pericarp	157.647104	216140.0817	3261.720598	577845.0041	12883.93261	6419349.527	67.48348316	5099.883746	592.0203977	20162.51333	277.8176536	604975.5597
WT(tc)	15	pericarp	68.04023063	144939.7542	3498.022014	175584.6295	203254.8887	7383377.025	64.63077846	10377.35613	311.7228411	25808.06975	18335.64589	368210.6724
WT(tc)	19	pericarp	385.3730568	93194.63755	6279.193836	6157.488816	250735.8969	29036462.18	69.48924118	5102.99177	563.9062884	316.5956991	20857.15479	2318702.322
WT(tc)	24	pericarp	1117.612127	25827.0374	1032.672697	2485.727439	597528.4506	10073498.45	1308.729505	2497.244088	483.2090249	705.8174046	84877.16433	1378806.054
WT(tc)	7	endosperm	35.13381413	32694.26223	3152.34279	1988786.964	483.0162181	673135.6181	19.62606116	1137.0036	237.8131336	102799.0207	77.59750489	17646.15482
WT(tc)	11	endosperm	32.00479134	47978.96409	600.3955859	1147920.235	9179.034366	677820.4633	4.41497048	1840.342152	83.31372219	61501.5787	1227.827857	39498.3102
WT(tc)	15	endosperm	75.95212156	82619.66076	202.917441	208664.7117	59600.60753	964589.4757	71.58500672	11055.29441	18.23323304	23166.18444	1533.324824	68728.99864
WT(tc)	19	endosperm	50.31276947	177535.7539	1426.796407	4459.241679	56656.72837	1619547.421	38.40392786	20490.47217	217.1741441	437.3504986	5050.952706	209282.3917
WT(tc)	24	endosperm	471.8847267	322968.7234	16010.12409	2821.566379	16130.39546	9060443.332	184.1293326	44969.44549	4930.328031	1685.586003	4377.226685	892631.8333
WT(tc)	15	embryo	174.8129613	11230.64681	139.9735008	26528.06355	2067.930276	2395939.726	136.8961264	1940.150449	81.3387932	3181.522795	285.4700369	146563.3473
WT(tc)	19	embryo	19.32847424	11477.1907	154.8305556	5471.478923	17133.35904	367130.8141	4.906241323	578.2145416	33.97361578	88.37405771	1230.38577	13392.64831
WT(tc)	24	embryo	14.46689599	5668.881201	424.0864403	1188.026072	2506.021415	611020.0909	6.929455755	642.7220925	90.18740698	302.604178	288.3519358	76490.94857
F6-15-3	7	pericarp	225.2651242	195137.883	2640.564087	71112.10399	142.5432023	10949775.37	22.16185919	21836.99868	469.334324	18694.86722	4.260635319	1034248.338
F6-15-3	11	pericarp	1199.851199	307721.3695	3801.065007	170468.6751	3932.136214	8727651.154	71.03953686	23319.82088	170.7316343	24159.05757	547.5803711	1071557.247
F6-15-3	15	pericarp	1173.761426	247304.0323	5909.193244	19001.98591	670537.6582	23578514.41	25.19348556	21585.41128	554.9918152	6666.276607	69974.40933	2048207.753
F6-15-3	19	pericarp	995.1637877	173795.117	2860.398717	3947.987645	180906.2754	11123883.45	103.3864626	24055.27431	1143.422353	353.0464256	28860.54486	401422.7639
F6-15-3	24	pericarp	1014.626389	55579.51729	3329.195932	1712.844075	777255.5335	20585006.4	187.3643922	7603.107802	754.2335327	598.9656188	115170.4012	2142503.892
F6-15-3	7	endosperm	647.0354344	52981.9803	3916.199346	516302.3497	26.55214054	632488.0798	41.42137675	6306.525622	506.5466681	45145.77227	8.027866147	87281.208
F6-15-3	11	endosperm	1631.235138	377405.4903	1144.011683	255668.4435	6466.033309	803918.7007	132.2266371	42721.05975	169.4210457	34663.64257	700.1811541	75798.59056
F6-15-3	15	endosperm	1083.510057	339334.0729	3807.317891	60367.81489	16922.18376	3751812.573	86.88325834	9218.124957	213.4824918	1996.330559	884.7996403	232642.0017
F6-15-3	19	endosperm	727.9781567	252856.7161	5344.142825	6140.090825	14277.56059	1814661.32	212.5885173	15242.70831	489.6706101	1190.374289	744.0033154	232443.5743
F6-15-3	24	endosperm	748.8120185	168261.2245	17714.15023	2176.195379	1877.197904	3894877.161	160.6649877	23686.52968	2325.883141	848.7781175	191.696551	378186.6852
F6-15-3	15	embryo	6.128746997	15041.73841	199.0337009	5291.200819	3528.035426	2592188.374	6.208604885	1370.685935	94.05853189	1795.153681	191.5667903	240688.4086
F6-15-3	19	embryo	6.661446847	12856.35437	258.9752606	3480.42989	4780.370898	1498708.475	6.023930808	1239.754976	77.10616892	687.7457109	474.5303307	119858.8281
F6-15-3	24	embryo	8.461219847	6799.999467	183.0922063	2349.749605	2096.522875	1014718.839	4.095219659	651.2566048	9.303260927	122.636579	116.1590609	80173.22561
F6-16-5	7	pericarp	3356.845848	386105.3351	1652.885849	88595.68337	145.5068801	7393228.375	459.6587672	16473.54876	494.4395819	10793.68056	29.33960071	889100.6965
F6-16-5	11	pericarp	5519.038187	369470.8504	2283.841295	43364.5713	1477.344529	5399506.382	540.9149587	16333.6614	510.9471304	8077.070016	80.23019632	526314.4416
F6-16-5	15	pericarp	7615.583578	808779.9172	5762.382102	131572.4102	734195.0257	9113341.43	995.8087949	40388.41927	184.7921768	14390.68004	41555.88025	831156.8226
F6-16-5	19	pericarp	4739.901665	361292.8481	2304.622003	2809.292298	83574.09269	15843767.48	349.2608175	6259.996673	483.126767	516.9893804	9424.856924	1504881.424
F6-16-5	24	pericarp	2324.468123	82977.22965	3681.83186	844.8499276	148238.2428	5729499.806	586.9146234	11167.71475	918.0937454	471.5281031	10806.06659	357160.0883
F6-16-5	7	endosperm	899.5558472	80968.14132	1666.836004	397293.6887	32.48260864	200665.4688	45.75670822	7882.724191	233.0580599	70995.1822	2.014116337	22206.92371
F6-16-5	11	endosperm	2438.260255	335108.0119	967.4362823	233040.2377	6124.677546	872487.7392	147.6792225	40223.47448	194.6661345	44376.13868	1636.663601	49278.06041
F6-16-5	15	endosperm	4039.889332	434007.3553	3485.592328	41107.96156	5123.647954	2093730.955	372.1664942	69782.30677	555.5869382	7586.564553	606.9192856	1527.066897
F6-16-5	19	endosperm	1158.158224	278317.3768	14123.07574	21428.49431	429.0466454	1669390.828	46.05591189	7155.055092	719.8906708	441.7783621	90.40766391	116083.4015
F6-16-5	24	endosperm	708.4776889	114936.5428	18288.59251	3035.359976	682.8235619	2426925.815	17.19475476	6842.590437	2043.438651	93.8258979	146.7811301	151122.6885
F6-16-5	15	embryo	303.2031569	27661.96449	199.2733027	16392.02084	2656.519428	1844588.908	19.86317555	3145.586561	13.34927359	966.1890255	469.4363592	80055.02219
F6-16-5	19	embryo	127.0910998	17426.47259	186.5220071	3325.949862	4105.343882	691437.4609	9.629565487	4256.333876	7.577262495	441.1436894	729.9600963	36542.01193
F6-16-5	24	embryo	192.3305241	15237.32605	268.2396733	1658.853786	1366.89552	1446037.926	35.27755882	847.0130583	35.93465135	194.683391	235.8743671	78765.96989
F6-18-6	7	pericarp	3973.634687	338093.4844	1261.11905	47102.66596	146.0208755	8107193.891	296.6396728	11830.46397	130.0695584	5717.717829	13.51778294	552865.0437
F6-18-6	11	pericarp	2377.305526	350480.6333	5182.117128	40512.70621	1554.635138	5922632	65.47030228	26088.43392	526.4566374	976.0892726	236.3584193	276078.9866
F6-18-6	15	pericarp	5258.649996	630953.6587	6786.905616	48782.72907	239072.4824	13906957.46	383.9805045	2775.569053	176.5787369	3523.83164	37111.69553	1126436.905
F6-18-6	19	pericarp	12937.84249	1069049.452	1892.718613	6253.648966	107808.1855	5184384.457	1017.375236	110817.5071	930.9302534	2355.854479	7138.118209	367590.6738
F6-18-6	24	pericarp	6436.864951	826323.1945	20481.84157	39848.95422	2697487.705	238143080.3	6471.145152	154152.1166	8238.274898	N/A	120627.4736	4622577.715
F6-18-6	7	endosperm	5498.502247	398203.9927	1370.511213	449839.0691	27.69389778	356151.0179	309.2175992	14832.48791	28.82891968	22187.11759	5.228920235	7222.73051
F6-18-6	11	endosperm	9493.434035	1135065.101	1953.339107	98264.28575	2586.234709	1061188.374	748.6257309	39040.64932	119.1163584	4201.977798	392.6868642	58712.91715
F6-18-6	15	endosperm	2422.612569	627659.6777	4043.234677	86488.26717	370.0081918	527812.554	203.4117285	40156.41278	685.8610836	378.7304693	20.41075345	16537.17637
F6-18-6	19	endosperm	4034.368572	625785.2394	30385.01727	14337.36861	707.6463324	3026524.976	147.2957788	72496.87249	3457.637399	1725.989029	193.8998997	57046.93838
F6-18-6	24	endosperm	475.5970871	126630.7185	24245.60416	2904.948072	1064.105234	2473796.824	36.79074525	4398.426593	1570.735503	901.181847	46.66367371	158059.7211
F6-18-6	15	embryo	8.478635953	17529.69814	311.9494906	5197.44774	1829.027243	553041.28	7.362550165	1656.163495	90.17861572	844.6603407	196.5527491	36467.75656
F6-18-6	19	embryo	867.4538874	79235.67002	347.7953016	3585.367568	5406.299985	1854412.277	190.0629458	7606.556802	70.08875259	867.5681665	356.4230631	71968.49704
F6-18-6	24	embryo	3.04533066	8268.750274	333.0892813	1705.242531	1794.962109	1418253.993	1.587349963	465.7270612	75.22886333	200.2401358	112.5192181	81001.93154
F6-25-5	7	pericarp	2568.705867	256340.2276	2382.490897	153313.0633	110.4914774	2914224.993	244.3456451	26581.97872	495.6846412	17374.53463	20.72760956	238766.5729
F6-25-5	11	pericarp	3332.447403	357869.8842	3688.47358	32158.91214	4444.181525	8347542.334	198.5787477	53176.87838	580.0096816	5047.423433	72.20950539	948307.4275
F6-25-5	15	pericarp	6633.38928	688036.7589	16788.85923	15658.2703	594833.9954	31558625.71	489.0837518	100729.6855	2070.196575	2426.165779	80554.83546	3428746.768
F6-25-5	19	pericarp	3667.902898	256237.439	3322.565392	3221.655082	217906.4709	7182571.621	235.450271	9567.500365	429.0081542	982.9110406	8115.36084	60463.07521
F6-25-5	24	pericarp	2784.365126	132918.0097	2940.879301	469.3661705	396664.2341	3069882.252	572.2494837	16548.82621	547.1305183	182.9132558	29741.21454	132806.6813
F6-25-5	7	endosperm	610.3937543	58447.03235	2265.317381	465238.8113	39.45459407	613810.4408	48.15745228	9156.553488	371.9035888	2876.145466	7.738180514	74503.57503
F6-25-5	11	endosperm	1480.575177	337975.8184	1155.279033	192856.0562	10176.77781	1393871.209	123.1093507	6574.450323	120.1031816	11963.62351	590.3041909	67843.24393
F6-25-5	15	endosperm	3479.544519	406950.4808	4213.099711	9838.145781	9654.967533	4698206.244	125.4254364	68617.72108	1004.623201	2980.002609	1427.983281	305605.9241
F6-25-5	19	endosperm	1937.430755	306050.7122	12835.43105	12836.70308	6051.688541	2344989.559	283.6713191	14602.48075	2411.942524	2033.459082	799.4382281	252064.4694
F6-25-5	24	endosperm	664.3557586	141565.5896	25793.79889	2347.318418	3214.334601	2185387.883	52.33055373	26845.17477	1327.030975	600.3801396	494.4999374	163581.8327
F6-25-5	15	embryo	119.5671806	19620.00083	348.8416178	4236.647125	4757.725391	2111459.059	18.05365362	1881.498171	59.07847777	56.42289741	598.5554556	334778.5218
F6-25-5	19	embryo	100.5656713	14811.30569	385.7383339	4146.878491	4796.049439	1072567.576	24.86498355	473.9206879	38.09623202	534.3035173	427.0278322	111165.67192
F6-25-5	24	embryo	92.78830133	14026.90955	252.0644486	1478.449036	4961.724569	1755328.246	26.21682376	1177.125007	59.75922362	293.5634307	377.5760361	90111.49644

Appendix 1: Black font: Absolute transcript levels of cell wall related genes in developing barley grain (in arbitrary units). Red font: Standard deviations from 3 technical replicates.

Line	DAP	*SSII*	*SBEI*	*SBEIIa*	*SBEIIb*	*GBSSIa*	*Iso1*	*LD*	*SuSy1*	*SSII*	*SBEI*	*SBEIIa*	*SBEIIb*	*GBSSIa*	*Iso1*	*LD*	*SuSy1*
WT Torrens	7	134896.0337	142.0414803	18889.85549	7868.812778	113195.0478	13658.68287	36749.06117	1560824.298	5800.5113	37.151939	316.6654	1493.1676	2733.7284	686.07436	3741.4671	49766.174
WT Torrens	11	377004.4969	413.263017	24350.58527	47950.16557	619008.3397	32112.97268	72934.59905	5869554.474	94226.733	178.68354	2991.6645	10545.32	56021.774	3754.8434	11976.763	178208.78
WT Torrens	15	319787.552	603.8835337	32862.99465	46498.11566	881019.5355	45779.82591	30599.1435	4590614.583	18341.705	32.764409	2134.7038	5709.582	39384.43	6493.2716	4725.2962	148383.01
WT Torrens	19	239712.4626	871.2422121	29067.39723	33585.0072	867031.8059	60013.88318	28240.91008	4060702.918	14168.394	197.14314	3267.0936	10452.496	131179.15	7939.2297	1251.8817	451206.65
WT Torrens	24	304926.3958	739.1156988	11334.62602	10684.61162	345886.0082	18538.46859	75172.4237	11518893.49	26257.385	345.72486	555.36701	2726.8123	25091.372	2429.8584	5112.797	1060991.3
WT Torrens	7	1657359.347	223.0224069	54063.17224	66113.11252	1123820.461	64103.47565	126299.7665	10591968.44	153976.81	38.892902	1196.7859	964.82656	32067.441	748.52231	6601.3353	741298.45
WT Torrens	11	1604012.136	1481.662674	125090.7552	247131.6742	3294297.851	67725.35244	203876.2143	11034592.42	17832.613	27.214745	3256.2127	19513.659	184863.62	2425.4802	7613.4427	672278.52
WT Torrens	15	785546.186	3300.168568	141962.1427	217278.9303	2421581.261	62002.60314	76517.01805	5645735.232	30843.237	141.37353	12736.133	8637.1582	137005.6	5749.9639	4455.5235	71617.493
WT Torrens	19	689269.4988	12286.05883	129774.4247	207072.2593	5741341.229	62767.35012	177977.007	2780390.766	21999.609	752.17949	5332.3314	19659.27	329176.52	3647.6217	13120.785	158419.76
WT Torrens	24	829876.2161	6956.36683	46448.1389	92700.20545	2619666.631	36749.56022	539268.9849	4912312.594	50566.026	240.00686	2802.5475	7430.0451	245736.82	3916.5421	19117.054	293164.16
WT Torrens	15	9308.871389	105.0607243	13821.22895	707.0865395	48802.1878	7587.413038	83583.7967	1587310.157	605.39192	11.379226	935.35255	112.1872	4722.8441	905.41549	5541.7411	64824.383
WT Torrens	19	7816.752762	61.36729371	15811.40705	19.97626722	6403.36337	3790.50298	65245.11032	547019.8945	126.91018	28.831978	1888.5052	0.3426573	625.79802	60.492658	6227.0674	55491.079
WT Torrens	24	20254.19169	68.67055262	15990.28431	56.82964055	846.4652003	2995.262294	24502.09784	409168.3589	3914.9673	8.1370895	1045.5938	23.875782	19.720273	515.41712	3210.6759	5538.1892
WT(tc)	7	1380622.634	764.0070872	18510.88703	33483.27303	848605.4153	86889.24532	55423.63552	10166980.15	129022.14	40.141555	962.60593	2838.671	49435.817	4157.6331	7611.0487	1881836
WT(tc)	11	484816.4818	848.6468362	39091.59874	103573.9348	1393738.389	53549.98595	68520.65677	5936494.982	80666.789	294.83852	3517.2661	15944.814	119071.83	1926.627	6474.0625	431440.35
WT(tc)	15	1121430.289	1606.73575	46650.84181	200660.0108	3701181.969	119250.4628	186729.9466	10087746.13	220835.85	599.55984	8518.397	16580.242	48974.946	6095.7844	28817.137	1512229.7
WT(tc)	19	1144419.784	2156.848512	12994.17016	102404.9594	590622.684	128104.3484	156646.1386	10549862.25	135734.08	370.90509	1057.4495	12270.211	45484.271	10356.532	11045.917	337698.1
WT(tc)	24	43548.49122	1220.43653	12812.45441	5038.452557	184220.9056	15438.99053	22302.27817	2517863.614	2679.45	963.30853	1949.3161	1436.3634	12587.619	230.82489	3595.4039	407183.29
WT(tc)	7	1016730.943	319.0868636	67614.74106	81318.39682	1811091.208	91294.95939	50033.40249	7853248.878	55427.842	44.998027	3728.9941	24466.093	150016.92	10535.625	7259.5094	459375.49
WT(tc)	11	1748315.821	1369.65831	136598.9331	303020.085	4575876.105	75966.69315	160917.6825	15682535.91	254146.15	129.1352	12007.551	26988.452	173458.11	7385.8542	4082.7098	484254.1
WT(tc)	15	1293664.797	5665.821649	134408.5639	508756.8646	5495871.681	82242.38593	289267.5388	11391936.75	221397.15	704.36571	17750.017	129152.51	167270.87	15423.004	45462.923	1219368.5
WT(tc)	19	390220.2221	21846.33411	136937.3429	406679.0373	3931462.337	151750.2766	376650.8433	3839292.971	52857.64	3244.0339	24191.161	16117.443	152091.49	21450.41	45841.119	419491.4
WT(tc)	24	1436942.213	29386.30514	81684.30658	186981.8925	4871792.361	102791.9323	1700236.291	11942947.21	162010.16	2683.1053	5777.5134	46852.814	136366.65	12658.574	158619.58	646982.85
WT(tc)	15	14925.62709	321.0661843	9581.022641	1903.617721	96124.89658	18845.32291	55785.54879	2435957.563	2673.4233	46.581024	1363.1907	574.38755	4334.5097	2030.7075	6969.4467	274626.56
WT(tc)	19	2131.641994	71.03269383	12356.55914	646.7214917	16335.53604	5172.625889	15788.96117	335217.8942	347.81047	21.974601	617.27002	147.27301	562.94799	397.31172	195.6912	20869.399
WT(tc)	24	4930.195092	29.40349104	14596.86526	38.69464873	925.0028166	2414.713889	5830.108904	170769.7508	837.575	15.469603	701.14667	10.980021	64.23809	198.31039	895.18966	5758.426
F6-15-3	7	370033.4104	8952.713408	18379.58627	1501.242401	79047.57996	19856.41182	63621.64479	2482248.388	27814.55	1238.6937	3114.4277	335.11503	1975.0306	3753.668	7173.0607	173943.72
F6-15-3	11	500522.8871	19105.10828	37274.96007	40555.96835	331483.311	24231.26091	67417.10961	6249982.529	21525.989	3227.3143	6025.4791	9000.3324	33960.173	2889.2001	7372.6511	552642.07
F6-15-3	15	178564.3066	17712.19455	11196.56858	10454.23339	311780.7796	26612.52423	146120.7971	16263038.3	462.35618	1460.4383	884.21325	2610.2243	27955.748	4171.1501	21540.358	497158.73
F6-15-3	19	85692.44625	40244.77415	17168.36807	29615.8831	281518.2108	27841.08139	40820.43935	4309919.711	15441.539	8322.0574	2324.0419	11019.196	10383.566	2450.1286	5594.5657	681913.5
F6-15-3	24	97178.3844	12764.41939	6108.600651	4065.538765	47619.98148	9608.909448	7907.215585	10176283.69	17371.536	505.8096	719.36701	2451.7423	10564.024	2104.0753	2394.4287	953752.2
F6-15-3	7	486242.1081	4174.962025	39541.76953	17765.79585	315664.7205	37971.17019	19927.9447	1490460.155	48155.97	444.4848	4138.1746	4224.329	20335.252	6291.7852	2016.5276	173037.88
F6-15-3	11	1029225.14	146607.4645	134509.4583	147295.6332	2412857.172	55906.82695	114373.6415	10575776.91	106857.96	25993.906	2671.2295	15487.393	96266.515	3590.3418	7187.6843	710530.12
F6-15-3	15	2850429.34	612755.581	100586.0431	373157.626	4213778.708	58448.25598	233584.879	28434911.75	211559.52	46050.789	3625.8135	30459.024	239651.41	4644.9553	12700.506	2623365.7
F6-15-3	19	1299158.451	1511744.982	70500.63521	262534.9098	4156617.333	41682.97911	448589.8406	15275971.96	35369.694	138430.86	3246.3364	30254.835	171140.79	2263.2265	67801.655	310353.21
F6-15-3	24	506028.1781	278726.8172	18723.46446	37451.14757	952362.3277	11085.58187	397925.0346	6168734.502	22671.369	24194.119	1264.0517	665.44252	92284.557	1333.7553	44618.305	436141.84
F6-15-3	15	14711.60657	5301.996869	13059.24274	41.61877191	9737.468689	7520.869205	168514.9728	2183074.908	2747.2169	1873.057	1813.8421	5.7495772	554.8237	1295.7816	10785.079	144907.72
F6-15-3	19	8629.546871	5204.651029	12558.69187	22.5983593	936.1707767	4101.522689	102857.9433	945145.0789	1008.3018	458.02781	1713.2883	16.172464	62.920829	434.93427	13868.789	97297.601
F6-15-3	24	8352.062775	2690.920696	14247.87046	30.05133969	188.2628045	2282.355056	23285.36894	347800.0637	1319.7352	288.11356	1466.8663	4.5285988	25.783548	300.93051	1982.5097	37080.868
F6-16-5	7	352509.6516	7340.956323	15733.34319	5263.686751	95276.70504	16677.50714	51732.9966	2790020.783	26862.536	162.56419	207.07707	2117.588	5709.1836	689.52411	3742.3947	341753.37
F6-16-5	11	161269.9602	7548.629453	17288.02216	12243.682	103066.7889	12842.32079	23073.55748	1812082.572	9558.7742	357.12677	1130.0414	786.43758	9025.9691	860.53736	3761.9107	88191.447
F6-16-5	15	633855.0389	76332.9749	29202.3158	102763.9958	1151637.34	53959.83822	55648.48678	9523558.333	103051.55	2832.8301	1975.459	14044.034	26041.163	7256.4152	7381.8794	489013.64
F6-16-5	19	94838.73662	13979.5554	9268.146064	4622.879619	127187.7005	17086.23634	14031.96093	6392456.475	17111.341	1869.6919	1036.5735	1625.6751	5334.0475	837.54438	2804.0468	421113.42
F6-16-5	24	50937.26363	3734.98051	10602.08758	690.7439734	9838.154273	6183.085208	16966.10436	3714374.414	3895.8855	371.12501	1111.6707	211.89722	563.93918	1011.6794	735.64317	493627.23
F6-16-5	7	405682.6454	7295.450669	45586.42284	23795.42294	336755.2437	32760.54989	16865.15056	1253778.786	2625.2371	854.26081	7554.3253	2389.79	28625.633	4457.1217	3167.8442	70580.145
F6-16-5	11	1034503.717	112662.5956	97644.99011	121897.7354	1378090.641	45289.61483	114549.3446	10306080	149194.53	18897.978	17642.804	21535.564	76828.478	7948.9167	10339.662	887961.94
F6-16-5	15	1057339.531	350682.8382	69179.14554	210920.8079	1980711.956	37274.67384	151243.8968	15041605.06	93310.473	53054.239	9160.6981	31302.512	105667.81	3501.1485	28820.193	1632640.9
F6-16-5	19	344000.1311	149702.4025	25598.304	75658.02457	1265612.423	18006.82989	55483.77381	4404521.934	64944.422	12467.092	1988.6292	9275.397	125734.41	996.36682	202.27182	246097.24
F6-16-5	24	271449.42	34190.36742	9410.29701	15716.36898	215040.611	6258.396162	65035.86048	2281552.429	36141.161	2269.482	489.6698	2818.5852	23356.856	282.13917	2776.8309	143498.79
F6-16-5	15	9309.95345	5835.779232	8536.032086	22.77801695	16373.70318	6815.545361	70294.04105	2054555.148	1491.5705	850.92605	969.21213	N/A	1588.1549	805.30401	10038.406	185493.07
F6-16-5	19	6673.878298	3550.384908	12583.57851	21.84332048	3812.225795	3080.804238	43006.15052	456520.3261	561.35416	675.52584	696.71429	2.8268129	192.77063	342.69729	2037.7006	26343.891
F6-16-5	24	11523.90645	2285.719552	13193.61819	15.98290543	178.5771181	2328.668784	32888.73678	614753.1166	1934.7883	60.866258	1517.2554	N/A	60.433757	205.90449	3014.7892	80847.233
F6-18-6	7	223306.8462	6328.115232	16390.63113	2639.08091	22630.95106	12673.20205	67579.53169	2953381.543	19347.249	457.37935	1915.469	459.42924	483.39003	534.97888	8602.0264	71014.471
F6-18-6	11	154088.0595	10253.08268	16442.25542	15750.81081	122415.4355	14289.85527	23051.8711	2843473.021	6044.2487	280.54564	728.95089	1026.0954	16853.065	670.7489	3108.8614	116574.33
F6-18-6	15	301434.0831	11959.52798	16669.96266	8439.985646	199002.1598	18086.04499	42912.60814	6845100.78	16917.221	313.91444	871.95639	661.99269	2673.431	1206.3759	6859.7089	150145.61
F6-18-6	19	45893.21123	8664.655485	1747.985102	3316.397424	7866.79319	14060.44119	18490.61997	2096377.803	6510.1668	1302.1764	194.56642	430.20535	1272.0903	1652.0594	6560.2316	71133.895
F6-18-6	24	1296957.575	62677.45642	9026.352441	54694.64305	523679.5029	77987.61563	100768.3685	91973817.21	120139.31	3038.7463	7113.6716	33149.96	49396.676	19313.175	93556.553	7162409.5
F6-18-6	7	479170.0446	7901.714989	47503.40414	16108.75796	343483.1547	43713.87242	28412.82608	2356655.638	24861.639	364.27808	1749.1006	1534.6816	56639.679	3772.5282	677.18958	112252.04
F6-18-6	11	705536.4732	39006.36251	50573.97491	100324.0458	859743.8417	31887.8318	115676.124	11816156.78	51374.121	394.92284	667.22662	9153.2486	2330.3525	1851.4451	16484.104	361635.05
F6-18-6	15	337793.1486	61446.14947	65818.76489	42521.10269	907002.0906	31804.17808	59839.41415	5313703.251	28679.254	2225.2926	1292.9998	6655.8714	23539.509	2381.567	1472.0605	41506.888
F6-18-6	19	710760.2877	92125.16864	39864.61568	113755.1809	1051498.853	25648.21225	78193.21305	9402947.205	66665.225	8278.1814	4394.411	12550.811	98204.027	3776.9658	51054.413	332825.48
F6-18-6	24	339531.6082	53381.58128	13537.35077	19923.44596	512324.786	7849.880293	89656.83755	4345445.685	24276.683	3636.0459	1322.8046	1418.6675	46440.432	713.24363	9153.1173	301009.83
F6-18-6	15	6660.441477	4191.710815	10299.11101	84.39295903	33232.64962	3706.288809	39169.00612	513473.1719	664.32807	471.34048	1100.6304	53.232887	3606.155	374.29681	224.3217	47993.532
F6-18-6	19	28857.77982	4159.872676	16202.85752	98.19829105	19027.72076	3185.236735	125165.8537	1115530.354	2426.8522	327.78802	556.55723	69.612148	810.62847	323.45019	10801.188	13349.98
F6-18-6	24	30710.05579	3322.619784	14086.97218	31.17220433	5239.109842	2418.577361	36842.08225	459295.7716	265.90498	186.72134	542.74441	10.802849	775.36948	130.0757	1563.9256	10946.048
F6-25-5	7	182895.3149	8530.924202	21432.40018	2299.597735	95091.42082	23942.76654	15651.48608	1154218.527	27932.328	1151.7576	2058.1844	652.6853	5733.1785	760.68369	1585.3158	114465.03
F6-25-5	11	129546.906	12242.63825	16040.25081	8419.595251	161462.1098	14927.669	35875.99497	3362752.012	20524.778	113.07494	1859.0657	302.52696	10302.533	1238.2334	4622.8309	421985.08
F6-25-5	15	345434.8348	29789.34418	14259.84254	19168.50426	270002.1478	30682.99875	27865.54024	7159280.529	41491.496	2703.108	1827.6371	4550.37	24025.667	6679.8747	16052.954	570378.87
F6-25-5	19	52854.57793	15239.69926	12432.89768	2104.83957	85676.59061	12912.03478	15713.97772	2935368.795	3259.2007	1310.3727	634.35747	777.46633	4512.4191	480.02603	8583.1372	102197.74
F6-25-5	24	22099.80149	5584.249404	12141.09112	202.4323475	19644.07204	7652.000052	5653.027464	1998443.526	4347.3361	419.98826	1133.602	97.173339	678.12871	677.64526	97.266865	178707.15
F6-25-5	7	616033.9987	6195.049183	40056.58169	12014.80518	321602.3957	36281.95661	32539.8714	2655253.506	71266.28	1217.8613	5839.3432	2421.6608	11291.304	368.14662	3287.4531	112744.9
F6-25-5	11	1337259.143	102455.3379	100169.4249	83614.41384	1833730.887	45441.45152	144316.1209	12162664.79	126512.47	5888.2736	3901.2565	2144.1036	131623.19	2163.0965	3570.4888	266891.92
F6-25-5	15	2099180.616	742819.3793	76783.26849	280746.9842	1982957.175	28015.7445	389011.6455	16439721.41	185968.2	92202.86	7870.3786	56894.21	174939.82	3679.091	43066.12	1943851.7
F6-25-5	19	553969.5974	338614.7115	28016.48768	33778.78912	1566379.247	17505.05767	141278.1477	5859611.827	95217.91	22610.422	2679.521	2517.6339	172069.05	1634.5852	18999.302	568402.64
F6-25-5	24	387967.9386	51438.34476	13883.22813	17527.3395	603575.6134	11130.13931	73295.82005	2657692.769	76494.943	7126.8599	1196.8944	2758.5678	64902.559	1497.9764	2465.1321	263050.76
F6-25-5	15	10278.03478	5381.147173	16520.05318	115.7917034	14655.71627	6914.427773	129177.4864	1747874.358	460.6514	676.32203	845.83968	52.687284	1955.3551	1167.8591	19346.811	218758.13
F6-25-5	19	5478.875194	3662.791556	13476.27846	18.75737184	1063.555744	3561.986633	90134.27576	711217.0157	355.54518	337.69981	1265.1201	3.2346613	143.80656	410.36459	6956.0012	23168.377
F6-25-5	24	16088.46252	2491.421758	13241.08828	139.6183372	637.7430689	2620.836697	41525.74237	651494.941	288.45491	184.59679	754.66978	28.735753	46.907403	248.35237	1031.6096	43935.093

Appendix 1: (Continued) Black font: Absolute transcript levels of starch metabolic genes in developing barley grain (in arbitrary units). Red font: Standard deviations from 3 technical replicates.

Line	DAP	*1SST*	*1FFT*	*6SFT*	*HORVU6H1G011260*	*HORVU2H1G109120*	*1SST*	*1FFT*	*6SFT*	*HORVU6H1G011260*	*HORVU2H1G109120*
WT Torrens	7	361.1832113	2506.934355	302946.3514	2733.794933	161.0224917	91.29236268	82.04545043	10619.82258	332.4731431	13.61351928
WT Torrens	11	210.5817947	688.0106767	40722.49371	17270.11038	3649.583771	85.11699937	149.6768913	3675.5543	2755.780185	637.4440324
WT Torrens	15	95.45080079	372.0988609	13810.97816	11418.33022	4381.31981	31.48022373	65.75060321	1025.644873	1167.744847	252.8859536
WT Torrens	19	94.98286651	209.1090468	5605.688101	17383.51988	31960.10227	144.2708133	143.011056	243.1385563	1166.757139	2113.54676
WT Torrens	24	69.07853874	371.4513065	7134.198173	15524.89739	287471.7681	N/A	100.2652274	1281.735179	1199.482418	27529.85931
WT Torrens	7	727.7249744	20.9490852	1362691.416	836.166556	54.63059912	66.96670649	13.24034924	16396.12058	45.20432393	10.915041
WT Torrens	11	48.82704794	13.35994424	3986.147868	660.8176363	92.21897912	5.193109821	3.962898836	485.2005377	34.71178009	11.96388871
WT Torrens	15	15.17314604	17.99880489	1103.374656	585.87994	55.03382317	11.69786569	17.76245827	294.0374859	11.36892451	16.62048578
WT Torrens	19	10.96300194	62.7216388	417.2871715	2145.574872	730.1239871	8.144128753	57.74452899	155.8824873	194.7858263	145.8215706
WT Torrens	24	84.43715647	40.69201495	1951.830206	2844.449574	4117.519324	75.57974882	N/A	420.0162014	130.8059427	527.9971466
WT Torrens	15	344.3907945	553.7743179	70807.77823	915.7982206	23.8702283	82.92639263	4.889684682	2693.028334	101.1371762	1.767837805
WT Torrens	19	229.689419	320.8448491	27120.70502	838.64742	112.5363554	11.20979058	37.7748288	872.134351	101.3860216	15.54074165
WT Torrens	24	282.8849476	373.8393219	11429.93304	1472.871345	1316.564568	15.79692082	33.01553976	1280.412438	233.1546605	157.8025711
WT(tc)	7	2118.132365	27369.56025	1067208.599	13321.13152	607.6450876	596.4407306	3206.727913	177194.4555	477.1942117	159.2417897
WT(tc)	11	301.4189521	17679.23412	58144.1889	5249.816962	486.1789382	162.4232324	1174.585973	2289.880256	267.3476905	54.68877547
WT(tc)	15	122.1617893	11884.54087	8054.880799	11561.76337	6834.022383	66.36041319	1126.012439	1010.643062	783.3713799	270.0772772
WT(tc)	19	108.0622798	3163.780883	14331.355	46766.13541	194987.1459	107.1844051	1063.977465	1144.000242	3421.381777	11369.46346
WT(tc)	24	229.7963605	3460.827554	12235.59304	5767.478147	171372.1135	238.6952794	780.4752509	269.370518	700.5723243	9274.16314
WT(tc)	7	240.1653516	1590.728392	1046974.359	247.6634599	44.49546907	93.240224	121.5820823	88389.6633	21.11024367	16.63421608
WT(tc)	11	42.24030368	7834.682607	27076.12874	701.9040217	104.9140015	17.98571505	548.5420566	906.9018652	100.6743642	9.929508902
WT(tc)	15	59.20746601	3166.992971	6280.039168	1164.615652	113.7959599	26.8346922	452.2104881	526.3100711	8.975559943	18.68660901
WT(tc)	19	90.50153881	620.5704853	535.8624495	2805.679374	784.0613835	6.269078013	212.54404	32.81530489	375.52398	23.30428065
WT(tc)	24	46.12407103	111.8964751	47958.20945	13889.3389	16364.92464	#DIV/0!	78.52019488	8155.631776	559.9511817	1406.150999
WT(tc)	15	288.0394976	631.666165	41084.97928	1349.593001	82.29309037	179.2424493	104.9696139	4064.33412	166.9798919	48.98070934
WT(tc)	19	64.17406078	841.5489858	3967.075671	203.4228247	87.05527168	3.986137954	91.25002271	80.16372724	2.975551625	2.274085095
WT(tc)	24	5.252280333	2147.78333	6948.420446	392.0465473	433.546229	6.713452257	35.95952438	869.7626586	30.88791059	56.00716616
F6-15-3	7	2315.662466	2085.27768	1052681.254	5031.840021	512.1040285	338.8197026	467.1253149	142402.1578	563.026334	49.37324458
F6-15-3	11	469.4886078	2718.247712	162012.4682	17679.39179	1276.379871	121.2297171	434.5056756	25844.95186	2667.37144	313.7728532
F6-15-3	15	2801.385819	361.8339157	8666.987704	112491.3463	71791.12078	754.7795075	191.2854126	2282.423909	18734.40811	462.3561756
F6-15-3	19	636.80722	993.968635	24325.34062	18182.25591	36643.38078	374.6753313	69.54087311	3798.350178	3705.981943	4798.738884
F6-15-3	24	364.5261551	953.9006197	8709.387554	16223.55817	439875.8556	164.2155467	497.9807253	1358.237865	3031.514596	53781.8687
F6-15-3	7	1350.200485	13.6307425	920924.787	258.2477281	59.20644573	156.5957797	6.707335278	93824.9107	28.96103613	7.726286417
F6-15-3	11	39.09624142	10.87609374	4344.546774	1060.949718	185.7229746	15.83414875	7.886244944	241.5355751	118.8298616	16.07522658
F6-15-3	15	84.51840992	20.55431299	1834.277298	4356.011085	1366.471542	41.42515168	N/A	587.6531061	292.424987	232.5119295
F6-15-3	19	91.20863244	183.5519497	1214.112714	328.5579899	176.1709364	30.55984048	0	410.395932	211.4410585	93.19764913
F6-15-3	24	147.6530741	369.1326852	6830.00934	1570.501376	4111.083448	79.62544736	257.6924076	1425.274436	98.17581265	215.5777191
F6-15-3	15	354.0536115	618.6704738	112500.5209	1795.724006	56.85540743	80.23928147	267.482716	18231.53387	243.7053996	33.52004455
F6-15-3	19	1052.12587	449.2482391	32351.91532	827.1463326	128.6435128	117.1751727	74.81668375	3498.520236	141.3990247	20.59110644
F6-15-3	24	477.1534038	406.355983	20072.52718	832.5325921	591.7683295	44.68458194	102.4377596	2360.919332	102.091377	78.84191739
F6-16-5	7	535.2440339	1486.050882	787511.1355	10437.53091	744.0055421	326.7127539	156.4349113	43470.48314	998.301171	208.4020542
F6-16-5	11	820.9973457	1722.433718	116411.2413	19541.49061	715.4762357	131.8892763	8.313614758	3249.197145	1125.156976	96.91451023
F6-16-5	15	1076.329908	738.5069647	49850.67686	30913.10675	20972.33918	548.5095819	250.7284717	13198.002	2269.666673	1296.740155
F6-16-5	19	2626.178235	612.381456	73957.93324	43608.51994	77957.03447	681.49293	123.9066421	10969.71005	21.58619542	8592.516979
F6-16-5	24	270.2037135	1804.289851	20268.10556	4069.326979	100002.3881	37.57941379	202.0857279	2804.142978	468.4626787	10611.33478
F6-16-5	7	332.5151181	15.56268133	264125.34	192.7329849	33.55582705	60.12854324	4.263555332	41075.58375	25.64475433	5.414558629
F6-16-5	11	134.4786084	38.50342933	8006.079491	798.7746707	185.7874872	27.947673	31.82814894	635.1585938	123.1883305	13.36505315
F6-16-5	15	125.6958439	51.03131766	3240.11794	1701.043922	963.2170207	91.17404946	14.68745849	370.5479561	246.5097823	59.69272401
F6-16-5	19	20.68126588	26.28043645	2778.589545	1111.692534	1376.367262	16.93248494	17.87121665	248.1719594	221.663052	101.3809706
F6-16-5	24	25.4100722	147.1366343	3595.361568	1159.884377	2550.655896	16.68738523	166.3480307	629.3636761	255.2471623	650.0756128
F6-16-5	15	497.004057	370.4518861	38789.94624	1066.546069	35.21342206	171.827609	76.35414299	5431.805559	85.36067709	20.70072118
F6-16-5	19	323.0427602	302.543514	22354.74498	469.3693382	29.81477993	35.68280422	54.81448451	4006.200827	75.32275772	4.086983526
F6-16-5	24	157.7226116	61.94099716	5129.296551	918.3414561	460.5701974	107.6692647	29.03820784	550.4428416	39.72904946	92.21095377
F6-18-6	7	51.98689126	3587.857586	613065.741	5216.150273	359.7322507	41.13246885	101.7745545	57863.1963	645.7316431	44.25373782
F6-18-6	11	20.59556988	1617.831689	137136.5142	7969.084998	721.295686	20.64920264	148.159621	15281.67992	824.5385793	109.5180242
F6-18-6	15	127.3335498	2191.764835	48808.03131	22045.84639	15861.97762	129.0863736	711.6246651	3786.808801	785.9840239	801.841689
F6-18-6	19	338.3957651	958.5100396	21036.89748	6665.698604	12352.88685	391.9669979	90.04787711	2170.619964	356.1080717	449.4181425
F6-18-6	24	21275.34798	7738.857907	61036.61713	102140.0755	2663976.384	11631.49453	5323.865699	4106.911675	12126.41515	122192.2721
F6-18-6	7	13.00567285	21.8840043	455609.9845	247.4889027	20.42232778	5.078987249	5.837945092	18636.0436	7.18993524	2.289674975
F6-18-6	11	19.63363272	15.20102911	12548.05818	511.7817119	230.4459535	13.42283023	8.409764913	1144.418695	63.2011897	4.390527224
F6-18-6	15	30.8303817	21.81143203	2390.707396	403.6348668	208.6116285	15.41327321	5.532923925	252.9247744	41.1469021	9.135387524
F6-18-6	19	124.5881522	25.37574117	4488.886272	1875.199903	1658.001524	90.57426352	10.45478526	1042.412951	268.042577	83.88906178
F6-18-6	24	13.65511894	26.37940363	2413.914706	734.0882291	2552.974291	0.025405831	12.1955399	77.41906755	169.3268384	145.8771218
F6-18-6	15	18.73954721	1085.557317	42441.64215	319.6236511	24.57669837	10.06755807	399.9983734	4244.136029	52.67565257	3.700235074
F6-18-6	19	17.2658431	624.8876476	67726.96795	716.4922661	134.7215639	9.835440349	105.680846	2854.655455	62.80829988	11.78759773
F6-18-6	24	9.643927458	408.1028361	12234.09886	637.4511812	165.4035332	12.06877852	10.26524158	486.0372085	50.57794904	11.33146364
F6-25-5	7	1137.325607	1200.57584	169184.5502	2219.454584	72.54133797	298.642237	96.40096523	15454.51702	95.97314952	18.08432238
F6-25-5	11	133.6581607	1046.250736	65508.81661	19661.96948	1219.601577	29.31639733	138.4271406	6554.656145	887.3897111	208.0350893
F6-25-5	15	518.4226665	579.5877848	353057.9401	31445.30928	50644.71801	192.0207616	393.7639156	31465.36169	4423.816135	7875.323436
F6-25-5	19	214.400772	260.7223417	23802.12594	12706.47674	25033.23172	169.7676022	124.1657055	2337.034898	1197.213524	1217.825199
F6-25-5	24	23.08297504	1336.14608	9182.752771	2188.905846	33912.87417	10.34021597	316.1393366	967.4688652	239.8204158	1649.664181
F6-25-5	7	443.4099809	34.67665629	717341.465	307.176386	51.07132816	91.82131524	25.18121624	97947.85065	30.17316491	6.577341605
F6-25-5	11	42.96802215	17.16309962	7886.400075	1431.285177	167.9699636	14.29912051	3.043394117	391.7562501	195.4112052	28.23350944
F6-25-5	15	375.2838043	42.9717221	9273.451457	2980.541704	1568.342685	74.75186086	45.40487319	682.3709208	418.7168381	321.853227
F6-25-5	19	52.11511919	25.96024921	5125.013796	3730.23156	1867.278233	20.32096155	20.0004502	298.3577637	281.84248	313.4004804
F6-25-5	24	213.153092	82.02757124	4457.810057	1735.740685	3961.498812	112.9605439	78.8462896	314.9468859	83.36101386	610.9190764
F6-25-5	15	765.5482193	313.0213872	110596.5218	930.1403064	81.20396335	52.23216048	99.62872097	8005.0298	141.2551717	21.7103382
F6-25-5	19	168.2261912	257.2280066	43768.79598	501.7118464	44.70666458	51.98683859	96.06037577	3900.761749	17.93274581	9.182919271
F6-25-5	24	16.92401153	147.9554097	8500.375945	1469.117408	1034.705591	6.785123962	23.01678276	451.3999089	49.27869747	16.01809338

Appendix 1: (Continued) Black font: Absolute transcript levels of fructan metabolic genes in developing barley grain (in arbitrary units). Red font: Standard deviations from 3 technical replicates.

Line	DAP	*CWINV*	*VIN*	*SUT1*	*SUT2*	*SPS*	*SPP*	*CWINV*	*VIN*	*SUT1*	*SUT2*	*SPS*	*SPP*
WT Torrens	7	127897.6128	69.8224811	83936.94348	6548.522443	323.3388091	39751.32494	1786.951466	2.675341684	8532.872705	216.5024458	21.76911739	443.6570547
WT Torrens	11	211663.2418	9304.951627	270767.3333	8279.679636	485.7199769	59503.62609	26353.81643	1075.4129	21475.2863	900.2724366	97.52436662	4099.648587
WT Torrens	15	156091.794	25660.28223	140165.5764	6538.170559	439.2217999	50332.29683	7807.890043	2092.581298	8849.052511	219.8008847	44.23063894	5017.115191
WT Torrens	19	382211.3231	32583.86616	331218.6251	11689.33528	669.5325645	101377.2261	27861.00519	6549.854986	32402.4365	1165.124065	109.4676469	7956.669401
WT Torrens	24	1029721.465	3209.736261	1493872.369	25453.57709	797.2832816	101158.4903	55834.97948	364.4507545	141225.2455	2756.149933	93.00825292	8662.678359
WT Torrens	7	1960.144635	63.92221429	95059.76436	1669.023122	127.1036213	17293.91037	64.67343022	14.78164596	4045.358414	113.9018905	9.701986837	1124.448383
WT Torrens	11	4348.686771	3682.944302	36704.83881	1967.55974	190.0273469	34117.81816	427.985083	207.0157065	2671.217251	128.8711044	29.80304005	1543.768156
WT Torrens	15	4710.671965	3884.466809	11323.10445	2283.880401	222.0519398	33746.01465	289.4057497	704.57136	1349.700247	59.80952196	17.74929059	2231.765409
WT Torrens	19	17374.87103	13156.288	9807.934135	5379.650445	301.5804041	64698.6532	2143.450085	356.115334	404.3501927	299.379128	75.36839419	3213.623536
WT Torrens	24	30790.36134	19151.36666	37743.92713	5571.255738	206.5061987	37561.85995	1913.589783	2384.571682	1658.06045	353.5424229	56.03248625	1299.936858
WT Torrens	15	2115.202024	617.434134	26182.02682	11259.41697	328.497868	13641.70386	169.425643	71.6087338	1170.352347	476.442408	23.22234144	104.189702
WT Torrens	19	830.2434831	56.84117339	24434.71947	5777.979492	294.5197896	15849.60676	131.9122296	12.73897994	2113.03862	213.8654875	25.56952684	605.5376923
WT Torrens	24	1519.443353	132.2038674	14796.92923	5630.749507	346.5530096	25504.2803	171.2729952	30.5216399	2150.891967	529.5696779	81.00858101	3077.925721
WT(tc)	7	1824591.348	792.0225205	1054649.957	33436.35063	1359.231539	142588.895	30985.27442	103.736062	68664.30313	1689.632566	62.4376338	8354.512486
WT(tc)	11	518441.9055	18867.29609	346445.4108	11186.31194	680.6832124	94559.92329	4635.876743	1782.992702	10404.74325	834.8437271	52.51958183	5262.508574
WT(tc)	15	222463.3143	143439.7882	275310.2182	8811.825675	338.6632133	79618.44932	6930.439477	11201.34992	22903.44171	138.018001	55.4526181	8184.974024
WT(tc)	19	308973.712	113146.4089	895120.792	13109.59363	449.6804189	30975.89056	29239.89987	13837.39624	59450.77736	1804.715357	54.8015688	1591.891832
WT(tc)	24	715739.6094	8655.191659	266071.6292	22924.56169	1087.519949	71925.98264	89740.15828	1129.740291	22105.33184	3800.60451	203.0385576	11007.38361
WT(tc)	7	3111.809083	88.08238075	54024.02752	1701.537257	228.331517	17966.59703	176.2310151	16.47934655	2283.494399	146.0992624	11.76847311	963.8348651
WT(tc)	11	5225.94403	2203.551521	43632.6344	1764.496962	199.9029427	31242.7725	570.0913419	492.5469905	2054.853421	243.3115272	17.80541953	2278.378145
WT(tc)	15	4022.03171	4441.970324	26906.3943	3299.744346	160.641505	41620.11248	667.90766	543.0505662	3056.42259	261.0392017	18.84224388	4749.671183
WT(tc)	19	13126.81954	22519.31678	14487.41494	6698.189181	319.7033425	72272.48653	1849.006527	2932.038008	2328.283067	889.9297625	46.38289383	9786.440604
WT(tc)	24	37378.33779	130133.6241	88158.91543	14243.13719	933.5062964	83187.69873	1050.574619	5653.713999	7482.7257	1347.958534	210.2052625	8565.76503
WT(tc)	15	2787.156836	447.584115	35154.13062	17289.75776	220.8779381	23908.09234	902.3340307	78.55572265	5236.118823	1905.415797	26.2553454	2218.176947
WT(tc)	19	450.4394032	109.0372788	12410.33506	6555.81294	222.8614955	14651.73281	114.1913338	31.47797909	1238.089934	527.9512744	20.92936175	1047.254547
WT(tc)	24	1223.232938	194.8305177	3472.565043	4933.896749	312.7488403	23801.65095	174.9839443	36.74680011	237.1511634	338.1213966	24.89097012	1292.991888
F6-15-3	7	93737.07145	26.15044542	95981.84629	8702.243794	614.8320139	58978.50525	11304.57629	21.45317875	7286.105913	1173.317123	106.3133225	3759.384105
F6-15-3	11	289202.2764	7810.152704	392875.3731	11867.44078	480.4816767	77238.99394	21437.61032	1831.207373	25525.84181	476.1535357	79.28292657	6762.64496
F6-15-3	15	540404.6327	14926.19391	1460797.7	26742.0162	1016.063277	193519.9888	59442.39105	797.4118423	6511.307477	2225.820585	208.9712058	10262.6461
F6-15-3	19	514712.4154	10553.19805	558315.5686	26851.09659	753.1453726	109535.742	76980.31894	1541.550052	79083.6909	2953.214341	172.0670528	1267.650833
F6-15-3	24	520243.1514	3174.379529	846558.3884	22853.64565	912.5161797	141907.8879	29876.62044	384.4958036	92592.40439	4638.596036	218.7564556	6211.58111
F6-15-3	7	1800.653526	8.71489529	25869.83099	978.6636235	239.8639915	8627.997376	74.19721116	4.46536462	2217.980114	125.9724887	72.39825615	982.7753783
F6-15-3	11	5263.114383	3359.777333	36182.53505	2049.916988	202.3766577	32178.76943	321.4359414	365.1426869	5672.777596	185.2635579	28.07756721	2757.640363
F6-15-3	15	5132.507353	8825.923707	152055.6617	3893.46677	218.2052805	62015.62901	1631.491584	544.862245	15358.30517	75.25457053	50.8380379	1047.400553
F6-15-3	19	6774.179378	15617.48983	63447.7906	4790.705886	171.2205959	75156.18011	1017.477252	1740.40648	6440.320277	736.1337059	29.60275595	6034.509348
F6-15-3	24	2902.43757	18693.93384	49379.40663	4024.600933	152.6627319	40035.07637	1371.853712	839.8384062	4432.002229	385.3324383	31.22772756	1167.39533
F6-15-3	15	289.4477768	93.34037356	70458.43015	12229.08334	155.946098	12482.5064	N/A	66.98387201	13428.46241	1397.645301	42.39588846	1408.453458
F6-15-3	19	210.7272792	30.47886293	32014.2683	7694.797766	210.4162886	23475.353	82.38666469	6.631500347	2964.612037	1285.555414	36.33916977	3232.681841
F6-15-3	24	314.3458517	170.2320007	5874.594977	4747.227807	199.7972158	21875.60757	160.4962694	7.248349686	771.6988986	514.6137746	13.69360143	2014.116898
F6-16-5	7	200376.1999	153.0808827	169334.2239	7634.442115	360.7860599	56785.96164	6060.122262	82.55759468	14628.73748	302.1507058	92.04232092	2891.682393
F6-16-5	11	168912.1575	4123.357395	210748.2894	8938.921515	399.7457092	57840.65673	305.9327395	679.0837513	11278.09332	1062.055473	93.94649071	885.8649697
F6-16-5	15	878936.3308	20436.26027	399308.8629	21319.62508	431.9863685	123251.5332	43599.87728	1782.432557	53895.07897	1474.686301	179.616963	7791.773302
F6-16-5	19	526090.4167	7783.492451	697451.3957	24115.69978	590.8086962	135145.1997	79928.60313	480.7700137	93375.37106	5107.46931	97.19175001	22668.60928
F6-16-5	24	176885.7418	2301.72603	310109.177	14140.305	526.0208539	95969.12176	10546.01435	597.5832638	32474.9738	612.2977216	144.8167759	5259.23571
F6-16-5	7	1324.988552	11.04258565	17942.42651	1185.815049	129.4962781	9899.374733	13.43130395	1.94351764	2887.95643	163.0020296	18.51220746	1484.765248
F6-16-5	11	2850.747892	2244.161906	40591.83896	1739.78119	171.8240169	22869.00208	282.1458768	253.8485537	5643.863589	258.5021055	38.87210176	3145.205085
F6-16-5	15	5021.786881	10972.38118	58708.6911	3753.742502	140.3019299	46928.0801	890.3240917	1234.633586	1832.480276	586.0041702	9.790114682	4197.670528
F6-16-5	19	2493.084106	21582.52422	23661.92799	3258.46606	140.7173244	51137.92993	338.8425812	1597.445543	2702.706398	214.5567047	19.48620923	5291.512925
F6-16-5	24	5614.394332	13732.14713	36755.78012	2860.548669	196.1216384	51058.52346	2704.19216	747.105033	2263.797186	128.9269342	127.9068048	4667.945111
F6-16-5	15	483.7008525	19.85863902	18477.94499	12719.32893	169.0949489	14576.28226	63.90280997	7.954965232	2862.974964	1826.494056	17.67412972	1243.425388
F6-16-5	19	89.78669834	8.765646739	9364.985525	6038.612998	180.604699	16488.15658	71.02250838	1.965451772	1049.793355	934.8898836	17.8536763	1135.993911
F6-16-5	24	636.7826949	239.5022936	15114.26926	5556.134711	252.7489951	26505.46741	164.7861001	16.9659659	1278.925618	264.618718	28.56779559	3120.047493
F6-18-6	7	175296.8534	4.098636912	247001.7849	8483.832448	354.7876457	47553.06562	9455.743649	2.607674231	20341.95457	1150.544612	49.50297126	2482.944983
F6-18-6	11	213492.8168	7306.636453	224236.2304	8390.271419	383.045444	61917.74956	4379.805536	829.7502699	24014.14244	979.7349943	117.5805132	1709.038088
F6-18-6	15	274613.7031	22452.36913	393618.5971	10745.0202	512.3704687	100753.5411	17176.35493	3060.800327	21257.40002	364.5660512	76.9329739	1176.758442
F6-18-6	19	658634.2489	3006.930082	274606.5671	22183.15248	562.8262564	112410.4101	49834.71226	607.045972	12143.8607	2127.62252	143.2926175	6596.650246
F6-18-6	24	12480796.64	29183.49883	9572430.702	192742.1858	170.7775116	681946.7002	151599.3009	4249.478547	710492.7184	14872.90458	N/A	99134.36305
F6-18-6	7	772.1766368	7.391535747	25560.93278	1369.861579	161.0875796	9794.3154	338.7966877	1.061866879	951.6269787	81.7928517	8.532821733	400.7948766
F6-18-6	11	1467.373054	1582.994251	55998.00968	1402.421954	101.1342181	19393.32739	387.5073816	323.7901731	2096.642822	65.48136671	15.4615418	978.2132741
F6-18-6	15	4828.239649	7657.241488	8394.044401	2312.321665	132.6474777	28062.78011	499.3464157	1415.18784	624.5708435	134.7424899	10.86911968	2076.931741
F6-18-6	19	916.3112766	26606.35233	56697.9392	3776.868426	193.4844123	85843.36274	344.1313883	6214.194124	1448.171955	619.0448231	28.56624589	9614.2189
F6-18-6	24	4057.346163	17104.99428	47360.10165	2366.009012	242.6556487	44771.86344	1438.264555	1091.382211	3928.068806	301.3625932	42.22353826	2974.346126
F6-18-6	15	1304.379217	504.5788998	5311.47687	7943.269188	162.3660781	10118.94499	380.1985473	29.00489562	579.3038934	588.3008038	15.86965978	1127.337561
F6-18-6	19	85.44339416	9.582215094	23063.90395	7398.816687	215.0616044	22452.4315	N/A	6.4499843	979.1411787	628.9344625	28.56523828	731.2750617
F6-18-6	24	405.278595	45.59437683	12235.52525	5614.248935	193.7600547	24807.67721	N/A	6.006954116	1729.462685	165.1220908	34.28114494	1306.244939
F6-25-5	7	194072.1417	29.91814564	81419.94202	8988.604456	378.1853181	49158.39491	9419.455393	8.988454213	6504.983744	1361.259253	19.87441264	3835.277296
F6-25-5	11	238791.8432	7396.019991	272296.4495	11850.58561	540.9902531	74235.69636	18834.30653	660.4676939	63656.41255	1037.459933	32.46282815	5722.320192
F6-25-5	15	968597.9377	31298.51299	1391860.557	32251.40115	772.0196857	186508.542	54205.9514	5467.162295	137126.1191	3580.373917	246.3707503	19218.17078
F6-25-5	19	449985.2342	3089.350454	369481.2314	17725.83031	635.5854563	103167.711	13261.46612	294.5588791	18794.27524	1411.377445	132.2754229	1857.899462
F6-25-5	24	320258.8637	2753.062291	186168.0999	19494.17114	708.2376633	100654.0454	23557.12543	181.7544226	5407.982459	1848.044563	240.9591856	12361.07253
F6-25-5	7	990.5950351	7.272118927	29622.1296	1039.920057	151.7008805	6940.212238	167.3916661	4.711867293	4293.855609	143.1214682	27.30390439	688.8359784
F6-25-5	11	4420.027216	2093.03915	46093.29392	1885.788985	160.07642	25265.58991	343.2530072	40.31963969	5922.60162	55.56458488	10.96460296	1603.533133
F6-25-5	15	6347.231578	6081.938943	123078.9389	2537.545113	75.2462556	42194.16202	1130.436906	65.75626235	16610.75975	320.5949673	42.51793793	5712.623017
F6-25-5	19	17329.51736	16796.53628	27348.67129	3672.990155	182.7718062	49443.85362	517.8733438	1180.155888	3085.514879	390.8982164	87.56985257	4894.06884
F6-25-5	24	4354.411881	17261.20159	37358.21054	2929.944662	222.6117773	132700.3199	1940.290917	2466.682612	6103.392117	252.7997294	74.5208902	7040.652718
F6-25-5	15	602.5630502	59.15330402	31896.54238	9909.847746	275.7814525	12646.2887	220.6190426	24.74909166	3026.300977	571.391828	55.20116368	1253.624624
F6-25-5	19	402.2467351	23.01127582	10763.15861	6826.662542	230.527462	15466.8567	135.0105892	8.503039056	179.125183	525.9704283	18.16630618	1009.455249
F6-25-5	24	455.2851943	203.5031502	22079.1218	5567.052511	236.0410619	28391.47667	15.62792467	31.53358111	458.4191238	145.5502221	19.64776076	2233.731483

Appendix 1: (Continued) Black font: Absolute transcript levels of sucrose metabolic genes in developing barley grain (in arbitrary units). Red font: Standard deviations from 3 technical replicates.

Line	DAP	*LTP 1*	*LTP 2*	*LTP 1*	*LTP 2*
WT Torrens	7	3421.286871	6971.956314	220.9792582	161.7215317
WT Torrens	11	65532.69402	66875.49092	1766.486307	2140.365757
WT Torrens	15	900586.7391	218211.4734	58020.44101	10527.41778
WT Torrens	19	7492184.013	202286.6292	562541.2524	13184.7239
WT Torrens	24	2981505.761	20781.59862	235971.9296	1383.993077
WT Torrens	7	219.2474419	12156.33282	32.31643195	779.5824267
WT Torrens	11	7589.58282	20292.68489	434.4744637	1947.763179
WT Torrens	15	55191.99308	18220.24276	3780.172703	1070.394732
WT Torrens	19	3787182.49	86554.37593	85851.44561	4589.678432
WT Torrens	24	12020635.49	77385.5545	557996.0975	4296.294943
WT Torrens	15	8976.254357	11241.79487	765.9365798	1004.461195
WT Torrens	19	9019.498021	1666.708062	745.110863	121.3114121
WT Torrens	24	251311.9893	5442.103397	11445.8729	395.5986068
WT(tc)	7	13023.7263	116850.5782	1360.664935	9211.420798
WT(tc)	11	18442.20969	138229.3755	2342.087501	12628.89219
WT(tc)	15	1366108.29	297714.7739	111241.7533	13687.70658
WT(tc)	19	5506563.258	589916.0097	404730.5925	35659.11938
WT(tc)	24	2068411.389	30743.9857	80261.6518	1315.396419
WT(tc)	7	365.8574909	9040.397078	50.38612694	682.28415
WT(tc)	11	1196.65181	14493.41021	29.78420795	295.2545517
WT(tc)	15	7605.084768	10368.35842	351.2025683	87.94852939
WT(tc)	19	1502141.205	47068.55411	101476.7495	2677.150712
WT(tc)	24	29670947.39	244110.794	964854.5444	5074.729824
WT(tc)	15	2331.295528	2745.155209	169.0915493	159.4430547
WT(tc)	19	5779.147681	1157.989388	310.8480311	111.7543203
WT(tc)	24	175952.0698	3283.369269	7275.740481	219.4131511
F6-15-3	7	1609.936762	4771.918724	242.3875827	708.6763731
F6-15-3	11	72342.85013	84003.95947	7759.577839	4818.791601
F6-15-3	15	634382.4728	477966.4225	44872.17493	19628.67679
F6-15-3	19	4787980.778	118041.2451	275943.3415	7955.025694
F6-15-3	24	831720.0296	34398.40341	127739.8451	2920.50723
F6-15-3	7	223.4241935	634.2904069	22.63303469	55.16573587
F6-15-3	11	20178.48326	16337.12545	242.7704758	1726.284372
F6-15-3	15	903985.0452	85177.53557	8301.067818	6813.399044
F6-15-3	19	3478031.337	121733.8779	212917.4718	1791.479753
F6-15-3	24	10033026.38	57299.93939	743612.7417	3835.095403
F6-15-3	15	5216.196684	1439.2839	482.8284012	129.341289
F6-15-3	19	5421.900227	1153.064557	332.8095435	94.17891434
F6-15-3	24	95735.61347	5012.828618	9027.939492	512.0708162
F6-16-5	7	12723.34419	10121.1761	348.411002	601.0553539
F6-16-5	11	73458.17292	63689.87703	5275.919041	6038.993775
F6-16-5	15	1138351.907	542628.3934	73092.4653	21598.5401
F6-16-5	19	511946.0128	129100.7566	25491.82538	9002.19406
F6-16-5	24	2283130.285	32722.22883	134395.6425	732.0515964
F6-16-5	7	200.2394274	2093.283092	30.55852355	82.14557599
F6-16-5	11	9334.442456	12096.58189	550.0805823	583.5361272
F6-16-5	15	980313.8439	133643.1672	15916.08626	3550.772603
F6-16-5	19	3729357.498	93569.50261	133712.5504	8366.380244
F6-16-5	24	10549219.17	41500.65847	536214.8192	2987.031993
F6-16-5	15	1459.917934	480.4036727	70.1099521	41.9419729
F6-16-5	19	3437.533388	762.7832909	305.9547765	60.44682497
F6-16-5	24	172207.1196	6721.31361	5391.689661	148.6941963
F6-18-6	7	1245.779351	5707.999757	184.5194096	172.8388111
F6-18-6	11	61735.5948	89296.72563	2387.884262	73.1307342
F6-18-6	15	685100.4637	245516.1209	35158.59057	20178.97031
F6-18-6	19	377296.3907	48230.88323	16107.59931	350.2000682
F6-18-6	24	10512657.66	2154534.852	934086.4367	123421.8409
F6-18-6	7	74.42640289	1504.335819	3.27168827	70.35669276
F6-18-6	11	10394.92235	19868.44537	309.9876135	735.7582812
F6-18-6	15	411439.0098	42440.76592	45322.28323	2714.156172
F6-18-6	19	12026454.51	164979.7449	1101621.693	8243.435534
F6-18-6	24	12927218.53	58291.91494	640615.3197	4814.062682
F6-18-6	15	20634.71135	6375.368652	173.4892411	518.759858
F6-18-6	19	36504.67297	1270.374709	2100.952643	120.6011272
F6-18-6	24	101002.2782	4045.368751	623.5437336	225.962518
F6-25-5	7	18986.85548	10854.68274	1059.850265	959.4540517
F6-25-5	11	25633.88476	60204.45041	1317.05382	4598.975654
F6-25-5	15	2228985.682	591614.7786	52605.74494	34257.51016
F6-25-5	19	569433.1419	40528.57043	35428.12897	1566.883618
F6-25-5	24	958219.458	19624.6731	51145.09236	1098.734955
F6-25-5	7	237.3241287	1609.25934	24.44518359	21.58021603
F6-25-5	11	2902.931006	8364.120188	78.48180605	708.9491749
F6-25-5	15	1182068.186	45040.79411	40337.21446	2944.009024
F6-25-5	19	4316001.938	94613.68234	69819.91551	4310.004266
F6-25-5	24	8805928.135	45908.79014	624843.2293	3810.421681
F6-25-5	15	3343.325523	897.0658775	314.0891915	50.79053558
F6-25-5	19	1902.373928	1174.010506	282.2787898	48.38457833
F6-25-5	24	50906.4837	4743.16803	3076.580568	427.2956042

Appendix 1: (Continued) Black font: Absolute transcript levels genes encoding lipid transfer protein 1 and 2 in developing barley grain (in arbitrary units). Red font: Standard deviations from 3 technical replicates.

Line	DAP	Tissue	*CslH1*	*CslJ*	*CslF3*	*CslF7*	*CslF8*	*CslF9*	*CslF10*	*CesA2*	*CesA3*	*CslH1*	*CslJ*	*CslF3*	*CslF7*	*CslF8*	*CslF9*	*CslF10*	*CesA2*	*CesA3*
WT	7	Pericarp	1,305	25	17,083	2,923	1,770	215,794	1,883	6,659,157	18,631	427	3	4,528	492	306	13,105	53	698,408	2,698
WT	11	Pericarp	178	11	399	3,771	2,016	58,259	1,232	11,218,324	12,540	21	8	346	1,599	182	11,001	501	1,633,847	3,193
WT	15	Pericarp	615	4	324	1,830	3,117	38,553	890	8,660,118	6,394	149	3	163	670	297	5,538	345	255,403	1,299
WT	19	Pericarp	533	10	219	1,236	2,071	1,241	624	5,599,693	4,958	59	1	151	394	286	372	411	537,925	1,581
WT	24	Pericarp	2,169	99	3,049	9,228	628	1,365	1,723	4,187,690	19,286	430	26	1,217	3,572	597	1,163	830	114,186	13,387
WT	7	Endosperm	677	26	233	729	921	726,760	343	396,803	9,411	46	2	232	145	130	49,354	116	24,028	884
WT	11	Endosperm	51	34	110	742	695	373,973	182	555,636	2,514	9	7	135	287	94	46,520	59	23,169	901
WT	15	Endosperm	16	9	257	717	508	89,296	457	829,944	4,304	2	3	146	332	220	11,099	197	30,608	252
WT	19	Endosperm	431	4	345	1,351	1,138	2,060	939	2,354,426	8,730	91	2	345	68	609	357	121	81,690	1,699
WT	24	Endosperm	1,810	12	695	5,122	625	1,082	1,694	1,181,760	6,009	600	5	655	2,518	758	822	652	110,552	872
OUM125	7	Pericarp	252	8	207	440	972	62,711	296	6,279,658	6,432	76	4	72	19	54	1,833	22	603,548	5,145
OUM125	11	Pericarp	72	13	9	463	579	24,001	2,033	3,898,920	2,437	19	1	1	173	64	879	2,519	222,332	339
OUM125	15	Pericarp	739	14	280	961	881	621	1,584	2,801,035	2,345	267	12	373	109	204	344	888	297,771	281
OUM125	19	Pericarp	2,443	77	4,060	11,935	2,280	1,604	6,067	8,274,238	9,835	400	71	3,473	3,818	1,106	1,142	1,703	546,025	1,094
OUM125	24	Pericarp	5,400	76	117	1,146	659	448	833	1,551,418	1,475	238	19	133	92	59	321	215	62,489	61
OUM125	7	Endosperm	597	23	38	282	537	673,631	102	367,398	2,041	54	1	22	125	40	43,127	36	37,652	1,740
OUM125	11	Endosperm	154	20	59	300	442	422,000	244	389,118	780	38	3	66	90	50	14,286	26	22,441	34
OUM125	15	Endosperm	2	13	593	1,528	939	5,115	2,191	1,186,740	4,220	N/A	9	521	523	272	815	742	149,850	428
OUM125	19	Endosperm	17	4	836	2,489	364	547	451	599,457	1,597	5	1	636	795	49	395	57	111,750	129
OUM125	24	Endosperm	347	143	280	5,687	761	378	1,544	776,924	18,673	82	3	70	1,339	636	164	552	65,201	6,273

Appendix 2: Black font: Absolute transcript levels of cell wall related genes in developing barley grain (in arbitrary units). Red font: Standard deviations from 3 technical replicates.

Line	DAP	Tissue	*Endo E1*	*Gsl2*	*CslA6*	*HORVU1Hr1G080720*	*HORVU5Hr1G013550*	*UGPase*	*Endo E1*	*Gsl2*	*CslA6*	*HORVU1Hr1G080720*	*HORVU5Hr1G013550*	*UGPase*
WT	7	Pericarp	73	75,408	10,279	497,884	2,559	295,005	24	7,409	929	37,079	262	4,442
WT	11	Pericarp	16,339	71,219	1,983	1,010,295	1,557	281,956	658	9,610	199	94,137	178	21,300
WT	15	Pericarp	120,175	52,814	1,435	812,972	1,163	171,113	11,948	2,376	138	73,866	100	8,598
WT	19	Pericarp	199,497	40,132	120	417,981	894	108,951	18,328	2,548	10	43,366	208	4,936
WT	24	Pericarp	150,091	72,046	81	392,483	2,318	144,940	8,518	4,618	80	17,564	465	12,256
WT	7	Endosperm	34	10,221	22,209	53,049	1,050	171,914	24	754	534	3,694	65	12,095
WT	11	Endosperm	3,867	9,272	11,899	54,632	361	182,376	235	740	1,086	4,294	44	13,914
WT	15	Endosperm	6,699	9,132	4,272	37,105	133	107,973	250	344	569	5,241	36	6,388
WT	19	Endosperm	4,972	22,791	354	46,392	222	145,933	678	1,479	50	3,468	37	12,350
WT	24	Endosperm	1,530	13,873	154	19,177	794	61,561	547	1,568	18	3,532	105	1,668
OUM125	7	Pericarp	625	48,686	919	456,260	1,090	103,370	72	1,059	64	11,068	114	6,420
OUM125	11	Pericarp	1,970	25,954	1,000	289,406	617	65,100	106	916	100	18,405	79	5,367
OUM125	15	Pericarp	128,986	29,413	94	257,339	670	62,606	13,917	1,129	10	15,827	76	4,107
OUM125	19	Pericarp	149,287	70,604	39	609,706	2,013	188,962	8,762	3,078	43	44,871	457	3,132
OUM125	24	Pericarp	111,445	22,276	53	132,167	1,042	48,773	10,523	709	6	9,560	164	1,292
OUM125	7	Endosperm	32	8,165	13,163	39,440	530	98,819	7	188	174	3,011	15	2,823
OUM125	11	Endosperm	109	7,548	9,835	31,492	347	95,622	3	231	507	4,742	34	4,860
OUM125	15	Endosperm	4,483	16,959	443	38,078	222	112,820	486	2,901	10	5,729	62	7,154
OUM125	19	Endosperm	2,741	8,458	35	14,120	58	67,805	78	438	8	2,075	11	7,706
OUM125	24	Endosperm	19,194	11,324	66	29,323	655	35,021	865	349	17	2,296	117	1,955

Appendix 2: (Continued) Black font: Absolute transcript levels of cell wall related genes in developing barley grain (in arbitrary units). Red font: Standard deviations from 3 technical replicates.

Line	DAP	Tissue	*GBSS 1a*	*GBSS 1b*	*SS 2*	*SBE 1*	*SBE 2a*	*SBE 2b*	*Limit Dextrinase*	*Isoamylase*	*AGPase*	*GBSS 1a*	*GBSS 1b*	*SS 2*	*SBE 1*	*SBE 2a*	*SBE 2b*	*Limit Dextrinase*	*Isoamylase*	*AGPase*
WT	7	Pericarp	135,286	54,593	11,404	3,618	28,911	148,077	60,736	23,308	84,435	2,364	4,353	266	268	1,479	18,369	11,772	768	7,785
WT	11	Pericarp	223,611	10,642	8,521	5,915	23,196	204,114	28,464	21,033	43,798	26,080	948	2,467	437	1,940	25,663	4,544	2,159	2,763
WT	15	Pericarp	294,749	3,156	4,093	13,424	40,222	215,715	61,228	32,448	74,479	18,617	365	129	143	1,832	8,240	6,849	1,247	1,020
WT	19	Pericarp	177,940	1,476	3,399	19,131	25,635	80,649	224,413	17,420	46,983	13,877	54	416	1,698	991	2,827	3,961	558	1,644
WT	24	Pericarp	168,219	2,413	5,973	18,575	18,572	80,155	437,595	11,156	64,769	7,682	395	1,320	838	778	1,816	62,128	631	5,332
WT	7	Endosperm	427,031	1,624	903	2,879	78,168	492,948	40,562	36,664	509,881	36,631	292	164	254	6,520	23,193	4,683	2,439	34,027
WT	11	Endosperm	1,152,719	202	400	19,048	144,323	1,122,014	246,277	37,093	740,817	32,241	27	8	835	13,226	49,992	21,249	652	61,235
WT	15	Endosperm	1,096,534	100	213	116,223	109,405	1,041,345	531,386	34,672	508,603	104,838	45	77	66	13,090	45,329	20,631	4,685	22,370
WT	19	Endosperm	1,315,856	521	456	295,166	79,905	395,917	1,862,713	35,916	482,742	39,063	120	54	8,405	615	41,147	108,432	2,322	38,046
WT	24	Endosperm	409,339	725	666	143,203	52,079	206,512	2,253,524	15,122	359,887	10,333	170	206	5,050	499	16,114	51,190	514	31,513
OUM125	7	Pericarp	30,101	28,207	11,555	2,020	12,217	29,225	33,690	6,404	28,971	1,837	1,154	506	177	204	1,408	2,568	389	2,038
OUM125	11	Pericarp	33,328	7,286	5,395	1,288	10,871	29,465	29,376	3,725	23,016	3,387	387	183	83	1,195	1,926	4,316	227	2,437
OUM125	15	Pericarp	96,160	848	2,660	10,885	14,035	43,578	110,496	10,692	28,840	8,857	91	409	833	654	2,690	11,491	442	2,762
OUM125	19	Pericarp	596,824	4,235	3,899	79,084	18,847	94,100	329,979	26,126	31,331	35,124	259	1,504	4,513	1,286	9,217	38,530	623	2,737
OUM125	24	Pericarp	85,062	903	2,607	14,394	3,235	18,202	377,561	3,520	14,737	2,768	173	257	784	236	505	11,167	756	334
OUM125	7	Endosperm	279,755	1,296	544	2,085	46,961	368,208	27,345	30,935	345,487	6,813	89	43	87	1,103	5,154	3,715	1,596	22,823
OUM125	11	Endosperm	449,611	483	402	5,707	63,992	529,872	86,153	26,985	318,609	16,410	42	22	541	1,275	66,860	5,776	1,055	8,897
OUM125	15	Endosperm	1,283,793	499	394	270,530	71,273	274,414	511,119	27,964	341,260	62,233	132	105	22,319	7,901	43,472	51,686	1,531	38,618
OUM125	19	Endosperm	447,059	61	191	126,617	49,476	87,321	1,195,137	10,592	229,423	51,576	30	12	2,816	3,719	8,551	29,697	1,610	9,379
OUM125	24	Endosperm	184,919	349	926	63,337	7,188	26,675	1,558,015	4,330	58,588	8,694	134	200	4,496	368	1,782	64,487	473	569

Appendix 2: (Continued) Black font: Absolute transcript levels of starch metabolic genes in developing barley grain (in arbitrary units). Red font: Standard deviations from 3 technical replicates.

Line	DAP	Tissue	*1-SST*	*1-FFT*	*6-SFT*	*HORVU6H1G011260*	*HORVU2H1G109120*	*1-SST*	*1-FFT*	*6-SFT*	*HORVU6H1G011260*	*HORVU2H1G109120*
WT	7	Pericarp	27,770	3,481	768,830	12,674	4,898	2,415	201	52,413	677	982
WT	11	Pericarp	4,893	3,085	59,084	43,393	27,982	459	723	7,800	3,743	3,603
WT	15	Pericarp	3,143	1,802	26,007	10,664	38,092	323	140	1,820	556	2,114
WT	19	Pericarp	537	752	692	6,102	120,432	71	260	16	186	10,185
WT	24	Pericarp	439	1,911	1,326	6,161	224,314	495	482	382	5,238	16,321
WT	7	Endosperm	13,968	374	465,562	957	388	1,311	43	34,968	108	127
WT	11	Endosperm	849	741	6,059	1,033	209	65	8	539	175	31
WT	15	Endosperm	184	378	1,097	1,166	450	47	60	104	205	64
WT	19	Endosperm	125	270	80	2,647	2,377	133	191	50	488	350
WT	24	Endosperm	337	341	36	3,547	2,170		122	18	212	499
OUM125	7	Pericarp	7,775	1,685	278,916	6,776	5,300	712	89	14,156	429	253
OUM125	11	Pericarp	1,906	1,516	31,755	5,634	3,052	75	164	2,240	316	310
OUM125	15	Pericarp	187	622	252	4,944	132,564	106	47	127	414	14,369
OUM125	19	Pericarp	230	1,982	854	11,138	121,732	41	1,492	191	2,815	6,022
OUM125	24	Pericarp	83	237	930	2,613	150,802	60	85	204	771	8,454
OUM125	7	Endosperm	5,676	661	273,684	817	136	107	20	15,671	92	9
OUM125	11	Endosperm	1,577	534	40,315	1,000	74	131	49	1,437	63	6
OUM125	15	Endosperm	262	684	1,079	1,868	1,848	146	235	295	N/A	142
OUM125	19	Endosperm	52	294	299	143	1,189	41	312	102	N/A	149
OUM125	24	Endosperm	100	352	2,083	506	18,508	47	34	386	683	1,308

Appendix 2: (Continued) Black font: Absolute transcript levels of fructan metabolic genes in developing barley grain (in arbitrary units). Red font: Standard deviations from 3 technical replicates.

Line	DAP	Tissue	*CWINV 1*	*VIN*	*SUT 1*	*SUT 2*	*CWINV 1*	*VIN*	*SUT 1*	*SUT 2*
WT	7	Pericarp	44,045	753	414,917	22,046	1,941	29	22,182	587
WT	11	Pericarp	24,191	19,930	688,526	17,746	2,397	2,735	27,955	1,707
WT	15	Pericarp	20,555	44,933	198,684	11,851	2,444	860	13,994	803
WT	19	Pericarp	14,600	27,894	125,435	9,582	1,583	1,943	2,329	434
WT	24	Pericarp	86,984	29,345	129,188	20,343	4,683	1,807	4,395	561
WT	7	Endosperm	481	175	65,388	2,917	193	17	1,263	181
WT	11	Endosperm	45	2,985	57,788	2,926	21	53	5,079	146
WT	15	Endosperm	463	1,470	20,919	3,163	59	75	1,480	21
WT	19	Endosperm	99	20,400	17,468	6,711	84	2,478	284	412
WT	24	Endosperm	82	23,718	17,354	3,719	35	2,886	507	793
OUM125	7	Pericarp	31,042	233	200,839	12,410	1,715	7	1,330	917
OUM125	11	Pericarp	14,435	582	123,640	6,133	614	79	3,381	140
OUM125	15	Pericarp	5,489	30,711	89,850	5,734	323	2,202	4,753	562
OUM125	19	Pericarp	16,665	56,323	279,822	14,793	402	5,184	10,395	940
OUM125	24	Pericarp	2,055	38,338	80,736	7,166	176	374	3,528	552
OUM125	7	Endosperm	235	89	46,371	2,099	21	26	1,229	65
OUM125	11	Endosperm	221	647	39,689	2,034	14	21	1,268	160
OUM125	15	Endosperm	47	2,616	13,863	7,074	37	151	1,436	736
OUM125	19	Endosperm	21	1,236	4,263	4,051	30	100	194	191
OUM125	24	Endosperm	44	5,562	22,021	7,622	34	425	1,684	928

Appendix 2: (Continued) Black font: Absolute transcript levels of sucrose metabolic genes in developing barley grain (in arbitrary units). Red font: Standard deviations from 3 technical replicates.

----------End of Thesis----------